New N-donor Ligands for Asymmetric Catalysis

Ready, Christopher

Award date:
2013

Awarding institution:
University of Bath

New N-donor ligands for Asymmetric Catalysis

Christopher W. Ready

A thesis submitted for the degree of Doctor of Philosophy

Department of Chemistry
University of Bath
June 2013

Contents

Acknowledgements

First and foremost I would like to thank Dr Matthew Jones for providing me with the opportunity to undertake this PhD project within his group. His guidance and advice, patience and enthusiasm, his nicknames, wrong names, and "kicks-up-the-backside", have been invaluable.

The University of Bath and the EPSRC is thanked for their financial support. Dr John Lowe is thanked for his assistance with NMR issues and advice. Dr Anneke Lubben and Mr Christian Rehbein are gratefully acknowledged for their help with mass spectrometry, and Ms Anneke Klapwijck for working with me in the lab.

A noteworthy thanks must go to Mr Jeff Summers, without whose inspirational and exciting teaching would not have seen me take this path, and Mrs Iris Law, Nanny, without whose guidance wouldn't have seen me take this path for so long.

Many members of the Jones and Davidson groups, past and present, are thanked especially; Dr Emma Whitelaw, for all your support, in the lab and office, and also outside of the department. Dr Kirsty Mokebo for all the coffee. Dr Justin O'Byrne is hugely thanked for his humour. But also his help, motivation, and. Dr Chris Hawkins is thanked for being a great friend, being someone who will always stop and listen no matter how frivolous the issue.

The following people are thanked for making everyday fun and enjoyable; Ben Jeffery is thanked for his advice, help, ideas, dates, apples, and Ryvita, and badger spotting. Lois Manton is gratefully thanked for her encouragement, help, and muesli. Tom Forder for cheering the place up. Rhodri Owen, Marek Lewandowski and Dr Stuart Hancock are thanked for being the best office-mates for putting up with me using the office as a dressing room. David Liptrot is thanked for being my weekend lab buddy and Ben Hodges as my personal career's advisor.

My new friends at the Universitatea Babes-Bolyai, Cluj-Napoca, Romania, for welcoming me and letting me work and write in the department. Special mentions go to Dr Ana-Maria Preda and Ana Toma for being very polite when tasting my cupcakes.

A very special thanks go to my parents for their support, understanding and love, Mum, whose mince pies became legendary and were invaluable as bribes for Matthew, and Dad, for never being too far from his email and rescuing me from many financial complications. Without you both I would never have gotten this far. Andrew is acknowledged for popping his head up every so often and sharing some enchilada's with me, you would never guess we were studying at the same university, shame about the subject. Nick, Wifey, is thanked for being genuinely interested in my research whenever I would phone home or visit home, good luck in the correct subject at university. Also Mr Brian Law for proof reading a foreign language. Greg Price and Nick, Wifey, Smith are thanked for not only the lads holidays during my PhD but for also getting my through my Undergraduate degree. Ryan Davies is thanked for being a really amazing and true friend, for all the BBQs and shocking television series we chose to follow, this is an understatement and words cannot be put onto paper for how remarkable a mate you are. Wishey cannot be forgotten for her endless roast chickens and refreshing affect when visiting the department. Joe Lazell and Emily Workman are also thanked for their support.

Dr Ioana Barbul is kindly thanked for all her assistance with presenting my crystal structures, no really thanked for all her help with my crystal structures, showing me how to use the TGA device, helping with my NMR spectra, and a lot of proof reading, restructuring, spelling and grammar correcting, and more. Finally I would like to thank Ioana for all her support, advice, patience, distractions, motivation, and love that she has given me throughout my PhD and beyond into the next stages of my life.

Abstract

Faster, cleaner, cheaper, better processes for industrially relevant chemicals is at the forefront of many areas of chemical research. The development of selective catalysts is important in many fields, classically; pharmaceutical chemistry and drug development, agricultural chemistry and biological activity, cosmetic chemistry and specific fragrances. But, selective catalysis is also important in many other areas including polymerisation and the fine tuning of a polystyrene, and of growing environmental importance; biodegradable and biocompatible plastics from sustainable sources. The former areas are looking towards heterogeneous systems that are tolerant to an array of substrates for a varied range of classic reactions, including asymmetric Michael reaction, Henry reaction, hydroformylation, hydrogenation, hydrosilylation reactions to name a few, to generate important chemical building blocks. An example of the latter point is the stereocontrolled production of polylactide *via* the ring-opening polymerisation (ROP) of the racemic cyclic ester lactide (*rac*-LA), with current industrial metal initiators chosen for the ROP of LA lacking chiral discrimination. This thesis, divided into four chapters, will investigate various ligands as homogeneous analogues containing a variety of transition metals for organically important reactions and the ROP of *rac*-LA.

Chapter 1 introduces the importance of chirality and catalysis alongside the interests of heterogeneous systems. A review of the current literature is presented for the benchmark reactions undertaken in this thesis. Also introduced in this chapter is the ring-opening polymerisation of *rac*-LA, the importance of biopolymers, mechanism and methods involved in the preparation and characterisation of polylactic acid, alongside a review of the current literature.

Chapter 2 investigates the preparation of an array of chiral pyridine containing Schiff base homogeneous ligands, as analogues to heterogeneous systems. The sterics about the chiral centre of the ligands have been varied. These ligands were trialled against benchmark reactions, and the activity and selectivity analysed. Furthermore, a selection of heterogeneous catalysts have been trialled for the same benchmark reactions.

Chapter 3 describes the development of chiral Schiff base complexes, and Salalen based complexes, for the ROP of *rac*-LA, where the sterics and electronics of the ligand have been varied. The metal centre of these initiators includes titanium, hafnium, zirconium and aluminium, and the initiators investigated under solution and melt polymerisation conditions.

Chapter 4 provides details of the reaction procedures for the synthesis of starting materials, ligands and complexes. Benchmark reaction conditions for the asymmetric Henry reaction and asymmetric hydrogenation reaction is detailed along with that of the polymerisation reaction.

Glossary of Abbreviations

Me	methyl
Et	ethyl
^{i}Pr	isopropyl
Cy	cyclohexyl
Ph	phenyl
OTf	triflate
COD	1,5-cyclooctadiene
THF	tetrahydrofuran
DIPA	diisopropylamine
MP	1-methyl pyrrolidine
NMR	nuclear magnetic resonance
br	broad
s	singlet
d	doublet
t	triplet
q	quartet
m	multiplet
dd	double doublet
ppm	parts per million
J	coupling constant
CP	cross polarisation
MAS	magic angle spinning
MS	mass spectrometry
ESI	electro-spray ionisation
HPLC	high performance liquid chromatography
GPC	gel permeation chromatography
XRD	x-ray diffraction
CD	circular dichroism
EPR	electron paramagmentic resonance
FDA	Food and Drug Administration
ee	enantiomeric excess
PEG	polyethylene glycol
g_e	(Landé) g-factor
μ_B	Bohr magneton
B_0	external magnetic field strength
h	Planck constant
ν	frequency
λ	wavelength

IPA	isopropylalcohol
LA	lactic acid or lactide
PLA	polylactic acid or polylactide
ROP	ring-opening polymerisation
k_p	polymerisation rate constants
k_{int}	rate of initiation
k_{prop}	rate of propagation
k_{app}	apparent rate of propagation
PDI	polydispersity index
M_w	weight average molecular weight
M_n	number average molecular weight
M_n (theo.)	theoretical number average molecular weight
P_r	probability of *racemic* enrichment
P_m	probability of *meso* enrichment
rac-LA	racemic-lactide
"i"	isotactic
"s"	syndiotactic
$[LA]_o$	initial concentration of lactide
$[LA]_t$	concentration of lactide at a specific time, t
fac	facial
mer	meridional
ROMP	ring-opening metathesis polymerisation
MAO	methylaluminoxane

Glossary of ligands used herein

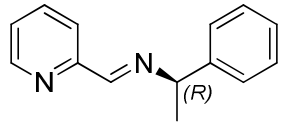 **2IM**	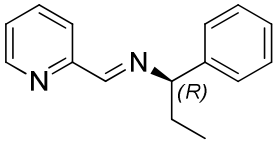 **2IE**	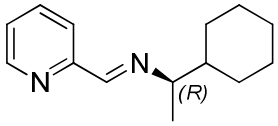 **2IC**
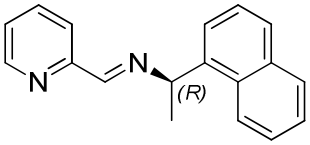 **2IN**	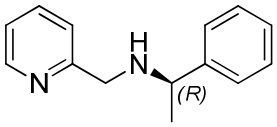 **2AM**	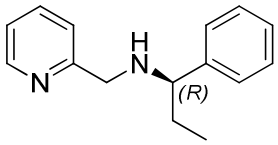 **2AE**
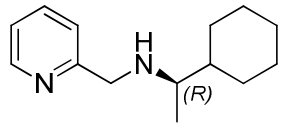 **2AC**	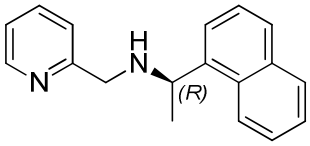 **2AN**	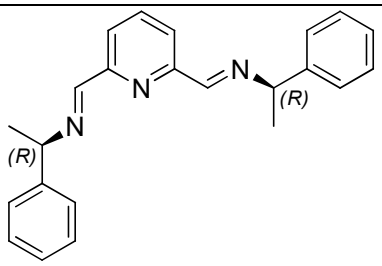 **3IM**
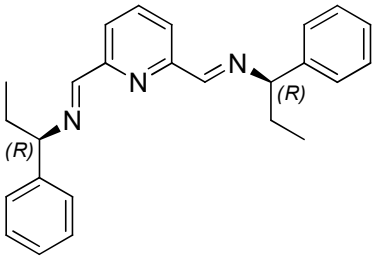 **3IE**	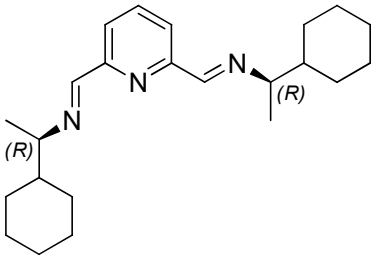 **3IC**	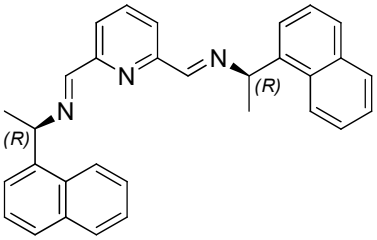 **3IN**
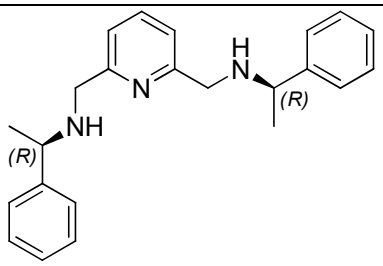 **3AM**	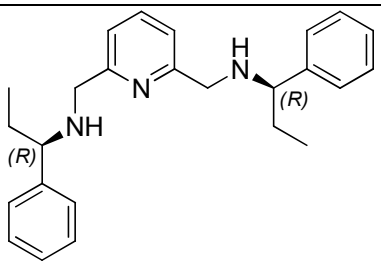 **3AE**	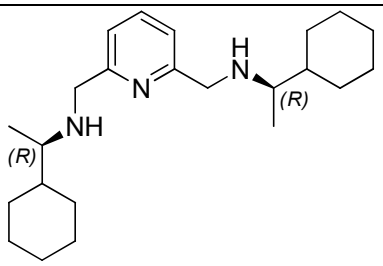 **3AC**
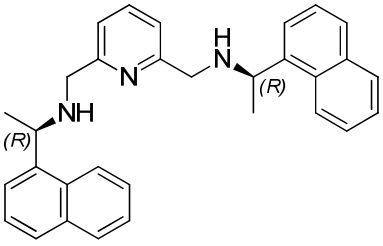 **3AN**	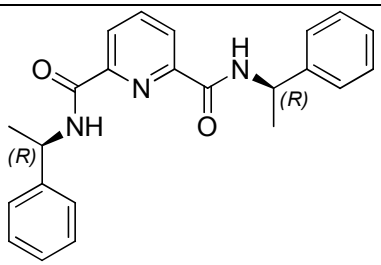 **3NOMe**	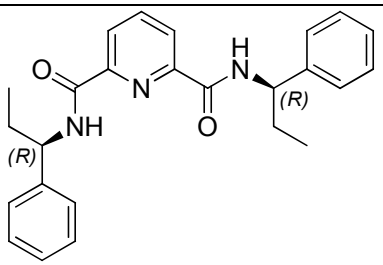 **3NOEt**

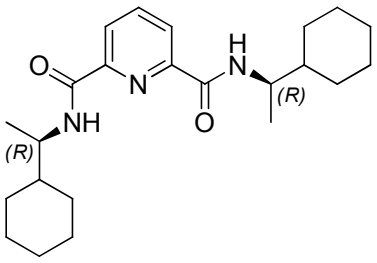 **3NOCy**	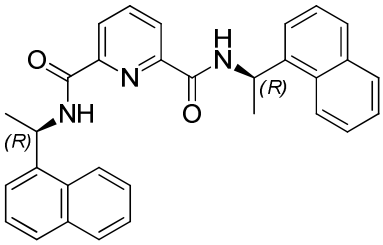 **3NONap**	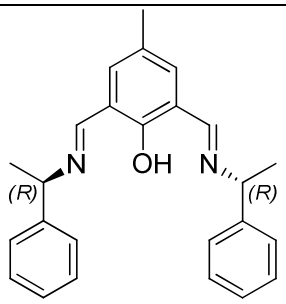 **2R**
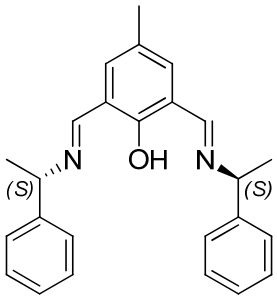 **2S**	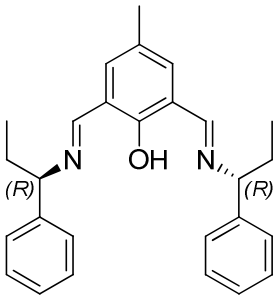 **2E**	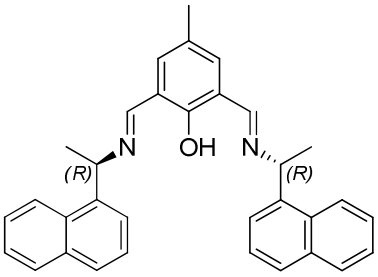 **2N**
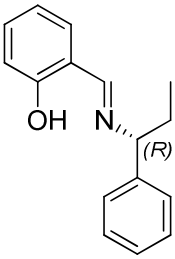 **EH**	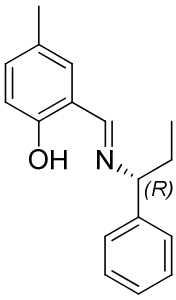 **E5**	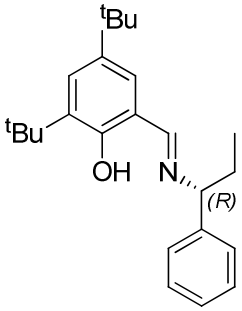 **EB**
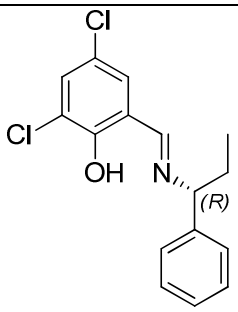 **EC**	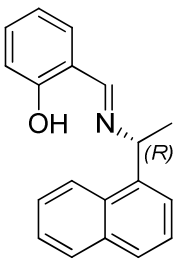 **NH**	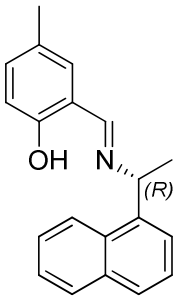 **N5**
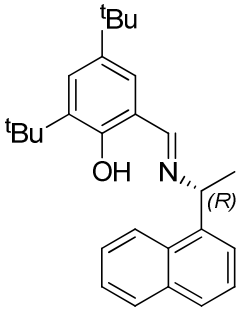 **NB**	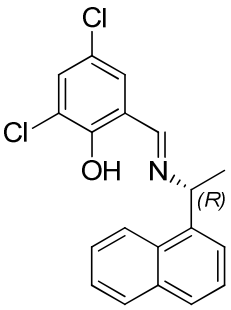 **NC**	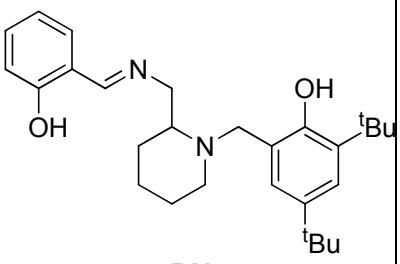 **BH**

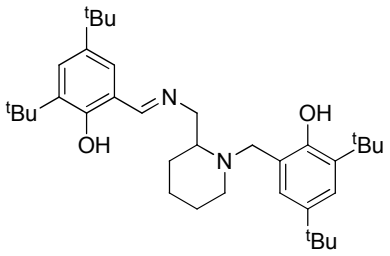 **BB**	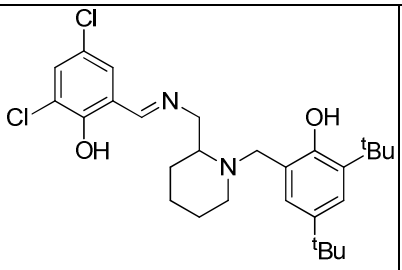 **BC**	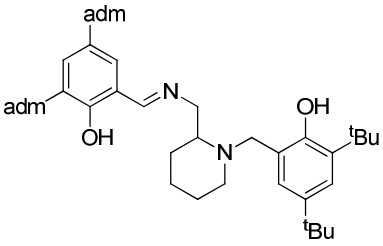 **BA**
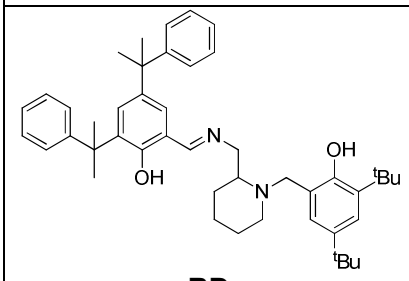 **BD**	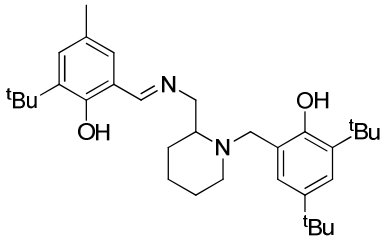 **BM**	

Chapter 1

Introduction

1.1. Asymmetric Catalysis

1.1.1. Importance of Chirality

Pharmaceutical, agriculture, biological, fragrance and materials chemistry all have an important relationship with stereochemistry. This can be as simple as two enantiomers having different odours, (-)-(*R*)-carvone being spearmint and (+)-(*S*)-carvone being caraway. However, the best known and greatly "appreciated" relationship is in the context of drug-receptor interactions as most biological targets are chiral[1]. This is no more so than for the drug thalidomide, Figure 1.1.

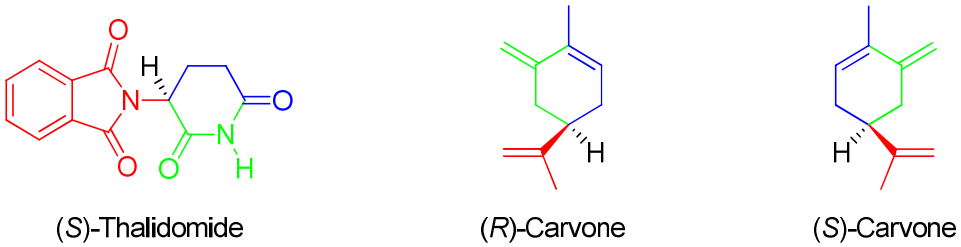

(*S*)-Thalidomide (*R*)-Carvone (*S*)-Carvone

Figure 1.1. Different chiral enantiomers exhibiting different characteristics

Marketed as a sedative and prescribed to alleviate morning sickness during the mid 50's, thalidomide exists as two enantiomers, and in 1961 was withdrawn after it was discovered that the (*S*)-enantiomer, Figure 1.1, caused birth defects[2]. Grünenthal, the German company which developed thalidomide recently issued an apology (Stock, H. Sept 2012, Stolberg, Germany). However, thalidomide has now found new uses under the trade name Thalomid[3], as a treatment for leprosy[4] and multiple myelomas[5]. Research is still underway into thalidomide's treatment of other tumours[6-10].

The importance of chirality and asymmetric synthesis is also recognised by the change in the US Food and Drugs Administration, FDA, (1988) requiring further analysis and information on any chiral substance[11]. As of 2006, 80 % of small molecules approved by the FDA were chiral of which three quarters were single enantiomers[12]. However, there are rare cases where a drug is sold or dispensed as a racemic mixture. The (*S*)-isomer of ibuprofen, Figure 1.2, is the isomer responsible for pain relief and the (*R*)-enantiomer inert, yet ibuprofen is

normally sold as a 50:50 mixture, because racemisation of the inert enantiomer is enzyme-catalysed in our bodies.

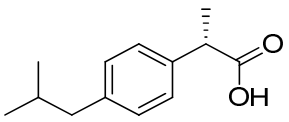

Figure 1.2. Pain relieving ibuprofen (S)-enantiomer

These moves by the FDA therefore highlight the importance of stereocontrol in new synthesis, and an important aspect of asymmetric synthesis is asymmetric catalysis. In 2001 the Nobel Prize in chemistry was awarded to William S Knowles, Ryoji Noyori and K. Barry Sharpless, for "the development of catalytic asymmetric synthesis" and the field is growing and evolving still[13].

Figure 1.3. 2001 Nobel Prize winners in the field of chemistry, William S Knowles, Ryoji Noyori and K. Barry Sharpless 2001

1.1.2. **Asymmetric Synthesis**

Enantiopure products can be achieved via asymmetric catalysis, chiral pool synthesis and by the use of chiral auxiliaries. Chiral pool synthesis is straight forward in that a chiral starting material is used with achiral reagents such that it retains its chirality[14-21]. Pictured below, Figure 1.4, shows the preparation of *S*-sulcatol from *S*-glutamic acid reported by Mori[22].

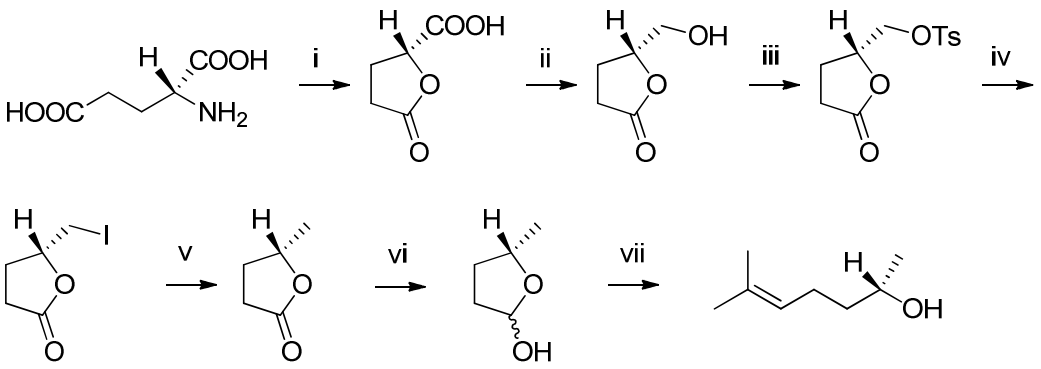

Figure 1.4. Preparation of the aggregation pheromone, Sulcatol, in the Scolytid Beetle from the readily available, enantiopure, glutamic acid[22].
i) HNO_2, 85 %; iia) thyonil chloride; iib) $NaBH_4$, dry diglime, 70 %; iii)TsCl, Py, -10°C; iv) LiI, reflux acetone, 9h; v) Ra-Ni W_7, $CaCO_3$, EtOH, 49 %; vi) i-Bu_3AlH, n-hexane/THF, -60°C, aq.NH_4Cl 73 %; $NaCH_2SOCH_3$/DMSO, $(CH_3)_2CBrPPh_3$[22]

It represents an attractive strategy if the starting material is available, relatively inexpensive for its enantiopure form and if the starting material has similar selectivity to the desired product. Typical starting materials are amino acids or sugars. However, the limitations are that the number of reactions with preserved chirality might be limited and the reactions required are extensive, the above reaction requires upwards of 17 reagents to afford the product, while costs can accumulate especially if the starting material is not a natural occurring enantiomer.

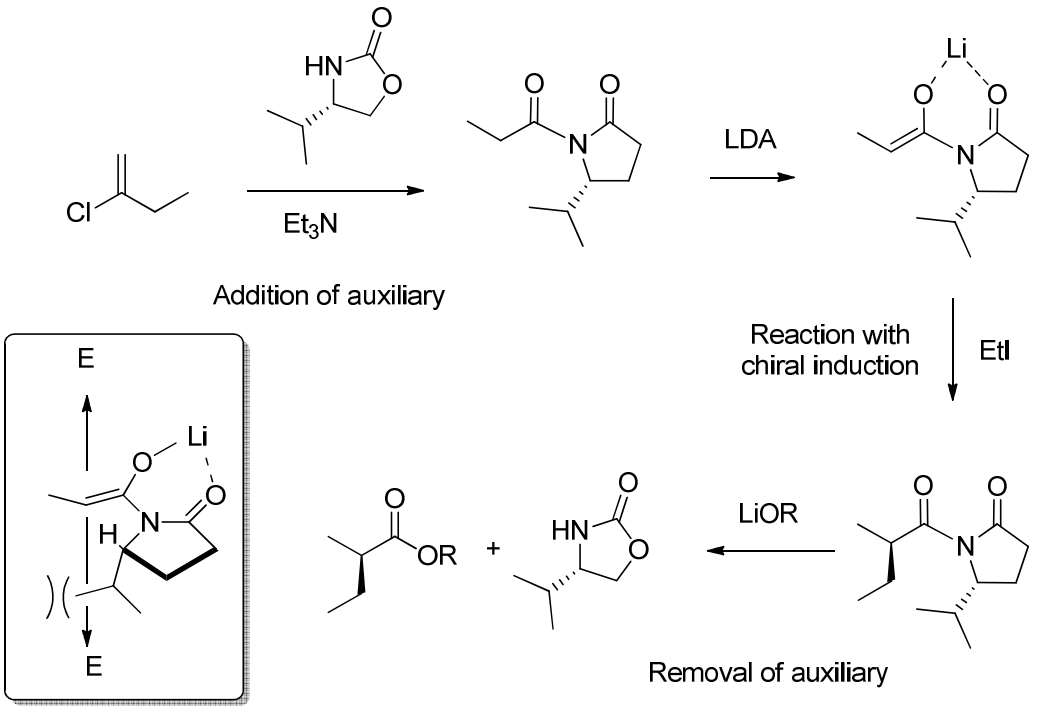

Figure 1.5. Enantioselective enolate alkylation via oxazolidinone auxiliary with a 3D representation of the chiral induction [23,24]

Chiral auxiliaries proceed by inducing enantioselectivity, Figure 1.5. Typically a chiral molecule, auxiliary, is incorporated into the structure of the starting material and physically blocks one trajectory, leaving the desired face open to attack. The chiral auxiliary is then carried through the reaction and removed either in a subsequent step or during work up.

In a sense chiral auxiliaries can be likened to protecting groups in organic chemistry, and as such suffer from the same problem. They increase the number of steps in the reaction, addition and removal, which increases cost and decreases yield. One of the most famous and extensively used chiral auxiliaries is that reported by Evans et al.[23,24], and as such have prompted interest from different research groups reporting structural alternatives to Evans oxazolidinone, Figure 1.6. However, it is important to remember that with such changes the cleavage chemistry can be different, resulting in a possible different diastereoselectivity.

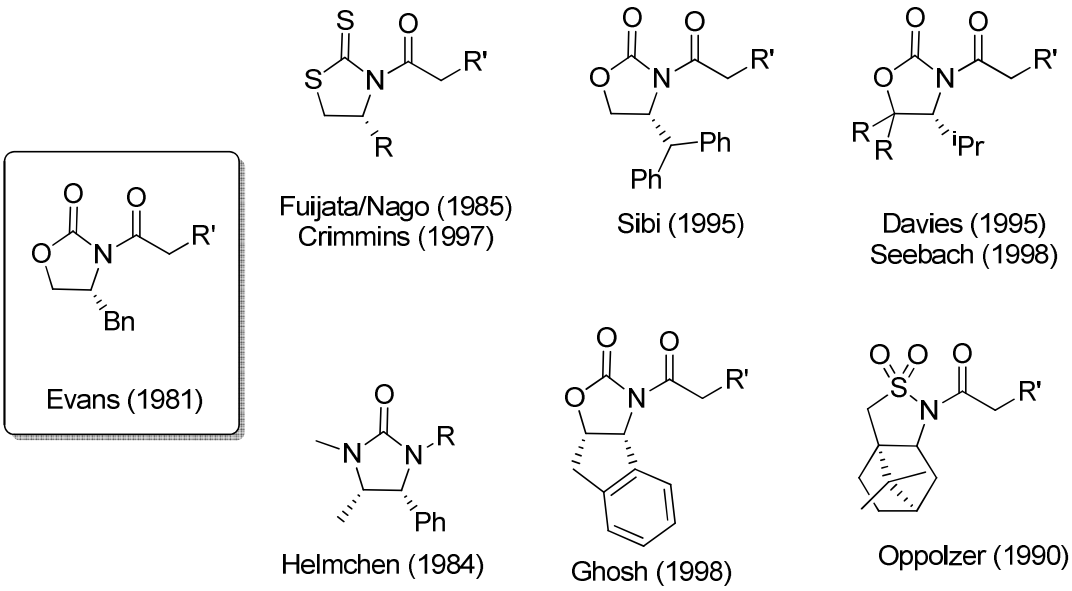

Figure 1.6. Few examples of Evan's oxazolidinone inspired chiral auxiliries

Chiral oxazolidines have been utilised for a broad range of asymmetric transformations, yielding a library of chiral building blocks, medicinally important compounds, natural products and antibodies. Used in the α-alkylation of enolate and the aldol reaction, Figure 1.7, two very important organic carbon-carbon forming reactions, selective enolisation to form the Z-enolates, Z:E >100 was possible with either lithium and sodium amide bases, alternatively dibutylboryl trifluorosulfonate.

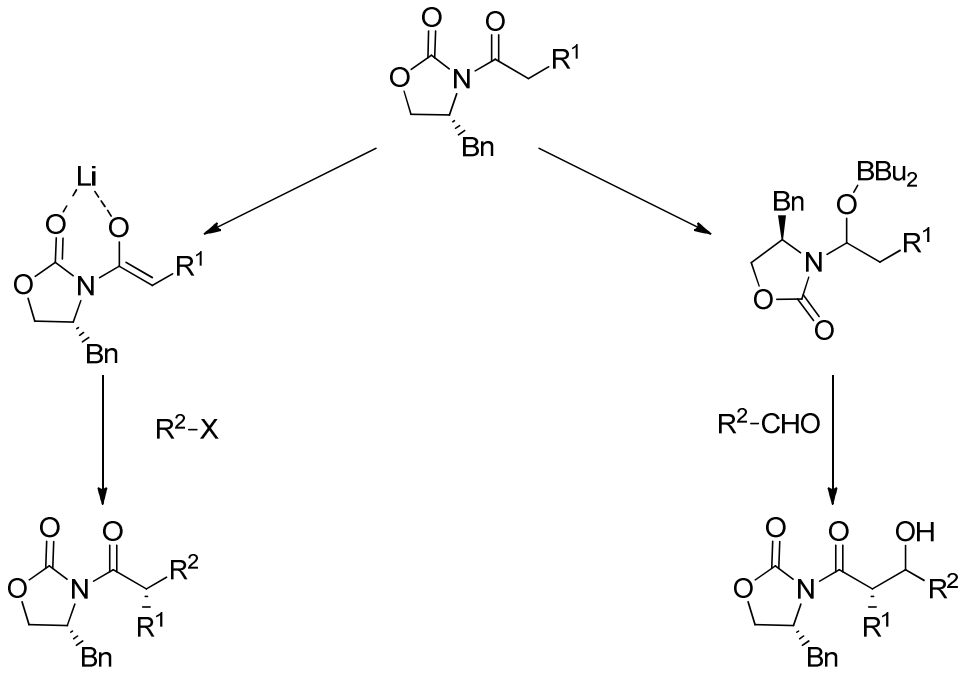

Figure 1.7. Initial asymmetric alkylation[23] (left pathway) and asymmetric aldol[16] reactions (right pathway)

Work on the Aldol reaction also achieved excellent diastereoselectivity. The original work reported in 1981 mediated by boron or titanium gave the syn product. However in an extension of this work (1990) configuration of the chiral centre depended on the reagent used, such the same auxiliary can produce either diastereomer, summarised in Figure 1.8.

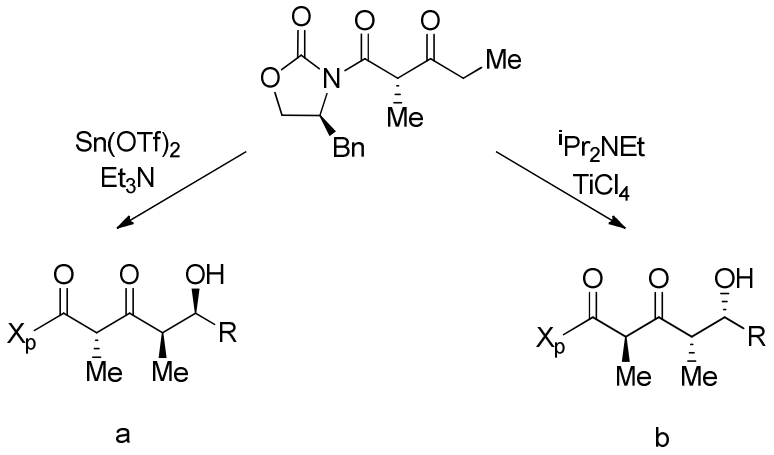

Figure 1.8. An example of varying diastereoselectivity by using different reagents

Enolisation Condition	Aldehyde	Yield (%)	Ratio a:b
$Sn(OTf)_2$, Et_3N	Isobutyraldehyde	83	95:5
$TiCl_4$, ^iPrNEt		86	<1:99
$Sn(OTf)_2$	2-methyl	77	95:5
$TiCl_4$, ^iPrNEt	acrylaldehyde	64	2:98
$Sn(OTf)_2$	Propionaldehyde	71	79:21
$TiCl_4$, ^iPrNEt		86	<1:99
$Sn(OTf)_2$	Benzaldehyde	85	89:11
$TiCl_4$, ^iPrNEt		81	4:96

Table 1.1. Aldol reactions reported by Evans[24] 1-1.1 equiv of aldehyde except for 2-methylacrylaldehyde were yield was obtained with 3-5 equivalents. Ratios determined by HPLC

The work conducted by Evans' is impressive because the reported selectivities are very high for a range of enolates, Table 1.1. Moreover, the results were reproducible and predictable enabling a fine tuning process of the reaction to reach high selectivities by changing one of the R substituents. Further praise can be given as the addition and removal of the auxiliary is straightforward with no risk of racemisation and the auxiliary can be recycled.

Disadvantages to using chiral auxiliaries, however, are that a stoichiometric quantity of the auxiliary is required which can be expensive, even if recycling is possible, when compared to chiral catalysis. Another disadvantage is the extra steps can over complicate the reaction and even reduce stereoselectivity as a result of racemisation. While Evan's reported no complications due to the addition and removal of the chiral auxiliary, this is not always the case. Meyers et al.[25] used a lithio-methoxy chelate as a chiral auxiliary to prepare chiral α-monosubstituted carboxylic acids,

Figure 1.9. When it was the case that R^2 was a phenyl group, racemisation was observed as a result of the greater activity of the α-benzyl proton.

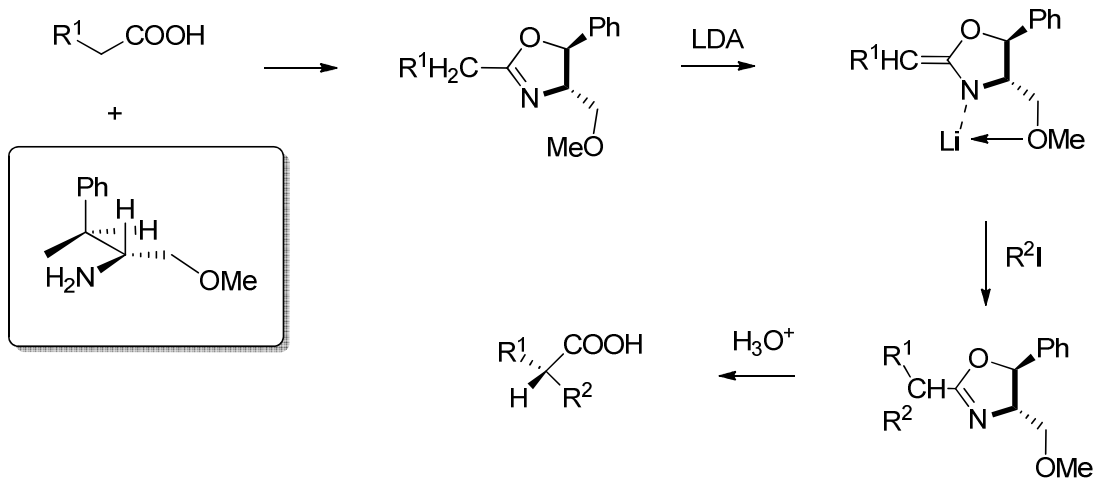

Figure 1.9. Preparation of α-monosubstituted carboxylic acids reported by Meyers[25]

The possibility of racemisation is a common concern when working with chiral auxiliaries. Considerations have to be taken when selecting the removal reaction, to avoid this risk and maintaining the desired geometry at the newly prepared chiral centre. As such this can dictate how the reaction is used and also limit the number of useable substrates for a given auxiliary.

Chiral catalysts have the advantage over chiral auxiliaries in that they are required on a substoichiometric level, have greater flexibility with regards to the substrates that can be utilised and there is no danger of racemisation of the product as there is no cleavage step, and in some cases the selectivity achieved is superior. An ideal stereoselective catalytic transformation would proceed to 100 % conversion with complete chemo-, stereo-, and regio-control under the minimum amount of solvent, with the minimal requirement of additives, like co-catalysts, under laboratory temperatures and pressures, forming no waste by-products, using inexpensive recoverable catalysts, at low loading.

A simplified means to picture asymmetric catalysis is that of a reaction between an achiral substrate which is prochiral and a reagent which when added yields a pair of enantiomers. As in traditional catalysis, the reaction cannot occur if the activation energy barrier is not overcome, and the addition of a catalyst provides a new route via a lower activation energy, to the product, and in the case of prochiral substrates, a racemic mixture. By employing a chiral catalyst, this new, lower energy pathway can be for a single enantiomer, or as represented in Figure 1.10, offering two reaction pathways with lower activation barriers. For a

successful enantiospecific catalysts the energy difference between the two activation energy barriers, ΔΔG, should be high. As drawn there will be a preference for the *S* enantiomeric product.

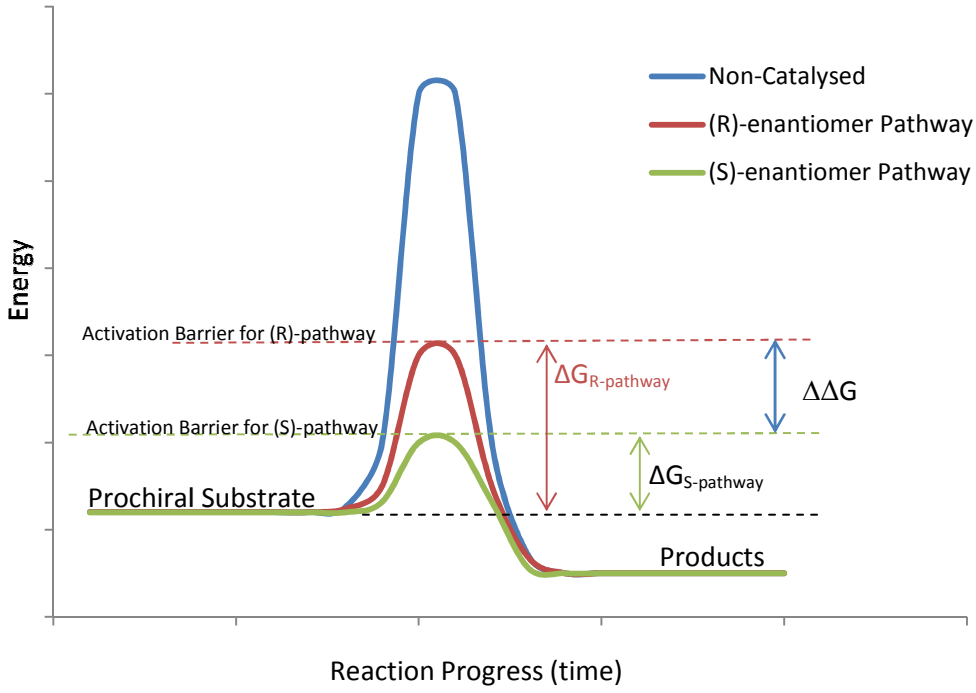

Figure 1.10. Energy reaction profile for a prochiral substrate

However, as catalysis is not as simple as a single pathway, asymmetric synthesis is not a straight forward as there are often many competing diastereomeric pathways.

A good example of this principle is given in "Fundamentals of Asymmetric Catalysis"[26]. Silyl ketene acetals show poor reactivity with acetic anhydride with conversion after 60 hours being less than 2 %, as such the activation barrier is great. The addition of a ferrocene based catalyst in Figure 1.11, planar, chiral derivative, below stoichiometric amounts, substantially decreases the activation energy barrier, complete conversion after 18 mins. Enantioselectivity is determined in the last step of the reaction where the *N*-acyl-catalyst can attack to either the top face or bottom of the enolate substrate which gives rise of a mixture of enantiomers. The energy difference between these two diastereomeric pathways dictates enantiomeric excess, with top face approach being more favourable.

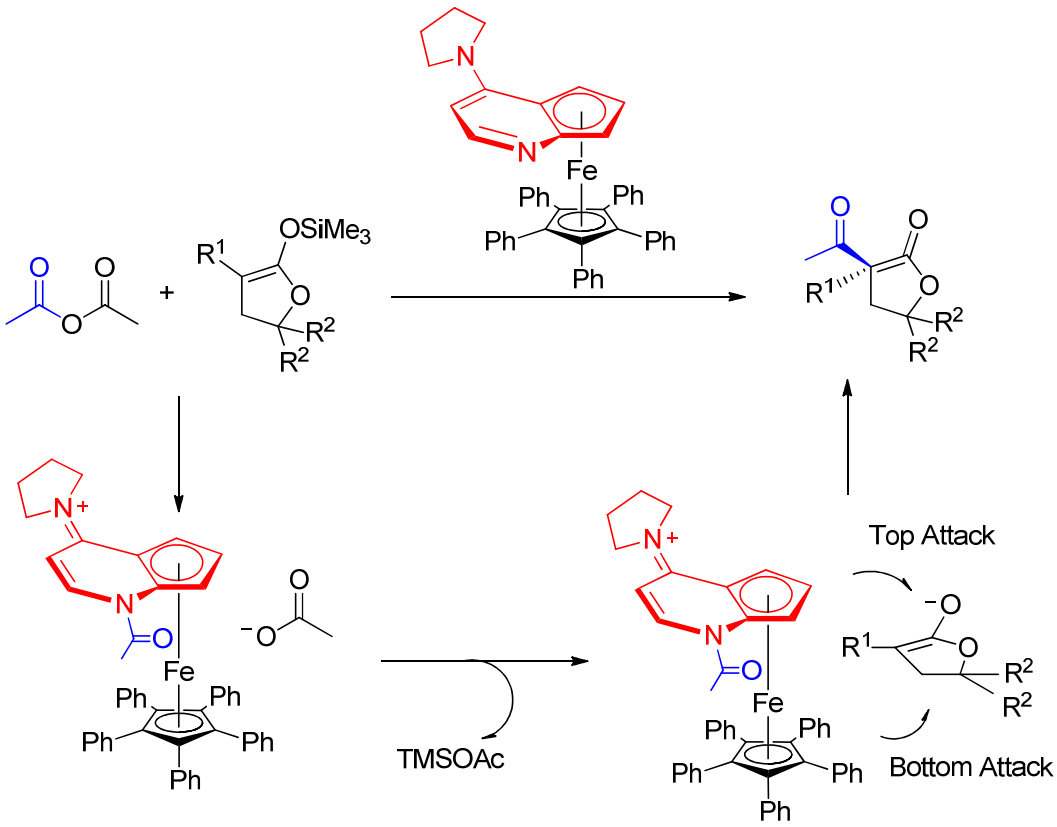

Figure 1.11. Reaction scheme for the substituted ferrocene catalysed reaction of acetic anhydride with a silyl ketene acetal[26]

It is seen in the literature and is commented herein, that the best selectivities are achieved at low temperatures, or are improved upon cooling a reaction. With reference to the energy profile diagram, Figure 1.10, if the difference in energy between diastereomeric reaction pathways is comparatively large (> 2.0 kcal/mol) then high enantiomeric excess can be achieved at moderate temperatures (room temperature).

R^1	R^2	Yield (%)	ee (%)
Ph	Me	80	90
4-(MeO)C_6H_4	Me	78	95
4-(F_3C)C_6H_4	H	84	90
2-(Me)C_6H_4	Ne	89	95
1-Naphthyl	Me	82	99
2-Thienyl	Me	84	76
3-Thienyl	Me	86	87
3-Thienyl	H	73	90

Table 1.2. Substrate tolerance for the addition of acetic anhydride to different substituted silyl ketene acetals

However, as the case more commonly encountered, if the energy gap is small, at room temperature the reaction will give a poor selectivity. Low temperatures will improve the selectivity because $\Delta G = -RT\ln K$, where K is the enantiomeric ratio and ΔG is the free energy difference between transition-states. This is shown, in a simplistic manner assuming a two-state model with only two diastereomeric pathways, in Table 1.3.

		Reaction temperature (°C)							
		60	40	25	0	-20	-50	-78	-100
ΔG (kcal/mol)	0.1	8	8	8	9	10	11	12	14
	0.2	15	16	17	18	20	22	25	28
	0.5	36	38	40	43	46	51	57	62
	1.0	64	67	69	7	76	81	86	90
	1.4	78	81	83	86	88	92	95	97
	1.8	88	90	91	93	95	97	98	99
	2.2	93	94	95	97	98	98.6	99.4	99.6
	2.0	96	97	98	98	98.8	99.4	99.8	99.8
	3.0	98	98	98.8	99.2	99.4	99.8	99.9	> 99.9
	3.4	98.8	99.2	99.4	99.6	99.8	99.9	>99.9	> 99.9

Table 1.3. Enantiomeric excess (%) at different temperatures and ΔG, adapted from[26]

Other factors which can enhance or inhibit enantiomeric selectivity include chemical additives, choice in solvent, as well as the reaction concentration or pressure.

1.1.3. **Heterogeneous Catalysis**

In contrast to the extensive developments of homogeneous systems for asymmetric reactions, heterogeneous asymmetric catalysts have had considerably less consideration, this is despite the historical example of a silk-palladium composite as the first heterogeneous enantioselective catalyst more than 50 years ago[27]. Now with increased demand for single enantiomers combined with environmental concerns and the rising price of catalytically important metals, there has been rapid development and growth in the area[28], such that there are many examples of heterogeneous systems for as many reactions as there are homogeneous; e.g. Carbonyl-ene, Michael Addition, Oxidation, Epoxidation, Sulfoxidation, Hydrogenation, Henry Reaction.

Heterogeneous systems have the advantage over homogeneous in that work up tends to be easier, with reduced contamination of the chiral product, easier recovery, recycling and reuse of often costly catalysts, which is a primary driving forces for their research. Comparing heterogeneous catalysts with homogeneous catalysts give a range of advantages and disadvantages. Firstly, they can operate at higher reaction temperatures as they are limited only by the stability of the catalyst, whereas homogeneous systems are more often limited by the solvent which is employed, enabling reduced reaction temperatures and achieving greater conversions. Transfer of heat can however become an issue due to the varied heat capacities of reactants and heterogeneous catalysts. This increased stability also contributes to the ease of separation for reuse and recycling as the possibility of destruction or poisoning of the catalyst is reduced. This can especially be seen with air sensitive complexes[29] such as iridium or rhodium catalysts, or those with ligands that incorporate phosphines[30-34].

Diffusion of reactants to the catalytic site is an issue for heterogeneous catalysts. Whereas homogeneous counterparts can easily diffuse with the starting materials, heterogeneous systems require the substrates to diffuse to the active site, subsequently reduced activity is often observed[35]. It is also possible that the support, with its high surface area, can interfere with the active site, changing it physically or impeding the substrates access. This latter point can be used to our advantage, however, when size selection is an important factor for subsequent

reactions in multistep synthesis. Selectivity is also hampered, especially enantioselectivity[36], as the chosen support may be active for catalysis of the reaction. While correct selection and implementation of different supports can be of benefit to selectivity, it is seldom observed and rare[37].

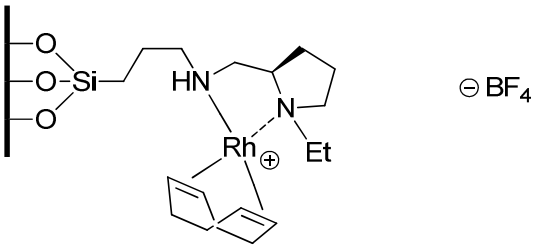

Figure 1.12. Heterogeneous rhodium catalyst prepared by Raja et al. which displays improved enantioselectivity upon heterogenisation.[37]

As mentioned, catalyst separation is a huge benefit of heterogeneous catalysts via filtering or settling mobile heterogeneous catalysts or by flushing immobilised heterogeneous catalysts with a solvent or carrier gas. This type of heterogeneous catalyst system is preferred in industry as it allows the possibility of a continuous flow process[38-40]. Continuous flow can also tackle the heat transfer issue and diffusion problem thereby increasing efficiency[39,41]. A schematic representation is shown below, Figure 1.13, where a feedstock, and the reaction media, are moved through the reactor by a pump. This could be an HPLC pump for small scale liquid reactions, or an argon tank to provide a carrier gas for gaseous reactions. This will then pass a packed reactor bed, containing the heterogenised catalyst, or a series of reactors in parallel. Analysers built into the flow can monitor ongoing reactions before passing the reaction media onto the next stage or allowing the product for collection[42-44].

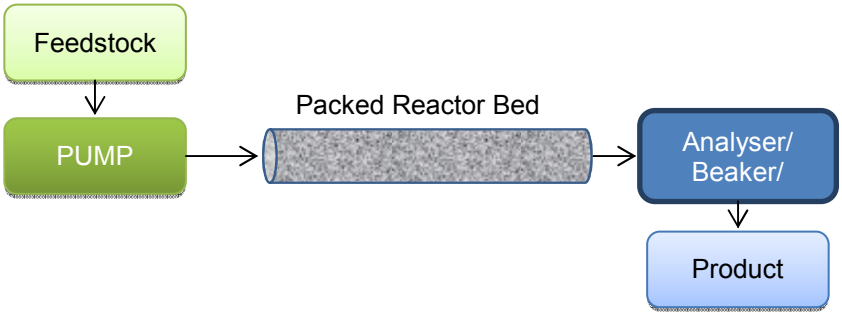

Figure 1.13. Schematic continuous flow reactor

Separation is an important processes industrially as the cost of these catalysts are usually very high. The costs of addition steps and reagents to remove

catalyst, expensive machinery or having to treat the catalyst as a reagent when removal is impossible (polymerisations) is significant and that is before the catalyst is recycled for a subsequent reaction, with typical separation in industry being distillation. A lot of waste is generated and energy required for these processes in homogeneous catalysis unlike heterogeneous where separation and recycling are comparatively straightforward and at most reactivation of the heterogeneous catalyst system is needed. Modification of heterogeneous systems is difficult, with active sites not being as well defined as their homogeneous counterparts, and fine tuning and characterisation of a heterogeneous catalysts being very difficult. It is also more difficult to follow the progress of a heterogeneous system, compared to its homogeneous analogue, resulting in the mechanism remaining elusive. As a result, it is common in the literature to immobilise homogeneous catalysts on heterogeneous supports, like silica zeolites or polymers and to perform mechanistic studies on the homogeneous system.

1.1.4. **Catalyst Immobilisation**

Turning a homogeneous complex into a heterogeneous system addresses the issue of separation and recycling, enabling its use multiple times, while maintaining its high level of selectivity and activity. There are a number of strategies to achieve immobilisation and different supports, inorganic, organic polymeric, dendrimeric, organic-inorganic coordination polymers, and different reactions will suit different supports.

The choice of support is dictated by activity, enantioselectivity, stability, productivity, reuse and recyclability. A perfect immobilised system would display conversion and selectivity at a comparable rate, or better, than its homogeneous analogue, while being easily recoverable and immediately reusable over numerous cycles. However, this is often not the case and a varied range of difficulties can occur. As commented, activity decreases, or ceases, often as a result of constraints around the active site of the newly immobilised catalyst, alternatively during the heterogenising process the geometry of the then homogeneous catalyst is altered resulting in decreased enantioselectivity. This is much the case when using a silica supported catalysts. However, there are examples of increased enantioselectivity[37].

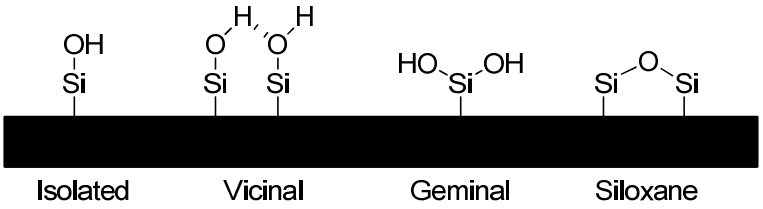

Figure 1.14. The different types of possible silicon groups on the surface of silica[45]

The silica surface is covered in hydroxy-like groups, silanols. Different types of these silanols can be encountered on a silica surface which are very reactive, particularly in acid catalysed processes, but not enantioselective, Figure 1.14. This additional achiral activity is observed as a decrease in enantiomeric excess. Silica supported catalysts can be treated to remove, or cap, the reactive silanol groups[46,47] as can polymeric supports, where it is also important to select as inert a polymer as possible. A typically capping agent is trimethylchlorosilane[48] which reacts with the silanols rendering them inert.

To avoid these complications, it is common practice to use a spacer or linker moiety of ample distance to tether the complex to the support. The result would be that the active site can move away from the solid surface, minimising disturbances on geometry, and into the reactant phase, enabling better diffusion[49]. The difference in reactivity and selectivity has been demonstrated by Lee et al.[50], who prepared a cinchona alkaloid mesoporous silica-supported catalyst with different linker lengths, screened against the asymmetric dihydroxylation of alkenes. As the distance from the silica surface to the active site increases, the enantioselectivity improves up to comparable results with the homogeneous counterpart.

The recurrent consideration towards stability enabling reuse of the catalyst is import. Poor stability in the spacer molecule or incompatibility of the support with the solvent/reactant will result in metal leaching or destruction of the heterogeneous system, like strong acids, oxidising or reducing agents, high temperature or pressures.

1.1.5. **Inorganic Supports**

By far the most common means of heterogenising a catalyst in the literature, this method supports the catalyst onto an insoluble solid. Catalysts can be anchored or tethered by several discrete approaches, covalently bonded and non-covalently bonded, into the internal pores or onto the exterior surface. This is shown pictorially in Figure 1.15. The covalently bonded tethering is considered the strongest linkage between support and catalyst, explaining why it is the preferred type, minimising leaching of the catalyst during repeated reaction and as a result maintaining activity. The disadvantage of using a covalent system is that it requires an extra degree of functionality to create the attachment between support and catalyst. The alternative non-covalent immobilisation, does not require this extra functionality and is generally easier to prepare. Adsorption of a chiral catalyst onto the surface of a support is relatively straightforward and can be sufficient to afford a heterogeneous system, but not very stable when only interacting *via* van der Waals forces, leaching is often observed to varying degrees even when stronger hydrogen bonding is present. Electrostatic interactions are also sufficient to immobilise an ionic homogeneous chiral catalyst. In this instant a support would be either anionic or cationic and the catalyst held by ion-pairing. Lastly, the metal complex can also be entrapped within a solid matrix, assuming sufficient space for the catalytic system in the tunnels or pores of the material, like the defined cages of a porous solid or by forming a polymeric network around the complex. The main disadvantage here is that the designing and synthesis of the heterogeneous system can be difficult, and substrate diffusion issues are more likely to occur[51,52].

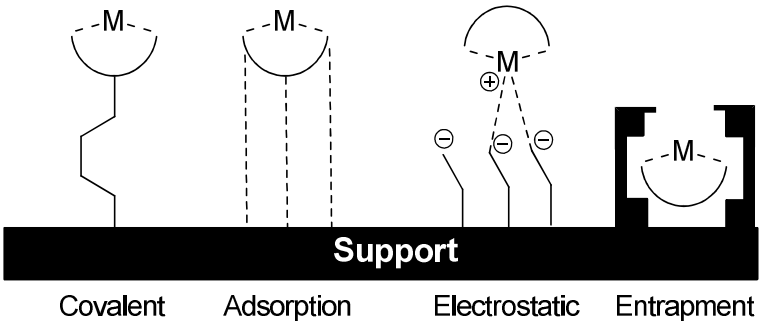

Figure 1.15. Schematic representation of the possible heterogenising strategies

As mentioned, inorganic solid supports encompass silica, mesoporous solids (pore diameters of 2-50 nm, for example MCM-41, SBA-15) but also

zeolites and clays have been utilised for heterogenising a wide variety of chiral homogeneous catalysts[53-57]. Each support has its advantages and disadvantages which need to be considered when designing a heterogeneous system. Silica has an extended structure and an incredibly large surface area, typically 500 m^2 g^{-1}. This can be utilised to prepare a highly concentrated number of active sites within a minimum amount of support and there are many examples in the literature. The silica materials also have high mechanical and thermal stability as such the system can withstand harsher conditions, prolonged reaction times, and as they are a non-compressible material adds to their ideal standing as a flow process catalyst[58,59].

1.1.6. **Benchmark Reactions - Asymmetric Nitroaldol Reaction**

The nitroaldol reaction or Henry reaction is a classical and very powerful carbon-carbon bond forming organic reaction[60,61]. The "key step" in many syntheses affording important functionality and in more complex synthetic ventures facilitating the joining of two molecular fragments, under mild conditions, with the formation of a maximum of two asymmetric centres[62,63].

The addition of a nitro-alkyl compound to a carbonyl, yields a nitroalcohol. The β-nitroalcohol product is then in a prime position for further reactions such as dehydration, yielding a conjugated nitroalkene, denitration, to give an alcohol, oxidation giving an α-nitroketone, which can be further denitrated to afford a new ketone, and reduction, producing a β-aminoalcohol. It is also possible to remove the nitro-group to leave a new carbonyl *via* the Nef reaction, generating an α-hydroxy carboxylic acid[64,65]. Retro-aldol cleavage, induced by a base is also possible reversing the addition and forming the starting materials. Following any further reaction of the nitroalcohol, it is important to note that epimerisation of the chiral centre can occur.

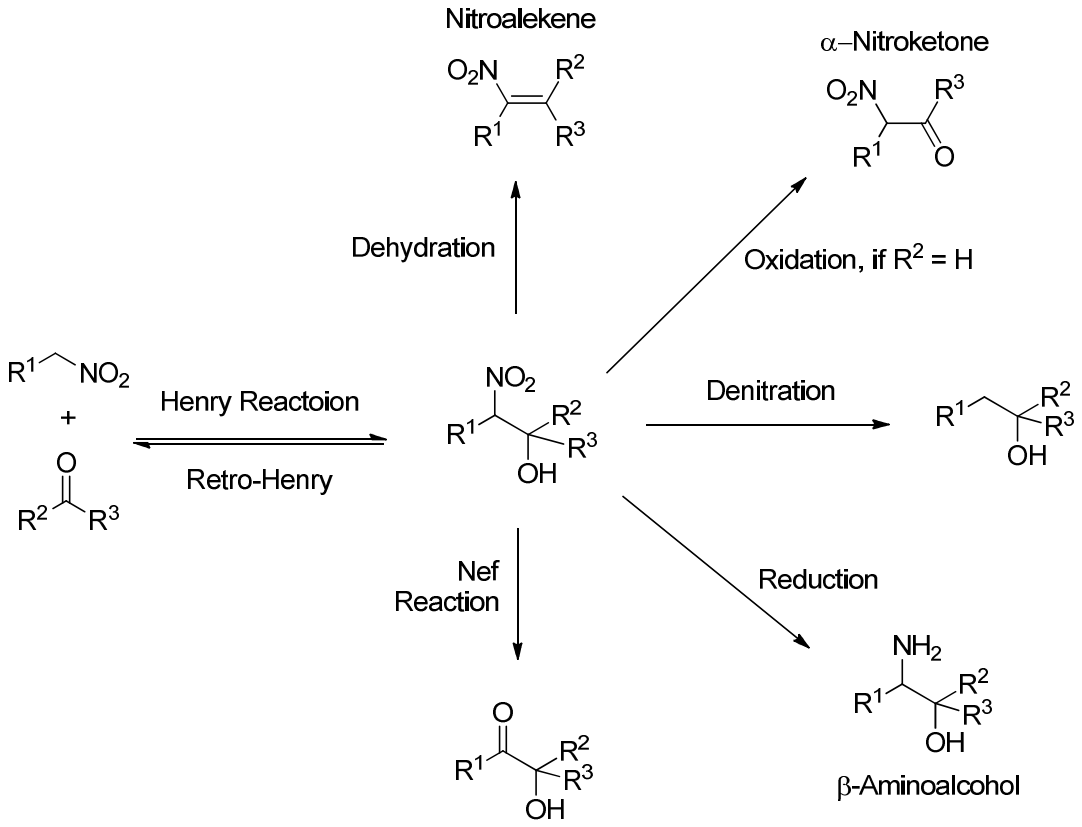

Figure 1.16. Schematic representation of the synthetic importance of the Henry Reaction

A base is typically used in order to deprotonate the α-carbon position on the nitroalkane, which is the most important step in the mechanism, forming a resonance stabilised anion. The aldehyde or ketone facilitates the alkylation of the nitroalkane to form the diastereomeric β-nitro alkoxide, which is protonated by either the earlier protonated base or by deprotonation of another nitroalkane, to yield the β-nitroalcohol,

Figure 1.17. However. there are examples of the Henry reaction proceeding without the need for a base[64,66,67].

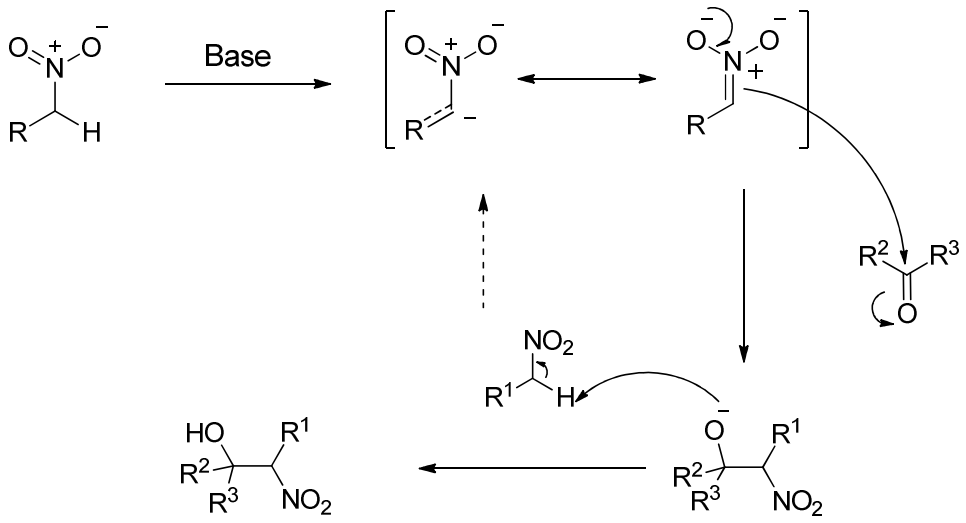

Figure 1.17. Mechanism for the base promoted nitroaldoll reaction.

Stereocontrol in the nitroaldol reaction is a constant challenge, as two chiral centres give rise to syn and anti stereoisomers which is complicated to control[68]. Chiral auxiliaries, as introduced earlier, have not been extensively developed as a general method because of the inability to covalently bond to either the pronucleophilic nitroalky or aldehyde substrate[69-72]. This leaves chiral catalysts to meet the ever-increasing demand for stereochemically pure aminoalcohols by the pharmaceutical industry[62,73] and natural product synthesis[62,74,75], Figure 1.18.

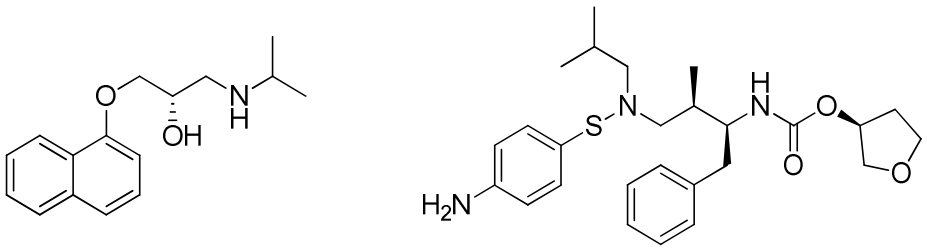

Figure 1.18. Left; More active enantiomer of the β-adrenoceptor antagonist propranolol
Right; Amprenavir, GSK, HIV protease inhibitor

There has been a recent high demand for selective Henry reactions, and given the popularity of the reaction, it is surprising that, besides years of research to implement asymmetry, no significant success was achieved until recently[76]. As with all asymmetric catalytic reactions, examples of biocatalysts, organocatalysts and metal complexes are present in the literature with the latter being the most common. This trend towards metal complexes is a likely result of the catalysts ability to coordinate substrates. Copper(II) systems dominate the literature for the

asymmetric Henry reaction due to their availability, low cost, and their relatively non toxic nature.

It was not until late in the 20th century and early in the 21st that chiral catalysts were extensively developed. Shibasaki et al.[77-81] are often credited with the most remarkable advancement in the topic. Reporting the first metal-chiral ligand complex in the first efficient method for the enantioselective nitroaldol reaction, by exploiting the general principle of a two-centre catalysis[82-84]. The group employed (*S*)-(2,2')-binaphthol with lanthanum alkoxide, Figure 1.19, and by designing a system comprising of two sites of opposite character, in this case an acidic site and basic site, a chiral metal/ligand catalyst can activate each starting material in close proximity. The acidic site activates the aldehyde while the basic site activates the nitroalkane, Figure 1.21. This activation of substrates enable lower loading of the catalyst, as little as 1 mol % can facilitate the reaction at temperatures between -5 and -30 °C within 5 days achieving high selectivities.

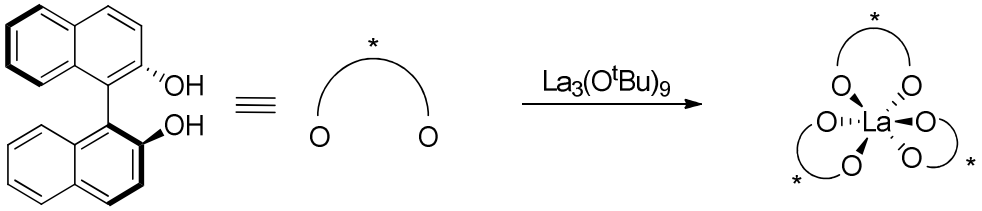

Figure 1.19. Shibasaki's asymmetric lanthanum-BINOL catalyst

Shibasaki's system was later refined by insertion of substituents at the 6,6' -positions of the BINOL skeleton[85-90], Figure 1.20. This improved both enantio- and the anti/syn selectivities when groups such as CN and SiC=C where inserted, achieving syn/anti rations of up to 94:6 and enantiomeric excess of up to 97 %[91-93]. However, simply adding a methyl did not see any significant improvement.

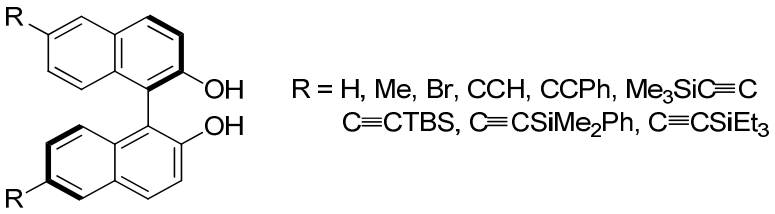

Figure 1.20. Sibasaki's second generation ligands for Ln-based catalyst.

R	Yield (%)	ee (%)
H	72	62
Me	84	63
$Et_3SiC{\equiv}C$	84	85

Table 1.4. Performance of a selection of second generation catalysts against the nitroaldol reaction

Further studies found that addition of water and BuLi to make LiOH gave an improved catalyst system resulting in shorter reaction times[80]. More efficient nitronate formation through transfer of hydrogen enhances the rate of reaction as it is thought to be the rate-limiting step of the catalytic cycle.

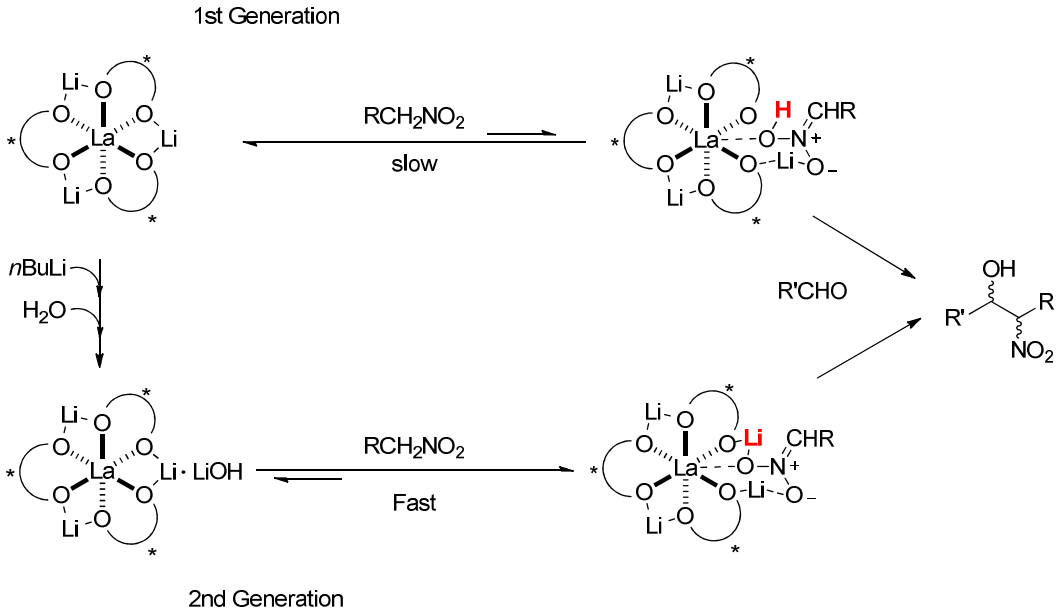

Figure 1.21. Mechanism proposed by Shibasaki, 1st generation vs 2nd generation (modifications are highlighted in red)

Catalyst Generation	Aldehyde R'	Temperature (°C)	Yield (%)	*syn:anti*	ee (%)
1st	Me	-30	25	70:30	62
2nd	Me	-30	83	89:11	94
1st	Et	-40	< 5		
2nd	Et	-40	84	95:5	95

Table 1.5. Comparison of 1st generation *vs* 2nd Shibasaki catalysts with two different aldehydes

In 2006 Shibasaki along with Matsunaga published promising results for the Henry reaction of ketones, a still challenging area[94]. Needing the kinetic

resolution (a means of differentiating two enantiomers in a racemic mixture via the differences in their reaction rates) of nitroaldols with BINOL/biphenol mixed La-Li heterobimetallic complexes as the catalytic resolution agent[94]. Conversions were achieved in the range of 50 - 69 %, and high selectivities, 80 - 97 %. However, low temperatures are still required.

Trost et al.[95,96] applied their novel asymmetric catalyst, which combines a dinuclear zinc centred complex with a chiral semi-azacrown ligand, Figure 1.22, that had already shown promise in the enantioselective direct aldol reaction, against the nitroaldol reaction. The ligand is easily prepared from proline and can be tuned for structural and electronic variations.

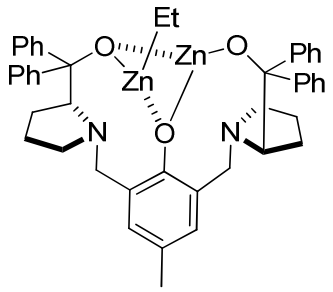

Figure 1.22. Trost's dinuclear zinc complex

This was one of the first zinc catalysed examples and this novel family of dinuclear zinc complexes appear to function in a similar manner to that of Shibasaki's work *via* "cooperative activation". Like the work of Shibasaki, high yields and selectivities were obtained with a slightly higher but still attractive loading, 5 mol %, in a more reasonable timescale, 24 hrs, at -35 $^{\circ}$C. Trost proposed that one of the zinc alkoxides behaves as a Brønsted base, generating a zinc nitronate, and the second zinc acts as a Lewis acid, activating the aldehyde, Figure 1.23, in a similar mechanism to that proposed by Shibasaki, Figure 1.21.

Conversions of 56 - 90 % were achieved and ee's of up to 93 %, but more interestingly with the use of zinc catalysts the doors to reactions are opened. The system utilises a Zn^{2+} centre, just like class II adolase ensymes, as such there is every possibility to conduct the reaction in an aqueous medium, and have lead to the development to an efficient preparation of β-receptor agonists, (-)-denopamine and (-)-arbutamine[96].

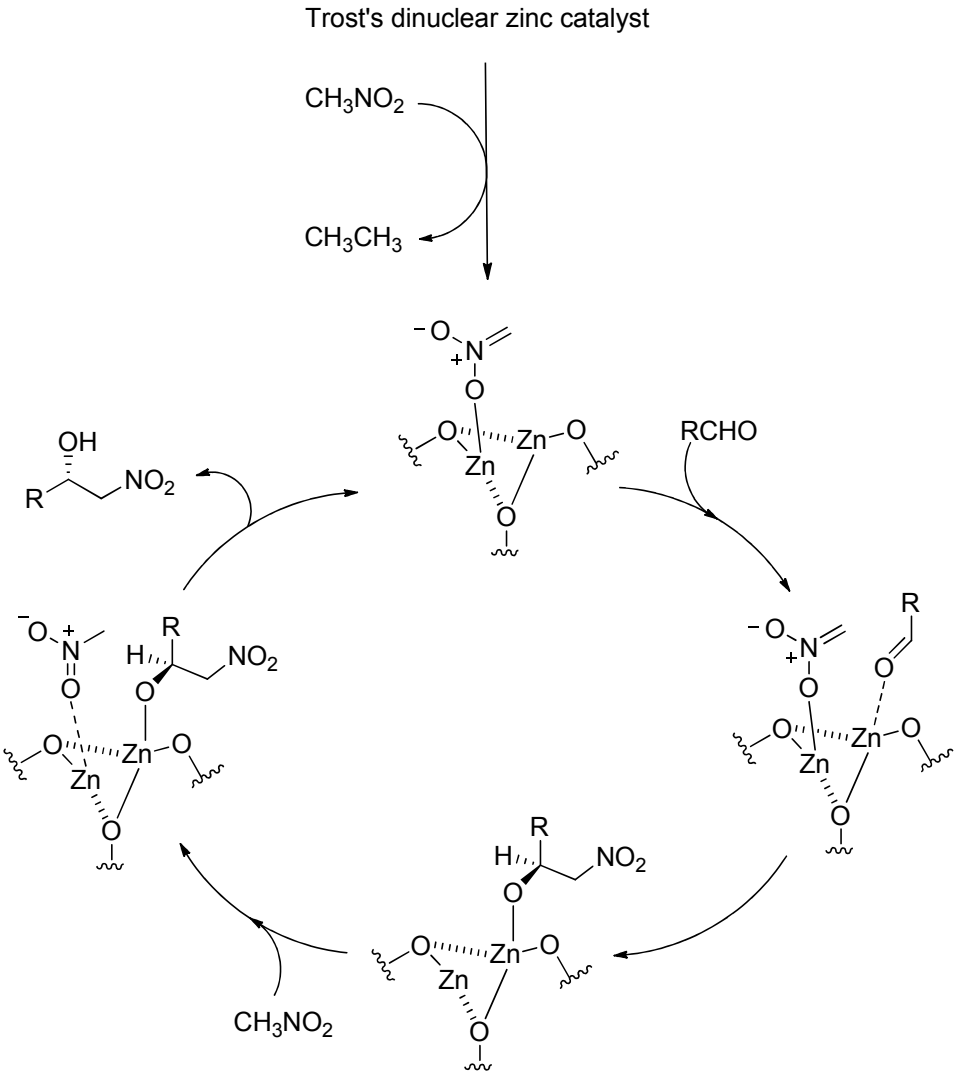

Figure 1.23. Mechanism proposed by Trost et al., catalyst simplified omitting the semi-azacrown

Equiv's CH_3NO_2	Catalyst loading	Temperature (°C)	Solvent	Yield (%)	ee (%)
10	5	5	THF	69	78
10	5	-20	THF	68	85
10	5	-20	Toluene	68	57
10	5	-20	CH_2Cl_2	75	51
2	5	-20	Et_2O	20	55
2	5	-20	THF:dioxane 4:1	17	86
10	5	-78 then -20	THF	75	85
10	2.5	-78 then -20	THF	44	85
6	5	-78 then -20	THF	70	86

Table 1.6. Trost Henry reaction optimisation results

R	Yield (%)	ee (%)	R	Yield (%)	ee (%)
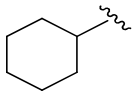	75	85	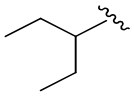	90	92
	58	88		88	93
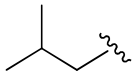	84	87	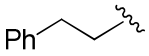	59	84
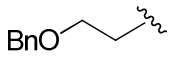	56	86	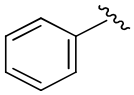	75	91
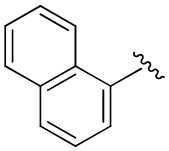	71	93	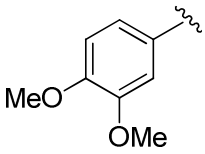	69	78
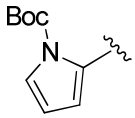	79	90			

Table 1.7. Substrate tolerance for Trost dinuclear zinc system.

In the early work of Trost, the importance of temperature and solvent was also explored, Table 1.6. The study also investigated the substrate tolerance of this system by varying the R group of the aldehyde with linear, branched, cyclic and protected alkyls as well as aromatics, summarised in Table 1.7. α-Branched aldehydes proved the easiest, giving high yields and enantiomeric excesses, 75 - 80 % and 85 - 93 %, however greater equivalents of nitromethane and more concentrated conditions were required to get good conversions and selectivities for other derivatives.

Continuing with Lewis acidic chiral catalyst systems, Evans et al., acknowledging the early work of Shibasaki and Trost, reported a new Henry catalyst with a mildly Lewis acidic metal complex incorporating a reasonably basic, charged ligand[66]. The group proposed that this type of system allows the deprotonation of the nitroalkane **I**, as the lead up to the aldol addition process **II**. To meet these conditions, metal acetate complexes were screened with a chiral bidentate ligand, without the need of a base promoter[97].

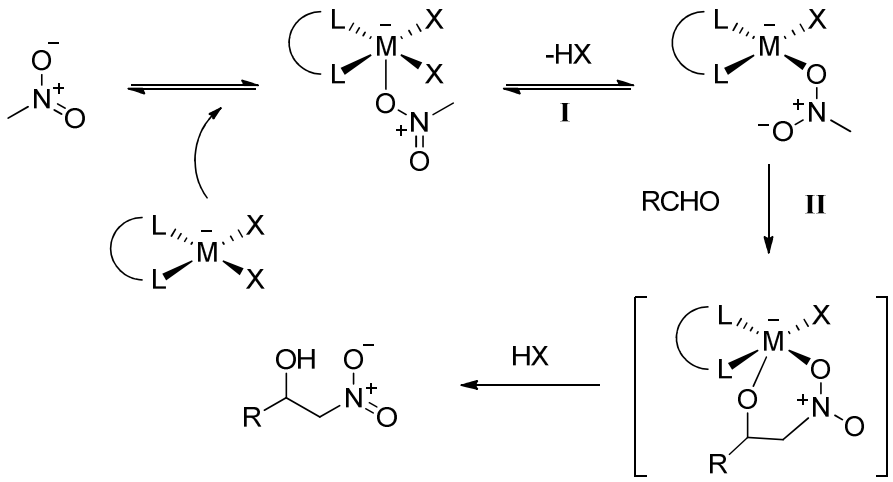

Figure 1.24. Proposed mechanism by Evans et al[97].

The leading system emerged as a copper(II) acetate bis(oxazoline) complex, a general example can be seen in Figure 1.25. Addition of nitromethane to both aromatic and aliphatic aldehydes was achieved in high yields, 70 - 95 %, and impressive selectivities were obtained, 87 - 94 %. What is very appealing of Evan's work is that these high selectivities were achieved at ambient temperatures, as such higher selectivities could potentially be achieved at lower temperatures while accounting for longer reaction times, (benzaldehyde and nitromethane addition stored at 0 °C for 10 days yielded the nitroalcohol at 81 % and with an ee of 96 %) and vice versa, elevating the temperature reduced the reaction rate at a cost to selectivity, 40 °C brought the ee down to 79 % with an increase in side reactions.

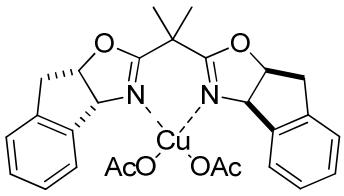

Figure 1.25. CuBOX prepared by Evans et al[66]

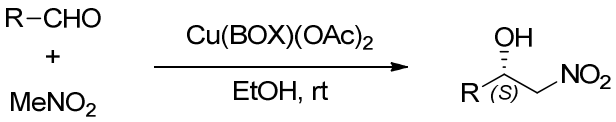

Figure 1.26. Reaction scheme for the substrate screen undertaken by Evans et al[66]

R	Time (hrs)	Yield (%)	ee (%)
Ph	22	76	94
2-MeC_6H_4	42	72	93
2-$MeOC_6H_4$	27	91	93
2-NOC_6H_4	4	86	89
2-ClC_6H_4	15	88	91
1-naphthyl	15	66	87
4-FC_6H_4	45	70	92
4-ClC_6H_4	21	73	90
4-PhC_6H_4	20	70	91
$PhCH_2CH_2$	2	81	90
i-Bu	48	86	92
t-Bu	96	83	94
i-Pr	48	86	94
n-Bu	48	87	93
cyclohexyl	48	95	93

Table 1.8. Substrate screen with Evans copper(II) acetate bis(oxazoline) complex

Chiral ligands were screened with $Cu(OAc)_2$ and the reaction conditions optimised displaying that catalyst loading could be lowered, and the reaction could be run at higher concentrations, up to 1.0 M, without affecting ee. Further substrate screening was conducted, Table 1.8, and it was established that aldehydes incorporating either electron withdrawing groups or donating, gave high selectivities and yields, as did branched and unbranched aliphatic aldehydes. Moreover, the group attempted large scale reactions for 2-$MeOC_6H_4$ with nitromethane at 50 mmol with 1 mol % catalyst loading, 0.1 M concentration for 56 hours, afforded the nitroalcohol with an isolated yield of 92 % and an enantiomeric excess of 94 %.

The general trends established by the discussed groups lead to the same generalisation that these current catalytic systems are ideal for aldehydes, however, ketones are somewhat slower and the reaction with nitroalkanes reversible, also the enantioface differentiation proves to be difficult as the two groups either side of the carbonyl become more similar. One notable exception is Christensen's et al.[98] work with α-keto esters and nitromethane, Figure 1.27.

Promoted by another example of a bis(oxazoline) copper complex and also base, triethylamine, 20 mol % of both complex and base. High enantioselectivities are achieved, however results vary depending on the stoichiometry and the reaction does not occur if either the catalyst or base is absent.

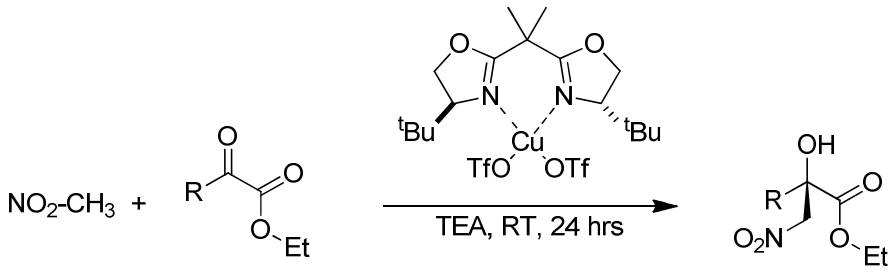

Figure 1.27. Nitro aldol reaction between an α-keto ester and nitromethane.

Interestingly Christensen also reported some of the early observations of varying other factors and their influence on the nitroaldol reaction. Varying the base type would influence not only the yield but also the selectivity, Table 1.9.

Base	Yield (%)	ee (%)
Et_3N	95	92
N-Me-morpholine	65	83
$PhNMe_2$	14	9
Bn_3N	10	14
EtN^iPr_2	31	69
Pyridine	6	13
K_2CO_3	95	27

Table 1.9. Variation of selectivity and conversion of the henry reaction as a result of chosen base.

It could be thought that one specific base is best to use as a promoter for the nitroaldol reaction, however as consideration to time *vs* temperature is important, as is metal salt and ligand type, choosing the right base may vary from each substrate combination. Base is important in the Henry reaction as a means to activate the nitroalkane, via deprotonation, before it binds to the metal centre with aldehyde/ketone[98,99]. Therefore it is safe to assume different bases will facilitate the activation of different substrates. Another consideration to make is the base and metal combination as some bases may interact with the metal more than the nitroalkane, changing the rate of substrate activation.

The system established by Evans "is good" as it operates under mild conditions, avoiding the need for low temperatures, and with more preferable solvents, for example ethanol. Other systems for the nitroaldol reaction, designed with Evan's "activation principle" in mind were those by Zhou et al.[100] and Pedro et al.[101]. Zhou described a dinuclear copper(II) complex with modest enantioselectivity, 45 - 64 %, Figure 1.28, while Pedro reported a series of camphor derived iminopyridine-copper(II) acetate catalysts for the reaction of nitromethane with o-anisaldehyde. Good yields were achieved but only modest enantiomeric excess, 7 - 61 %, under the conditions used by Evans, and a maximum selectivity of 86 % was only achieved at a temperature of -65 °C after 70 hours.

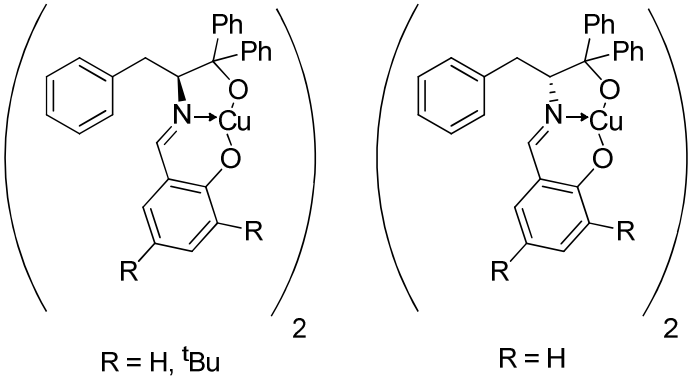

Figure 1.28. Dinuclear complexes prepared by Zhou et al. [100]

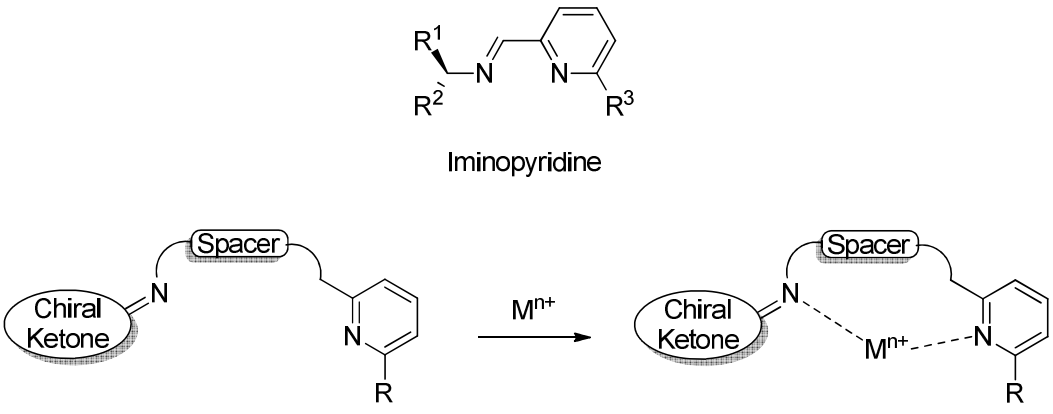

Figure 1.29. Iminopyridine type ligands prepared by Pedro and a generalisation for the modular building of these types of ligands

Maheswaran et al. further developed copper(II) systems with chiral diamine ligands by taking (-)-sparteine[102]. Sparteine is a very versatile chiral

agent and many catalytic systems have been prepared with it or with its derivatives, Mg[103], Li[104-106], Pd[107-109], Zn[110,111], Cu[112-114]. The systems were prepared with two copper(II) salts, acetate and chloride, and applied to the addition of nitromethane to a range of aromatic and aliphatic aldehydes. Reasonable to very good yields were observed, 70 - 95 % and selectivities, 73 - 97 %, were afforded at room temperature with a 20 mol % catalyst loading.

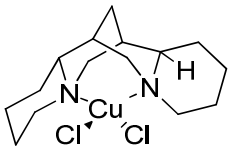

Figure 1.30. Copper(II) (-)-sparteine catalyst employed by Maheswaran[102]

The diacetatato[(-)-sparteine-N,N'] copper(II) catalyst directly, without the need for a basic co-catalyst or promoter, exhibited enantiomeric selectivity, < 4 %. Its dichloro counterpart on the other hand was unable to catalyse the reaction alone, however a small amount of NEt_3, 1.5-6 mol %, was efficient to facilitate the addition with good selectivity, 73 % (86 % ee at 0 °C). Maheswaran also demonstrated the sensitivity of their designed system to the amount of NEt_3 used. The difference of reactivity between the diaceto and dichloro copper(II) complexes were attributed to the significant differences in bond angles and torsion angles around the copper(II) site as determined from the respective crystal structures.

After the development of circular dichroism spectroscopy, there was a boost to the development of systems for the nitroaldol reaction as it provided a means to achieve high-throughput screening, HTS, of the efficiency of catalysts, and new diamine-copper(I) complexes were identified[115] prepared using the combinatorial approach[115-119]. Yanagisawa's group paired a CD spectrometer with a HTS system and synthesised a few chiral amines supported on polymer beads, Figure 1.31, which were used in turn to prepare the desired green solid supported Cu(II) catalysts. These were then used to examine their ability to catalyse the Henry reaction, and due to CD being sensitive to both yield and selectivity, only the systems which meet the criteria give strong signals. The best example to come from this work is with the C_2-symmetric copper catalyst, Figure 1.31, achieving

impressive yields and selectivities against varied aldehydes, at room temperature, in isopropyl alcohol with loadings as low as 1 mol %.

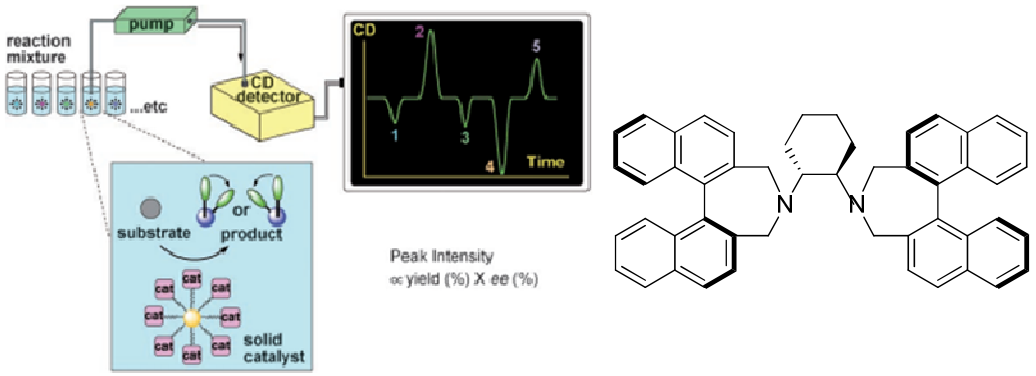

Figure 1.31. Schematic of the system developed by Yanagisawa et al.[115] and an example of the ligands employed

While the emphasis for the Henry reaction may have been on copper or zinc complexes a variety of transition metals have been explored, including, but not limited to, cobalt, chromium, rhodium and the lanthanides. Chromium(II) complexes with ketoimine and salen ligands were developed by Yamada and co-workers in 2004[116,120], and were found to be good catalysts when Hünig's base, N,N-Diisopropylethylamine, was used as a co-catalyst achieving high yields in the range of 72 - > 99 % and good selectivities, 73 - 92 %.

Kowalczyk et al. developed a chromium(III) complex based on Jacobsen-type, sterically-modified salen ligand[121]. The benefit of this system was that the salen ligands were easy to prepare and were fairly stable. Sterics and electronic influences of the ligand were easily varied by simple modifications of the salicylidene unit, Figure 1.32, and variations at the 3,3' -positions have been studied extensively [122-124]. This type of system appealed to Kowalczyk and at the time only cobalt(II) and heterobimetallic Pd/La salen complexes were useful in the nitroaldol reaction. Moreover, the salen-chromium(III) complex was commercially available.

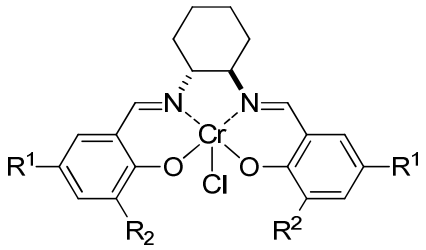

Figure 1.32. Chromium complex presented by Kowalczyk

These systems afforded the nitroalcohol product over a wide range of conversions, 16 - 78 % yield, and gave modest enantioselectivity, 19 - 93 %, under harsh conditions of -78 and -20 °C temperatures over 20.5 hours. Optimisation for the most successful complex was undertaken before the catalyst was screened to ascertain its substrate sensitivity. The system worked well with aromatic substrates, 80 - 94 % ee, slightly less effective with electron withdrawing group substituted benzaldehydes, 80 - 86 %.

In 2012 Schulz and his group published results of a chromium-salen complex[125] which had previously been polymerised to make an example of an asymmetric heterogeneous catalyst[126]. Further modification of the Jacobsen-type salen ligand by the addition of a thiophene affords new chiral thiophene-salen ligands, Figure 1.33.

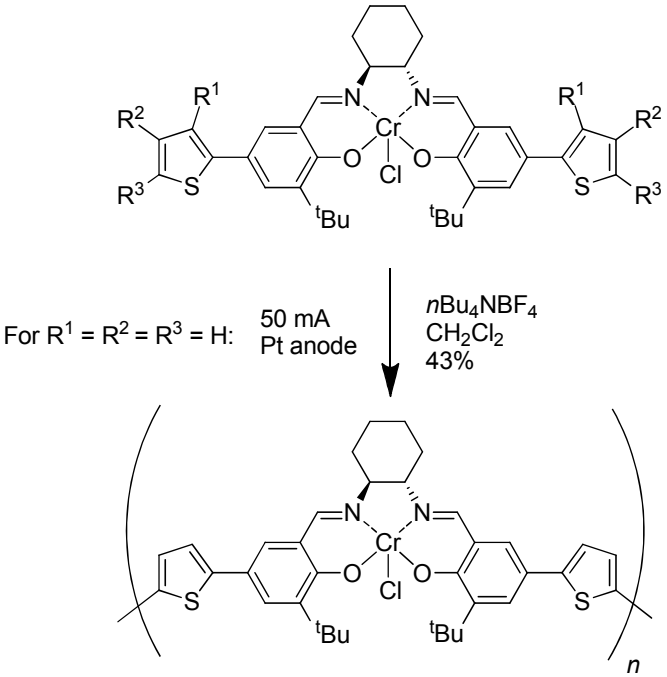

Figure 1.33. Chiral thiophene-salen chromium complex

These poly-salen chromium complexes still need more research, however, as while active and selective in their monomer form, 79 % yield and 93 % ee, this was not retained and conversion suffered greatly, 5 %, and selectivity dropped, to 0 %. But with other systems there was an increase in activity and yield, from 74 to 99 % yield and enantiomeric excess from 34 to 65 %. One limitation is that the polymers cannot be prepared metal free[127].

Kiyooka et al., discovered an early example of the rhodium catalysed nitroaldol reaction[128]. The group was investigating the Mukaiyma aldol reaction using rhodium complexes, Figure 1.34. Attempting to improve on their poor yield for the reaction of silyl keten acetal with benzaldehyde in CH_2Cl_2 by changing the solvent for nitroethane, resulted in the change of the course of the reaction, and the Henry product was formed in good yield, up to 82 %. While research has continued with PGM based catalysts in the Henry reaction, they are limited, with reasons likely to be associated to cost and availability of PGM salts.

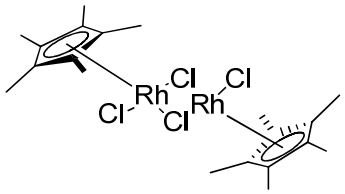

Figure 1.34. The rhodium complex [{Rh(C_5Me_5)Cl_2(μ-Cl)$_2$]

Another variable in the nitroaldol reaction not yet discussed is the range of nitroalkanes that can be used. Blay et al. in 2008 showed that addition of aldehydes to a series of functionalised nitroalkanes was indeed possible[129]. Utilising another copper(II) system with dinitrogen-chelating ligands, bromonitromethane was added in excellent yields, 72 - 99 %, and good enantioselectivities, 81 - 98 %, however diastereoselectivity range widely, 8 - 74 %. Incorporation of a bromonitroalkane is significant as the additional functionality clearly results in additional functionality in the nitroalcohol, 2-bromo-2-nitroalkan-1-ol, which is an important step to some natural products, for example antibacterial-, antifungal-, and antialgal-agents.

As described earlier, the catalysts previously discussed have all been examples of Lewis acid asymmetric catalysts where the enantioselectivity is induced as a result of the "organisational ability" of a metal centre to create an

effective asymmetric environment. Brønsted bases have also been shown to catalyse the asymmetric nitroaldol reaction, and certain cinchona alkaloids [130-132] and guanidine bases [133-136] have been reported, however selectivities are still lacking in these systems, >50 % ee[133,135], however improvements are being reported for organocatalysts especially with advances in the parent aza-Henry reaction[137], addition of a nitroalkane to an imine. In this context a protonated chiral bisamialine ligand as well as a chiral derivative of thiourea [131,138] have been found to catalyse the reaction of nitroalkanes with N-Boc and N-phosphenyl imines respectively achieving high selectivities.

1.1.7. **Benchmark Reaction - Asymmetric Hydrogenation, AH**

Hydrogenation is a very common reaction, indeed at an early stage of scientific education we are introduced to the large scale application of hydrogenation in the processing of fats and oils. With "trans fat" being implicated in heart disease and other circulatory problems, chemistry and biology crossover in secondary school to teach this important reaction.

The importance of AH was globally recognised in 2001 by the awarding of the Nobel Prize in chemistry to Knowles and Noyori as mentioned earlier. The journey to this stage, however, started in 1968 when Knowles et al. published their work on the asymmetric hydrogenation of alkenes with the use of a chiral rhodium metal catalyst[139]. In Knowles Nobel Lecture[140], he describes the issues faced by industry with the production of chiral compounds, employing "biochemical reactions or making racemic mixtures followed by laborious resolutions... [with] the project costs doubled". A cheaper alternative was needed to meet this new demand for optically pure and biologically important compounds.

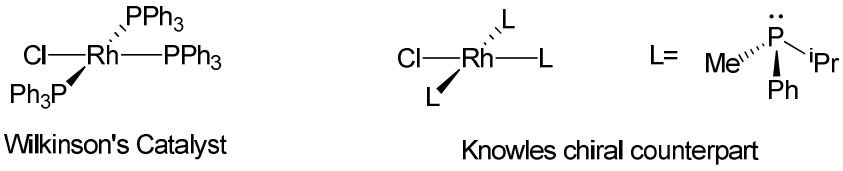

Figure 1.35. Trisphosphine rhodium catalysts used for hydrgenation

Knowles acknowledged the discovery by Sir G. Wilkinson (also a Nobel Laureate, 1973) of the first homogeneous catalyst for the hydrogenation of

unhindered olefins[141,142] by a chloro-tris(triphenyl-phosphine) rhodium complex, Figure 1.35 left. Rates were comparable to the well-studied and known heterogeneous counterpart. Knowles set out to replace Wilkinson's triphenylphosphine component with a chiral doppelganger to selectively hydrogenate the prochiral olefin α-phenylacrylic acid, Figure 1.36. This was achieved with an enantiomeric excess, ee, of 15 % utilising methylpropylphenyl phosphine, Figure 1.35 right.

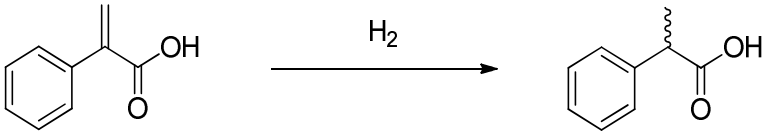

Figure 1.36. Direct hydrogenation of 2-phenylprop-2-enoic acid

Unimpressive by today's standards, Knowles persisted where others in the field had failed. Knowles held the position of research director at Monsanto Pharmaceuticals, and the discovery at a similar time to Knowles work, that an incredibly large dose of the amino acid L-DOPA, was seen as a possible clinical treatment to Parkinson's disease[143]. This would prove to be the driving force in the early stages of Knowles' work. Monsanto were manufacturing a racemic intermediate which Hoffman-LaRoche would in turn need to be resolved and deprotected to affording L-DOPA, Figure 1.37. Knowles wanted to use the "golden opportunity" provided by the prochiral enamide as a means to commercialise his new technology. A straightforward test reaction, highlighted in Figure 1.37, easily analysed for efficiency was to be used in a simple structure *vs* activity study, which would also introduce the concept of fine tuning, Table 1.10.

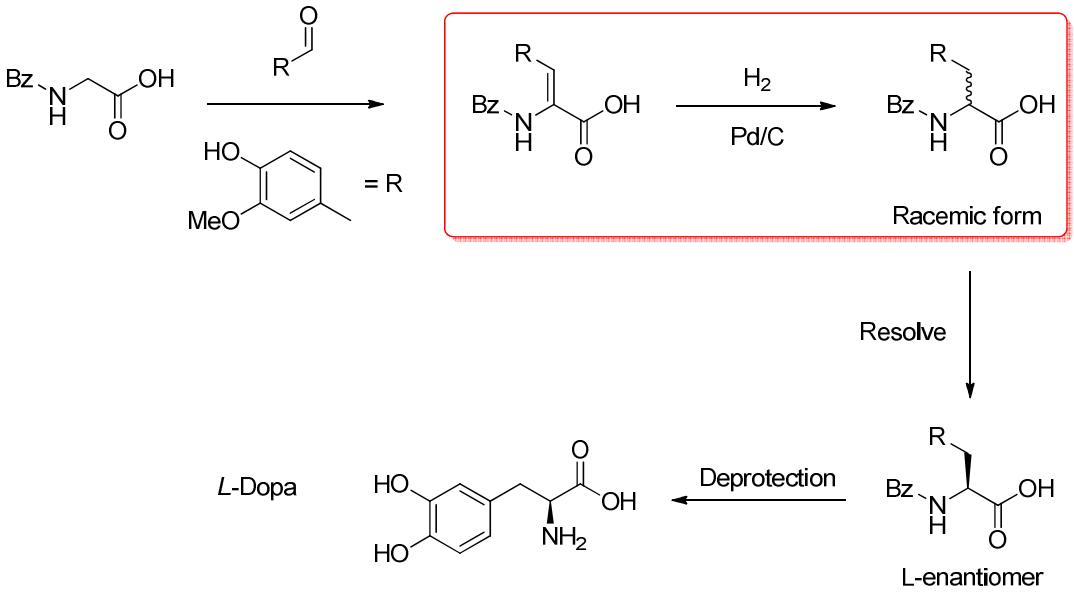

Figure 1.37. Hoffman LaRoche L-Dopa Process; Test reaction employed for Knowles' structure vs activity study, highlighted in red

They had achieved impressive selectivity on the 6th variant of their chiral ligand. Once the group had recovered from their shock, more luck was to fall in their lap in the form of a manufacturing plant becoming available. CAMP was put into the L-DOPA reaction scheme of Figure 1.37 and a simplified reaction starting from vanillin was developed, Figure 1.38. Used in a solid and air stable complex at ratios of 20,000:1 "this super expensive complex was used at close to throwaway levels"[140]

Phosphine		ee (%)
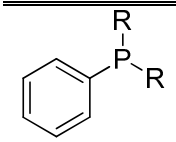	$[CH_2CH^*(Me)(Et)]_2$	1
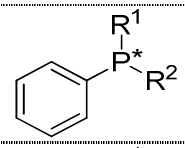	Me, ^{n}Pr	28
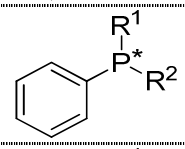	Me, ^{i}Pr	28
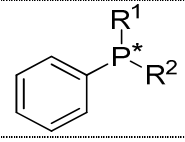	Me, Cyclohexyl	32
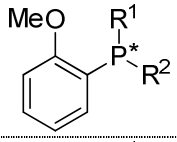	Me, Phenyl (PAMP)	58
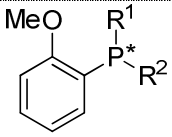	Me, Cyclohexyl (CAMP)	88

Table 1.10. Chiral phosphines employed by Knowles for AH, in sequential order.

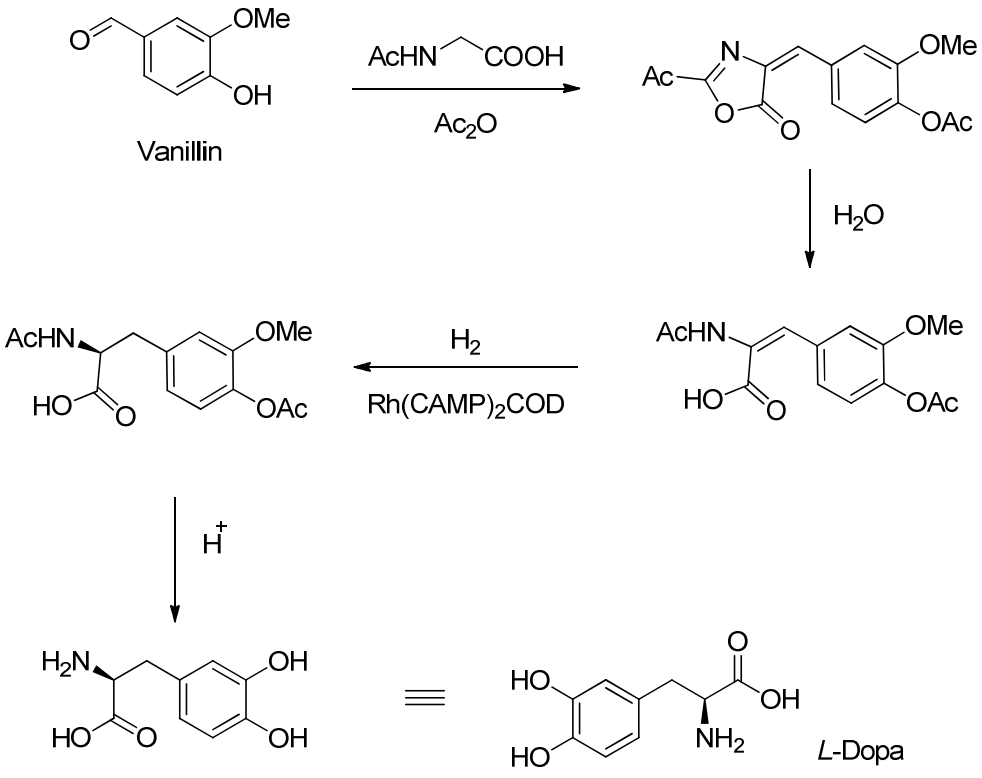

Figure 1.38. Monsanto L-Dopa process

Noyori, sharing the prize with Knowles, is a strong believer of catalysis and green chemistry stating "our ability to devise straightforward and practical chemical syntheses is indispensable to the survival of our species"[144]. Noyori's work with AH introduced the ligand BINAP, Figure 1.39, a ligand which would later find applications in a vast magnitude of selective reactions and decades later still generate exciting results.

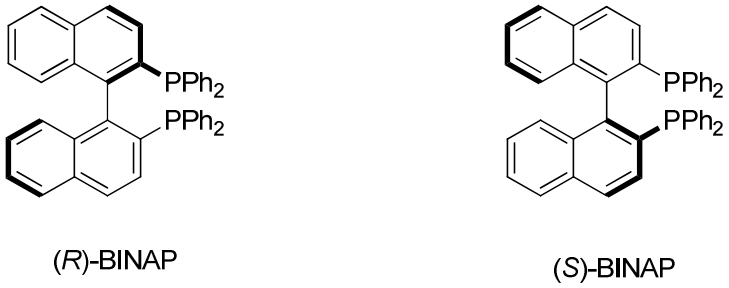

Figure 1.39. Both enantiomers of the chiral disphosphine ligand prepared by Noyori

A fully aromatic, axially dissymetric C_2-diphosphine which could be fine tuned by various substitutions around the aromatic rings. While lacking a stereogenic atom, chirality results from the restricted rotation. The disadvantage at the time of its discovery, was the difficulties in obtaining the ligand as an optically pure ligand[145-147]. After 6 years of work in 1980 the results were first published[148,149] of a rhodium-BINAP complex achieving up to 100 % enantiomeric excess in the hydrogenation of α-(acylamino)acrylic acids affording amino acids with high levels of conversion, 93 - 99 %.

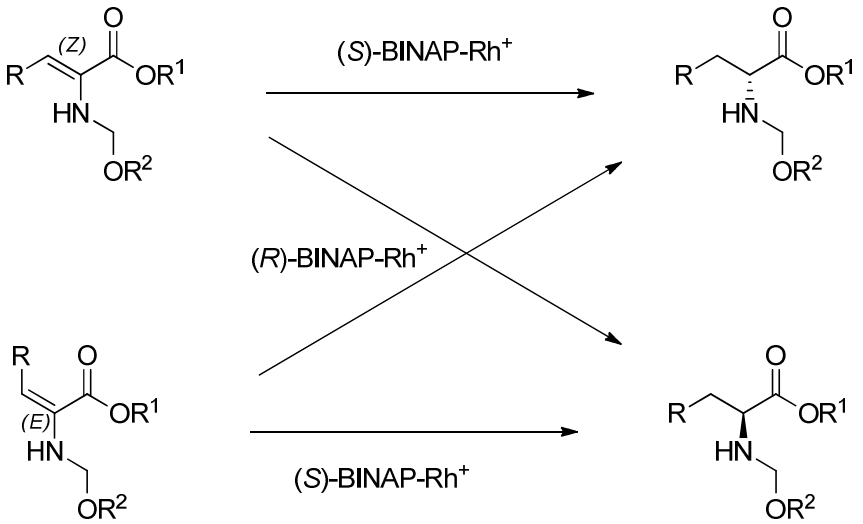

Figure 1.40. Noyori's successful asymmetric hydrogenation of α-(acylamino)acrylic acids with rhodium BINAP catalysts

Both enantiomers of BINAP were used with rhodium and it was significant because the conformation of the resulting amino acid could be controlled by employing the appropriate BINAP enantiomer[150], Figure 1.40. Moreover, as a result of the rotation about the binaphthyl C(1)-C(1') pivot and C(2 or 2')-P bonds, BINAP can harbour a range of transition metals, a factor which has seen the incredibly wide range of uses and applications of BINAP[151].

BINAP was also successfully employed with Ru(II) for AH of a range of functionalised olefins, displaying enantioselective hydrogenation of allylic[152] and homoallylic alcohols and α,β- and α,γ-unsaturated carboxylic acids[153]. Achieving up to 100 % conversion and high selectivities, 83 - 97 %, with product configuration being controlled by BINAP enantiomer, a selection of the results are summarised in Table 1.11. The list of possible substrates was extended further to include various ketones[154], again with impressive conversion, 93 - 97 % and selectivities, 90 - 100 %. A selection of substrates is summarised in Table 1.11. The pattern of conformer control was again repeated with a typical catalyst loadings of 10,000:1 being employed.

Substrate	R^1, R^2, R^3	ee (%)	R^1, R^2, R^3	ee (%)
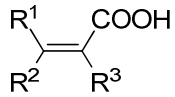	H, Me, Me	94	Me, $CH_2COOCMe$, H	95
	Ph, Me, H	85	H, Me, CH_2OH	97
	H, H, Ph	92	H, $CH_2COOCMe$, Me	95
	Me, CH_2OH, H	93	Me, CH_2CH_2OH, H	93
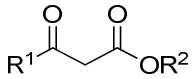	Me, Me	99	Me, ^{t}Bu	98
	Me, ^{i}Pr	98	n-Bu, Me	98
	Et, Me	100	Ph, Et	85

Table 1.11. Asymmetric Hydrogenation of a range of different substrates with Ru(II)-BINAP

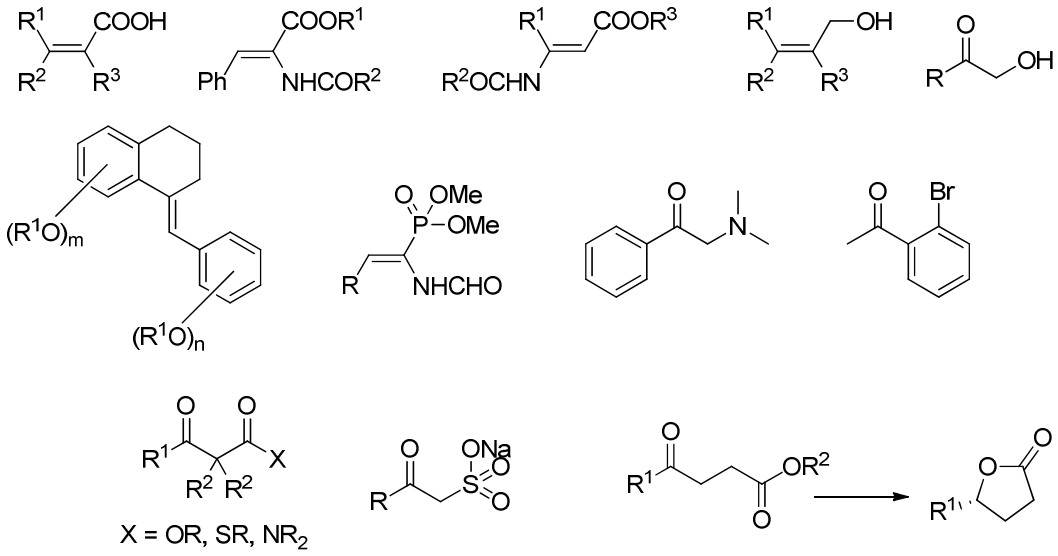

Figure 1.41. Different substrates reduced selectively by Noyori's Ru-BINAP system

This Ru-BINAP system has also been employed in synthetically useful reactions, and is able to produce a selection of important drug precursors and pharmaceuticals, for example (*S*)-naproxen, a nonsteriodal anti-inflammatory

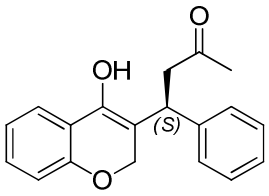

Figure 1.42. Naproxen

Kagan's[155,156] work with DIOP, Figure 1.43, a bidentate disphosphine should also be included as a pioneering study of AH as the field has exploded with the use of bidentate, and especially C_2-symmetrical diphosphines, up to the turn of the century with rhodium, ruthenium and iridium. Monodentate phosphorous containing chiral ligands experienced renewed interest in the AH of dehydroamino acids after the discovery of conveniently synthesised novel enantiopure ligands with P-O and P-N bonds, and as such examples of phosphines, phosphonites, phosphinites, phosphoramidites and phosphite chiral monodentate ligands are present in the literature. There are however two main disadvantages with these systems, which can lead to difficulties in handling and reusing them as well as making the recycling complicated: (*i*) the inclination of the phosphine group to oxidise and (*ii*) the metals used so far are expensive platinum group metals which can be air and moisture sensitive.

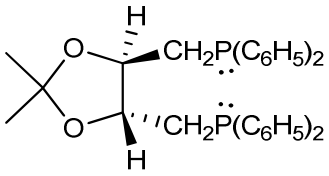

Figure 1.43. Kagan's diphosphine, DIOP

The choice of metal for AH is limited in comparison to the multitudinous number of chiral ligands available[157,158] with the platinum group metals being the leading systems especially rhodium, ruthenium and iridium. Palladium may appear as an unlikely alternative as it is a PGM, but it is somewhat cheaper than those already stated, Pd = 747.50 $/oz while Rh = 1215.00 $/oz[159], and being a PGM shares a lot of the chemistry already studied[160]. Furthermore, with heterogeneous palladium catalysts being well studied and one of the more successful systems in the hydrogenation of unsaturated double bonds[161], it might come as a surprise that AH with Pd complexes remained under developed until 2001[162].

Since then work has been published on the hydrogenation of varied substrates including imines, enamines, olefins, ketones, and heteroarenes, as well as fairly significant tandem reactions. Amii, Uneyama et al.[163] reported the palladium catalysed AH of fluorinated iminoesters for the synthesis of fluoroamino acids, using BINAP as the chiral ligand, Figure 1.44. High yields were obtained for a range of substrates, 69 - 99 %, with enantioselectivity for the best part being high, 30 - 88 %. Selectivity was shown to have a large dependence on solvent, with non-fluorinated alcohols experiencing a significant drop in selectivity and conversion, as did varying the palladium source, $PdCl_2$ or $Pd_2(dba)_3$.

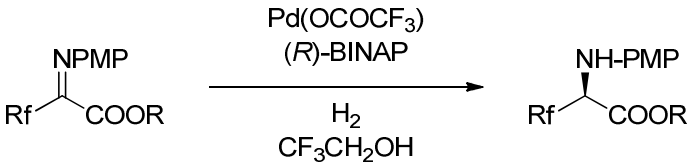

Figure 1.44. Uneyama et al. preparation of amino acids with a Pd-BINAP catalyst, the amine protecting group p-methoxyphenyl abbreviated to PMP

A strong advocate of palladium catalysed AH, Zhou et al.[164] recently reported further advances on reduction of fluoro-imino esters, and in contrast to Uneyama who stated that an α-ester group was required in order to achieve good

conversion and enantiomeric excess, achieved good yields without them. This could be enhanced by including molecular sieves, 4 Å, and thus the scope widened to include alky substituted fluorinated imines, those bearing longer perfluoroalkyl chains and even difluoro substrates, with selectivities across all those screened reasonably good, 69 - 88 %.

Zhou et al. are prolific in the study of asymmetric hydrogenation with palladium and followed the work on fluorinated amino acid precursors with non-fluorinated imines utilising a palladium (*S*)-SegPhos ((*S*)-(-)-5,5'-bis(diphenylphosphino)-4,4'-bi-1,3-benzodioxole, commercially available from Sigma Aldrich) system achieving yields in the range of 70 - 98 % with high enantiomeric excess, 87 - 99 %[164]. Reactions covered to date include the asymmetric reduction of N-tosylimines, acyclic and cyclic sulfonamides, cyclic imines, cyclic sulfamidates, ketimies, trisubstituted enamines, exocyclic enamines, cyclic arylsulfonamidoacrylates to name a few[165-171].

Another variation to what has been described so far is using a hydride source which is not hydrogen gas. While hydrogen gas is a clean and renewable hydride source, there can be safety issues when used on large scales at considerable pressures. Sodeoka et al.[172] utilised ethanol as a hydride source for the asymmetric system. They obtained high yields, 85 - >99 %, and moderate selectivities, 74 - 96 %, under these much milder conditions, and found applications in the production of (*S*)-warfarin, an important anticoagulation drug.

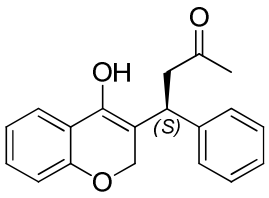

Figure 1.45.The anticoagulant, warfarin

Kegan, Knowles and Noyori encouraged the study of asymmetric catalysis and what followed over the consequential thirty years was a plethora of phosphine containing chiral complexes enabling the selective formation of C-H, C-C, C-O, C-N bonds[173-178], however few have found industrial applications. This is likely due to the cost of metal salts and chiral phosphines, the difficulties in handling and recycling due to their low stability to oxidation. Nitrogen containing ligands

have been scarce in the literature during the 70's and 80's and interestingly the first asymmetric catalysts were heterogeneous systems such as palladium on silk fibroin for asymmetric reduction[27,179,180]. This however changed in the 90's when the need for easy and inexpensive handling, separation, reuse and recycling was becoming paramount. Nitrogen containing ligands looked promising, moreover they showed greater opportunities for supported catalysis than their phosphine counterparts as evident in the literature today. One key advantage is that they are less susceptible to oxidation.

Mixed NP-ferrocenyl ligands were demonstrated by Cullen et al.[181-183] and gave enantioselectivity of up to 84 % in the AH of acetamido cinnamic acid with rhodium, Figure 1.46. However, it was shown that selectivity and conversion were seemingly controlled by the phosphorous centre with exchange of the $P(Ph)_2$ for $P(^tBu)_2$ increasing activity and reversing configuration.

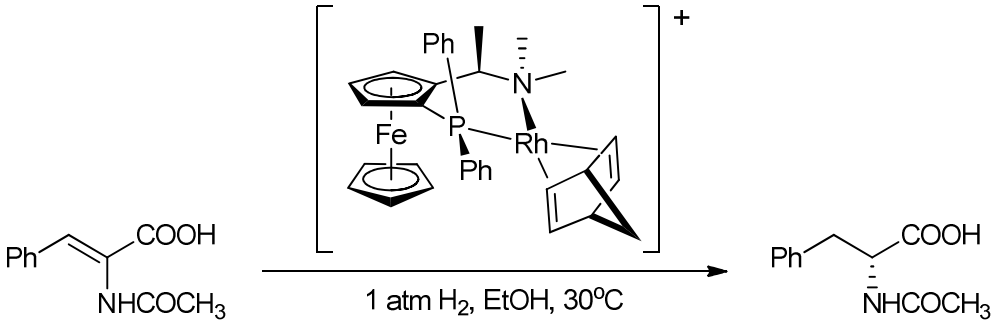

Figure 1.46. Cullen's rhodium complex and screening reaction

Iglesias et al.[184] reported a phosphine free ligand for AH in the form of N-heterocyclic carbene and (*S*)-proline incorporating pincer ligands, stating that lower toxicity makes carbene ligands safer to be used instead of phosphine ligands. Reasonable selectivities, 41 - 99 % ee, were obtained for the hydrogenation of diethyl 2-benzylidenesuccinate, with Rh(I), Pd(II) and Au(III) catalysts, however this was not seen for the hydrogenation of diethyl itaconate with enantiomeric excess in the range 0 - 15 % obtained under mild conditions.

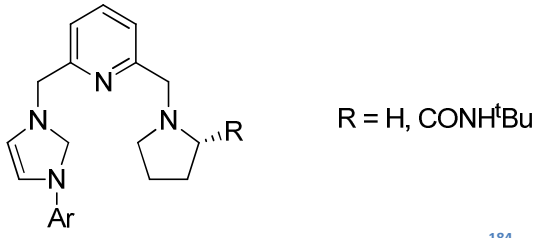

Figure 1.47. Pincer ligands reported by Iglesias[184]

Major results for a phosphine free ligand were found for sp^2-nitrogen containing ligands, such as Pfaltz et al.'s use of semicorrins[185], Figure 1.48. Here, aromatic ketones were reduced by the transfer of a hydride giving alcohols with good selectivities, up to 91 %. Gladiali demonstrated the asymmetric transfer hydrogenation of acetophenone with 3-alkyl phenonthroline and potassium hydroxide as a co-catalyst[186]. More moderated selectivities were achieved, 63 % ee. An improved selectivity for the same reaction was published by Pinel et al.[187] using a 1,2-diamino-1,2-diphenyl ethane, Figure 1.48, and rhodium system, increasing selectivity to 67 % for acetophenone and acquiring 99 % ee for methyl phenylglyoxylate.

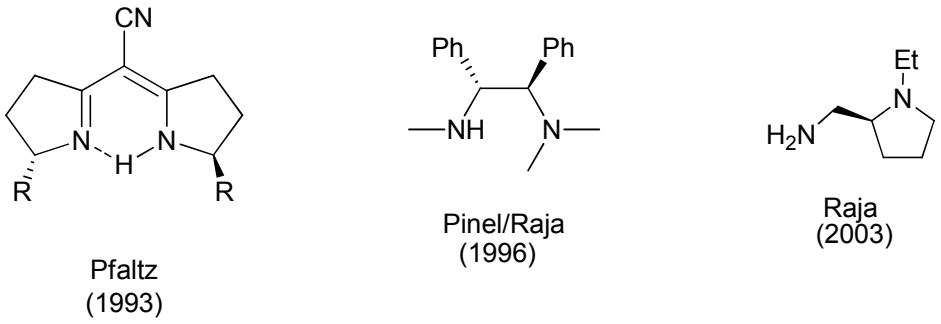

Figure 1.48. Phosphine free ligands

This 1,2-diamino-1,2-diphenyl ethane was also employed by Raja et al[37]. along with another chiral bidentate amine ligand, (*S*)-(-)-2-aminomethyl-1-ethyl pyrrolidine, Figure 1.48, for the AH of olefins will palladium and rhodium. Raja reported that complete conversion was achieved, with optical purity reaching up to 93 % ee for the reduction of α-phenyl cinnamic acid, Table 1.12. However this was not the "key feature" of the work presented, instead it was the enhancement of selectivity by heterogenising these palladium and rhodium catalysts. The work also screened the more commercially relevant reaction of methyl benzoylformate to prepare methyl mandelate where the selectivity was boosted from quite low levels to impressive levels, Table 1.13.

Amine	Metal and diene	Catalyst State	Conversion (%)	ee (%)
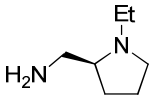	Rh(I), COD	Homogeneous	74	93
		Heterogeneous	80	96
	Rh(I), NBD	Homogeneous	88	64
		Heterogeneous	99	91
	Pd(II), allyl	Homogeneous	100	76
		Heterogeneous	93	93
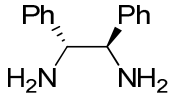	Pd(II), allyl	Homogeneous	95	79
		Heterogeneous	75	88
	Rh(I), COD	Homogeneous	57	81
		MCM-41	98	93
		Cabosil	95	79

Table 1.12. Asymmetric hydrogenation of α-phenyl cinnamic acid.

Metal and diene	System State	Conversion (%)	ee (%)
Rh(I), COD	Homogeneous	95	0
	Heterogeneous	98	91
Rh(I), NBD	Homogeneous	85	18
	Homogeneous (293 K)	56	69
	Heterogeneous	100	99
Pd(II), allyl	Homogeneous	100	87
	Heterogeneous	97	87

Table 1.13. Asymmetric hydrogenation of methyl benzoyl formate with the ligand(*S*)-(-)-2-aminomethyl-1-ethyl pyrrolidine performed in methanol at 313 K unless otherwise stated

This work and subsequent work on heterogenised catalysts has shown that enantioselectivity can be improved in comparison to their homogeneous analogues. Constraints to the accessibility of the active site by bulky substrates is critical as the element by which enantioselectivity is enhanced. This was also demonstrated by Raja via the use of a concave MCM-41, 93 % ee, and a convex cabosil, 79 % ee indicating the positive benefits the support can offer. These were similar to results reported by Thomas et al.[188-190] with a palladium-phosphine catalyst located at the walls of a mesoporous silica support.

1.2. Stereoselective Biopolymers

Polymerisation has been an interesting topic of research for many decades, but with dwindling stocks and increasing prices of oil, pressure from government legislation and public awareness, a sustainable alternative to polyolefins has been now become the vanguard of research[191].

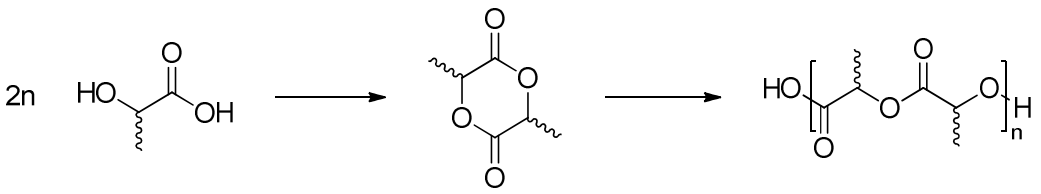

Figure 1.49 Preparation of Polylactic acid from the cyclic lactide

Polylactide, also known as polylactic acid, (PLA) is a starch derived polymer and it has become one of the most important synthetic biodegradable polymers investigated[192]. Part of the lactone family, lactide (LA) is a cyclic ester that can be polymerised to make polyesters, a widely used and important polymer. The monomer is produced by the fermentation of glucose, derived from starch harvested typically from corn or sugar beet[193]. The lactide monomer, a cyclic dimer, is prepared by thermal degradation of oligo-lactic acid, prepared from condensation polymerisation of lactic acid. In the presence of an initiator the monomer is opened and grows into the polymer, while hydrolysis of the ester bond returns lactic acid. This "disposal" of the polymer chain into natural products is important for biomedical applications, where avoiding the need of a second bout of surgery is of great benefit, and lactic acid is naturally broken down in the human metabolism, Krebs cycle. Biodegradation of this lactic acid returns water and carbon dioxide, the plants feedstock.

The life cycle of PLA, summarised in Figure 1.51, involves a significant energy input, fermentation of the feedstock, synthesis of the monomer, fabrication, ect, and where this is derived from fossil fuels, it has been proposed to offer no better carbon balance than polyolefins[194]. Natureworks LLC, who are the largest producer of PLA, off-set their non-renewable carbon emissions by purchasing wind energy certificates, thereby claiming carbon neutrality. Polylactide was first recognised in 1932 by Carothers et al[195], but not developed because of its low stability in humid conditions. In the 1970's the advantages and applications of PLA were recognised as a degradable polyester and the development of medical products, sutures, stents, fibres, began. With market pressures for sustainable plastics and improvements to monomer production enabling cost reductions, the 1990's saw the start of PLA used in consumer articles, fibre technology and packaging, as well as more intricate and complex medical instruments, scaffold for tissue engineering[196] ranging from liver to bone grafts.

The physical properties of PLA are often compared to polystyrene, PS, it has a high modulus and strength but low toughness, with stereochemistry of the monomer giving rise to PLA having a varied crystallinity. Isotactic, pure poly(D/L-Lactide) is a crystalline thermoplastic compared to the amorphous atactic PLA. Tacticity is the common characteristic of the polymeric material used for comparison and reflects the order of repeating side groups along the polymer chain, an example of this can be seen for polystyrene, with isotacticity achieved when all the phenyl ring are on the same side of the polymer chain, and atacticity when no order is observed. Tacticity of PLA will be discussed further below.

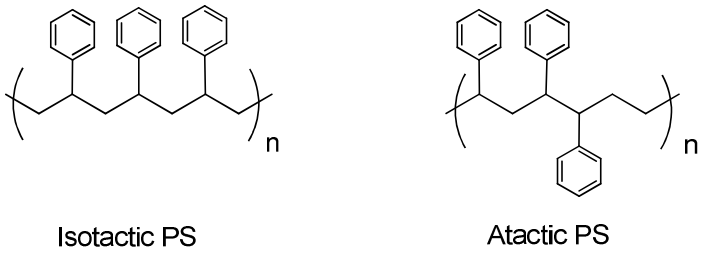

Figure 1.50. Representation of tacticity within polystyrene

In all tacticity PLA exhibits good oil resistance, low temperature heat sealability, good barrier to aromas, and can be processed by injection thermoforming, film casting and multifibre spinning[197]. A draw back still facing the widespread use of PLA is monomer preparation, efficient recycling of products, fine tuning of physical properties for different applications. It should also be noted, that although systems used for the polymerisation of PLA can be called catalysts and initiators interchangeably, they are not true catalysts as the system gets incorporated into the polymeric structure (as the end group).

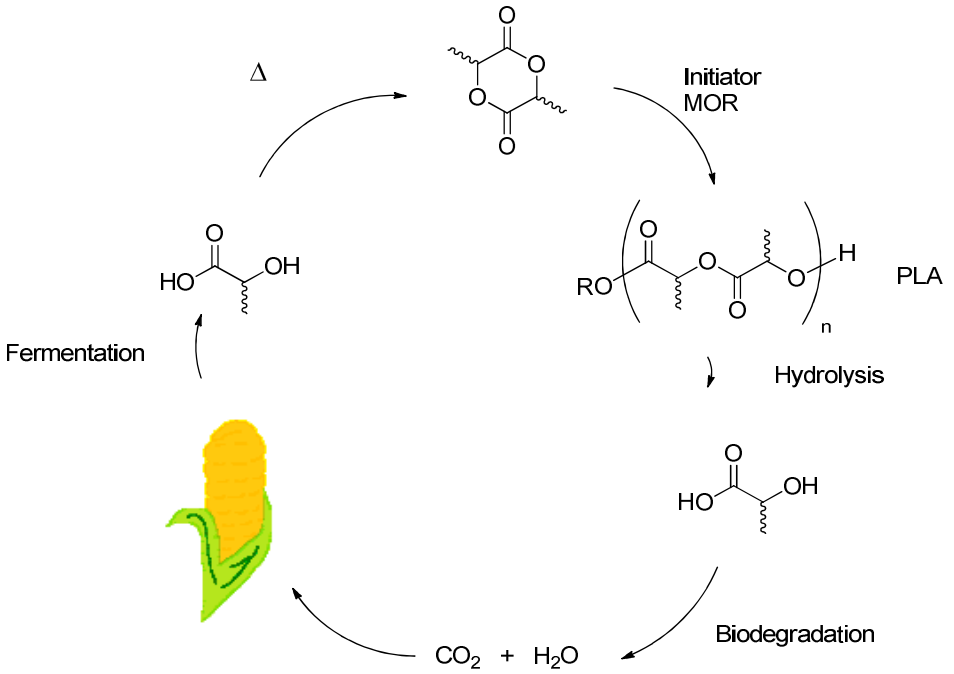

Figure 1.51 Lactide Life cycle from Corn through, lactide, PLA, lactic acid and carbon dioxide and water to be taken up by the corn.

1.2.1. **Polymerisation of Lactide**

Of the two methods to prepare PLA, ring-opening polymerisation is the more widely used[198]. While condensation polymerisation of lactide should be the cheaper method, it is an equilibrium reaction, and the water by product can be difficult to separate from the growing polymer chain, with the need for coupling agents and adjuvants adding to the cost and limiting the weight of the resulting polymer. Ring-opening polymerisation, ROP, allows for higher molecular weight in comparison and generally offers better control of the polymer[198]. As described previously, each lactide monomer unit is a cyclic unit comprised of two lactic

acid molecules, and the driving force, thermodynamically, is the enthalpy of polymerisation, specifically the relief of ring strain as a consequence of two ester moieties and a planar configuration[199,200] with $\Delta H = 22.1$ kJmol^{-1} for 1M solutions at room temperature, overcoming the unfavourable entropy of polymerisation[199].

The preferred complex for commercial production of PLA is tin octanoate, $Sn(Oct)_2$, also known as stannous octanoate or tin(II) *bis*(2-ethylhexanoate), but zinc powder and aluminium isopropoxide are also used (Figure 1.52). $Sn(Oct)_2$ is an ideal initiator as it is commercially available, readily soluble in many common organic solvents, soluble in melt conditions, easy to handle, and very reactive with reaction times in bulk polymerisation at 140-180 °C ranging from a few hours down to a few minutes. Control of the polymer is good with high molecular weights being achieved, 10^5-10^6 Da.

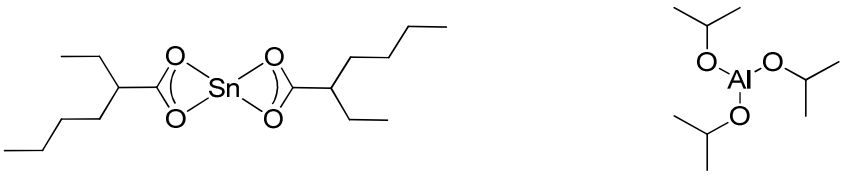

Figure 1.52. Structure of tin octanoate and aluminium isopropoxide

The disadvantage to $Sn(Oct)_2$ is that, with most synthetic polymers, any and all additives are still present in the sample. Although approved by the US Food and Drug Administration, Sn(II) readily oxidises to Sn(IV) which is highly toxic, limiting uses in biomedical applications but also raising concern for the build up of these toxic tin compounds at landfill sites and potentially domestic composting bins. Alternatives used to produce PLA are typically inferior to $Sn(Oct)_2$, with aluminium alkoxides being effective but less active, 125 - 180 °C bulk reaction times of several days, producing lower molecular weight polymer, > 10^5 Da [201], and often requiring an induction period. With evidence supporting a link between aluminium and Alzheimer's disease[191,202] and aluminium ions absent from the human metabolism, this metal is not suitable for biomedical applications. Zinc can be considered as a potentially non-toxic initiator, with zinc powered performing as well as $Al(O^iPr)_3$ and numerous zinc salts have been investigated[203,204].

1.2.2. **Polymerisation Mechanism**

As with many processes it is important to understand the mechanism, how lactide is ring opened to produce PLA. Dittrich and Schulz[205] first devised that there is a three-step coordination insertion mechanism of cyclic esters and in the 1980's the $Al(O^iPr)_3$ initiated polymerisation of lactide was reported by both Kricheldorf[206] and Teyssié[207] independently, further supported this experimentally[201,208] and theoretically[209,210]. Anionic (Figure 1.53) and cationic (Figure 1.54) mechanisms have been reported but polymer produced in this method would appear not to compare to that prepared by coordination and insertion mechanism.

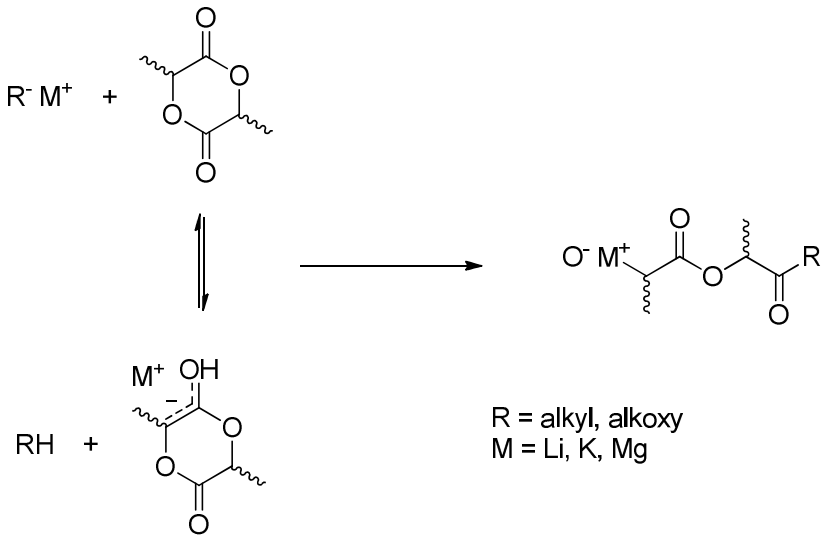

Figure 1.53. Anionic Mechanism for the production of PLA[191]

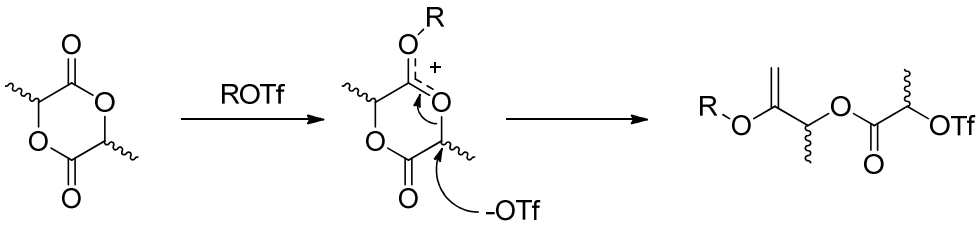

Figure 1.54. Cationic Mechanism for the production of PLA[191]

The coordination-insertion mechanism is one that is similar to all polymerisations, as shown in Figure 1.55, with an initiation (**I**) step, followed by multiple propagation (**II**), and finally termination (**III**). Monomer inserts into one of the alkoxide bonds, having previously been coordinated by the Lewis-acidic metal centre. This step proceeds by nucleophilic addition of the alkoxy group on

the carbonyl carbon. Acyl-oxygen cleavage opening the ring, with the polymer propagated by addition of further lactide molecules. Termination is achieved by hydrolysis of the active metal alkoxide bond giving rise to a hydroxyl end group.

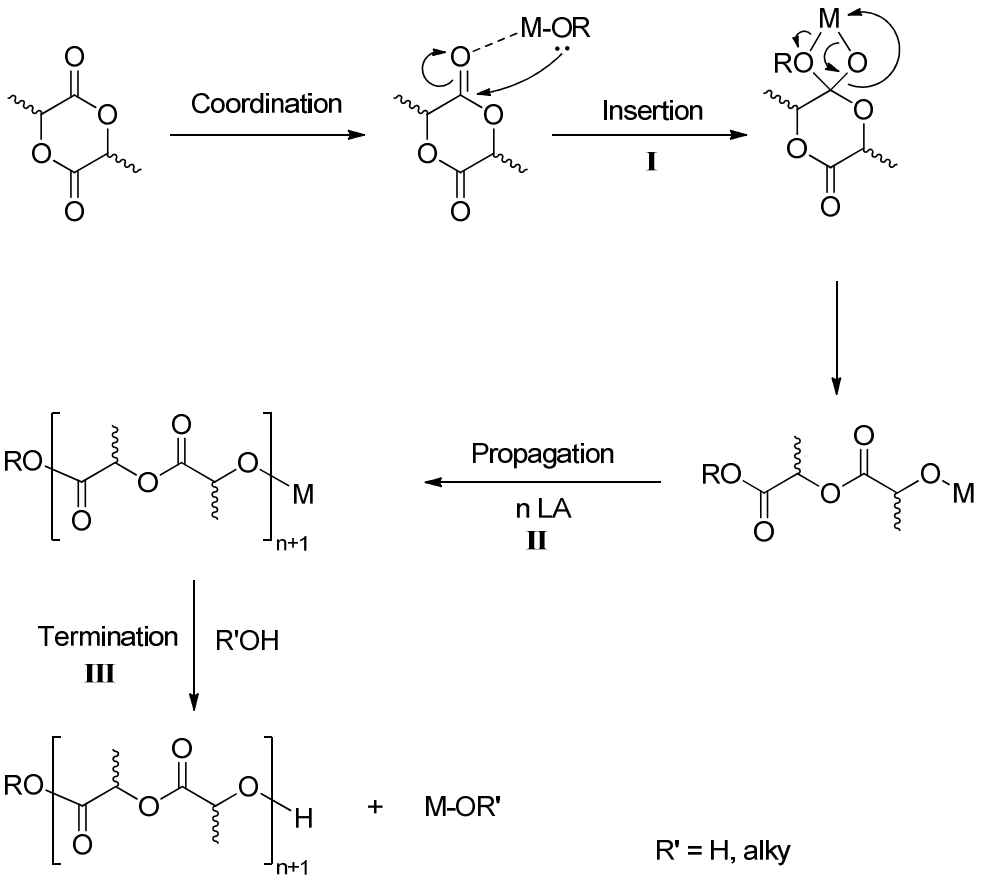

Figure 1.55 Coordination-insertion Mechanism for the ring opening polymerisation of lactide[191]

Further investigation by Gibson et al [211] using DFT analysis, report that the polymerisation proceeds by two major transition states when taking into account the ring opening of two consecutive lactide molecules, which is also present in other coordinative initiating systems [211]. Polyesters are susceptible to side reactions, mainly inter- and intramolecular transesterification, leading to shorter polymer chains, macrocyclic structures and chain redistributions[212,213], Figure 1.56 and Figure 1.57.

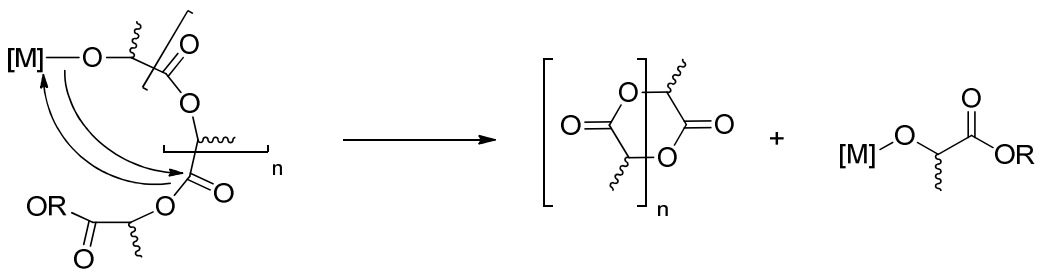

Figure 1.56. Intramolecular transesterification reaction

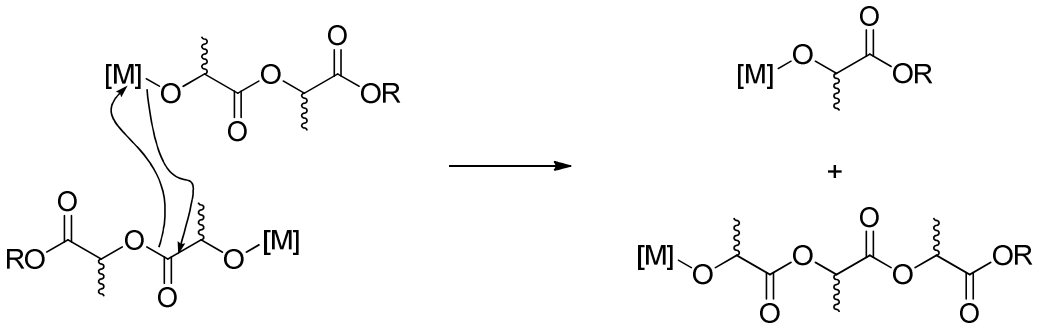

Figure 1.57. Intermolecular Transesterification reaction

Transesterification and other side reactions will affect molecular weight, and the molecular weight distribution. Monitoring the degree of transesterification can be achieved by MALDI ToF MS (Matrix-Assisted Laser Desorption/Ionisation Time of Flight Mass Spectrometry). A very soft ionisation technique commonly used for polymers but also biomolecules and large organic molecules which can be fragmented by more standard ionisation techniques. MALDI ToF MS measures the distribution of molecular weight within a polymeric sample and gives an indication to the presence of cyclic polymer, intramolecular transesterification. The resulting spectra gives the molecular weight distribution by mass against intensity with each peak separated by the mass of the repeating unit, 144 mass units for LA, in the case of a controlled and clean polymeric sample. If side reactions occur, transesterification, it is common to see an extra series of peaks that appear in the spectra separated by 72 mass units, the new repeating unit size. This can be seen in Figure 1.58, a MALDI ToF spectrum of PLA initiated by propyl alcohol (a) and a zoomed in fragment (b) displaying PLA with a repeat unit of 144.14 and a m/z of n × 144, 56 ($M_{Pry\text{-}OH}$) and 39 (M_{K+}) series 1, while series 2 has the repeat unit of half a lactide, 72.07, complete with end groups.

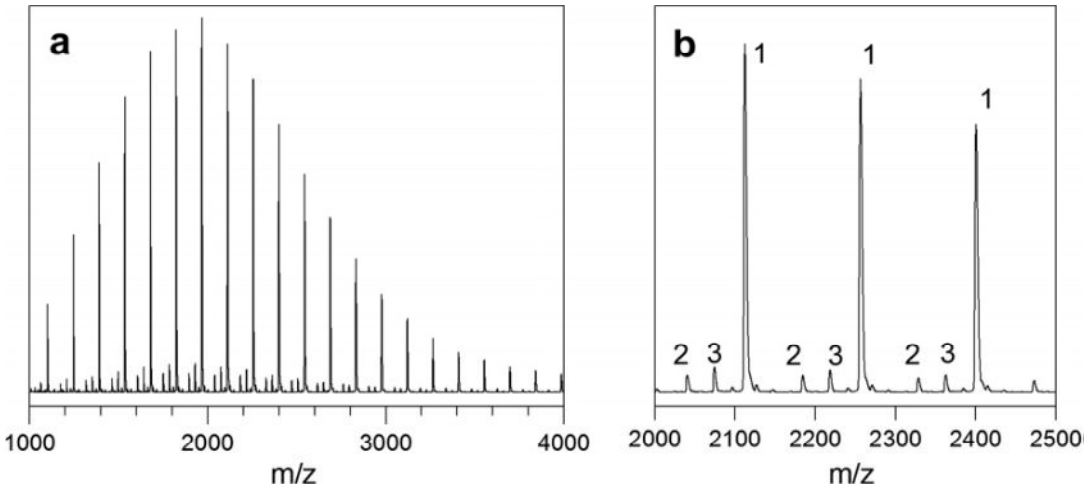

Figure 1.58. Images reproduced from work published by Basko and Bednarek[214]

1.2.3. **Polymerisation Rates**

The performance of a catalyst system is often characterised by the resulting molecular weight of the polymer produced and coordination-insertion systems are no different. Molecular weight depends primarily on the ratio of rate of propagation to the rate of initiation. That is to say that if the k_{prop} is greater than k_{ini}, many polymer chains make up the sample, and the observed M_n value will differ significantly to the theoretical M_n. If k_{ini} is greater than k_{prop} then the polymerisation will be well controlled and this will result in a narrow molecular weight distribution. Theoretical molecular weight, $M_{n(theo)}$, is calculated from conversion multiplied by the mass of one repeat unit, multiplied by the ratio of monomer to initiator, Equation 1.

$$M_{n(theo)} = \left((Conversion\,\% \times 144) \times \frac{[Monomer]}{[Initiator]} \right) + (end\ groups)$$

Equation 1. Calculation of theoretical M_n

$k_{ini} >> k_{prop}$ = Narrow MWD and good fit to $M_{n(theo)}$

$k_{ini} << k_{prop}$ = Wide MWD and poor fit to $M_{n(theo)}$

Different catalyst systems are compared to one another and evaluated based also on their activity, which is derived from analysis of the polymerisation rate constants, $k_{(poly)}$. The majority of LA polymerisation reactions follow a second order rate law, Equation 1.2.1, where k_p is the rate of propagation, $[Lactide]_0$ is the initial lactide concentration, $[I]_0$ is the initial initiator

concentration and n is the order in initiator concentration/aggregation number. However, it is the practice to carry out pseudo first order rate experiments to determine k_{app}, the apparent rate of propagation, Equation 1.2.2, which takes into account the concentration of impurities, such as water which kills initiator, in order to accurately calculate k_p. Applying pseudo first order kinetic to the concentration of monomer, [monomer] generates Equation 1.2.3. Therefore plotting the natural logarithms of the concentration of monomer, against time affords k_{app}.

1. $\frac{-d[LA]}{dt} = k_p[Lactide]_0[Initiator]_0^n$
2. $k_{app} = k_p[I]_0^n$
3. $\frac{-d[LA]}{dt} = k_{app}[LA]_0$

Equation 1.2. Formula used to calculate rate constants

If only k_{app} is used, a distorted value for the initiators activity and mechanism is obtained so it is imperative to determine k_p.

1.2.4. **Polymer Analysis -GPC**

It has been shown that M_n can be calculated theoretically, and compared to the experimental value, M_n. Molecular weight is determined by Gel Permeation Chromatography. Unlike HPLC discussed earlier and other chromatography techniques where separation of a sample is a result of chemical or physical interactions, GPC works on the principle of size exclusion chromatography, where the hydrodynamic volume separates analytes. Cross-linked polystyrene beads of various pore size are packed into a column, a polymeric sample is loaded onto this column dissolved in a solvent, typically THF, and the column is flushed with solvent. Smaller polymer chains enter the pores more easily than larger chains, thereby increasing their retention time, the path taken is longer, whereas larger chains spend little to no time in these pores and are eluted quickly (Figure 1.59).

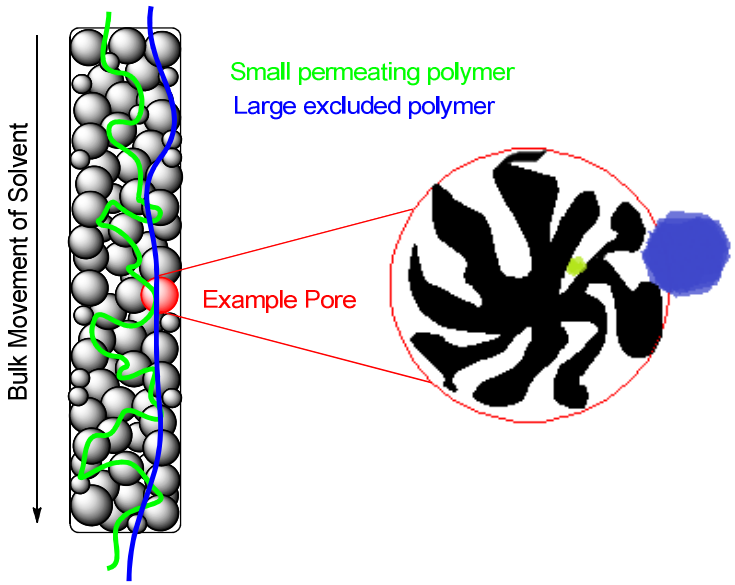

Figure 1.59. Schematic diagram of a GPC column exerting the size exclusion principle

The concentration by size of polymer in the eluting solvent is monitored by detectors and a retention time assigned. Using a calibration curve of time versus molecular weight for known polystyrene standards generates M_n (observed). Because the hydrodynamic volume of PS is different to PLA it is routine to apply a correction factor to the molecular weight value. Multiplying by 0.58 accounts for such differences[215]. Different detectors can be used, those that are concentration sensitive and those that are molecular weight sensitive. Concentration sensitive are UV, IR, RI and differential refactometer, while molecular weight sensitive are low angle light scattering and multi angle light scattering, which give a molecular weight distribution of the polymer as a function of retention volume[216].

GPC provides the weight average molecular weight, M_w and the number average molecular weight, M_n and from these the polydispersity index can be calculated as the ratio of the M_w to M_n. PDI is a measure of molecular weight distribution and is one factor used to compare initiators.

$$M_n = \frac{\sum N_i M_i}{\sum N_i}$$

$$M_w = \sum W_i M_i \text{ where } W_i = \frac{N_i M_i}{\sum N_i M_i}$$

$$PDI = \frac{M_w}{M_n}$$

Equation 3. Determination of M_n M_w and PDI where N_i is the number of molecules of mass M_i

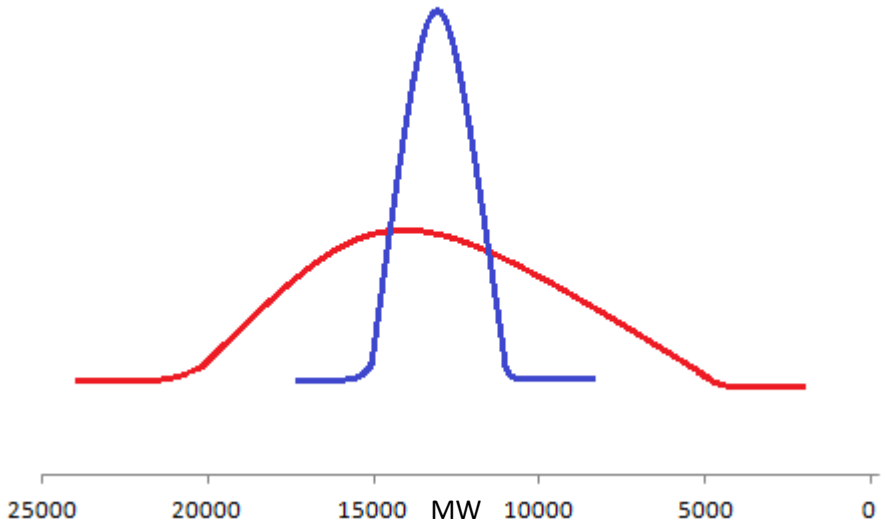

Figure 1.60. Example GPC trace showing in blue a polymer with narrow PDI and in red a sample with poorer control and a broader PDI

1.2.5. **Polymer Analysis - Stereochemistry**

PLA and other poly(alpha-hydroxy acids) and poly(hydroxyalkanoates) are an additionally attractive class of polymers because of the presence of an asymmetric carbon atom in the monomer unit. It has been demonstrated that stereochemical structure has a strong influence on both the physical and chemical properties, with stereochemistry of the monomer giving rise to PLA having a varied crystallinity. Vert et al[217,218] has shown that physical, degradation and mechanical properties of polylactide are strongly influenced by their configurational structure. Lactide has two stereocentres and as such can exist in three forms, *D*-Lactide, *D*-LA (*R, R*), *L*-lactide, *L*-LA (*S, S*) and *meso*-lactide, *meso*-LA (*R*, *S*). *L*-lactide is the naturally occurring form and studies will often screen initiators against it, while *rac*-lactide consists of a 50:50 mix of *L* and *D* enantiomer.

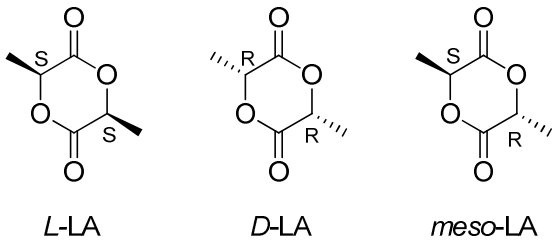

Figure 1.61. Possible stereo forms of lactide

Meso-LA can produce either syndiotactic PLA, where the *R* and *S* chiral centres alternate, or heterotactic, where pairs of *R* alternate with pairs of *S*. Heterotactic PLA can also be produced from *rac*-LA which can also produce isotactic PLA, where *R* follows *R* and *S* follows *S*. Isotactic polymer can be further divided into pure isotactic, with only *R*/*S*, diblock isotactic, where *R* follows *R* until all *D*-lactide is consumed then *S* follows *S* until complete, and finally multiblock, where there are discreet 'blocks' of *R* following *R* and *S* following *S*. Isotactic diblock polymers are also known as stereocopolymers, and as well as being prepared from a racemic monomer mixture, can also be a result of polymerisation of various enantiomerically enriched monomers[219]. The final possibility is atactic when there is no perceived stereoregularity. Possibly tacticities are shown in Figure 1.62.

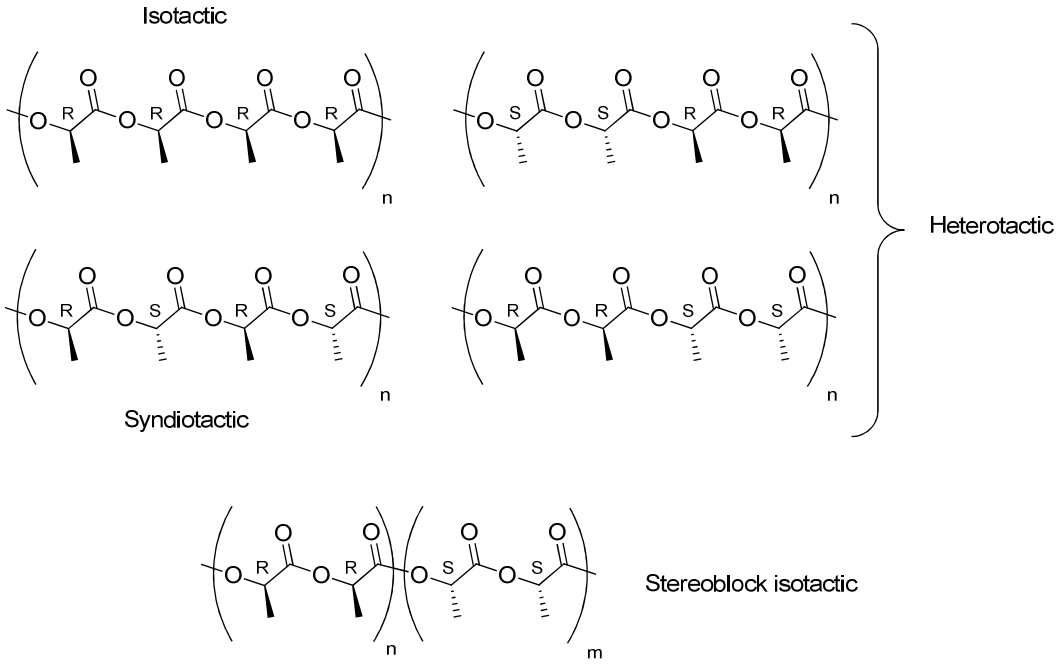

Figure 1.62 Different tacticity of PLA prepared from either rac- or meso-LA

The physical properties of PLA are strongly dependent upon their stereochemical composition. As such in the past melting and glass-transition temperature have been used to characterise the stereoregularity of PLA. Poly(*D*-Lactide) or poly(*L*-lactide) is a highly crystalline thermoplastic with a T_m around 180 °C, heterotactic PLA displays some degree of crystallinity at 130 °C and atactic PLA is amorphous with a T_g of around 60 °C. So when a purely isotactic

polymer is contaminated with meso-lactide, the melting point and crystallinity decrease, however poly(*D/L*-lactide) can be surpassed, with stereoblock isotactic PLA reporting a T_m of 230 °C. Stereosequence is determined quantitatively by Homonuclear Decoupled NMR spectroscopy, HNDNMR, focussing on the methine region and/or the carbonyl region of the ^{13}C $\{^1H\}$ NMR. If consecutive chiral centres are equivalent, *R* following *R* or *S* following *S*, then they are given the symbol i for isotactic, alternatively if they are non equivalent they are given the symbol s, syndiotactic. Any for structural/repeat units will give rise to a combination of i and s, and these tetrads are the focus of HNDNM. Isotactic PLA can only have one possible combination of tetrads, which give rise to the iii resonance, as such the methine region of the HNDNMR would give a single resonance, Figure 1.63.

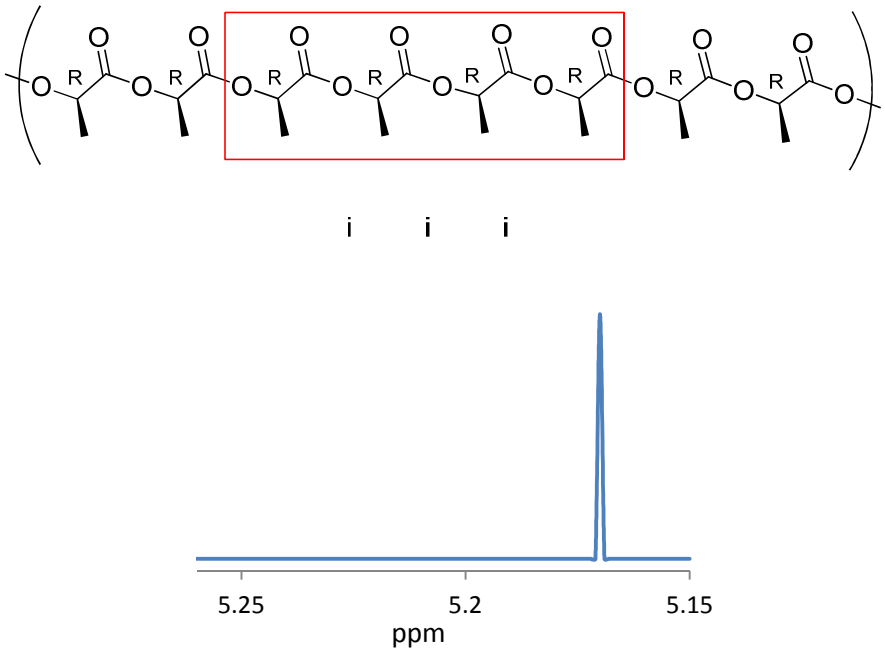

Figure 1.63. Top; Example of an isotactic PLA sample, and assignment of consecutive stereocentres giving rise to iii tetrad and below; Expected NMR trace of methine region in HNDNMR.

Heterotactic PLA, with its alternation of stereocentre "pairs" would give rise to alternative i and s labelling, thus resulting in two possible tetrads, isi and sis. The HNDNMR of this polymer would have two resonances, shown in Figure 1.64.

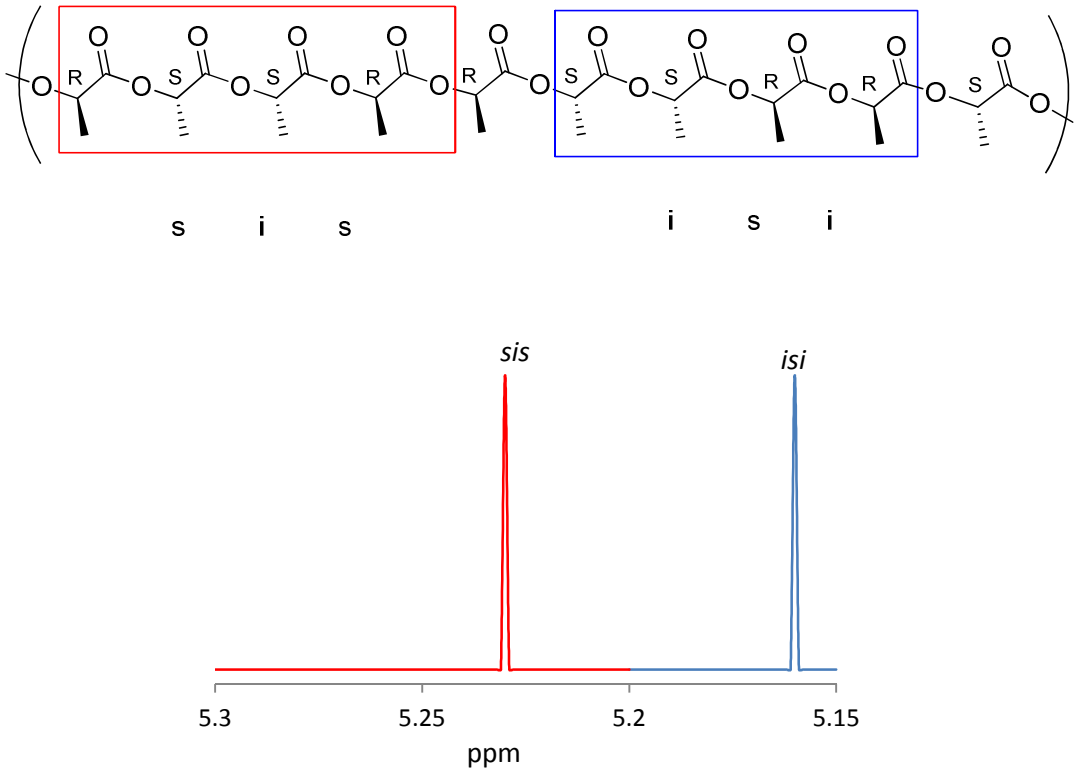

Figure 1.64. Top; Example of a heterotactic PLA sample, and assignment of consecutive stereocentres giving rise to isi and sis tetrad and below; Expected NMR trace of methine region in HNDNMR.

With no stereoregularity in atactic PLA there is a random orientation of the methyl groups. This gives rise to five possible combinations of tetrads, sis, sii, iis, iii, or isi in the ration 1: 1:1:3:2, Figure 1.65.

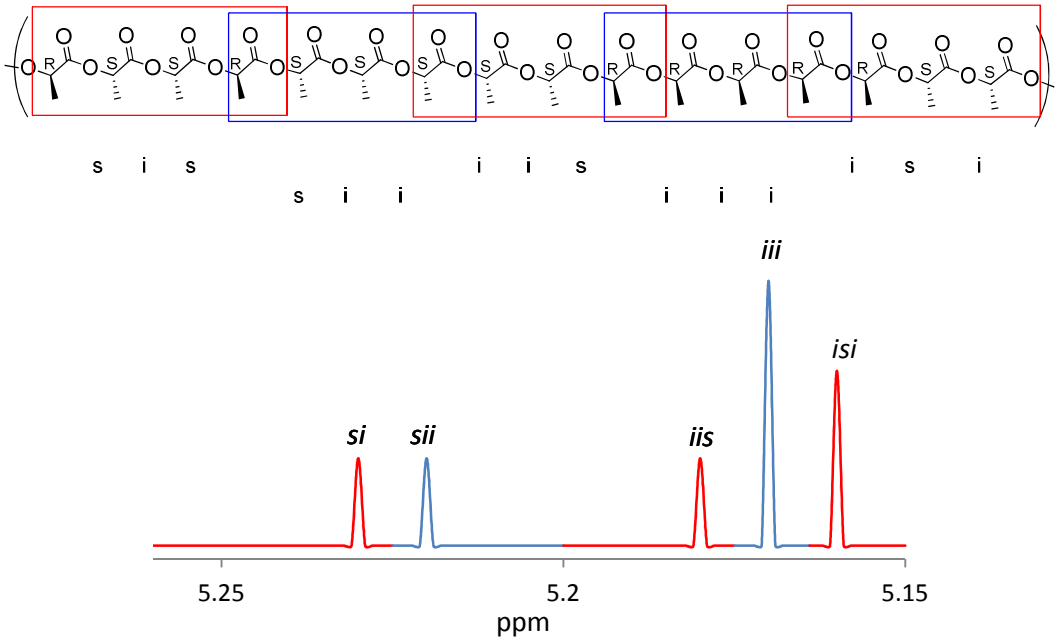

Figure 1.65. Top; Example of an atactic PLA sample, and assignment of consecutive stereocentres giving rise to five possible tetrads and below; Expected NMR trace of methine region in HNDNMR.

These five possible tetrads present in PLA prepared from *rac*- or *meso*-LA can be determined from a Bernoullian distribution[220], and the probability of the tetrad appearing in the HNDNMR spectra can be calculated from such, giving rise to the equations in Table 1.14. Avoiding the need to use simultaneous equations and to ease calculations [sis] is normally calculated (for *rac*-LA) and used to determine the stereoregularity or tacticity of the polymeric sample, with the value of P_r, probability of racemic enhancement, (P_m for meso-lactide). When the P_r value is 1, then there is a hundred percent chance that the neighbouring stereocentre will be racemic, leading to heterotactic PLA. If the P_r value is 0 then there is no chance that the subsequent chiral centre at any point in the polymer chain, being racemic, therefore isotactic. If the probability of racemic enrichment is 0.5, then there is a 50:50 chance that the following centre being different is suggestive of atactic PLA.

	Probability	
tetrad	***rac*-LA**	***meso*-LA**
[iii]	$P_m^2 + P_rP_m/2$	0
[iis]	$P_rP_m/2$	0
[sii]	$P_rP_m/2$	0
[sis]	$P_r^2/2$	$(P_m^2 + P_rP_m)/2$
[sss]	0	$P_r^2 + P_rP_m/2$
[ssi]	0	$P_rP_m/2$
[iss]	0	$P_rP_m/2$
[isi]	$(P_r^2 + P_rP_m)/2$	$P_m^2/2$

Table 1.14. Probabilities for possible tetrads based on Bermoullian statistics[220]

1.2.6. **Aluminium Initiators**

The pioneering work that opened up the area of single site metal centre polymerisation of lactide as a biodegradable plastic is typically credited to Inoue and Aida, (porhyrin)AlX and Zn initiators, Spassky's subsequent work, and Coates (salen)-AlX compounds.

In 1981 metalloporphyrins were utilised for the living polymerisation, polymerisation with a continuous propagation step, of epoxides and block copolymers with controlled chain lengths[221,222], PDI for ethylene oxide ~ 1.10, 1,2-butene oxide ~ 1.10, and 1,2-butene oxide-propylene oxide block copolymer ~ 1.20.

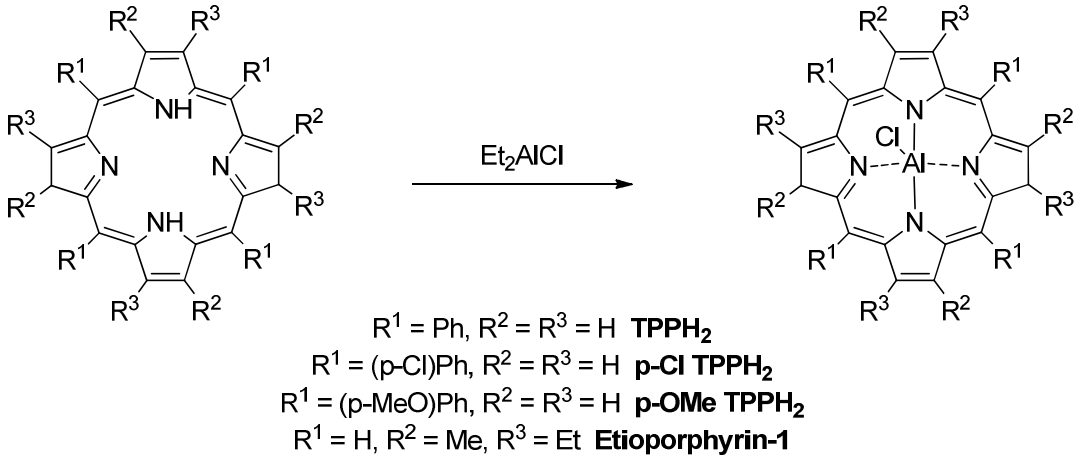

Figure 1.66 Aida and Inoue early (porphyrin)AlCl complexes[221]

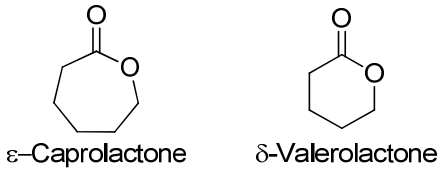

Figure 1.67. Cyclic esters similar to lactide

In 1987[223,224] these aluminium porphyrins were used to polymerise δ-valerolactone and ε-caprolactone, Figure 1.67, two cyclic esters in the same family as lactide. The Al(III) complexes were excellent catalysts for the polymerisation of lactones. Although inactive on their own, when used in tandem with MeOH to generate (TPP)AlOMe, 51 % conversion of 200 equivalents of valerolactone was achieved after >80 mins (50 °C solvent free), with very narrow PDI and when used with methanol for the polymerisation of caprolactone went to 65 % conversion after 3 hours (room temperature) with a PDI of 1.07. The number of aluminium initiators were increased in 1994 to incorporate Phthalocyanine, tetraazaannulene, and Schiff bases, Figure 1.68, for the ROP of epoxides[225]. Narrow PDI was maintained as the equivalents of epoxide were increase and molecular weight increased linearly.

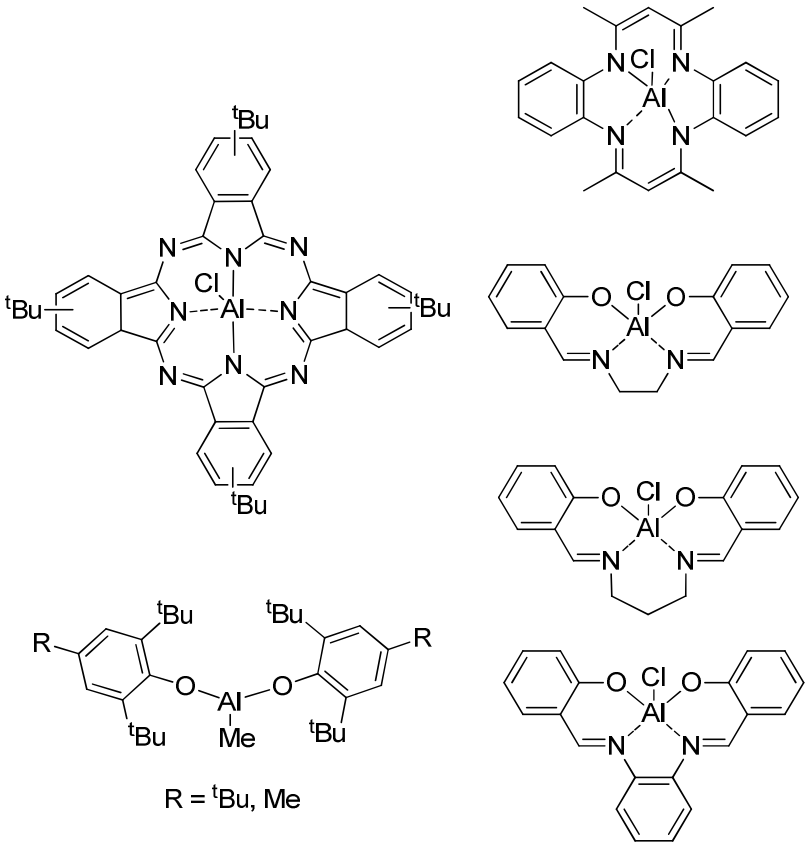

Figure 1.68. Selection of Aluminium catalysts with Schiff base, phthalocyanine and tetraazaannulene ligands

Aluminium alkoxides are the preferentially used initiators, but Schiff base aluminium alkoxides can be used too. These display characteristics of living polymerisation, but secondary reactions occur in the last stage of polymerisation with a broadening of the molecular weight distribution, this can be attributed to transesterification reactions.

Previous to Spassky's work, stereoselective PLA prepared from *rac*-LA had not been reported[226]. The group prepared a chiral aluminium alkoxide initiator derived from a chiral Schiff base incorporating a binaphthyl moiety, which are known and "powerful" tools in asymmetric chemistry[227]. PLA made in olution at 70 °C found good conversions, 65 % after 22 hrs with predictable M_n and narrow PDI. At high conversions the PDI increases, indicative of transesterification. Most significantly, the polymer was optically active and it was established that the R,R-LA enantiomer is preferentially polymerised in *rac*-LA[228].

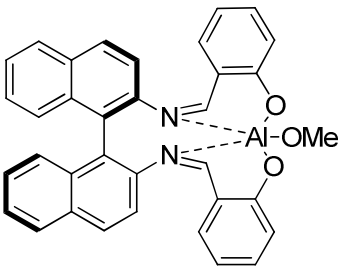

Figure 1.69. Aluminium Schiff base initiator incorporating (R)-Binaphtyl ligand[228]

Further examination by circular dichroism, and DSC concluded that the *R*-SalBinaphtAlOCH$_3$ initiator preferentially polymerises *D*-LA, and that this consumption of identical configuration or "same spatial configuration" as the chiral ligand is termed as homosteric when applied to monomers containing a single asymmetric carbon atom cycle[226,229]. This work was also explored by Baker and Smith[230] who utilised the racemic ligand in preparation of an aluminium initiator for the ROP of racemic lactide, replacing the OMe with an O^{i}Pr. It was reported that PLLA and PDLA were prepared from a living polymerisation of *rac*-LA, with the chiral binaphthyl ligand controlling the vital step in the coordination insertion mechanism[230,231]. However, Coates et al. re-evaluated this work and came to the conclusion that the modified racemic complex did not produce a mixture of PLLA and PDLA but in fact an isotactic stereoblock polymer[232].

Reverse-stereocontrol was reported by Feijen et al. with chiral aluminium isopropoxides based on Jacobsen's ligand, under solution conditions[233]. This complex had a significant preference towards *L*-lactide over *D*-Lactide with a reported rate ratio, k_L/k_D of 14.

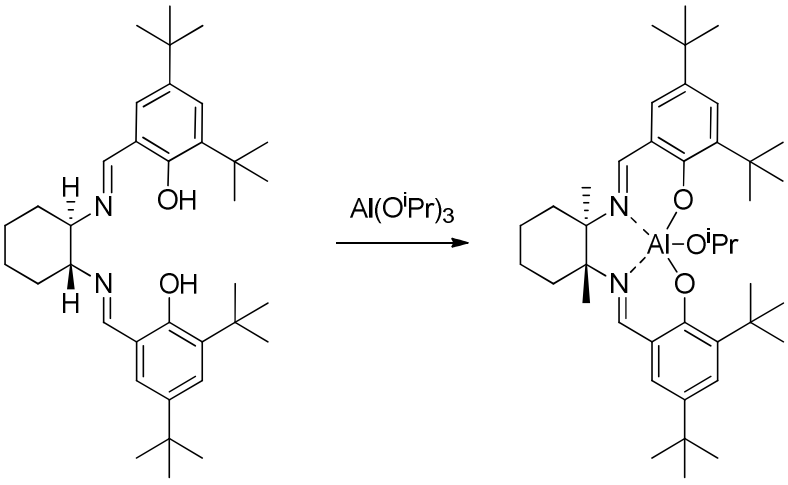

Figure 1.70. Preparation of chiral salen aluminium complex from Jacobsen's ligand

The benefit of using Jacobsen ligand is that it is an inexpensive commercial starting material and can be used to provide high isospecificity without the need of modification, and control the polymerisation of lactide at higher temperatures both in solution and under melt conditions[233]. Furthermore, the ROP of *rac*-LA *via* the (*R*,*R*) salen aluminium complex produces isotactic stereoblock PLA *via* an enantiomorphic site control mechanism[234].

Nomura et al.[231] achieved good stereoselectivity from an achiral aluminium complex, similar to Spassky's (Figure 1.71).

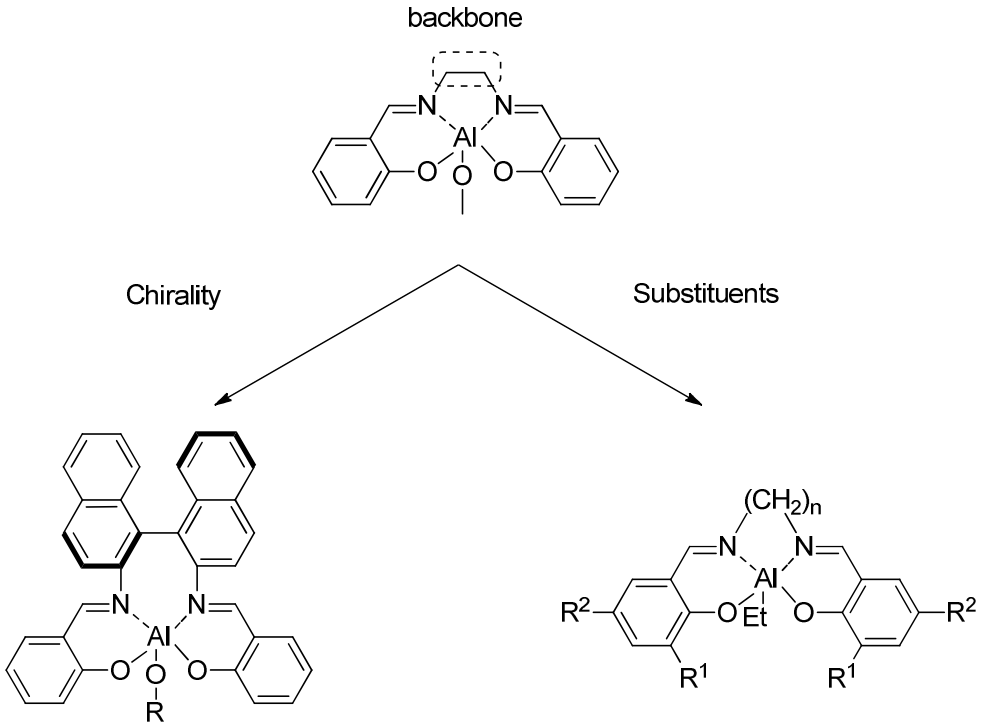

Figure 1.71. Spassky's Aluminium complex (Left) compared to those prepared by Nomura (Right)

High crystallinity in the polymeric material was achieved by chain-end stereocontrolled polymerisation of *rac*-lactide. That is to say that with an absence of chirality in the complex, the last inserted monomer in the growing polymer chain determines stereoselectivity. The initiating species in this work is generated *in situ* by addition of an alcohol to the Al-Et moiety. Polymers were prepared in solution at 70 °C with an alcohol to initiator ratio of 1:1. When the back bone was $-(CH_2)_3-$ compared to $-(CH_2)_2-$, reactivity was much higher and increasing the size of the R groups lead to a greater isotacticity, and a further increase to activity.

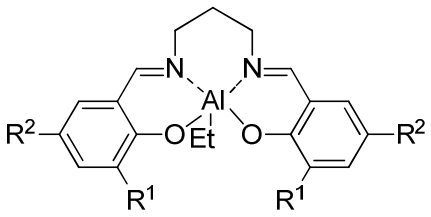

R^1 = Ph, R^2 = H	R^1 = R^2 = ^{t}Bu
time = 1.3hr	time = 14 hr
Mn = 20,000	Mn = 22,000
PDI 1.11	PDI 1.06
P_{meso} = 0.81	P_{meso} = 0.91

Figure 1.72. Comparison of increasing R groups around the aluminium complex

One more interesting example of metal initiators are complexes operating with a parallel site stereocontrolled synthesis of PDLA and PLLA from *rac*-LA. In this instance each enantiomer of the initiator preferentially polymerises one lactide enantiomer. As such, unlike kinetic resolution of monomer with a homochiral catalyst were tacticity can be dependent on conversion, the *D*/*L* ratio is kept constant and high enantioselectivites achieved.

One important criteria for consumer plastics is that they are clear, and the complexes reported above have been based on salen ligands, known for their bright yellow appearance which "stains" the polymer. In an industrial and commercial process, this is unadvantageous as it requires an additional decolourisation step during production. Gibson et al. developed a range of salan complexes producing colourless polymer of high stereocontrol and good PDI[235].

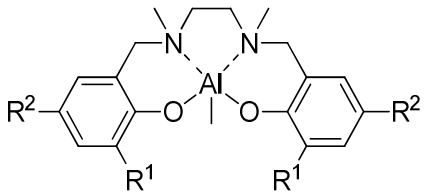

Figure 1.73. Aluminium salan complex prepared by Gibson et al.[235]

These are based on tetradentate phenoxyamine ligands and ROP *rac*-LA with a reported unprecedented degree of stereocontrol. Interesting in this work, rate decreases as the phenoxide alkyl substituent increases, H, Me, ^{t}Bu, but the dichloro equivalent is more active, 94 % in 21 hrs compared to the dimethyl substituted counterpart, attributed to greater electrophilicity of the aluminium centres. Additionally, the probability of racemic enrichment is reversed, R^1 = H

for a P_r of 0.21 and R^2 = Cl P_r = 0.96. At the time reported to the first example of an aluminium catalyst producing heterotactic PLA.

1.2.7. **Group(I) Initiators**

Initiators incorporating group(I) metals, all show a degree of activity but poor control with side reactions, enolisation and epimerisation, due to the strong ionic character of the compounds [236-243]. Some alkoxide complexes display greater control, Kasperczyk et al [243] reported commercial grade lithium tert-butoxide with good conversion achieving a polymer with an M_n of 40,000 $gmol^{-1}$ from an initial initiator to monomer ratio of 1:400. Stereocontrol was also demonstrated with a heterotactic bias from *rac*-LA and a P_r of 0.76. Reducing the temperature and analysis at lower conversion, saw improved selectivity due to reduced transesterification [242,243] .

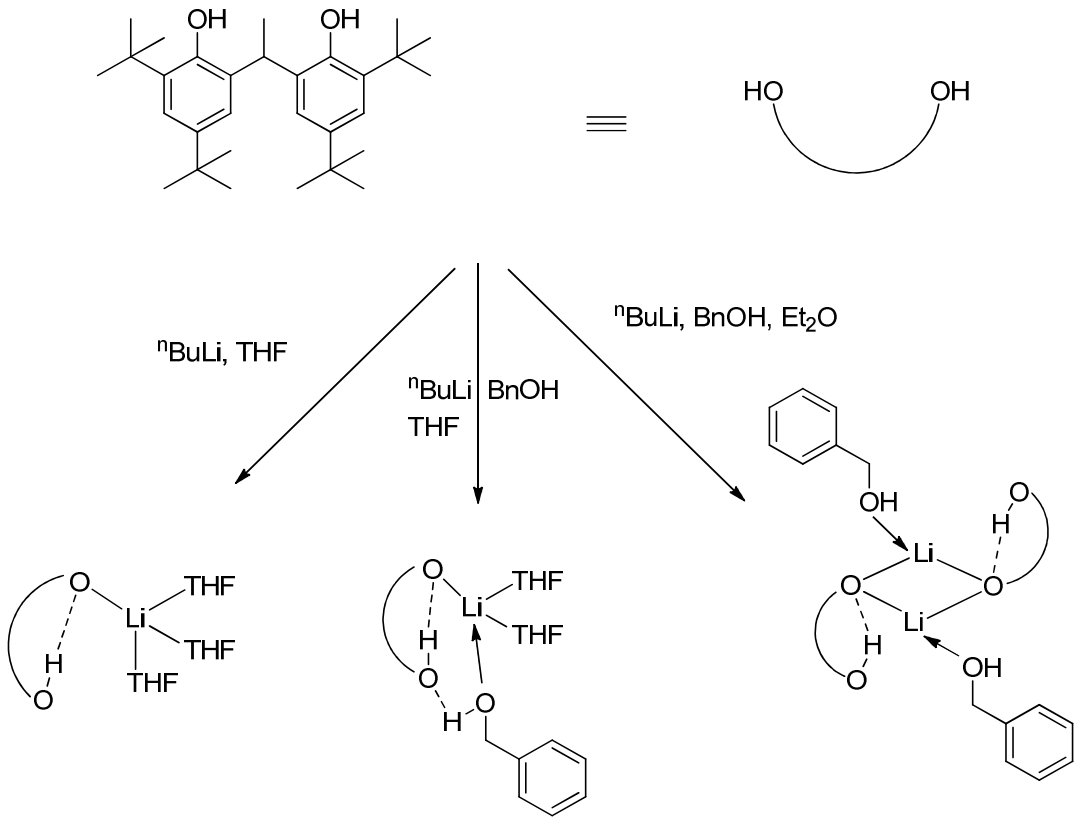

Figure 1.74. Preparation of initiator, Lin et al[244]

A draw back that these group I alkoxides face is their tendency to aggregate, complicating structural analysis and introducing solubility issues. With

the above study Kasperczyk also demonstrated that potassium *tert*-butoxide was active, but when crown ether was introduced the control was improved, due most likely to improved solubility but at a cost to the rate; $k_{p(KO^tBu)} = 5.9 \times 10^{-3} M^{-1}s^{-1}$ compared to $k_{p(K18\text{-crown-6})} = 0.53 \times 10^{-3} M^{-1}s^{-1}$ [237]. Lin et al[244,245] used ancillary ligands, bis(phenolate)'s, to control the aggregation of lithium alkoxides, Figure 1.74, and displayed good control with no epimerization.

Recently Miller et al[246] reported a comparison between a series of Group I and II complexes with 2,6-di-tert-butyl-4-methylphenol (BHT) as the ligand. In the presence of benzyl alcohol as initiator, high activities were observed with the sodium complex outperforming the others in bulk polymerisation reactions. The group also studied the variation in the C_{ipso}-O-metal angle (159.3 - 180.0°) and suggested that there is a "shallow potential energy well for bond angle deviation"[246] and were able to support this with DFT calculations. The significance of this is that the variable angle controls the electrostatic charge on the metal centre and this fluxionality means that the metal can alternate to activate the monomer as a strong Lewis acid (C_{ipso}-O-metal linear) and as a weaker Lewis acid increases lability (C_{ipso}-O-metal bent) giving rise to the activity of these complexes.

1.2.8. **Group(II) and Zinc Initiators**

Compared together as they display closely related properties and in often cases utilising the same ligand system, group(II) metals and zinc complexes are attractive due to their low toxicity, being present in many metalloenzymes, in vivo and the environment, and having a high level of activity. Initial investigations focused on the application of heterogeneous oxides, alkoxides, halides, amino acid salts, and carboxylates of calcium, magnesium, and zinc as initiators[247]. However, while displaying some activity, they were generally slow and hindered by epimerisation, for example Feijen et al[248] reported work based on commercially available calcium dimethoxide under solvent free conditions at 120 °C, but only achieved modest conversion with poor control, with evidence of significant racemisation of *L*-LA, attributed to the formation of aggregates.

Heteroleptic Group II and zinc complexes on the other hand have demonstrated impressive activities and interesting selectivities have been observed, for three major ligand types; β-diketiminates, BDI, tri(pyrazolyl)borates, and phenoxy-amines. Coates et al [220,249] observed incredible results for BDI complexes of magnesium and zinc isopropoxide (Figure 1.75). Excellent activities and very high heteroselectivity were observed for both *rac* and *meso*-LA, P_r 0.90 and P_m 0.76. This impressive performance is not seen when the initiating group is an amide, acetate nor alkyl, likely due to k_{ini} being greater than k_{prop}.

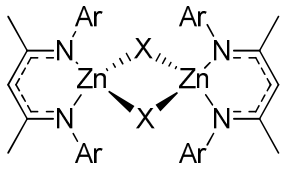

Ar = 2,6-^{i}PrC$_6$H$_3$, 2,6-PrC$_6$H$_3$, 2,6-Et$_2$C$_6$H$_3$,
X = Et, N(SiMe$_3$)$_2$, OAc, lactate, O^{i}Pr

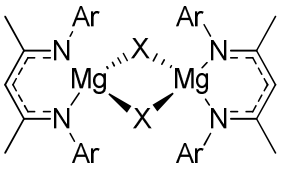

Ar = 2,6-^{i}PrC$_6$H$_3$
X = O^{i}Pr

Figure 1.75. BDI complexes of Coates et al[220,249]

The second factor effecting rate and stereocontrol is the substituents of the BDI aryl rings, with both rate and stereochemistry decreasing in the order ^{i}Pr > Et > Pr. Magnesium complexes prepared also showed greater activity but with reduced control and stereoselectivity.

Chisholm et al [250-252] presented work of very similar BDI complexes, with increased steric bulk around the metal. Efficient initiators for polymerisation of *rac*-LA in THF with zinc and magnesium and good heterotactic bias, was also extended to include calcium. Single point kinetic studies and competition experiments with one equivalent of LA showed that the relative order of activities for the BDI complexes was Ca > Mg > Zn [253-255].

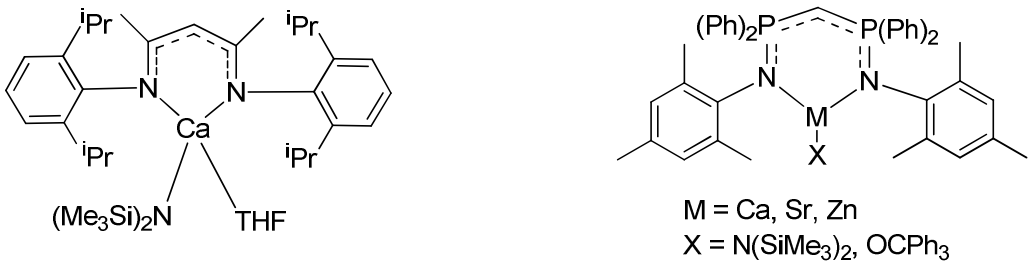

Figure 1.76. Example of BDI complexes reported by Chisholm et al[250-252]

Further investigations of BDI's include DFT analysis proposing a two transition state polymerisation [211] and ligand system derivatives, including the introduction of heteroatoms into the backbone.

Tris(pyrazolyl)borate, Tp, metal alkoxides were also prepared by Chisholm's group(Figure 1.77), in the form ^{t}BuTpMOR where M = Mg, Ca, Zn and R = Et, all showed promising results [254-257]. Kinetic studies revealed the same order of activity for these complexes as those for BDI complexes, Ca > Mg > Zn with one hundred equivalents fully converted in 1min, 1hr and 6days respectively[254]. It was proposed that the difference in polarity of the M-OR bond correlates to the activity[257]. A final consideration in the study with Tp's and Ca is the very good heterotactic bias seen for the polymerisation of *rac*-LA in THF, P_r = 0.90. This, however, decreases when the solvent is changed to CH_2Cl_2, signifying a possible correlation between a solvents coordinating ability and heteroselectivity[255].

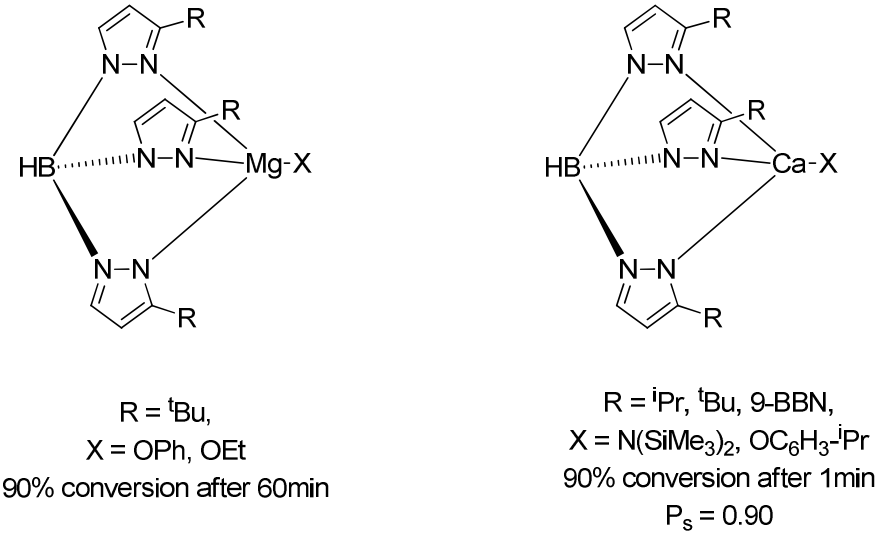

Figure 1.77. Tris(pyrazolyl)borates prepared by Chisholm et al[255,257]

Phenoxy-diamine, bis(phenoxy diamine), phenoxyimine amine, and phenoxy imine complexes have demonstrated their usefulness as ROP initiators and offer some interesting relationships between structure and activity being[258-262].

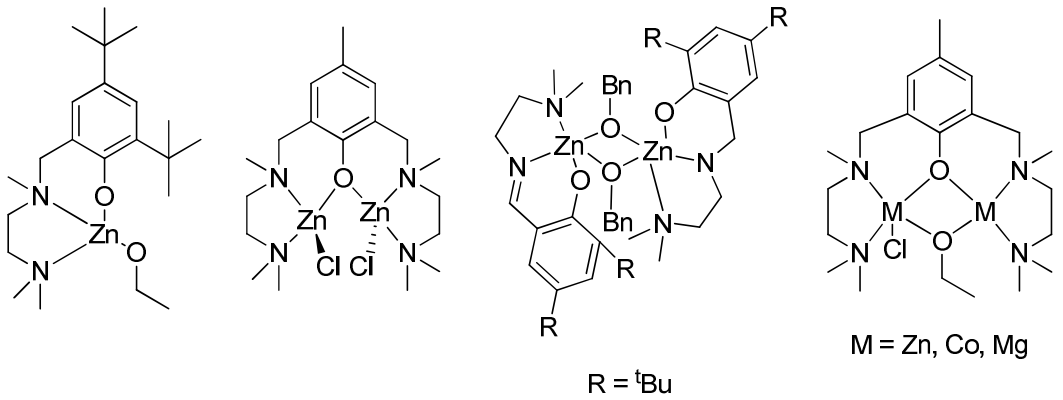

Figure 1.78. Left to right, Williams[258], Williams[259], Chen[261], Breyfogle[262]

Binuclear metal alkoxides were very active and controlled catalysts however the order of activity was reversed when compared to what has already been seen, with Zn > Mg > Ca [259-261]. It has been rationalised as the complexes possessing a different rate determining step in the coordination-insertion mechanism, being either the coordination of the carbonyl to the metal or insertion/ring opening of the LA. BDI and Tp complexes gave a lower coordination number so it can be expected that $k_{carbonyl}$ faster than $k_{insertion/RO}$ therefore their relative rates are due to increasing polarity of the M-OR bond. The phenoxy diamine zinc ethoxide prepared by Williams et al[258], Figure 1.78, displayed incredible activity. A dimer in the solid state, PSGE NMR spectroscopy confirms a mononuclear structure in solution. Good stereocontrol at very low initiator concentrations, 1500:1, and a considerably faster system than its phenoxy imine amine counterpart reported by Chen et al[261], Figure 1.78, and these results are summarised in Table 1.15.

	Phenoxy diamine[258]	Phenoxy imine amine[261]
$[LA]_0/[I]_0$	1500	150
Temperature (^oC)	25	25
Solvent	DCM	Tol
Time (min)	18	80
Conversion (%)	93	93
M_n	130,000	21,500
PDI	1.34	1.08

Table 1.15. Comparison of initiator performances on the ring opening polymerisation of lactide

1.2.9. Group(III) and Lanthanide Initiators

With both group(III) and lanthanides having no known toxicity issues, with moderate Lewis acidity and reasonable activity they are considered attractive initiators. Combine this with Lanthanides' ability to polymerise a diverse range of monomers[263] and you would expect a great number of studies. However, due to difficulties in handling and characterisation of lanthanides, as well as solubility issues and the formation of aggregates their investigation has so far been limited.

DuPont researchers discovered homoleptic yttrium alkoxides[264] in the form $Y(OCH_2CH_2NMe_2)_3$ as one of the most active initiators with $k_{app} = 0.5\ s^{-1}$, curiously exhibiting a zero order dependence on the initial concentration of LA. Spassky et al[265] examined a series of $Ln_5(\mu\text{-}O)(OR)_{13}$ clusters and reported that their activity decreased with decreasing ionic radius La > Sm > Y > Yb, 106.1, 96.4, 90.0, 85.8 pm respectively.

Highly active tris(alkoxide)-lanthanide systems, were prepared from aliphatic alcohols and $Ln(OAr)_3$ complexes previously too bulky to allow efficient polymerisation. An example of which is the work conducted by Stevels et al[266,267] who prepared tris(iso-propoxide)yttrium from tris(2,6-di-tert-butyl phenoxy)yttrium with isopropanol (IPA), Figure 1.79. This initiator displayed impressive activity, $k_p = 0.32\ M^{-1}\ s^{-1}$, when compared to the Yttrium cluster, was controlled and showed iso-propoxy ester end groups in the polymeric sample. Okuda et al[268] reported that yttrium complexes of a 1,ω-dithialkanediyl bridged bis(phenolate), Figure 1.79, displayed improved rates and control when the

alkoxide was prepared in situ upon the addition of IPA, k_p = 2.3 ×10^{-4} M^{-1} s^{-1} increases to 6.96 M^{-1} s^{-1}. A common practice of many groups to achieve improvements to initiators.

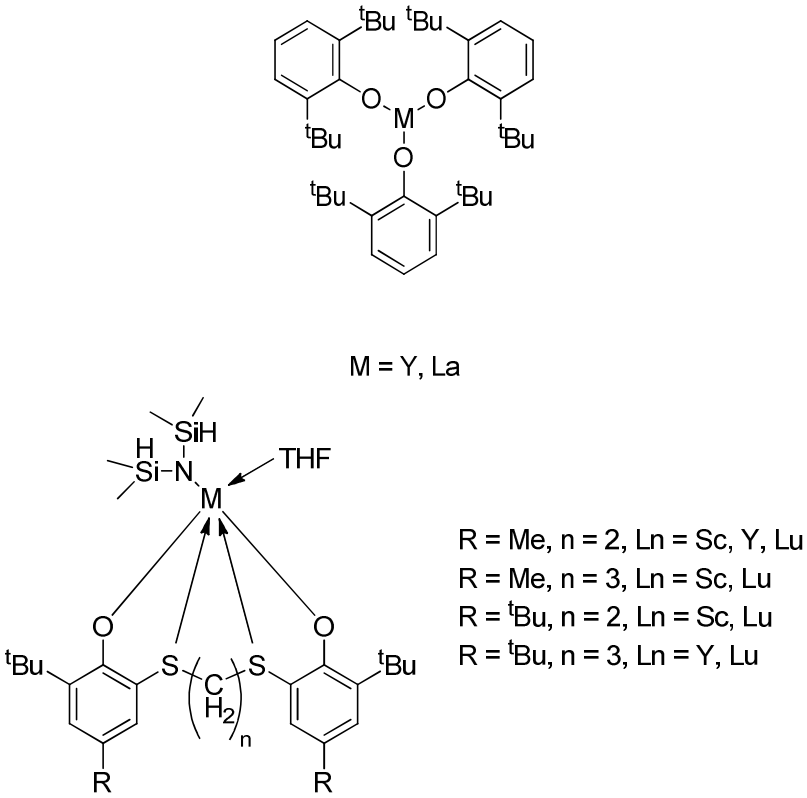

Figure 1.79 Top; Stevels initiators Bottom; Okuda's initiators

The design of ligands in group(III) and lanthanide complexes is also an important factor for the rate of polymerisation and control. Salen, guanidinate and 1,4,7-triazacyclononane macrocycle complexes of yttrium all display good activity, achieving completion after a few hours (1 mM loading), however bis(oxazolinate), bis(thiophosphinic amide), bis(phenolate) and amidinate complexes are reported to be much faster[232,268-275], going to completion in minutes under the same loadings, and "soft" thio-based initiators reportedly faster still[268,271,272,276].

Bis(phenoxy) amine yttrium complexes were first reported for the ROP of LA by Carpentier et al[273]. Such initiators showed good stereocontrol and a heterotactic bias, P_r = 0.8, which improved when the polymerisations were conducted in THF over toluene. Selectivity also improved with bulky substituents (ortho- and para- cumyl groups, P_r = 0.90)

Okuda et al's[271] work with chiral ligands of 1,ω-dithialkanediyl bridged bis(phenolate)'s also encompassed scandium complexes displaying again impressive stereocontrol, P_r = 0.95. The same trends were observed with increasing bulk increasing selectivity, however what was more important was the dithialkane bridge length, with propyl bridges or longer being vital for high stereocontrol. In this report the tert-butoxy-*R*-lactate complex, a model complex from the catalytic cycle was isolated as a dimer with a single ligand configuration, (Λ Δ). This scandium complex has a fluxional ligand configuration and stereocontrol is achieved from the rapid conversion pair with high lactide enantiomer selectivity. That is to say that the Δ-isomer selected for the *R*-LA but underwent fast isomerisation prior to insertion of the following monomer unit as did the Λ-isomer select *S*-LA and again isomerise to the Δ-isomer, leading to heterotacticty.

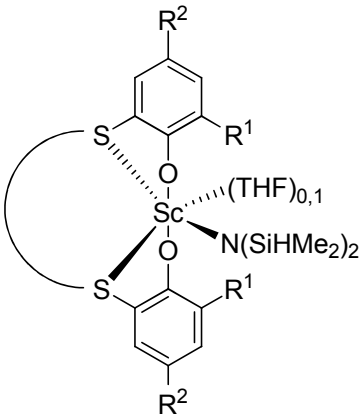

Bridge		R^1	R^2
C_2	$-(CH_2)_2-$	^{t}Bu	Me
	$-(CH_2)_2-$	cumyl	cumyl
	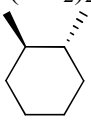	^{t}Bu	Me
C_3	$-(CH_2)_3-$	^{t}Bu	Me
C_4	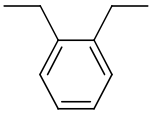	^{t}Bu	Me
	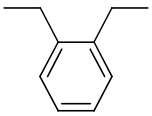		Me
	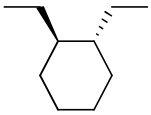	^{t}Bu	Me

Figure 1.80. A selection of Okuda's chiral bridged initiators

Very recently in 2012 Okuda published more variation of this 1,ω-dithialkanediyl bridged bis(phenols) having the -OSSO- tertadentate, a single methyl space, and also cyclo alkanes again complexed to yttrium and scandium, summarised in

Figure 1.80.

Li et al[277] incorporated potentially active ligand back bones that were previously utilised for ethylene and/or α-olefin polymerisation, such as polydentate phenolate, with high performances. A recently reported bis(alkyl) complex incorporating phosphido pincer ligands they had previously complexed to group(IV) metals with good success for highly isotactic polypropylene and poly(1-hexene)[277]. Anilidopyridyl-pyrolide and anilidopyridyl-indolide ligands, Figure 1.81, with yttrium and scandium that have been used as ROP initiators achieving a probability of racemic enhancement of 0.84, unfortunately with poor control over molecular weight.

Complete conversion of the Y complexes were achieved within minutes at room temperature dependant on solvent, CH_2Cl_2 > Tol ≥ THF, a similar observation to other groups, with scandium equivalents displaying lower activities. M_n values were close to expected, in most cases, Y-1-THF, Figure 1.81, = 25.7 and found 25.4, however PDI ranges from 1.54 to 2.23 attributed to transesterification, not uncommon in group(III) initiators, and analysis of low conversion polymeric samples by ESI-MS confirmed the occurrence of intramolecular side reactions.

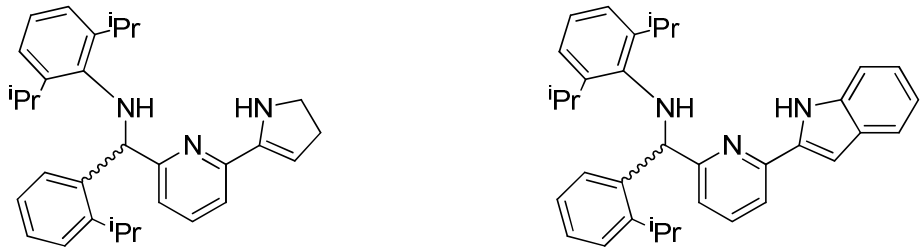

Figure 1.81 Left; Anilidopyridyl-pyrrolide ($1H_2$) Right; Anilidopyridyl-indolide ($2H_2$)

Polymerisations under solvent free conditions were investigated and good conversions, 87 %, suggest that these complexes are stable at high temperatures, with activities following the same order as solution experiments. Selectivity does suffer, P_r = 0.59, but this is not unusual for bulk reactions. An interesting entry to this report was an investigation to the coordination effect, as such Y-1-$(THF)_2$ was performed in toluene at 20 °C with the addition of ten equivalents of pyridine. A noticeable increase in control was observed with M_n values recorded being closer to theoretical and a narrowing of the PDI, 1.54 - 2.23 down to 1.67 - 2.02, with P_r increasing.

Also under investigation within the same group are complexes of group(III) metals with soft second row coordinating donor groups, sulphur and phosphorous. Mazzeo et al[278] report the use of tridentate phosphido-diphosphine ligands with Sc and Y, Figure 1.82. Arguably better control was demonstrated when compared to the -NNN- complexes described above with a PDI ranging from 1.20 to 1.66 depending on catalyst and conditions. Higher conversion is achieved in a matter of minutes at room temperature and M_n values are in agreement with theoretical, Table 1.16.

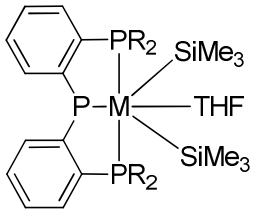

M = Y, Sc
R = ^{i}Pr, Ph

Figure 1.82. Complexes screened by Mazzeo et al [278].

Time /min	eq Monomer	Conversion	M_n	$M_{n(theo)}$	PDI
15	100	84	14.9	12.1	1.27
15	200	85	25.8	24.5	1.23
30	300	80	36.7	34.6	1.25
60	400	82	42.9	47.3	1.27
60	500	78	46.9	56.2	1.26

Table 1.16 Performance comparision at increasing monomer:initiator ratio, complex M=Y and R=Ph

These were very active like other NO multidentate ligands with reasonable control. However, not avoiding side reactions; with MALDI ToF MS confirming transesterification, the Yttrium complex with R = Ph was also screened for very high molecular weight polymer and utilised at a 1000:1 LA:I ratio, successfully 99 % conversion was obtained in 3 hrs at room temperature.

Examples of chiral ligands and group(III) metals or lanthanides are limited. Zi et al.[279] developed chiral biaryl-based, NNO- donor ligands which were active for the ROP of *rac*-LA at room temperature, Figure 1.83. These were also complexed to group(IV) metals as well as screened against the enatioselective hydroamination and cyclisation.

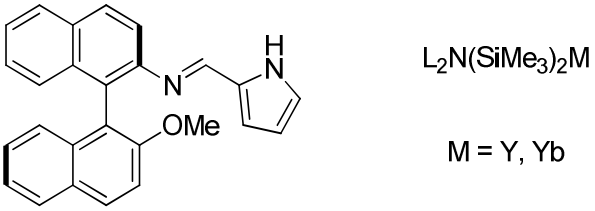

Figure 1.83. (*R*)-2-(pyrrol-2-ylmethyleneamino)-2'-methoxy-1,1'-binaphthyl ligand LH, and initiator.

Higher conversion is achieved with THF compared to polymerisation in toluene as expected, and good control was reported with PDI in the range of 1.23-1.29. Probability of meso linkages was reported to be in the range of 0.54-0.62 indicating an isotactic bias. Recently Carpentier et al[280] reported developments of chiral Yttrium, Lanthanum, Neodymium amido complexes, Figure 1.84, from cheap, readily available and enantiomerically pure (*S*)-(2-hydroxymethyl)pyrrolidine.

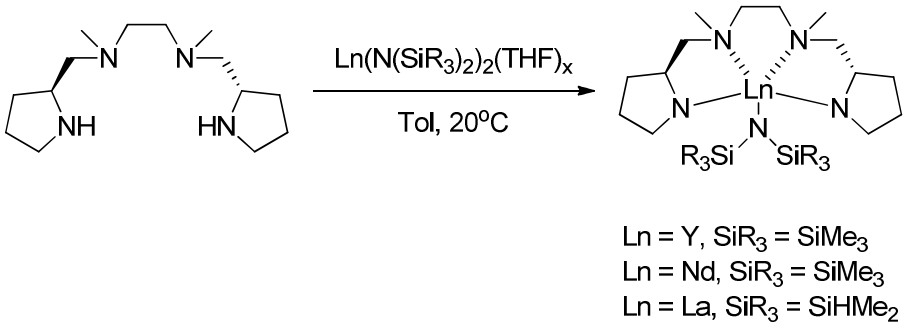

Figure 1.84 Preparation of Lanthanide complexes with S)-(2-hydroxymethyl)pyrrolidine

Conversion of 200 equivalents of LA was completed within 15mins at room temperature with the Yttrium complex. A reasonable degree of control was demonstrated, PDI 1.32 - 1.72, but it was also commented that there was a low initiation efficiency due to the M_n observed being greater than the theoretical value. Isotactic enrichment with a P_{meso} of up to 70 % was observed. Chiral ligands of this type have also been used by Carpentier's group, with zinc, for the asymmetric hydrosilylation of ketones[281], but also complexed with group(IV) metals and screened for the polymerisation of ethylene.[282] Such metal initiators will be discussed now.

1.2.10. **Group(IV) Initiators**

In view of the well-known and significant number of similarities in the chemistries of tin and titanium, it is surprising that there had been no previous investigations before 2002 with the publication of work from Verkade's group[283-285]. This may be a result of the trend in group(IV) initiators being slow, slower than those seen for other main group or lanthanide species, with rates comparable to aluminium complexes, 100 equivalents typically requiring reaction times of 24 hrs. Titanium complexes are more common in the literature, however it has been demonstrated that greater activity and stereocontrol can be achieved with Zirconium and Hafnium initiators[247,286,287]. Approximately, the order of activity for different ligands is as such; diamine bis(phenolates) > bulky alcohol/phenol clusters > salens > atranes > tellurium bis(phenolates) > amine bis(phenolates) > trisphenolates[284-293].

Amine trisphenolates had caught the eye of different groups, complexed to main group elements[294,295], iron(III)[296], with Kol et al.[297] taking amine trisphenolates and complexing them to titanium, Figure 1.85. Davidson et al.[298] demonstrated the preparation of heterotactic PLA under melt conditions with different group(IV) metal amine trisphenolate complexes, at the time considered a first. As previously discussed solvent free, bulk, melt, polymerisation is the industrially preferred method for PLA production, and the limit prior to this report was the long reaction times, 48 hrs, required for Al and Ge complexes at high temperatures[233,299]. The trisphenolates accomplished 95 % conversion within half an hour, more impressively with high stereocontrol, $P_r > 0.9$.

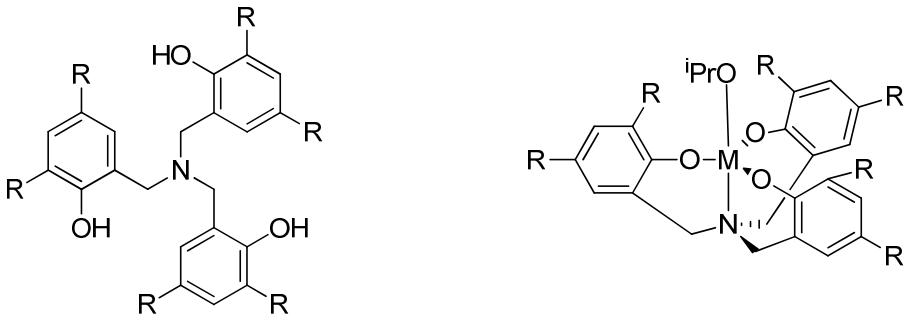

Figure 1.85 Kol et al. M = Ti, R = Me, ^{t}Bu Davidson et al. M = Zr, Hf, Ti, R = ^{t}Bu

The complexes from Figure 1.85 were isolated as monomeric complexes with the bulky ligand adopting a propeller like, C_3 symmetry. Analysis of the

microstructure revealed that the titanium initiator produced atactic PLA with an M_n value of 37,100 g mol^{-1} for 50 % conversion after 30 mins, (300:1 [LA]:[I]). Zirconium showed highest activity reaching almost 80 % conversion after 6 minutes maintaining control and stereoselectivity, observed M_n of 32,200 g mol^{-1} being in agreement to that of theoretical value, 33,700 g mol^{-1}, a narrow PDI of 1.22, and high selectivity P_r = 0.96. Further investigations with this Zirconium complex revealed it to be a living polymerisation, initiated by isopropoxide with minimal transesterification. Kinetic studies also demonstrated that the rate constants for polymerisation of *rac*-LA 4.2 $\times 10^{-3}$ min^{-1}, were seven times faster than that for (*S*,*S*)-LA, 0.6 $\times 10^{-3}$ min^{-1}.

Davidson et al. has also published work on amine bis(phenolates) comparing titanium, zirconium and hafnium, undertaking the first comparison of different group(IV) metals, with the same ligand group[286]. Contrary to previous work, where bulky ligands have shown to be more effective than sterically unhindered, this work demonstrated that improved activity and control is achieved with sterically less demanding ligands in combination with Zr(IV) and Hf(IV).

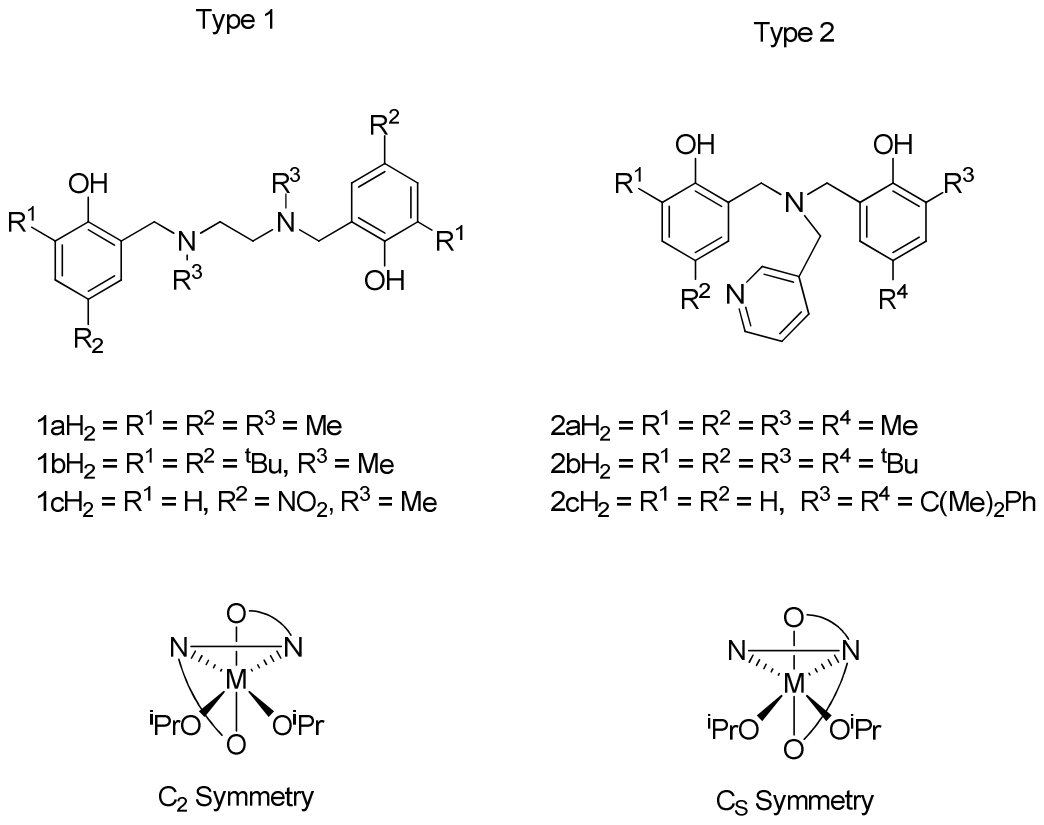

Figure 1.86 Tetradentate amine bis(phenolate ligands and their structural motifs[298]

When screened for the ROP of *rac*-LA, titanium complexes were mostly inactive under solution polymerisation conditions and produced only atactic polymer under solvent free conditions after two hours. By contrast, zirconium and hafnium analogues produced polymeric material of varying isotactic enrichment when less bulky ligands were utilised. This was attributed to the structural difference in the metal complexes with the tetradentate ligands falling into two categories with their complexes forming either C_2 or C_S symmetry. Type 1 ligands favour a fac-fac coordination of these achiral ligands which leads to a *pseudo*, chiral, C_2 symmetric complexes of Δ or Λ forms. On the other hand, bulkier type 2 ligands have *pseudo* C_S symmetry and as such nonchiral complexes. It is thought that this difference influences the stereoselectivity by the chain end mechanism. Comparing Zr and Hf with Ti, the difference giving rise to isotactic rather than atactic is the ability of the metal to chelate the growing polymer chain, with the heavier group(IV) metals preferring higher coordination numbers than Ti, favouring addition of *D*- or *L*-LA.

	Type 1		**Type 2**	
	Melt	**Solution**	**Melt**	**Solution**
time (hrs)	2	2	2	2
Yield (%)	55	>99	45	>99
M_n[a]	6050	9150	440	7100
PDI[a]	1.47	1.17	1.27	1.11
P_r[b]	0.30	0.25	0.45	0.40

Table 1.17 Comparison of initiators of $Zr(O^iPr)_2$ (1a/2a) for polymerisation of rac-LA. Melt conditions; 300eq LA, 130 °C, solvent free, Solution conditions; 100eq LA, 10mL Tol, 110 °C. [a] Determined from GPC using PS as the reference, [b] Determine from the ^{1}H homonuclear decouple NMR ($CDCl_3$) analysis.

Harada et al.[300] developed a series of titanium complexes having tellurium-bridged chelating bis(aryloxo) ligands, which were screened for the polymerisation of ethylene with great success, and investigated against polar monomers, namely cyclic esters; capralactone, valeralactone, and L-LA. The best system reported by Harada was the dimeric tellurium complex, containing a chloro group, carried out in anisole as solvent, chosen for its high boiling point and appropriate polarisability, at 100 °C in a 200:1 LA:I ratio. 84 % conversion was achieved after 32 hours, M_n from 24,200 $gmol^{-1}$ and a very narrow PDI of

1.08 for L-LA. This narrow PDI is indicative of no transesterification of hydroxy terminated PLA.

Atranes are well studied tricyclic, 5 membered ring molecules. Variations include silatranes, boratranes and phosphatranes. Verkade et al.[301] developed titanatranes, titanium containing atranes, Figure 1.87.

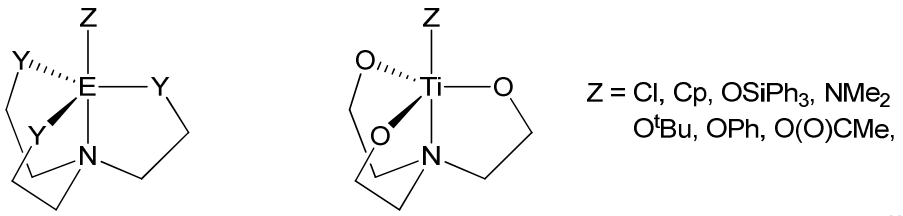

Figure 1.87 Left; General structure of an atrane Right; Titanatranes developed by Verkade[301]

Ten years after the group first reported titanatranes, further development came in widening the scope of these structures, by adjusting the "spacer" and found these to be active for the ROP of *rac*-LA in both solution and melt conditions[284]. A first for titanatranes to contain different ring sizes, which are demonstrated to influence the activity and control in bulk polymerisation, with increasing number of 5-membered rings there is a correlation to increasing activity, conversion after 24 hrs ranges from 68 % up to 96 %, and polydispersity index, 1.43 to 1.97. This is attributed to transesterification which leads to bimodal molecular weight distributions, a shoulder or side tail observed in the GPC trace.

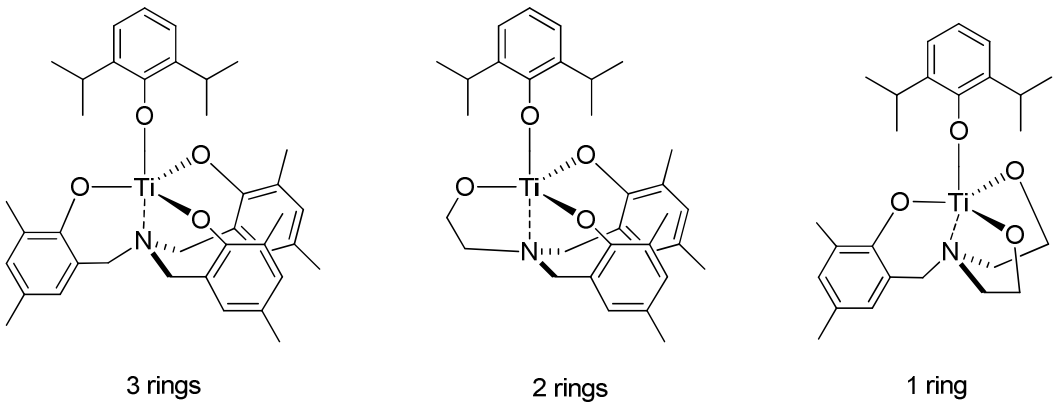

Figure 1.88. Titanatranes with decreasing number of 5-membered rings.

No. rings	Yield (%)	M_w	M_n	PDI
3	69	29,300	19,400	1.43
2	79	30,700	18,70	1.50
1	91	30,800	20,000	1.56
0	99	44,500	25,400	1.75

Table 1.18. Summarised results for the ROP of *rac*-LA with titanatranes of different ring numbers

Further developments saw the preparation of titanatranes but from $TiCl_x(O^iPr)_{(4-x)}$, because the ideal criteria for developing a catalyst had two conditions, firstly there had to be an alkoxide, because they have been proven to be the initiator of choice. The second condition was that the initiating alkoxide group should dissociate with relative ease from the metal centre in the beginning of the polymerisation, such that it could initiate LA polymerisation acting as an end group and therefore controlling the molecular weight. The *trans* Ti-N bond in alkoxy titanatranes could possibly labialise the *trans* axial OR bond, and therefore well suited.

Under solvent free conditions, as the number of chloro groups increases and isopropoxides decrease, a general trend in increasing molecular weight and narrowing of the PDI is observed. This decrease in PDI as x increases, (in $TiCl_x(O^iPr)_{4-x}$) was also observed during solution polymerisation and so greater control is assumed[289]. This could be attributed to the chloro titanium alkoxides which allow only one isopropoxide group to dissociate. For the polymeric material produced a heterotactic bias was demonstrated.

Salen ligands complexed with Al have been extensively studied, as previously discussed. Gibson et al. undertook a detailed study "drawing" on parallel investigations with such Al systems[290]. Various salen ligands, Figure 1.89, were prepared by established reaction of the desired salicylaldehyde with either 1,2-ethylenediamine of (1*R*,2*R*)-diaminocyclohexane, this choice in diamine back bone would later display the importance to activity, stereocontrol and polymerisation control.

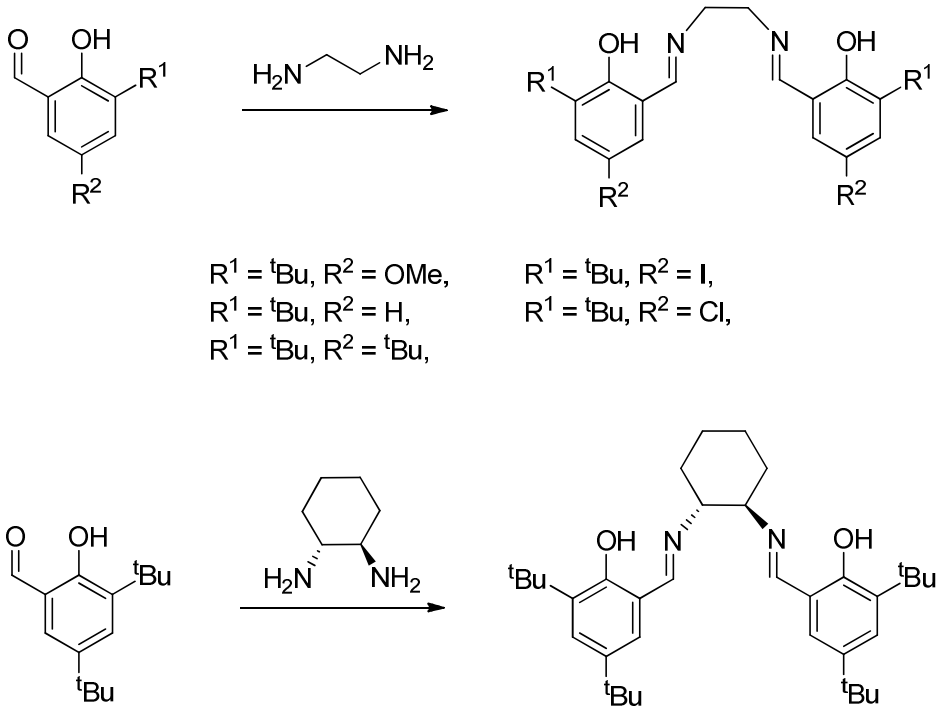

Figure 1.89. Salen ligands prepared by Gibson et al[290].

Reaction with titanium(IV) isopropoxide yielded complexes of a *trans*-planar geometry for 1,2-ethyldiamine whereas a β-*cis* geometry is adopted for *RR*-cyclo complexes. For symmetric tetradentate ligands like Gibson's, three geometries are possible as the ligand "wraps" around the metal. This difference was believed to lead to the varying activity of the cyclo complex, 57 % conversion after 24 hrs in solution at 70 °C compared with 66 - 97 %. All polymeric samples prepared had narrow PDI's, 1.11-1.21 with M_n values demonstrating that one PLA chain grows from each titanium centre, reflecting the sterically busy metal coordination sphere from *ortho*-tert-butyl groups on the phenoxy units.

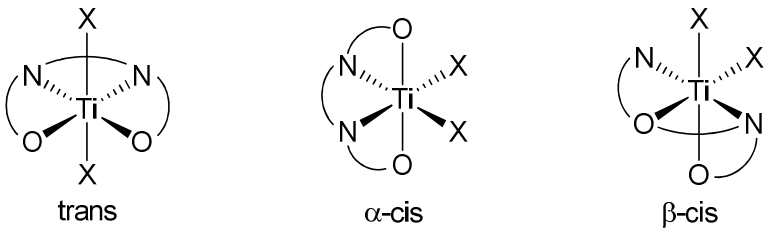

Figure 1.90. The three possibily ligand configurations around the titanium metal

Kinetic investigations confirm that the rate of propagation are comparable with analogous aluminium complexes, [^{t}Bu-salen-^{t}Bu]Ti(O^iPr)$_2$ for example has a k_{app} of 2.59 ×10^{-5} s^{-1}, whereas [^{t}Bu-salen-^{t}Bu]AlMe/$PhCH_2OH$ system k_{app} of 0.13

$\times 10^{-5}$ s^{-1} which is an order in magnitude larger[302] but still slower than Mg, Zn, Y systems. Variation of the substituents around the phenoxy rings showed, electron-withdrawing groups in the para position reduce the activity of the initiator. When R_2 = OMe k_{app} = 6.17 $\times 10^{-5}$ but when R_2 = Cl, k_{app} = 2.16 $\times 10^{-5}$. This is quite a contrast compared to Al(salen) initiators, where halides in the *para* position lead to greatly enhanced activity[302,303] which as of yet has been unexplained.

Kim[304] reported chiral tridentate Schiff base titanium complexes, Figure 1.91, with good activity but no stereocontrol was demonstrated, however bidentate chiral Schiff bases that were investigated with titanium and zirconium by Davidson et al.[305,306], extending the scope of N,O- chelating ligands, did demonstrate a heterotactic bias.

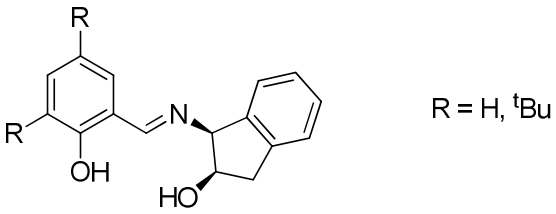

Figure 1.91. Tridentate chiral schiff bases prepared by Kim et al.

R, *S* and *rac*- methylbenzylamine were added to different salicylaldehydes, affording the chiral ligand with X-ray diffraction confirming the chiral centre, with the intramolecular OH---N hydrogen bond determining conformation. Desired complexes were prepared by reacting ligands with Ti or Zr(IV) alkoxides, and all were six-coordinate, *pseudo*-octahedral complexes with α-*cis* geometry. The N,O-chelation gives rise to Δ and Λ chirality at the metal centre, however only one diastereomer is observed in the solid state. Previous to this study it was reported that two diastereomers are observed in solution NMR for the (*R*-**1**)Ti(O^iPr)$_2$, Figure 1.92, and related complexes. A fluxional process on the NMR timescale, isopropoxide and Schiff base ligand peaks are broad. Further investigation of solution dynamics revealed a number of diastereomers.

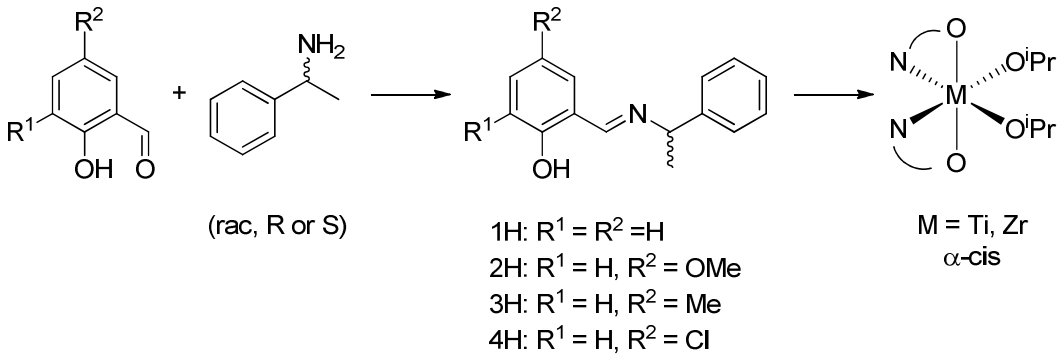

Figure 1.92. Preparation of chiral Schiff base complexes by Davidson

The titanium Schiff base complexes were inactive for ROP LA at 80 °C in toluene, while good activity was observed for the zirconium counterparts, supposedly irrespective of ligand. 35 - 43 % conversion was achieved after 2 hrs at 80 °C and 45 - 69 % conversion at 20 °C for 24 hrs. GPC analysis confirmed good control, PDI 1.08-1.23, however MALDI ToF revealed that transesterification was occurring to a small degree. Stereocontrol of the resulting polymer was good with analysis of the methine region of the HNDNMR spectra revealing moderate heterotactic bias, $P_r \sim 0.7$. Like with other studies, lowering the temperature improved P_r and eliminated cyclic by-products. Solvent free polymerisation saw titanium initiation being a possibility, however no selectivity was observed and zirconium initiators were less controlled, PDI 1.10-2.45, conversion after 30 mins 80 - 97 %.

Recently Kol[307] et al. published work, which came out of their interest of -ONNO- tertadentate ligands, of N,O- chelating, half ligand, bis(aniline-phenolate) complexes of Titanium, hafnium, and zirconium. These complexes, exhibit a *cis*-N/*trans*-O binding of the ligand, similar geometries observed by Davidson and other reported salen complexes. Five stereoisomers are possible, and again with low temperature NMR (-30 °C) confirming the fluxional complex undergoing a facile interconversion of two C_2 symmetric enantiomers. Further reductions in temperature increased "complication". Polymerisation of *rac*-LA at 130 °C in the melt resulted in PLA with a M_n value half of what was expected, suggesting a pair of growing polymer chains per metal centre. Zirconium and Hafnium were more active than Titanium, PDI ranging from1.10-1.80 indicating some backbiting, and a heterotactic bias which improves upon lower temperature polymerisation.

1.2.11. **Tin Initiators**

Straightforward and simple tin containing catalysts for the ring opening polymerisation of lactide are present in the literature, Sn(II) carboxylates and Sn(IV) dialkyl dialkoxide, and indeed tin octanoate still dominates as the industrially accepted initiator[308]. Gibson et al. prepared a range of elegant Sn(II) complexes with β-diketiminate ligands, Figure 1.93. Polymerisation of *rac*-LA at ambient temperatures in CH_2Cl_2 gives high levels of conversion at a catalyst loading of 1 mol %, and complete conversion to PLA after 96 hours. Elevating the temperature to 60 °C and using a more suitable solvent (toluene) achieved 85 % conversion after 4 hours with heterotactic fortification[309]. The drop in activity and selectivity, in comparison to its Zinc cousin, is attributed to the lower electrophilicity of tin. The living character is confirmed by the linear correlation between increasing M_n with decreasing catalyst loading[310].

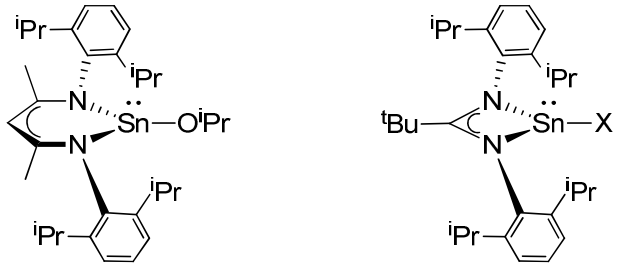

Figure 1.93. Sn(II) complexes prepared by Gibson et al.; Left, β-diketiminate complex, Right, tert-butylamidinate complex

Heterotactic enrichment was also reported more recently when Gibson et al. used tert-butylamidinate ligands[311], Figure 1.93. As before, the reactions were well controlled with narrow PDI's and M_n being close to expect. These complexes did exhibit greater activity, obtaining complete conversion in 37.5 % of the time required for the β-diketiminate ligands at 60 °C, when X was an isopropanol. When X was NMe_2 or $N(SiMe_3)_2$ reaction times were 3 and 4 hours respectively[311].

Schiff bases have also been employed for tin complexes by Gibson et al[312]. These iminophenols were trailed against the polymerisation of *rac*-LA. MALDI-ToF analysis revealed that the PLA chains prepared bore Me_2N end groups, resulting from the reversible migration within the ligand of the -NMe_2

group and as such initiate polymerisation. Treatment of the primary ligand with 1,1-diphenylethanol afforded inactive tin complexes.

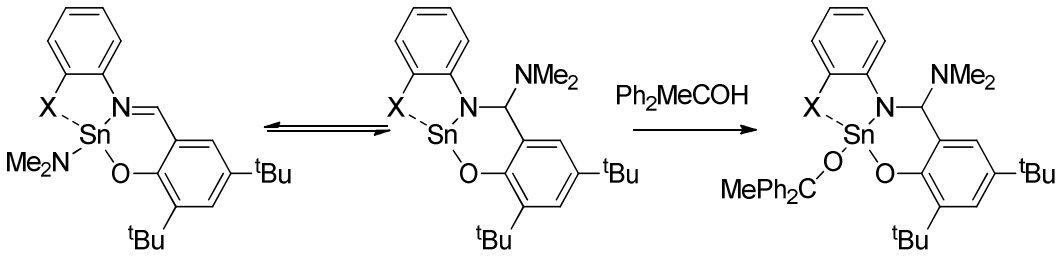

Figure 1.94. Tin complexes employed by Gibson, displaying the interchangeable position of the -NMe_2 group

Lastly, Fauré et al.[313] have reported an "almost" stannatrane, tin containing atrane, with a pair of five-membered rings. These were utilised in the bulk copolymerisation of *rac*-LA and glycolide, at 140 °C achieving 90 % conversion after just 20 mins. High molecular weights were achieved with reasonable PDI, (M_n 85,200 g mol^{-1}, PDI 1.9).

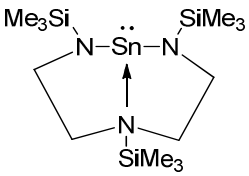

Figure 1.95. Diamindoamine ligands prepared by Fauré

1.2.12. **Bismuth Initiators**

Impressive results were obtained by Pepto-Bismol as an initiator for the ROP of LA, comparable activity to tin(II) octanoate, during a study by Chisholm et al.[314], of over the counter antacides and dietary supplements. The active ingredient in this drug, bismuth subsalicylate, was identified as the initiating species, although not mononuclear as such resulting in a bimodal molecular weight distribution. Polymerisation with the pure compound afforded PLA with good PDI, 1.35-1.41 and a significant heterotactic enhancement, P_r 0.78-0.82. The similarity between Bi(III) alkanoates and Sn(II) octanoates was also noted by Kricheldorf et al[315].

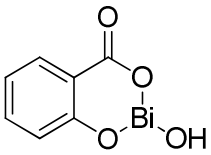

Figure 1.96. Bismuth subsalicylate, the active ingredient in Pepto-Bismol

1.2.13. **References**

(1) Mannschreck, A.; Kiesswetter, R.; von Angerer, E. *J. Chem. Educ.* **2007**, *84*, 2012.
(2) Rouhi, M. *Chemical & Engineering News Archive* **2005**, *83*, 122.
(3) Support®, C. P.; Vol. 2013.
(4) Shah, J. H.; Swartz, G. M.; Papathanassiu, A. E.; Treston, A. M.; Fogler, W. E.; Madsen, J. W.; Green, S. J. *J. Med. Chem.* **1999**, *42*, 3014.
(5) Rajkumar, S. V.; Blood, E.; Vesole, D.; Fonseca, R.; Greipp, P. R. *Journal of Clinical Oncology* **2006**, *24*, 431.
(6) Byrne, J. C.; Downes, M. R.; O'Donoghue, N.; O'Keane, C.; O'Neill, A.; Fan, Y.; Fitzpatrick, J. M.; Dunn, M. J.; Watson, R. W. G. *J. Proteome Res.* **2008**, *8*, 942.
(7) Chowdhury, G.; Murayama, N.; Okada, Y.; Uno, Y.; Shimizu, M.; Shibata, N.; Guengerich, F. P.; Yamazaki, H. *Chem. Res. Toxicol.* **2010**, *23*, 1018.
(8) Cornely, K.; Bennett, N. *J. Chem. Educ.* **2001**, *78*, 759.
(9) Lepper, E. R.; Ng, S. S. W.; Gütschow, M.; Weiss, M.; Hauschildt, S.; Hecker, T. K.; Luzzio, F. A.; Eger, K.; Figg, W. D. *J. Med. Chem.* **2004**, *47*, 2219.
(10) Muntané, J. *Chem. Res. Toxicol.* **2011**, *24*, 1610.
(11) De Camp, W. H. *Chirality* **1989**, *1*, 2.
(12) Thayer, A. M. *Chemical & Engineering News Archive* **2007**, *85*, 11.
(13) Groysman, S.; Goldberg, I.; Kol, M.; Goldschmidt, Z. *Organometallics* **2003**, *22*, 3793.
(14) Sundram, U. N.; Albizati, K. F. *The Journal of Organic Chemistry* **1991**, *56*, 2622.
(15) Marinetti, A.; Buzin, F.-X.; Ricard, L. *The Journal of Organic Chemistry* **1997**, *62*, 297.
(16) Amberg, M.; Bergsträsser, U.; Stapf, G.; Hartung, J. *The Journal of Organic Chemistry* **2002**, *73*, 3907.
(17) Blaser, H. U. *Chem. Rev.* **2002**, *92*, 935.
(18) Hollingsworth Rawle, I.; Wang, G. In *Carbohydrate Synthons in Natural Products Chemistry*; American Chemical Society: 2002; Vol. 841, p 85.
(19) Khan, F. A.; Sudheer, C. *Org. Lett.* **2002**, *10*, 3029.
(20) Tanaka, K.; Takeishi, K.; Noguchi, K. *J. Am. Chem. Soc.* **2002**, *128*, 4586.
(21) Lo, H.-J.; Chang, Y.-K.; Yan, T.-H. *Org. Lett.* **2012**, *14*, 5896.
(22) Mori, K. *Tetrahedron* **1975**, *31*, 3011.
(23) Evans, D. A.; Ennis, M. D.; Mathre, D. J. *J. Am. Chem. Soc.* **1982**, *104*, 1737.
(24) Evans, D. A.; Clark, J. S.; Metternich, R.; Novack, V. J.; Sheppard, G. S. *J. Am. Chem. Soc.* **1990**, *112*, 866.
(25) Meyers, A. I.; Knaus, G.; Kamata, K.; Ford, M. E. *J. Am. Chem. Soc.* **1976**, *98*, 567.
(26) Kirsch, S. F. *Angewandte Chemie International Edition* **2009**, *48*, 2450.
(27) Akamatsu, A.; Izumi, Y.; Akabori, S. *Bull. Chem. Soc. Jpn.* **1961**, *34*, 1067.
(28) Vankelecom, I. F. J.; Jacobs, P. A. In *Chiral Catalyst Immobilization and Recycling*; Wiley-VCH Verlag GmbH: 2007, p 19.
(29) B. De, B.; Lohray, B. B.; Sivaram, S.; Dhal, P. K. *Tetrahedron: Asymmetry* **1995**, *6*, 2105.
(30) Gao, H.; Angelici, R. J. *J. Mol. Catal. A: Chem.* **1999**, *149*, 63.
(31) Schmid, L.; Kröcher, O.; Köppel, R. A.; Baiker, A. *Microporous Mesoporous Mater.* **2000**, *35–36*, 181.
(32) Rohr, M.; Günther, M.; Jutz, F.; Grunwaldt, J.-D.; Emerich, H.; Beek, W. v.; Baiker, A. *Applied Catalysis A: General* **2005**, *296*, 238.
(33) Yan, L.; Ding, Y. J.; Zhu, H. J.; Xiong, J. M.; Wang, T.; Pan, Z. D.; Lin, L. W. *J. Mol. Catal. A: Chem.* **2005**, *234*, 1.
(34) Cai, M.; Sha, J.; Xu, Q. *J. Mol. Catal. A: Chem.* **2007**, *268*, 82.

(35) Xiang, S.; Zhang, Y.; Xin, Q.; Li, C. *Chem. Commun.* **2002**, *0*, 2696.
(36) Kureshy, R. I.; Ahmad, I.; Khan, N.-u. H.; Abdi, S. H. R.; Pathak, K.; Jasra, R. V. *Tetrahedron: Asymmetry* **2005**, *16*, 3562.
(37) Jones, M. D.; Raja, R.; Thomas, J. M.; Johnson, B. F. G.; Lewis, D. W.; Rouzaud, J.; Harris, K. D. M. *Angewandte Chemie International Edition* **2003**, *42*, 4326.
(38) Glasnov, T. N.; Findenig, S.; Kappe, C. O. *Chemistry – A European Journal* **2009**, *15*, 1001.
(39) Wegner, J.; Ceylan, S.; Kirschning, A. *Chem. Commun.* **2011**, *47*, 4583.
(40) Park, Y.-M.; Lee, D.-W.; Kim, D.-K.; Lee, J.-S.; Lee, K.-Y. *Catal. Today* **2008**, *131*, 238.
(41) Richardson, J. T.; Remue, D.; Hung, J. K. *Applied Catalysis A: General* **2003**, *250*, 319.
(42) Jas, G.; Kirschning, A. *Chemistry – A European Journal* **2003**, *9*, 5708.
(43) Hodge, P. *Curr. Opin. Chem. Biol.* **2003**, *7*, 362.
(44) Kirschning, A.; Solodenko, W.; Mennecke, K. *Chemistry – A European Journal* **2006**, *12*, 5972.
(45) Rechavi, D.; Albela, B.; Bonneviot, L.; Lemaire, M. *Tetrahedron* **2005**, *61*, 6976.
(46) Lee, J.-M.; Kim, J.; Shin, Y.; Yeom, C.-E.; Lee, J. E.; Hyeon, T.; Moon Kim, B. *Tetrahedron: Asymmetry* **2010**, *21*, 285.
(47) Pathak, K.; Bhatt, A. P.; Abdi, S. H. R.; Kureshy, R. I.; Khan, N.-u. H.; Ahmad, I.; Jasra, R. V. *Tetrahedron: Asymmetry* **2006**, *17*, 1506.
(48) Cazes, J. *Encyclopedia of Chromatography*; CRC Press, 2009.
(49) Peerlings, H. W. I.; Meijer, E. W. *Chemistry – A European Journal* **1997**, *3*, 1563.
(50) Lee, H. M.; Kim, S.-W.; Hyeon, T.; Kim, B. M. *Tetrahedron: Asymmetry* **2001**, *12*, 1537.
(51) Alvarez, R.; Hourdin, M.-A.; Cavé, C.; d'Angelo, J.; Chaminade, P. *Tetrahedron Lett.* **1999**, *40*, 7091.
(52) Minutolo, F.; Pini, D.; Petri, A.; Salvadori, P. *Tetrahedron: Asymmetry* **1996**, *7*, 2293.
(53) Nakahata, M.; Imaida, M.; Ozaki, H.; Harada, T.; Tai, A. *Bull. Chem. Soc. Jpn.* **1982**, *55*, 2186.
(54) Blaser, H.-U.; Boyer, S. K.; Pittelkow, U. *Tetrahedron: Asymmetry* **1991**, *2*, 721.
(55) Herold, P.; Indolese, A. F.; Studer, M.; Jalett, H. P.; Siegrist, U.; Blaser, H. U. *Tetrahedron* **2000**, *56*, 6497.
(56) Blaser, H.-U.; Jalett, H.-P.; Spindler, F. *J. Mol. Catal. A: Chem.* **1996**, *107*, 85.
(57) Cederbaum, F.; Lamberth, C.; Malan, C.; Naud, F.; Spindler, F.; Studer, M.; Blaser, H.-U. *Adv. Synth. Catal.* **2004**, *346*, 842.
(58) Annis, D. A.; Jacobsen, E. N. *J. Am. Chem. Soc.* **1999**, *121*, 4147.
(59) Fan, Q.-H.; Li, Y.-M.; Chan, A. S. C. *Chem. Rev.* **2002**, *102*, 3385.
(60) Henry, L. *Bull. Soc. Chim. Fr.* **1895**, *13*.
(61) Henry, L. *C. R. Acad. Sci. Ser. C.* **1895**.
(62) Luzzio, F. A. *Tetrahedron* **2001**, *57*, 915.
(63) Rosini, G. In *Comprehensive Organic Synthesis*; Editor-in-Chief: Barry, M. T., Ian, F., Eds.; Pergamon: Oxford, 1991, p 321.
(64) Arai, T.; Watanabe, M.; Yanagisawa, A. *Org. Lett.* **2007**, *9*, 3595.
(65) Palomo, C.; Oiarbide, M.; Laso, A. *Eur. J. Org. Chem.* **2007**, *2007*, 2561.
(66) Evans, D. A.; Seidel, D.; Rueping, M.; Lam, H. W.; Shaw, J. T.; Downey, C. W. *J. Am. Chem. Soc.* **2003**, *125*, 12692.
(67) Zhang, G.; Yashima, E.; Woggon, W.-D. *Adv. Synth. Catal.* **2009**, *351*, 1255.
(68) Lecea, B.; Arrieta, A.; Morao, I.; Cossío, F. P. *Chemistry – A European Journal* **1997**, *3*, 20.
(69) Solladie-Cavallo, A.; Khiar, N. *The Journal of Organic Chemistry* **1990**, *55*, 4750.

(70) Kudyba, I.; Raczko, J.; Jurczak, J. *The Journal of Organic Chemistry* **2004**, *69*, 2844.
(71) Soengas, R. G.; Estévez, J. C.; Estévez, R. J. *Org. Lett.* **2003**, *5*, 4457.
(72) Hanessian, S.; Devasthale, P. V. *Tetrahedron Lett.* **1996**, *37*, 987.
(73) Sasai, H.; Itoh, N.; Suzuki, T.; Shibasaki, M. *Tetrahedron Lett.* **1993**, *34*, 855.
(74) Poupart, M.-A.; Fazal, G.; Goulet, S.; Mar, L. T. *The Journal of Organic Chemistry* **1999**, *64*, 1356.
(75) Ono, N. In *The Nitro Group in Organic Synthesis*; John Wiley & Sons, Inc.: 2002, p 30.
(76) Palomo, C.; Oiarbide, M.; Mielgo, A. *Angewandte Chemie International Edition* **2004**, *43*, 5442.
(77) Shibasaki, M. *Comprehensive Asymmetric Catalysis, Supplement 1*, 2004.
(78) Shibasaki, M. *Comprehensive Asymmetric Catalysis*, 1999.
(79) Sasai, H.; Suzuki, T.; Arai, S.; Arai, T.; Shibasaki, M. *J. Am. Chem. Soc.* **1992**, *114*, 4418.
(80) Arai, T.; Yamada, Y. M. A.; Yamamoto, N.; Sasai, H.; Shibasaki, M. *Chemistry – A European Journal* **1996**, *2*, 1368.
(81) Sasai, H. W., Shizue; Suzuki, Takeyuki; Shibasaki, Masakatsu *Org. Synth.* **2004**, *10*.
(82) Shibasaki, M.; Yoshikawa, N. *Chem. Rev.* **2002**, *102*, 2187.
(83) Shibasaki, M.; Kanai, M.; Funabashi, K. *Chem. Commun.* **2002**, *0*, 1989.
(84) Rowlands, G. J. *Tetrahedron* **2001**, *57*, 1865.
(85) Sasai, H.; Watanabe, S.; Shibasaki, M. *Enantiomer* **1997**, *2*, 267.
(86) Shibasaki, M.; Sasai, H.; Arai, T. *Catalytic asymmetric carbon-carbon bond-forming reaction utilizing rare earth metal complexes*, 1997.
(87) Shibasaki, M.; Matsunaga, S. *Chem. Soc. Rev.* **2006**, *35*, 269.
(88) Chen, Y.; Yekta, S.; Yudin, A. K. *Chem. Rev.* **2003**, *103*, 3155.
(89) Yamamoto, H.; Futatsugi, K. *Angewandte Chemie International Edition* **2005**, *44*, 1924.
(90) Mikami, K.; Terada, M.; Matsuzawa, H. *Angewandte Chemie International Edition* **2002**, *41*, 3554.
(91) Iseki, K.; Oishi, S.; Sasai, H.; Shibasaki, M. *Tetrahedron Lett.* **1996**, *37*, 9081.
(92) Sasai, H.; Tokunaga, T.; Watanabe, S.; Suzuki, T.; Itoh, N.; Shibasaki, M. *The Journal of Organic Chemistry* **1995**, *60*, 7388.
(93) Sasai, H.; Suzuki, T.; Itoh, N.; Shibasaki, M. *Tetrahedron Lett.* **1993**, *34*, 851.
(94) Tosaki, S.-y.; Hara, K.; Gnanadesikan, V.; Morimoto, H.; Harada, S.; Sugita, M.; Yamagiwa, N.; Matsunaga, S.; Shibasaki, M. *J. Am. Chem. Soc.* **2006**, *128*, 11776.
(95) Trost, B. M.; Yeh, V. S. C. *Angewandte Chemie International Edition* **2002**, *41*, 861.
(96) Trost, B. M.; Yeh, V. S. C.; Ito, H.; Bremeyer, N. *Org. Lett.* **2002**, *4*, 2621.
(97) Johnson, J. S.; Evans, D. A. *Acc. Chem. Res.* **2000**, *33*, 325.
(98) Christensen, C.; Juhl, K.; Hazell, R. G.; Jørgensen, K. A. *The Journal of Organic Chemistry* **2002**, *67*, 4875.
(99) Ginotra, S. K.; Singh, V. K. *Org. Biomol. Chem.* **2007**, *5*, 3932.
(100) Gan, C.; Lai, G.; Zhang, Z.; Wang, Z.; Zhou, M.-M. *Tetrahedron: Asymmetry* **2006**, *17*, 725.
(101) Blay, G.; Climent, E.; Fernández, I.; Hernández-Olmos, V.; Pedro, J. R. *Tetrahedron: Asymmetry* **2006**, *17*, 2046.
(102) Maheswaran, H.; Prasanth, K. L.; Krishna, G. G.; Ravikumar, K.; Sridhar, B.; Kantam, M. L. *Chem. Commun.* **2006**, *0*, 4066.
(103) Okamoto, Y.; Urakawa, K.; Yuki, H. *Journal of Polymer Science: Polymer Chemistry Edition* **1981**, *19*, 1385.
(104) Norsikian, S.; Marek, I.; Klein, S.; Poisson, J. F.; Normant, J. F. *Chemistry – A European Journal* **1999**, *5*, 2055.
(105) Lautens, M.; Gajda, C.; Chiu, P. *J. Chem. Soc., Chem. Commun.* **1993**, *0*, 1193.

(106) Klein, S.; Marek, I.; Poisson, J.-F.; Normant, J.-F. *J. Am. Chem. Soc.* **1995**, *117*, 8853.
(107) Trost, B. M.; Dietsch, T. J. *J. Am. Chem. Soc.* **1973**, *95*, 8200.
(108) Kang, J.; Oh Cho, W.; Cho, H.; Geun *Tetrahedron: Asymmetry* **1994**, *5*, 1347.
(109) Togni, A. *Tetrahedron: Asymmetry* **1991**, *2*, 683.
(110) Mimoun, H.; de Saint Laumer, J. Y.; Giannini, L.; Scopelliti, R.; Floriani, C. *J. Am. Chem. Soc.* **1999**, *121*, 6158.
(111) Jana, S.; Sherrington, D. C. *Angewandte Chemie International Edition* **2005**, *44*, 4804.
(112) Zhang, Y.; Yeung, S.-M.; Wu, H.; Heller, D. P.; Wu, C.; Wulff, W. D. *Org. Lett.* **2003**, *5*, 1813.
(113) Rajca, A.; Wang, H.; Bolshov, P.; Rajca, S. *Tetrahedron* **2001**, *57*, 3725.
(114) Smrcina, M.; Lorenc, M.; Hanus, V.; Sedmera, P.; Kocovsky, P. *The Journal of Organic Chemistry* **1992**, *57*, 1917.
(115) Arai, T.; Watanabe, M.; Fujiwara, A.; Yokoyama, N.; Yanagisawa, A. *Angewandte Chemie International Edition* **2006**, *45*, 5978.
(116) Kogami, Y.; Nakajima, T.; Ashizawa, T.; Kezuka, S.; Ikeno, T.; Yamada, T. *Chem. Lett.* **2004**, *33*, 614.
(117) Berkessel, A.; Gröger, H. In *Asymmetric Organocatalysis*; Wiley-VCH Verlag GmbH & Co. KGaA: 2005, p i.
(118) Dalko, P. I.; Moisan, L. *Angewandte Chemie International Edition* **2004**, *43*, 5138.
(119) Choudary, B. M.; Ranganath, K. V. S.; Pal, U.; Kantam, M. L.; Sreedhar, B. *J. Am. Chem. Soc.* **2005**, *127*, 13167.
(120) Kogami, Y.; Nakajima, T.; Ikeno, T.; Yamada, T. *Synthesis* **2004**, *2004*, 1947.
(121) Kowalczyk, R.; Kwiatkowski, P.; Skarżewski, J.; Jurczak, J. *The Journal of Organic Chemistry* **2008**, *74*, 753.
(122) Larrow, J.; Jacobsen, E. In *Organometallics in Process Chemistry*; Springer Berlin Heidelberg: 2004; Vol. 6, p 123.
(123) Larrow, J. F.; Jacobsen, E. N.; Gao, Y.; Hong, Y.; Nie, X.; Zepp, C. M. *The Journal of Organic Chemistry* **1994**, *59*, 1939.
(124) Larrow, J. F.; Jacobsen, E. N. *Org. Synth.* **1998**, *75*, 1.
(125) Zulauf, A.; Mellah, M.; Guillot, R.; Schulz, E. *Eur. J. Org. Chem.* **2008**, *2008*, 2118.
(126) Zulauf, A. s.; Mellah, M.; Schulz, E. *The Journal of Organic Chemistry* **2009**, *74*, 2242.
(127) Kingsborough, R. P.; Swager, T. M. *Advanced Materials* **1998**, *10*, 1100.
(128) Kiyooka, S.-i.; Tsutsui, T.; Maeda, H.; Kaneko, Y.; Isobe, K. *Tetrahedron Lett.* **1995**, *36*, 6531.
(129) Blay, G.; Hernandez-Olmos, V.; Pedro, J. R. *Chem. Commun.* **2008**, *0*, 4840.
(130) Li, H.; Wang, B.; Deng, L. *J. Am. Chem. Soc.* **2005**, *128*, 732.
(131) Okino, T.; Nakamura, S.; Furukawa, T.; Takemoto, Y. *Org. Lett.* **2004**, *6*, 625.
(132) Yoon, T. P.; Jacobsen, E. N. *Angew. Chem.* **2005**, *117*, 470.
(133) Chinchilla, R.; Nájera, C.; Sánchez-Agulló, P. *Tetrahedron: Asymmetry* **1994**, *5*, 1393.
(134) Sohtome, Y.; Hashimoto, Y.; Nagasawa, K. *Adv. Synth. Catal.* **2005**, *347*, 1643.
(135) Allingham, M. T.; Howard-Jones, A.; Murphy, P. J.; Thomas, D. A.; Caulkett, P. W. R. *Tetrahedron Lett.* **2003**, *44*, 8677.
(136) Ma, D.; Pan, Q.; Han, F. *Tetrahedron Lett.* **2002**, *43*, 9401.
(137) Westermann, B. *Angewandte Chemie International Edition* **2003**, *42*, 151.
(138) Nugent, B. M.; Yoder, R. A.; Johnston, J. N. *J. Am. Chem. Soc.* **2004**, *126*, 3418.
(139) Knowles, W. S.; Sabacky, M. J. *Chemical Communications (London)* **1968**, *0*, 1445.
(140) Knowles, W. S. *Angewandte Chemie International Edition* **2002**, *41*, 1998.

(141) Osborn, J. A.; Wilkinson, G.; Young, J. F. *Chemical Communications (London)* **1965**, *0*, 17.
(142) Osborn, J. A.; Jardine, F. H.; Young, J. F.; Wilkinson, G. *Journal of the Chemical Society A: Inorganic, Physical, Theoretical* **1966**, *0*, 1711.
(143) Barbeau. A *CMAJ* **1969**, *101*, 59.
(144) Noyori, R. *Chem. Commun.* **2005**, *0*, 1807.
(145) Brown, K. J.; Berry, M. S.; Waterman, K. C.; Lingenfelter, D.; Murdoch, J. R. *J. Am. Chem. Soc.* **1984**, *106*, 4717.
(146) Takaya, H.; Mashima, K.; Koyano, K.; Yagi, M.; Kumobayashi, H.; Taketomi, T.; Akutagawa, S.; Noyori, R. *The Journal of Organic Chemistry* **1986**, *51*, 629.
(147) Cai, D., Payack, J. F., Bender, D. R., Hughes, Verhoeven, T. R., Reider, P. J. *Org. Synth.* **1999**, 6.
(148) Miyashita, A.; Yasuda, A.; Takaya, H.; Toriumi, K.; Ito, T.; Souchi, T.; Noyori, R. *J. Am. Chem. Soc.* **1980**, *102*, 7932.
(149) Toriumi, K.; Ito, T.; Takaya, H.; Souchi, T.; Noyori, R. *Acta Crystallographica Section B* **1982**, *38*, 807.
(150) Ohta, T.; Takaya, H.; Noyori, R. *Inorg. Chem.* **1988**, *27*, 566.
(151) Akutagawa, S. *Applied Catalysis A: General* **1995**, *128*, 171.
(152) Kitamura, M.; Kasahara, I.; Manabe, K.; Noyori, R.; Takaya, H. *The Journal of Organic Chemistry* **1988**, *53*, 708.
(153) Ohta, T.; Takaya, H.; Kitamura, M.; Nagai, K.; Noyori, R. *The Journal of Organic Chemistry* **1987**, *52*, 3174.
(154) Kitamura, M.; Tokunaga, M.; Ohkuma, T.; Noyori, R. *Tetrahedron Lett.* **1991**, *32*, 4163.
(155) Dang, T. P.; Kagan, H. B. *Journal of the Chemical Society D: Chemical Communications* **1971**, *0*, 481.
(156) Kagan, H. B.; Dang Tuan, P. *J. Am. Chem. Soc.* **1972**, *94*, 6429.
(157) Tang, W.; Zhang, X. *Chem. Rev.* **2003**, *103*, 3029.
(158) Minnaard, A. J.; Feringa, B. L.; Lefort, L.; de Vries, J. G. *Acc. Chem. Res.* **2007**, *40*, 1267.
(159) Inc, I. 2013.
(160) Hartley, F. R. *Volume 11: Chemistry of the Platinum Group Metals: Recent Developments, 1st Edition*; Elsevier Science, 1991.
(161) *Org. Process Res. Dev.* **2001**, *5*, 669.
(162) In *Handbook of Asymmetric Heterogeneous Catalysis*; Wiley-VCH Verlag GmbH & Co. KGaA: 2008, p I.
(163) Abe, H.; Amii, H.; Uneyama, K. *Org. Lett.* **2001**, *3*, 313.
(164) Chen, M.-W.; Duan, Y.; Chen, Q.-A.; Wang, D.-S.; Yu, C.-B.; Zhou, Y.-G. *Org. Lett.* **2010**, *12*, 5075.
(165) Tu, T.; Zhou, Y.-G.; Hou, X.-L.; Dai, L.-X.; Dong, X.-C.; Yu, Y.-H.; Sun, J. *Organometallics* **2003**, *22*, 1255.
(166) Wang, Y.-Q.; Lu, S.-M.; Zhou, Y.-G. *Org. Lett.* **2005**, *7*, 3235.
(167) Wang, Y.-Q.; Lu, S.-M.; Zhou, Y.-G. *The Journal of Organic Chemistry* **2007**, *72*, 3729.
(168) Wang, Y.-Q.; Yu, C.-B.; Wang, D.-W.; Wang, X.-B.; Zhou, Y.-G. *Org. Lett.* **2008**, *10*, 2071.
(169) Yu, C.-B.; Wang, D.-W.; Zhou, Y.-G. *The Journal of Organic Chemistry* **2009**, *74*, 5633.
(170) Wang, D.-S.; Chen, Q.-A.; Li, W.; Yu, C.-B.; Zhou, Y.-G.; Zhang, X. *J. Am. Chem. Soc.* **2010**, *132*, 8909.
(171) Wang, D.-S.; Ye, Z.-S.; Chen, Q.-A.; Zhou, Y.-G.; Yu, C.-B.; Fan, H.-J.; Duan, Y. *J. Am. Chem. Soc.* **2011**, *133*, 8866.
(172) Tsuchiya, Y.; Hamashima, Y.; Sodeoka, M. *Org. Lett.* **2006**, *8*, 4851.
(173) Miyaura, N.; Suzuki, A. *Chem. Rev.* **1995**, *95*, 2457.

(174) Muci, A.; Buchwald, S. In *Cross-Coupling Reactions*; Miyaura, N., Ed.; Springer Berlin Heidelberg: 2002; Vol. 219, p 131.
(175) Negishi, E.-i.; Anastasia, L. *Chem. Rev.* **2003**, *103*, 1979.
(176) Tietze, L. F.; Ila, H.; Bell, H. P. *Chem. Rev.* **2004**, *104*, 3453.
(177) Beccalli, E. M.; Broggini, G.; Martinelli, M.; Sottocornola, S. *Chem. Rev.* **2007**, *107*, 5318.
(178) Lyons, T. W.; Sanford, M. S. *Chem. Rev.* **2010**, *110*, 1147.
(179) Akabori, S.; Sakurai, S.; Izumi, Y.; Fujii, Y. *Nature* **1956**, *178*, 323.
(180) Sajiki, H.; Ikawa, T.; Yamada, H.; Tsubouchi, K.; Hirota, K. *Tetrahedron Lett.* **2003**, *44*, 171.
(181) Togni, A.; Venanzi, L. M. *Angewandte Chemie International Edition in English* **1994**, *33*, 497.
(182) Cullen, W. R.; Einstein, F. W. B.; Huang, C.-H.; Willis, A. C.; Yeh, E. S. *J. Am. Chem. Soc.* **1980**, *102*, 988.
(183) Cullen, W. R.; Woollins, J. D. *Can. J. Chem.* **1982**, *60*, 1793.
(184) Boronat, M. r.; Corma, A.; González-Arellano, C.; Iglesias, M.; Sánchez, F. l. *Organometallics* **2009**, *29*, 134.
(185) Pfaltz, A. *Acc. Chem. Res.* **1993**, *26*, 339.
(186) Gladiali, S.; Pinna, L.; Delogu, G.; De Martin, S.; Zassinovich, G.; Mestroni, G. *Tetrahedron: Asymmetry* **1990**, *1*, 635.
(187) Pinel, C.; Gendreau-Diaz, N.; Bréhéret, A.; Lemaire, M. *J. Mol. Catal. A: Chem.* **1996**, *112*, L157.
(188) Thomas, J. M.; Maschmeyer, T.; Johnson, B. F. G.; Shephard, D. S. *J. Mol. Catal. A: Chem.* **1999**, *141*, 139.
(189) Thomas, J. M.; Johnson, B. F. G.; Raja, R.; Sankar, G.; Midgley, P. A. *Acc. Chem. Res.* **2002**, *36*, 20.
(190) Thomas, J. M. *Angewandte Chemie International Edition* **1999**, *38*, 3588.
(191) Dechy-Cabaret, O.; Martin-Vaca, B.; Bourissou, D. *Chem. Rev.* **2004**, *104*, 6147.
(192) Gupta, A. P.; Kumar, V. *Eur. Polym. J.* **2007**, *43*, 4053.
(193) Jacobsen, S.; Fritz, H. G.; Degée, P.; Dubois, P.; Jérôme, R. *Polymer Engineering & Science* **1999**, *39*, 1311.
(194) Mecking, S. *Angewandte Chemie International Edition* **2004**, *43*, 1078.
(195) Carothers, W. H.; Dorough, G. L.; Natta, F. J. v. *J. Am. Chem. Soc.* **1932**, *54*, 761.
(196) Chen, G.; Ushida, T.; Tateishi, T. *Macromol. Biosci.* **2002**, *2*, 67.
(197) Sessolo, M.; Bolink, H. J. *Advanced Materials* **2011**, *23*, 1829.
(198) Södergård, A.; Stolt, M. In *Poly(Lactic Acid)*; John Wiley & Sons, Inc.: 2010, p 27.
(199) Duda, A.; Penczek, S. *Macromolecules* **1990**, *23*, 1636.
(200) van Hummel, G. J.; Harkema, S.; Kohn, F. E.; Feijen, J. *Acta Crystallographica Section B* **1982**, *38*, 1679.
(201) Degée, P.; Dubois, P.; Jérŏme, R.; Jacobsen, S.; Fritz, H.-G. *Macromol. Symp.* **1999**, *144*, 289.
(202) Vol. 2013.
(203) Kricheldorf, H. R.; Damrau, D.-O. *Macromol. Chem. Phys.* **1997**, *198*, 1753.
(204) Kreiser-Saunders, I.; Kricheldorf, H. R. *Macromol. Chem. Phys.* **1998**, *199*, 1081.
(205) Dittrich, V. W.; Schulz, R. C. *Die Angewandte Makromolekulare Chemie* **1971**, *15*, 109.
(206) Kricheldorf, H. R.; Berl, M.; Scharnagl, N. *Macromolecules* **1988**, *21*, 286.
(207) Dubois, P.; Jacobs, C.; Jerome, R.; Teyssie, P. *Macromolecules* **1991**, *24*, 2266.
(208) Degée, P.; Dubois, P.; Jérŏme, R. *Macromol. Symp.* **1997**, *123*, 67.
(209) Eguiburu, J. L.; Fernandez-Berridi, M. J.; Cossío, F. P.; Román, J. S. *Macromolecules* **1999**, *32*, 8252.

(210) von Schenck, H.; Ryner, M.; Albertsson, A.-C.; Svensson, M. *Macromolecules* **2002**, *35*, 1556.
(211) Marshall, E. L.; Gibson, V. C.; Rzepa, H. S. *J. Am. Chem. Soc.* **2005**, *127*, 6048.
(212) Baran, J.; Duda, A.; Kowalski, A.; Szymanski, R.; Penczek, S. *Macromol. Symp.* **1997**, *123*, 93.
(213) Penczek, S.; Duda, A.; Szymanski, R. *Macromol. Symp.* **1998**, *132*, 441.
(214) Basko, M.; Bednarek, M. *Reactive and Functional Polymers* **2012**, *72*, 213.
(215) Biela, T.; Duda, A.; Penczek, S. *Macromol. Symp.* **2002**, *183*, 1.
(216) Trathnigg, B. *Prog. Polym. Sci.* **1995**, *20*, 615.
(217) Vert, M. C., F; Leary, J; Christel, P; *Makromol. Chem. Suppl.* **1981**, *5*, 30.
(218) Li, S. M.; Vert, M. *Macromolecules* **1994**, *27*, 3107.
(219) Spassky, N. *Makromolekulare Chemie. Macromolecular Symposia* **1992**, *53*, 367.
(220) Chamberlain, B. M.; Cheng, M.; Moore, D. R.; Ovitt, T. M.; Lobkovsky, E. B.; Coates, G. W. *J. Am. Chem. Soc.* **2001**, *123*, 3229.
(221) Aida, T.; Inoue, S. *Macromolecules* **1981**, *14*, 1166.
(222) Aida, T.; Inoue, S. *Macromolecules* **1981**, *14*, 1162.
(223) Shimasaki, K.; Aida, T.; Inoue, S. *Macromolecules* **1987**, *20*, 3076.
(224) Endo, M.; Aida, T.; Inoue, S. *Macromolecules* **1987**, *20*, 2982.
(225) Sugimoto, H.; Kawamura, C.; Kuroki, M.; Aida, T.; Inoue, S. *Macromolecules* **1994**, *27*, 2013.
(226) Spassky, N.; Leborgne, A.; Momtaz, A.; Sepulchre, M. *Journal of Polymer Science: Polymer Chemistry Edition* **1980**, *18*, 3089.
(227) Whitesell, J. K. *Chem. Rev.* **1989**, *89*, 1581.
(228) Wisniewski, M.; Borgne, A. L.; Spassky, N. *Macromol. Chem. Phys.* **1997**, *198*, 1227.
(229) Spassky, N. L., A. ; Sepulchre, M. *Pure. Appl. Chem.* **1981**, *53*, 1735.
(230) Radano, C. P.; Baker, G. L.; Smith, M. R. *J. Am. Chem. Soc.* **2000**, *122*, 1552.
(231) Nomura, N.; Ishii, R.; Akakura, M.; Aoi, K. *J. Am. Chem. Soc.* **2002**, *124*, 5938.
(232) Ovitt, T. M.; Coates, G. W. *J. Am. Chem. Soc.* **2002**, *124*, 1316.
(233) Zhong, Z.; Dijkstra, P. J.; Feijen, J. *Angewandte Chemie International Edition* **2002**, *41*, 4510.
(234) Zhong, Z.; Dijkstra, P. J.; Feijen, J. *J. Am. Chem. Soc.* **2003**, *125*, 11291.
(235) Hormnirun, P.; Marshall, E. L.; Gibson, V. C.; White, A. J. P.; Williams, D. J. *J. Am. Chem. Soc.* **2004**, *126*, 2688.
(236) Xie, W.; Chen, D.; Fan, X.; Li, J.; Wang, P. G.; Cheng, H. N.; Nickol, R. G. *Journal of Polymer Science Part A: Polymer Chemistry* **1999**, *37*, 3486.
(237) Kricheldorf, H. R.; Boettcher, C. *Makromolekulare Chemie. Macromolecular Symposia* **1993**, *73*, 47.
(238) Sipos, L.; Zsuga, M.; Kelen, T. *Polymer Bulletin* **1992**, *27*, 495.
(239) Jedliński, Z.; Wałach, W.; Kurcok, P.; Adamus, G. y. *Die Makromolekulare Chemie* **1991**, *192*, 2051.
(240) Billouard, C.; Carlotti, S.; Desbois, P.; Deffieux, A. *Macromolecules* **2004**, *37*, 4038.
(241) Bhaw-Luximon, A.; Jhurry, D.; Spassky, N.; Pensec, S.; Belleney, J. *Polymer* **2001**, *42*, 9651.
(242) Bero, M.; Dobrzyński, P.; Kasperczyk, J. *Journal of Polymer Science Part A: Polymer Chemistry* **1999**, *37*, 4038.
(243) Kasperczyk, J. E. *Macromolecules* **1995**, *28*, 3937.
(244) Hsueh, M.-L.; Huang, B.-H.; Wu, J.; Lin, C.-C. *Macromolecules* **2005**, *38*, 9482.
(245) Ko, B.-T.; Lin, C.-C. *J. Am. Chem. Soc.* **2001**, *123*, 7973.
(246) Chen, H.-Y.; Mialon, L.; Abboud, K. A.; Miller, S. A. *Organometallics* **2012**, *31*, 5252.
(247) Platel, R. H.; Hodgson, L. M.; Williams, C. K. *Polymer Reviews* **2008**, *48*, 11.

(248) Zhong, Z.; Ankoné, M. J. K.; Dijkstra, P. J.; Birg, C.; Westerhausen, M.; Feijen, J. *Polymer Bulletin* **2001**, *46*, 51.
(249) Cheng, M.; Attygalle, A. B.; Lobkovsky, E. B.; Coates, G. W. *J. Am. Chem. Soc.* **1999**, *121*, 11583.
(250) Ayala, C. N.; Chisholm, M. H.; Gallucci, J. C.; Krempner, C. *Dalton Trans.* **2009**, *0*, 9237.
(251) Chisholm, M. H.; Huffman, J. C.; Phomphrai, K. *Journal of the Chemical Society, Dalton Transactions* **2001**, *0*, 222.
(252) Chisholm, M. H.; Gallucci, J.; Phomphrai, K. *Inorg. Chem.* **2002**, *41*, 2785.
(253) Chisholm, M. H.; Phomphrai, K. *Inorg. Chim. Acta* **2003**, *350*, 121.
(254) Chisholm, M. H.; Gallucci, J.; Phomphrai, K. *Chem. Commun.* **2003**, *0*, 48.
(255) Chisholm, M. H.; Gallucci, J. C.; Phomphrai, K. *Inorg. Chem.* **2004**, *43*, 6717.
(256) Chisholm, M. H.; Eilerts, N. W. *Chem. Commun.* **1996**, *0*, 853.
(257) Chisholm, M. H.; Eilerts, N. W.; Huffman, J. C.; Iyer, S. S.; Pacold, M.; Phomphrai, K. *J. Am. Chem. Soc.* **2000**, *122*, 11845.
(258) Williams, C. K.; Breyfogle, L. E.; Choi, S. K.; Nam, W.; Young, V. G.; Hillmyer, M. A.; Tolman, W. B. *J. Am. Chem. Soc.* **2003**, *125*, 11350.
(259) Williams, C. K.; Brooks, N. R.; Hillmyer, M. A.; Tolman, W. B. *Chem. Commun.* **2002**, *0*, 2132.
(260) Chisholm, M. H.; Gallucci, J. C.; Zhen, H.; Huffman, J. C. *Inorg. Chem.* **2001**, *40*, 5051.
(261) Chen, H.-Y.; Tang, H.-Y.; Lin, C.-C. *Macromolecules* **2006**, *39*, 3745.
(262) Breyfogle, L. E.; Williams, C. K.; Young, J. V. G.; Hillmyer, M. A.; Tolman, W. B. *Dalton Trans.* **2006**, *0*, 928.
(263) Yakovenko, M. V.; Trifonov, A. A.; Kirillov, E.; Roisnel, T.; Carpentier, J.-F. *Inorg. Chim. Acta* **2012**, *383*, 137.
(264) McClain, S. J. F., T. M.; Drysdale, N. E. *Polym. Prep.* **1992**, 463.
(265) Simic, V.; Spassky, N.; Hubert-Pfalzgraf, L. G. *Macromolecules* **1997**, *30*, 7338.
(266) Stevels, W. M.; Ankoné, M. J. K.; Dijkstra, P. J.; Feijen, J. *Macromolecules* **1996**, *29*, 3332.
(267) Stevels, W. M.; Ankoné, M. J. K.; Dijkstra, P. J.; Feijen, J. *Macromolecules* **1996**, *29*, 6132.
(268) Ma, H.; Spaniol, T. P.; Okuda, J. *Dalton Trans.* **2003**, *0*, 4770.
(269) Aubrecht, K. B.; Chang, K.; Hillmyer, M. A.; Tolman, W. B. *Journal of Polymer Science Part A: Polymer Chemistry* **2001**, *39*, 284.
(270) Ovitt, T. M.; Coates, G. W. *J. Am. Chem. Soc.* **1999**, *121*, 4072.
(271) Ma, H.; Spaniol, T. P.; Okuda, J. *Angewandte Chemie International Edition* **2006**, *45*, 7818.
(272) Ma, H.; Okuda, J. *Macromolecules* **2005**, *38*, 2665.
(273) Cai, C.-X.; Amgoune, A.; Lehmann, C. W.; Carpentier, J.-F. *Chem. Commun.* **2004**, *0*, 330.
(274) Amgoune, A.; Thomas, C. M.; Roisnel, T.; Carpentier, J.-F. *Chemistry – A European Journal* **2006**, *12*, 169.
(275) Alaaeddine, A.; Amgoune, A.; Thomas, C. M.; Dagorne, S.; Bellemin-Laponnaz, S.; Carpentier, J.-F. *Eur. J. Inorg. Chem.* **2006**, *2006*, 3652.
(276) Hodgson, L. M.; White, A. J. P.; Williams, C. K. *Journal of Polymer Science Part A: Polymer Chemistry* **2006**, *44*, 6646.
(277) Li, G.; Lamberti, M.; Mazzeo, M.; Pappalardo, D.; Roviello, G.; Pellecchia, C. *Organometallics* **2012**, *31*, 1180.
(278) Mazzeo, M.; Lamberti, M.; D'Auria, I.; Milione, S.; Peters, J. C.; Pellecchia, C. *Journal of Polymer Science Part A: Polymer Chemistry* **2010**, *48*, 1374.
(279) Zi, G.; Wang, Q.; Xiang, L.; Song, H. *Dalton Trans.* **2008**, *0*, 5930.
(280) Grunova, E.; Kirillov, E.; Roisnel, T.; Carpentier, J.-F. *Dalton Trans.* **2010**, *39*, 6739.

(281) Bette, V.; Mortreux, A.; Savoia, D.; Carpentier, J.-F. *Tetrahedron* **2004**, *60*, 2837.
(282) Carpentier, J.-F.; Martin, A.; Swenson, D. C.; Jordan, R. F. *Organometallics* **2003**, *22*, 4999.
(283) Kim, Y.; Kapoor, P. N.; Verkade, J. G. *Inorg. Chem.* **2002**, *41*, 4834.
(284) Kim, Y.; Verkade, J. G. *Organometallics* **2002**, *21*, 2395.
(285) Kim, Y.; Jnaneshwara, G. K.; Verkade, J. G. *Inorg. Chem.* **2003**, *42*, 1437.
(286) Chmura, A. J.; Davidson, M. G.; Jones, M. D.; Lunn, M. D.; Mahon, M. F.; Johnson, A. F.; Khunkamchoo, P.; Roberts, S. L.; Wong, S. S. F. *Macromolecules* **2006**, *39*, 7250.
(287) Gendler, S.; Segal, S.; Goldberg, I.; Goldschmidt, Z.; Kol, M. *Inorg. Chem.* **2006**, *45*, 4783.
(288) Kim, Y.; Verkade, J. G. *Macromol. Rapid Commun.* **2002**, *23*, 917.
(289) Kim, Y.; Verkade, J. G. *Macromol. Symp.* **2005**, *224*, 105.
(290) Gregson, C. K. A.; Blackmore, I. J.; Gibson, V. C.; Long, N. J.; Marshall, E. L.; White, A. J. P. *Dalton Trans.* **2006**, *0*, 3134.
(291) Gregson, C. K. A.; Gibson, V. C.; Long, N. J.; Marshall, E. L.; Oxford, P. J.; White, A. J. P. *J. Am. Chem. Soc.* **2006**, *128*, 7410.
(292) Russell, S. K.; Gamble, C. L.; Gibbins, K. J.; Juhl, K. C. S.; Mitchell, W. S.; Tumas, A. J.; Hofmeister, G. E. *Macromolecules* **2005**, *38*, 10336.
(293) Takashima, Y.; Nakayama, Y.; Watanabe, K.; Itono, T.; Ueyama, N.; Nakamura, A.; Yasuda, H.; Harada, A.; Okuda, J. *Macromolecules* **2002**, *35*, 7538.
(294) Motekaitis, R. J.; Martell, A. E.; Koch, S. A.; Hwang; Quarless, D. A.; Welch, M. J. *Inorg. Chem.* **1998**, *37*, 5902.
(295) Chandrasekaran, A.; Day, R. O.; Holmes, R. R. *J. Am. Chem. Soc.* **2000**, *122*, 1066.
(296) Hwang, J.; Govindaswamy, K.; Koch, S. A. *Chem. Commun.* **1998**, *0*, 1667.
(297) Kol, M.; Shamis, M.; Goldberg, I.; Goldschmidt, Z.; Alfi, S.; Hayut-Salant, E. *Inorg. Chem. Commun.* **2001**, *4*, 177.
(298) Chmura, A. J.; Davidson, M. G.; Frankis, C. J.; Jones, M. D.; Lunn, M. D. *Chem. Commun.* **2008**, *0*, 1293.
(299) Chmura, A. J.; Chuck, C. J.; Davidson, M. G.; Jones, M. D.; Lunn, M. D.; Bull, S. D.; Mahon, M. F. *Angewandte Chemie International Edition* **2007**, *46*, 2280.
(300) Nakayama, Y.; Watanabe, K.; Ueyama, N.; Nakamura, A.; Harada, A.; Okuda, J. *Organometallics* **2000**, *19*, 2498.
(301) Menge, W. M. P. B.; Verkade, J. G. *Inorg. Chem.* **1991**, *30*, 4628.
(302) Hormnirun, P.; Marshall, E. L.; Gibson, V. C.; Pugh, R. I.; White, A. J. P. *Proceedings of the National Academy of Sciences* **2006**, *103*, 15343.
(303) Cameron, P. A.; Jhurry, D.; Gibson, V. C.; White, A. J. P.; Williams, D. J.; Williams, S. *Macromol. Rapid Commun.* **1999**, *20*, 616.
(304) Lee, J.; Kim, Y.; Do, Y. *Inorg. Chem.* **2007**, *46*, 7701.
(305) Chmura, A. J.; Cousins, D. M.; Davidson, M. G.; Jones, M. D.; Lunn, M. D.; Mahon, M. F. *Dalton Trans.* **2008**, *0*, 1437.
(306) Johnson, A. L.; Davidson, M. G.; Lunn, M. D.; Mahon, M. F. *Eur. J. Inorg. Chem.* **2006**, *2006*, 3088.
(307) Stopper, A.; Goldberg, I.; Kol, M. *Inorg. Chem. Commun.* **2011**, *14*, 715.
(308) Gruber, P.; O'Brien, M. In *Biopolymers Online*; Wiley-VCH Verlag GmbH & Co. KGaA: 2005.
(309) Dove, A. P.; Gibson, V. C.; Marshall, E. L.; White, A. J. P.; Williams, D. J. *Chem. Commun.* **2001**, *0*, 283.
(310) Dove, A. P.; Gibson, V. C.; Marshall, E. L.; Rzepa, H. S.; White, A. J. P.; Williams, D. J. *J. Am. Chem. Soc.* **2006**, *128*, 9834.
(311) Nimitsiriwat, N.; Gibson, V. C.; Marshall, E. L.; White, A. J. P.; Dale, S. H.; Elsegood, M. R. J. *Dalton Trans.* **2007**, *0*, 4464.

(312) Nimitsiriwat, N.; Marshall, E. L.; Gibson, V. C.; Elsegood, M. R. J.; Dale, S. H. *J. Am. Chem. Soc.* **2004**, *126*, 13598.
(313) Fauré, J.-L.; Gornitzka, H.; Réau, R.; Stalke, D.; Bertrand, G. *Eur. J. Inorg. Chem.* **1999**, *1999*, 2295.
(314) Balasanthiran, V.; Beilke, T. L.; Chisholm, M. H. *Dalton Trans.* **2013**.
(315) Kricheldorf, H. R.; Bornhorst, K.; Hachmann-Thiessen, H. *Macromolecules* **2005**, *38*, 5017.

Chapter 2

Asymmetric Catalysts Based on Amines

2.1. Background

The purpose of the work described in this section was to generate a library of chiral ligands, as homogeneous models to heterogenised ligands, that could then be complexed with a wide variety of transition metals. These complexes are then screened to assess their performance against a range of asymmetric organic transformations. The results from this evaluation can be compared and the most promising reaction further developed and can be used to optimise the design of heterogeneous systems.

2.2. Ligand Design

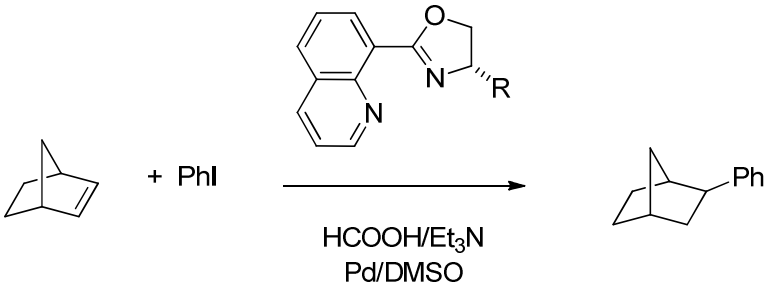

Figure 2.1. Reaction scheme for the hydroarylation of norobornene as reported by Chen et al[1]

Chan et al.[1] reported their discovery of chiral discrimination for the hydroarylation of norobornene using quinolinyl-oxazolines palladium(II) complexes. It was therefore hypothesised that novel chiral ligands could be obtained from the condensation reaction between 2,6-pyridinedicarboxaldehyde and chiral amines, Figure 2.2. Heterogenisation to silica before complexation to a palladium source would yield an assay of chiral heterogeneous catalysts. The benefit of using 2,6-pyridinedicarboxaldehyde is that a straightforward reaction with a chiral amine generates a chiral bidentate ligand, and the second aldehyde moiety can react with the appropriately functionalised tether of a silica support (eg, 3-aminopropyltrimethoxysilane)

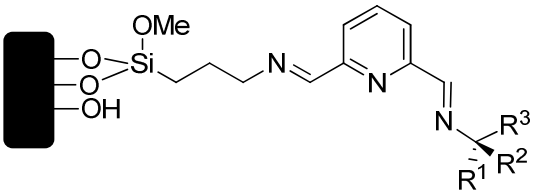

Figure 2.2. General structure of heterogeneous systems described herein.

Due to the issues discussed in chapter one of the difficulties working with heterogeneous systems, analogous homogeneous ligands will be prepared, complexed and screened against the standard reactions to assess the best systems to explore heterogeneously. The 2,6-pyridinecarboxaldehyde can be prepared from the commercially available 2,6-pyridinedimethanol by oxidation with manganese dioxide. Addition of this molecule to a chiral amine results in a mixture of mono and bi-condensed Schiff base molecules as well as unreacted starting material. As such to explore the scope fully, 2,6-pyridinedicarboxaldehyde is reacted with two equivalents of chiral amine to ensure full condensation, along with 2-pyridinecarboxaldehyde with one equivalent to prepare a homogeneous ligand more akin to the proposed heterogeneous system, Figure 2.3.

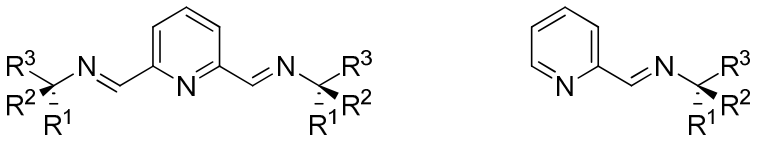

Figure 2.3. General structure of the homogeneous analogues described herein.

2.2.1. Homogeneous Analogues

Four chiral amines were chosen based on their availability, safety, cost and degree of functionality, the ligands that they afforded are detailed in Figure 2.4. As such, (*R*)-(+)-α-methyl benzylamine was chosen as a standard and is commonly used in the literature to introduce chirality in a cheap and clean means to a ligand. (*R*)-(+)-ethyl benzylamine was chosen to offer an increase in flexibility around the chiral centre in the form of an alkyl chain. (*R*)-(+)-methyl naphthylamine was selected to explore the additional rigidity surrounding the chiral centre, while (*R*)-(+)-methyl cyclohexylamine was introduced to compare an aromatic substituent vs. a non-aromatic version. The nature of these chiral amines is such that they were stored at low temperature and exposed to air sparingly to avoid racemisation or water incorporation. ^{1}H and ^{13}C $\{^{1}H\}$ NMR spectroscopy and mass spectrometry confirms a successful reaction. Figure 2.4 also includes the scheme for the preparation of 2,6-pyridinedicarboxaldehyde from the oxidation of 2,6-pyridinedimethanol by manganese dioxide in chloroform.

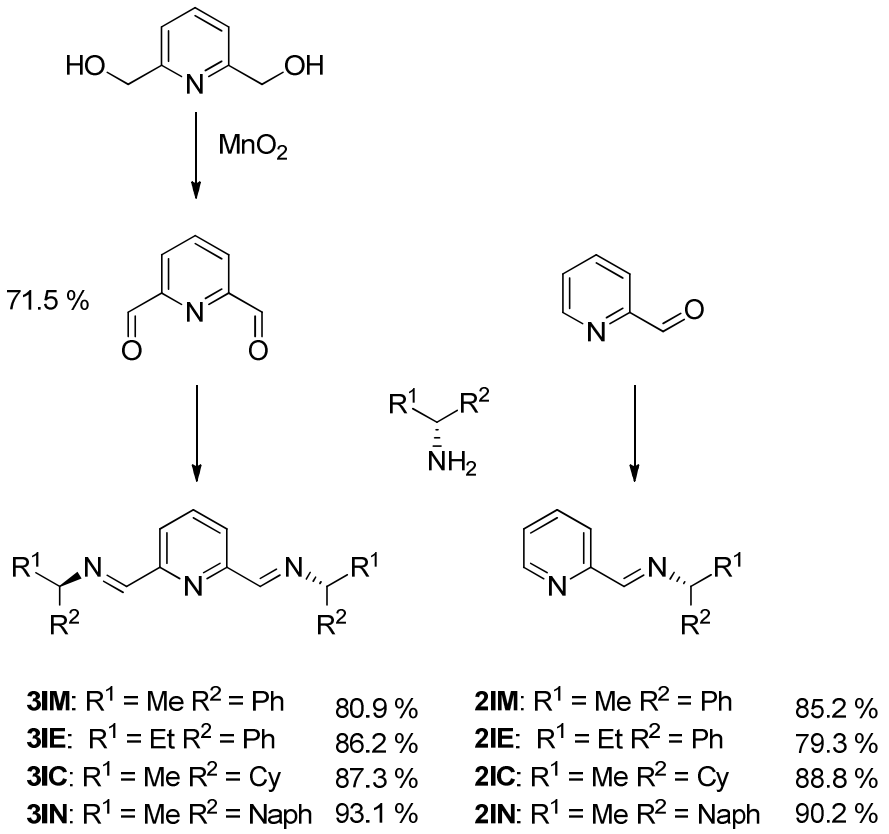

3IM: R^1 = Me R^2 = Ph	80.9 %	**2IM**: R^1 = Me R^2 = Ph	85.2 %
3IE: R^1 = Et R^2 = Ph	86.2 %	**2IE**: R^1 = Et R^2 = Ph	79.3 %
3IC: R^1 = Me R^2 = Cy	87.3 %	**2IC**: R^1 = Me R^2 = Cy	88.8 %
3IN: R^1 = Me R^2 = Naph	93.1 %	**2IN**: R^1 = Me R^2 = Naph	90.2 %

Figure 2.4. Homogeneous analogues prepared in this study.

The presence of an imine group in the ligands may be poorly suited for certain catalytic processes, for example catalytic asymmetric hydrogenation. In this reaction there is a chance that these imine groups may be reduced to amines, thus potentially altering the catalyst and ultimately the catalytic results. It may also be a possibility that the additional stabilisation resulting from heterogenisation to an inorganic support protects the imine bounds from such reduction. To investigate the stability of such ligands for these applications, the ligands were reduced prior to complex preparation, producing the amine-containing counterpart series of ligand systems. The reaction scheme can be seen in Figure 2.5.

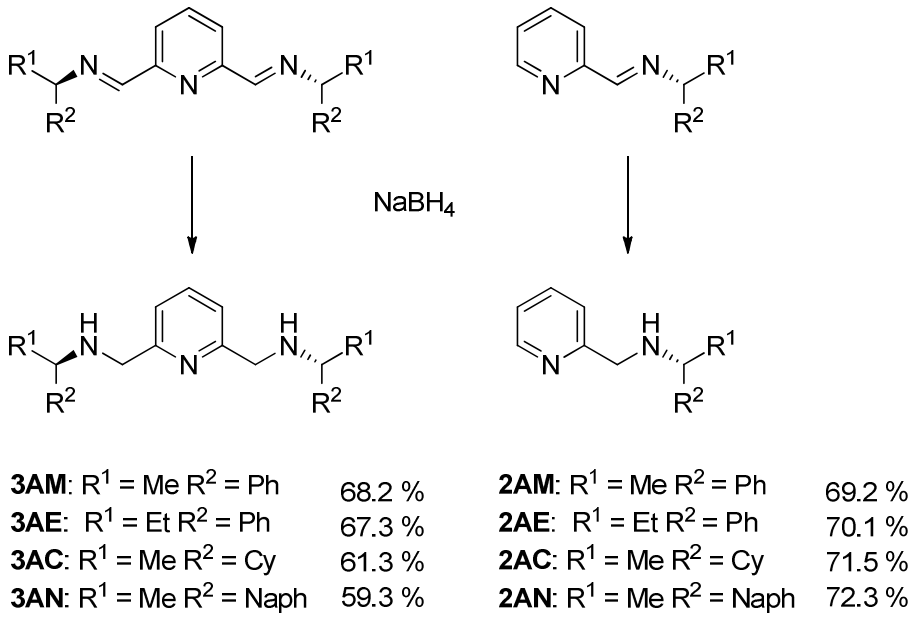

3AM: R^1 = Me R^2 = Ph	68.2 %	**2AM**: R^1 = Me R^2 = Ph	69.2 %
3AE: R^1 = Et R^2 = Ph	67.3 %	**2AE**: R^1 = Et R^2 = Ph	70.1 %
3AC: R^1 = Me R^2 = Cy	61.3 %	**2AC**: R^1 = Me R^2 = Cy	71.5 %
3AN: R^1 = Me R^2 = Naph	59.3 %	**2AN**: R^1 = Me R^2 = Naph	72.3 %

Figure 2.5. Reduction of homogeneous ligands to the corresponding amines containing analogues investigated in this chapter

These ligands were characterised by ^{1}H and ^{13}C $\{^{1}H\}$ NMR spectroscopy and mass spectrometry with all characterisation indicating that the reaction had been accomplished successfully. Comparing the physical aspects of the ligands provided an immediate if qualitative indication of success; the amine ligands were much less viscous in comparison with their imine counterparts which were rather viscous, likely due to less hydrogen bonding. The amine Schiff bases prepared from 2-pyridinecarboxaldehyde would also be less intense in colour. Figure 2.6 shows the NMR spectra for ligands containing (*R*)-methyl benzylamine, **2IM** and **2AM**. Comparing the spectra, it can clearly be seen that the imine resonance at 8.38 ppm is absent upon reduction from **2IM** (blue) to **2AM** (red), and a new resonance is present at 3.60 ppm (red), corresponding to the new CH_2-NH environment. The resonance quartet resulting from the chiral centre now appears more upfield.

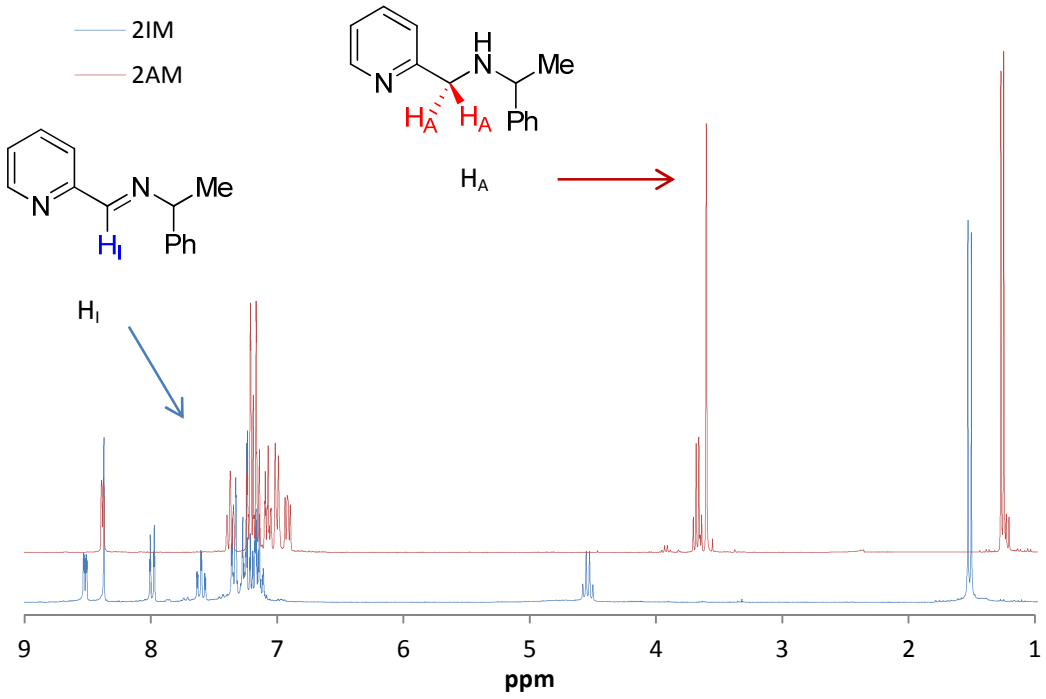

Figure 2.6.The offset ^{1}H NMR spectra of the imine ligand 2IM(blue), and its reduced amine version 2AM (red)

2.2.2. Conclusions

Sixteen ligands have been prepared and characterised representing a novel selection of chiral bis-pyridine chiral Schiff base ligands. This group has the potential to be expanded by different chiral amines than the four discussed, and variation of the pyridine backbone. All ligands were screened against two benchmark reactions, the asymmetric nitroaldol reaction and asymmetric hydrogenation reaction, with their activity and selectivity determined from NMR spectroscopy and HPLC respectively. The best systems were optimised and heterogenised to silica to assess their performance as asymmetric heterogeneous catalysts, which in turn were optimised to obtain the best selectivity and conversion.

2.3. Asymmetric Nitroaldol Reaction

The ligands described in section 2.1 of this chapter were screened against the nitroaldol reaction. As discussed in the introduction, the Henry reaction is an important carbon-carbon bond forming reaction, with the product providing a wide scope for subsequent modifications, due to conversion of the nitro moiety,

into other function groups. Copper(II) complexes are seen to dominate the literature for this reaction, which formulates the starting point in this investigation, however the drawbacks have been the need for high catalyst loadings, non-ambient reaction conditions (decreased temperature, lengthy reaction times, non-ideal solvent system) and substrate specificity. It is therefore clear that there is a niche in the area for an undemanding and efficient catalyst. As discussed before and displayed below, the asymmetric nitroaldol reaction is not limited to copper(II) complexes, with examples of zinc(II) lanthanum(III), iron (II/III) & cobalt(II) present in the literature[2-7]. Heterogeneous systems for this reaction remain limited, despite the work of Yanagisawa et al[8]. and his high-through put CD HPLC device, but success has been found with catalysts supported on dendrimers, PEG polymers and Wang type resins [9-11].

2.3.1. Copper(II) Complexes

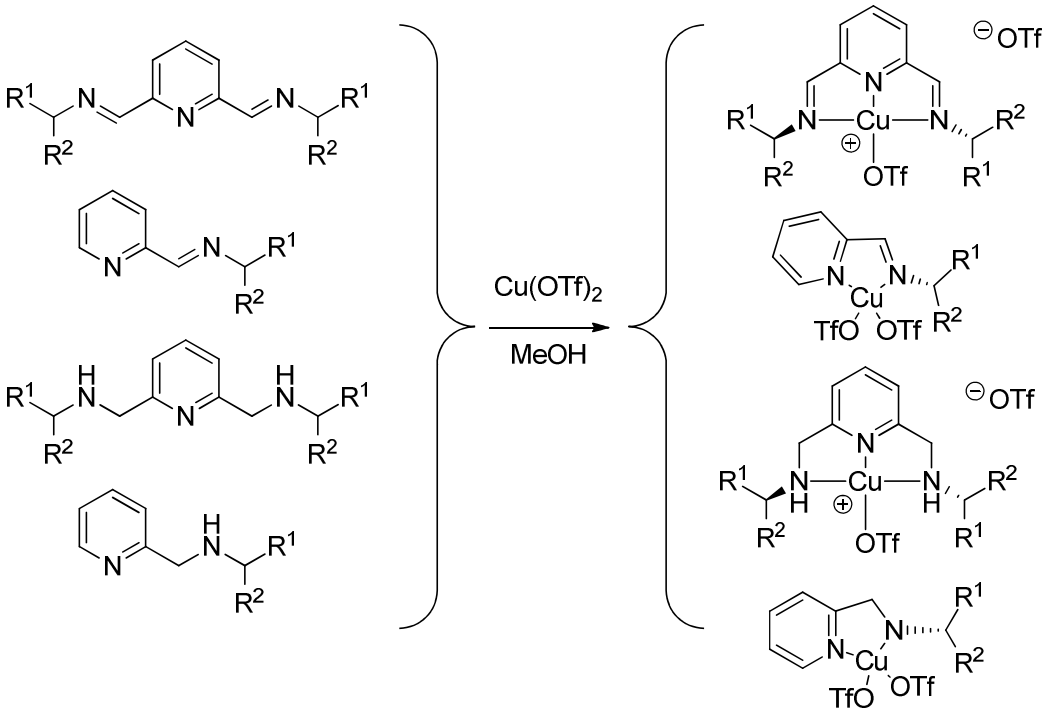

Cu(3IM)(OTf)$_2$: R^1 = Me, R^2 = Ph
Cu(3IE)(OTf)$_2$: R^1 = Et, R^2 = Ph
Cu(3IC)(OTf)$_2$: R^1 = Me, R^2 = Cy
Cu(3IN)(OTf)$_2$: R^1 = Me, R^2 = naph

Cu(2IM)(OTf)$_2$: R^1 = Me, R^2 = Ph
Cu(2IE)(OTf)$_2$: R^1 = Et, R^2 = Ph
Cu(2IC)(OTf)$_2$: R^1 = Me, R^2 = Cy
Cu(2IN)(OTf)$_2$: R^1 = Me, R^2 = naph

Cu(3AM)(OTf)$_2$: R^1 = Me, R^2 = Ph
Cu(3AE)(OTf)$_2$: R^1 = Et, R^2 = Ph
Cu(3AC)(OTf)$_2$: R^1 = Me, R^2 = Cy
Cu(3AN)(OTf)$_2$: R^1 = Me, R^2 = naph

Cu(2AM)(OTf)$_2$: R^1 = Me, R^2 = Ph
Cu(2AE)(OTf)$_2$: R^1 = Et, R^2 = Ph
Cu(2AC)(OTf)$_2$: R^1 = Me, R^2 = Cy
Cu(2AN)(OTf)$_2$: R^1 = Me, R^2 = naph

Figure 2.7. Reaction scheme for the formation of copper(II) complexes

The reaction scheme detailed above shows the method used for preparation of copper(II) homogeneous analogues for the asymmetric nitroaldol reaction, Figure 2.7. These complexes were characterised by mass spectrometry, elemental analysis and electron paramagnetic resonance, EPR, spectroscopy. Where possible, the complexes were characterised by single crystal X-ray diffraction.

While the reaction mixtures were stirred overnight, confirmation of successful complexation is almost instant via a vivid colour change, to blue, turquoise, or green depending on the imine/amine nature, bi-/tridentate binding, and aromaticity of the ligand employed. As copper(II) complexes are paramagnetic (resulting from its d^9 electron configuration and an unpaired electron giving rise to magnetic susceptibility) standard NMR spectroscopic techniques are redundant. EPR spectroscopy, however, requires an unpaired electron. Basic concepts are analogous to NMR, but instead of exciting the spins of atomic nuclei, electron spins are excited, with each electron having a spin quantum number, s= ½, and magnetic moment, $m_s = +½$ and $-½$.

When an external magnetic field of strength B_0 is applied, the magnetic moment of the electron aligns itself either parallel ($m_s = -½$) or antiparallel ($m_s = ½$), much like the spins of a proton in ^{1}H NMR. Each alignment will have a specific energy and the difference between the lower and upper state is $\Delta E = g_e \mu_B B_0$, where g_e is the (Landé) g-factor, and μ_B is the Bohr magneton. The inclusion of B_0 means that there is direct proportionality between the splitting of the energy levels and the magnetic field strength. This can be seen pictorially in Figure 2.8.

The unpaired electron can transfer between the lower and upper state by absorbing or emitting a photon of energy hv, such that $\Delta E = hv$. In practice microwaves are used in the 9000-10000 MHz range, with a fixed magnetic field, 3500 G, however it is also possible for the frequency to be fixed while the field strength is scanned. When either frequency or field scanning fulfil the equation $hv = g_e \mu_B B_0$ the unpaired electrons can transfer between their spin states, and a net

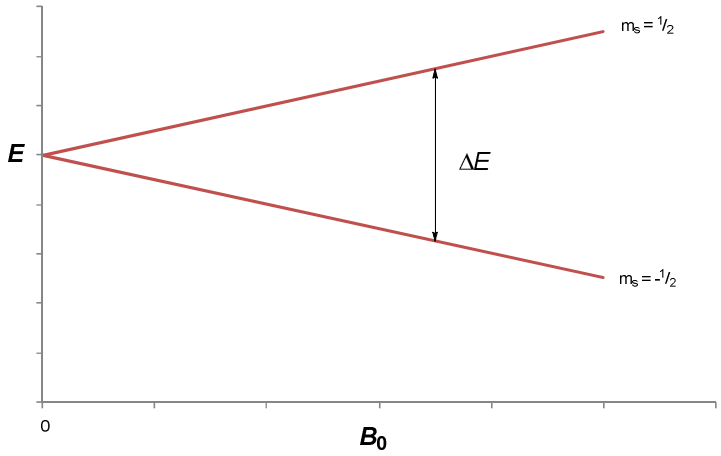

Figure 2.8. Schematic of unpaired electron splitting when an external magnetic field is applied.

absorbance is observed, (this is due to a greater population in the lower state, Maxwell-Boltzmann distribution) and transformed into the spectra.

EPR spectra were recorded for the two complexes, Cu(**3IM**)$(OTf)_2$ and Cu(**2IM**)$_2(OTf)_2$, submitted in their purified form and analysed as powders, and are presented below with their simulated spectra, using Bruker XSophe computer simulation software (version 1.1.4). The spectra were recorded in the solid-state for variable temperatures at the X-band, (ν = 9.4 GHz, λ = 30 mm and B_0 = 0.33T, and the Q-band (ν = 34 GHz, λ = 8.5 mm and B_0 = 1.25 T) microwave frequencies, with simulations being generated using Bruker's XSophe software package.

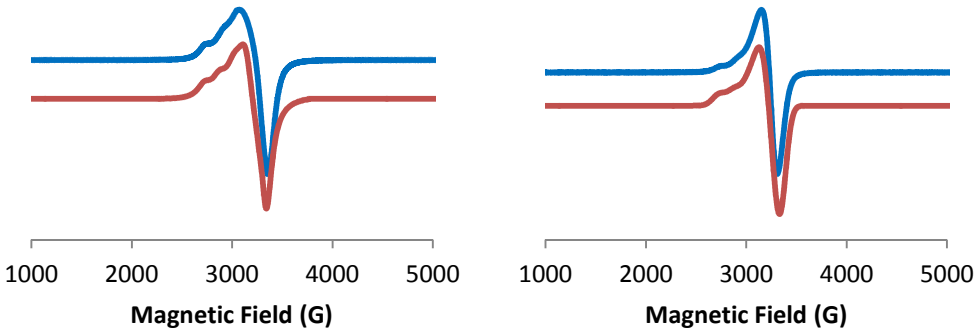

Figure 2.9. X-band EPR spectrum of Cu(3IM)(OTf)2 at 5 K (left) and 200 K (right), experimental (blue) and simulated (red)

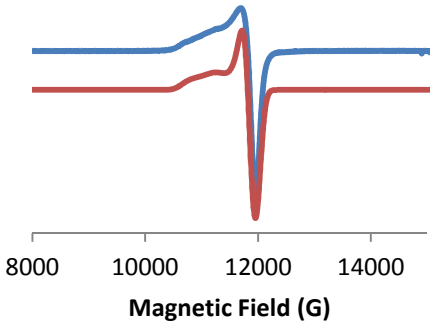

Figure 2.10. Q-band EPR spectrum of Cu(3IM)$(OTf)_2$ at 200 K, experimental (blue) and simulated (red)

As can be seen in Figure 2.9 and Figure 2.10, the experimental values are in close agreement with the simulated spectra for Cu(**3IM**)$(OTf)_2$, and also agree with literature values for similar complexes[12,13], as are that of Cu(**2IM**)$_2(OTf)_2$, Figure 2.11 and Figure 2.12.

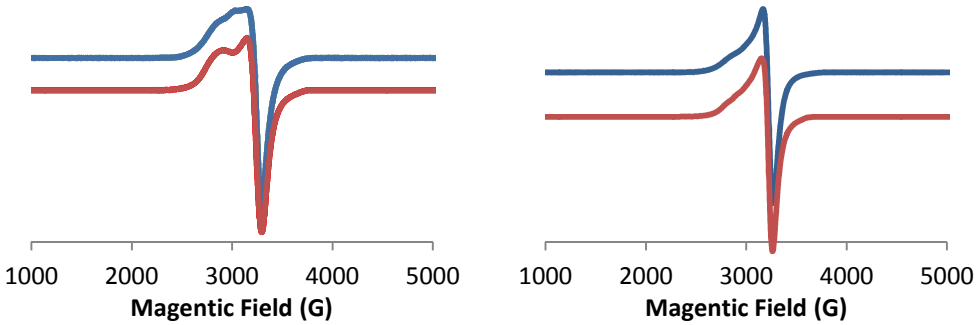

Figure 2.11. X-band EPR spectrum of Cu(2IM)$_2(OTf)_2$ at 5 K (left) and 20 K (right), experimental (blue) and simulated (red)

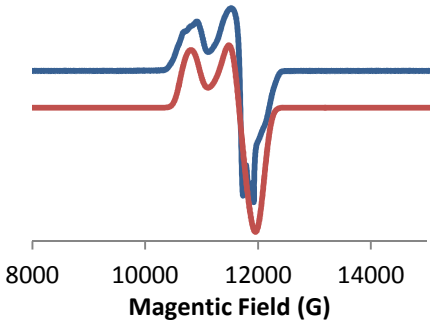

Figure 2.12. Q-band EPR spectrum of Cu(3IM)$(OTf)_2$ at 200 K, experimental (blue) and simulated (red)

The Table 2.below gives the g values and A values from the EPR spectra of the two compounds. g values can be thought of as chemical shifts while the A value, the hyperfine coupling constant, can be compared to the J value from standard NMR spectroscopy.

Complex	Band	gx, gy, gz	Ax, Ay, Az (G)
Cu(**3IM**)$(OTf)_2$	X	2.07, 2.07, 2.27	20, 20, 148
	Q	2.06, 2.06, 2.23	40, 40, 180
Cu(**2IM**)$_2(OTf)_2$	X	2.08, 2.08, 2.27	0, 0, 100
	Q	2.04, 2.09, 2.26	60, 60, 85

Table 2.1. Summarised results for the EPR spectroscopy of two copper homogeneous catalysts. X band = 9.4 GHz while Q band = 34 GHz. Recorded at 200 K

It should be noted that the second complex to be analysed by EPR, Figure 2.11 and Figure 2.12, was not in a one to one ratio of ligand to metal but indeed two to one. This was not intentionally prepared, however, was the only example to yield crystals suitable for XRD, Figure 2.13. This is likely due to the difficult nature of growing crystals of chiral complexes resulting from the limited number of symmetry groups possible.

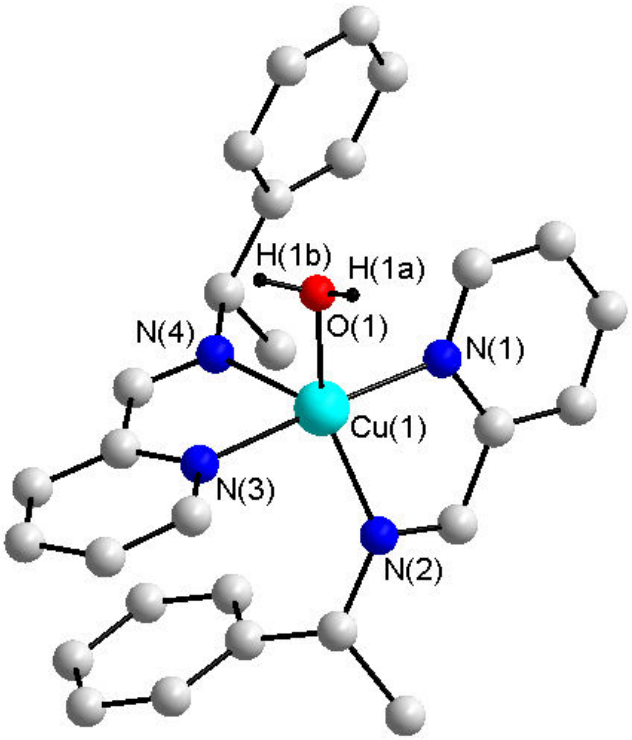

Figure 2.13. Molecular structure of $Cu(2IM)_2(OTf)_2$, two triflate counterions and the hydrogen atoms have been removed for clarity.

Specific bond lengths and angles are given below, Table 2.2.

Bond Lengths (Å)		Bond Angles (^{0})	
Cu(1)-N(1)	1.9869(13)	N(1)-Cu(1)-N(3)	176.09(5)
Cu(1)-N(3)	2.0356(12)	N(1)-Cu(1)-O(1)	90.06(5)
Cu(1)-O(1)	2.0023(13)	N(3)-Cu(1)-O(1)	93.73(5)
Cu(1)-N(2)	2.0533(13)	N(1)-Cu(1)-N(2)	81.04(5)
Cu(1)-N(4)	2.2490(13)	N(3)-Cu(1)-N(2)	95.95(5)
		O(1)-Cu(1)-N(2)	152.80(5)
		N(1)-Cu(1)-N(4)	99.69(5)
		N(3)-Cu(1)-N(4)	78.89(5)
		O(1)-Cu(1)-N(4)	97.42(5)
		N(2)-Cu(1)-N(4)	109.35(5)

Table 2.2. Selected bond lengths and angles for $Cu(2IM)_2(OTf)_2$

An absolute structure parameter of 0.000(5) is indicative of an enantiopure compound, the space group is $P2_1$ and the crystal system is monoclinic. Copper(II) centres can adopt a variety of structural motifs, square planar, octahedral, and in this case trigonal pyramidal. In this case the trigonal pyramidal is presented with a N(1)-Cu(1)-N(3) bond angle of 176.09(5) ^{0}, showing a slight deviation from the ideal value of 180 ^{0}, and a N(1)-Cu(1)-O(1) bond angle of 90.05(5) ^{0}.

No other crystals suitable for XRD were obtained, despite purposeful procedures to grow dual ligand barring complexes. The ligand structure along with multiple examples from the elemental analysis show that the complexes are somewhat hydrophilic with some examples becoming tacky losing crystallinity if exposed to air for prolonged periods of time (weeks). This may affect catalytic activity and selectivity, however the purpose of this study is to find efficient, stable and more practical complexes. Indeed non-distilled solvents were to be utilised and with the reaction vessels sealed, no attempts to exclude air and moisture were undertaken. The first round of screening was to test the sixteen copper(II) chiral complexes prepared against the nitroaldol coupling of nitromethane to benzaldehyde, the reaction scheme is detailed below, Figure 2.14.

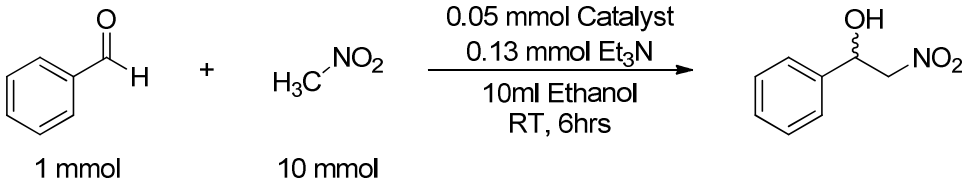

Figure 2.14. Initial conditions for the asymmetric nitroaldol reaction evaluated in this study, herein referred to as the Standard

As with many examples, base was included as co-catalyst to facilitate the deprotonation of the nitroalkane, as discussed in the introduction, which is required for the ensuing addition of the nitroalkane to the δ-positive carbon of the aldehyde. Following reaction optimisation in the literature[14], triethylamine was chosen as base and used at a 13 mol % ratio, ethanol as the reaction solvent, and 6 hours as the reaction time. The results can be seen in Table 2.3.

The results show that the complexes prepared are reasonably active for the Henry reaction on the whole. Improvement can be seen when using the amine containing homogeneous bidentate ligands when compared to their imine counterparts, with conversion increasing by up to 38 %. This is likely due to the additional basic character of the ligand as a whole in its amine form that compared to imine, and the amount of base present has been shown to have a direct correlation with conversion. The short comings in complete conversion can be a result of impurities in starting materials, solvents or catalysts, or simply non-optimal reaction conditions.

Enantiomeric excesses are poor, unable to achieve a selectivity bias of more than 10 %. With such low chiral discrimination it is hard to draw concrete conclusions when comparing different classes of complex, however there is a clear variation in the bidentate ligands when concerning the imine or amine character. The imine containing variants have considerably low ee, 0.1 - 2 %, upon reduction of the imine bond to prepare the amine ligand, a jump in selectivity is observed, 1.8 - 8.2 with the most impressive improvement, and indeed best in this screening, to the ethyl-benzylamine. This can be again attributed to the additional basicity in the complex from the amine groups, however we see the reverse trend for the tridentate complexes.

Ligand	[a]Conversion (%)	[b]ee (%)	Yield (%)
2IM	75.2	0.5	0.4
2IE	67.6	0.1	0.7
2IC	71.4	2.0	1.4
2IN	45.7	0.5	2.3
2AM	88.5	2.5	2.2
2AE	90.9	8.2	7.5
2AC	89.3	5.7	5.1
2AN	84.0	1.7	1.4
3IM	87.7	5.1	4.5
3IE	52.4	0.9	0.5
3IC	88.5	2.3	2.0
3IN	90.9	7.2	6.5
3AM	83.3	0.4	0.3
3AE	82.6	0.6	0.5
3AC	80.0	1.5	1.2
3AN	82.6	1.0	0.8

Table 2.3. Results for the nitroaldol reaction between benzaldehyde, 1.0 mmol, and nitromethane, 10 mmol catalysed by various chiral copper(II) complexes generate from coordination with copper(II) triflate, with triethylamine as co-catalyst, 100:5:13 aldehyde:catalyst:base, ethanol used as solvent and the reaction was kept at room temperature for 6 hours. [a]Conversion determined by ^{1}H NMR spectroscopy, [b]ee determined by chiral-HPLC OD-H column, with an error of ± 2%.

It is important to note that during a blank run, in which Et_3N, nitromethane and benzaldehyde were stirred in ethanol for 6 hr, a conversion of approximately 10 % was achieved. Triethylamine is therefore clearly able to deprotonate the nitroalkane and as such the catalyst's influence over the coordination of the nitromethane is lessened as will be the ensuing coordination of the benzaldehyde. This will ultimately result in decreased selectivity, expressed as a drop in enantiomeric excess. This is supported in the literature by the trend in selectivity and basicity, with an increased basicity of the ligand compared to the Et_3N, leading to deprotonation by the complex and as such greater control by the chiral ligand.[15]

Following the standard screening for the nitroaldol, further screens were conducted to achieve improved enantioselectivity while maintain catalytic

activity, and are detailed below. The first concern is the variation of counter-ion in the copper(II) complex. If deprotonation of the nitromethane was exclusively achieved by the complex, then it would give rise to an increase in the selectivity of the reaction. A selection of ligands were selected and complexed with copper(II) chloride and copper(II) acetate *in situ* before being screened against the standard reaction conditions. They are presented below along with the corresponding copper(II) triflate catalyst screen, Table 2.4.

Copper Salt	Ligand	[a]Conversion (%)	[b]ee (%)	[c]Yield (%)
Copper(II) Triflate	2IM	75.2	0.5	0.4
	2AM	88.5	2.5	2.2
	3IM	87.7	5.1	4.5
	3AM	83.3	0.4	0.3
Copper(II) Acetate	2IM	46.3	11.0	5.1
	2AM	55.2	2.2	1.2
	3IM	54.6	10.2	5.6
	3AM	36.0	27.4	9.9
Copper(II) Chloride	2IM	66.2	18.7	12.4
	2AM	57.1	3.9	2.2
	3IM	37.3	21.7	8.1
	3AM	74.1	1.5	1.1

Table 2.4. Results for the nitroaldol reaction between benzaldehyde, 1.0 mmol, and nitromethane, 10 mmol catalysed by various chiral copper(II) complexes with triethylamine as co-catalyst, 100:5:13 aldehyde:catalyst:base, ethanol used as solvent and the reaction was kept at room temperature for 6 hours. [a]Conversion determined by ^{1}H NMR spectroscopy, [b]ee determined by chiral-HPLC OD-H column, with an error of ± 2%. Complexes were prepared *in situ*.

The conversion decreases as the loosely coordinated triflate ion is replaced with the stronger acetate and chloride. The drop off can be significant, 2AM, from triflate to the alternatives or step down, 3AM, from triflate to acetate onto chloride, and the conversions range by some 20 %. The bidentate imine ligand was trailing in activity for the copper(II) triflate complex, and remains to be one of the poorest catalysts. However, no obvious patterns or trends can be identified. The enantioselectivity is improved upon variation of the counter-ion in general, where the triflate was rather poor, the acetate manages an enantiomeric excess of 27 %, while the chloride achieves about 22 %. Interestingly, for these new copper

complexes, the best enantioselectivity is often associated with the catalysts exhibiting low conversion; Cu(**3AM**)$(AcO)_2$ conversion = 36 %, ee = 27 %, Cu(**3IM**)Cl_2 conversion = 37 %, ee = 22 %.

It has been discussed that the nitroaldol reaction can be catalysed with varying degrees of success and the choice of the ligand and transition metal is critical. The catalytic activity of iron(II) chloride, cobalt(II) chloride, and europium(III) triflate was then explored with a selection of ligands. The complexes were prepared *in situ* with colour changes being used as indicators for successful complexation, as is common practice for this kind of *in situ* synthesis. Iron is seeing growing interest due to its availability, biocompatibility, low toxicity, and expense, and is seeing applications in lots of catalytic reactions replacing expensive metals. Cobalt is another metal that has shown promise in the asymmetric nitroaldol reaction. Yamada et al. developed ketoimine[4] and salen[5] ligands which were coordinated to cobalt(II) and were good catalysts for the nitroaldol reaction for a range of different aldehydes and nitromethane (albeit under poor conditions requiring very low temperatures, -78 to - 40 ^{0}C, extended reaction times, 40-144 h, and Hünig's base). Lanthanide group metals have also been employed in the asymmetric nitroaldol reaction from quite an early stage in the development of this reaction. Shibasaki reported a lanthanum-lithium binaphthol catalyst[16]. The results are given below with the standard condition screen for comparison.

Metal Salt	Ligand	[a]Conversion (%)	[b]ee (%)	[c]Yeild (%)
Copper Triflate	2IM	75.2	0.5	0.4
	2AM	88.5	2.5	2.2
	3IM	87.7	5.1	4.5
	3AM	83.3	0.4	0.3
Cobalt Chloride	2IM	70.4	2.2	1.5
	2AM	73.0	1.3	0.9
	3IM	74.6	0.9	0.7
	3AM	76.3	1.0	0.8
Iron Chloride	2IM	43.7	0.3	0.1
	2AM	11.8	4.5	0.5
	3IM	32.1	0.6	0.2
	3AM	39.5	3.6	1.4
Europium Triflate	2IM	45.2	0.8	0.4
	2AM	64.9	0.6	0.4
	3IM	28.2	5.2	1.5
	3AM	46.9	0.4	0.2

Table 2.5. Results for the nitroaldol reaction between benzaldehyde, 1.0 mmol, and nitromethane, 10 mmol, catalysed by various transition metal complexes with triethylamine as co-catalyst, 100:5:15 aldehyde:catalyst:base, ethanol used as solvent and the reaction was kept at room temperature for 6 hours. [a]Conversion determined by ^{1}H NMR spectroscopy, [b]ee determined by chiral-HPLC OD-H column, with an error of ± 2%. Complexes were prepared *in situ*.

The cobalt complexes behaved quite similarly for amine or imine, bi- or tri-dentate. Conversion was quite similar, 73.5 % on average, and is the closest to our standard reaction system that has been trialled so far. Both iron chloride and europium triflate complexes show a decrease in activity and a greater range of conversion than both the copper and cobalt complexes. Enantiomeric excess was still poor, with just one example matching that previously experienced in the standard system, Eu(**3IM**)$(OTf)_3$. For both the iron and europium systems, a drop in conversion is paired with minor enantioselectivity, however, whereas for the europium system, an ee of 5 % and conversion of 28 % stands out from the remainder, < 1 % ee, > 45 % conversion, the next closest iron system has a conversion over three times that of the most selective catalyst.

So far the reaction conditions have remained constant whilst the catalyst was altered. This proved to be unfruitful, so improvements to enantioselectivity were sought by optimising the reaction conditions. This could be possibly achieved by a variety of ways, base concentration and type, solvent effects, reaction time and temperature. Varying reaction time is problematic, as increasing duration will probably increase conversion, however it leaves the product exposed to possible racemisation, or may favour non-selective competing catalysis of the substrate, reducing enantiomeric excess. Reducing reaction time will have a detrimental impact upon conversion however there is the possibility of improving selectivity, but adjustments can be time consuming to find the ideal balance, unless continuous monitoring was possible without affecting the reaction vessel. Due to the product having a yellow colour, compared to the colourless starting material, it could be possible to measure the reaction progress as a correlation against colour with a UV-detector. Measuring enantiomeric excess, however, is difficult as samples would have to be removed and worked up before being subjected to chiral-HPLC.

Easier variations to the reaction are the base, solvent, nitroalkane and temperature as previously discussed. The Henry reaction requires base to deprotonate the nitroalkane. However, some groups have published catalytic systems where by the ligand is of sufficient basicity to deprotonate the nitroalkane. If the ligand systems employed in this study are sufficiently basic, screening the reaction in the absence of base could provide significant increases to selectivity as a chiral base is doing the work. As such the basic character of the ligand systems employed will be evaluated in a base free Henry reaction. Christensen[15] and Pennaforte[17], have also demonstrated the importance of selecting the correct base for a given catalyst. As such, two additional bases were selected and screened, 1-methyl pyrrolidine, MP, and diisopropylamine, DIPA, the results are detailed below alongside the results of the standard reaction for comparison. Also included in this series were a selection of the best performing non-copper(II) triflate complexes to investigate if any improvements were universal or specific to one system.

Base	System	[a]Conversion (%)	[b]ee (%)	Base	System	[a]Conversion (%)	[b]ee (%)
Tri-ethyl amine	Cu(2IM)(OTf)	75.2	0.5	MP	Cu(2IM)(OTf)	32.9	3.2
	Cu(2AM)(OTf)	88.5	2.5		Cu(2AM)(OTf)	55.2	0.2
	Cu(3IM)(OTf)	87.7	5.1		Cu(3IM)(OTf)	34.4	24.1
	Cu(3AM)(OTf)	83.3	0.4		Cu(3AM)(OTf)	55.2	7.4
	Cu(2IM)(Cl)	66.2	18.7		Cu(2IM)(Cl)	35.8	6.5
	Cu(3IM)(Cl)	37.3	21.7		Cu(3IM)(Cl)	61.0	9.5
	Eu(2IN)(OTf)	51.2	36.0		Eu(2IN)(OTf)	48.8	7.5
	Cu(3AM)(AcO)	36.0	27.4		Cu(3AM)(AcO)	56.5	42.0
No Base	Cu(2IM)(OTf)	0	-	DIPA	Cu(2IM)(OTf)	34.2	5.7
	Cu(2AM)(OTf)	0	-		Cu(2AM)(OTf)	44.6	7.3
	Cu(3IM)(OTf)	0	-		Cu(3IM)(OTf)	56.2	17.8
	Cu(3AM)(OTf)	0	-		Cu(3AM)(OTf)	38.6	0.3
	Cu(2IM)(Cl)	-	-		Cu(2IM)(Cl)	51.5	6.7
	Cu(3IM)(Cl)	-	-		Cu(3IM)(Cl)	73.0	5.6
	Eu(2IN)(OTf)	-	-		Eu(2IN)(OTf)	37.9	5.0
	Cu(3AM)(AcO)	-	-		Cu(3AM)(AcO)	56.5	25.2

Table 2.6. Results for the nitroaldol reaction between benzaldehyde, 1.0 mmol, and nitromethane, 10 mmol, catalysed by various transition metal complexes with various bases as co-catalyst, 100:5:15 aldehyde:catalyst:base, MP, 1-methyl pyrrolidine, DIPA, diisopropylamine, ethanol used as solvent and the reaction was kept at room temperature for 6 hours. [a]Conversion determined by ^{1}H NMR spectroscopy, [b]ee determined by chiral-HPLC OD-H column, with an error of ± 2%. Complexes were prepared *in situ*.

The base free catalyst evaluation shows that additional base is required in these reactions, and the basic character of the ligands in the complex is not sufficient to deprotonate the nitroalkane. As the systems did not undergo catalysis selectivity while inherently be zero and was not recorded. Moreover due to the failure of the standard complexes base-free screening was abandoned. Stronger bases like diisopropylamine and 1-methyl pyrrolidine would be expected to increase the conversion relative to the weaker triethylamine. However, the results in general show a decrease in the conversion of the reaction compared to the standard copper triflate complexes. This trend is not applicable to all the catalysts screened, as Cu(**3IM**)(Cl) and Cu(**3AM**)(AcO) experience an increase in conversion, and the decrease in conversion varies from system to system.

Changing the base has a varied effect on the enantioselectivity of the catalytic reaction. Where before we have seen drops in conversion being associated with better enantiomeric excess, examples are also present in this

optimisation study, with the **3IM** standard complex dropping in activity with an increase in selectivity, and a further drop resulting in higher enantioselectivity still. The vice versa is also observed with increasing activity upon changing base and decreasing enantioselectivity. However, changing the base can impact on the conversion (and hence selectivity). The best system in this variation of the reaction conditions is the copper(II) acetate with the tridentate-amine containing a chiral ligand, Cu(**3AM**)(AcO). The new bases improve the conversion compared to triethylamine by about 20 % and while diisopropylamine slightly decreases enantioselectivity, 1-methyl pyrrolidine significantly increased the chiral discrimination, 42 %. However there is no conclusive relation between enantiomeric excess and conversion.

Reducing the reaction temperature is a common technique in the literature to improve enantioselectivity[18]. By reducing the temperature of the system it is hoped that, any difference in activation barrier for one enantiomer will become more pronounced. Often to compensate for this drop in conversion, extended reaction times are employed. This introduces logistical difficulties in maintaining a constant reduced temperature, -78 ^{o}C, for long periods of time, 72 hrs. An ice bath was chosen, to achieve 0 ^{o}C, and the catalyst along with base and benzaldehyde were chilled before nitromethane from the fridge was added and the reaction started. The results are displayed below along with the standard room temperature screens for comparison. A selection of the best performing catalysts were also included in this variant.

System	Room temperature		Ice Bath	
	[a]Conversion (%)	[b]ee (%)	[a]Conversion (%)	[b]ee (%)
Cu(2IM)(OTf)	75.2	0.5	7.30	6.5
Cu(2AM)(OTf)	88.5	2.5	50.4	2.8
Cu(3IM)(OTf)	87.7	5.1	33.4	12.0
Cu(3AM)(OTf)	83.3	0.4	54.6	17.0
Cu(2IM)(Cl)	66.2	18.7	45.2	63.0
Cu(3IM)(Cl)	37.3	21.7	0	-
Eu(2IN)(OTf)	51.2	36.0	37.6	3.6
Cu(3AM)(AcO)	36.0	27.4	0	-

Table 2.7. Results for the nitroaldol reaction between benzaldehyde, 1.0 mmol, and nitromethane, 10 mmol catalysed by various transition metal complexes with triethylamine as co-catalyst, 100:5:13 aldehyde:catalyst:base, ethanol used as solvent and the reaction was kept at 0 ^{0}C via a melting ice bath for 6 hours. [a]Conversion determined by ^{1}H NMR spectroscopy, [b]ee determined by chiral-HPLC OD-H column, with an error of ± 2%. Complexes were prepared *in situ*, and chilled prior to reaction.

For the same period of time, the conversions at 0 ^{0}C are lower than for those conducted at room temperature as expected. The drops in activity are not however consistent across the range of catalysts trialled, suggesting that certain catalysts might be intrinsically slower than others, Cu(**2IM**)(OTf) experiences a large decrease in conversion, some 90 % whereas others 22 %. The imines appear to perform less effectively than their amine counter parts when complexed to copper(II) triflate, likely due to the more basic character of the amine, as commented before. For complexes with a low activity at room temperature, no conversion is seen at the reduced temperature. Enantiomeric excess is improved in all cases bar that for Eu(OTf)(**2IN**). The increase is consistent with the proposed theory of accessing only one reaction pathway resulting in an enantiomerically enriched product. As with conversion, there are no patterns to this increase, with some experiencing a large increase and others less so. For the standard copper(II) triflate complexes the enantiomeric excesses are still rather low, however the copper(II) chloride complex has an impressive selectivity with a modest yield.

Due to the basic character of the chiral ligand, an investigation was undertaken to explore the possibility of using the ligand itself as a replacement for the bases used so far. As such, the complex was prepared *in situ*, and then an additional amount of ligand was added at the same molar ratio as the standard reactions, for six hours. The reaction did not proceed as expected, with an intense peak in the HPLC trace replacing the pair of peaks associated with the enantiomeric products. NMR spectra of the crude reaction mixture was also lacking the proton environments associated with the desired product. Attempts at purifying and isolating this side product proved unsuccessful via TLC or silica column purification. Repeating the reaction to yield more crude mixture at an elevated reaction time resulted in the unexpected formation of crystals within two of the catalyst screens, Cu(**2IM**)$(OTf)_2$ and Cu(**3AM**)$(OTf)_2$. Assuming that it was that of the catalyst, the unit cell was checked against those that had already yielded crystals, however the two values did not match. A full analysis of the crystal by single crystal XRD gave the structure below, Figure 2.15, with important bond lengths and angles in Table 2.9.

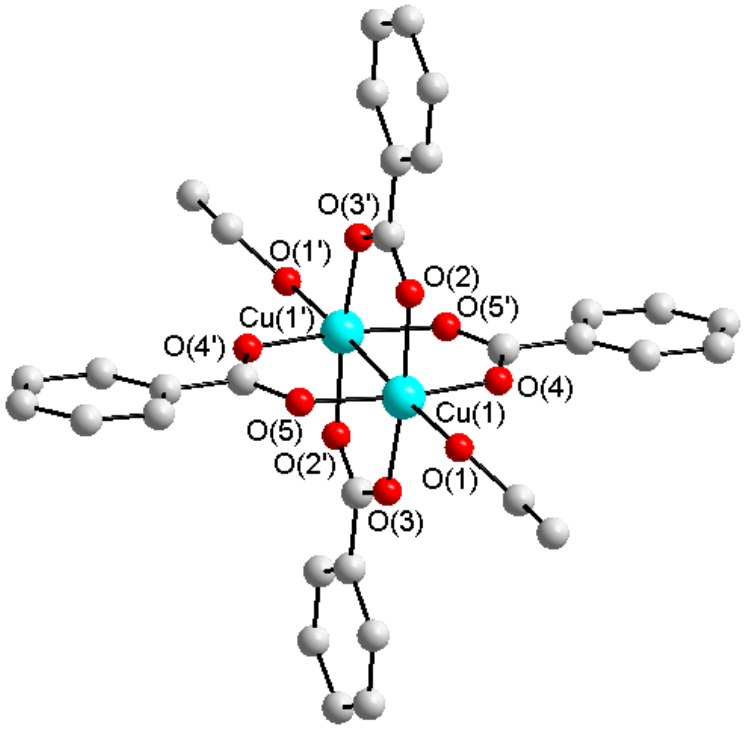

Figure 2.15. Solid-state structure of an asymmetric Henry reaction intermediate. Hydrogen atoms removed for clarity

Bond Length (Å)		Bond Angles (°)	
Cu(1) - Cu(1')	2.5788(1)	Cu(1)-O(2)-C(3)	124.841(4)
Cu(1) - O(1)	2.1392(1)	Cu(1)-O(3)-C(3)	122.919(3)
Cu(1) - O(2)	1.9503(1)	O(2)-C(3)-O(3)	28.133(2)
Cu(1) - O(3)	1.9465(1)	Cu(1)-O(4)-C(3)	
Cu(1) - O(4)	1.9346(1)	Cu(1)-O(5)-C(3)	
Cu(1) - O(5)	1.9425(1)	Cu(1)-O(3)-C(3)	

Table 2.8. Selected bond lengths and angles for the Henry reaction intermediate

The solid structure is represented by a centrosymmetric dimer of a pair of copper atoms and four benzoic acid molecules coordinating through the carboxylato oxygen atoms. There is a centre of inversion in the middle of the Cu(1)-Cu(1') distance, with symmetry generating the other half. Similar structures report the coordinated copper ion's at a distance of 2.623 Å, the difference denoting a stronger bond between the two copper ions and this is a likely result of the absence of nitro groups in the compared examples. As in these structures that reported above, the ligand has one oxygen of each carboxylato groups coordinated to each copper ion. In other examples the structures are prepared with water in place of ethanol, and the bond distance for the Cu-O is longer as a result. This is somewhat unexpected and would explain the sharp new peak in the HPLC trace. Benzoic acid can be prepared from benzaldehyde via the Cannizzaro reaction, a base catalysed disproportionation reaction resulting in benzoic acid and benzylalcohol.

In a final attempt to access high enantioselectivity under mild conditions, a different ligand was prepared, from pyridine-2,6-dicarbonyl dichloride and two equivalents of each chiral amine, in the presence of triethylamine, as shown in Figure 2.16.

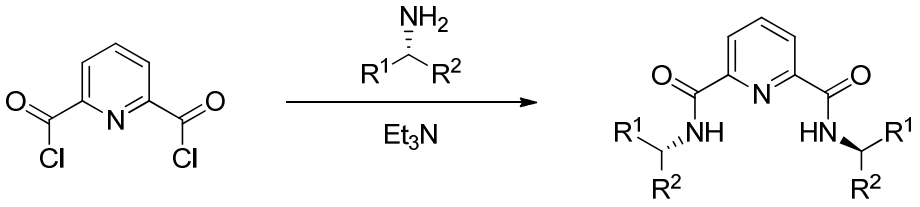

3NOMe: R^1 = Ph, R^2 = Me
3NOEt: R^1 = Ph, R^2 = Et
3NOCy: R^1 = Cy, R^2 = Me
3NONap: R^1 = naph, R^2 = Me

Figure 2.16. Preparation of 3NOX ligands

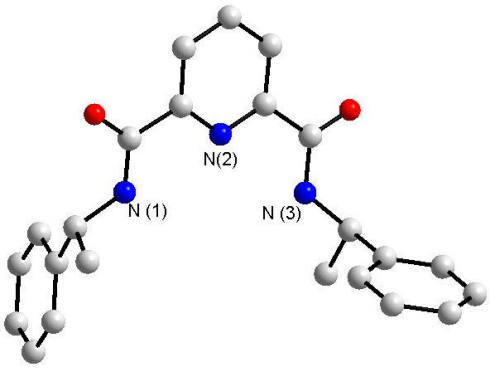

Figure 2.17. Crystal structure of ligand 3NOMe, all hydrogen atoms have been removed for clarity

Bond Length (Å)		Bond Angle (°)	
N(1)-C(15)	1.336(3)	C(15)-N(1)-C(16)	121.08(19)
N(1) - C(16)	1.469(3)	C(5)-N(2)-C(1)	117.29(18)
N(2) - C(1)	1.340(3)	C(6)-N(3)-C(7)	121.71(19)
N(2) - C(5)	1.340(3)		
N(3) - C(6)	1.341(3)		
N(3) - C(7)	1.464(3)		

Table 2.9. Selected bond lengths and angles for ligand 3NOMe

One example of this ligand gave crystals suitable for single crystal X-ray diffraction. The structure from which is given in Figure 2.17, while the important bond lengths and angles have been summarised in Table 2.9. The data collected classes the structure as that of the monoclinic, $P2_1$ space group. Bond lengths and angles are in line with typical values.

The ligands prepared were complexed to copper(II) triflate *in situ* and screened for the asymmetric nitroaldol reaction. The results are shown below, Table 2.10.

Ligand	[a]Conversion (%)	[b]ee (%)
3NOMe	15.3	0
3NOEt	11.1	0
3NOCy	11.5	0
3NONap	9.8	0

Table 2.10. Results for the nitroaldol reaction between benzaldehyde, 1.0 mmol, and nitromethane, 10 mmol catalysed by various chiral copper(II) complexes with triethylamine as co-catalyst, 100:5:13 aldehyde:catalyst:base, ethanol used as solvent and the reaction was kept at room temperature for 6 hours. [a]Conversion determined by ^{1}H NMR spectroscopy, [b]ee determined by chiral-HPLC OD-H column, with an error of ± 2%

The new class of ligand showed very limited catalytic activity toward to nitroaldol reaction. Further attempts with counter-ion variation, metal variation and increasing reaction time did not give any positive results. These ligands were therefore not further developed.

2.3.2. Conclusions

Sixteen chiral ligands were prepared and complexed to copper(II) triflate as standard. These catalysts were screened against the Henry reaction between benzaldehyde and nitromethane with triethylamine used as co-catalyst. The initial results demonstrated reasonable to high levels of conversion (88 - 36 %), however enantiomeric excess was poor. Various methods were employed to improve on the results obtained. These included varying the catalyst and varying the reaction conditions.

Changing the counter-ion from the standard triflate to a chloride or acetate generally lowered conversion and increased selectivity, while varying the metal centre to include iron, cobalt and europium, had a much more varied impact on both conversion and chiral discrimination. Reducing the temperature had the expected effect of improving selectivity while reducing reactivity. Surprising, varying the base to 1-methyl pyrrolidine and diisopropylamine, resulted in poorer conversion and improved selectivities, further studies are necessary. Using the basic character of the ligand to promote the reaction highlighted a potential issue

where a reaction intermediate or side product, containing benzoic acid, was isolated rather than the nitroalcohol product, this matter being attributed to the Cannizzaro reaction.

A second set of ligands was prepared incorporating a carbonyl group in the ligand backbone, however this ligand type proved inactive for the nitroaldol reaction.

2.4. Asymmetric Hydrogenation Reaction

2.4.1. Background

Hydrogenation is of high importance for the synthesis of organic molecules as highlighted in the Introduction. The eight chiral imine ligands prepared above along with the eight chiral amine ligands were hence complexed to palladium, commercially used in catalytic hydrogenation. It proved important to compare the differences in activity and conversion between the imine containing complexes and the amine, as the conditions used in the benchmark reactions had the potential to reduce the imine ligand, resulting in either the deactivation of the catalyst, or conversion into the other catalyst type (amine). It should be noted, that catalyst free experiments were conducted[19] as control runs for all benchmark reactions.

2.4.2. Preparation of Palladium Complexes

The ligands prepared above, Figure 2.4 and Figure 2.5, were to be complexed with palladium sources, generating systems for asymmetric hydrogenation of a range of substrates as inspired by literature. All the ligands described were complexed to palladium, generating a novel series of systems. The reaction scheme is detailed below, Figure 2.18. The resulting homogeneous catalysts were analysed by multinuclear NMR spectroscopy, mass spectrometry, elemental analysis and single crystal X-ray diffraction when possible.

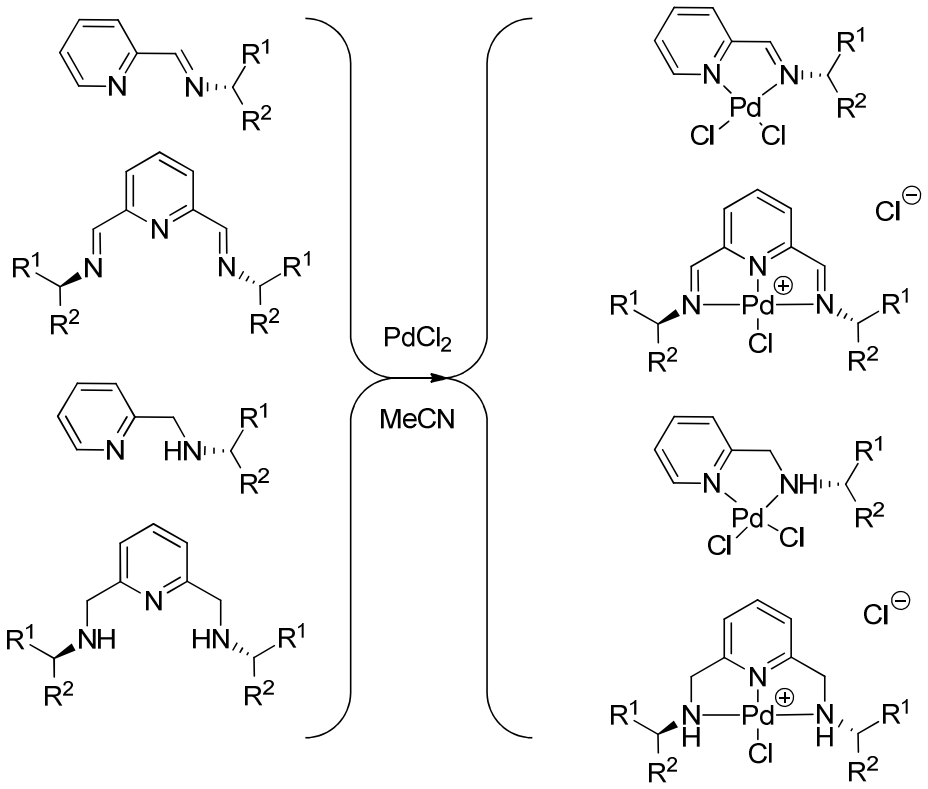

Pd(**2IM**)Cl_2: R^1 = Me R^2 = Ph
Pd(**2IE**)Cl_2: R^1 = Et R^2 = Ph
Pd(**2IC**)Cl_2: R^1 = Me R^2 = Cy
Pd(**2IN**)Cl_2: R^1 = Me R^2 = Naph

Pd(**2AM**)Cl_2: R^1 = Me R^2 = Ph
Pd(**2AE**)Cl_2: R^1 = Et R^2 = Ph
Pd(**2AC**)Cl_2: R^1 = Me R^2 = Cy
Pd(**2AN**)Cl_2: R^1 = Me R^2 = Naph

Pd(**3IM**)Cl_2: R^1 = Me R^2 = Ph
Pd(**3IE**)Cl_2: R^1 = Et R^2 = Ph
Pd(**3IC**)Cl_2: R^1 = Me R^2 = Cy
Pd(**3IN**)Cl_2: R^1 = Me R^2 = Naph

Pd(**3AM**)Cl_2: R^1 = Me R^2 = Ph
Pd(**3AE**)Cl_2: R^1 = Et R^2 = Ph
Pd(**3AC**)Cl_2: R^1 = Me R^2 = Cy
Pd(**3AN**)Cl_2: R^1 = Me R^2 = Naph

Figure 2.18. Preparation of palladium complexes from the sixteen chiral ligands prepared above

The ^{1}H NMR spectrum for Pd(**2IE**)Cl_2 is shown in Figure 2.19, along with the free ligand for comparison. Close examination does not highlight significant discrepancies, which is to be expected as the palladium source does not provide any additional proton environments. The main difference in the aliphatic and aromatic region results from a reduction of mobility of the chiral amine arm. When the ligand binds to the metal, the majority of the rotation about the nitrogen-carbon bond is removed, thus fixing the atoms of the chiral ligand, with the CH_2 group ortho to the pyridine nitrogen being diastereotopic. This has the effect on the spectra of reducing the resonance intensity, with less protons in the equivalent environment, and additional signals, due to the diastereotopic positions.

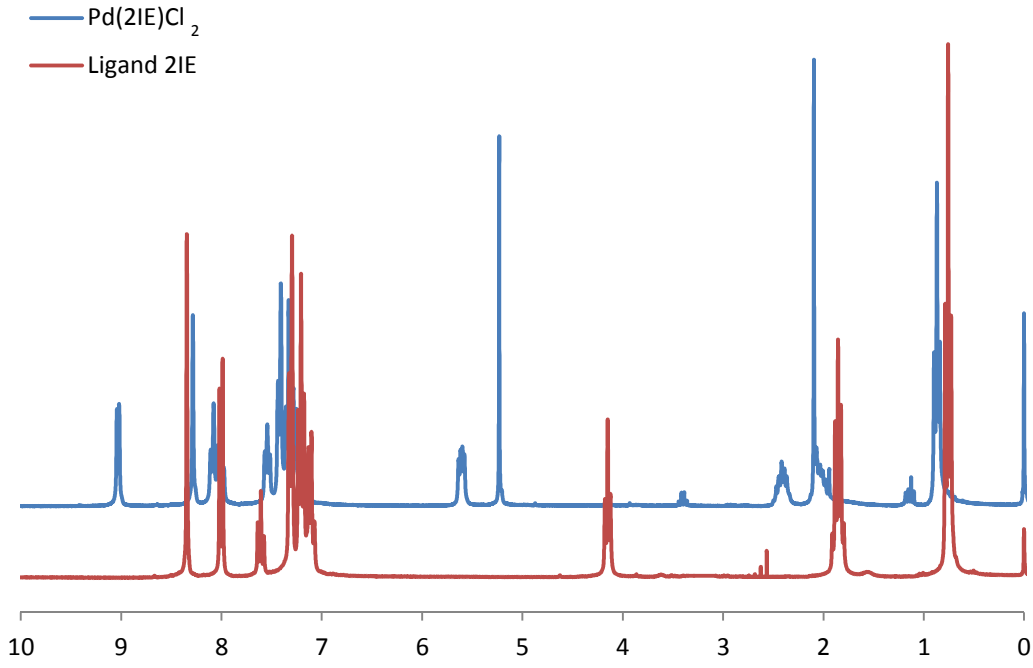

Figure 2.19. NMR spectra for the palladium complex $Pd(2IE)Cl_2$

The tridentate amine containing ligands, and to a degree the bidentate amine ligands, exhibit an additional degree of complexity in their NMR spectra. Upon coordination to a metal, the nitrogen atom of the pendant arm becomes a chiral centre, having four non-equivalent groups bonded to itself. For the bidentate, 2N, enantiomerically pure (*R*)-ligands this results in two diastereomers, S_NR_C or R_NR_C. While the tetradentate, 3N, enantiomerically pure (*R*-)ligands can now orientate themselves into one of three geometries, $S_{N1}R_{C1}S_{N2}R_{C2}$, $R_{N1}R_{C1}R_{N2}R_{C2}$, $R_{N1}R_{C1}S_{N2}R_{C2}$ (which is equivalent to $S_{N1}R_{C1}R_{N2}R_{C2}$). These are shown below, Figure 2.20.

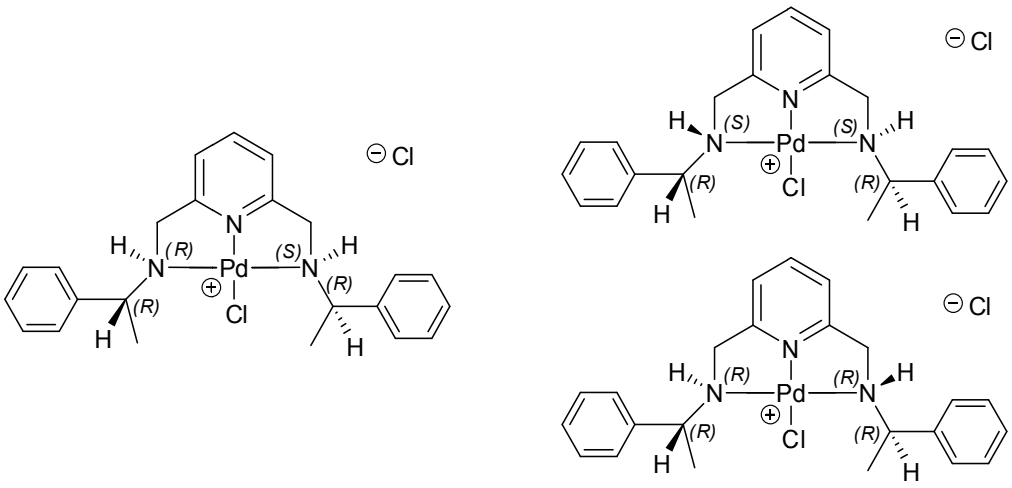

Figure 2.20. Possible configuration for a tridentate amine containing ligand

Attention is drawn to the fact that three configurations are possible for enantiomerically pure ligands, because if the racemic amine was used to prepare the ligands, then the number of possible geometries is far greater. This paired with the "locking" of the amine upon complexation results in multiple resonances from the formation of diastereotopic hydrogen atom environments. These isomers are all NMR inequivalent and complicate solution state NMR spectra as a consequence of these stereoforms all being present

A selection of single crystals suitable for X-ray diffraction were grown and the structures are shown below. Only one example of a bidentate imine-containing chiral ligand complexed to palladium chloride was successfully crystallised and the structure of Pd(**2IC**)Cl_2 is shown below, Figure 2.21, with selected bond distances and angles listed in Table 2.11.

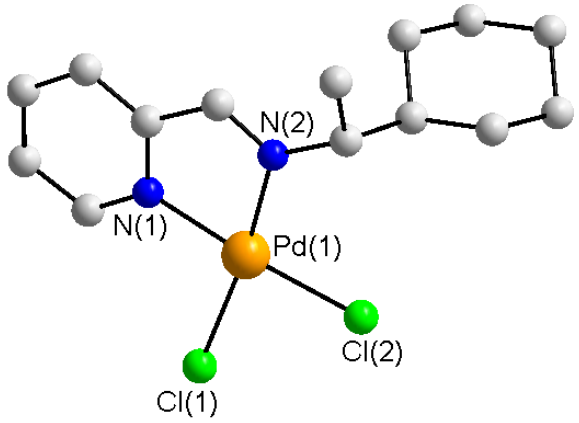

Figure 2.21. The solid-state structure for Pd(2IC)Cl_2. All hydrogen atoms have been removed for clarity

Length (Å)		Angle (^{0})	
Pd(1)-N(1)	2.026(4)	N(1)-Pd(1)-N(2)	80.75(17)
Pd(1)-N(2)	2.034(4)	N(1)-Pd(1)-Cl(1)	94.07(12)
Pd(1)-Cl(1)	2.2863(12)	N(2)-Pd(1)-Cl(1)	172.57(11)
Pd(1)-Cl(2)	2.2885(17)	N(1)-Pd(1)-Cl(2)	175.74(12)
		N(2)-Pd(1)-Cl(2)	95.40(14)
		Cl(1)-Pd(1)-Cl(2)	89.94(5)

Table 2.11. Selected bong lengths (Å) and bond angles (^{0}) for the solid-state structure of Pd(2IC)Cl_2

The data collected shows that the structure belongs to the monoclinic *P*2 space group. The absolute structure parameter is -0.02(4), which indicates that the complex is enantiomerically pure. The bond lengths and angles are in agreement with literature values of similar complexes[20-23].

The Cl(1)-Pd(1)-Cl(2) angle is very close to 90° suggesting that the geometry around the palladium atom is distorted square planar, which is expected. The cause of this distortion raised from the N(1)-Pd(1)-N(2) bond angle which is smaller than 90°, due to the strain imposed by the ligand, and the remaining N-Pd-Cl angles compensate for this short coming, 95.40(14) ° and 94.07(12)°, totalling 360.2° around the palladium atom. The Pd-Cl bond lengths, 2.28 Å, are less than the sum of their covalent radii, Σcov(Pd, Cl) 2.41 Å, suggesting some degree of polar character.

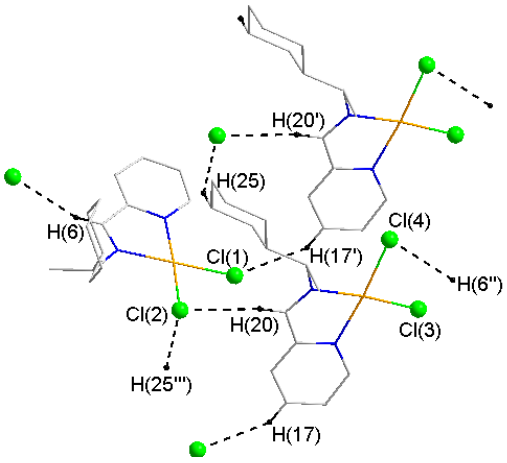

Figure 2.22. Crystal structure of Pd(2IC)Cl_2 showing the hydrogen bonding.

In the crystal, the chlorine atoms interact intermolecularly with hydrogen atoms from neighbouring molecules [Cl(1)···H(17') 2.7403(15) Å, Cl(2)···H(20)

2.8604(14) Å, Cl(2)···H(25’’’) 2.6255(18) Å, Cl(4)···H(6’’) 2.6493(15) Å], Figure 2.22, to form a two-dimensional layer-type arrangement along bisecting line of axes *a* and *b*, Figure 2.23.

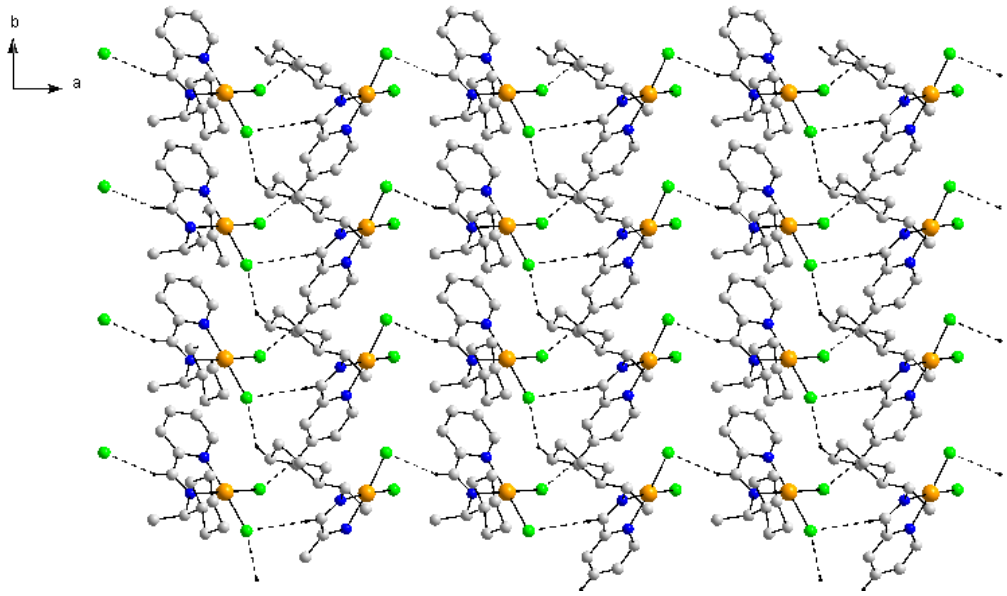

Figure 2.23. Supramolecular structure of Pd(2IC)Cl_2

Pd(**2AN**)Cl_2 was unobtainable as a single crystal resulting in the incomplete collection of crystals for this subgroup of ligands. Pd(**2AM**)Cl_2 is detailed below, Figure 2.24, with selected bond lengths and angles in Table 2.12.

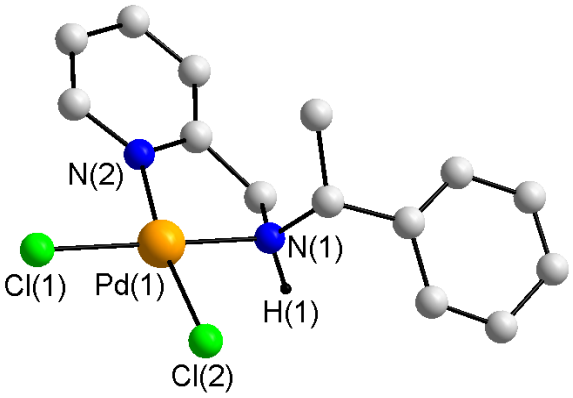

Figure 2.24. Solid-state structure for Pd(2AM)Cl_2. The hydrogen atoms, not involved in hydrogen bonding, have been omitted for clarity

It should be noted that convergence was optimised after accounting for 35 % twinning about the reciprocal *a* axis. Residual electron density maxima are in non-chemically significant regions of the difference Fourier map. A molecule of

Et_2O was also present in the asymmetric unit and this has been omitted for clarity along with the hydrogen atoms.

Length (Å)		Angle (°)	
Pd(1)-N(1)	2.007(5)	N(2)-Pd(1)-N(1)	82.5(2)
Pd(1)-N(2)	2.060(5)	N(2)-Pd(1)-Cl(1)	94.86(16)
Pd(1)-Cl(1)	2.3036(16)	N(1)-Pd(1)-Cl(1)	176.44(17)
Pd(1)-Cl(2)	2.3063(18)	N(2)-Pd(1)-Cl(2)	171.11(16)
		N(1)-Pd(1)-Cl(2)	89.38(16)
		Cl(1)-Pd(1)-Cl(2)	93.43(6)

Table 2.12. Selected bond lengths (Å) and bond angles (^{0}) for the solid-state structure of Pd(2AM)Cl_2

The crystal studied for Pd(**2AM**)Cl_2 experienced a degree of twinning. As such two or more crystals intergrowning to one another. The data collected states that the structure belongs to the monoclinic $P2_1$ space group. The absolute structure parameter is -0.04(4), it can therefore be said that the complex is enantiomerically pure. The bond lengths and angles are in agreement with literature values[24] of similar complexes; Pd(1)-N(1) 2.007(5) Å compared to 2.0250(17) Å, and Pd(1)-Cl(1) 2.3036(5) Å vs. 2.3103(6) Å while N(1)-Pd(1)-N(2) angle of 82.5(2) ^{0} is in close agreement with 81.988(66) ^{0} and that of N(1)-Pd(1)-Cl(1) 176.44(17) ^{0} vs. 177.101(48) ^{0}.

It should be noted, that complexation with **2AM**, compared to the structure of Pd(**2IC**)Cl_2, Figure 2.21, has created a new chiral centre at the coordinating nitrogen atom from the pendant arm and the possibility of an *R* or *S* configuration. The solid structure above has an *S* configuration and the control of this centre is attributed to the chirality of the amine used[24]. Comparing the solid-state structure to the solution-state, it is possible to see multiple diastereomers in the ^{1}H NMR spectra, which has the effect of complicating an otherwise straightforward spectrum.

The crystal structure for Pd(**2AE**)Cl_2 is shown below, Figure 2.25, with the data indicating that the structure belongs again to the monoclinic $P2_1$ space group, just as Pd(**2AM**)Cl_2. An absolute structure parameter of -0.016(17) is

indicative of an enantiomerically pure complex. The recorded bond lengths and angles, Table 2.13, are in concurrence with literature values of similar complexes[24-27].

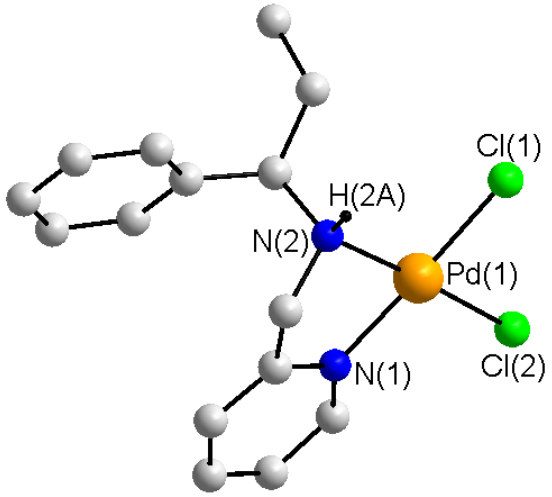

Figure 2.25. Solid state structure for Pd(2AE)Cl_2, hydrogen atoms, not involved in hydrogen bonding, were removed for clarity.

Length (Å)		Angle (°)	
Pd(1)-N(1)	2.0285(15)	N(1)-Pd(1)-N(2)	81.88(6)
Pd(1)-N(2)	2.0565(15)	N(1)-Pd(1)-Cl(1)	172.92(4)
Pd(1)-Cl(1)	2.2824(5)	N(2)-Pd(1)-Cl(1)	92.34(5)
Pd(1)-Cl(2)	2.3082(4)	N(1)-Pd(1)-Cl(2)	94.23(4)
		N(2)-Pd(1)-Cl(2)	175.43(5)
		Cl(1)-Pd(1)-Cl(2)	91.705(18)

Table 2.13. Selected bond lengths (Å) and bond angles (^{0}) for the solid state structure of Pd(2AE)Cl_2

With the modification between **2AM** and **2AE** being outside of the coordination sphere of the metal, it should be expected for the bond lengths and angles to be the same and such is the case, however the configuration at the new chiral centre is *R* as opposed to *S*. Again, in the solution-state diastereomers are observed from the ^{1}H NMR spectroscopy.

Finishing this subgroup of complexes is Pd(**2AC**)Cl_2, Figure 2.26, and our first deviation from the monoclinic space group experienced so far, with the collected information indicating that the structure belongs to the orthorhombic $P2_12_12_1$ space group, with all three lattice vectors intersecting at a 90° angle.

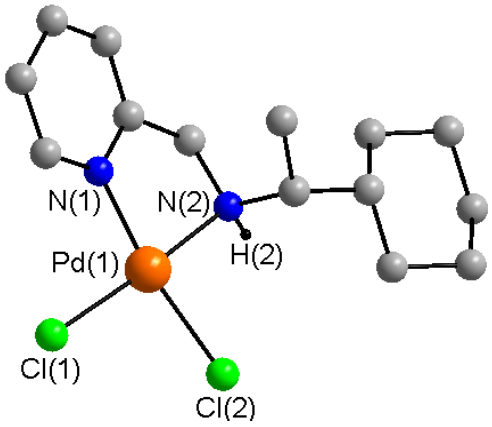

Figure 2.26. Two crystallographic unique palladium centres where observed. One carbon atom was isotropically refined, Hydrogen atoms, not involved in hydrogen bonding, and a CH_2Cl_2 molecule have been removed for clarity.

The absolute structure parameter, -0.05(9), indicates that the complex is enantiomerically pure, and all lengths and bonds, Table 2.14, are in agreement with literature values[24].

Length (Å)		Angle (°)	
Pd(1)-N(1)	2.045(12)	N(1)-Pd(1)-N(2)	82.0(5)
Pd(1)-N(2)	2.038(11)	N(1)-Pd(1)-Cl(1)	94.9(4)
Pd(1)-Cl(1)	2.301(4)	N(2)-Pd(1)-Cl(1)	176.8(3)
Pd(1)-Cl(2)	2.305(4)	N(1)-Pd(1)-Cl(2)	171.7(4)
		N(2)-Pd(1)-Cl(2)	89.7(3)
		Cl(1)-Pd(1)-Cl(2)	93.30(14)

Table 2.14. Selected bond lengths (Å) and bond angles (^{0}) for the solid state structure of Pd(2AC)Cl_2

Two tridentate ligands, both amine containing, afforded suitable crystals for single crystal X-ray diffraction, the "standard" Pd(**3AM**)Cl_2 and the more sterically bulky Pd(**3AN**)Cl_2. The first is shown below, Figure 2.27. Selected bond lengths and bond angles are listed in Table 2.15.

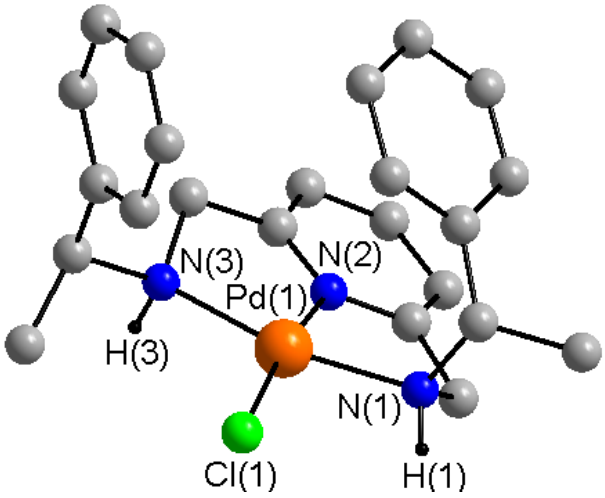

Figure 2.27. Two palladium centres are present, only one shown for use.
The Cl^- anions and the water of crystallisation have been removed for clarity.

The structure above belongs to the triclinic *P1* space group as evident from the data collected. An absolute structure parameter of -0.04(4) is indicative of an enantiomerically pure complex. The recorded bond lengths and angles are in concurrence with literature values of similar complexes[28,29]. The Pd(II) centre was, as expected, in a square planar geometry as illustrated by the N(1)-Pd(1)-Cl(1) angles of 92.8(3) °.

Length (Å)		Angle (°)	
Pd(1)-N(2)	1.939(8)	N(2)-Pd(1)-N(1)	81.5(4)
Pd(1)-N(1)	2.029(9)	N(2)-Pd(1)-N(3)	80.1(4)
Pd(1)-N(3)	2.081(8)	N(1)-Pd(1)-N(3)	161.4(3)
Pd(1)-Cl(1)	2.309(3)	N(2)-Pd(1)-Cl(1)	172.5(3)
		N(1)-Pd(1)-Cl(1)	92.8(3)
		N(3)-Pd(1)-Cl(1)	105.8(2)

Table 2.15. Selected bond lengths (Å) and bond angles (^{0}) for the solid state structure of $Pd(3AM)Cl_2$

The tridentate amine ligands create an additional pair of chiral centres upon complexation, at the pendant arm nitrogen atoms. For the above structure, the N(1) atom has an *S* configuration, while the N(3) atom has an *R* configuration, while those at Pd(2) are reversed with N(4) having an *R* configuration and N(6) an *S*. This would suggest that there are two diastereomers in the solid state, as stated earlier.

The palladium solid-structure for Pd(**3AM**)Cl_2, as well as all amine containing ligands presented here, would infer a straightforward, simple and single solution-structure. However, multiple diastereomers are observed in the solution state ^{1}H NMR spectra of this class of compounds. The possible diastereomers of Pd(**3AE**)Cl_2 are shown in Figure 2.28.

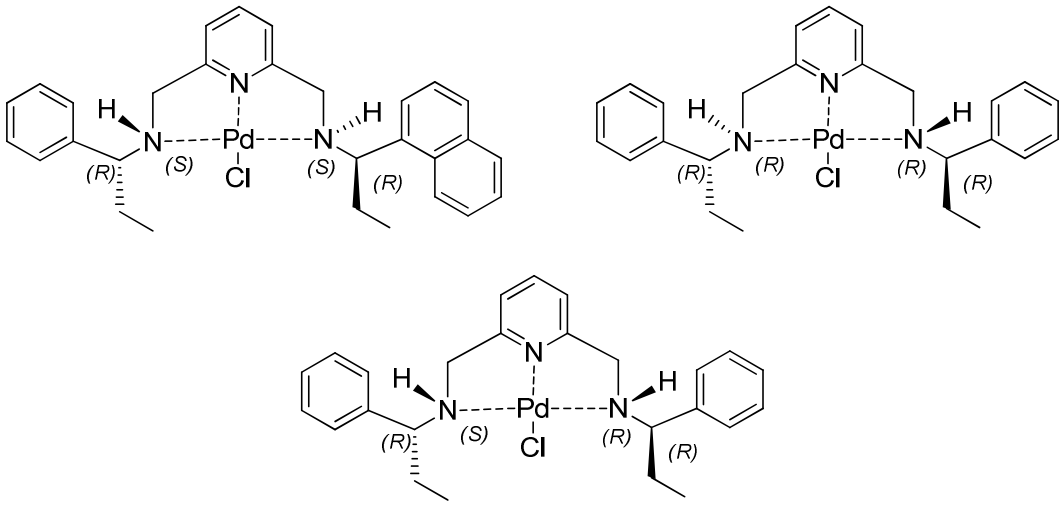

Figure 2.28 Three possible diastereomers present in solution for Pd(3AE)Cl_2

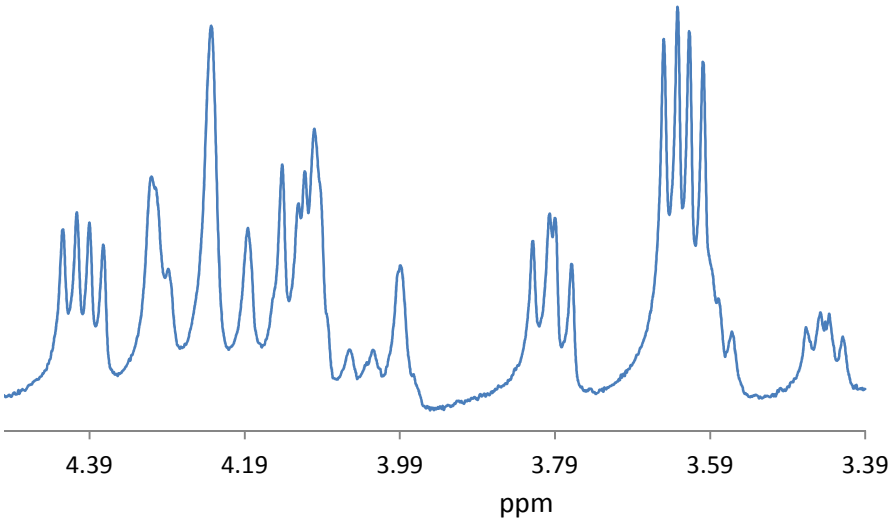

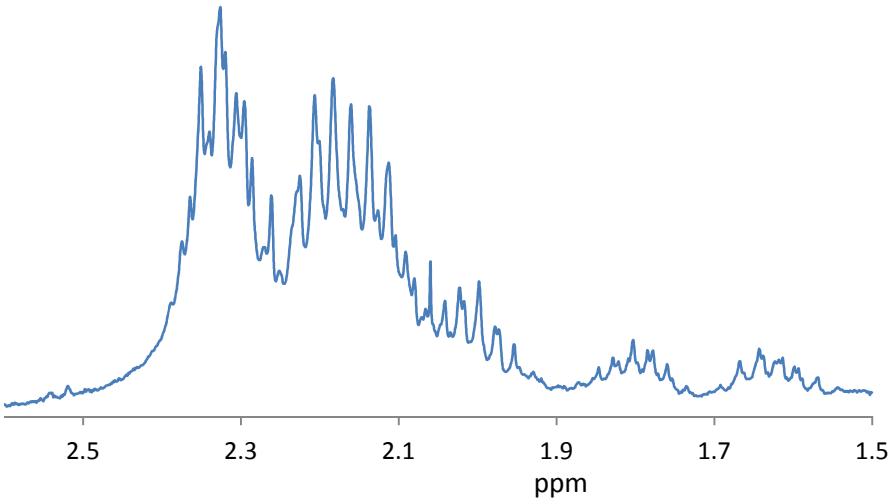

Figure 2.29. Selections of the ^{1}H NMR spectrum for Pd(3AM)Cl_2. The exact assignment cannot be achieved due to mixture of compounds.

Each diastereomer has inequivalent proton environments, the presence of which results in difficult peak assignment of the ^{1}H NMR spectrum, as can be seen from the two regions of the ^{1}H NMR spectrum of Pd(**3AE**)Cl_2 shown in Figure 2.29. The electronegative region of the ^{1}H NMR spectrum (3.4 - 4.4 ppm) for the free ligand contains the resonance signals for the environments neighbouring the amine-nitrogen, containing a pair of resonance signals, a singlet and a triplet, of 2 H and 1 H respectively. However, the same region from the ^{1}H NMR spectrum of the palladium complex is more complicated as a result of the diastereomers. While typically, for the higher field aliphatic region it would be expected to see a quartet for the -CH_2- of the ethyl chain. However, due to the different diastereomers present, the region between 1.5 and 2.5 ppm contains several more complexly split resonances.

The crystal structure of Pd(**3AN**)Cl_2 is shown below, Figure 2.30, and selected bond distances and angles are reported in Table 2.16.

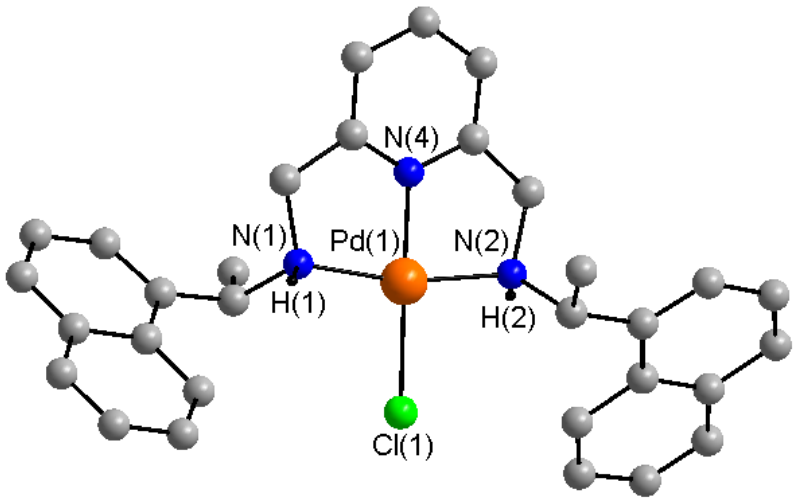

Figure 2.30 The non-coordinated Cl anion has been removed for clarity as have two half occupied MeOH moieties and a water molecule, along with some hydrogen atoms, not involved in the hydrogen bonding network

Length (Å)		Angle (°)	
Pd(1)-N(2)	1.936(5)	N(2)-Pd(1)-N(3)	83.9(2)
Pd(1)-N(3)	2.053(6)	N(2)-Pd(1)-N(1)	83.6(2)
Pd(1)-N(1)	2.052(5)	N(3)-Pd(1)-N(1)	167.4(2)
Pd(1)-Cl(1)	2.3172(14)	N(2)-Pd(1)-Cl(1)	177.2(4)
		N(3)-Pd(1)-Cl(1)	96.15(16)
		N(1)-Pd(1)-Cl(1)	96.35(15)

Table 2.16. Selected bond lengths (Å) and bond angles (^{0}) for the solid state structure of $Pd(3AN)Cl_2$

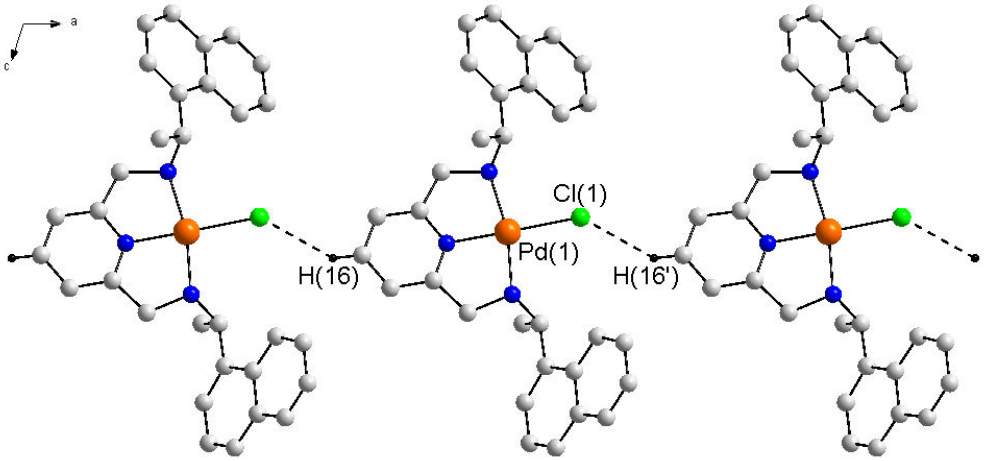

Figure 2.31. Crystal structure of $Pd(3AN)Cl_2$ showing the intermolecular interactions.

Unlike the previous complex, Pd(**3AM**)Cl_2, the complex prepared with **3AN**, in the solid state crystal structure with two new chiral centres with the same configuration, *S*, of at the nitrogen atom of each of the pendant arms. This structure is also monoclinic, whereas the previous triclinic, and belongs to the $P2_1$ space group. An absolute structure parameter of 0.00(5) indicates that the structure is enantiomerically pure. Bond lengths and angles are in close agreement with the similar structure recorded, similar structures in the literature, and literature values[28,29].

2.4.3. Direct Hydrogenation

The palladium complexes developed above were screened for the asymmetric hydrogenation of olefins, with dimethyl itaconate chosen as the primary substrate, the reaction scheme is shown in Figure 2.32. The proposed mechanism for which can be seen in Figure 2.33.

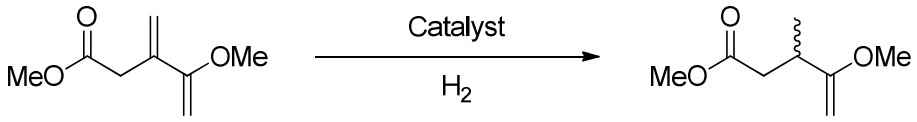

Figure 2.32. Reaction scheme for the direct asymmetric hydrogenation of dimethyl itaconate

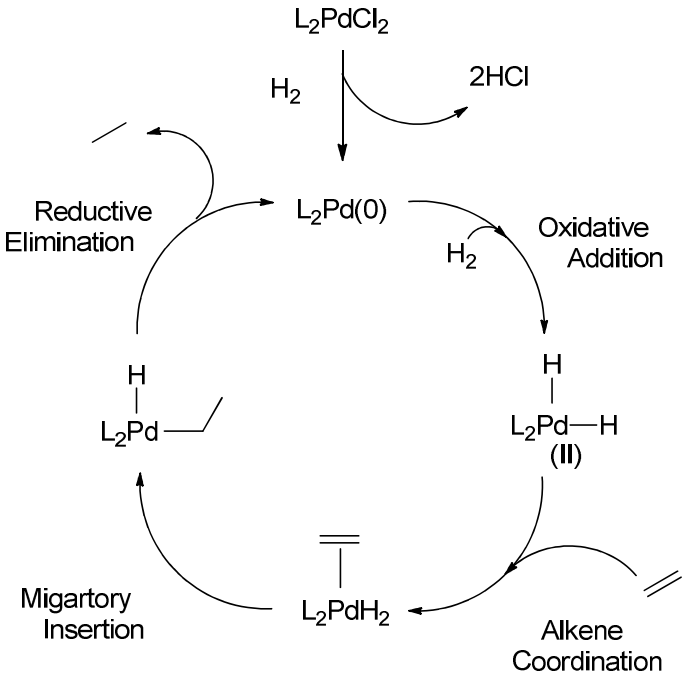

Figure 2.33. Schematic representation of the mechanism for direct hydrogenation by a palladium(II) catalyst

Firstly, the Pd(II) is reduced to Pd(0) before hydrogen gas is oxidatively added, to the Pd(0) species generating a hydride complex, now Pd(II). This is followed by coordination of the alkene forming the π-coordinated Pd(II) system, which is followed in step by migratory insertion of a hydride into the C=C bond. The final step, closing the catalytic cycle, is reductive elimination, generating the alkane product and the catalytically active starting material.

The goal was to select the most promising catalysts and investigate the substrate sensitivity of these catalysts. Dimethyl itaconate was chosen due to its stability, solubility and availability. More importantly, the spectroscopic differences between dimethyl itaconate and its reduction product, dimethyl succinate, are striking, thus allowing the conversions and selectivity to be readily determined. Firstly, the proton environments due to the unsaturation in the substrate are more downfield toward the aromatic region of the spectrum, centred around 6 ppm. Also geminal splitting is encountered as the terminal protons of the carbon unsaturation being inequivalent, resulting in them being unique. This pair of peaks merge and shift considerable upfield in the product structure appearing at around 1ppm spilt as a result of the second additional proton on the tertiary carbon. Secondly, the racemic product can be easily separated by chiral high performance liquid chromatography (HPLC) *via* the chiral Daicel OD-H column.

The initial screen was carried out in a Parr high pressure bomb reactor, a closed vessel, with the reaction mixture contained in a glass sleeve and a mechanical metallic stirrer. Hydrogen gas addition is controlled and monitored by taps and a pressure gauge. The catalyst screen encompassed all the palladium catalysts prepared above and the results are shown in Table 2.17.

Catalyst	Time (h)	[a]Pressure (bar)	[b]Conversion (%)	[c]ee (%)	Yield (%)
Pd(**3IM**)Cl_2	24	5	> 99	0	0
Pd(**3IE**)Cl_2	24	5	100	1	1
Pd(**3IC**)Cl_2	24	5	> 99	2	2
Pd(**3IN**)Cl_2	24	5	> 99	4	4
Pd(**2IM**)Cl_2	24	5	99	5	5
Pd(**2IE**)Cl_2	24	5	100	0	0
Pd(**2IC**)Cl_2	24	5	100	2	0
Pd(**2IN**)Cl_2	24	5	> 99	3	3
Pd(**3AM**)Cl_2	24	5	100	4	4
Pd(**3AE**)Cl_2	24	5	99	3	3
Pd(**3AC**)Cl_2	24	5	100	1	1
Pd(**3AN**)Cl_2	24	5	100	3	3
Pd(**2AM**)Cl_2	24	5	100	1	1
Pd(**2AE**)Cl_2	24	5	100	2	2
Pd(**2AC**)Cl_2	24	5	100	0	0
Pd(**2AN**)Cl_2	24	5	> 99	2	2

Table 2.17. Results for the direct hydrogenation of dimethyl itaconate with various chiral palladium(II) complexes and H_2 gas, 100:1 substrate:catalyst, methanol used as solvent and the reaction was kept at room temperature. The reaction vessel was purged 3 times with hydrogen gas, to exclude air, before being kept under an ambient pressure, by a hydrogen filled party balloon. [a]Conversion determined by ^{1}H NMR spectroscopy, [b]ee determined by chiral-HPLC OD-H column, with an error of ± 2%.

Upon initial observation conversions are all very high, with no variation when using a bi-dentate vs tri, nor amine vs imine. However, no chiral discrimination is detected. In reality, the reaction conditions are too harsh for the catalytic systems developed. The reaction mixture prior to reaction is typically a clear yellow solution, with the catalyst and substrate both dissolving in methanol. Post-reaction, the solution mixture is colourless with a black precipitate.

Background reactivity of hydrogen with dimethyl itaconate was ruled out as the culprit to this impressive activity but poor enantiomeric excess, with a catalyst free reaction under the same conditions only converting around 5 % of

the substrate. A black precipitate has been encountered by different groups working with PGM[30,31], indeed preparing iridium complexes is difficult as "iridium black" is a phenomenon which occurs from instability in the complexes[32]. Research has been conducted on the purposeful formation of palladium black for the formation of nanoparticles[33-35] fuel cells[36,37] and as a heterogeneous catalyst[38]. However the palladium systems prepared are stable in an open vessel, dissolved in reaction grade methanol for prolonged periods of time. Indeed, the majority of single crystals characterised by XRD were prepared by evaporation of solvent in this open manner. Palladium black can be used as a catalyst for hydrogenation reactions as it is a sponge-like, coarse, form of elemental palladium. The large surface area which is offered is ideal for hydrogen adsorption. However, a black precipitate of elemental palladium is also referred to colloquially as palladium black within the literature, having been fashioned from the decomposition of a palladium(II) complex. To fully ascertain the precise nature of this deactivation control experiments involving Pd nanoparticles on SiO_2 could be trialled. However, the focus of this work was to prepare catalysts for enantioselective processes. Due to the very low ee's this line of enquiry was abandoned. However, previous work in the Jones group[19] showed similar results with similar ligands. Time permitting, one could also investigate tests with Pd(0) on different supports, (Pd/C, Pd/Si, Pd/Al_2O_3 etc.).

Investigating the reaction mechanism can shed light upon the matter. While the vast majority of organopalladium studies are centred on the use of Pd(II) but also Pd(0), and in several publications the active catalyst is not clearly outlined[39,40]. As such a general cycle of reactivity can be proposed where the Pd(II) complex can switch with the coordinated Pd(II)-substrate transition state, by ligand substitution, insertion, β-hydride elimination, which undergoes reductive elimination generating a Pd(0) species before oxidation or oxidative addition regenerates the Pd(II) catalyst.

In summary, decomposition of the palladium(II) compounds resulted in elemental palladium(0), palladium black. Under the reaction conditions present this would catalyse the non-selective reduction of dimethyl itaconate to high conversions. It was hoped that conducting the reaction under more mild conditions would circumvent the formation of palladium black, to afford the

asymmetric hydrogenation of dimethyl itaconate. As such, the catalysts prepared above were repeated on the bench, in a round bottom flask, under an atmosphere of hydrogen. The results are given in Table 2.18.

Catalyst	Time (h)	Pressure (bar)	[a]Conversion (%)	[b]ee (%)	Yield (%)
Pd(**3IM**)Cl_2	24	1	5.0	-	-
Pd(**3IE**)Cl_2	24	1	5.5	-	-
Pd(**3IC**)Cl_2	24	1	4.1	-	-
Pd(**3IN**)Cl_2	24	1	12	3	0.4
Pd(**2IM**)Cl_2	24	1	7.7	2	0.2
Pd(**2IE**)Cl_2	24	1	11	1	0.1
Pd(**2IC**)Cl_2	24	1	6.9	-	-
Pd(**2IN**)Cl_2	24	1	20	3	0.6
Pd(**3AM**)Cl_2	24	1	10	1	0.1
Pd(**3AE**)Cl_2	24	1	8	5	0.4
Pd(**3AC**)Cl_2	24	1	8.7	3	0.3
Pd(**3AN**)Cl_2	24	1	18	4	0.7
Pd(**2AM**)Cl_2	24	1	16	2	0.3
Pd(**2AE**)Cl_2	24	1	8.9	0	0
Pd(**2AC**)Cl_2	24	1	25	2	0.5
Pd(**2AN**)Cl_2	24	1	28	1	0.3

Table 2.18. Results for the direct hydrogenation of dimethyl itaconate with various chiral palladium(II) complexes and H_2 gas, 100:1 substrate:catalyst, methanol used as solvent and the reaction was kept at room temperature. The reaction vessel was a glass round bottom flask complete with suba seal, with hydrogen gas being delivered by latex balloon. The system was purged for a few seconds with hydrogen gas, to exclude air, before being sealed. [a]Pressure is assumed to be 1 bar, investigations on the pressure of typical latex balloons show that the pressure remains fairly constant at 1.08 bar once the latex has begun stretching, however it is possible for solvent vapours to mix with the hydrogen and destroy the polymer matrix, [b]Conversion determined by ^{1}H NMR spectroscopy, [b]ee determined by chiral-HPLC OD-H column, with an error of ± 2%.

A significant drop in conversion is observed and could be linked to the absence of any background reduction which previously contributed 5%, however as seen from the blank Parr reactor run, the contribution is rather small, and would not account for such short comings. Another explanation for the drop in conversion can be attributed to the availability of hydrogen, in the pressurised reaction there is 20 times as much reducing agent, and the pressure would ensure

that it dissolves to a degree into the solvent. Under a balloons pressure of hydrogen and in accordance with Henry's law, the amount of hydrogen in the solvent would be less. The tridentate complexes are somewhat less active than their bidentate complement, this could be attributed to the initial activation of the molecular hydrogen, as commented on above, the removal of a ligand for substrate coordination, or the steric bulk around the palladium metal. With only one metal-chloride, activation of H_2 becomes more specific, unlike in the bidentate systems where there are two possible means to form a metal-hydride. The size of the **3N** ligands may be a factor, with the second chiral amine moiety becoming more of a hindrance when it comes to coordination of the alkene, adjusting the geometry to accommodate the incoming substrate before a nitrogen atom dissociates. For all but one case, the amine containing ligands are more active than their imine counterparts. One possible cause could be reduction of the ligand prior to reaction, or the rigidity of the imine double bond when it comes to dissociation. These differences were not further investigated as they are small variations but more importantly, enantioselectivity is again poor, and at this stage, selectivity ranks higher than activity.

The problem of palladium black is still present, and clearly visible when purging the system. While hydrogen gas is bubbled through the catalytic mixture, the palladium precipitate appears. When the system has been purged and left under hydrogen, the rapid decomposition of the catalyst ceases, however after the full time allocated for the reaction to proceed, additional palladium black had formed. This rapid decomposition of the catalyst while purging the system explains the low enantiomeric excesses expressed in the Parr reactor, where the purging process uses much more hydrogen. It is highly possible that the complete catalyst present in the reactor vessel is decomposed before the system is taken to pressure and left to react for the desired time (24 h).

Two approaches were taken to overcome this issue and develop an asymmetric hydrogenation system, redesign of the ligand and redesign of the reaction. Employing transfer hydrogenation removes molecular hydrogen from the system, typically using a secondary alcohol as a hydrogen source, Figure 2.34. This is attractive industrially as it eliminates the need for an explosive gas under

pressure[41]. Heterogeneous asymmetric transfer hydrogenation systems are limited in the literature so successful systems would be highly sought after.

2.4.4. Transfer Hydrogenation

The ligands introduced above are once again complexed with palladium and screened for the asymmetric transfer hydrogenation of ketones (acetophenone). Isopropanol was chosen as the hydrogen source and potassium hydroxide was present in a low concentration, 4.3 $\times 10^{-5}$ mol dm^{-3}, as shown in Figure 2.34.

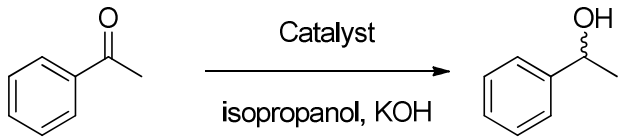

Figure 2.34. Asymmetric transfer hydrogenation of acetophenone

Acetophenone was chosen due to the spectroscopic differences of the starting material and product, enabling straightforward calculation of the conversion from ^{1}H NMR and enantiomeric excess from chiral-HPLC. The ^{1}H NMR spectra, Figure 2.35, show the singlet of the methyl group in acetophenone at 2.6 ppm being split in the secondary alcohol product with chemical shift 1.5 ppm. Integration and comparison of these two peaks facilitates calculation of conversion.

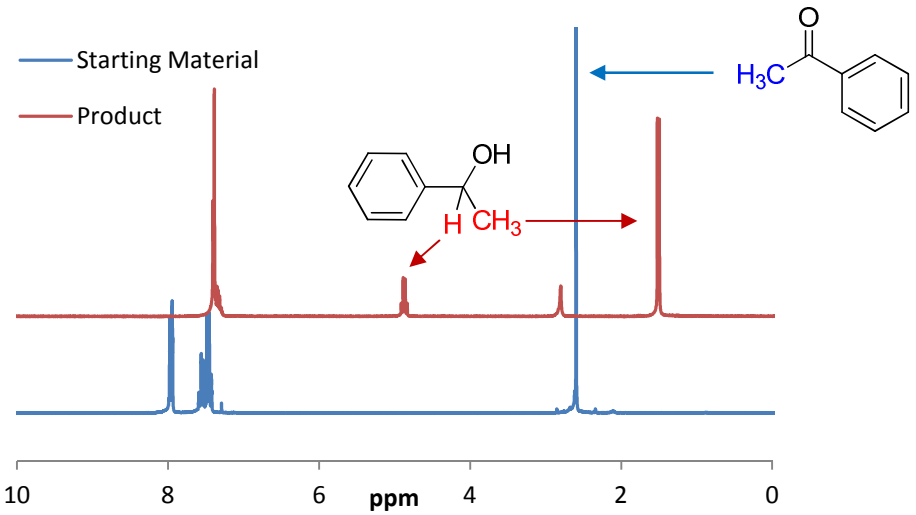

Figure 2.35. Comparison of 1H NMR spectra for the asymmetric transfer hydrogenation of acetophenone

Table 2.19, over the page, shows the results obtained for the transfer hydrogenation of acetophenone with the palladium complexes prepared earlier. Low to no conversion is observed which is not unusual for palladium complexes and is indeed in accordance with literature, which agree that these are poor catalysts[42]. Due to the prevalence of palladium complexes in the literature for the direct hydrogenation of ketones, it would suggest that the method employed here is non-compatible with the complexes described herein. The reactions were repeated at an extended reaction time with the hope of yielding more material to better ascertain the selectivity of the complexes. In general, greater conversion was achieved however the conversion did not increase linearly, suggesting that the catalysts perform at varying rates. Enantiomeric excess is poor, and comparisons between catalysts cannot be made due to such low values and the errors involved. The use of a strong hydroxide, even at low concentrations, encourages decomposition of the catalyst rendering it catalytically inactive, which can go to explain some of the low conversion. This is not the case for all PGM metals, with rhodium and ruthenium the more common options for the transfer hydrogenation reaction[43-49]. As a continuation to attempt to yield a successful catalytic complex for heterogenisation, rhodium complexes were prepared from the 2N series of amine and imine ligands, and will be discussed now.

Catalyst	Time (h)	Conversion (%)[a]	ee (%)[b]	Yeild (%)
Pd(**3IM**)Cl_2	24	8	0	0
	48	12	1	0.1
Pd(**3IE**)Cl_2	24	5	2	0.1
	48	26	1	0.3
Pd(**3IC**)Cl_2	24	11	0	0
	48	28	0	0
Pd(**3IN**)Cl_2	24	10	3	0.3
	48	23	4	0.9
Pd(**2IM**)Cl_2	24	8	3	0.2
	48	32	3	1.0
Pd(**2IE**)Cl_2	24	18	2	0.4
	48	51	1	0.5
Pd(**2IC**)Cl_2	24	15	1	0.3
	48	29	1	0.3
Pd(**2IN**)Cl_2	24	12	3	0.4
	48	35	1	0.4
Pd(**3AM**)Cl_2	24	10	2	0.2
	48	23	3	0.7
Pd(**3AE**)Cl_2	24	9	4	0.4
	48	44	3	1.3
Pd(**3AC**)Cl_2	24	12	0	0
	48	35	2	0.7
Pd(**3AN**)Cl_2	24	9	2	0.2
	48	21	1	0.2
Pd(**2AM**)Cl_2	24	11	1	0.1
	48	28	4	1.1
Pd(**2AE**)Cl_2	24	10	0	0
	48	31	1	0.3
Pd(**2AC**)Cl_2	24	24	5	1.2
	48	46	5	2.3
Pd(**2AN**)Cl_2	24	22	6	1.3
	48	51	4	2.0

Table 2.19. Results for the transfer hydrogenation of acetophenone with various chiral palladium(II) complexes, isopropanol as a hydrogen source and KOH as a co-catalyst 100:1:1 substrate:catalyst:KOH, 4.29×10^{-5} mol dm^{-3} KOH in isopropanol solution used as solvent and the reaction was kept at room temperature. [a]Conversion determined by ^{1}H NMR spectroscopy, [b]ee determined by chiral-HPLC OD-H column, with an error of ± 2%.

2.4.5. Preparation of Rhodium Complexes

Following the poor performance of the palladium catalysts prepared, other platinum group metals were employed which have reported success for the transfer hydrogenation reaction[43-49]. The reaction scheme for the preparation of rhodium(I) complexes can be seen below, Figure 2.36.

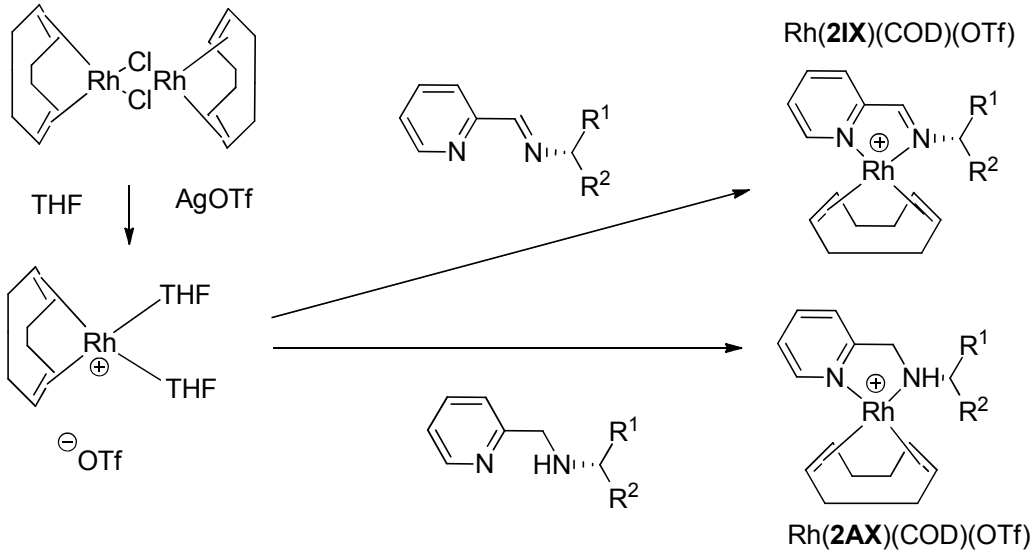

Rh(**2IM**)(COD)(OTf): R^1 = Me R^2 = Ph
Rh(**2IE**)(COD)(OTf): R^1 = Et R^2 = Ph
Rh(**2IC**)(COD)(OTf): R^1 = Me R^2 = Cy
Rh(**2IN**)(COD)(OTf): R^1 = Me R^2 = Naph

Rh(**2AM**)(COD)(OTf): R^1 = Me R^2 = Ph
Rh(**2AE**)(COD)(OTf): R^1 = Et R^2 = Ph
Rh(**2AC**)(COD)(OTf): R^1 = Me R^2 = Cy
Rh(**2AN**)(COD)(OTf): R^1 = Me R^2 = Naph

Figure 2.36. Preparation of Rhodium(I) complexes

The resultant complexes were characterised by ^{1}H and ^{13}C $\{^{1}H\}$ NMR spectroscopy, mass spectrometry, and elemental analysis. Attempts were made at growing crystals suitable for X-ray diffraction, with one complex yielding such. The solid state structure for Rh(**2IM**)(COD)(OTf) is shown below, Figure 2.37

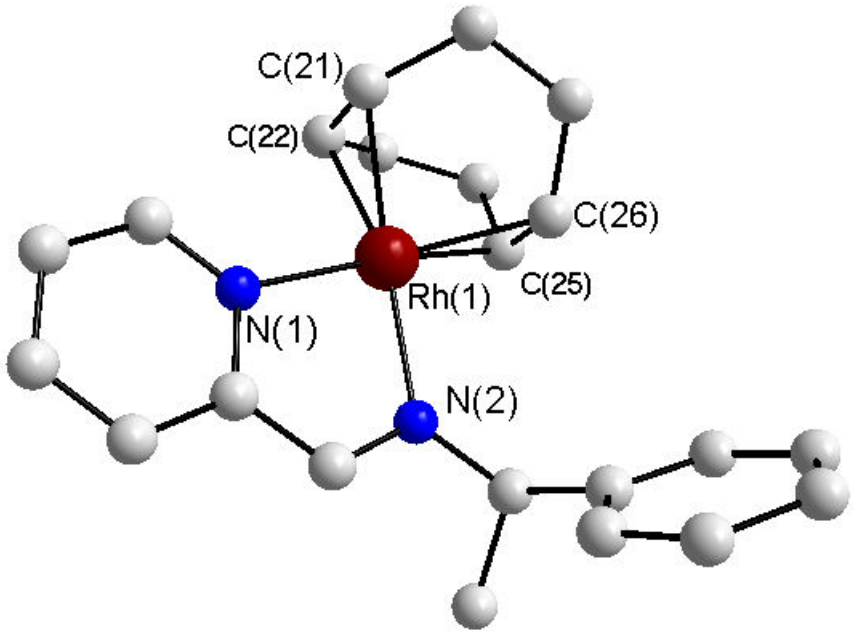

Figure 2.37. Solid state structure for Rh(2IM)(COD)(OTf). One triflate molecule removed along with all hydrogen atoms for clarity.

Bond Length (Å)		Bond Angle (°)	
Rh(1)-N(1)	2.086(6)	N(1)-Rh(1)-N(2)	79.0(2)
Rh(1)-N(2)	2.122(6)	N(1)-Rh(1)-C(25)	166.3(3)
Rh(1)-C(25)	2.129(11)	N(2)-Rh(1)-C(25)	99.0(3)
Rh(1)-C(22)	2.138(7)	N(1)-Rh(1)-C(22)	95.3(3)
Rh(1)-C(21)	2.141(8)	N(2)-Rh(1)-C(22)	158.9(3)
Rh(1)-C(26)	2.142(7)	C(25)-Rh(1)-C(22)	81.7(4)
		N(1)-Rh(1)-C(21)	94.8(4)
		N(2)-Rh(1)-C(21)	162.2(4)
		C(25)-Rh(1)-C(21)	90.9(5)
		C(22)-Rh(1)-C(21)	37.3(4)
		N(1)-Rh(1)-C(26)	156.8(3)
		N(2)-Rh(1)-C(26)	96.7(3)
		C(25)-Rh(1)-C(26)	36.6(4)
		C(22)-Rh(1)-C(26)	96.1(4)
		C(21)-Rh(1)-C(26)	82.4(4)

Table 2.20. Selected bond lengths and angles for Rh(2IM)(COD)(OTf)

The crystal belongs to the $P2_12_12_1$ space group and has an orthorhombic crystal system. The absolute structure parameter is descriptive of an

enantiomerically pure crystal with a value of 0.01(6). The bond lengths and angles are in agreement with literature values[50-52], and the Rh(I) centre is in a square planer geometry as expected for such complexes.

The eight complexes prepared were screened for the asymmetric transfer hydrogenation of acetophenone with isopropanol as the hydrogen source. The results are given in Table 2.21.

Catalyst	Time (hrs)	[a]Conversion (%)	[b]ee (%)
Rh(**2IM**)COD	24	53	10
Rh(**2IE**)COD	24	64	11
Rh(**2IC**)COD	24	51	9
Rh(**2IN**)COD	24	52	13
Rh(**2AM**)COD	24	31	15
Rh(**2AE**)COD	24	68	12
Rh(**2AC**)COD	24	73	10
Rh(**2AN**)COD	24	58	10

Table 2.21. Results for the transfer hydrogenation of acetophenone with various chiral rhodium(I) complexes, isopropanol as a hydrogen source and KOH as a co-catalyst 100:1:1 substrate:catalyst:KOH, 4.29×10^{-5} mol dm^{-3} KOH in isopropanol solution used as solvent and the reaction was kept at room temperature for the duration specified. [a]Conversion determined by ^{1}H NMR spectroscopy, [b]ee determined by chiral-HPLC OD-H column, with an error of ± 2%.

As can be seen from Table 2.21, the activity of these catalysts, compared with their palladium counterparts Table 2.19, is generally better with conversion being mild to moderate. The amine containing complexes would appear to perform better, however the difference is marginal. Selectivity however is still somewhat low, with little chiral discrimination observed. These catalysts were also trial for the direct hydrogenation, however similar results were obtain as those to the palladium complexes.

2.4.6. Chiral Phosphino-ligands

The second approach to prepare chiral discriminating palladium complexes and overcome the decomposition of the catalyst leading to palladium black was to redesign the ligand. Incorporation of a phosphorus atom into the ligand will result in the ligand binding more strongly to the Pd(II) centre, as a result of the increased strength between Pd-P and Pd-N. The new ligands prepared are detailed in Figure 2.38, prepared from the amine condensation of 2-(diphenylphosphino)benzaldehyde with each chiral amine.

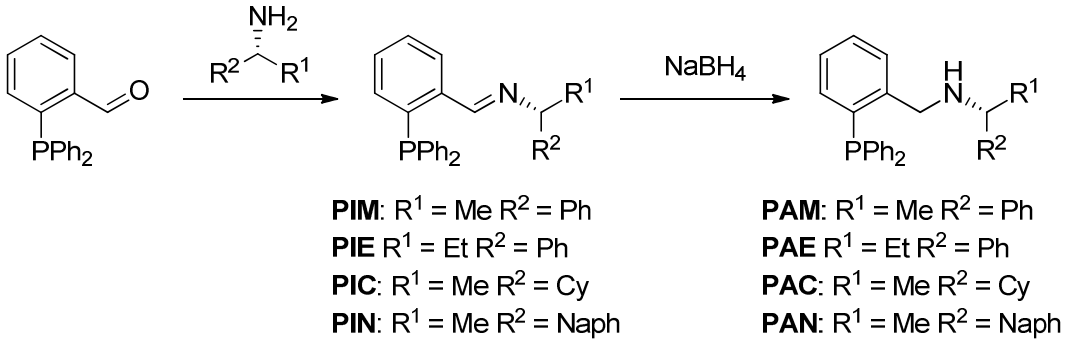

Figure 2.38. Preparation of 2-2-(diphenylphosphino)benzaldehyde derived chiral ligands.

As with the previous ligand set, the imine double bond could potentially be reduced under the conditions employed in the benchmark reactions. To cover this possibility, the chiral phosphino-imine ligands were reduced with sodium borohydride yielding four additional chiral phosphino-amine ligands. The new series of ligands were characterised by multinuclear NMR spectroscopy and mass spectrometry. The introduction of a phosphine brings in the difficulties as described in chapter 1, and the ligands were handled accordingly. Complexes with palladium chloride were prepared, and characterised by multinuclear NMR spectroscopy and elemental analysis, and from such analysis complexes of the form Pd(**PIX**)Cl_2 and Pd(**PAX**)Cl_2 were formed. These complexes were screened against the direct hydrogenation of dimethyl itaconate. The results are given in Table 2.22.

Catalyst	Pressure (bar)	[a]Conversion (%)	[b]ee (%)
Pd(**PIM**)Cl_2	5	99	6
	1	20	5
Pd(**PIE**)Cl_2	5	100	7
	1	18	6
Pd(**PIC**)Cl_2	5	100	5
	1	32	6
Pd(**PIN**)Cl_2	5	98	5
	1	26	5
Pd(**PAM**)Cl_2	5	100	2
	1	31	4
Pd(**PAE**)Cl_2	5	100	3
	1	41	7
Pd(**PAC**)Cl_2	5	100	5
	1	26	5
Pd(**PAN**)Cl_2	5	>99	1
	1	28	3

Table 2.22. Results for the direct hydrogenation of dimethyl itaconate with various chiral palladium(II) complexes and H_2 gas, 100:1 substrate:catalyst, methanol used as solvent and the reaction was kept at room temperature. The reaction vessel was purged 3 times with hydrogen gas, to exclude air, before being kept under at the desired pressure. [a]Conversion determined by ^{1}H NMR spectroscopy, [b]ee determined by chiral-HPLC OD-H column, with an error of ± 2%.

All eight chiral phosphino palladium complexes proved to be very active for the direct hydrogenation of dimethyl itaconate at 5 bar. While the formation of palladium black was lessened when comparing the post reaction mixtures, it was not completely eradicated. The enantiomeric excess on face value appear to be improved compared to the chiral pyridyl based complexes, however the values are still very low and susceptible to error. It would appear that even the small amount of palladium black being produced by decomposition of the catalyst is enough to non-selectively catalyse the reaction to near completion. Reducing the pressure of the hydrogen gas down to one atmosphere, has the result of reducing conversion and, qualitatively, reducing the formation of palladium black. However, this reduction does not correspond to an increase in chiral discrimination and therefore it can be assumed that these catalysts do not impart any selectivity in the direct hydrogenation reaction of alkenes.

Using the same reasoning as before, it was hoped that the complexes prepared may fair better with the transfer hydrogenation reaction of acetophenone. The results for the 24 hour reaction screen are given in Table 2.23.

Catalyst	Time (hrs)	[a]Conversion (%)	[b]ee (%)
Pd(**PIM**)Cl_2	24	28	6
Pd(**PIE**)Cl_2	24	0	7
Pd(**PIC**)Cl_2	24	10	5
Pd(**PIN**)Cl_2	24	30	5
Pd(**PAM**)Cl_2	24	30	2
Pd(**PAE**)Cl_2	24	28	6
Pd(**PAC**)Cl_2	24	9	7
Pd(**PAN**)Cl_2	24	26	2

Table 2.23. Results for the transfer hydrogenation of acetophenone with various chiral palladium(II) complexes, isopropanol as a hydrogen source and KOH as a cocatalyst 100:1:1 substrate:catalyst:KOH, 4.29×10^{-5} mol dm^{-3} KOH in isopropanol solution used as solvent and the reaction was kept at room temperature for the duration specified. [a]Conversion determined by ^{1}H NMR spectroscopy, [b]ee determined by chiral-HPLC OD-H column, with an error of ± 2%.

Conversion ranges from mild to poor, as has been seen previously, and chiral discrimination is too low to accurately draw any comparisons. These phosphino ligands were also complexed to rhodium as per the reaction scheme in Figure 2.36, and trailed for the asymmetric transfer hydrogenation reaction. The results obtained were in line with what has been seen for the pyridyl ligands, in that there was an improvement to conversion, however no significant change in selectivity.

2.4.7. Conclusions

Thirty two chiral complexes were prepared and screened for the hydrogenation reaction, using hydrogen gas, direct hydrogenation, or isopropanol as a hydrogen source, transfer hydrogenation. Due to the harsh reductive power of hydrogen gas, the palladium(II) complexes swiftly decomposed, completely at 5 bar and partially at 1 bar, resulting in the formation of elemental palladium black. This would then become the more active catalyst and catalyse the hydrogenation reaction to completion with no chiral discrimination.

Attempts were made at overcoming this issue. Replacing the direct hydrogen source with an alcohol indeed prevented the decomposition of the palladium complexes, however they proved to be inactive for the transfer hydrogenation reaction. Incorporation of a phosphino group, into the chiral ligand, to form a stronger interaction between ligand and metal was envisioned to produced a catalyst which would exhibit a greater performance. Decomposition was reduced, however there was not a significant improvement upon enantiomeric excess.

Rhodium complexes were prepared, as the literature suggested that they are more effective catalysts for the transfer hydrogenation reaction. However, the performance of these catalysts was very similar to their palladium counterparts.

2.5. Heterogeneous Catalysts

2.5.1. Preparation of Heterogeneous Complexes

In parallel to the preparation of homogenous analogues, the heterogeneous ligands were prepared. The heterogeneous systems were prepared using a covalent synthetic method[53-56], and is detailed in Figure 2.39. This covalent immobilisation sees the chiral ligand being built up on the support by a series of synthetic steps. As described in Chapter One, and seen in the literature, the mesoporous material MCM-41 is the inorganic support of choice. However, large scale applications using MCM-41 could become expensive and as such the commercially available Davisil-623 60 Å pore diameter porous silica (35-70 micron, 450 m^2 g^{-1} surface area) was utilised as standard.

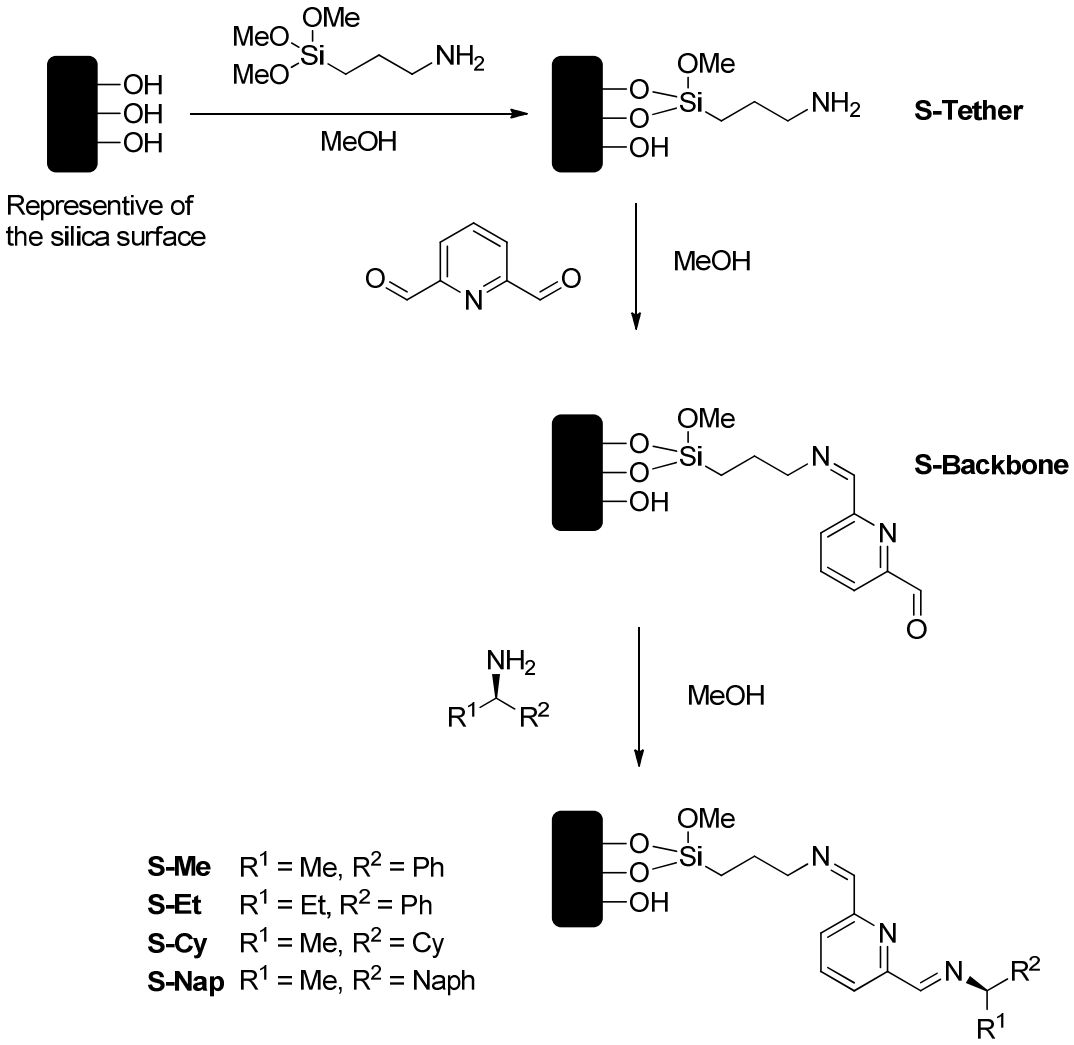

Figure 2.39. Method of preparing the heterogeneous ligands discussed herein.

Additional of various metal salts ($PdCl_2$, $Cu(OTf)_2$) afforded the solid supported heterogeneous catalyst, Figure 2.40. S is used to denote that it is a supported ligand, catalyst or compound. Me, Et, Cy, or Nap denotes which chiral amine is used to generate the chiral ligand, and then later Pd, Rh, or Cu is such as to show which metal is complexed to the heterogeneous ligand. At each stage of preparation the heterogeneous ligands were characterised by ^{13}C $\{^1H\}$ CP/MAS solid state NMR spectroscopy, elemental analysis, and thermogravimetric analysis.

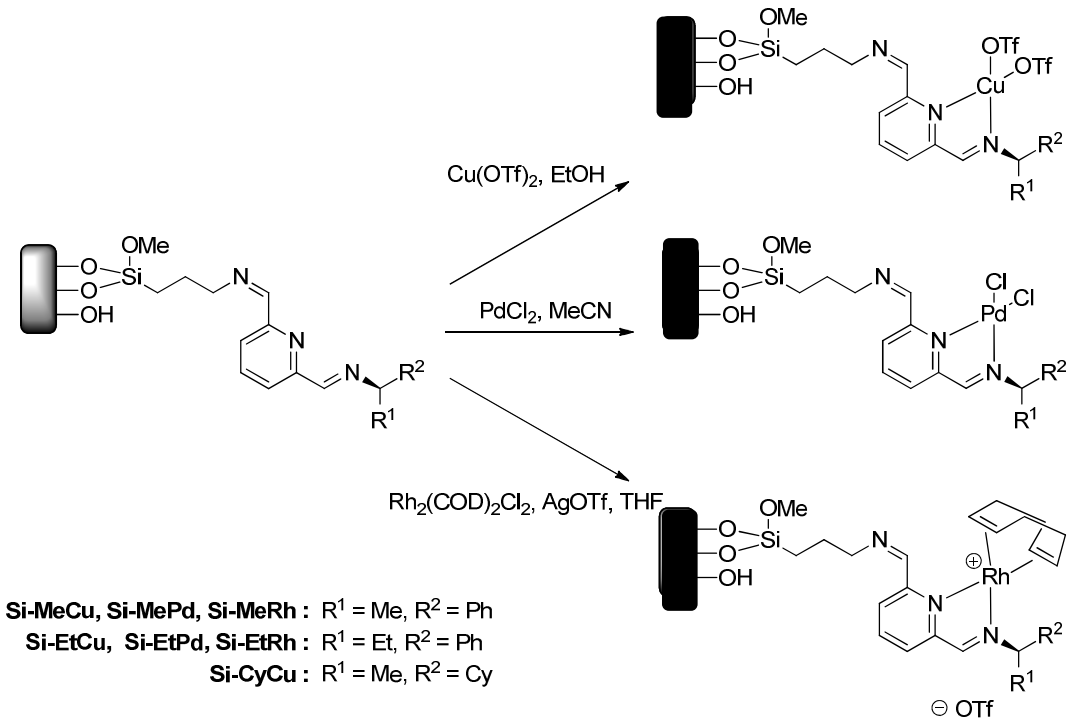

Figure 2.40. Complexation of heterogeneous ligands

Thermogravimetric analysis, TGA, of compounds is important characterisation technique for many different "disciplines" giving insights to the chemical and physical properties of a compound or material. The thermal characterisation of a chemical compound is important for CVD precursors for example, where knowledge of the reaction process is vital as is determining the properties of the resulting materials. However, information on sublimation, absorption, adsorption, desorption, chemisorption, vaporisation, desolvation, dehydration and decomposition can be obtained using this characterisation technique. TGA analysis involves the heating of a sample under a variety of atmospheres, including air, nitrogen and argon among others, on a sensitive spring balance. Either the heat can be raised at a steady gradient over time and the decomposition recorded as a % weight lose, or alternatively, the sample can be taken to a desired temperature and held while decomposition is monitored over time (a function of temperature or a function of time). It is a useful technique for heterogenised systems as it can demonstrate the development of the organic ligand on the thermally stable inorganic support. TGA was used to characterise the heterogeneous ligands during preparation as well as their complexation and these are described below. In each case the sample was placed in a ceramic

crucible before being loaded on the balance. It is then taken to 50 °C and held steady before applying the temperature gradient.

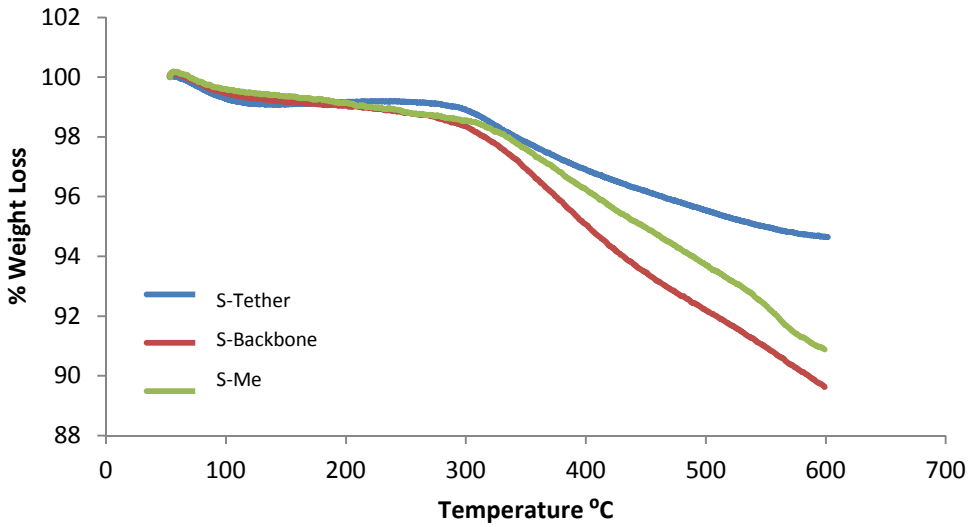

Figure 2.41. Thermogravimetric analysis for the preparation of the heterogeneous ligand from (*R*)-methyl benzylamine

The TGA curves above, Figure 2.41, shows the thermal decomposition of the developing heterogeneous ligand over time. Each curve has a similar shape with the loss of solvent occurring up to a temperature of 100 ^{0}C. **S-Tether** is thermally stable up to a temperature of 300 ^{0}C before a slow and steady decomposition occurs with the percentage weight loss in close agreement with calculated values. Addition of 2,6-pyridine dicarboxaldehyde generates **S-Backbone** and the decomposition follows a similar path with an initial drop before remaining steady until 300 ^{0}C. Decomposition is quicker than that of **S-Tether** likely due to the availability of decomposable material, and this additional organic matter results in an increased percentage loss as expected. Imine condensation between **S-Backbone** and (*R*)-methyl benzylamine generates the heterogeneous ligand, **S-Me**. The ligand is still thermally stable until 300 ^{0}C and decomposes by a slow and steady path. Interestingly, the percentage loss is less than that of **S-Backbone** where it would be expected to be greater as there is additional organic material. This shortcoming may be a result of imine hydrolysis, not observed in the homogenous analogues as it proceeds by an acid catalysed mechanism. Condensation of the chiral amine to generate the heterogeneous ligand results in the by-product water and as discussed previously, the untreated silica surface has

the acidic silanols creating the conditions required for imine hydrolysis, the mechanism of which can be seen below, Figure 2.42.

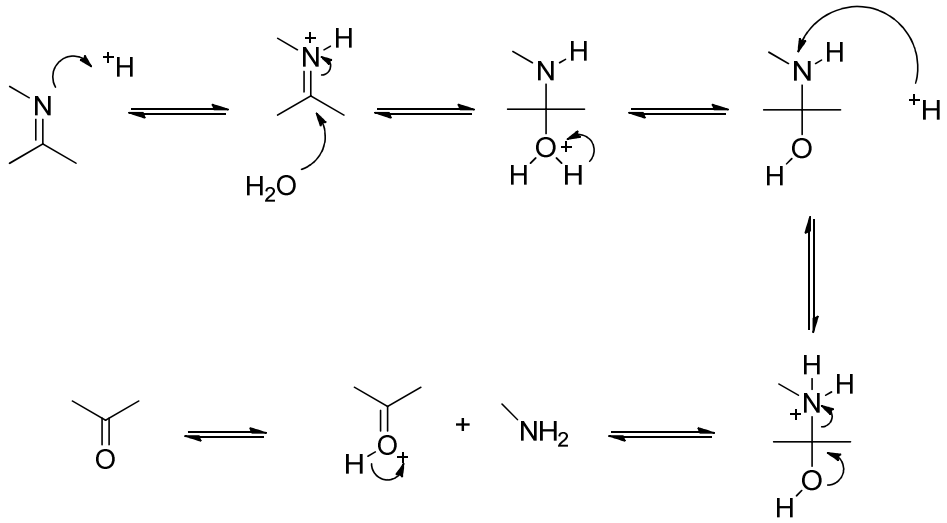

Figure 2.42. Acid catalysed mechanism for imine hydrolysis, a reverse of imine condensation

A second explanation could be that the decomposition is not complete at 600 ^{0}C. Indeed, the traces have a similar gradient suggesting that decomposition occurs at a similar rate, however, whereas **S-Tether** can clearly be seen to start tailing off, but **S-Backbone** and **S-Me** are continuing to decompose steadily, and the final decomposition product has not yet been reached. At elevated temperatures, above 600 ^{0}C it is possible that the **S-Backbone** trace will tail off and plateau earlier than the **S-Me** as expected. This explanation for the short coming in the TGA trace can be backed up by the solid-state NMR spectra, confirming successful synthesis, and the elemental analysis, where the composition percentages increase upon build up of the ligand. As such repeated experiments at higher temperatures and longer duration were not necessary.

As stated earlier, characterisation of heterogeneous catalysts is difficult with normal spectral techniques being unsuitable. Solid-state ^{13}C $\{^{1}$H$\}$ CP/MAS (cross polarisation/magic angle spinning) NMR spectroscopy can be used to analyse the surface of a solid-supported compound, behaving in a similar manner to solution NMR spectroscopy in that a spin interacts with an external magnetic field. However, solid-state NMR spectroscopy is more technically demanding resulting from the anisotropic nature of the chemical shift due to the interactions being orientation dependant, and the sample being immobile. In solution NMR

spectroscopy, Brownian motion leads to an averaging of these anisotropic interactions. This can be overcome by spinning the sample at the magic angle spinning, 54.74° at frequencies from 1 to 20 kHz, which can increase the resolution by narrowing the broad lines, and averaging the chemical shift more to with the isotropic. Various solid-state ^{13}C {^{1}H} CP/MAS NMR spectra are displayed below and discussed in turn.

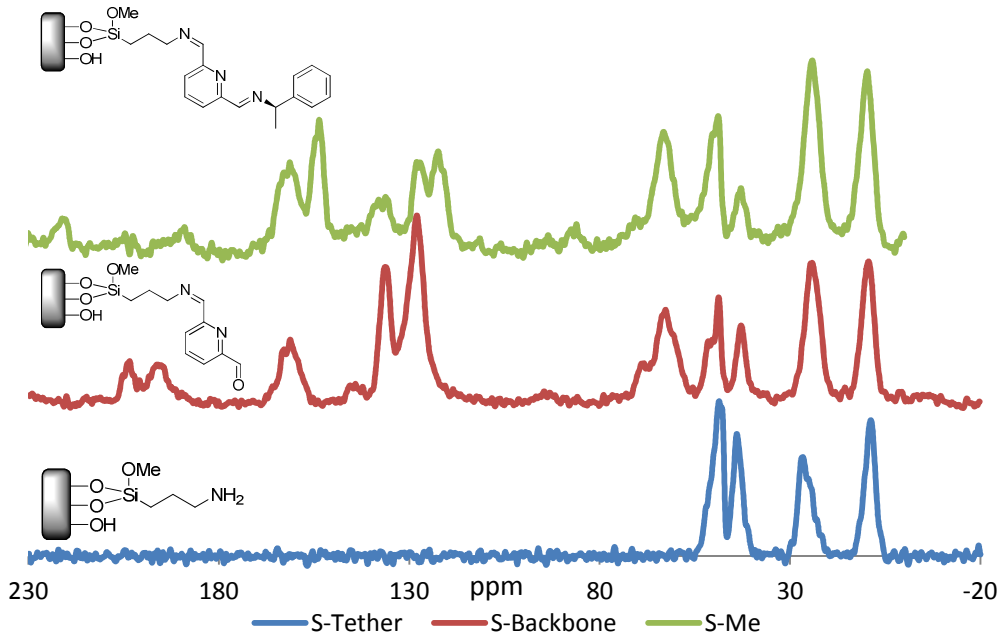

Figure 2.43. Solid-state ^{13}C NMR spectra for the development of the heterogeneous ligand S-Me.

Figure 2.43 shows the spectra at each step of the development of the heterogeneous ligand as detailed above, Figure 2.39. In the tether supported spectrum, **S-Tether**, the resonances at 9 ppm corresponds to CH_2Si, 24 ppm to -CH_2- and 43 ppm to -CH_2N group. The peak at 49 ppm results from the OMe groups still present from the aminopropylmethoxysilane, the tethering moiety. These tether resonances are consistently present throughout the synthesis of the ligand. Imine condensation between the tether and pyridine dialdehyde gives rise to the spectra labelled **S-Backbone**. Additional resonances in the aromatic region are present as expected, 120 - 140 ppm with the signal at ~160 ppm corresponding to the carbon bound to the nitrogen-imine. The aldehyde resonance is present at around 200 ppm, and the amine resonance from the tether has almost disappeared giving rise to the resonance at 62 ppm, corresponding to $CH_2C{=}N$, and some side bands also contribute to this region. With the remaining aliphatic resonances resulting from the iminopropyl tether. The second imine condensation

generates **S-Me** by addition of (*R*)-methyl benzylamine in solution. The aldehyde peak previously seen at 200 ppm is now absent therefore it can be concluded that the synthesis step was successful. Additional intensity at ~162 ppm provides additional evidence for the second imine, CH=N, present. The resonances at 154 ppm can now be assigned to the carbon atoms neighbouring the pyridine nitrogen atom, while the signals at 122 and 136 ppm arising from the remaining carbons in that ring as seen from **S-Backbone**. The resonance at 128 ppm can be assigned to the terminal phenyl ring and this is confirmed when comparing the spectra of **S-Me** and **S-Et** (phenyl rings in the chiral amine) to that of **S-Cy** (a cyclohexyl ring in the chiral amine). This replacement of a phenyl ring with a cyclohexyl removes the 128 ppm signal from the spectra. The quaternary carbon from the phenyl contributes to the signal at 136 ppm. The aliphatic region remains relatively unchanged as would be expected with the tether not being involved in this step, however a clear signal from the methyl of the chiral amine is absent. It is possibly within the resonances at 24 ppm and additional intensity in that area would add additional evidence to this statement.

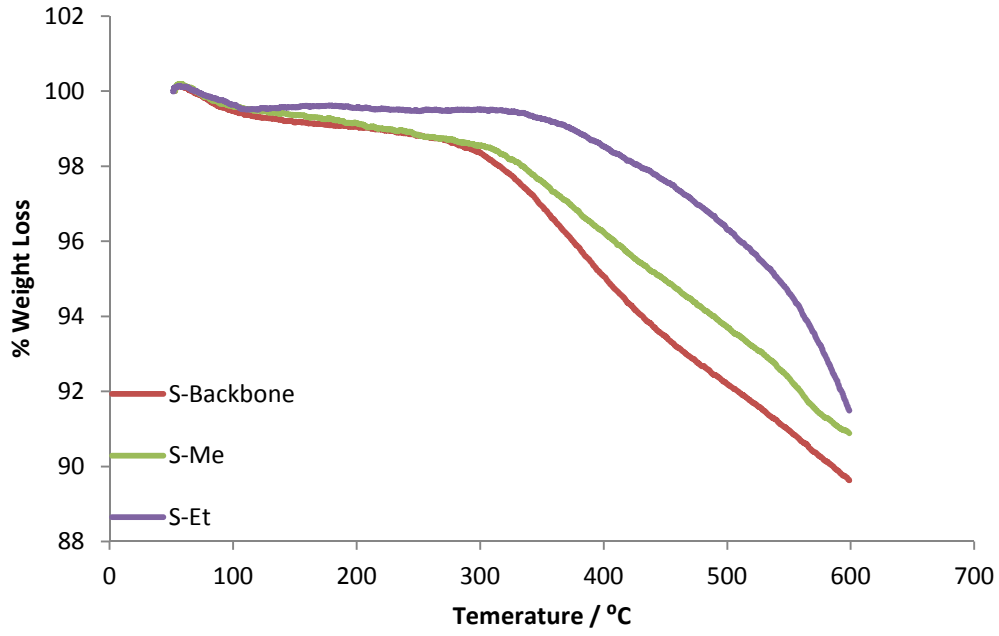

Figure 2.44. Graph displaying the TGA of different heterogeneous ligands for comparison.

Comparison of the **S-Me** to **S-Et** heterogeneous ligands show some stark differences, Figure 2.44. Replacement of the methyl group on the chiral amine with an ethyl would appear to provide additional stability with decomposition not

starting until 350 ^{0}C. However, once started, decomposition is fairly rapid and by 600 ^{0}C percentage loss is at a similar level. Again we do not seen the final decomposition weight however solid-state NMR spectroscopy and elemental analysis confirms that they were successfully prepared.

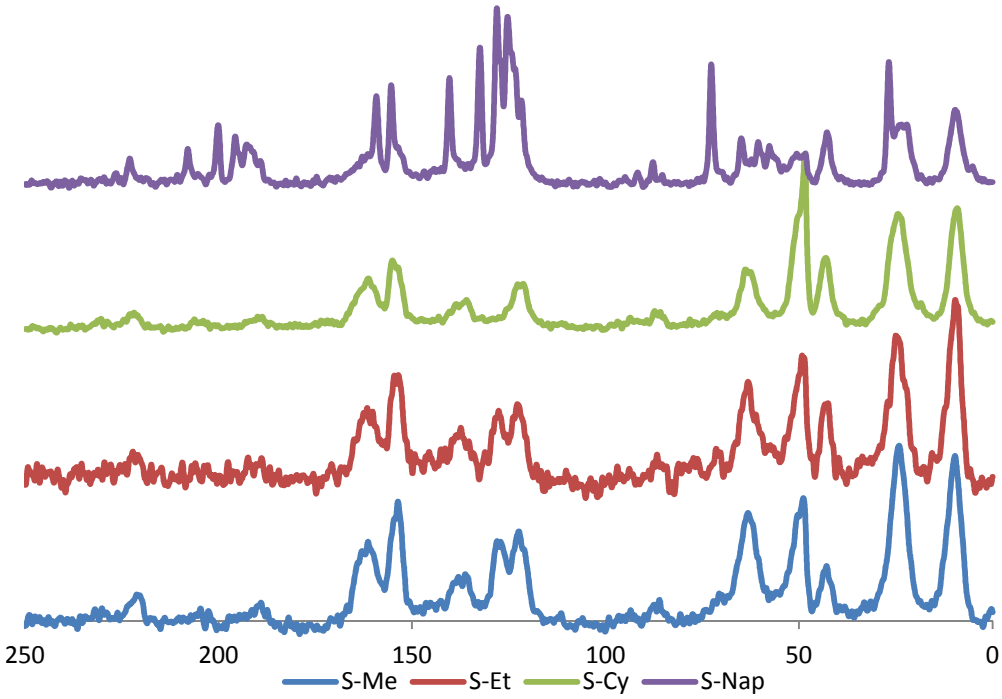

Figure 2.45. Solid-state ^{13}C NMR spectra for each heterogeneous ligand.

Comparing the ^{13}C {^{1}H} CP/MAS NMR spectra of the four different ligands, Figure 2.45, shows some similarities, stark differences, and more evidence for the success and failure of synthesis between **S-Backbone** and the different chiral amines. Firstly, the resonances resulting from the tether, are all clearly present in each of the four spectra, indicating that addition of the chiral amine has no effect on it, and it remains unchanged for the most part. Spectra for **S-Me** and **S-Et** should be similar and indeed this is the case with matching terminal phenyl signals, absent aldehyde, and additional intensity in the imine region. Like **S-Me**, **S-Et** lacks a clearly distinguishable -CH_2- and -CH_3 pair of signals. It is likely that these are also under the tether resonances.

S-Cy shares similarities, and common features with those of **S-Me** and **S-Et**. The peak at 128 ppm is not present, which in turn confirms it to be from a terminal phenyl in the other spectra. The solution spectrum of cyclohexane would

allude to having quite an impact upon the low frequency part of the spectrum, and there is indeed an additional signal at 43 ppm and extra intensity at ~25 ppm, relative to other resonances in this spectrum, and the same resonance in the spectra for **S-Me** and **S-Et** with the signal at 10 ppm also enhanced.

The spectrum of **S-Nap** shows a stark difference to the others. The sharpness of the signals is usually indicative of crystalline material suggesting they arise from a component not involved with the surface. As such the chiral amine may not have successfully condensed with the backbone supported component and is residing in a crystalline fashion on the silica surface. This was the case upon repeated synthetic attempts. One thing that can be taken away from the spectrum of **S-Nap** is that the methyl from the chiral amine does indeed sit within the 25 ppm band (26.7 ppm here).

Below is reported the TGA graphs for the complexation of **S-Me** to palladium chloride, rhodium cyclooctadiene, and copper triflate, Figure 2.46.

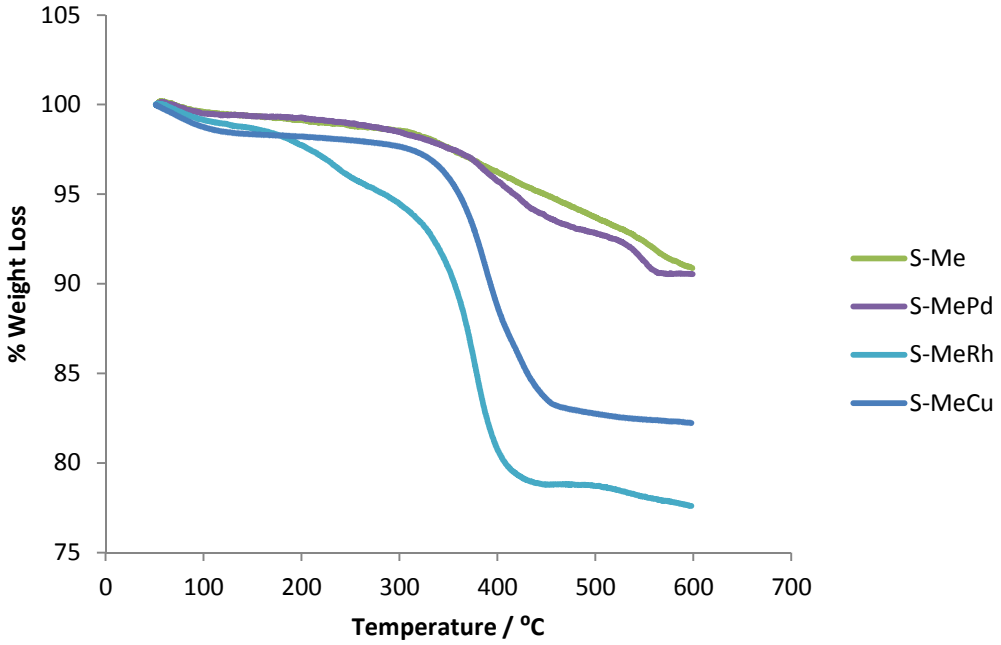

Figure 2.46. Thermogravimetric Analysis of different heterogeneous systems based on (*R*)-methyl benzylamine

There is a significant difference here between what has been seen for **S-MeRh** and **S-MeCu** as to what has been seen before and indeed **S-Me** and **S-MePd**. This is a result of the large organic counter ions, COD in **S-MeRh** and

triflate in **S-MeCu**, whereas **S-MePd** is only decomposable addition comes from chlorine. Complexation with palladium chloride also affects the decomposition process as where before there was a steady decomposition, two steps can now be observed. Decomposition follows that of the ligand until 400 ^{0}C where upon the rate increases before levelling off and dropping again at about 550 ^{0}C. **S-MeCu** remains thermally stable until 350 ^{0}C where there is a quick and steady decomposition before levelling, while **S-MeRh** follows a similar pattern besides the steady start to the trace. The increasing percentage loss from palladium to copper to rhodium follows the pattern in increasing decomposable material in the counter ion. Thermogravimetric analysis was carried out for other palladium, copper, and rhodium complexes and followed the same patterns as discussed.

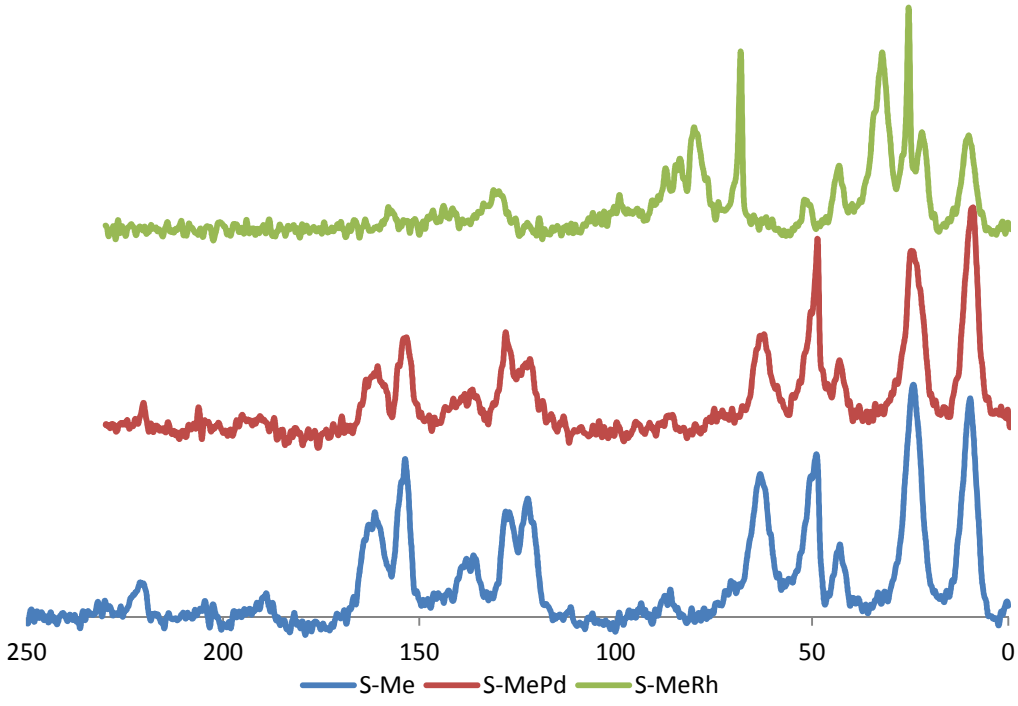

Figure 2.47. Solid-state ^{13}C NMR for S-Me and its complexes with palladium and rhodium.

The spectra above, Figure 2.47, show the sample **S-Me** after it has been complexes to palladium(II) and rhodium(I), as bar the reaction scheme above, Figure 2.40. The addition of $PdCl_2$ should have a very minor effect on the spectrum with no new carbon environments being introduced, nor any removed as a result of complexation. This is indeed the case, as can be seen, with both the spectra looking similar. The rhodium complex would provide additional signals in the aliphatic region as a result of the COD counter ligand, and the resulting does

look different, however it should be noted that the sharp resonances at ~25 and 68 ppm result from additional THF and should be ignored in this comparison. Resonances at 30 ppm result from the -CH_2- moieties in the COD as do the resonances at ~90 ppm. Resonances in the aromatic region are at a reduced intensity which is unsurprising, but still present, as are the peaks resulting from the tether. Spectra for palladium and rhodium complexes were also obtained with **S-Et** and followed the same patter as discussed. The complexes containing copper(II) were not analysed by solid-state NMR spectroscopy due to being paramagnetic. Instead these were investigated by EPR spectroscopy, the spectra are displayed below, having been recorded by, Dr Floriana Tuna at the University of Manchester.

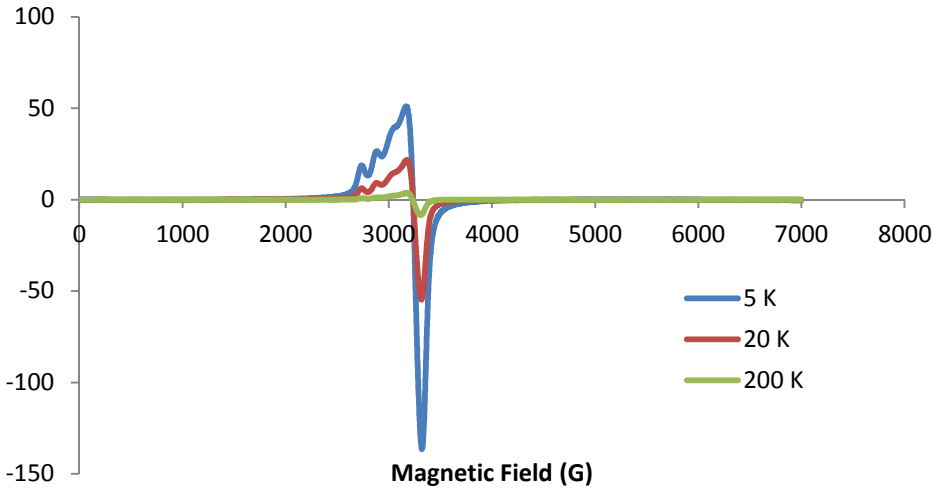

Figure 2.48. Overlaid EPR spectra for the X-band of S-MeCu

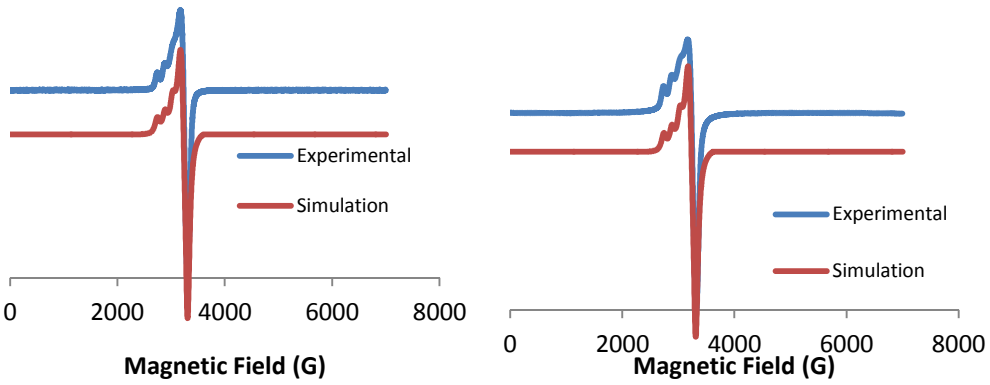

Figure 2.49. Left; X-Band experimental and simulated EPR spectra for S-MeCu at 200 K and, Right; X-Band experimental and simulated EPR spectra for S-MeCu at 5 K

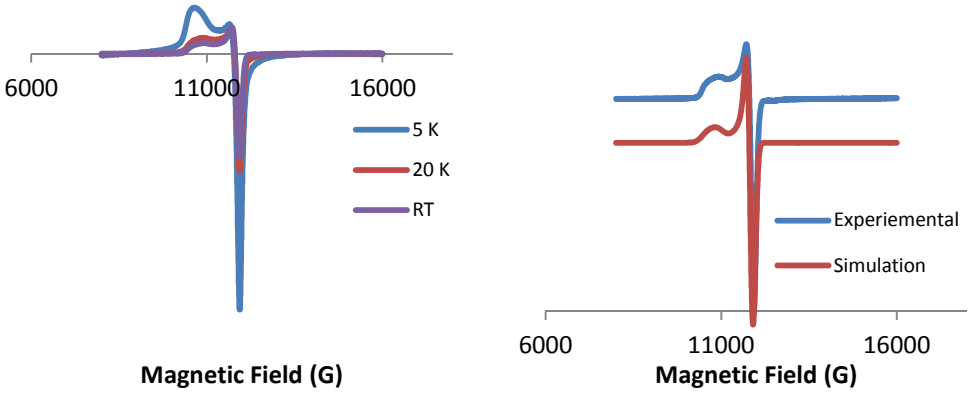

Figure 2.50. Left; Overlaid EPR spectra for the Q-band of S-MeCu and Right; Q-Band experimental and simulated EPR spectra for S-MeCu at 200 K

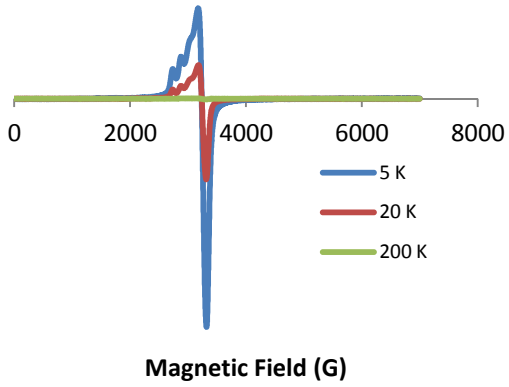

Figure 2.51. Overlaid EPR spectra for the X-band of S-EtCu

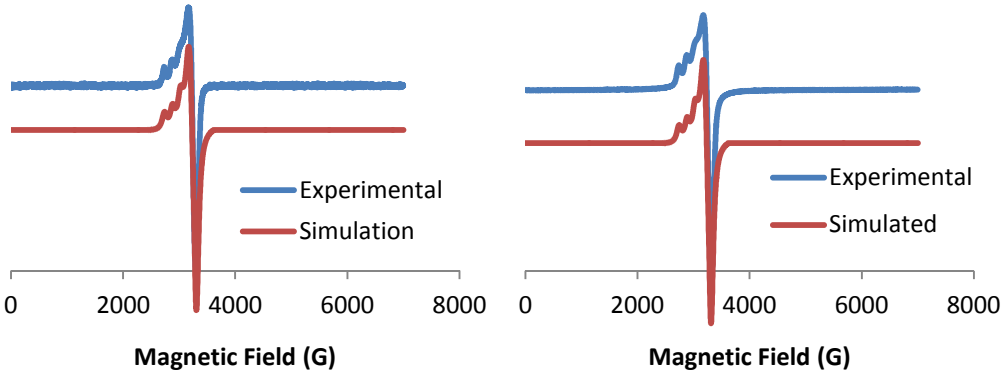

Figure 2.52. Left; X-Band experimental and simulated EPR spectra for S-EtCu at 200 K and Right; X-Band experimental and simulated EPR spectra for S-EtCu at 5 K

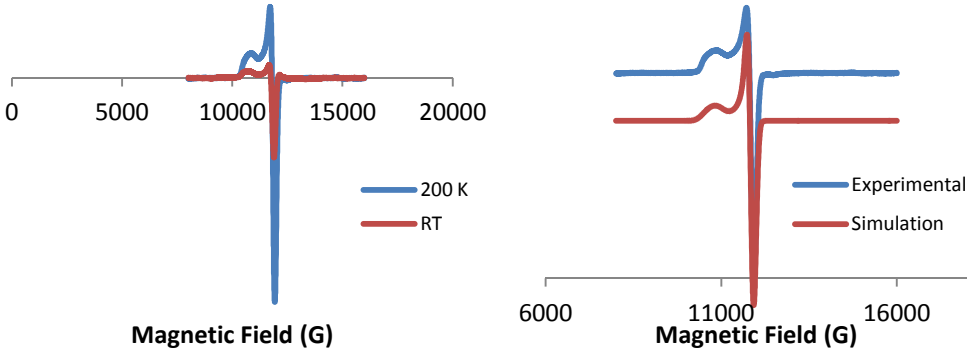

Figure 2.53. Left; Overlaid EPR spectra for the Q-band of S-EtCu and
Right; Q-Band experimental and simulated EPR spectra for S-EtCu at 200 K

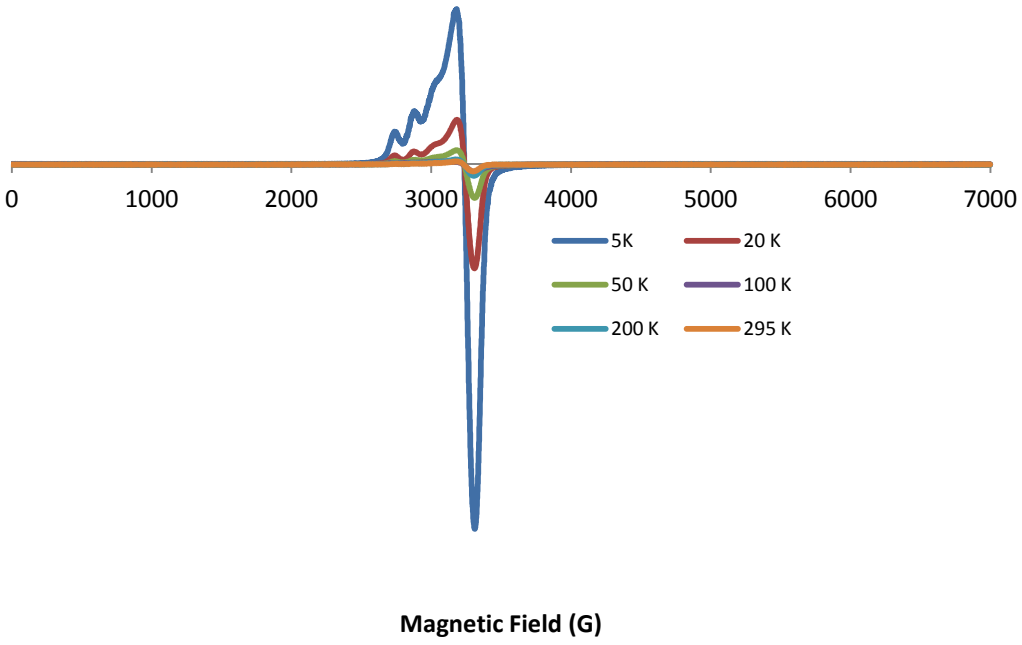

Figure 2.54, Overlaid EPR spectra for the X-band of S-CyCu

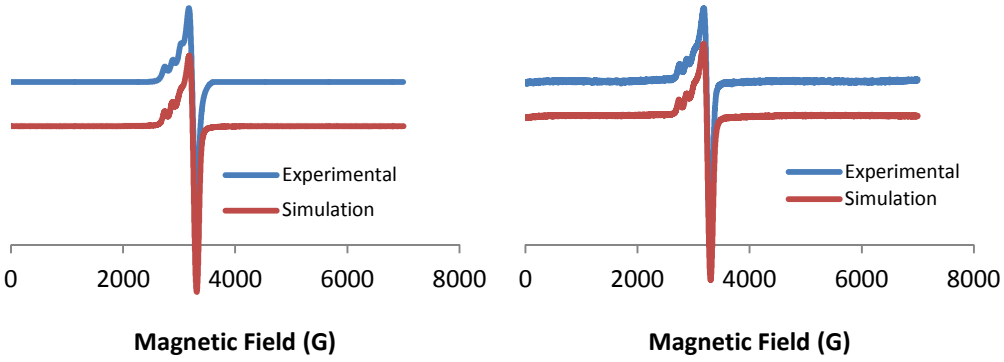

Figure 2.55 Left; X-Band experimental and simulated EPR spectra for S-CyCu at 200 K and Right; X-Band experimental and simulated EPR spectra for S-CyCu at 5 K

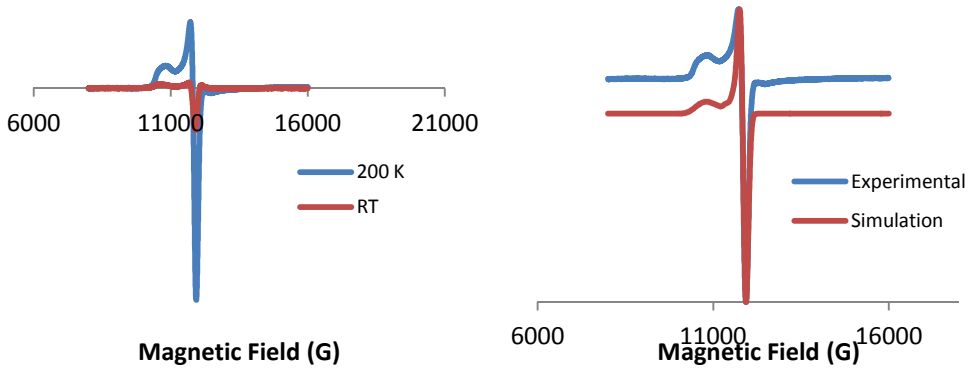

Figure 2.56 Left; Overlaid EPR spectra for the Q-band of S-CyCu and Right; Q-Band experimental and simulated EPR spectra for S-CyCut at 200 K

Catalyst	Band	gx, gy, gz	Ax, Ay, Az, (G)
S-MeCu	X	2.067, 2.067, 2.272	20, 20, 140
	Q	2.058, 2.058, 2.272	20, 20, 140
S-EtCu	X	2.063, 2.063, 2.272	20, 20, 140
	Q	2.056, 2.056, 2.270	20, 20, 140
S-CyCu	X	2.067, 2.067, 2.280	20, 20, 148
	Q	2.057, 2.057, 2.273	20, 20, 140

Table 2.24. Collected values for all three heterogeneous copper complexes. Values are those recorded at 200 K, the X-band at 9.40 GHz and the Q-band at 34.12GHz

The values obtained are in close agreement with the homogeneous analogues submitted for EPR spectroscopy, and also with literature values of similar compounds[12,14].

2.5.2. Catalysis with Heterogeneous Complexes

The heterogeneous catalysts successfully prepared and characterised were screened against the benchmark reactions discussed previously, the asymmetric Henry reaction, asymmetric direct hydrogenation and asymmetric transfer hydrogenation. These reactions have had varying degrees of success with heterogeneous ligands in the literature[9,11,57-60].

The nitroaldol reaction, as discussed before, can be catalysed by a wide range of different metals, and a vast number of ligands have been reported. However unfavourable conditions are often required, with low temperature, long reaction times, and high catalyst loadings necessary to obtain good results. Heterogeneous systems are limited, with the greatest area of interest coming from polymer supported catalysts[9,57,58], and those immobilised onto resins[59] and dendrimers[11,60]. The homogeneous analogues, screened previously, displayed a varying range of activity and selectivity. It is hoped that the heterogeneous systems would afford better selectivities while maintaining conversion. The benchmark nitroaldol reactions were prepared as standard with benzaldehyde and nitromethane as the reagents and triethylamine employed as the basic co-catalyst. The reactions were stirred for 6 hours, before volatiles removed by rotary evaporation. The results are shown below, Table 2.25.

Heterogeneous System	[a]Conversion (%)	[b]ee (%)	Yield (%)
S-MeCu	81	0	0
S-EtCu	72	0	0
S-CyCu	32	1	0.3

Table 2.25. Results for the nitroaldol reaction between benzaldehyde, 1.0 mmol, and nitromethane, 10 mmol, catalysed by various chiral heterogeneous copper(II) complexes with triethylamine as co-catalyst, 100:5:13, aldehyde:catalyst:base, ethanol used as solvent and the reaction was kept at room temperature for 6 hours. [a]Conversion determined by ^{1}H NMR spectroscopy, [b]enantiomeric excess determined from chiral-HPLC OD-H column, with an error of ± 2%.

Despite the restricted diffusion of catalyst with reagents, the conversion is improved with the exception of **S-CyCu**. Whether this is purely a result of the catalytic metal centre, or additional catalysis from the support it is uncertain as no selectivity was observed as with the homogeneous analogues. An explanation could be reaction of the nitroalcohol product catalysed by the acidic sites of the

silica support followed by addition of a second nitroalkane resulting in a 1,3-dinitro alkane, Figure 2.57. These molecules have been found to be key building blocks in the preparation of HIV-protease inhibitors amongst other biologically important intermediates. These 1,3-dinitro alkanes have been produced from heterogeneous primary amine and tertiary amine catalysts in the literature, with the acidic silanol surfaces amplifying the activity. Heterogeneous catalysts of this type were not further developed for the nitroaldol reaction.

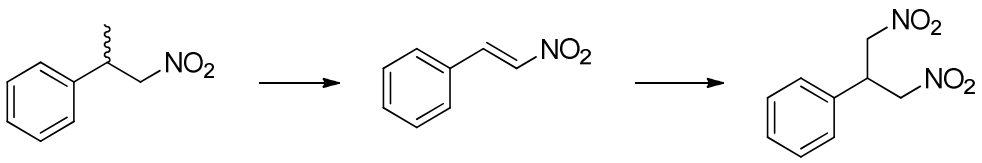

Figure 2.57. Acid catalysis of the nitroalcohol product from the Nitroaldol reaction, followed by addition of nitromethane

While direct hydrogenation heterogeneous catalysts are present in the literature, the same cannot be said for transfer hydrogenation catalysts[41], where a lack of systems has created a niche in this area of research. The homogeneous analogues to the heterogeneous catalysts performed poorly under the direct hydrogenation reaction with the complex being reduced by the hydrogen gas, resulting in the formation of palladium black. This in turn catalysed the reaction at elevated pressure non-asymmetrically, resulting in the racemic mixture. At 1 atm, decomposition of the catalyst was not as severe, but activity was significantly reduced, with no clear increase to selectivity. It is therefore hoped that the inorganic support, will provide an additional degree of protection to the catalyst, as such decomposition is lessened or ideally eliminated which should result in the chiral complex being the catalyst and chiral discrimination being exhibited. Homogeneous systems screened against the transfer hydrogenation also performed poorly, with conversion and selectivity being low. With the trend in catalyst immobilisation being that activity drops, as a result of reduced diffusion, and selectivity drops, as a result of surface interactions and possible catalyst modification upon heterogenisation. However, examples have been reported where enantioselectivity is improved upon immobilisation, and it is hoped that this will be seen with these systems.

The palladium heterogeneous catalysts were trailed for the direct hydrogenation of dimethyl itaconate under 5 bar and 1 bar of hydrogen gas, while the rhodium catalysts were screened against the transfer hydrogenation reaction, with isopropanol as the hydrogen source and potassium hydroxide as co-catalyst. The results for direct hydrogenation reaction is given in Table 2.26.

Heterogeneous System	Pressure (bar)	[a]Conversion (%)	[b]ee (%)
S-MePd	5	100	2
	1	8	0
S-EtPd	5	> 99	1
	1	5	0

Table 2.26. Results for the direct hydrogenation of dimethyl itaconate with various chiral palladium(II) heterogeneous complexes and H_2 gas, 100:1 substrate:catalyst, methanol used as solvent and the reaction was kept at room temperature. The reaction vessel was purged 3 times with hydrogen gas, to exclude air, before being kept under an ambient pressure, by a hydrogen filled balloon, or raised to 5 bar. [a]Conversion determined by ^{1}H NMR spectroscopy, [b]ee determined by chiral-HPLC OD-H column, with an error of ± 2%..

The reaction at 5 bar again went to completion however no selectivity was exhibited by either system employed. The degree of palladium black precipitation appeared to have decreased, however it would appear that very little is needed to catalyse the reaction to completion with no chiral discrimination. Reducing the pressure to 1 atm, has the same effect as seen with the homogeneous analogues. Palladium black is mostly formed during purging of the system, however under ambient pressure activity significantly reduces, this is likely due to the inability to get both reactant and hydrogen at the active site of the catalyst. For these low conversions it is impossible to accurately ascertain an enantiomeric excess.

Heterogeneous System	Time (hrs)	[a]Conversion (%)	[b]ee (%)
S-MeRh	24	6	1
	48	15	1
S-EtRh	24	7	3
	48	34	2

Table 2.27. Results for the transfer hydrogenation of acetophenone with various chiral palladium(II) complexes, isopropanol as a hydrogen source and KOH as a co-catalyst 100:1:1 substrate:catalyst:KOH, 4.29×10^{-5} mol dm^{-3} KOH in isopropanol solution used as solvent and the reaction was kept at room temperature. [a]Conversion determined by ^{1}H NMR spectroscopy, [b]ee determined by chiral-HPLC OD-H column with an error of ± 2%.

The heterogeneous systems reported in here performed to a similar level as their homogeneous counterparts. Conversion has decreased as might be expected, and no chiral discrimination is observed with these systems.

2.5.3. Conclusion

Not all heterogeneous ligands were successfully prepared with the bulkiest proving difficult, and solid-state NMR spectroscopy suggesting that the ligand was present on the surface support rather than attached to it. The remaining were characterised with confidence and complexed to different metals before being screened against the benchmark reactions used previously.

For the nitroaldol reaction, conversion was generally high with the exception of **S-CyCu**, however no chiral discrimination is observed. This performance is attributed to the acidic surface of the inorganic support reacting with the desired product.

Heterogeneous palladium complexes appear to protect the catalyst from decomposition by hydrogen gas, however the small amount present, either from the decomposition of the heterogeneous catalyst, or leeching of the metal, is sufficient to complete the reaction at higher pressures. In either case, no chiral discrimination is observed, nor when rhodium heterogeneous catalysts are trailed for the transfer hydrogenation.

2.6. Future Work

It is unfortunate that only mild to moderate selectivities were exhibited for the catalysts used in the asymmetric nitroaldol reaction, as it is an ideal reaction for high throughput screening, HTS. This has been previously reported by Yanagisawa et al.[8] who used a circular dichroism, CD, spectrometry to evaluate a range of chiral amines supported on polymer beads and complexed to different copper salts. The heterogeneous catalysts were contained in reaction vessels with the reactants and a sample taken for analysis by the CD spectrometer. A signal response results from both product activity and selectivity, with a low yield resulting in an insignificant peak, while a high yield and high selectivity resulting in a maximum intensity. High activity without enantiomeric excess results in no

signal. This can be seen in Figure 2.58. Typical CD Trace for a HTS system, where each peak is the result of a different catalyst.

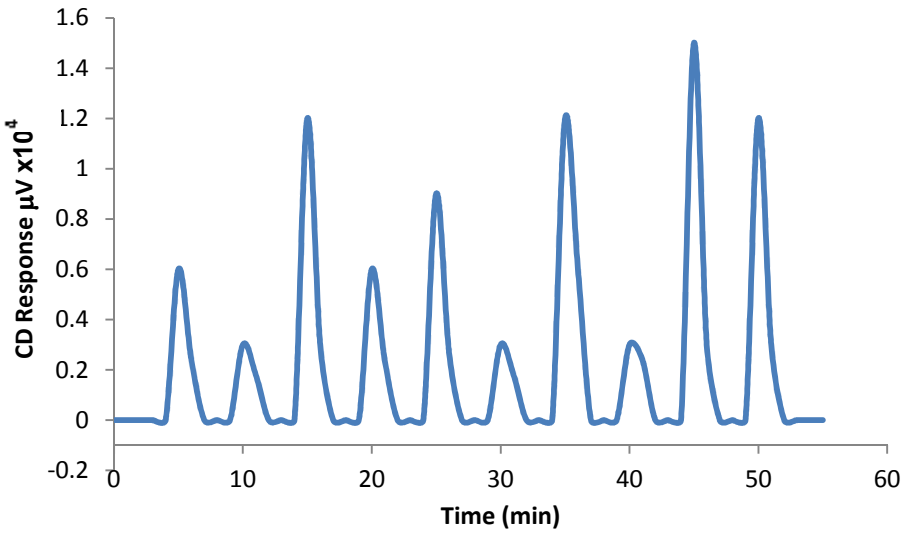

Figure 2.58. Typical CD Trace for a HTS system, where each peak is the result of a different catalyst.

Had the complexes reported in Chapter 2, Section 1, shown a greater performance then HTS would have been investigate as Yanagisawa but in a slightly modified manner. Rather than screening a selection of heterogeneous catalyst in separate reaction vessels, one heterogeneous catalyst would be prepared and pack in a HPLC-style column. Substrate tolerance would then be screened using an HPLC autosampler. Vials containing different aldehydes would be loaded up into the autosampler tray, while the system solvent would contain the nitroalkane. It is then envisioned that the aldehyde would be selected and injected onto the catalytic column and pumped through with the reaction media. A CD spectrometer at the end of the column would then detect the effectiveness of the catalyst. The HTS could then be further developed to include multiple solvent reservoirs of different nitroalkanes, that could be automatically selected and pumped through the system as the reaction media.

The benefit is that numerous experiments would not have to be conducted by the scientist, and moreover, the system could be run continuously with exchange of the catalytic column to test other heterogeneous catalysts, given that the solvent reservoirs are topped up and there is sufficient aldehyde in the autosampler.

One disadvantage is that the reusability, recyclability and turnover rate, of the heterogeneous system being screened would need to be fully understood, as erroneous results would be obtained if the heterogeneous system leeched overtime, or became inactive or blocked from side reactions. Other issues would surely arise from implementing such a complicated system, such as calibrating the system, ensuring the correct wavelength was chosen for detection of each different chiral product and designing of the automation program. However these would all be part of the challenge, and there is evidence in the literature of groups working on different HTS systems, pairing different devises, chiral-HPLC, UV-vis, mass spectrometry etc., for their needs.[61-66]

Other interesting work which is currently receiving interest, and could be investigated with the work presented here, involves combinatorial methods for the development of enantioselective homogeneous catalysts. Here libraries and arrays of catalysts are prepared in parallel rather than one at a time, an approach modified from the development of enantioselective enzymes[67]. Moreover, silsesquioxanes were introduced in Chapter 1 as being able to bridge the gap between homogeneous and heterogeneous catalysts. Attempts were made at preparing a selection however, issues arose when trying to get a 1:1 reaction between the silsesquioxane and the typical dialdehydes used in this thesis, resulting in a mixture of non-, mono- and di-addition. This issue was encountered when a 1:1 reaction was investigated between the dialdehyde and chiral amine, the aim of which was to then reacted this and generate the silsesquioxane ligand. Due to the poor performance of the heterogeneous catalysts and moderate selectivities of the homogeneous catalysts, this route was not developed further. Future work in the area would potentially involve attempts at a mono-protection of the dialdehyde, reaction with either the silsesquioxane or chiral amine, deprotection and then completion of synthesis.

Had the heterogeneous systems performed greater, exhibiting high levels of selectivity at near to complete conversion investigations into the complete characterisation of the solid material would have been important. Measuring of the pore volume and total surface area via BET analysis. This information could be used as a second source of fine tuning the heterogeneous catalyst through size

exclusion of substrates, or aid in enantiomeric selectivity by fixing the shape of the reaction centre.

2.7. References

(1) Wu, X.-Y.; Xu, H.-D.; Zhou, Q.-L.; Chan, A. S. C. *Tetrahedron: Asymmetry* **2000**, *11*, 1255.
(2) Trost, B. M.; Yeh, V. S. C. *Angewandte Chemie International Edition* **2002**, *41*, 861.
(3) Trost, B. M.; Yeh, V. S. C.; Ito, H.; Bremeyer, N. *Org. Lett.* **2002**, *4*, 2621.
(4) Kogami, Y.; Nakajima, T.; Ashizawa, T.; Kezuka, S.; Ikeno, T.; Yamada, T. *Chem. Lett.* **2004**, *33*, 614.
(5) Kogami, Y.; Nakajima, T.; Ikeno, T.; Yamada, T. *Synthesis* **2004**, *2004*, 1947.
(6) Choudary, B. M.; Ranganath, K. V. S.; Pal, U.; Kantam, M. L.; Sreedhar, B. *J. Am. Chem. Soc.* **2005**, *127*, 13167.
(7) Palomo, C.; Oiarbide, M.; Laso, A. *Eur. J. Org. Chem.* **2007**, *2007*, 2561.
(8) Arai, T.; Watanabe, M.; Fujiwara, A.; Yokoyama, N.; Yanagisawa, A. *Angewandte Chemie International Edition* **2006**, *45*, 5978.
(9) Bandini, M.; Benaglia, M.; Sinisi, R.; Tommasi, S.; Umani-Ronchi, A. *Org. Lett.* **2007**, *9*, 2151.
(10) Kehat, T.; Portnoy, M. *Chem. Commun.* **2007**, 2823.
(11) Gaab, M.; Bellemin-Laponnaz, S.; Gade, L. H. *Chemistry – A European Journal* **2009**, *15*, 5450.
(12) Becker, M.; Heinemann, Frank W.; Knoch, F.; Donaubauer, W.; Liehr, G.; Schindler, S.; Golub, G.; Cohen, H.; Meyerstein, D. *Eur. J. Inorg. Chem.* **2000**, *2000*, 719.
(13) Abry, S.; Thibon, A.; Albela, B.; Delichere, P.; Banse, F.; Bonneviot, L. *New J. Chem.* **2009**, *33*, 484.
(14) Jones, M. D.; Cooper, C. J.; Mahon, M. F.; Raithby, P. R.; Apperley, D.; Wolowska, J.; Collison, D. *Journal of Molecular Catalysis A: Chemical* **2010**, *325*, 8.
(15) Christensen, C.; Juhl, K.; Hazell, R. G.; Jørgensen, K. A. *The Journal of Organic Chemistry* **2002**, *67*, 4875.
(16) Sasai, H.; Watanabe, S.; Shibasaki, M. *Enantiomer* **1997**, *2*, 267.
(17) Pennaforte, E. V.; Costa, J. S.; Silva, C. A.; Saraiva, M. C.; Pereira, V. L. P. *Lett. Org. Chem.* **2009**, *6*, 110.
(18) Kirsch, S. F. *Angewandte Chemie International Edition* **2009**, *48*, 2450.
(19) Cooper, C. **2012**.
(20) Roberto Pioquinto-Mendoza, J.; Martínez-Otero, D.; Andrade-López, N.; Alvarado-Rodríguez, J. G.; Salazar-Pereda, V.; Sánchez-Cabrera, G.; Zuno-Cruz, F. J. *Polyhedron* **2013**, *50*, 289.
(21) Pelagatti, P.; Carcelli, M.; Costa, M.; Ianelli, S.; Pelizzi, C.; Rogolino, D. *J. Mol. Catal. A: Chem.* **2005**, *226*, 107.
(22) Zhang, H.; Enman, J.; Conrad, M.; Manning, M.; Turner, C.; Wheaton, S.; Vogels, C.; Westcott, S.; Decken, A.; Baerlocher, F. *Transition Metal Chemistry* **2006**, *31*, 13.
(23) Rülke, R. E.; Delis, J. G. P.; Groot, A. M.; Elsevier, C. J.; van Leeuwen, P. W. N. M.; Vrieze, K.; Goubitz, K.; Schenk, H. *J. Organomet. Chem.* **1996**, *508*, 109.
(24) Grach, G.; Pieters, G. g.; Dinut, A.; Terrasson, V.; Medimagh, R.; Bridoux, A.; Razafimahaleo, V.; Gaucher, A.; Marque, S.; Marrot, J. r. m.; Prim, D.; Gil, R.; Planas, J. G.; Viñas, C.; Thomas, I.; Roblin, J.-P.; Troin, Y. *Organometallics* **2011**, *30*, 4074.

(25) Grach, G.; Dinut, A.; Marque, S.; Marrot, J.; Gil, R.; Prim, D. *Org. Biomol. Chem.* **2011**, *9*, 497.
(26) Brancatelli, G.; Saporita, M.; Drommi, D.; Nicolò, F.; Faraone, F. *J. Organomet. Chem.* **2007**, *692*, 5598.
(27) Strong, E. T. J.; Cardile, S. A.; Brazeau, A. L.; Jennings, M. C.; McDonald, R.; Jones, N. D. *Inorg. Chem.* **2008**, *47*, 10575.
(28) Arnaiz, A.; Cuevas, J. V.; Garcia-Herbosa, G.; Carbayo, A.; Casares, J. A.; Gutierrez-Puebla, E. *Journal of the Chemical Society, Dalton Transactions* **2002**, *0*, 2581.
(29) Tang, F.; Qu, F.; Khusnutdinova, J. R.; Rath, N. P.; Mirica, L. M. *Dalton Trans.* **2012**, *41*, 14046.
(30) Li, Y.; El-Sayed, M. A. *The Journal of Physical Chemistry B* **2001**, *105*, 8938.
(31) Nakamura, S.; Yasui, T. *J. Catal.* **1971**, *23*, 315.
(32) Fuentes, J. A.; France, M. B.; Slawin, A. M. Z.; Clarke, M. L. *New J. Chem.* **2009**, *33*, 466.
(33) Hueso, J. L.; Sebastian, V.; Mayoral, A.; Uson, L.; Arruebo, M.; Santamaria, J. *RSC Advances* **2013**.
(34) Huang, H.; Wang, X. *Phys. Chem. Chem. Phys.* **2013**.
(35) Xie, M.; Zhang, F.; Long, Y.; Ma, J. *RSC Advances* **2013**.
(36) Zhu, Y.; Khan, Z.; Masel, R. I. *J. Power Sources* **2005**, *139*, 15.
(37) Yu, X.; Pickup, P. G. *J. Power Sources* **2008**, *182*, 124.
(38) van de Sandt, E. J. A. X.; Wiersma, A.; Makkee, M.; van Bekkum, H.; Moulijn, J. A. *Applied Catalysis A: General* **1997**, *155*, 59.
(39) Tang, W.; Zhang, X. *Chem. Rev.* **2003**, *103*, 3029.
(40) *Org. Process Res. Dev.* **2001**, *5*, 669.
(41) Song, C. E.; Lee, S.-g. *Chem. Rev.* **2002**, *102*, 3495.
(42) Costa, M.; Pelagatti, P.; Pelizzi, C.; Rogolino, D. *J. Mol. Catal. A: Chem.* **2002**, *178*, 21.
(43) Kirss, R. U.; Eisenberg, R. *Inorg. Chem.* **1989**, *28*, 3372.
(44) Himeda, Y.; Onozawa-Komatsuzaki, N.; Sugihara, H.; Arakawa, H.; Kasuga, K. *J. Mol. Catal. A: Chem.* **2003**, *195*, 95.
(45) Matharu, D. S.; Morris, D. J.; Kawamoto, A. M.; Clarkson, G. J.; Wills, M. *Org. Lett.* **2005**, *7*, 5489.
(46) Ma, Y.; Liu, H.; Chen, L.; Cui, X.; Zhu, J.; Deng, J. *Org. Lett.* **2003**, *5*, 2103.
(47) Hashiguchi, S.; Fujii, A.; Takehara, J.; Ikariya, T.; Noyori, R. *J. Am. Chem. Soc.* **1995**, *117*, 7562.
(48) Ikariya, T.; Blacker, A. J. *Acc. Chem. Res.* **2007**, *40*, 1300.
(49) Thorpe, T.; Blacker, J.; Brown, S. M.; Bubert, C.; Crosby, J.; Fitzjohn, S.; Muxworthy, J. P.; Williams, J. M. J. *Tetrahedron Lett.* **2001**, *42*, 4041.
(50) Jones, M. D.; Raja, R.; Thomas, J. M.; Johnson, B. F. G.; Lewis, D. W.; Rouzaud, J.; Harris, K. D. M. *Angewandte Chemie International Edition* **2003**, *42*, 4326.
(51) Murata, K.; Ikariya, T.; Noyori, R. *The Journal of Organic Chemistry* **1999**, *64*, 2186.
(52) Jones, M. D.; Almeida Paz, F. A.; Davies, J. E.; Johnson, B. F. G.; Klinowski, J. *Acta Crystallographica Section E* **2003**, *59*, m1091.
(53) Corma, A.; Fuerte, A.; Iglesias, M.; Sánchez, F. *J. Mol. Catal. A: Chem.* **1996**, *107*, 225.
(54) Huang, L.; Kawi, S. *J. Mol. Catal. A: Chem.* **2004**, *211*, 23.
(55) Gao, H.; Angelici, R. J. *J. Mol. Catal. A: Chem.* **1999**, *149*, 63.
(56) Sarkar, B. R.; Mukhopadhyay, K.; Chaudhari, R. V. *Catal. Commun.* **2007**, *8*, 1386.
(57) Bergbreiter, D. E.; Tian, J.; Hongfa, C. *Chem. Rev.* **2009**, *109*, 530.
(58) Angulo, B.; García, J. I.; Herrerías, C. I.; Mayoral, J. A.; Miñana, A. C. *The Journal of Organic Chemistry* **2012**, *77*, 5525.

(59) Wang, J.-L.; Li, X.; Xie, H.-Y.; Liu, B.-K.; Lin, X.-F. *J. Biotechnol.* **2010**, *145*, 240.
(60) Méry, D.; Astruc, D. *Coord. Chem. Rev.* **2006**, *250*, 1965.
(61) Taran, F.; Gauchet, C.; Mohar, B.; Meunier, S.; Valleix, A.; Renard, P. Y.; Créminon, C.; Grassi, J.; Wagner, A.; Mioskowski, C. *Angew. Chem.* **2002**, *114*, 132.
(62) Taran, F.; Gauchet, C.; Mohar, B.; Meunier, S.; Valleix, A.; Renard, P. Y.; Créminon, C.; Grassi, J.; Wagner, A.; Mioskowski, C. *Angewandte Chemie International Edition* **2002**, *41*, 124.
(63) Evans, M. A.; Morken, J. P. *J. Am. Chem. Soc.* **2002**, *124*, 9020.
(64) Reetz, M. T. *Angew. Chem.* **2002**, *114*, 1391.
(65) Reetz, M. T.; Becker, M. H.; Klein, H.-W.; Stöckigt, D. *Angew. Chem.* **1999**, *111*, 1872.
(66) Reetz, M. T. *Angewandte Chemie International Edition* **2002**, *41*, 1335.
(67) Reetz, M. T. *Angewandte Chemie International Edition* **2001**, *40*, 284.

Chapter 3

Ring Opening Polymerisation of *rac*-Lactide

3. Ring Opening Polymerisation of *rac*-Lactide

To further explore the extent for which ligands of the type prepared in Chapter 2 could be utilised with various transition metals, the ring opening polymerisation of racemic lactide was introduced as a new benchmark reaction. The importance of this reaction has been highlighted in the introduction along with the past and present literature precedent. The work of Karl Ziegler[1] and Giulio Natta[2-4] was recognised with the awarding of the chemistry Nobel prize in 1963. Ziegler had discovered the first titanium-based catalyst, while Natta utilised them for the preparation of stereo regular polymers of propylene, Figure 3.1. In 2010 is was reported that Ziegler-Natta and related catalysts produced a total which exceed 100 million metric tons of alkene based plastics, elastomers and rubbers[5]. Indeed a study conducted by Alberta Energy[6] of the polypropylene market alone, highlighted the increase in demand, worldwide, for polypropylene went from 6.4 million metric tons in 1983 to 38.6 metric tons in 2004, while the global polypropylene capacity is predicted "to extend by more than 23.5 million tons by 2019"[7]. More interestingly, is that heterogeneous supported catalysts currently dominate the industry[8]. As such, development of heterogeneous catalysts for the selective ROP of *rac*-LA might be an attractive area of work.

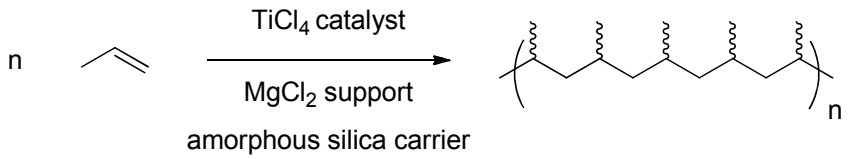

Figure 3.1. Typical conditions for the preparation of polypropylene from a heterogeneous catalyst system

3.1. Background

Methyl benzylamine is a readily available, optically active and affordable starting material to a wide range of chiral ligands. Davidson et al.[9], as previously discussed and prepared a selection of chiral Schiff bases from methyl benzylamine and salicylaldehyde complexed to zirconium and titanium. For the ROP of *rac*-LA the zirconium complexes afforded heterotactically bias PLA in solution at room and elevated temperatures as well as in the melt.

The first section in this chapter details the synthesis and complexation of a group of phenolic bis-Schiff base ligands complexed to group(IV) metals and

aluminium. The objective is to improve upon Davidson's results by incorporation of a second chiral arm in the ligand, increasing stereocontrol while at least maintaining good control over polymerisation and high levels of activity. This second chiral amine moiety is expected to be non-coordinating and as such aid in the selectivity of monomer coordination at the metal centre, potentially resulting in an isotactic polymer.

The ligands described in Section 3.2 are an extended version of Davidson's chiral Schiff base with a second imine at the alternative *ortho*-position of the salicylaldehyde leading to a second chiral centre. Such ligands are novel, bar 2*R*/*S* which proved unsuccessful for the asymmetric transfer hydrogenation of acetophenone in water, 10% conversion and 9 % enantiomeric excess, and has also been shown to self assemble into supramolecular helices when complexed to zinc(II)[10].

The second section looks at Schiff base ligands more akin to the literature precedent with just one arm. Davidson et al.[9,11] prepared a range with different amines but did not explore any additional chiral amines, nor exploited them for the ROP of *rac*-LA. In this section increased flexibility and rigidity at the chiral centre of Schiff base ligands are explored, widening the scope of metals employed and investigating the effects of sterics and electronics *via* variation around the salicylaldehyde phenol. The intention is twofold, firstly to replicate the success reported by other groups with chiral Schiff bases in terms of activity, control and selectivity, but to also feedback any positive steric or electronic effects back into the chiral phenolic bis-Schiff base ligands from the first section.

The final section of this chapter explores the effect of chirality in Salalen ligands which are defined as half salen and half salan ligands. A relatively new family of ligand that have been developed over the last decade in a response, initially, to the very increasing demand of group(IV) metal coordinating ligands for olefin polymerisation. Kol, highlighting the two structural factors of "symmetry of metal complex and the geometrical relationship of labile groups"[12] and introduced Salan ligands as [ONNO] type ligands, Figure 3.2. These had a tendency to wrap around the group(IV) metals they were complexed to, forming an octahedral complex with C_2-symmetry, one of which is reported to be the first

living polymerisation initiator producing isotactic polyolefins[13-15]. Thought to be the result of *cis*- labile groups, the salen counterpart complexes orientate such as to have *trans*- labile groups and this attributed to their poorer performances. However, as described in the introduction chapter, imine phenolate ligands, or "half-Salen units" are successful and highly active catalysts for polymerisation of lactide, and are impressive for the polymerisation of propylene[16].

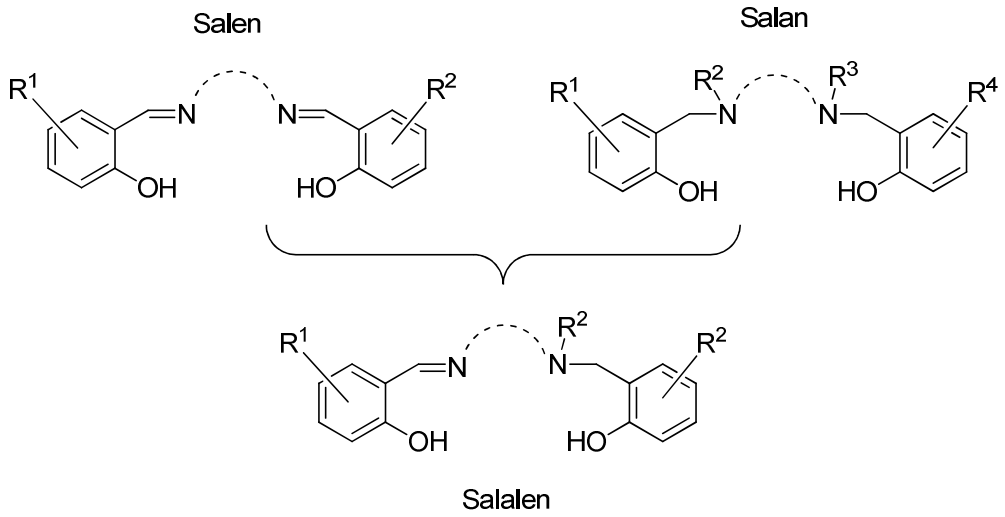

Figure 3.2. Schematic structures of Salen, Salan and Salalen ligands.

Pairing the activity of Salen and the selectivity of Salan, in a group(IV) complex has generated an optimised ligand for olefin polymerisation[17]. could then be trialled for ROP of *rac*-LA. However, since these Salalen ligands were introduced by Kol as potentially powerful polymerisation initiator, the research took a different turn. By taking the "spacer" or "backbone" and incorporating one or two chiral centres generated novel Salalen's shown in Figure 3.3.

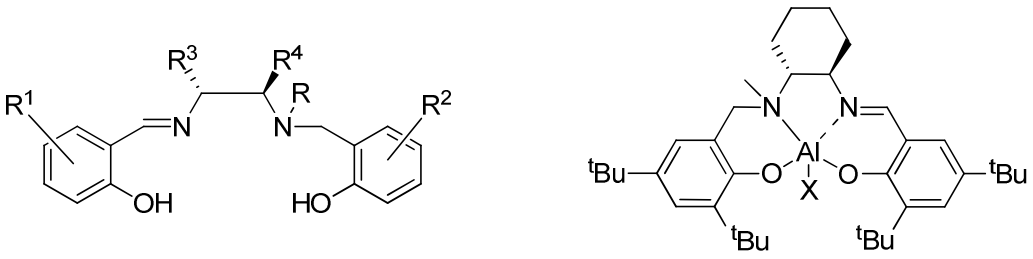

Figure 3.3. Left; general form of chiral Salalen's in the literature. Right; most commonly encountered chiral Salalen complex.

Catalysts of this type have found many of applications in the asymmetric hydrophosphrylation reaction of aldehydes and aldimines, asymmetric epoxidations, asymmetric sulfimidatio, asymmetric oxidation, asymmetric

transamination, asymmetric Simmons-Smith reaction and asymmetric hydrosilylation reactions[18-31]. The first reports of polymerisation, were those of a chromium catalyst pitted against the copolymerisation of epoxides and carbon dioxide in 2009 by Nakano et al[32]. It was not until 2011 that Kol et al.[17] reported his Salalen for the polymerisation of hexene and propylene, and despite extensive research into the ROP of *rac*-LA by Salen and Salan systems, examples initiated by Salalens are rare. Jones et al.[33,34] recently reported unsymmetrical group(IV) complexes with Salalen's, producing PLA with narrow PDI's, 1.07-1.82, and isotacticity of P_m = 0.75 in 2010.

In the final section of this chapter, a novel series of chiral asymmetric salalen complexes are prepared, with varied sterics and electronics around the aromatic ring of the salen component, and screened for the ROP of *rac*-LA.

3.2.Chiral Bis-Phenolic Schiff Base Initiators

Following from the work described in chapter two, 2,6-pyridine dicarboxaldehyde was exchanged for a di-aldehyde of similar appearance, which however incorporated a hydroxy group as such enabling complexation to group(IV) metals and aluminium.

3.2.1. Preparation of Ligands

A series of phenolic bis-Schiff Base chiral ligands were prepared using different chiral amines and 2,6-diformyl-p-cresol. Oxidation of 2,6-bis(hydroxymethyl)-p-cresol afforded the starting material and a simple imine condensation reaction formed the desired ligand. The sterics of each ligand in the series were varied by altering the substituents on the amine. All four ligands discussed in this section were prepared as shown in, Figure 3.4. Characterisation was obtained by ^{1}H, $^{13}C\{^{1}H\}$ NMR spectroscopy and high resolution mass spectrometry.

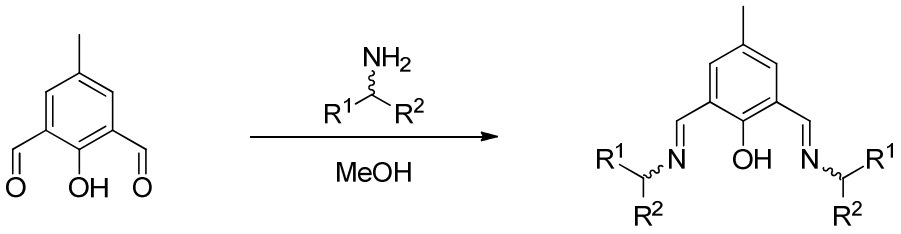

2NR-H = (*R*) R^1 = Me, R^2 = Ph **2NE**-H = (*R*) R^1 = Et, R^2 = Ph
2NS-H = (*S*) R^1 = Me, R^2 = Ph **2NN**-H = (*R*) R^1 = Me, R^2 = Naph

Figure 3.4. Preparation of bis-Schiff base Ligands

3.2.2. Complexation to Group(IV) Metals and Trimethyl Aluminium

The ligands prepared in Figure 3.4 were complexed to group(IV) metal alkoxides in a 2:1 stoichiometry of the appropriate ligand and metal salt, while the aluminium complexes were prepared in a 1:1 stoichiometric ratio after the 2:1 attempts failed, as confirmed by NMR spectroscopy. For zirconium and hafnium isopropoxides complexation was facilitated in CH_2Cl_2, whereas titanium isopropoxide and trimethyl aluminium complexes were prepared in toluene. This is shown schematically below, Figure 3.5.

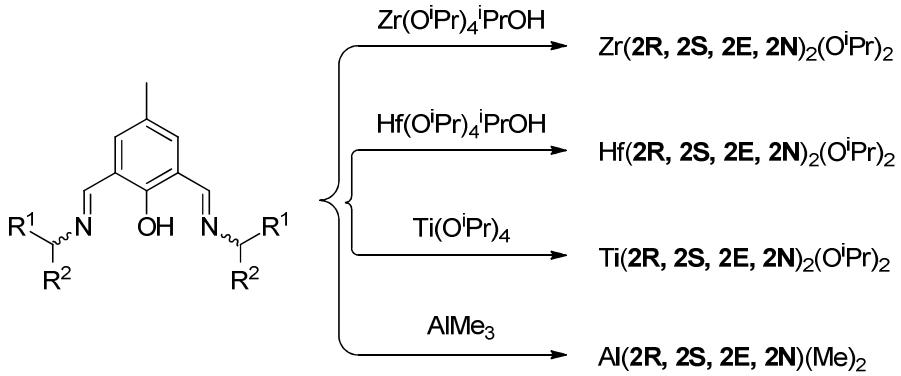

2R-H = (*R*) R^1 = Me, R^2 = Ph **2E**-H = (*R*) R^1 = Et, R^2 = Ph
2S-H = (*S*) R^1 = Me, R^2 = Ph **2N**-H = (*R*) R^1 = Me, R^2 = Naph

Figure 3.5. Complexes prepared from phenolic bis-Schiff Base chiral ligands

The complexes were characterised by ^{1}H NMR, $^{13}C\{^1H\}$ NMR spectroscopy, and elemental analysis. All the complexes are shown to be monometallic, as evidenced by single crystal X-ray diffraction, with group(IV) metals able to incorporate a pair of ligands into their structure. For the aluminium complex only one ligand was coordinated to the metal, despite repeated attempts at a 2:1 coordination. Suitable crystals were grown for the complexes of Zr(**2R**)$_2$(O^{i}Pr)$_2$ and Zr(**2S**)$_2$(O^{i}Pr)$_2$ and these are reported below.

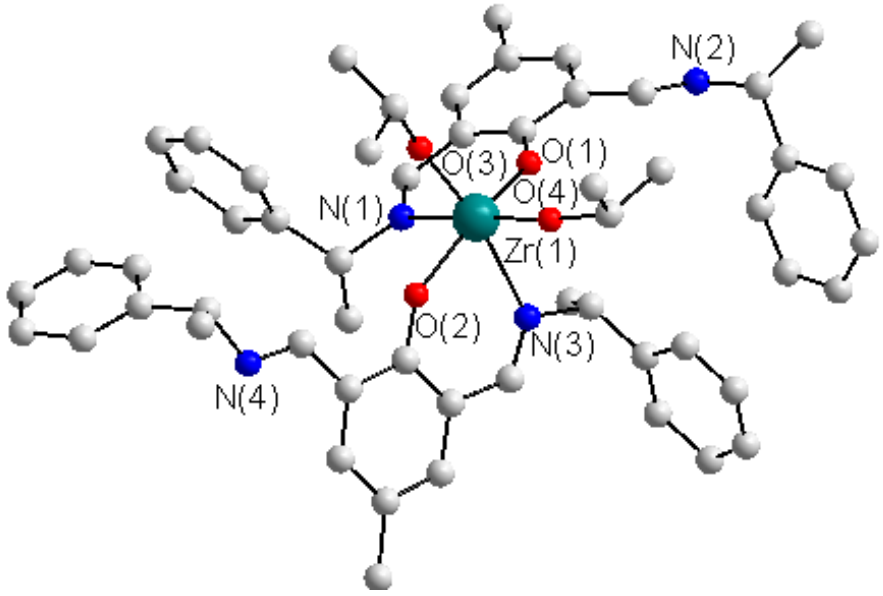

Figure 3.6. Molecular structure of $Zr(2R)_2(O^iPr)_2$, two molecules present in the unit cell, only one shown for clarity, hydrogen atoms omitted for clarity

Bond Length (Å)		Bond Angle (^{0})	
Zr(1)-O(4)	1.934(2)	O(4)-Zr(1)-O(3)	100.51(10)
Zr(1)-O(3)	1.946(2)	O(4)-Zr(1)-O(1)	93.91(9)
Zr(1)-O(1)	2.0512(19)	O(3)-Zr(1)-O(1)	101.35(8)
Zr(1)-O(2)	2.0537(19)	O(4)-Zr(1)-O(2)	101.80(9)
Zr(1)-N(1)	2.405(3)	O(3)-Zr(1)-O(2)	93.33(8)
Zr(1)-N(3)	2.418(3)	O(1)-Zr(1)-O(2)	156.18(8)
Zr(1) -N(2)	5.9347 (30)	O(4)-Zr(1)-N(1)	168.51(9)
Zr(1)-N(4)	5.9371 (31)	O(3)-Zr(1)-N(1)	88.34(9)
N(1)-C(8)	1.295(4)	O(1)-Zr(1)-N(1)	77.04(8)
N(1)-C(9)	1.507(4)	O(2)-Zr(1)-N(1)	84.82(8)
N(2)-C(18)	1.262(4)	O(4)-Zr(1)-N(3)	85.41(10)
N(2)-C(19)	1.473(4)	O(3)-Zr(1)-N(3)	169.05(9)
		O(1)-Zr(1)-N(3)	87.31(9)
		O(2)-Zr(1)-N(3)	76.35(9)

Table 3.1. Selected bond lengths and bond anlges for $Zr(2R)_2(O^iPr)_2$

The crystal isolated belongs to the triclinic system with a *P1* space group, and an absolute structure parameter of -0.006 (17). In the solid state, the

zirconium centre is observed as adopting a *pseudo*-octahedral geometry with the O(4)-Zr(1)-N(1) bond angle distorted from linearity, just short of 170 ^{0} while the O(1)-(Zr(1)-O(2) angle 156.18(8)^{0}. The distances between the zirconium centre and N(2) and N(4) are approximately 6 Å and this compares to a bond distance of approximately 2.5 Å of N(1) and N(3) which are coordinated to the metal centre. The imine and amine bond lengths correspond well to literature values[11,35-37] for similar complexes. The bond distances of the iso-propoxides are smaller than that of the phenoxy, again as expected.

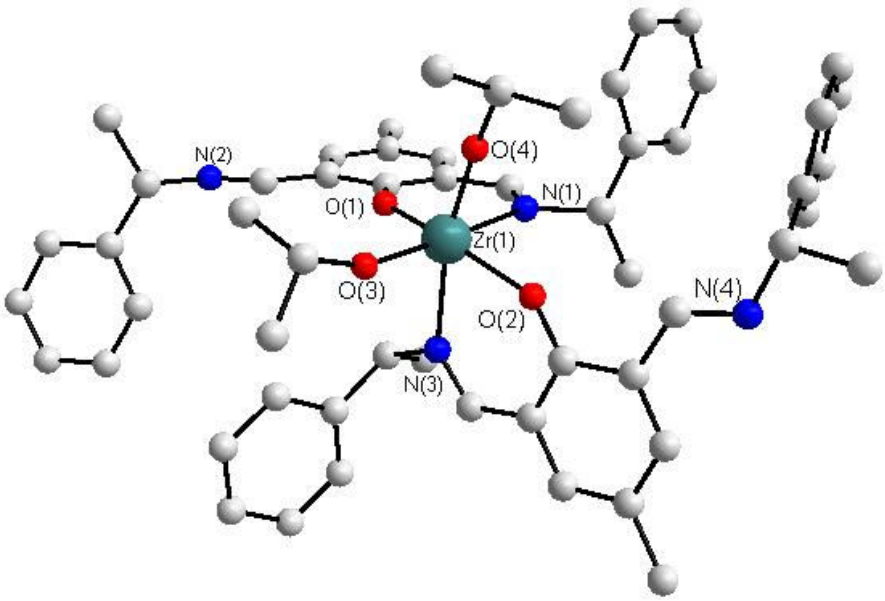

Figure 3.7. Solid state structure of $Zr(2S)_2(O^iPr)_2$

The structure above is in the same crystal system, triclinic, as that of $Zr(\mathbf{2R})_2(O^iPr)_2$, Figure 3.6, and belongs to the same space group *P1*. The absolute structure parameter of -0.024(17) indicates an enantiomerically pure crystal. The zirconium centre is observed as adopting a pseudo-octahedral geometry The O(3)-Zr(1)-N(1) bond angle distorted from linearity, just short of 170 ^{0} while the O(1)-(Zr(1)-O(2) angle 155.31(8)^{0}. It has also be highlighted that the distances between the zirconium metal and N(2) and N(4) are significantly greater than the bonding distance and are therefore non coordinating. The bond lengths and angles are comparable to the earlier crystal structure and literature values[11,35-37].

Bond Length (Å)		Bond Angle (^{0})	
Zr(1)-O(4)	1.940(2)	O(4)-Zr(1)-O(3)	99.19(9)
Zr(1)-O(3)	1.9470(19)	O(4)-Zr(1)-O(1)	101.11(9)
Zr(1)-O(1)	2.0533(18)	O(3)-Zr(1)-O(1)	94.39(8)
Zr(1)-O(2)	2.054(2)	O(4)-Zr(1)-O(2)	93.50(9)
Zr(1)-N(1)	2.404(3)	O(3)-Zr(1)-O(2)	102.87(8)
Zr(1)-N(3)	2.413(3)	O(1)-Zr(1)-O(2)	155.31(8)
Zr(1)-N(2)	5.9467(24)	O(4)-Zr(1)-N(1)	85.91(9)
Zr(1)-N(4)	5.9467(24)	O(3)-Zr(1)-N(1)	169.98(8)
		O(1)-Zr(1)-N(1)	76.10(8)
		O(2)-Zr(1)-N(1)	85.31(8)
		O(4)-Zr(1)-N(3)	168.46(8)
		O(3)-Zr(1)-N(3)	89.11(8)
		O(1)-Zr(1)-N(3)	86.12(8)
		O(2)-Zr(1)-N(3)	76.74(8)

Table 3.2. Selected bond distances and angles for the solid state structure of $Zr(2S)_2(O^iPr)_2$

For the pair of crystals isolated, two different structural isomers are observed. As most zirconium complexes, the isopropoxides occupy the *cis* geometry but due to the bidentate chiral ligands we experience optical isomerisation. This is shown in Figure 3.8, where, just like chiral isomers, the two molecules are non-superimposable with each other, being mirror images. This is often experienced in coordination chemistry where multiple, dual chelating ligands are used and are given the prefixes delta and lambda, Δ for a right handed propeller twist and Λ for a left handed twist.

The chemical formula of all the complexes was confirmed using elemental analysis. Crystals isolated confirmed the presence of Λ and Δ diastereomers and the preference of the isopropoxide groups for cis orientation. The presence of these isomers resulted in peak assignment in the ^{1}H NMR spectrum being difficult and as a result, variable temperature ^{1}H NMR spectroscopy was employed to probe an potential equilibrium of the isomers in solution. The aim was to see a shift in the equilibrium to one, more dominant, isomer as the temperature was reduced. Unfortunately, investigations were unsuccessful and the intensity of the resonances did not change as the temperature changed suggesting that the isomers

were not in equilibrium. Thus, in solution both the diastereomers are formed in approximately 50:50 ratios.

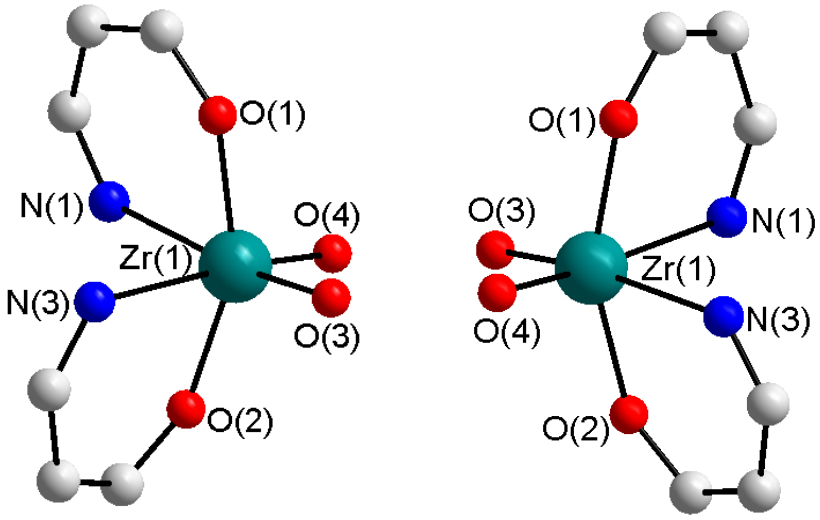

Figure 3.8. Metal centres of the above crystals, displaying the Λ-cis geometry of $Zr(2S)_2(O^iPr)_2$ on the left and the Δ-cis geometry of $Zr(2R)_2(O^iPr)_2$.

3.2.3. Ring Opening Polymerisation of *rac*-Lactide.

The complexes prepared above, were screened as initiators for the ROP of *rac*-LA under solvent free conditions and in solution. The catalyst labelling has been abbreviated, for representation in the tables included herein, to a three character code. The first character is representative of the metal centre, the second character is that of the common moiety (in this case the dialdehyde), while the final character is an abbreviation of the variant moiety (in this case the chiral amine). As such the complex $Zr(\mathbf{2R})_2(O^iPr)_2$, picture in Figure 3.6, becomes **Z2R**. Later examples, where the chiral amine remains constant while the salicylaldehyde, follow a similar abbreviation pattern and will be explained in due course.

The monomer feedstock was purified, by two methods; i) simple recrystallisation in toluene and ii) recrystallisation followed by a double sublimation. These two methods of monomer purification were both used to investigate the complexes stability to the impurities often found in the monomer as a result of the processes involved in its preparation. Group(IV) alkoxide complexes as prepared above have been shown to be susceptible to contaminants.

For the solution polymerisations, reactions were undertaken in 5 ml of toluene at a temperature of 80°C with a monomer:initiator ratio of 100:1. Polymerisations were carried out for a reaction time of 24 hours with either 0.7 g or 0.5 g or *rac*-LA. The melt polymerisations were performed in the absence of any solvent, at a temperature of 130°C for 2 hours. The monomer:initiator ratio used was 300:1 employing 1 g of *rac*-LA

3.2.4. Titanium Initiators

Titanium initiators were screened for the ROP or *rac*-LA in toluene at 80°C for 24 hours. Unfortunately, the polymerisations after this time did not produce any significant amount of polymeric material, results are reported in Table 3.3 below, only oligomeric PLA being obtained which was below the detection limit of the GPC. As discussed in Chapter 1, the theoretical M_n is calculated as the product between conversion and repeat unit size, while P_r is determined from the ^{1}H homonuclear decoupled NMR spectra.

Entry	Initiator	Lactide	Conversion[a] (%)	M_n[b]	M_w[b]	M_n (theo.)	PDI[b]	P_r[c]
1	T2R	reXtal	12	-	-	1,750	-	-
2		Sub	10	-	-	1,450	-	-
3	T2S	reXtal	13	-	-	1,850	-	-
4		Sub	9	-	-	1,300	-	-
5	T2E	reXtal	27	-	-	3,900	-	-
6		Sub	16	-	-	2,300	-	-
7	T2N	reXtal	17	-	-	2,450	-	-
8		Sub	16	-	-	2,300	-	-

Table 3.3. ROP results for titanium bis-phenolic Schiff base initiators in toluene at 80°C for 24hrs with 0.7 g of *rac*-LA, LA:Ini = 100:1. [a]Conversion determined *via* ^{1}H NMR, [b]determined from GPC referenced to PS in THF, [c]calculated from the ^{1}H homonuclear decoupled NMR analysis.

Under the more industrially relevant melt conditions, the same titanium initiators showed some activity, at 130°C after 2 hours, monomer:initiator ratio of 300:1. The results are shown in Table 3.4.

Entry	Initiator	Lactide	Conversion[a] (%)	M_n[b]	M_w[b]	M_n (theo.)	PDI[b]	P_r[c]
1	T2R	reXtal	29	3,800	4,200	12,500	1.10	0.50
2		Sub	41	4,250	4,600	17,700	1.08	0.51
3	T2S	reXtal	15	-	-	-	-	-
4		Sub	36	4,900	5,550	15,550	1.13	0.50
5	T2E	reXtal	32	15,600	16,400	13,800	1.05	0.52
6		Sub	13	-	-	-	-	-
7	T2N	reXtal	62	8,500	12,000	26,800	1.41	0.50
8		Sub	65	8,950	12,450	28,100	1.39	0.51

Table 3.4. ROP results for titanium bis-phenolic Schiff base initiators under solvent free conditions at 130°C for 2hrs with 1.0 g of *rac*-LA, LA:Ini = 300:1. [a]Conversion determined *via* ^{1}H NMR, [b]determined from GPC referenced to PS in THF, [c]calculated from the ^{1}H homonuclear decoupled NMR analysis.

The benchmark catalyst that we can compare the work herein is that of Davidson et al[11]. The titanium initiators prepared above performed poorly for the ROP of *rac*-LA. The initiators were generally inactive under the milder solution polymerisation conditions, struggling to achieve a conversion greater than 30 %. Moreover, the converted monomer was not polymeric, but rather oligomeric, and as such was lost during the methanol wash of the crude material, which is the standard procedure to remove unreacted monomer.

Inactivity of a titanium initiator has been experienced in the literature[11]. Davidson et al.[11] prepared a selection of chiral Schiff bases of similar design to those prepared above. In their investigation, the titanium complexes prepared were inactive under solution conditions, however, when polymerisation was conducted under the more industrially relevant method in the absence of solvent, moderate conversions were obtained, likely due to the higher temperatures of polymerisation, however the polymeric material was atactic. This is the case with the chiral -bis-phenolic Schiff base ligands presented in this section. As the data in Table 3.3, the initiators to begin to show a degree of activity with the **T2N** initiator performing best, converting two thirds of the monomer present into PLA. However, in each case, the polymeric material was produced with no apparent selectivity resulting in atactic polymer. M_n values are generally in poor agreement with theoretical values, with the exception of **T2E**, and can be said that the

polymerisation is inadequately controlled by these titanium initiators. The polymer weight distributions are narrow, as described by PDI, suggesting minimal transesterification and other side reactions. **T2N** stands out from the other initiators under melt polymerisation. The calculated values for M_n are somewhat greater than those observed and the PDI is moderate but reasonable.

The results are generally not very promising, with poor performance likened to similar catalysts[11], and no conclusions can be made about the initiators stability regarding the monomer's purity. Using other group(IV) metals proved promising in the literature[11,36] and as such it was decided that Zr(IV) and Hf(IV) would be investigated.

3.2.5. Zirconium Initiators

Zirconium initiators were trailed for the ROP or *rac*-LA in toluene at 80°C for 24 hours. High conversions were achieved with good polymerisation control and a slight heterotactic bias, results are reported in Table 3.5 below.

Entry	Initiator	Lactide	Conversion[a] %	M_n[b]	M_w[b]	M_n (theo.)	PDI[b]	P_r[c]
1	Z2R	reXtal	97	11,650	14,000	14,000	1.20	0.59
2		Sub	99	11,400	14,000	14,300	1.23	0.60
3	Z2S	reXtal	94	13,000	15,200	13,550	1.17	0.59
4		Sub	100	13,200	15,200	14,400	1.15	0.59
5	Z2E	reXtal	96	13,100	15,300	13,900	1.17	0.61
6		Sub	98	13,800	18,650	14,100	1.19	0.61
7	Z2N	reXtal	91	12,600	15,250	13,100	1.21	0.59
8		Sub	95	12,050	14,350	13,400	1.19	0.59

Table 3.5. ROP results for zirconium bis-phenolic Schiff base initiators in toluene at 80°C for 24hrs with 0.7 g of *rac*-LA, LA:Ini = 100:1. [a]Conversion determined *via* ^{1}H NMR, [b]determined from GPC referenced to PS in THF, [c]calculated from the ^{1}H homonuclear decoupled NMR analysis.

Table 3.6 below details the results for the melt polymerisation of *rac*-lactide with the chiral-bis-phenolic Schiff base zirconium complexes. The reactions were conducted in sealed ampules for two hours at a temperature of 130 °C. The resulting polymeric material was dissolved in dichloromethane and quenched with methanol. It should be noted, that the observed M_n can exceed the theoretical value as the polymerisation is living, as discussed in detail below. The

observed M_n can exceed the predicted value (M_n theo.) due to the living nature of these initiators, which is proven below, and the way in which the theoretical M_n is calculated. The assumption is made that the monomer is evenly distributed amongst the initiators. In the case of initiator deactivation, the initiator:monomer ratio effectively increases which has the observed result of increased M_n .

Entry	Initiator	Lactide	Conversion[a] %	M_n[b]	M_w[b]	M_n (theo.)	PDI[b]	P_r[c]
1	2RZ	reXtal	99	43,000	52,900	42,750	1.23	0.59
2		Sub	100	44,150	53,400	43,200	1.21	0.60
3	2SZ	reXtal	99	42,850	52,300	42,750	1.22	0.60
4		Sub	99	42,600	51,100	42,750	1.20	0.59
5	2EZ	reXtal	99	51,650	70,750	42,750	1.37	0.59
6		Sub	100	50,050	68,050	43,200	1.36	0.58
7	2NZ	reXtal	99	49,250	68,950	42,750	1.40	0.58
8		Sub	98	50,950	70,800	42,350	1.39	0.59

Table 3.6. ROP results for zirconium bis-phenolic Schiff base initiators in the absence of solvent at 130 °C for 2hrs with 1.0 g of *rac*-LA, LA:Ini = 300:1. [a]Conversion determined *via* ^{1}H NMR, [b]determined from GPC referenced to PS in THF, [c]calculated from the ^{1}H homonuclear decoupled NMR analysis.

The performance of the zirconium initiators, compared to titanium, is significantly improved. For the solution polymerisation, Table 3.5, M_n is in very good agreement with theoretical values, and is indicative of single polymer chain propagated by each metal centre, and the rate of initiation being greater than the rate of propagation. However, there is no noticeable trend between control and the sterics introduced by the chiral amine. The short comings between the observed value and the calculated value, entries 5 - 8, can be explained as a result of side reactions and catalyst deactivation from the impurities in the monomer feed. Good control of the polymerisation is also confirmed by the low PDI values, suggesting that side reactions like transesterification and back biting are kept to a minimum. The P_r values obtained from the homonuclear decoupled NMR indicate that there is a mild heterotactic bias, which would appear to be unaffected by the steric bulk about the chiral centre of the ligand.

Another important point is that the difference between polymerisation of the sublimed lactide *vs* the recrystallised lactide. Sublimation is very energy intensive, requiring reduced pressures and high temperatures. It is also not

logistically feasible on an industrial scale, and as such the industrial standard is recrystallisation. The results from Table 3.5 indicate that, in solution, the zirconium initiators are stable to the impurities in the monomer, with there being no noticeable difference the two purification methods employed. PDI is slightly lower for the sublimed monomer, but the difference is insignificant. Selectivity differences between sublimed *vs.* recrystallised are not significant and do not justify the energy intensive purification process.

The melt polymerisation reactions, Table 3.6, improve on the conversion compared to their solution counterparts, reaching in some cases complete conversion over the two hour time frame. This is a good sign, as the melt polymerisation reaction mixture can become more viscous as the molten monomer becomes longer polymer chains with a higher melting point. Control is maintained, with M_n values again being in close agreement with the calculated values, however PDI has increased slightly. This is not unusual as the elevated temperature and the increased concentration of impurities relative to initiator can result in side reactions such as, chain transfer and transesterification.

Further analysis of the polymeric material was obtained by employing MALDI-ToF mass spectrometry. A sample of the polymerisation product produced by $Zr(\mathbf{2E})_2(O^iPr)_2$ was submitted and the resulting spectra can be seen below, Figure 3.9 and Figure 3.10.

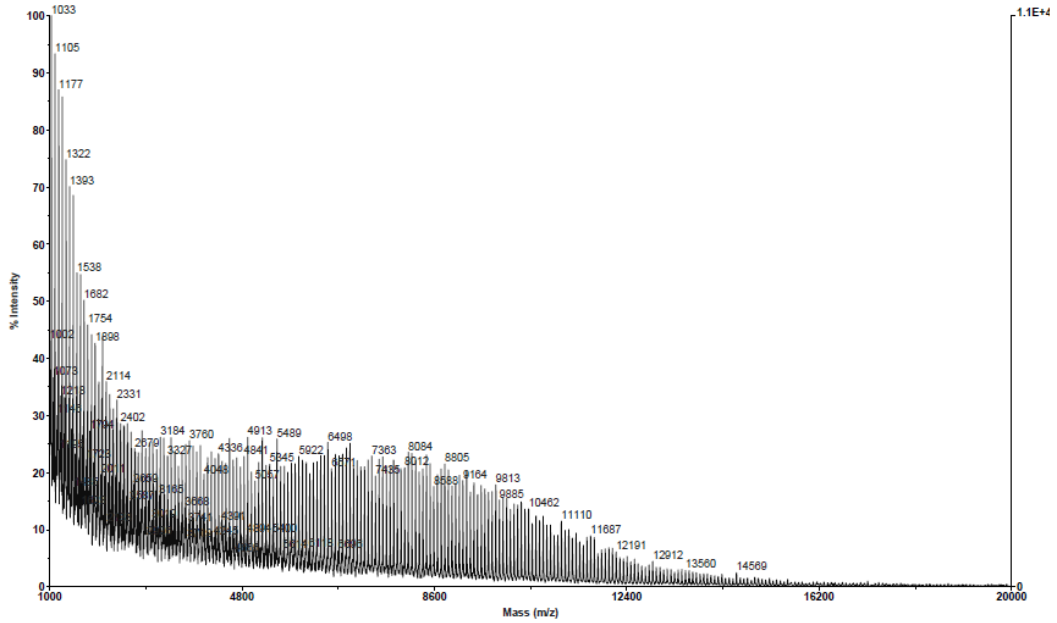

Figure 3.9. MALDI-ToF mass spectrum for the polymeric material produced by $Zr(2E)_2(O^iPr)_2$. Samples ionised with Na^+.

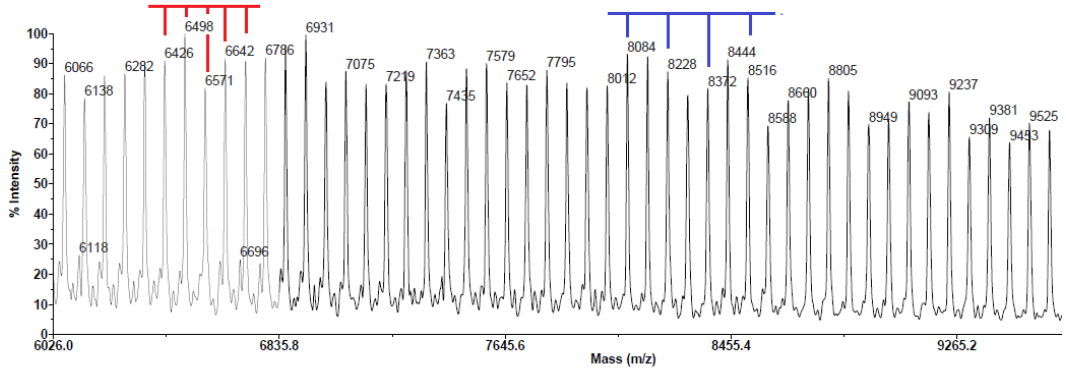

Figure 3.10. Zoomed in view of the same MALDI-ToF above, highlighting in blue, the repeating unit of a lactide molecule, 144 g mol^{-1}, and in red a repeating unit of mass 72 g mol^{-1} indicative of cyclic polymers. Samples ionised with Na^+.

The MALDI-ToF mass spectrum shows that the polymers contain an isopropoxide end group, confirming that the reaction proceeds *via* a coordination and insertion mechanism at the high mass range, high M_n. There is evidence of cyclic oligomers at low M_n suggesting that transesterification and back biting do occur but on a limited scale.

The nature of polymerisation was further investigated with $Zr(\mathbf{2E})_2(O^iPr)_2$, due to its high level of activity. The polymerisation was repeated at greater monomer to initiator ratios than the standard 100:1. The results from this catalyst loading experiment can be seen in Figure 3.11.

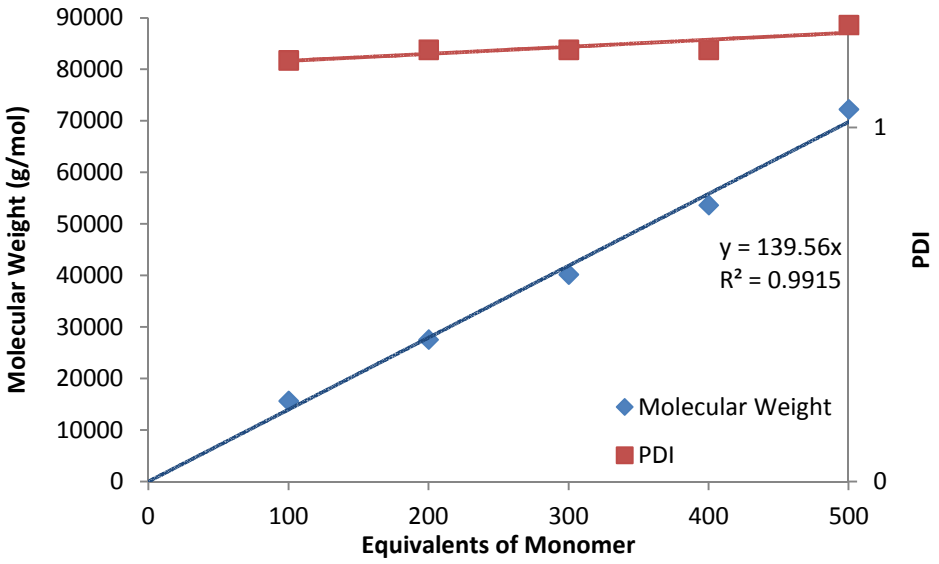

Figure 3.11. Plot of polymeric analysis against the monomer:initiator ratio, for the polymerisation or *rac*-LA at 80 °C for 24 hours in toluene, the catalyst for each polymerisation was $Zr(2E)_2(O^iPr)_2$

It can be clearly seen that the molecular weight of the resulting polymeric sample increases linearly with an increased monomer:initiator ratio, and the initiator maintains good control despite the increased concentration. This correlation between monomer concentration and M_n supports the controlled "living" nature of polymerisation for these initiators, moreover it means that a desired M_n can be achieved *via* monomer concentration choice. The gradient of the line plotted for M_n against the ratio of monomer:initiator is 139.56 Da, which is just short of the monomer repeat unit 144 Da, supporting further evidence for single chain propagation. A near constant PDI is indicative of a well controlled polymerisation.

3.2.6. Hafnium Initiators

The four hafnium initiators were trailed for the ROP or *rac*-LA in toluene at 80°C for 24 hours, Table 3.7, and also under the more industrially relevant melt conditions, Table 3.8.

Entry	Initiator	Lactide	Conversion[a] %	M_n[b]	M_w[b]	M_n (theo.)	PDI[b]	P_r[c]
1	2RH	reXtal	98	11,650	14,000	14,000	1.20	0.58
2		Sub	99	11,400	14,000	14,300	1.23	0.60
3	2SH	reXtal	98	13,000	15,200	13,550	1.17	0.58
4		Sub	99	13,200	15,200	14,400	1.15	0.59
5	2EH	reXtal	97	13,100	15,300	13,900	1.17	0.61
6		Sub	98	13,800	18,650	14,100	1.19	0.61
7	2NH	reXtal	94	12,600	15,250	13,100	1.21	0.57
8		Sub	96	12,050	14,350	13,400	1.19	0.58

Table 3.7. ROP results for hafnium bis-phenolic Schiff base initiators in toluene at 80°C for 24hrs with 0.7 g of *rac*-LA, LA:Ini = 100:1. [a]Conversion determined *via* ^{1}H NMR, [b]determined from GPC referenced to PS in THF, [c]calculated from the ^{1}H homonuclear decoupled NMR analysis.

Entry	Initiator	Lactide	Conversion[a] %	M_n[b]	M_w[b]	M_n (theo.)	PDI[b]	P_r[c]
1	H2R	reXtal	99	43,000	52,900	42,750	1.23	0.58
2		Sub	99	44,150	53,400	43,200	1.21	0.59
3	H2S	reXtal	98	42,850	52,300	42,750	1.22	0.58
4		Sub	98	42,600	51,100	42,750	1.20	0.58
5	H2E	reXtal	100	51,650	70,750	42,750	1.37	0.59
6		Sub	99	50,050	68,050	43,200	1.36	0.58
7	H2N	reXtal	98	49,250	68,950	42,750	1.40	0.57
8		Sub	97	50,950	70,800	42,350	1.39	0.57

Table 3.8. ROP results for hafnium bis-phenolic Schiff base initiators in the absence of solvent at 130 °C for 2hrs with 1.0 g of *rac*-LA, LA:Ini = 300:1. [a]Conversion determined *via* ^{1}H NMR, [b]determined from GPC referenced to PS in THF, [c]calculated from the ^{1}H homonuclear decoupled NMR analysis.

The hafnium initiators are highly active for the ROP of *rac*-LA both in solution and under solvent free conditions. This is in contrast to the titanium initiators, however, it is the same behaviour that we have seen with the zirconium initiators, and this difference has been reported previously with similar initiators[11]. M_n is in good agreement with theoretical values and with a reasonably narrow polydispersity index it can be confidently said that side reactions, backbiting and transesterification are kept to a minimum while a single chain is propagated per metal centre. P_r values are maintained upon changing from zirconium to hafnium, and once again there is no apparent correlation between amine choice and tacticity. The resulting PLA has a moderate degree of

heterotactic enrichment which can be seen by an increase in the isi and sis tetrads as discussed in Chapter 1.

Upon changing to the harsher reaction conditions of the melt polymerisation, it would be expected to see a drop in the control of polymerisation, due to the increased concentration of impurities relative to catalyst and the elevated temperatures. However, the hafnium initiators trialled above, Table 3.8, maintain a high level of control. PDI has broadened slightly and selectivity is very slightly reduced.

For the Zr(IV) and Hf(IV) initiators, there is no noticeable difference between using the monomer feeds of different purity. The short comings in M_n and any broad PDI are not decreased upon polymerisation of the sublimed lactide. This indicates that the initiators have a tolerance to the impurity concentration. This is important because sublimation is an energy intensive process and difficult to do on a large scale, whereas recrystallisation is the industrial standard.

3.2.7. Aluminium Initiators

Following the expressed tolerance of the initiators to the impurities in the monomer feed, sublimed *rac*-lactide was omitted for future tests. To generate an alkoxide, stoichiometric amount of benzyl alcohol was added prior to polymerisation to generate the initiating species *in situ*. The initiators were trialled for the ROP or *rac*-LA in toluene at 80°C for 24 hours, the results for which are given in Table 3.9.

Entry	Initiator	Conversion[a] %	M_n[b]	M_w[b]	M_n (theo.)	PDI[b]	P_r[c]
1	A2R	89	12,950	15,400	12,800	1.19	0.50
2	A2S	90	13,800	14,800	13,000	1.07	0.49
3	A2E	94	14,200	18,200	13,550	1.28	0.49
4	A2N	65	14,600	22,050	9,400	1.51	0.51

Table 3.9. ROP results for aluminium bis-phenolic Schiff base initiators in toluene at 80°C for 24hrs with 0.7 g of *rac*-LA, LA:Ini = 100:1. [a]Conversion determined *via* ^{1}H NMR, [b]determined from GPC referenced to PS in THF, [c]alculated from the ^{1}H homonuclear decoupled NMR analysis.

Below, Table 3.10, displays the results for the aluminium initiated ROP of *rac*-LA under the industrially relevant melt conditions, 130 °C for two hours in the absence of solvent.

Entry	Initiator	Conversion[a] %	M_n[b]	M_w[b]	M_n (theo.)	PDI[b]	P_r[c]
1	A2R	94	41,200	50,300	40,600	1.22	0.50
2	A2S	89	39,000	46,000	38,450	1.18	0.49
3	A2E	97	49,550	64,400	41,900	1.30	0.50
4	A2N	78	34,050	46,300	33,700	1.36	0.51

Table 3.10. ROP results for hafnium bis-phenolic Schiff base initiators in the absence of solvent at 130 °C for 2hrs with 1.0 g of *rac*-LA, LA:Ini = 300:1. [a]Conversion determined *via* ^{1}H NMR, [b]determined from GPC referenced to PS in THF, [c]alculated from the ^{1}H homonuclear decoupled NMR analysis.

The aluminium initiators deviate from the consistent performance that had been seen with zirconium and hafnium, however they are active unlike the titanium initiators. In solution, conversion is relatively high with the exception of **A2N,** entry 4, which also experiences a broad polydispersity index. This may be due to the difficult nature of preparing the initiating group *in situ* from benzyl alcohol and the aluminium complex, a greater susceptibility towards monomer impurities not previous experienced by the group(IV) initiators or by a greater degree of transesterification and back biting. It is possible to prepare and isolate the active initiator during the synthetic procedure, however it involves additional synthetic steps and purification moreover the complex is less stable. The other initiators behave well, however less consistent than previously seen. The two initiators, **2RA** and **2SA**, would be expected to behave very similar due to the difference in the structure of the initiator being the chirality of the amine, however there appears to be a mild difference between their catalytic performance.

The selectivity for these initiators under solution conditions is poor, with only atactic polymer being produced. This expectantly is not improved upon changing the polymerisation to solvent free conditions. Activity has been maintained, while control decreased slightly. **2NA** is still under performing compared to the others, however, it is more in line with its counterparts and produces a polymer with an M_n in good agreement with the calculated value for one chain propagating per metal centre.

3.2.8. Conclusions

Four chiral bis-phenolic Schiff base ligands were prepared from enantiopure chiral amines and 2,6-bis(hydroxymethyl)-p-cresol. These were complexed to various group(IV) metals in a two-to-one ratio, while they were complexed to aluminium in a one-to-one ratio, after unsuccessful attempts to generate the two-to-one initiator.

The twelve group(IV) initiators were screened for the ROP or *rac*-LA under solution and melt conditions. The titanium initiators were mostly inactive for the solution polymerisation, however they did show activity at elevated temperatures. In either case, atactic polymer was produced. Zirconium and hafnium initiators were active in both solvent free and solution conditions. A mild heterotactic bias is observed and high levels of control are maintained. Aluminium initiators are active, however produced atactic PLA.

Further investigation with $Zr(\mathbf{2E})_2(O^iPr)_2$ ascertained that a coordination insertion mechanism was being followed, with mild back-biting and transesterification, as explained in Chapter 1, occurring at low M_n, as observed from the MALDI-ToF mass spectrum. A catalyst loading experiment highlighted the living nature of the polymerisation, which maintained control at higher monomer concentrations and predictable polymerisation.

3.3. Chiral Phenolic Schiff Base Initiators

Following the success of the bis-Schiff base ligands modification of the ligand was anticipated to offer the ability to achieve greater selectivity.

3.3.1. Preparation of Ligands

Two series of chiral phenolic Schiff base ligands were prepared from (*R*)-α-ethyl benzylamine and (*R*)-α-methyl-2-naphthalenemethylamine and different salicylaldehydes where prepared. 5-methylsalicylaldehyde and 3,5-di-tert-butyl-2-hydroxybenzaldehyde were prepared from their corresponding phenols by a straight forward *ortho*-formylation reaction, Figure 3.12.

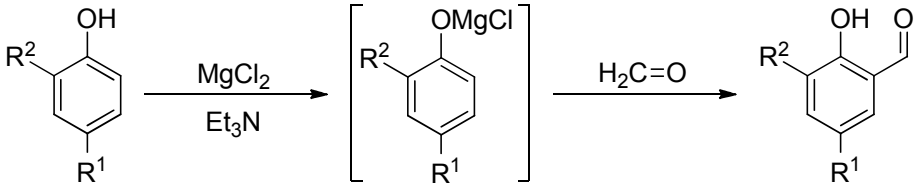

Figure 3.12. Formylation reaction generating salicylaldehydes

A simple imine condensation between chiral amine and salicylaldehyde afforded the desired ligand, varying sterics and electronics by different substitutions around the phenol ring of the salicylaldehyde. Each set of four ligands discussed within this section were prepared as shown in Figure 3.13 and characterised by ^{1}H, $^{13}C\{^{1}H\}$ NMR spectroscopy and high resolution mass spectrometry.

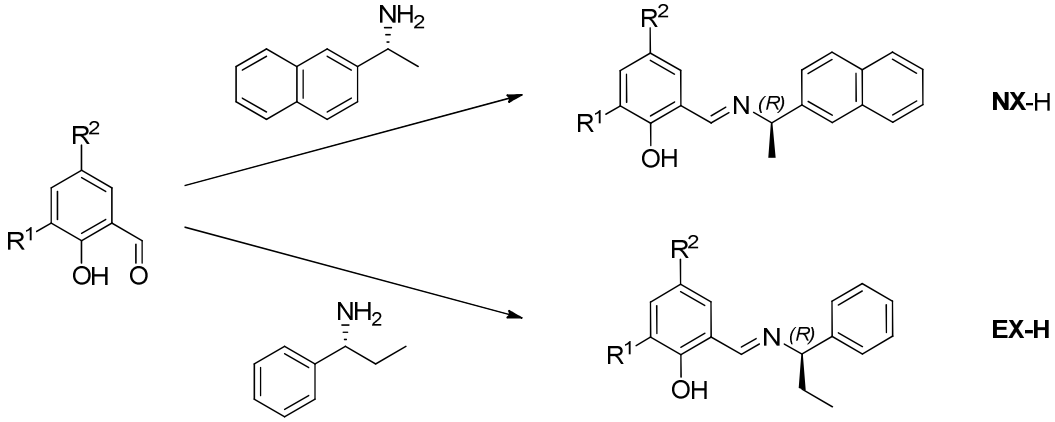

EX	**NX**-H
EH-H: $R^1 = R^2 = H$	**NH**-H: $R^1 = R^2 = H$
E5-H: $R^1 = H$, $R^2 = Me$	**N5**-H: $R^1 = H$, $R^2 = Me$
EB-H: $R^1 = R^2 = {}^{t}Bu$	**NB**-H: $R^1 = R^2 = {}^{t}Bu$
EC-H: $R^1 = R^2 = Cl$	**NC**-H: $R^1 = R^2 = Cl$

Figure 3.13. Preparation of chiral Schiff base ligands.

Of these ligands, **NB**-H produced crystals suitable for X-ray diffraction. The solid state structure is given below, Figure 3.14, along with selected bond lengths and bond angles, Table 3.11.

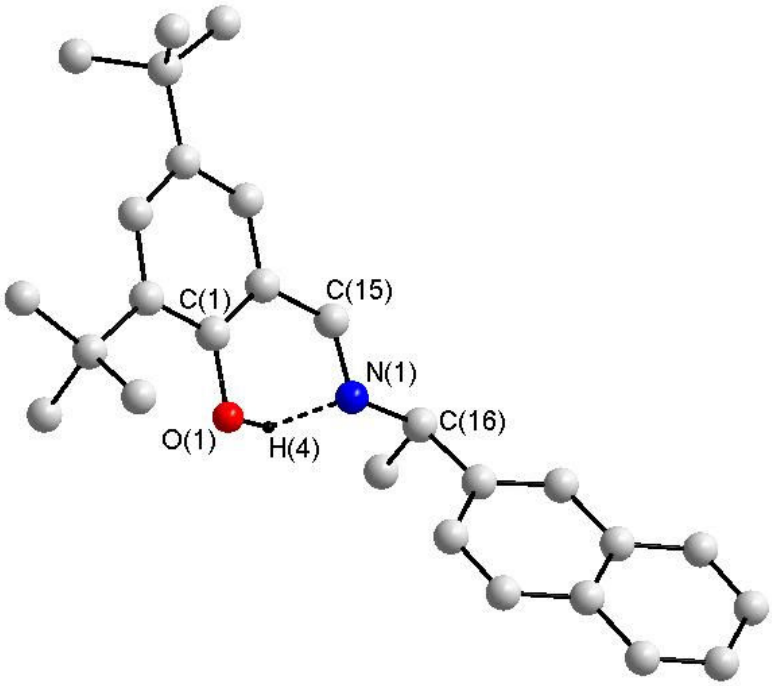

Figure 3.14. Solid state structure for the phenolic Schiff base chiral ligand NB-H, hydrogen atoms have been removed for clarity, except those involved in intramolecular hydrogen bonding, with the dashed line representing said bond.

Bond lengths (Å)	
O(1)-C(1)	1.3679(1)
N(1)-C(15)	1.2795(1)
N(1)-C(16)	1.4672(1)

Table 3.11. Selected bond lengths for NB-H

H-Bond	D-H / Å	H···A / Å	D···A / Å	D-H-A / °
O1 H1 N1	0.8382(1)	1.8281(1)	2.6039(1)	153.207(1)

Table 3.12. Hydrogen bond distances and angles in NB-H

From Table 3.11 it can been seen that the bond length between N(1) and C(15) is considerable shorter than that between N(1) and C(16). This is expected with {N(1)-C(15)} being an imine bond and the carbon sp^2 hybridised, while the more flexible, sp^3 hybridised amine bond of {N(1)-C(16)}. Intramolecular hydrogen bonding occurs between the proton of the phenoxy group and the nitrogen atom, and can be defined, as by Jeffrey[38], as "moderate, mostly electrostatic"[38] being in the range of 2.5 - 3.2 Å

3.3.2. Complexation to Group(IV) Metals and Trimethyl Aluminium

The ligands prepared above, Figure 3.13, were complexed to group(IV) metal alkoxides in a 2:1 stoichiometry of the appropriate ligand and metal salt. For zirconium and hafnium isopropoxides complexation was facilitated in CH_2Cl_2, whereas Titanium isopropoxide and trimethyl aluminium complexes were prepared in toluene. This is shown schematically below, Figure 3.15. Following the issues from the previous ligand set, no attempts were made at preparing a 2:1 ligand:aluminium complex, and as such the aluminium complexes were isolated and used in a 1:1 stoichiometry.

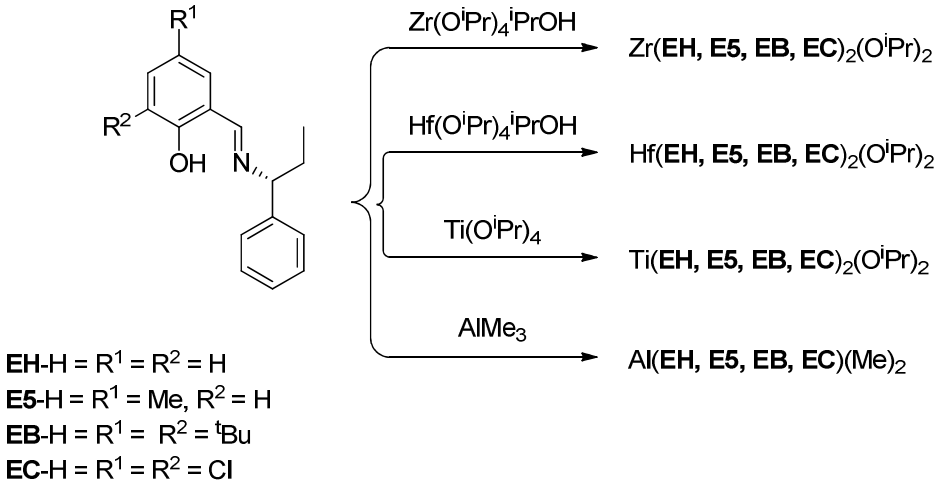

Figure 3.15. Complexes prepared from chiral Schiff bases incorporating (*R*)-ethyl benzylamine.

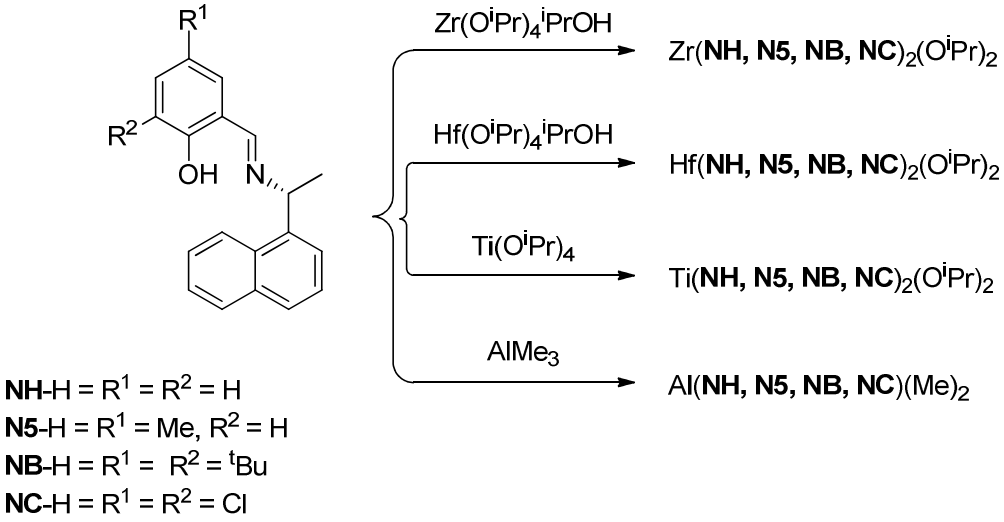

Figure 3.16. Complexes prepared for the ROP of *rac*-LA from the (R)- α-Methyl-2-Naphthalenemethylamine bearing Schiff base

All complexes were characterised by ^{1}H NMR, $^{13}C\{^{1}H\}$ NMR spectroscopy, and elemental analysis. All the complexes are shown to be monometallic with group(IV) metals able to incorporation a pair of ligands into their structure, while the aluminium one ligand, even with the increased steric bulk, with both increased rigidity, naphthyl containing, and increased flexibility, ethyl amine containing. Although numerous attempts were made, no crystals were grown suitable for single crystal XRD were obtained.

With the N,O-chelating character of the ligands employed, the geometry can result in the possibility five different isomeric structures. Group(IV) complexes most commonly position the isopropoxide groups in a cis position to one another, and as such with the resulting complex falling into a bis(η^2-*trans*-O,O) categories[9]. This complex can then form one of two diastereomers of either Δ or Λ chirality at the metal centre. This was experienced by Davidson et al.[11] where in the solid-state the complexes exhibited a single diastereomer, while in solution some structures exhibited both diastereomers characterised by ^{1}H and $^{13}C\{^{1}H\}$ NMR. This was also reported by Kol et al.[12,17] and is experienced in most of the zirconium and hafnium complexes as well as a selection of titanium complexes, with the isopropoxide chemical shifts being broad, fluxional process on the NMR timescale, or being multiple, indicating the presence of both diastereoisomers. This is a similar case as to what was observed previously in the 2NO ligand set with the solid-state structures for Zr(**2R**)$_2$(O^iPr)$_2$ and Zr(**2S**)$_2$(O^iPr)$_2$, Figure 3.6, Figure 3.7 and Figure 3.8.

3.3.3. Ring opening polymerisation of *rac*-Lactide

The abbreviations for the initiators found in the tables of polymerisation data herein, are based on the same three character coding as seen with the previous polymerisation. The first character is representative of the metal, the second that of the constant moeity in the ligand (in this case the chiral amine) and the third that of the varying moeity in the ligand (here now the saliclyaldehyde). Thus, **TN5** is the abbreviation for titanium initiators complexed to the ligand prepared from (*R*)-(+)-methyl naphthylamine and 5-methylsalicylaldehyde.

3.3.4. Titanium Initiators

Davidson's study in 2008 and our own study described earlier with the 2NO ligands, reported that titanium complexes with these chiral Schiff bases were only active under solvent free conditions and afforded atactic PLA. Interestingly for the ethyl benzylamine and methyl naphthylamine variations of these ligands, the titanium initiators do indeed appear to be active in the milder solution conditions. Table 3.13 shows the results for titanium initiators screened against the ROP of *rac*-LA in toluene at 80 °C.

Entry	Initiator	Conversion[a] %	M_n[b]	M_w[b]	M_n (theo.)	PDI[b]	P_r[c]
1	TEH	10	-	-	1,450	-	0.54
2	TE5	97	8,100	13,850	13,950	1.71	0.45
3	TEB	85	2,100	6,900	12,250	3.28	0.47
4	TEC	94	7,450	14,950	13,550	2.01	0.50
5	TNH	97	13,300	14,150	13,950	1.06	0.56
6	TN5	94	9,800	11,050	13,550	1.13	0.51
7	TNB	73	7,700	8,800	10,500	1.14	0.49
8	TNC	96	7,550	8,250	41,400	1.09	0.51

Table 3.13. ROP results for T(EH, E5, EB, EC) in toluene at 80°C for 24hrs with 0.7 g of *rac*-LA, LA:Ini = 100:1. [a] Conversion determined *via* ^{1}H NMR, [b] determined from GPC referenced to PS in THF, [c] calculated from the ^{1}H homonuclear decoupled NMR analysis.

Under the more industrially relevant melt conditions, the same titanium initiators proved to be active and the results are displayed in Table 3.14

Entry	Initiator	Conversion[a] %	M_n[b]	M_w[b]	M_n (theo.)	PDI[b]	P_r[c]
1	TEH	99	31,900	54,400	42,750	1.71	0.50
2	TE5	97	33,250	37,000	41,900	0.49	0.51
3	TEB	94	35,500	56,450	40,600	1.59	0.49
4	TEC	95	34,550	47,000	41,100	1.36	0.48
5	TNH	94	36,250	56,550	40,600	1.56	0.55
6	TN5	98	37,050	54,800	42,350	1.48	0.50
7	TNB	72	29,500	48,700	31,100	1.65	0.49
8	TNC	79	33,550	60,750	34,000	1.81	0.52

Table 3.14. ROP results for T(EH, E5, EB, EC) in toluene at 130°C for 2hrs with 1.0 g of *rac*-LA, LA:Ini = 300:1. [a] Conversion determined *via* ^{1}H NMR, [b] determined from GPC referenced to PS in THF, [c] calculated from the ^{1}H homonuclear decoupled NMR analysis.

In solution (Table 3.13) **TEH**, was a poor example of an initiator only achieving 10 % conversion and the remaining entries produces a poor quality polymer sample with high PDI's and observed M_n values lower than expected. The PDI for **TEB** is rather high, 3.28, and is combined with a very low M_n value, indicating oligomers are produced rather than polymeric material. It is highly likely that a large degree of transesterification is ongoing in this reaction as well as back biting and other side reactions. Selectivity of these initiators was mostly poor with slight enrichments of an otherwise atactic polymer. The naphthyl initiators in contrast appear to be more controlled with narrow molecular weight distributions, and M_n values in better agreement with those calculated for isopropoxide initiated single chain polymerisation. Selectivity, however, is not improved upon the bulkier and more rigid chiral amine, reporting similar values seen as seen in solution and previous studies.

Conducting the reaction at the elevated temperature to achieve melt polymerisation sees all the titanium initiators being active. Polymer weight distribution is still poor for the Ti(**EX**)$_2$(O^iPr)$_2$ initiators but M_n values obtained correlated better with calculated values, the short comings are in line with those reported by Davidson et al. who used very pure, twice sublimed *rac*-lactide[11]. This would suggest that the catalysts are stable to contaminants in the monomer feedstock and deactivation may result from other sources. In each case atactic PLA was produced, indicating that the ligand is not influencing the chirality of the polymer.

3.3.5. Zirconium Initiators

The two tables below give the results for the ROP of *rac*-LA for zirconium(IV) chiral Schiff bases as prepared Figure 3.5. Table 3.15 gives the results for the polymerisation carried out in toluene at 80 °C for 24 hrs, while Table 3.16 gives the results obtained for polymerisation in the absence of solvent, conducted at 130 °C for two hours.

Entry	Initiator	Conversion[a] %	M_n[b]	M_w[b]	M_n (theo.)	PDI[b]	P_r[c]
1	ZEH	97	11,950	16,950	13,950	1.42	0.54
2	ZE5	97	9,250	14,450	13,950	1.56	0.60
3	ZEB	93	8,450	19,350	13,400	2.29	0.54
4	ZEC	99	12,850	15,750	14,250	1.22	0.61
5	ZNH	94	28,750	37,250	13,550	1.29	0.51
6	ZN5	87	23,750	25,500	12,550	1.07	0.60
7	ZNB	32	4,450	4,800	4,600	1.08	0.52
8	ZNC	21	25,550	29,200	3,000	1.14	0.59

Table 3.15. ROP results for zirconium phenolic Schiff base initiators in toluene at 80°C for 24hrs with 0.7 g of *rac*-LA, LA:Ini = 100:1. [a] Conversion determined *via* ^{1}H NMR, [b] determined from GPC referenced to PS in THF, [c] calculated from the ^{1}H homonuclear decoupled NMR analysis.

Entry	Initiator	Conversion[a] %	M_n[b]	M_w[b]	M_n (theo.)	PDI[b]	P_r[c]
1	ZEH	95	34,500	52,950	41,050	1.54	0.54
2	ZE5	96	41,700	62,950	41,450	1.51	0.61
3	ZEB	94	22,550	45,200	40,600	2.00	0.54
4	ZEC	96	83,100	107,000	41,450	1.29	0.61
5	ZNH	35	20,500	26,050	15,100	1.27	0.50
6	ZN5	87	73,700	111,350	37,600	1.51	0.59
7	ZNB	68	31,650	41,800	29,400	1.32	0.53
8	ZNC	93	87,950	126,300	40,200	1.44	0.60

Table 3.16. ROP results for zirconium phenolic Schiff base initiators in toluene at 130°C for 2hrs with 1.0 g of *rac*-LA, LA:Ini = 300:1. [a] Conversion determined *via* ^{1}H NMR, [b] determined from GPC referenced to PS in THF, [c] calculated from the ^{1}H homonuclear decoupled NMR analysis.

Conversion of lactide to polymer is high within the ethyl ligand set, slight variations resulting from the steric hindrance around the metal centre. This has a more significant effect for the naphthyl bearing complexes. Reduced steric hindrance in the salicylaldehyde coincides with a reduction in activity. Mn values for the **ZEX** complexes are in the same region as the theoretical values and it can be therefore assumed that polymerisation is preceding in a reasonable controlled manner with one chain being propagated per metal centre. If this were not the case then it would be expected to be a greater variation between the two values. The differences can be attributed to catalyst deactivation by impurities in the monomer. The difference between the observed Mn values and the theoretical M_n's may imply that the rate of initiation is slow compared to the rate of propagation. The Mn values for the **ZNX** initiators are on the other side of the

calculated values, with **ZNC** reporting an incredible high value when its poor conversion is taken into account. The PDI for this entry remains narrow, as such the high Mn is unlikely a result of side reactions including chain transfer, which would result in longer chains than predicted. It is most likely that serious catalyst deactivation has occurred in these cases.

Interestingly the PDI's for the complexes with a more rigid environment around the chiral centre are lower than those with the additional flexibility about the chiral centre. It could be said that the environment at the metal centre protects the polymer chain from transesterification and other side reactions, however given the size that the polymer chains reach it is hard to imagine that the catalyst can protect the length of the growing chain. Indeed this may be the case in the local vicinity of the metal, and possibly this is where the majority of side reactions occur. The distribution of molecular weights for the polymeric sample increases when the harsher conditions of melt polymerisation are employed, as expected.

Where the titanium initiators are typically atactic, the zirconium complexes display a slight bias towards heterotactic, a level which is maintained during melt polymerisation. The better performing initiators appear to be those incorporating the 3,5-dichlorosalicylaldehyde, **ZEC**, and methyl-substituted salicylaldehyde, **ZE5**, a pattern that is repeated when the chiral amine is changed. The electron withdrawing effect of the di-chloro ligand is a clear variation to the remaining ligands, however the methyl substituted would be ranked between the two remaining complexes in terms of steric hindrance.

3.3.6. Hafnium Initiators

Complexation with hafnium isopropoxide isopropanol adduct generated eight complexes which were screened for the ROP of *rac*-LA. The results for the solution polymerisation are given in, Table 3.17. The polymerisations were carried out in toluene, at 80 °C, for twenty four hours, before the reaction was quenched with methanol, volatiles removed and the polymeric material analysed.

Entry	Initiator	Conversion[a] %	M_n[b]	M_w[b]	M_n (theo.)	PDI[b]	P_r[c]
1	HEH	100	7,000	9,100	14,400	1.31	0.56
2	HE5	96	15,400	19,150	13,800	1.24	0.56
3	HEB	96	8,100	10,650	13,800	1.32	0.47
4	HEC	96	15,300	17,600	13,800	1.15	0.60
5	HNH	96	2,990	37,350	13,800	1.25	0.58
6	HN5	100	16,550	18,850	14,400	1.14	0.57
7	HNB	39	3,650	7,200	5,600	1.98	0.53
8	HNC	80	13,150	18,200	11,500	1.20	0.58

Table 3.17. ROP results for hafnium phenolic Schiff base initiators in toluene at 80°C for 24hrs with 0.7 g of *rac*-LA, LA:Ini = 100:1. [a] Conversion determined *via* ^{1}H NMR, [b] determined from GPC referenced to PS in THF, [c] calculated from the ^{1}H homonuclear decoupled NMR analysis.

Table 3.17 displays the data for the solvent free melt polymerisation tests with the hafnium complexes described earlier. The polymerisations were quenched after 2 hours having been held at 130 °C.

Entry	Initiator	Conversion[a] %	M_n[b]	M_w[b]	M_n (theo.)	PDI[b]	P_r[c]
1	HEH	91	53,100	87,800	39,300	1.65	0.57
2	HE5	97	55,450	86,500	41,900	1.56	0.54
3	HEB	97	57,700	88,600	41,900	1.48	0.54
4	HEC	98	52,950	57,700	42,350	1.09	0.50
5	HNH	100	51.950	66,000	43,200	1.27	0.52
6	HN5	94	52,800	78,150	40,600	1.48	0.53
7	HNB	65	32,050	50,000	28,100	1.56	0.55
8	HNC	81	34,600	43,250	35,000	1.25	0.49

Table 3.18. ROP results for hafnium phenolic Schiff base initiators in toluene at 130°C for 2hrs with 1.0 g of *rac*-LA, LA:Ini = 300:1. [a] Conversion determined *via* ^{1}H NMR, [b] determined from GPC referenced to PS in THF, [c] calculated from the ^{1}H homonuclear decoupled NMR analysis.

The hafnium initiators prepared with the ethylbenzylamine containing Schiff bases have good activity achieving high levels of conversion under solution and solvent free conditions. The variation of steric bulk or electronegative substitution around the phenoxy moiety appears to have little effect upon conversion for this group(IV) metal series. This in general agrees with results seen for other trials. The sterically hindered **HEB** complex demonstrated poor polymerisation control with the observed M_n value varying to the theoretical by almost half. Being at half of what was expected does raise the question as to whether or not two propagating polymer chains are initiated from one metal

centre, rather than the typical single growing chains observed hitherto. It is indeed a possibility as the complexes have two potential initiating groups, however the discrepancy may result from deactivation of the complex, due to impurities in the monomer or solvent. **HEH** goes to complete conversion but has an observed M_n one half of expected value. Being less sterically hindered it is easier to imagine two growing chains than for the **HEB** initiator. In both cases PDI is high but not substantially, suggesting that transesterification amongst other side reactions are kept under control.

Both **HE5** and **HEC**, perform to similar standards. Observed M_n's are better correlated with theoretical values and the higher values a likely result due to catalyst deactivation. The selectivity of these complexes is moderate with the highest selectivity being **HEC**, achieving a P_r value of 0.6. Repeating the experiments at the more industrially relevant, but harsher melt conditions, Table 3.18, impressively maintains the high levels of conversion and mild selectivities. M_n values for **HEH**, **HE5**, and **HEB** are higher than calculated, with the differences between observed and expected can again be explained by a combination of catalyst deactivation due to impurities in the unpurified, and industrially relevant, monomer feed, and a greater degree of transesterification resulting from the scale of the reaction. Polydispersity increases to slightly more significant levels as a result of increasing side reactions.

Changing the chiral amine for the more rigid naphthyl containing amine has a significant effect when used in combination with the sterically bulky salicylaldehyde. **HNB** has a poor activity performance, only obtaining 39% conversion. The less hindered **HN5** and **HNH** perform in a similar manner to their ethylbenzylamine brethren achieving high levels of conversion, however the least sterically hindered ligand in this set behaves in a similar manner to its ethyl counterpart in that that M_n observed is considerably different to the theoretical value of M_n.

Changing to melt increases the reported M_n values with them being greater than expected values. With the increased ratio of monomer to initiator, we also have an increase ratio of impurities to catalyst and such, deactivation can be more severe. However, for in the solvent free polymerisation one polymer chain is

propagated by each metal centre, as with the solution polymerisation. In general the distribution of molecular weights is greater as is often the case, and generally speaking selectivity has suffered from the harsher conditions.

The study by Davidson et al. into similar chiral ligands did not included hafnium complexes and so no direct comparisons can be made, but comparing to the zirconium results obtained it can be confidently proposed that the additional sterics, either flexible of rigid about the chiral centre are detrimental to polymerisation performance.

3.3.7. Aluminium Initiators

The two tables below present the results for the ROP of *rac*-LA by the eight chiral phenolic ligands prepared above, complexed to trimethyl aluminium. The catalyst lacks an initiating group and therefore benzyl alcohol is added, in a one to one ratio with the catalyst, prior to polymerisation to generate one initiating group on each aluminium centre. Table 3.19 presents the data for the solution polymerisation, while Table 3.20 displays the data obtained from the melt polymerisation reaction.

Entry	Initiator	Conversion[a] %	M_n[b]	M_w[b]	M_n (theo.)	PDI[b]	P_r[c]
1	AEH	35	9,800	12,050	5,050	1.65	0.45
2	AE5	90	98,450	151,650	12,950	1.54	0.40
3	AEB	88	14,550	22,100	12,650	1.52	0.45
4	AEC	85	9,250	11,250	12,250	1.22	0.47
5	ANH	95	25,550	29,200	13,700	1.15	0.65
6	AN5	95	14,650	15,900	13,700	1.09	0.60
7	ANB	86	18,400	20,550	12,400	1.12	0.39
8	ANC	83	216,400	287,550	11,950	1.13	0.49

Table 3.19. ROP results for aluminium phenolic Schiff base initiators in toluene at 80°C for 24hrs with 0.7 g of *rac*-LA, LA:Ini = 100:1. [a] Conversion determined *via* ^{1}H NMR, [b] determined from GPC referenced to PS in THF, [c] calculated from the ^{1}H homonuclear decoupled NMR analysis.

Entry	Initiator	Conversion[a] %	M_n[b]	M_w[b]	M_n (theo.)	PDI[b]	P_r[c]
1	AEH	12	-	-	-	-	-
2	AE5	97	84,250	85,950	41,900	0.43	0.42
3	AEB	95	97,900	164,450	41,050	1.68	0.34
4	AEC	90	32,750	48,100	38,900	1.47	0.44
5	ANH	80	33,200	36,200	34,550	1.09	0.51
6	AN5	95	59,600	75,100	41,050	1.26	0.50
7	ANB	92	53,950	95,550	39,750	1.77	0.45
8	ANC	100	67,700	84,650	43,200	1.25	0.39

Table 3.20. ROP results for aluminium phenolic Schiff base initiators in toluene at 130°C for 2hrs with 1.0 g of *rac*-LA, LA:Ini = 300:1. [a] Conversion determined *via* ^{1}H NMR, [b] determined from GPC referenced to PS in THF, [c] calculated from the ^{1}H homonuclear decoupled NMR analysis.

Another metal not considered in similar work was aluminium, and as commented before, aluminium initiators generally match the activity of their group(IV) metal counterparts but often demonstrate superior selectivity giving rise to isotactic PLA or stereoblock isotactic PLA.

Interesting results are obtained in solution, Table 3.19, with the least sterically hindered complex performing poorly and not producing a significant amount of polymer for further analysis. This appears to be a similar case under solvent free conditions, however, the other catalysts performed better with good conversions. **AE5**, Table 3.19, under solution conditions produced a polymer with an M_n value 7.5 times greater than expected, while achieving 90% conversion. This could be due to difficulties in preparing the alkoxide *in-situ*. This could be overcome by preparing the aluminium initiator from the catalyst prior to polymerisation requiring additional synthetic steps and purification. The remaining polymeric samples for solution conditions are consistent with one propagating polymer chain with benzyl alcohol end group in place of the isopropoxide previously seen. In solution we observe a moderate isotactic bias for complexes **AE5**, **AEB** and **AEC**. Interestingly, the complexes **ANH** and **AH5** afford heterotactic PLA in solution. This illustrates the subtle nature of the polymerisation.

The aluminium initiators in the melt polymerisation perform in a similar manner to the solution experiments. M_n is in a reasonable agreement with theoretical values, with the differences being explained by catalyst deactivation

and side reactions as previously discussed. The polydispersity index is greater as transesterification and back biting become more predominant, not unusual for the harsher conditions employed in melt polymerisation. Interestingly the PDI for the more "rigid" ligand set is narrower than that of the more flexible, suggesting that this is conducive to coordination of the growing polymer chain. Where traditionally, tacticity is reduced by the elevated temperature, a selection of these complexes become more selective, generating polymeric material with an isotactic bias. However, this enrichment is still rather mild.

3.3.8. Conclusions

Eight new chiral Schiff base ligands were successfully prepared and characterised. These were complexed to group(IV) metals and aluminium before being screened as initiators for the ROP of *rac*-LA. All showed some level of activity towards the reaction, and tolerance to impurities in the monomer feed, avoiding the need to use sublimed lactide.

The titanium initiators performed better in solution compared to their bis-phenolic counterparts, Section 3.2, however only atactic polymer was produced and there was evidence for significant side reactions, amplified at the more industrially relevant melt conditions. The zirconium and hafnium initiators performed better, and achieved mild heterotactic bias, which was on the whole maintained when changing from solution to melt polymerisation. The aluminium initiators had a greater variance in performance, some of this is attributed to the difficult nature of preparing the initiator *in situ*. Noteworthy was the mild to moderate isotactic bias observed.

3.4. Chiral Salalen Initiators

After the mixed results obtained from the chiral salen initiators, attention was turned to salalen ligands, which are half salan and half salen type ligands. Using the skills and knowledge developed with the previous sets of chiral ligands, a new set were synthesised, complexed to group(IV) metals as well as aluminium, and trialled for the ROP of *rac*-LA in solution and solution free conditions. It is

hoped that incorporation of a chiral centre into the structure of the ligand, and in close proximity to the metal centre, will result in improved chiral discrimination and access isotactic PLA.

As with the previous ligands and initiators in this chapter, the three letter code is representative of; firstly the metal used, secondly the amine type employed in the ligand and thirdly the salicylaldehyde used to prepare the ligand. For example **ZBM** is the zirconium(IV) complex of the chiral ligand incorporating the 2-(aminomethyl)piperidine with the 5-*tert*-butyl-2-hydroxy-3-methylbenzaldehyde.

3.4.1. Preparation of Chiral Salalen Ligands

A series of chiral salalen ligands were synthesised from a chiral 2-(aminomethyl)piperidine as a backbone and different salicylaldehydes. 3,5-di-*tert*-butyl-2-hydroxybenzaldehyde was prepared from its corresponding phenol by a straight forward *ortho*-formylation reaction, as above, Figure 3.12.

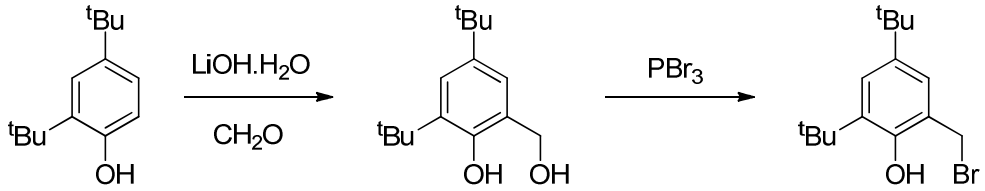

Figure 3.17. Modified Mannich affording 3,5-di-*tert*-2-hydroxybenzyl bromide.

A modified version of the Mannich reaction prepares the aryl bromide, Figure 3.17, and a simple imine condensation between chiral 2-(aminomethyl)piperidine and salicylaldehyde prepares the salen component. An S_N2 reaction between the two results in the salalen ligand, Figure 3.18.

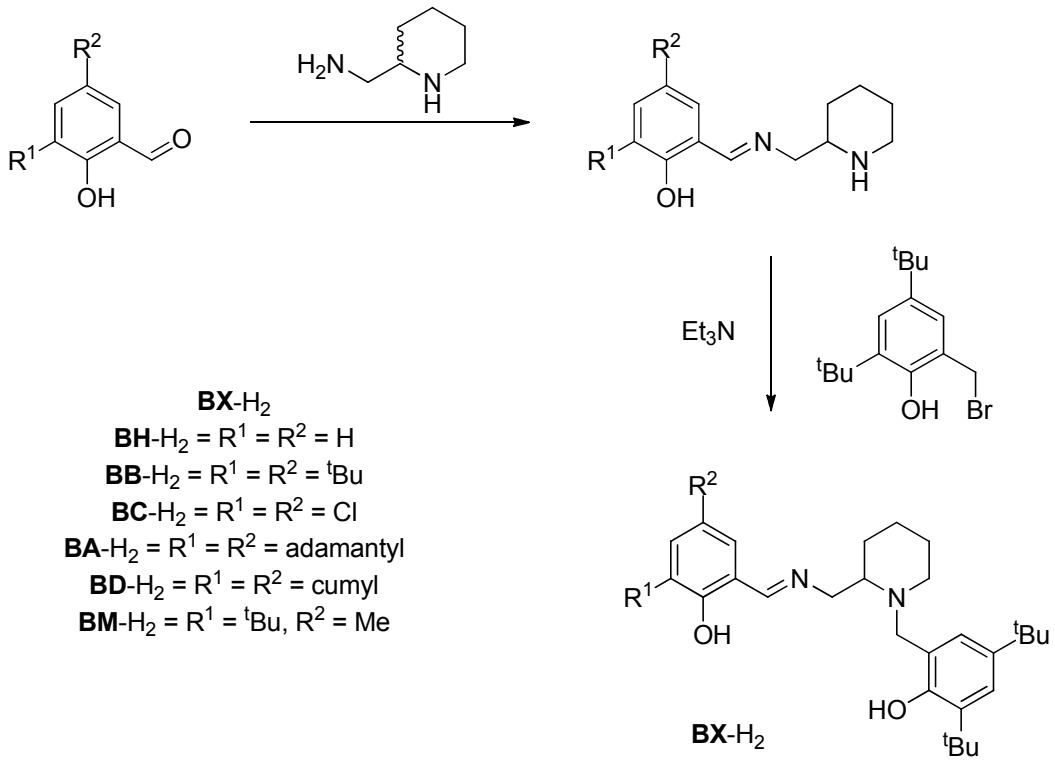

Figure 3.18. Synthesis of chiral salalen ligands

The sterics and electronics were varied around the salen aromatic ring *via* different substituents and all ligands were characterised by ^{1}H, $^{13}C\{^{1}H\}$ NMR spectroscopy and high resolution mass spectrometry.

3.4.2. Complexation to Group(IV) metals and Aluminium

The ligands prepared in Figure 3.18 were complexed to group(IV) metal alkoxides in a 1:1 stoichiometry, as well as trimethyl aluminium. For zirconium and hafnium isopropoxides complexation was facilitated in dichloromethane, whereas titanium isopropoxide and trimethyl aluminium complexes were prepared in toluene. This is shown schematically below, Figure 3.19.

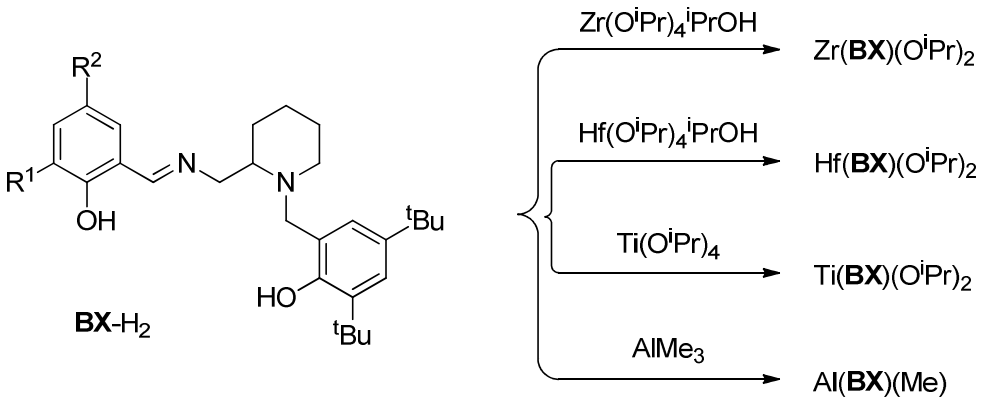

Figure 3.19. Complexes synthesised using chiral salalen ligands

The group(IV) complexes were characterised by ^{1}H NMR, ^{13}C{^{1}H} NMR spectroscopy, and elemental analysis. The ^{1}H NMR spectra for zirconium and hafnium, and in some cases titanium, were complex with multiple peaks and overlapping resonances. This is attributed to the different binding modes possible. Salan and Salen ligands typically bind *fac-fac* and *mer-mer*, but Salalen ligands can wrap around the metal diastereospecifically, giving rise to possible *fac-fac*, *mer-mer*, *fac-mer*, or *mer-fac* geometries, Figure 3.20. This is further complicated by the presence of a chiral centre in the racemic ligand, and the diastereotopic nature of the -CH_2- moieties. From NMR spectroscopic analysis, it is clear that multiple isomers are present in solution.

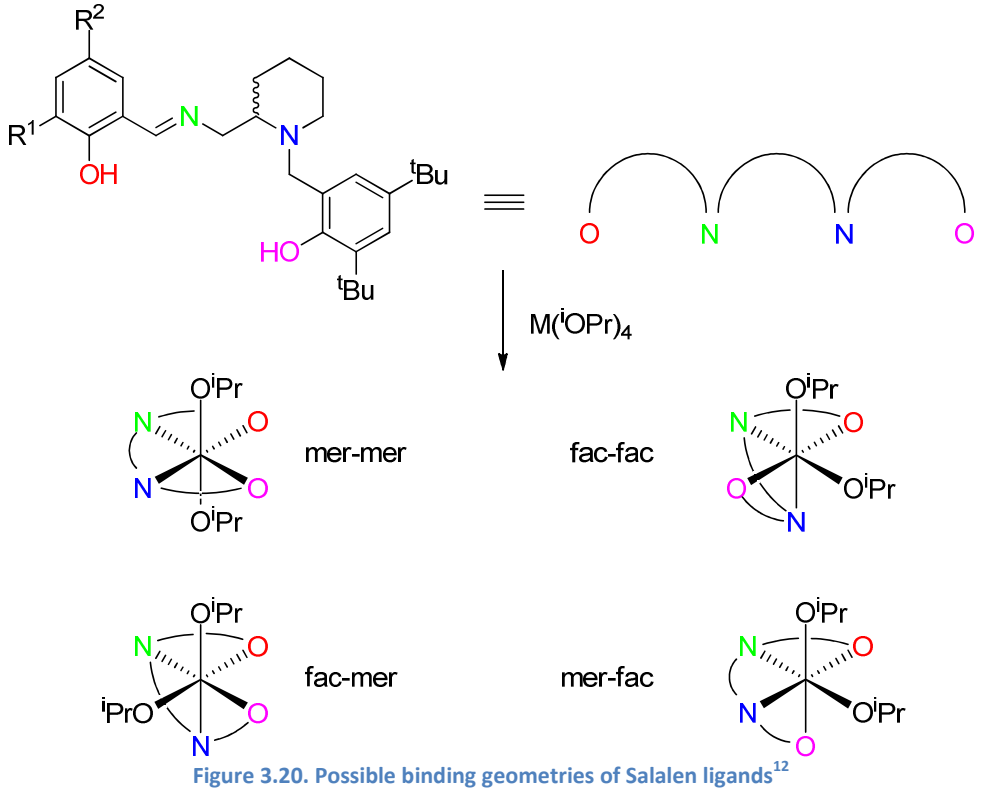

Figure 3.20. Possible binding geometries of Salalen ligands[12]

3.4.3. Ring opening polymerisation of *rac*-Lactide

The six chiral salalen ligands were complexed to four transition metals, generating twenty four novel complexes. These are trialled as initiators for the ROP of *rac*-LA, the results for which can be found below.

3.4.4. Titanium Initiators

The solution polymerisation of *rac*-LA in toluene at 80 °C was undertaken by all titanium initiators prepared for 24 hours, the results are shown in Table 3.21.

Entry	Initiator	Conversion[a] %	M_n[b]	M_w[b]	M_n (theo.)	PDI[b]	P_r[c]
1	TBH	85	13,000	15,750	12,250	1.21	0.49
2	TBB	94	11,400	17,400	13,550	1.53	0.51
3	TBC	62	8,600	9,250	8,950	1.08	0.60
4	TBA	95	11,250	15,450	13,700	1.37	0.51
5	TBD	95	13,550	21,000	13,700	1.55	0.50
6	TBM	95	14,050	19,350	13,700	1.38	0.52

Table 3.21. ROP results for titanium salalen initiators in toluene at 80°C for 24hrs with 0.5 g of *rac*-LA, LA:Ini = 100:1. [a] Conversion determined *via* ^{1}H NMR, [b] determined from GPC referenced to PS in THF, [c] calculated from the ^{1}H homonuclear decoupled NMR analysis.

Under the more industrially relevant melt conditions, the same titanium initiators were utilised in a 300:1 monomer to initiator ratio at 130 °C. Table 3.22 below details the results.

Entry	Initiator	Conversion[a] %	M_n[b]	M_w[b]	M_n (theo.)	PDI[b]	P_r[c]
1	TBH	92	51,850	68,850	39,750	1.33	0.52
2	TBB	73	31,550	42,250	31,550	1.21	0.55
3	TBC	80	30,200	34,150	34,550	1.33	0.52
4	TBA	36	18,550	24,950	15,550	1.35	0.61
5	TBD	81	34,600	40,200	35,000	1.17	0.53
6	TBM	91	41,500	54,950	39,300	1.33	0.51

Table 3.22. ROP results for titanium salalen initiators in toluene at 130°C for 2hrs with 1.0 g of *rac*-LA, LA:Ini = 300:1. [a] Conversion determined *via* ^{1}H NMR, [b] determined from GPC referenced to PS in THF, [c] calculated from the ^{1}H homonuclear decoupled NMR analysis.

Activity for these titanium initiators is generally high but falling short of full conversion. Interestingly, unlike previously seen, steric bulk from the substituents of the salen component appears to have promoted activity, while an absence of, or introducing electronegativity hinders activity. M_n, on the whole, is in accordance with theoretical values, and the slight variation attributed to catalyst deactivation by impurities in the monomer, and the observed M_n values are consistent with one polymer chain being propagated per metal centre. Relatively lower conversion for **TBC** has been comment on but it exhibits the best control with a very narrow PDI, while the remaining initiators have reasonable dispersities. This could be the result of transesterification and back-biting becoming more frequent as the concentration of monomer decreases at higher conversion.

P_r for these complexes appears to be influenced by electronic effects more so than steric bulk around the salen unit, with the organic substituted complexes behaving like other titanium initiators in the literature and producing atactic PLA, the chlorine containing ligand afforded a P_r of 0.6, indicating a mild heterotactic bias. In the absence of solvent conversion are more varied. This is due to two factors, the stability of the complex to the temperatures required to melt the monomer, 130 °C, and the mobility of the initiator and propagated chain in the molten monomer. This latter point can go some of the way to explain the drop in activity of the adamantyl containing complexes, and indeed it is a trend repeated regardless of metal employed. On the whole, control is unchanged by the new polymerisation conditions and M_n is again in close agreement to theoretical values with the exception being **TBH**, which expresses an elevated M_n, possibly resulting from additional transesterification. However, the PDI remain reasonably unaffected.

The polymer produced from the complexes is generally atactic however the heterotactic selectivity observed by **TBC** in the solution is, while **TBA** is now slightly more selective. Stereoselective bias in solution and melt conditions has been paired with poor conversion, it is therefore possible to say that for the more active complexes, the initiators are overly active and their thirst for conversion dominates selectivity.

3.4.5. Zirconium Initiators

All the zirconium initiators isolated were trailed for the ring opening polymerisation of *rac*-LA, under solution conditions, Table 3.23, and the more industrially favoured solvent free conditions, Table 3.24. Solution polymerisation was carried out for twenty four hours as above and in toluene, whereas the melt reactions were terminated after two hours. In each case, methanol was added to quench the reaction.

Entry	Initiator	Conversion[a] %	M_n[b]	M_w[b]	M_n (theo.)	PDI[b]	P_r[c]
1	ZBH	81	1,150	2,550	11,650	2.27	0.53
2	ZBB	82	6,700	7,250	11,800	1.08	0.52
3	ZBC	82	12,650	7,250	11,800	1.14	0.59
4	ZBA	92	8,200	8,800	13,250	1.08	0.43
5	ZBD	90	8,000	10,550	12,950	1.32	0.50
6	ZBM	100	2,900	4,200	14,400	1.46	0.41

Table 3.23. ROP results for zirconium salalen initiators in toluene at 80°C for 24hrs with 0.5 g of *rac*-LA, LA:Ini = 100:1. [a] Conversion determined *via* ^{1}H NMR, [b] determined from GPC referenced to PS in THF, [c] calculated from the ^{1}H homonuclear decoupled NMR analysis.

Entry	Initiator	Conversion[a] %	M_n[b]	M_w[b]	M_n (theo.)	PDI[b]	P_r[c]
1	ZBH	100	34,800	46,350	43,200	1.33	0.52
2	ZBB	93	25,100	27,300	40,200	1.35	0.53
3	ZBC	100	34,800	73,850	43,200	2.12	0.55
4	ZBA	23	34,800	46,300	9,950	1.33	0.43
5	ZBD	96	34,100	51,000	41,450	1.50	0.52
6	ZBM	92	2,900	4,200	39,750	1.46	0.38

Table 3.24. ROP results for Zr(BH, BB, BC, BA, BD, BM) in toluene at 130°C for 2hrs with 1.0 g of *rac*-LA, LA:Ini = 300:1. [a] Conversion determined *via* ^{1}H NMR, [b] determined from GPC referenced to PS in THF, [c] calculated from the ^{1}H homonuclear decoupled NMR analysis.

ZBM, entry 6 Table 3.23, went to complete conversion, however data collected from GPC indicates that although complete, the monomer was not converted to polymeric material but oligomers. Though it may be selective with a P_r of 0.4 a M_n of 2,900 g mol^{-1} equates to about 40 repeat units (20 lactide molecules) significantly lower than expected. This is also exhibited by **ZBH**, entry 1 Table 3.23, and seeing as complete conversion is not achieved in this trail, it means that side reactions are ongoing at a competing rate to polymerisation, or that the rate of termination is fast enough when compared to the rate of

propagation to cause issues, resulting in a large PDI. Entries 2, 4 and 5 from Table 3.23, (**ZBB**, **ZBA** and **ZBD**), have more acceptable PDI values, but still M_n is lower than expected. In this instance it might become the case that the complexes' ability to coordinate the growing chain has a finite limit after which the polymer is terminated and a new chain initiated (two isopropyl groups present on the metal). The salalen ligand with the chloro groups in the salen unit is the only example that is in agreement with its theoretical M_n value. Of these four possible polymeric samples atactic character is seen for the moderately hindered initiators, while the highly hindered have slight isotactic character, and the electronic variant a slight heterotactic bias. It has been shown that zirconium(IV) complexes can achieve high P_r values, 0.96 - 0.98, however similar salalens to those presented here did not match this level of selectivity either. In comparison to these non-chiral flexible salalens the activity and control was unchanged by varying the diamine backbone.[33,34]

Polymerisation under the more industrially favoured solvent free conditions saw PDI predictably increase as the control of polymerisation is reduced. However, under these conditions **ZBH**, entry 1 of Table 3.24, behaves better with a narrowing of the PDI and a shift from short chain oligomers to truly polymeric material. Transesterification and back-biting are still present as M_n is lower than calculated. Entry 6, Table 3.24 (**ZBM**) produces oligomeric material with increased isotacticity. The moderately hindered ligands are again lower in number average molecular weight and if the argument from the solution trail still stood, the value should not vary much, with it increasing at the same rate as the catalyst loading it is suggestive of different factors are in control. A different theory is that two polymer chains are being propagated by the metal complex and the short comings between the observed M_n value and the calculated value are a result of catalyst deactivation. This can be seen effectively with **ZBB**, entry 2 Table 3.23, M_n = 6,700 g mol^1 and the theoretical value for single chain propagation is 11,800 g mol^1. If two chains were propagated, then the recalculated theoretical M_n value would be 5,900 g mol^1 and a variation of around 10 % would be acceptable for a combination of catalyst deactivation and experimental error. The adamantyl variant is least converted as already discussed and maintains its isotactic bias, while the chlorine containing variant loses its selectivity and has a broader PDI.

3.4.6. Hafnium Initiators

Table 3.25 and Table 3.26 detail the results for the screening of the six hafnium complexes prepared with the salalen ligands described above under solvent and solvent free conditions.

Entry	Initiator	Conversion[a] %	M_n[b]	M_w[b]	M_n (theo.)	PDI[b]	P_r[c]
1	HBH	100	4,400	5,950	14,400	1.35	0.47
2	HBB	43	27,400	29,600	6,200	1.08	0.43
3	HBC	100	12,300	15,800	14,400	1.28	0.49
4	HBA	82	8,400	9,150	11,800	1.09	0.47
5	HBD	55	5,150	5,500	7,900	1.07	0.51
6	HBM	98	2,250	3,750	14,150	1.67	0.47

Table 3.25. ROP results for hafnium salalen initiators in toluene at 80°C for 24hrs with 0.5 g of *rac*-LA, LA:Ini = 100:1. [a] Conversion determined *via* ^{1}H NMR, [b] determined from GPC referenced to PS in THF, [c] calculated from the ^{1}H homonuclear decoupled NMR analysis.

The solution ROP of *rac*-LA, Table 3.25, was conducted in toluene at 80 °C for 24 hours before being quenched with methanol. A ^{1}H NMR spectrum of the crude material was examined to ascertain the conversion, the washed product was analysed by GPC and ^{1}H homonuclear decoupled NMR spectroscopy yielding the polymer characteristics. A similar work up schedule was followed for the solvent free reactions, Table 3.26, after the polymeric material had been dissolved in dichloromethane to remove it from the reaction flask.

Entry	Initiator	Conversion[a] %	M_n[b]	M_w[b]	M_n (theo.)	PDI[b]	P_r[c]
1	HBH	19	-	-	8,200	-	-
2	HBB	100	16,350	27,100	43,200	1.65	0.50
3	HBC	89	40,.700	53,950	38,450	1.33	0.49
4	HBA	77	19,700	21,050	33,250	1.07	0.42
5	HBD	80	30,800	35,400	34,550	1.15	0.55
6	HBM	97	40,500	54,250	41,900	1.34	0.47

Table 3.26. ROP results for hafnium salalen initiators in toluene at 130°C for 2hrs with 1.0 g of *rac*-LA, LA:Ini = 300:1. [a] Conversion determined *via* ^{1}H NMR, [b] determined from GPC referenced to PS in THF, [c] calculated from the ^{1}H homonuclear decoupled NMR analysis.

The hafnium complexes appear to be less consistent than their group(IV) brothers with examples of complete conversion and poor conversion, and activity

levels not being maintained in solvent free conditions. In solution, **HBH** produces oligomers as did its zirconium analogue, with a M_n value considerably lower than its theoretical value. Upon polymerisation in the melt activity drops considerably with no polymeric material being isolatable, suggesting what is converted is of very low molecular weight. The harsher conditions of melt polymerisation take a significant effect on **HBM**, entry 6, as well. While the monomer is ring opened and apparently polymerised from the ^{1}H NMR spectrum and conversion, there is no detectable polymeric material in the GPC trace, Figure 3.21. **HBM** had also performed poorly in solution, preparing only oligomers, the absence of solvent and increased reaction time has resulted in even less control of the ROP of *rac*-LA.

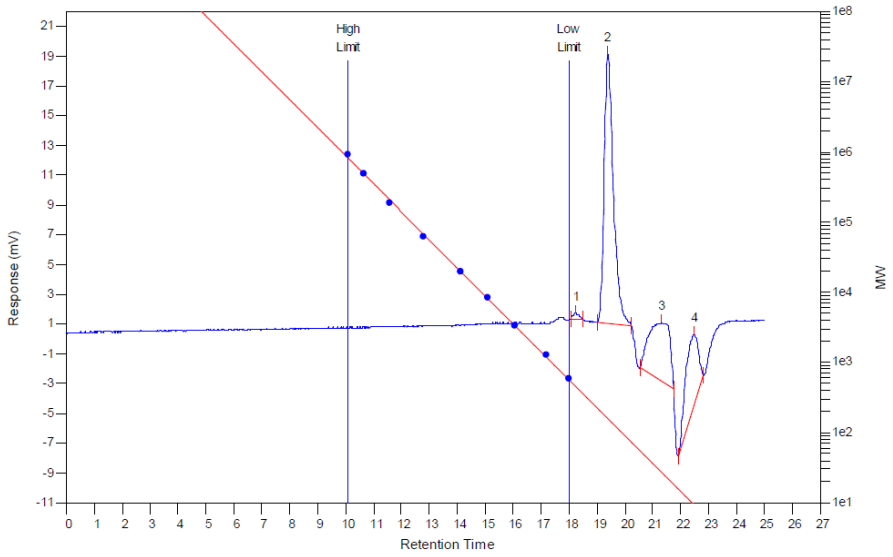

Figure 3.21. GPC trace of the polymeric sample prepared from HBM under melt conditions, sample dissolved in THF, and calibrated to PS standards.

The electronic substituent complex behaves as previously seen with a high level of conversion and a M_n value in line with theoretical values, signifying controlled polymerisation from a single propagation per metal. This activity and control is lost under solvent free conditions and polymeric material was not isolated. The most sterically hindered complex prepared had a narrow PDI which did not broaden under melt polymerisation. M_n is lower than calculated and under the solvent free conditions a slight isotactic bias is observed. Selectivity in general seems to be lacking for the hafnium complexes, this is unusual as zirconium and hafnium complexes tend to behave in a similar manner. Indeed, similar ligand systems complexed to hafnium used have experienced low molecular weights and

slight to moderate isotacticity with room temperature polymerisation in dichloromethane bringing the M_n in better agreement and improving selectivity.

3.4.7. Aluminium Initiators

Aluminium chiral Schiff base complexes have been used before by Spassky et al.[39] to produce isotactic PLA and since then an array of aluminium complexes have been reported with salen and salan ligands dominating the field. The inclusion of aluminium complexes is hoped to maintain or surpass activity seen for the group(IV) initiators while improving on selectivity, possible accessing stereoblock isotactic PLA. The six salalen ligands were complexes to aluminium and tested in solution, Table 3.27, and melt, Table 3.28, polymerisation of *rac*-LA.

Entry	Initiator	Conversion[a] %	M_n[b]	M_w[b]	M_n (theo.)	PDI[b]	P_r[c]
1	ABH	100	65,600	88,300	14,400	1.35	0.53
2	ABB	35	5,700	5,900	5,050	1.04	0.49
3	ABC	36	21,700	22,300	5,200	1.03	0.53
4	ABA	90	16,300	19,550	12,950	1.20	0.50
5	ABD	92	22,050	23,600	13,250	1.07	0.53
6	ABM	84	15,000	16,550	12,100	1.10	0.51

Table 3.27. ROP results for aluminium salalen initiators in toluene at 80°C for 24hrs with 0.5 g of *rac*-LA, LA:Ini = 100:1. [a] Conversion determined *via* ^{1}H NMR, [b] determined from GPC referenced to PS in THF, [c] calculated from the ^{1}H homonuclear decoupled NMR analysis.

Entry	Initiator	Conversion[a] %	M_n[b]	M_w[b]	M_n (theo.)	PDI[b]	P_r[c]
1	ABH	70	53,100	81,200	30,250	1.53	0.48
2	ABB	81	54,700	72,600	35,000	1.33	0.49
3	ABC	70	71,600	89,350	30,250	1.25	0.48
4	ABA	81	53,500	64,200	35,000	1.20	0.49
5	ABD	90	56,500	74,350	38,900	1.32	0.54
6	ABM	100	50,400	80,450	43,200	1.60	0.56

Table 3.28. ROP results for aluminium salalen initiators in toluene at 130°C for 2hrs with 1.0 g of *rac*-LA, LA:Ini = 300:1. [a] Conversion determined *via* ^{1}H NMR, [b] determined from GPC referenced to PS in THF, [c] calculated from the ^{1}H homonuclear decoupled NMR analysis.

Once again there is no distinct pattern in the activity of solution polymerisation of *rac*-LA whereas the solvent free polymerisations vary less and

are generally higher than expected. The low conversion of **ABB** in solution produces a polymer with M_n in close agreement with calculated values, whereas the similarly poor performance of the **ABH** derivative has a rather large observed M_n, indeed greater than the monomer initiator ratio, with a very narrow PDI. This may result from issues in measuring the very small amount of benzyl alcohol required to initiate the polymerisation and to ensure its mixture with the complex, as previously commented on, for other aluminium initiated polymerisations. One way to avoid this complication is to include an additional step in the synthesis of these aluminium complexes where, after coordination of the ligand to the metal, benzyl alcohol is added replacing the Al-Me bond with an Al-O-Bn, which acts as our initiating group. In general, PDI's are narrower for the solution polymerisation which is to be expected. Limitations to complete conversion in the melt can be attributed to the fact that the growing polymer chain causes the mixture to be more viscous. As the reaction progresses, stirring becomes sluggish and eventually ceases.

Unfortunately, selectivity was not displayed by these complexes unlike similar reported aluminium salalen complexes or other chiral systems. Strain imposed on the flexibility of the imine-amine backbone may hinder the reorganisational ability of the initiator to coordinate the growing chain. Indeed from previous studies, additional steric bulk at the metal centre from the amine results in more atactic character. The incorporation of a chiral centre at the metal would also appear to have a non-effect on stereocontrol, unlike what has been seen with structurally chiral ligands and aluminium complexes. It was hoped that chirality at the metal centre would impose additional stereochemistry however it appears that the coordination of the growing chain is more important.

3.4.8. Conclusions

The salalen initiators prepared above did not have the runaway success as previously seen with these types of ligand[12,17,33,34]. This is unlikely due to the different geometries adopted by the ligand and metal in solution as this kind of behaviour has been seen before for initiators which performed well[34]. It is hard to imagine that the racemic mixture of ligands would have a great impact on the performance of polymerisation, and it was hoped that this would improve the

selectivity[40]. One of the biggest structural differences in the salalen ligands investigated here is the reduced flexibility and free rotation at the salan half of the ligand, by incorporating a piperidine. This would impose restrictions on the initiators reorganisational ability during the coordination and insertion of monomers.

Trends were observed as with the previous sets of initiators. Solution polymerisation is more controlled than melt polymerisation as seen from narrower polydispersity indexes, where side reactions and back-biting are kept to a minimal. On the whole, conversion is high, with a few exceptions, however it has been commented that high levels of conversion cannot always be associated with high levels of polymerisation. Of the group(IV) metals, zirconium appears to be the most efficient but with tacticity ranging from slightly isotactic, to mildly heterotactic, while titanium initiators generally produce atactic PLA.

3.5. Future Work

The world cannot switch to plant based plastics overnight. Industrial processes are designed for petroleum based polymers, and the majority of the post-production, for example of vulcanisation, relies on oil based functionality of the polymer chain. An advantageous step towards reducing our dependence on petroleum based plastics would be to develop plant based polymers which could be used in the already established industrial process.

Ziegler Natta catalysts have been used for the polymerisation of most polymers encountered today, and typical homogeneous catalysts are titanium, hafnium or zirconium initiators used with methylaluminoxane (MAO), and while typically metallocenes, oxygen and nitrogen mutlidentate ligands, such as those reported in this chapter, can be used[41]. An investigation of group(IV) metals prepared in this chapter against the polymerisation of alkenes would be undertaken. Development of the MAO assisted polymerisation of a variety of increasingly complex, and more importantly industrially relevant, alkenes would hopefully lead to an optimised system for co-polymerisation as such dienes, which are common additives industrially to produce useful functionality on the polymer chain.

The significance of this is that the polymerisation of a diene would leave one unsaturation in the polymer chain, which could then be cross-linked by traditional methods. The challenging work would then come from developing this ring-opening metathesis polymerisation system to work alongside the ROP of *rac*-LA. While the initiators would ideally be those that had already shown aptitude to the polymerisation of plant based monomer feedstock's, the introduction of MAO, or any other organoaluminium co-catalyst is likely to affect the ROP.

However, if successful, a biopolymer that could be post-modified by conventional techniques could be a vital stepping stone to controlling our oil consumption.

3.6. References

(1) Ziegler, K.; Holzkamp, E.; Breil, H.; Martin, H. *Angew. Chem.* **1955**, *67*, 541.
(2) Natta, G.; Pino, P.; Corradini, P.; Danusso, F.; Mantica, E.; Mazzanti, G.; Moraglio, G. *J. Am. Chem. Soc.* **1955**, *77*, 1708.
(3) Natta, G. *J. Am. Chem. Soc.* **1962**, *84*, 4995.
(4) Natta, G.; Pasquon, I.; Zambelli, A. *J. Am. Chem. Soc.* **1962**, *84*, 1488.
(5) Chadwick, J. C. In *Encyclopedia of Polymer Science and Technology*; John Wiley & Sons, Inc.: 2002.
(6) Alberta, C. *Polypropylene Market Study*, 2004.
(7) Ceresana; 2nd Edition ed. 2012; Vol. 2013, p A market study conducted by the market intelligence and consulting company Ceresana.
(8) Malpass, D. B.; Band, E. I. In *Introduction to Industrial Polypropylene*; John Wiley & Sons, Inc.: 2012, p 59.
(9) Johnson, A. L.; Davidson, M. G.; Lunn, M. D.; Mahon, M. F. *Eur. J. Inorg. Chem.* **2006**, *2006*, 3088.
(10) Prabhakar, M.; Zacharias, P. S.; Das, S. K. *Inorg. Chem.* **2005**, *44*, 2585.
(11) Chmura, A. J.; Cousins, D. M.; Davidson, M. G.; Jones, M. D.; Lunn, M. D.; Mahon, M. F. *Dalton Trans.* **2008**, *0*, 1437.
(12) Yeori, A.; Gendler, S.; Groysman, S.; Goldberg, I.; Kol, M. *Inorg. Chem. Commun.* **2004**, *7*, 280.
(13) Busico, V.; Cipullo, R.; Ronca, S.; Budzelaar, P. H. M. *Macromol. Rapid Commun.* **2001**, *22*, 1405.
(14) Busico, V.; Cipullo, R.; Friederichs, N.; Ronca, S.; Togrou, M. *Macromolecules* **2003**, *36*, 3806.
(15) Tshuva, E. Y.; Goldberg, I.; Kol, M. *J. Am. Chem. Soc.* **2000**, *122*, 10706.
(16) Gibson, V. C.; Spitzmesser, S. K. *Chem. Rev.* **2002**, *103*, 283.
(17) Press, K.; Cohen, A.; Goldberg, I.; Venditto, V.; Mazzeo, M.; Kol, M. *Angewandte Chemie International Edition* **2011**, *50*, 3529.
(18) Egami, H.; Katsuki, T. *J. Am. Chem. Soc.* **2007**, *129*, 8940.
(19) Saito, B.; Egami, H.; Katsuki, T. *J. Am. Chem. Soc.* **2007**, *129*, 1978.
(20) North, M.; Usanov, D. L.; Young, C. *Chem. Rev.* **2008**, *108*, 5146.
(21) Suematsu, H.; Katsuki, T. *J. Am. Chem. Soc.* **2009**, *131*, 14218.

(22) Xu, Z.-J.; Fang, R.; Zhao, C.; Huang, J.-S.; Li, G.-Y.; Zhu, N.; Che, C.-M. *J. Am. Chem. Soc.* **2009**, *131*, 4405.
(23) Zhou, X.; Shang, D.; Zhang, Q.; Lin, L.; Liu, X.; Feng, X. *Org. Lett.* **2009**, *11*, 1401.
(24) Ziegler, J. E.; Du, G.; Fanwick, P. E.; Abu-Omar, M. M. *Inorg. Chem.* **2009**, *48*, 11290.
(25) Darensbourg, D. J. *Inorg. Chem.* **2010**, *49*, 10765.
(26) Egami, H.; Oguma, T.; Katsuki, T. *J. Am. Chem. Soc.* **2010**, *132*, 5886.
(27) Fujisaki, J.; Matsumoto, K.; Matsumoto, K.; Katsuki, T. *J. Am. Chem. Soc.* **2010**, *133*, 56.
(28) Kember, M. R.; White, A. J. P.; Williams, C. K. *Macromolecules* **2010**, *43*, 2291.
(29) Wojaczyńska, E.; Wojaczyński, J. *Chem. Rev.* **2010**, *110*, 4303.
(30) Li, W.; Qin, S.; Su, Z.; Yang, H.; Hu, C. *Organometallics* **2011**, *30*, 2095.
(31) Liao, S.; Čorić, I.; Wang, Q.; List, B. *J. Am. Chem. Soc.* **2012**, *134*, 10765.
(32) Nakano, K.; Nakamura, M.; Nozaki, K. *Macromolecules* **2009**, *42*, 6972.
(33) Whitelaw, E. L.; Loraine, G.; Mahon, M. F.; Jones, M. D. *Dalton Trans.* **2011**, *40*, 11469.
(34) Whitelaw, E. L.; Davidson, M. G.; Jones, M. D. *Chem. Commun.* **2011**, *47*, 10004.
(35) Cohen, A.; Yeori, A.; Kopilov, J.; Goldberg, I.; Kol, M. *Chem. Commun.* **2008**, *0*, 2149.
(36) Chmura, A. J.; Davidson, M. G.; Frankis, C. J.; Jones, M. D.; Lunn, M. D. *Chem. Commun.* **2008**, *0*, 1293.
(37) Sergeeva, E.; Kopilov, J.; Goldberg, I.; Kol, M. *Chem. Commun.* **2009**, *0*, 3053.
(38) Minch, M. J. *J. Chem. Educ.* **1999**, *76*, 759.
(39) Wisniewski, M.; Borgne, A. L.; Spassky, N. *Macromol. Chem. Phys.* **1997**, *198*, 1227.
(40) Spassky, N.; Leborgne, A.; Momtaz, A.; Sepulchre, M. *Journal of Polymer Science: Polymer Chemistry Edition* **1980**, *18*, 3089.
(41) In *Handbook of Transition Metal Polymerization Catalysts*; John Wiley & Sons, Inc.: 2010, p i.

Chapter 4

Experimental

4. Experimental

4.1. General Considerations

All manipulations involving metal complexes were conducted under an atmosphere of dry argon or dry nitrogen using standard Schlenk and glove-box techniques as appropriate. Solvents were taken from an MBraun SPS solvent system.

The solution ^{1}H, $^{13}C\{^{1}H\}$, and $^{31}P\{^{1}H\}$ NMR experiments were prepared at room temperature unless otherwise stated, in Young's NMR tubes for air sensitive compounds, otherwise Wilmad 5mm NMR Tubes were used. Spectra were recorded on Bruker Advance -250, 300, 400 or500 MHz FT-NMR spectrometers. Samples were dissolved in $CDCl_3$ or MeOD and spectra were referenced to the residual solvent peak. For air sensitive compounds, $CDCl_3$ was pre-treated and distilled from calcium hydride prior to use. Coupling constants are given in Hertz while chemical shifts are quoted as δ values in ppm. ^{1}H homonuclear decoupled NMR was also carried out at room temperature. Solid-state ^{13}C $\{^{1}H\}$ CP/MAS (cross polarisation/magic angle spinning) NMR spectroscopy were recorded using a Varian VNMRS 400 MHz machine, at the University of Durham, operating at 100.56 MHz with a spin rate of 10,000 Hz. Cross-polarisation pulse sequence was used with a contact time of 3.0 ms and recycle delay of 1.0 s, with a two pulse phase modulation. Spectra reference to tetramethylsilane. All spectra collected at room temperature.

High resonance mass spectrometry, MS, was recorded on a micrOTOF electro spray quadrupole time of flight, ESI-TOF, spectrometer. Samples were recorded in positive mode having been dissolved in methanol. MALDI-TOF Mass Spectra of polymeric products were submitted to the EPSRC National Mass Spectrometry Service Centre, Swansea, UK. The samples were dissolved in THF and analysed by positive MALDI in linear and reflectron modes using Dithranol matrix with LiCl as an additive to promote $[M^{+}Li]^{+}$ or NaOAc.

EPR spectroscopy samples were submitted to the University of Manchester and performed using a Bruker EMX instrument. X band operating at 9.4 GHz, while Q band at 34.0 GHz. Spectra recorded at temperatures stated.

Simulations were performed using Bruker XSophe computer simulation software (version 1.1.4).

Gel Permeation Chromatography, GPC, analysis was performed on a Polymer Laboratories PL-GPC 50 integrated system using a PLgel 5 μm MIXED-D 300 × 7.5mm column at 35°C using GPC-grade THF as the solvent under a flow rate of 1.0 mL min^{-1}. The polydispersity index, PDI, was determined from the number average molecular weight, M_n, and weight average molecular weight, M_w ratio. Polymeric samples were referenced to ten polystyrene standards, with narrow molecular weights in the range of M_w 580 - 6035000 g mol^{-1}.

X-ray crystallographic data were collected on a Nonius Kappa CCD area detector diffractometer using Mo-Kα radiation (λ = 0.71073 Å) with a constant temperature of 150(2) K throughout. All structures were solved by direct methods and refined on (all) F^2 data using the SHELXL-97 suite of programs[1]. Hydrogen atoms were included in idealised position and refined using the riding model. Experimental parameters and relevant information with regards to the structure's solution and refinement are given in the appendices.

Elemental analysis was carried out by Mr. A. K. Carver at the Department of Chemistry at the University of Bath, on an Exeter Analytical CE440 Elemental Analyzer and by Mr. S. Boyer at the Elemental Analysis Service, London Metropolitan University, using a Carlo Erba 1108 Elemental Analyser and Carlo Erba Flash 2000 Elemental Analyser. It should be noted that not every complex can present elemental analysis, and in the cases where it is reported, values are not always in close agreement with calculated values. This is due to the elemental analysis not being performed under rigorous conditions and hence not precise.

4.2. Chapter 2

4.2.1. Synthetic Procedures

Preparation of 2,6-Pyridinedicarboxaldehyde: To a suspension of activated manganese(IV) oxide (86.94 g, 1 mol) in chloroform (200 mL) was added 2,6-pyridinedimethanol (13.92 g, 0.1 mol) with stirring. The resulting mixture was refluxed over night and the ensuing suspension vacuum filtered through Celite to remove the manganese(IV) oxide and any unreacted starting

material. Solvent was removed by rotary evaporation to yield a white solid (9.63 g, 71.5 %). 1H NMR (CDCl3) 9.21 (2H, s, CH=O), 8.06 (1H, s, Ar-H), 7.89 (2H, t, Ar-H). 13C 1H NMR (CDCl3) 123.12 (Ar-H), 123.85 (Ar-H), 135.23 (Ar-H), 149.75(Ar-C), 150.21 (Ar-C), 187.58 (CH=O). m/z ion M+H calc. 136.0399, found 136.0345.

Peparation of 3IM: To a solution of 2,6-Pyridinedicarboxaldehyde (0.56 g, 4.13 mmol) in methanol (20 mL) was added *(R)*-(+)-α-Methylbenzylamine (1.0 g, 8.25 mmol) with stirring. The mixture was allowed to react over night before solvent was removed by rotary evaporation. Any traces of water were removed by gentle heating under reduced pressure to yield an off-white oil (1.14 g, 80.9%). **^{1}H NMR** ($CDCl_3$) 1.72 (6H, d, J=6.6, CH-C*H*$_3$) 4.74 (2H, q, J=6.6, C*H*-CH_3) 7.3-7.56 (10H, m Ar-*H*) 7.70 (1H, t, J=7.7, py-*H*) 8.22 (2H, dd, J=7.9, 0.6, py-*H*) 8.63 (2H, s, C*H*=N). **^{13}C{^{1}H} NMR** ($CDCl_3$) 24.54, 69.59, 122.38, 126.71, 127.04, 128.51, 136.98, 144.46, 154.44, 160.16. **m/z** ion M+H calc. 342.1927, found 342.1927.

Peparation of 3IE: To a solution of 2,6-Pyridinedicarboxaldehyde (0.5 g, 3.7 mmol) in methanol (20 mL) was added *(R)*-(+)-α-Ethylbenzylamine (1.0 g, 7.4 mmol) with stirring. The mixture was allowed to react over night before solvent was removed by rotary evaporation. Any traces of water were removed by gentle heating under reduced pressure to yield an off-white oil (1.18 g, 86.2%). **^{1}H NMR** ($CDCl_3$) 0.76 (6H, t, J=7.4, CH-C*H*$_3$), 1.85 (4H, qn, J=7.2, C*H*$_2$-CH_3) 4.15 (2H, t, J=6.8, C*H*-CH_2) 7.07-7.32 (10H, m, Ar-*H*) 7.58-7.64 (1H, m, py-*H*) 8.00 (2H, d, J=7.6, py-*H*) 8.34 (2H, s, C*H*=N). **^{13}C{^{1}H} NMR** ($CDCl_3$) 11.07, 31.35, 77.02, 122.28, 126.99, 127.08, 128.38, 136.88, 143.79, 154.36, 160.42. **m/z** ion M+H calc. 370.2283, found 370.2399.

Peparation of 3IC: To a solution of 2,6-Pyridinedicarboxaldehyde (0.53 g, 3.93 mmol) in methanol (20 mL) was added *(R)*-(−)-α-Methylcyclohexanemethylamine (1.0 g, 7.86 mmol) with stirring. The mixture was allowed to react over night before solvent was removed by rotary evaporation. Any traces of water were removed by gentle heating under reduced pressure to yield an off-white oil (1.22 g, 87.3%). **^{1}H NMR** ($CDCl_3$) 0.73-1.84 (22H, m cy-*H*) 1.17 (6H, d, *J*=6.6, CH-C*H*$_3$) 3.06 (2H, qn, *J*=6.5, C*H*-CH_3) 7.70

(1H, m, py-*H*) 7.97 (2H, d, *J*=7.9, py-*H*) 8.27 (2H, s, C*H*=N). **^{13}C{^{1}H} NMR** ($CDCl_3$) 19.79, 26.23, 26.39, 26.56, 29.76, 29.93, 43.61, 71.78, 121.99, 136.98, 154.55, 159.54. **m/z** ion M+H calc. 354.2909, found 354.2973.

Peparation of 3IN: To a solution of 2,6-Pyridinedicarboxaldehyde (0.39 g, 2.92 mmol) in methanol (20 mL) was added *(R)*-(+)-α-Methyl-2-naphthalenemethylamine (1.0 g, 5.84 mmol) with stirring. The mixture was allowed to react over night before solvent was removed by rotary evaporation. Any traces of water were removed by gentle heating under reduced pressure to yield an off-white oil (1.2 g, 93.1%). **^{1}H NMR** ($CDCl_3$) 1.63 (6H, d, J=6.6, CH-C*H*$_3$) 4.75 (2H, q, J=6.6, C*H*-CH$_3$) 7.32-7.42 (4H, m, Ar-*H*) 7.48-7.55 (2H, m, Ar-*H*) 7.71-7.80 (9H, m, Ar-*H*) 8.09 (2H, d, J=7.9, py-*H*) 8.47 (2H, s, C*H*=N). **^{13}C{^{1}H} NMR** ($CDCl_3$) 24.42, 69.59, 122.43, 125.07, 125.22, 125.50, 125.97, 127.59, 127.86, 128.17, 132.68, 133.47, 136.98, 141.84, 154.44, 160.35. **m/z** ion M+H calc. 442.2283, found 442.2335.

Peparation of 2IM: To a solution of *(R)*-(+)-α-Methylbenzylamine (1.0 g, 8.25 mmol) in methanol (20 mL) was added 2-Pyridinecarboxaldehyde (0.88 g, 8.25 mmol) with stirring. The mixture was allowed to react over night before solvent was removed by rotary evaporation. Any traces of water were removed by gentle heating under reduced pressure to yield an off-white oil (1.48 g, 85.2%). **^{1}H NMR** ($CDCl_3$) 1.51 (3H, d, *J*=6.6 CH-C*H3)* 4.54 (1H, q, *J*=6.6 N-C*H*), 7.10-7.32 (5H, m, Ar-*H*) 7.35 (1H, s, Ar-H) 7.60 (1H, m, Ar-*H*) 7.97-8.01 (1H, dt, *J*=7.9, 1.1, Ar-*H*) 8.37 (1H, s C*H*=N) 8.51-8.53 (1H, m, Ar-*H*). **^{13}C{^{1}H} NMR** ($CDCl_3$) 24.34, 69.38, 121.20, 124.45, 125.90, 126.77, 127.04, 128.32, 136.10, 144.35, 149.09, 154.54, 160.20. **m/z** ion M+H calc. 211.1235, found 211.124.

Peparation of 2IE: To a solution of *(R)*-(+)-α-Ethylbenzylamine (1.0 g, 7.4 mmol) in methanol (20 mL) was added 2-Pyridinecarboxaldehyde (0.79 g, 7.4 mmol) with stirring. The mixture was allowed to react over night before solvent was removed by rotary evaporation. Any traces of water were removed by gentle heating under reduced pressure to yield an off-white oil (1.32 g, 79.3%). **^{1}H NMR** ($CDCl_3$) 0.94 (3H, t, *J*=7.3, CH2-C*H3*) 2.02 (2H, qn, *J*=7.3, CH-C*H2*-CH3) 4.32 (1H, t, *J*=6.8, N-C*H*) 7.25-7.42 (5H,m, Ar-*H)* 7.50-7.51 (1H, m, py-*H*) 7.73-7.80 (1H, m, Ar-*H*) 8.16 (1H, d, *J*=7.5, Ar-*H*) 8.48 (1H, s, N=C*H*) 8.67 (1H, ddd,

J=4.9, 1.7, 0.9, Ar-*H*). **^{13}C ^{1}H NMR** ($CDCl_3$) 10.62, 30.85, 76.86, 121.31, 124.50, 126.85, 127.06, 128.29, 136.31, 143.76, 149.16, 154.61, 160.56. **m/z** ion M+H calc. 225.1392, found 225.1384.

Peparation of 2IC: To a solution of *(R)*-(−)-α-Methylcyclohexanemethylamine (1.0 g, 7.86 mmol) in methanol (20 mL) was added 2-Pyridinecarboxaldehyde (0.84 g, 7.86 mmol) with stirring. The mixture was allowed to react over night before solvent was removed by rotary evaporation. Any traces of water were removed by gentle heating under reduced pressure to yield an off-white oil (1.52 g, 88.8%). **^{1}H NMR** ($CDCl_3$) 0.70-1.11 (5H, m cy-*H*) 1.14 (3H, d, *J*=5.0 CH-CH_3) 1.32-1.78 (6H, m, cy-*H*) 3.02 (1H, qn, *J*=6.6, C*H*-N), 7.15-7.20 (1H, m, py-*H*) 7.6 (1H, dt, *J*=7.7, 1.9, py-*H*) 7.91 (1H, d, *J*=7.94, Ar-*H*) 8.22 (1H, s, C*H*=N) 8.51-8.54 (1H, m, py-*H*). **^{13}C{^{1}H} NMR** ($CDCl_3$) 19.45, 25.90, 26.06,26.23, 29.40, 29.56, 43.29, 71.36, 120.96, 124.10, 136.10, 149.00, 154.57, 159.34. **m/z** ion M+H calc. 217.1705, found 217.1702.

Peparation of 2IN: To a solution of *(R)*-(+)-α-Methyl-2-naphthalenemethylamine (1.0 g, 5.84 mmol) in methanol (20 mL) was added 2-Pyridinecarboxaldehyde (0.63 g, 5.84 mmol) with stirring. The mixture was allowed to react over night before solvent was removed by rotary evaporation. Any traces of water were removed by gentle heating under reduced pressure to yield an off-white oil (1.38 g, 90.2%). **^{1}H NMR** ($CDCl_3$) 1.16 (3H, d, *J*=6.6 CH-CH_3) 4.26 (1H, q, *J*=6.5, C*H*-N) 6.70-6.76 (1H, m, Ar-*H*) 6.87-6.92 (2H, m, Ar-*H*) 7.05 (1H, dd, *J*=8.5, 1.6, Ar-*H*) 7.17 (2H, ddd, *J*=7.7, 5.8, 2.1, Ar-*H*) 7.31 (2H, d, *J*=3.2, Ar-*H*) 7.58 (1H, d, *J*=7.9, Ar-*H*) 7.98 (1H, s, C*H*-N) 8.08 (1H, d, *J*=4.7, Ar-*H*). **^{13}C{^{1}H} NMR** ($CDCl_3$) 24.39, 69.49, 121.36, 124.57, 124.91, 125.13, 125.45, 125.83, 127.47, 127.75, 128.03, 132.56, 133.36, 136.34, 141.85, 149.20, 154.60, 160.51. **m/z** ion M+H calc. 261.1392, found 261.1466.

Peparation of 3AM: To a solution of 3IM (1.14 g, 3.34 mmol) in methanol (20 mL) was added sodium borohydride (1.26 g, 33.38 mmol) with stirring. The mixture was allowed to react over night before the solvent was removed by rotary evaporation. The residue was dissolved in chloroform and washed with water (3 x 20 mL) to remove the sodium salt. The organic phase was dried over magnesium sulphate before the solvent was removed by rotary

evaporation. Any traces of water were removed by gentle heating under reduced pressure to yield an off-white oil (0.79 g, 68.2%). **^{1}H NMR** ($CDCl_3$) 1.28 (6H, d, J=6.4, CH-C*H*$_3$) 2.20 (2H, br s, CH_2-N*H*) 3.62 (4H, s, C*H*$_2$-NH) 3.70 (2H, q, *J*=6.8 NH-C*H*) 6.91 (1H, d, *J*=7.5 Ar-*H*) 7.08-7.14 (2H, m, Ar-*H*) 7.16-7.28 (8H, m, Ar-*H*) 7.37 (1H, t, J=7.7, py-*H*). **^{13}C{^{1}H} NMR** ($CDCl_3$) 24.22, 52.64, 57.62, 120.15, 126.50, 126.68, 128.18, 136.38, 145.17, 158.91. **m/z** ion M+H calc. 346.2283, found 346.2299.

Peparation of 3AE: To a solution of 3IE (1.18 g, 3.19 mmol) in methanol (20 mL) was added Sodium borohydride (1.21 g, 31.88 mmol) with stirring. The mixture was allowed to react over night before solvent was removed by rotary evaporation. The residue was dissolved in chloroform and washed with water (3 x 20 mL) to remove the sodium salt. The organic phase was dried over magnesium sulphate before the solvent was removed by rotary evaporation. Any traces of water were removed by gentle heating under reduced pressure to yield an off-white oil (0.8 g, 67.3%). **^{1}H NMR** ($CDCl_3$) 0.73 (6H, d, *J*=7.3, CH-C*H*$_3$), 1.52-1.77 (4H,m, C*H*$_2$-CH_3) 2.21 (2H, br s, CH_2-N*H*), 3.43 (2H, dd, *J*=7.5, 6) 3.59 (ABq, 4H, $\Delta\delta_{AB}$=0.05, J_{AB}=14.2 Hz, C*H*$_2$-NH) 6.89 (2H, d, *J*=7.5, py-*H*) 7.09-7.24 (10H, m, Ar-*H*) 7.36 (1H, t, *J*=7.5, py-*H*). **^{13}C{^{1}H} NMR** ($CDCl_3$) 10.61, 30.93, 52.58, 64.41, 120.16, 126.72, 127.29, 128.06, 136.33, 143.69, 159.02. **m/z** ion M+H calc. 374.2596, found 374.2592.

Peparation of 3AC: To a solution of 3IC (1.22 g, 3.43 mmol) in methanol (20 mL) was added Sodium borohydride (1.3 g, 34.31 mmol) with stirring. The mixture was allowed to react over night before solvent was removed by rotary evaporation. The residue was dissolved in chloroform and washed with water (3 x 20 mL) to remove the sodium salt. The organic phase was dried over magnesium sulphate before the solvent was removed by rotary evaporation. Any traces of water were removed by gentle heating under reduced pressure to yield an off-white oil (0.75 g, 61.3%). **^{1}H NMR** ($CDCl_3$) 0.87-1.40 (10H, m, cy-*H*) 0.97 (6H, d, *J*=6.2, CH-C*H*$_3$) 1.53-1.73 (12H, m, cy-*H*) 1.92 (2H, br s, CH_2-N*H*) 2.38-2.48 (2H, m, C*H*-CH_3) 3.83 (ABq, 4H, $\Delta\delta_{AB}$=0.13, J_{AB}=14.2 Hz C*H*$_2$-NH) 7.0-7.1 (2H, m, py-*H*) 7.41-7.50 (1H, m, py-*H*). **^{13}C{^{1}H} NMR** ($CDCl_3$) 16.30, 26.22,

26.25, 26.35, 27.67, 29.39, 42.62, 52.32, 56.93, 119.80, 136.08, 159.08. **m/z** ion M+H calc. 358.3222, found 358.3206.

Peparation of 3AN: To a solution of 3IN (1.2 g, 2.72 mmol) in methanol (20 mL) was added Sodium borohydride (1.03 g, 27.18 mmol) with stirring. The mixture was allowed to react over night before solvent was removed by rotary evaporation. The residue was dissolved in chloroform and washed with water (3 x 20 mL) to remove the sodium salt. The organic phase was dried over magnesium sulphate before the solvent was removed by rotary evaporation. Any traces of water were removed by gentle heating under reduced pressure to yield an off-white oil (0.72 g, 59.3%). **^{1}H NMR** ($CDCl_3$) 1.41 (6H, d, *J*=6.6 Hz, CH-C*H*$_3$) 2.4 (2H, br s, CH_2-N*H*) 3.73 (ABq, 4H, $\Delta\delta_{AB}$=0.04, J_{AB}=14.2 Hz, C*H*$_2$-NH) 4.57 (4H, q, *J*=6.3 Hz, C*H*-CH_3) 6.91 (2H, d, *J*=7.9, Ar-*H*) 7.28-7.38 (7H, m, Ar-*H*) 7.60-7.66 (4H, m, Ar-*H*) 7.70-7.75 (2H, m, Ar-*H*) 8.01-8.05 (2H, m Ar-*H*). **^{13}C{^{1}H} NMR** ($CDCl_3$) 24.13, 52.61, 57.68, 120.06, 124.68, 125.08, 125.11, 125.58, 127.30, 127.40, 127.93, 132.51, 133.14, 136.27, 142.56, 158.77. **m/z** ion M+H calc. 446.2596, found 446.2577.

Peparation of 2AM: To a solution of 2IM (1.48 g, 7.03 mmol) in methanol (20 mL) was added Sodium borohydride (1.33 g, 35.15 mmol) with stirring. The mixture was allowed to react over night before solvent was removed by rotary evaporation. The residue was dissolved in chloroform and washed with water (3 x 20 mL) to remove the sodium salt. The organic phase was dried over magnesium sulphate before the solvent was removed by rotary evaporation. Any traces of water were removed by gentle heating under reduced pressure to yield an off-white oil (1.04 g, 69.2%). **^{1}H NMR** ($CDCl_3$) 1.26 (3H, d, *J*=6.4, CH-CH_3) 2.25 (1H, br, CH-N*H*) 3.61 (2H, s, C*H*-NH) 3.67 (ABq, 2H, $\Delta\delta_{AB}$=0.04, J_{AB}=11.0 Hz C*H*$_2$-NH) 6.92 (1H, dd, *J*=6.8, 5.7, py-*H*) 7.00 (1H, d, 7.5, py-*H*) 7.05-7.24 (5H, m, Ar-*H*) 7.37 (1H, t, *J*=7.5 py-*H*) 8.38-8.39 (1H, m, py-*H*). **^{13}C{^{1}H} NMR** ($CDCl_3$) 24.10, 52.64, 57.58, 121.37, 121.93, 126.35, 126.53, 128.04, 135.82, 145.02, 148.42, 159.42. **m/z** ion M+H calc. 213.1392, found 213.1388.

Peparation of 2AE: To a solution of 2IE (1.32 g, 5.86 mmol) in methanol (20 mL) was added Sodium borohydride (1.11 g, 29.32 mmol) with stirring. The mixture was allowed to react over night before solvent was removed by rotary

evaporation. The residue was dissolved in chloroform and washed with water (3 x 20 mL) to remove the sodium salt. The organic phase was dried over magnesium sulphate before the solvent was removed by rotary evaporation. Any traces of water were removed by gentle heating under reduced pressure to yield an off-white oil (0.93 g, 70.1%). **^{1}H NMR** ($CDCl_3$) 0.73 (3H, t, *J*=7.6 CH_2-C*H*$_3$) 1.53-1.77 (2H, m, C*H*$_2$-CH_3) 2.11 (1H, br, CH-N*H*) 3.40 (1H, t, J=6.8, C*H*-CH_2) 3.63 (ABq, 4H, $\Delta\delta_{AB}$=0.06, J_{AB}=14.0 Hz, C*H*$_2$-NH) 6.98-7.02 (1H, m py-*H*) 7.06 (1H, dd, J=7.5, py-*H*) 7.10-7.25 (5H, m, Ar-*H*) 7.46 (1H, td, J=7.5, 1.9, py-*H*) 8.43-8.45 (1H, m py-*H*). **^{13}C{^{1}H} NMR** ($CDCl_3$) 10.62, 30.94, 52.85, 64.61, 121.61, 122.25, 126.80, 127.37, 128.05, 128.12, 128.86, 136.08, 134.68, 149.08, 159.80. **m/z** ion M+H calc. 227.1548, found 227.1657.

Peparation of 2AC: To a solution of 2IC (1.52 g, 6.98 mmol) in methanol (20 mL) was added Sodium borohydride (1.32 g, 34.9 mmol) with stirring. The mixture was allowed to react over night before solvent was removed by rotary evaporation. The residue was dissolved in chloroform and washed with water (3 x 20 mL) to remove the sodium salt. The organic phase was dried over magnesium sulphate before the solvent was removed by rotary evaporation. Any traces of water were removed by gentle heating under reduced pressure to yield an off-white oil (1.09 g, 71.5%). **^{1}H NMR** ($CDCl_3$) 0.93 (3H, d, J=6.4, CH-C*H*$_3$) 0.96-1.35 (5H, m cy-*H*) 1.50-1.71 (6H, m, cy-*H*) 1.82 (1H, br s, CH-N*H*) 2.35-2.43 (1H, m, C*H*-CH_3) 3.78 (ABq, 4H, $\Delta\delta_{AB}$=0.011, J_{AB}=13.2 Hz C*H*$_2$-NH) 6.95-7.20 (2H, m py-*H*) 7.46 (1H, td, J=7.7, 1.9 py-*H*) 8.40-8.42 (1H, m, Ar-*H*). **^{13}C{^{1}H} NMR** ($CDCl_3$) 16.23, 26.06, 26.20, 26.31, 27.53, 29.39, 42.56, 52.54, 57.05, 121.16, 121.75, 135.6802, 148.60, 159.97. **m/z** ion M+H calc. 219.1861, found 219.2000.

Peparation of 2AN: To a solution of 2IN (1.38 g, 5.27 mmol) in methanol (20 mL) was added Sodium borohydride (1.0 g, 26.34 mmol) with stirring. The mixture was allowed to react over night before solvent was removed by rotary evaporation. The residue was dissolved in chloroform and washed with water (3 x 20 mL) to remove the sodium salt. The organic phase was dried over magnesium sulphate before the solvent was removed by rotary evaporation. Any traces of water were removed by gentle heating under reduced pressure to yield an

off-white oil (1.0 g, 72.3%). **^{1}H NMR** ($CDCl_3$) 1.56 (3H, d, J=6.8, CH-C*H*$_3$) 2.34 (1H, br s, CH_2-N*H*) 3.86 (2H, s NH-C*H*) 4.05 (1H, q, J=6.4 C*H*$_2$-NH) 7.03-7.33 (4H, m, Ar-*H*) 7.45-7.52 (3H, m, Ar-*H*) 7.62-7.65 (1H, m, Ar-*H*) 7.83-3.89 (3H, m, Ar-*H*) 8.62-8.63 (1H, m, Ar-*H*). **^{13}C{^{1}H} NMR** ($CDCl_3$) 23.99, 52.58, 57.61, 121.18, 121.73, 124.51, 124.80, 124.91, 125.38, 128.50, 135.58, 142.47, 148.68, 159.285. **m/z** ion M+H calc. 263.1548, found 263.1633.

Preparation of Cu(3IM)(SO_3CF_3)$_2$: To the ligand 3IM (0.0946 g, 0.28 mmol) in methanol (30 mL) was added copper(II) triflate (0.1 g, 0.28 mmol). The mixture was stirred over night before the solvent was removed by rotary evaporation. The product was dried under reduced pressure (0.17 g, 89.6 %). **m/z** ion M+ calc. 553.0693, found 533.070, corresponding to the correct, copper containing, isotope pattern. **Elemental analysis** of $C_{23}H_{23}N_3F_6O_9S_2Cu_1$, Expected C, 39.66; H, 3.86; N, 5.55. Found C, 39.3; H, 3.79; N, 5.48.

Preparation of Cu(3IE)(SO_3CF_3)$_2$: To the ligand 3IE (0.1024 g, 0.28 mmol) in methanol (30 mL) was added copper(II) triflate (0.1 g, 0.28 mmol). The mixture was stirred over night before the solvent was removed by rotary evaporation. The product was dried under reduced pressure (0.18 g, 88.3 %). **m/z** ion M+ calc. 581.1021, found 581.1017, corresponding to the correct, copper containing, isotope pattern. **Elemental analysis** of $C_{25}H_{27}N_3F_6O_8S_2Cu_1$, Expected C, 42.27; H, 4.07; N, 5.48. Found C, 42.6; H, 4.17; N, 5.56.

Preparation of Cu(3IC)(SO_3CF_3)$_2$: To the ligand 3IC (0.098 g, 0.28 mmol) in methanol (30 mL) was added copper(II) triflate (0.1 g, 0.28 mmol). The mixture was stirred over night before the solvent was removed by rotary evaporation. The product was dried under reduced pressure (0.18 g, 90.2 %). **m/z** ion M+ calc. 565.1642, found 565.1626, corresponding to the correct, copper containing, isotope pattern. **Elemental analysis** of $C_{23}H_{35}N_3F_6O_8S_2Cu_1$, Expected C, 39.97; H, 5.23; N, 5.59. Found C, 4.02; H, 5.4; N, 5.69.

Preparation of Cu(3IN)(SO_3CF_3)$_2$: To the ligand 3IN (0.1223 g, 0.28 mmol) in methanol (30 mL) was added copper(II) triflate (0.1 g, 0.28 mmol). The mixture was stirred over night before the solvent was removed by rotary evaporation. The product was dried under reduced pressure (0.19 g, 85. %). **m/z** ion M+ calc. 653.1016, found 653.1073, corresponding to the correct, copper

containing, isotope pattern. **Elemental analysis** of $C_{31}H_{27}N_3F_6O_6S_2Cu_1$, Expected C, 49.43; H, 3.39; N, 5.23. Found C, 48.7; H, 3.82; N, 5.15.

Preparation of Cu(2IM)$(SO_3CF_3)_2$: To the ligand 2IM (0.0584 g, 0.28 mmol) in methanol (30 mL) was added copper(II) triflate (0.1 g, 0.28 mmol). The mixture was stirred over night before the solvent was removed by rotary evaporation. The product was dried under reduced pressure (0.14 g, 85.7 %). The product was re-dissolved in methanol and diethyl ether (10:1) and cooled to -20^oC yielding crystals fit for single crystal XRD. **m/z** ion M+ calc. 421.998, found 421.9915, corresponding to the correct, copper containing, isotope pattern. **Elemental analysis** of $C_{28}H_{30}N_4F_6O_7S_2Cu_1$, Expected C, 44.6; H, 3.74; N, 6.9. Found C, 45.03; H, 3.78; N, 7.0.

Preparation of Cu(2IE)$(SO_3CF_3)_2$: To the ligand 2IE (0.0622 g, 0.28 mmol) in methanol (30 mL) was added copper(II) triflate (0.1 g, 0.28 mmol). The mixture was stirred over night before the solvent was removed by rotary evaporation. The product was dried under reduced pressure (0.12 g, 75.2 %). **m/z** ion M+ calc. 436.0124, found 436.0091, corresponding to the correct, copper containing, isotope pattern. **Elemental analysis** of $C_{30}H_{32}N_4F_6O_6S_2Cu_1$, Expected C, 48.2; H, 5.07; N, 6.66. Found C, 43.39; H, 5.34; N, 6.75.

Preparation of Cu(2IC)$(SO_3CF_3)_2$: To the ligand 2IC (0.060 g, 0.28 mmol) in methanol (30 mL) was added copper(II) triflate (0.1 g, 0.28 mmol). The mixture was stirred over night before the solvent was removed by rotary evaporation. The product was dried under reduced pressure (0.14 g, 89.3 %). **m/z** ion M+ calc. 428.0437, found 428.0393, corresponding to the correct, copper containing, isotope pattern. **Elemental analysis** of $C_{28}H_{44}N_4F_6O_8S_2Cu_1$, Expected C, 43.2; H, 5.07; N, 6.66. Found C, 43.39; H, 5.34; N, 6.75.

Preparation of Cu(2IN)$(SO_3CF_3)_2$: To the ligand 2IN (0.0722 g, 0.28 mmol) in methanol (30 mL) was added copper(II) triflate (0.1 g, 0.28 mmol). The mixture was stirred over night before the solvent was removed by rotary evaporation. The product was dried under reduced pressure (0.16 g, 92.3 %). **m/z** ion M+ calc. 472.0124, found 472.0108, corresponding to the correct, copper containing, isotope pattern. **Elemental analysis** of $C_{36}H_{32}N_4F_6O_6S_2Cu_1$, Expected C, 51.0; H, 3.88; N, 6.35. Found C, 51.73; H, 3.66; N, 6.26.

Preparation of Cu(3AM)(SO_3CF_3)$_2$: To the ligand 3AM (0.0957 g, 0.28 mmol) in methanol (30 mL) was added copper(II) triflate (0.1 g, 0.28 mmol). The mixture was stirred over night before the solvent was removed by rotary evaporation. The product was dried under reduced pressure (0.16 g, 84. %). **m/z** ion M+ calc. 557.1016, found 557.0936, corresponding to the correct, copper containing, isotope pattern. **Elemental analysis** of $C_{46}H_{54}N_6F_6O_6S_2Cu_1$, Expected C, 42.46; H, 3.85; N, 5.94. Found C, 42.4; H, 4.14; N, 5.95.

Preparation of Cu(3AE)(SO_3CF_3)$_2$: To the ligand 3AE (0.1035 g, 0.28 mmol) in methanol (30 mL) was added copper(II) triflate (0.1 g, 0.28 mmol). The mixture was stirred over night before the solvent was removed by rotary evaporation. The product was dried under reduced pressure (0.17 g, 81.3 %). **m/z** ion M+ calc. 585.1334, found 585.1291, corresponding to the correct, copper containing, isotope pattern. **Elemental analysis** of $C_{50}H_{62}N_6F_6O_6S_2Cu_1$, Expected C, 4.11; H, 4.25; N, 5.72. Found C, 44.6; H, 4.6; N, 5.86.

Preparation of Cu(3AC)(SO_3CF_3)$_2$: To the ligand 3AC (0.0991 g, 0.28 mmol) in methanol (30 mL) was added copper(II) triflate (0.1 g, 0.28 mmol). The mixture was stirred over night before the solvent was removed by rotary evaporation. The product was dried under reduced pressure (0.16 g, 81.2 %). **m/z** ion M+ calc. 569.196, found 569.196, corresponding to the correct, copper containing, isotope pattern. **Elemental analysis** of $C_{46}H_{78}N_6F_6O_6S_2Cu_1$, Expected C, 41.75; H, 5.47; N, 5.84. Found C, 41.6; H, 5.66; N, 5.81.

Preparation of Cu(3AN)(SO_3CF_3)$_2$: To the ligand 3AN (0.1234 g, 0.28 mmol) in methanol (30 mL) was added copper(II) triflate (0.1 g, 0.28 mmol). The mixture was stirred over night before the solvent was removed by rotary evaporation. The product was dried under reduced pressure (0.17 g, 78.3 %). **m/z** ion M+ calc. 657.1334, found 657.1306, corresponding to the correct, copper containing, isotope pattern. **Elemental analysis** of $C_{62}H_{62}N_6F_6O_6S_2Cu_1$, Expected C, 49.1; H, 3.87; N, 5.21. Found C, 49.7; H, 3.87; N, 5.21.

Preparation of Cu(2AM)(SO_3CF_3)$_2$: To the ligand 2AM (0.0589 g, 0.28 mmol) in methanol (30 mL) was added copper(II) triflate (0.1 g, 0.28 mmol). The mixture was stirred over night before the solvent was removed by rotary evaporation. The product was dried under reduced pressure (0.11 g, 70.6 %). **m/z**

ion M+ calc. 424.0123, found 424.017, corresponding to the correct, copper containing, isotope pattern. **Elemental analysis** of $C_{28}H_{34}N_4F_6O_7S_2Cu_1$, Expected C, 44.6; H, 3.73; N, 6.93. Found C, 47.2; H, 4.26; N, 6.97.

Preparation of Cu(2AE)$(SO_3CF_3)_2$: To the ligand 2AE (0.0628 g, 0.28 mmol) in methanol (30 mL) was added copper(II) triflate (0.1 g, 0.28 mmol). The mixture was stirred over night before the solvent was removed by rotary evaporation. The product was dried under reduced pressure (0.13 g, 80.4 %). **m/z** ion M+ calc. 438.0281, found 438.0227, corresponding to the correct, copper containing, isotope pattern. **Elemental analysis** of $C_{30}H_{36}N_4F_6O_6S_2Cu_1$, Expected C, 47.4; H, 4.7; N, 6.67. Found C, 47.2; H, 4.46; N, 6.88.

Preparation of Cu(2AC)$(SO_3CF_3)_2$: To the ligand 2AC (0.0606 g, 0.28 mmol) in methanol (30 mL) was added copper(II) triflate (0.1 g, 0.28 mmol). The mixture was stirred over night before the solvent was removed by rotary evaporation. The product was dried under reduced pressure (0.13 g, 81.6 %). **m/z** ion M+ calc. 430.0594, found 430.0554, corresponding to the correct, copper containing, isotope pattern. **Elemental analysis** of $C_{28}H_{47}N_4F_6O_{7.5}S_2Cu_1$, Expected C, 43.6; H, 5.53; N, 6.7. Found C, 43.66; H, 5.74; N, 6.79.

Preparation of Cu(2AN)$(SO_3CF_3)_2$: To the ligand 2AN (0.0728 g, 0.28 mmol) in methanol (30 mL) was added copper(II) triflate (0.1 g, 0.28 mmol). The mixture was stirred over night before the solvent was removed by rotary evaporation. The product was dried under reduced pressure (0.14 g, 79.9 %). **m/z** ion M+ calc. 474.0286, found , corresponding to the correct, copper containing, isotope pattern. **Elemental analysis** of $C_{40}H_{52}N_4F_6O_{10}S_2Cu_1$, Expected C, 49.6; H, 4.25; N, 5.13. Found C, 49.72; H, 5.17; N, 5.52.

Preparation of Pd(3IM)Cl_2: Palladium Chloride (100 mg, 0.56 mmol) in acetonitrile (50 mL) was added the ligand 3IM (193 mg, 0.56 mmol). The mixture was stirred for twenty four hours, or until all palladium chloride had dissolved, whichever came first. The solvent was removed by rotary evaporation before the product was dried under reduced pressure (234 mg, 80 %). **^{1}H NMR** ($CDCl_3$) 1.69-1.72 (6H, m, CH-C*H*$_3$) 4.52 (2H, q, J=6.6, C*H*-CH_3) 7.25-7.53 (10H, m Ar-*H*) 7.74 (1H, t, J=7.7, py-*H*) 8.12-8.19 (2H, m, py-*H*) 8.54 (2H, s, C*H*=N). **^{13}C{^{1}H} NMR** ($CDCl_3$) 24.89, 68.69, 122.87, 127.07, 127.71, 129.45, 137.12,

144.15, 154.94, 161.20. **m/z** ion M+ calc. 482.0615, found 482.6601, corresponding to the correct, palladium containing, isotope pattern. **Elemental analysis** of $C_{23}H_{25}N_3O_2Cl_2Pd_1$, Expected; C, 49.97, H 4.56, N 7.60. Found; C 50.15, H 4.10, N 7.40.

Preparation of Pd(3IE)Cl$_2$: Palladium Chloride (100 mg, 0.56 mmol) in acetonitrile (50 mL) was added the ligand 3IE (209 mg, 0.56 mmol). The mixture was stirred for twenty four hours, or until all palladium chloride had dissolved, whichever came first. The solvent was removed by rotary evaporation before the product was dried under reduced pressure (244 mg, 79 %). **^{1}H NMR** ($CDCl_3$) 0.74-0.78 (6H, m, CH-C*H*$_3$), 1.84 (4H, qn, J=7.2, C*H*$_2$-CH$_3$) 4.10-4.14 (2H, m, C*H*-CH$_2$) 7.00-7.33 (10H, m, Ar-*H*) 7.56-7.62 (1H, m, py-*H*) 8.10-8.12 (2H, m, py-*H*) 8.34 (2H, s, C*H*=N). **^{13}C{^{1}H} NMR** ($CDCl_3$) 10.89, 30.22, 121.92, 125.79, 127.19, 127.88, 137.24, 143.54, 154.37, 159.24. **m/z** ion M+ calc. 510.0928, found 510.1084, corresponding to the correct, palladium containing, isotope pattern. **Elemental analysis** of $C_{25}H_{27}N_3OCl_2Pd_1$, Expected; C, 54.91, H 4.98, N 7.68. Found C 55.03, H 4.84, N 7.79.

Preparation of Pd(3IC)Cl$_2$: Palladium Chloride (100 mg, 0.56 mmol) in acetonitrile (50 mL) was added the ligand 3IC (200 mg, 0.56 mmol). The mixture was stirred for twenty four hours, or until all palladium chloride had dissolved, whichever came first. The solvent was removed by rotary evaporation before the product was dried under reduced pressure (246 mg, 82 %). **^{1}H NMR** ($CDCl_3$) 0.73-1.84 (22H, m cy-*H*) 1.17 (6H, d, *J*=6.6, CH-C*H*$_3$) 3.06 (2H, qn, *J*=6.5, C*H*-CH$_3$) 7.70 (1H, m, py-*H*) 7.97 (2H, d, *J*=7.9, py-*H*) 8.27 (2H, s, C*H*=N). **^{13}C{^{1}H} NMR** ($CDCl_3$) 19.79, 26.23, 26.39, 26.56, 29.76, 29.93, 43.61, 71.78, 121.99, 136.98, 154.55, 159.54 **m/z** ion M+ calc. 530.8765, found 530.8805, corresponding to the correct, palladium containing, isotope pattern. **Elemental analysis** of $C_{23}H_{35}N_3OCl_2Pd_1$, Expected; C, 52.04, H 6.65, N 7.92. Found C 52.44, H 6.53, N 8.02.

Preparation of Pd(3IN)Cl$_2$: Palladium Chloride (100 mg, 0.56 mmol) in acetonitrile (50 mL) was added the ligand 3IN (249 mg, 0.56 mmol). The mixture was stirred for twenty four hours, or until all palladium chloride had dissolved, whichever came first. The solvent was removed by rotary evaporation before the

product was dried under reduced pressure (245 mg, 70 %). **^{1}H NMR** ($CDCl_3$) 1.63 (6H, d, J=6.6, CH-C*H*$_3$) 4.75 (2H, q, J=6.6, C*H*-CH$_3$) 7.32-7.42 (4H, m, Ar-*H*) 7.48-7.55 (2H, m, Ar-*H*) 7.71-7.80 (9H, m, Ar-*H*) 8.09 (2H, d, J=7.9, py-*H*) 8.47 (2H, s, C*H*=N). **^{13}C{^{1}H} NMR** ($CDCl_3$) 24.42, 69.59, 122.43, 125.07, 125.22, 125.50, 125.97, 127.59, 127.86, 128.17, 132.68, 133.47, 136.98, 141.84, 154.44, 160.35. **m/z** ion M+ calc. 584.4483, found 584.4493, corresponding to the correct, palladium containing, isotope pattern. **Elemental analysis** of $C_{31}H_{27}N_3O_{3.5}Cl_2Pd_1$, Expected; C, 55.17, H 4.03, N 6.23. Found C 55.07, H 4.12, N 5.98.

Preparation of Pd(2IM)Cl$_2$: To the ligand 2IM (119 mg, 0.56 mmol) in acetonitrile (50 mL) was added palladium chloride (100 mg, 0.56 mmol). The mixture was stirred for twenty four hours, or until all palladium chloride had dissolved, whichever came first. The solvent was removed by rotary evaporation before the product was dried under reduced pressure (177 mg, 81 %). **^{1}H NMR** ($CDCl_3$) 1.51 (3H, d, *J*=6.6 CH-C*H3)* 4.54 (1H, q, *J*=6.6 N-C*H*), 7.10-7.32 (5H, m, Ar-*H*) 7.35 (1H, s, Ar-H) 7.60 (1H, m, Ar-*H*) 7.97-8.01 (1H, dt, *J*=7.9, 1.1, Ar-*H*) 8.37 (1H, s C*H*=N) 8.51-8.53 (1H, m, Ar-*H*). **^{13}C{^{1}H} NMR** ($CDCl_3$) 24.34, 69.38, 121.20, 124.45, 125.90, 126.77, 127.04, 128.32, 136.10, 144.35, 149.09, 154.54, 160.20. **m/z** ion M+Na calc. 410.9453, found 410.9453, corresponding to the correct, palladium containing, isotope pattern. **Elemental analysis** of $C_{14}H_{14}N_2OCl_2Pd_1$, Expected; C, 43.38, H 3.64, N 7.23. Found C 44.02, H 3.50, N 7.03.

Preparation of Pd(2IE)Cl$_2$: To the ligand 2IE (127 mg, 0.56 mmol) in acetonitrile (50 mL) was added palladium chloride (100 mg, 0.56 mmol). The mixture was stirred for twenty four hours, or until all palladium chloride had dissolved, whichever came first. The solvent was removed by rotary evaporation before the product was dried under reduced pressure (179 mg, 79 %). **^{1}H NMR** ($CDCl_3$) 0.94 (3H, t, *J*=7.3, CH2-C*H3*) 2.02 (2H, qn, *J*=7.3, CH-C*H2*-CH3) 4.32 (1H, t, *J*=6.8, N-C*H*) 7.25-7.42 (5H,m, Ar-*H)* 7.50-7.51 (1H, m, py-*H*) 7.73-7.80 (1H, m, Ar-*H*) 8.16 (1H, d, *J*=7.5, Ar-*H*) 8.48 (1H, s, N=C*H*) 8.67 (1H, ddd, *J*=4.9, 1.7, 0.9, Ar-*H*). **^{13}C{^{1}H} NMR** ($CDCl_3$) 10.62, 30.85, 76.86, 121.31, 124.50, 126.85, 127.06, 128.29, 136.31, 143.76, 149.16, 154.61, 160.56. **m/z** ion M+Na calc. 424.9606, found 424.9629, corresponding to the correct, palladium

containing, isotope pattern. **Elemental analysis** of $C_{30}H_{32}N_4O_2Cl_2Pd_1$, Expected; C, 54.77, H 4.90, N 8.52. Found C 54.92, H 4.83, N 8.27.

Preparation of Pd(2IC)Cl_2: To the ligand 2IC (122 mg, 0.56 mmol) in acetonitrile (50 mL) was added palladium chloride (100 mg, 0.56 mmol). The mixture was stirred for twenty four hours, or until all palladium chloride had dissolved, whichever came first. The solvent was removed by rotary evaporation before the product was dried under reduced pressure (167 mg, 75 %). **m/z** ion M+Na calc. 414.9936, found 414.9945, corresponding to the correct, palladium containing, isotope pattern. **Elemental analysis** of $C_{28}H_{40}N_4O_1Cl_2Pd_1$, Expected; C, 53.73, H 6.44, N 8.95. Found C 54.29, H 6.23, N 7.96.

Preparation of Pd(2IN)Cl_2: To the ligand 2IN (147 mg, 0.56 mmol) in acetonitrile (50 mL) was added palladium chloride (100 mg, 0.56 mmol). The mixture was stirred for twenty four hours, or until all palladium chloride had dissolved, whichever came first. The solvent was removed by rotary evaporation before the product was dried under reduced pressure (171 mg, 69 %). **^{1}H NMR** ($CDCl_3$) 1.16 (3H, d, *J*=6.6 CH-C*H*$_3$) 4.26 (1H, q, *J*=6.5, C*H*-N) 6.70-6.76 (1H, m, Ar-*H*) 6.87-6.92 (2H, m, Ar-*H*) 7.05 (1H, dd, *J*=8.5, 1.6, Ar-*H*) 7.17 (2H, ddd, *J*=7.7, 5.8, 2.1, Ar-*H*) 7.31 (2H, d, *J*=3.2, Ar-*H*) 7.58 (1H, d, *J*=7.9, Ar-*H*) 7.98 (1H, s, C*H*-N) 8.08 (1H, d, *J*=4.7, Ar-*H*). **^{13}C{^{1}H} NMR** ($CDCl_3$) 24.39, 69.49, 121.36, 124.57, 124.91, 125.13, 125.45, 125.83, 127.47, 127.75, 128.03, 132.56, 133.36, 136.34, 141.85, 149.20, 154.60, 160.51. **m/z** ion M+Na calc. 460.9610, found 460.9622, corresponding to the correct, palladium containing, isotope pattern. **Elemental analysis** of $C_{18}H_{16}N_2OCl_2Pd_1$, Expected; C, 49.4, H 3.68, N 6.40. Found C 49.49, H 3.73, N 6.28.

Preparation of Pd(3AM)Cl_2: Palladium Chloride (100 mg, 0.56 mmol) in acetonitrile (50 mL) was added the ligand 3AM (195 mg, 0.56 mmol). The mixture was stirred for twenty four hours, or until all palladium chloride had dissolved, whichever came first. The solvent was removed by rotary evaporation before the product was dried under reduced pressure (218 mg, 74 %). **^{1}H NMR** ($CDCl_3$) 1.25-1.31 (6H, m, CH-C*H*$_3$) 2.21-2.24 (2H, m, CH_2-N*H*) 3.58 (4H, s, C*H*$_2$-NH) 3.57-3.61 (2H, m, NH-C*H*) 6.90-6.92 (1H, m, Ar-*H*) 7.10-7.18 (2H, m, Ar-*H*) 7.22-7.33 (8H, m, Ar-*H*) 7.35-7.39 (1H, m, py-*H*). **^{13}C{^{1}H} NMR** ($CDCl_3$)

24.32, 51.44 57.89, 121.85, 127.39, 127.89, 128.56, 136.54, 144.26, 159.09. **m/z** ion M+ calc. 486.0928, found 486.0927, corresponding to the correct, palladium containing, isotope pattern. **Elemental analysis** of $C_{23}H_{27}N_3OCl_2Pd_1$, Expected; C, 52.84, H 5.21, N 8.04. Found C 52.59, H 5.18, N 8.00.

Preparation of Pd(3AE)Cl$_2$: Palladium Chloride (100 mg, 0.56 mmol) in acetonitrile (50 mL) was added the ligand 3AE (211 mg, 0.56 mmol). The mixture was stirred for twenty four hours, or until all palladium chloride had dissolved, whichever came first. The solvent was removed by rotary evaporation before the product was dried under reduced pressure (227 mg, 73 %). **^{1}H NMR** ($CDCl_3$) 0.69 (6H, m, CH-C*H*$_3$), 1.53-1.75 (4H, m, C*H*$_2$-CH$_3$) 2.19-2.21 (2H, m, CH$_2$-N*H*) 3.20-3.59 (6H, m) 6.88-6.92 (2H, m, py-*H*) 6.95-7.23 (10H, m, Ar-*H*) 7.22 (1H, t, *J*=7.5, py-*H*). **^{13}C{^{1}H} NMR** ($CDCl_3$) 10.43, 25.11, 26.23, 30.93, 52.58, 63.44, 121.26, 127.51, 128.29, 128.56, 132.33, 133.54, 144.77, 158.58, 161.12. **m/z** ion M+ calc. 514.1241, found 514.1249, corresponding to the correct, palladium containing, isotope pattern. **Elemental analysis** of $C_{25}H_{31}N_3OCl_2Pd_1$, Expected; C, 54.51, H 5.67, N 7.63. Found C 54.32, H 5.57, N 7.20.

Preparation of Pd(3AC)Cl$_2$: Palladium Chloride (100 mg, 0.56 mmol) in acetonitrile (50 mL) was added the ligand 3AC (202 mg, 0.56 mmol). The mixture was stirred for twenty four hours, or until all palladium chloride had dissolved, whichever came first. The solvent was removed by rotary evaporation before the product was dried under reduced pressure (217 mg, 72 %). **^{1}H NMR** ($CDCl_3$) 0.81-1.41 (10H, m, cy-*H*) 0.86-0.88 (3H, m, CH-C*H*$_3$) 0.97 (3H, m, CH-C*H*$_3$) 1.48-1.75 (12H, m, cy-*H*) 1.88-1.92 (2H, m, CH$_2$-N*H*) 2.36-2.39 (2H, m, C*H*-CH$_3$) 3.34 (4H, m, C*H*$_2$-NH) 6.98-7.12 (2H, m, py-*H*) 7.40-7.50 (1H, m, py-*H*). **^{13}C{^{1}H} NMR** ($CDCl_3$) 15.29, 16.12, 25.42, 25.84, 26.25, 26.35, 26.84, 27.66, 29.48, 41.88, 53.13, 57.09, 118.70, 119.58, 137.50, 159.55, 160.18. **m/z** ion M+ calc. 498.1867, found 498.1878, corresponding to the correct, palladium containing, isotope pattern. **Elemental analysis** of $C_{23}H_{39}N_3OCl_2Pd_1$, Expected; C, 51.64, H 7.35, N 7.86. Found C 51.70, H 7.34, N 8.10.

Preparation of Pd(3AN)Cl$_2$: Palladium Chloride (100 mg, 0.56 mmol) in acetonitrile (50 mL) was added the ligand 3AN (252 mg, 0.56 mmol). The mixture was stirred for twenty four hours, or until all palladium chloride had

dissolved, whichever came first. The solvent was removed by rotary evaporation before the product was dried under reduced pressure (229 mg, 65 %). **^{1}H NMR** ($CDCl_3$) 1.40-1.42 (6H, m, CH-C*H*$_3$) 2.32-2.38 (2H, m, CH_2-N*H*) 3.59-3.62 (4H, m, C*H*$_2$-NH) 3.94 (4H, m) 6.93-6.96 (2H, m, Ar-*H*) 7.38-7.47 (7H, m, Ar-*H*) 7.55-7.60 (4H, m, Ar-*H*) 7.71-7.74 (2H, m, Ar-*H*) 8.00-8.10 (2H, m Ar-*H*). **^{13}C{^{1}H} NMR** ($CDCl_3$) 24.13, 25.69, 52.51, 57.68, 118.86, 119.54, 124.13, 124.79, 125.24, 125.57, 126.30, 126.85, 127.57, 133.55, 136.23, 136.63, 145.23, 141.65, 160.75, 161.87. **m/z** ion M+ calc. 586.1227, found 586.1241 corresponding to the correct, palladium containing, isotope pattern. **Elemental analysis** of $C_{31}H_{31}N_3OCl_2Pd_1$, Expected; C, 59.77, H 5.02, N 6.75. Found C 59.72, H 4.86, N 6.64.

Preparation of Pd(2AM)Cl$_2$: To the ligand 2AM (120 mg, 0.56 mmol) in acetonitrile (50 mL) was added palladium chloride (100 mg, 0.56 mmol). The mixture was stirred for twenty four hours, or until all palladium chloride had dissolved, whichever came first. The solvent was removed by rotary evaporation before the product was dried under reduced pressure (178 mg, 81 %). **^{1}H NMR** ($CDCl_3$) 1.12 (3H, d, *J*=6.4, CH-CH_3) 2.32 (1H, s, CH-N*H*) 3.58 (2H, s, C*H*-NH) 3.60-3.66 (2H, m, C*H*$_2$-NH) 6.94 (1H, d, *J*=6.8, py-*H*) 6.97-7.24 (6H, m, Ar-*H*) 7.35-7.39 (1H, m, py-*H*) 8.31-8.38 (1H, m, py-*H*). **^{13}C{^{1}H} NMR** ($CDCl_3$) 22.25, 51.12, 58.89, 121.73, 122.39, 126.07, 127.84, 135.82, 145.56, 147.32, 106.24. **m/z** ion M+Na calc. 410.9623, found 410.9630, corresponding to the correct, palladium containing, isotope pattern. **Elemental analysis** of $C_{14}H_{16}N_2O_4Cl_2Pd_1$, Expected; C, 37.07, H 3.56, N 6.18. Found C 36.72, H 3.38, N 6.67.

Preparation of Pd(2AE)Cl$_2$: To the ligand 2AE (128 mg, 0.56 mmol) in acetonitrile (50 mL) was added palladium chloride (100 mg, 0.56 mmol). The mixture was stirred for twenty four hours, or until all palladium chloride had dissolved, whichever came first. The solvent was removed by rotary evaporation before the product was dried under reduced pressure (182 mg, 80 %). **^{1}H NMR** ($CDCl_3$) 0.64 (3H, t, *J*=7.6 CH_2-C*H*$_3$) 1.55-1.80 (2H, m, C*H*$_2$-CH_3) 2.11 (1H, s, CH-N*H*) 3.36-3.40 (1H, m) 2.89-3.45 (4H, m, C*H*$_2$-NH) 6.94-7.00 (1H, m py-*H*) 7.03-7.11 (1H, m) 7.08-7.21 (5H, m, Ar-*H*) 7.40-7.45 (1H, m) 8.42-8.46 (1H, m). **^{13}C{^{1}H} NMR** ($CDCl_3$) 9.62, 11.17, 29.85, 53.79, 65.12, 121.56, 121.89, 122.52, 126.65, 127.37, 127.15, 127.23, 128.86, 129.23, 133.53, 150.28, 160.18. **m/z** ion

M+Na calc. 424.9780, found 424.9788, corresponding to the correct, palladium containing, isotope pattern. **Elemental analysis** of $C_{15}H_{18}N_2OCl_2Pd_1$, Expected; C, 44.63, H 4.49, N 6.94. Found C 44.44, H 4.38, N 6.89.

Preparation of Pd(2AC)Cl$_2$: To the ligand 2AC (124 mg, 0.56 mmol) in acetonitrile (50 mL) was added palladium chloride (100 mg, 0.56 mmol). The mixture was stirred for twenty four hours, or until all palladium chloride had dissolved, whichever came first. The solvent was removed by rotary evaporation before the product was dried under reduced pressure (177 mg, 79 %). **^{1}H NMR** ($CDCl_3$) 0.91 (3H, d, J=6.4, CH-C*H*$_3$) 0.80-1.36 (5H, m cy-*H*) 1.48-1.72 (6H, m, cy-*H*) 1.80-1.83 (1H, m, CH-N*H*) 2.35-2.43 (1H, m, C*H*-CH$_3$) 3.50-3.75 (4H, m) 6.99-7.28 (2H, m py-*H*) 7.44-7.47 (1H, m) 8.39-8.43 (1H, m, Ar-*H*). **^{13}C{^{1}H} NMR** ($CDCl_3$) 15.32, 25.96, 26.12, 26.48, 27.54, 28.53, 29.51, 42.60, 53.51, 56.55, 121.35, 121.84, 122.25, 136.02, 149.06, 160.53. **m/z** ion M+Na calc. 417.0093, found 417.0010, corresponding to the correct, palladium containing, isotope pattern. **Elemental analysis** of $C_{14}H_{22}N_2OCl_2Pd_1$, Expected; C, 42.50, H 5.60, N 7.08. Found C 42.99, H 5.26, N 7.10.

Preparation of Pd(2AN)Cl$_2$: To the ligand 2AN (148 mg, 0.56 mmol) in acetonitrile (50 mL) was added palladium chloride (100 mg, 0.56 mmol). The mixture was stirred for twenty four hours, or until all palladium chloride had dissolved, whichever came first. The solvent was removed by rotary evaporation before the product was dried under reduced pressure (174 mg, 70 %). **^{1}H NMR** ($CDCl_3$) 1.58 (3H, d, J=6.8, CH-C*H*$_3$) 2.30-2.35 (1H, m, CH$_2$-N*H*) 3.66 (2H, s NH-C*H*) 3.9-4.2 (1H, m, C*H*$_2$-NH) 7.03-7.36 (4H, m, Ar-*H*) 7.41-7.49 (3H, m, Ar-*H*) 7.59-7.68 (1H, m, Ar-*H*) 7.83-8.63 (4H, m, Ar-*H*). **^{13}C{^{1}H} NMR** ($CDCl_3$) 24.05, 53.48, 56.33, 121.56, 122.41, 125.11, 125.48, 125.80, 125.99, 126.28, 127.50, 136.22, 142.04, 148.12, 160.30 **m/z** ion M+Na calc. 460.9780, found 460.9787, corresponding to the correct, palladium containing, isotope pattern. **Elemental analysis** of $C_{18}H_{18}N_2OCl_2Pd_1$, Expected; C, 49.17, H 4.13, N 6.37. Found C 49.03, H 4.10, N 6.37.

Preparation of Rh(2IM)(COD)(OTf): Cyclooctadiene rhodium chloride dimer, $Rh_2COD_2Cl_2$, (100 mg, 0.20 mmol) was placed in a dry Schlenk and was repeatedly degassed and backfilled with nitrogen. This was dissolved in dry THF

(10 mL), before silver triflate was added (104 mg, 0.41 mmol). A second dry Schlenk was prepared, containing the ligand **2IM** (91 mg, 0.43 mmol) by repeated degassing and backfilling with Nitrogen. After the cyclooctadiene rhodium chloride dimer and silver triflate reaction mixture had been stirred for 30 mins the solution was cannula filtered into the Schlenk containing the ligand and this was stirred for a further hour. Hexane was added and decanted off the settled precipitate. The resulting complex was dried under reduced pressure, affording an orange solid (294 mg, 62 %). **^{1}H NMR** 1.48 (3H, d, *J*=6.6 CH-C*H*$_3$), 2.29-2.31 (8H, br m) 4.49-4.51 (1H, m N-C*H*), 7.08-7.26 (5H, m, Ar-*H*) 7.41 (1H, s, Ar-H) 7.59 (1H, m, Ar-*H*) 7.98-8.10 (1H, m, Ar-*H*) 8.38 (1H, s C*H*=N) 8.45-8.59 (1H, m, Ar-*H*). **^{13}C{^{1}H} NMR** ($CDCl_3$) 23.45, 29.83, 122.34, 124.51, 126.06, 126.97, 127.45, 128.36, 129.54, 135.87, 145.46, 150.27, 153.74, 160.35. **Elemental Analysis** of $C_{22}H_{28}N_2Cl_1Rh_1$, Expected; C 55.7, H 5.9, N 5.9. Found; C 55.6, H 5.8, N 5.9.

Preparation of Rh(2IE)(COD)(OTf): Cyclooctadiene rhodium chloride dimer, $Rh_2COD_2Cl_2$, (100 mg, 0.20 mmol) was placed in a dry Schlenk and was repeatedly degassed and backfilled with nitrogen. This was dissolved in dry THF (10 mL), before silver triflate was added (104 mg, 0.41 mmol). A second dry Schlenk was prepared, containing the ligand **2IE** (97 mg, 0.43 mmol) by repeated degassing and backfilling with Nitrogen. After the cyclooctadiene rhodium chloride dimer and silver triflate reaction mixture had been stirred for 30 mins the solution was cannula filtered into the Schlenk containing the ligand and this was stirred for a further hour. Hexane was added and decanted off the settled precipitate. The resulting complex was dried under reduced pressure, affording an orange solid (296 mg, 63 %). **^{1}H NMR** ($CDCl_3$) 0.91 (3H, t, *J*=7.3, CH2-C*H3*) 2.00-2.25 (10H, m) 4.32 (1H, m, N-C*H*) 4.56-4.58 (4H, m) 7.31-7.42 (5H, m, Ar-*H)* 7.49-7.52 (1H, m, py-*H*) 7.70-7.78 (1H, m, Ar-*H*) 7.99 (1H, d, *J*=7.5, Ar-*H*) 8.22 (1H, s, N=C*H*) 8.67 (1H, m, Ar-*H*). **^{13}C{^{1}H} NMR** ($CDCl_3$) 10.12, 29.56, 30.85, 75.99, 120.86, 123.73, 127.63, 128.41, 135.89, 143.24, 148.87, 155.16, 160.54 **Elemental Analysis** of $C_{23}H_{28}N_2Cl_1Rh_1$, Expected; C 58.7, H 6.1, N 6.. Found; C 58.5, H 6.1, N 6.1.

Preparation of Rh(2IC)(COD)(OTf): Cyclooctadiene rhodium chloride dimer, $Rh_2COD_2Cl_2$, (100 mg, 0.20 mmol) was placed in a dry Schlenk and was

repeatedly degassed and backfilled with nitrogen. This was dissolved in dry THF (10 mL), before silver triflate was added (104 mg, 0.41 mmol). A second dry Schlenk was prepared, containing the ligand **2IC** (93 mg, 0.43 mmol) by repeated degassing and backfilling with Nitrogen. After the cyclooctadiene rhodium chloride dimer and silver triflate reaction mixture had been stirred for 30 mins the solution was cannula filtered into the Schlenk containing the ligand and this was stirred for a further hour. Hexane was added and decanted off the settled precipitate. The resulting complex was dried under reduced pressure, affording an orange solid (319 mg, 69 %). **^{1}H NMR** ($CDCl_3$) 0.68-1.09 (5H, m cy-*H*) 1.25 (3H, d, *J*=5.0 CH-C*H*$_3$) 1.30-1.75 (6H, m, cy-*H*) 2.98-3.05 (9H, m), 3.90-3.95 (4H, m) 7.18-7.32 (1H, m, py-*H*) 7.45 (1H, d, *J*=7.7, py-*H*) 7.90-7.92 (1H, m, Ar-*H*) 8.26 (1H, s, C*H*=N) 8.68-8.75 (1H, m, py-*H*). **^{13}C{^{1}H} NMR** ($CDCl_3$) 18.55, 19.12, 21.68, 23.99 24.91, 25.86, 30.11, 44.84, 120.12, 121.55, 122.48, 123.47, 135.78, 151.23, 155.07, 160.43. **Elemental Analysis** of $C_{22}H_{32}N_2Cl_1Rh_1$, Expected; C 57.1, H 7.1, N 6.1. Found; C 57.9, H 6.8, N 6.3.

Preparation of Rh(2IN)(COD)(OTf): Cyclooctadiene rhodium chloride dimer, $Rh_2COD_2Cl_2$, (100 mg, 0.20 mmol) was placed in a dry Schlenk and was repeatedly degassed and backfilled with nitrogen. This was dissolved in dry THF (10 mL), before silver triflate was added (104 mg, 0.41 mmol). A second dry Schlenk was prepared, containing the ligand **2IN** (112 mg, 0.43 mmol) by repeated degassing and backfilling with Nitrogen. After the cyclooctadiene rhodium chloride dimer and silver triflate reaction mixture had been stirred for 30 mins the solution was cannula filtered into the Schlenk containing the ligand and this was stirred for a further hour. Hexane was added and decanted off the settled precipitate. The resulting complex was dried under reduced pressure, affording an orange solid (277 mg, 51 %). **^{1}H NMR** ($CDCl_3$) 1.18 (3H, d, *J*=6.6 CH-C*H*$_3$) 2.31-2.33 (8H, m) 4.05-4.12 (1H, m, C*H*-N) 4.49-4.56 (4H, m) 6.71-6.92 (3H, m, Ar-*H*) 7.12 (1H, m, Ar-*H*) 7.17 (2H, m, Ar-*H*) 7.16 (2H, d, *J*=3.2, Ar-*H*) 7.45 (1H, m, Ar-*H*) 7.97 (1H, s, C*H*-N) 8.08 (1H, s, Ar-*H*). **^{13}C{^{1}H} NMR** ($CDCl_3$) 23.39, 24.69, 24.88, 68.49, 120.36, 121.11, 123.75, 125.34, 125.39, 125.46, 126.40, 127.77, 127.89, 128.56, 131.50, 133.21, 137.74, 140.58, 150.49, 155.66, 161.41.**Elemental Analysis** of $C_{26}H_{32}N_2Cl_1Rh_1$, Expected; C 57.6, H 5.9, N 5.2. Found; C 57.1, H 5.9, N 5.2.

Preparation of Rh(2AM)(COD)(OTf): Cyclooctadiene rhodium chloride dimer, $Rh_2COD_2Cl_2$, (100 mg, 0.20 mmol) was placed in a dry Schlenk and was repeatedly degassed and backfilled with nitrogen. This was dissolved in dry THF (10 mL), before silver triflate was added (104 mg, 0.41 mmol). A second dry Schlenk was prepared, containing the ligand **2AM** (92 mg, 0.43 mmol) by repeated degassing and backfilling with Nitrogen. After the cyclooctadiene rhodium chloride dimer and silver triflate reaction mixture had been stirred for 30 mins the solution was cannula filtered into the Schlenk containing the ligand and this was stirred for a further hour. Hexane was added and decanted off the settled precipitate. The resulting complex was dried under reduced pressure, affording an orange solid (342 mg, 72 %). **^{1}H NMR** ($CDCl_3$) 1.20 (3H, d, *J*=6.4, CH-CH_3) 2.25-2.30 (9H, m) 3.61 (2H, s, C*H*-NH) 3.67 (2H, m, CH_2-NH) 5.11-5.23 (4H, m) 6.92 (1H, m) 7.10-7.12 (1H, m) 7.15-7.38 (6H, m, Ar-*H*) 8.26-8.31 (1H, m, py-*H*). **^{13}C{^{1}H} NMR** ($CDCl_3$) 10.25, 21.36, 22.84, 24.00, 51.64, 56.65, 71.23, 120.22, 120.54, 121.87, 121.99, 125.25, 126.35, 126.21, 127.85, 136.23, 144.74, 148.41, 160.23. **Elemental Analysis** of $C_{22}H_{28}N_2Cl_1Rh_1$, Expected; C 55.7, H 5.90, N 5.90. Found; C 56.3, H 5.8, N 6.0.

Preparation of Rh(2AE)(COD)(OTf): Cyclooctadiene rhodium chloride dimer, $Rh_2COD_2Cl_2$, (100 mg, 0.20 mmol) was placed in a dry Schlenk and was repeatedly degassed and backfilled with nitrogen. This was dissolved in dry THF (10 mL), before silver triflate was added (104 mg, 0.41 mmol). A second dry Schlenk was prepared, containing the ligand **2AE** (98 mg, 0.43 mmol) by repeated degassing and backfilling with Nitrogen. After the cyclooctadiene rhodium chloride dimer and silver triflate reaction mixture had been stirred for 30 mins the solution was cannula filtered into the Schlenk containing the ligand and this was stirred for a further hour. Hexane was added and decanted off the settled precipitate. The resulting complex was dried under reduced pressure, affording an orange solid (307 mg, 65 %). **^{1}H NMR** ($CDCl_3$) 0.69-0.72 (3H, m, CH_2-CH_3) 1.55-1.67 (2H, m, CH_2-CH_3) 2.05 (1H, br, CH-N*H*) 2.25-2.31 (8H, m) 3.40 (1H, t, J=6.8, C*H*-CH_2) 3.63 (ABq, 4H, $\Delta\delta_{AB}$=0.06, J_{AB}=14.0 Hz, CH_2-NH) 6.98-7.02 (1H, m py-*H*) 7.06 (1H, dd, J=7.5, py-*H*) 7.10-7.25 (5H, m, Ar-*H*) 7.46 (1H, td, J=7.5, 1.9, py-*H*) 8.43-8.45 (1H, m py-*H*). **^{13}C{^{1}H} NMR** ($CDCl_3$) 10.62, 30.94, 52.85, 64.61, 121.61, 122.25, 126.80, 127.37, 128.05, 128.12, 128.86, 136.08,

134.68, 149.08, 159.80.**Elemental Analysis** of $C_{23}H_{30}N_2Cl_1Rh_1$, Expected; C 58.51, H 6.42, N 5.93. Found; C 58.6, H 6.3, N 5.9.

Preparation of Rh(2AC)(COD)(OTf): Cyclooctadiene rhodium chloride dimer, $Rh_2COD_2Cl_2$, (100 mg, 0.20 mmol) was placed in a dry Schlenk and was repeatedly degassed and backfilled with nitrogen. This was dissolved in dry THF (10 mL), before silver triflate was added (104 mg, 0.41 mmol). A second dry Schlenk was prepared, containing the ligand **2AC** (94 mg, 0.43 mmol) by repeated degassing and backfilling with Nitrogen. After the cyclooctadiene rhodium chloride dimer and silver triflate reaction mixture had been stirred for 30 mins the solution was cannula filtered into the Schlenk containing the ligand and this was stirred for a further hour. Hexane was added and decanted off the settled precipitate. The resulting complex was dried under reduced pressure, affording an orange solid (318 mg, 66 %). **^{1}H NMR** ($CDCl_3$) 0.92-1.32 (8H, m) 1.48-1.70 (6H, m, cy-*H*) 1.85 (1H, br s, CH-N*H*) 2.02-2.52 (9H, m) 4.89-4.91 (4H, m) 7.02-7.22 (2H, m, py-*H*) 7.38 (1H, m) 8.38 (1H, s, Ar-*H*). **^{13}C{^{1}H} NMR** ($CDCl_3$) 16.32, 20.15, 25.86, 26.13, 27.55, 29.74, 43.65, 51.11, 120.36, 121.25, 122.17, 135.06, 149.71, 160.26. **Elemental Analysis** of $C_{22}H_{36}N_2Cl_1Rh_1$, Expected; C 54.8, H 7.5, N 5.8. Found; C 54.2, H 7.5, N 5.7.

Preparation of Rh(2AN)(COD)(OTf): Cyclooctadiene rhodium chloride dimer, $Rh_2COD_2Cl_2$, (100 mg, 0.20 mmol) was placed in a dry Schlenk and was repeatedly degassed and backfilled with nitrogen. This was dissolved in dry THF (10 mL), before silver triflate was added (104 mg, 0.41 mmol). A second dry Schlenk was prepared, containing the ligand **2AN** (113 mg, 0.43 mmol) by repeated degassing and backfilling with Nitrogen. After the cyclooctadiene rhodium chloride dimer and silver triflate reaction mixture had been stirred for 30 mins the solution was cannula filtered into the Schlenk containing the ligand and this was stirred for a further hour. Hexane was added and decanted off the settled precipitate. The resulting complex was dried under reduced pressure, affording an orange solid (290 mg, 55 %). **^{1}H NMR** ($CDCl_3$) 1.50-1.53 (3H, m, CH-CH_3) 2.14-2.51 (8H, m) 3.74 (2H, s NH-C*H*) 4.55-5.12 (5H, m) 6.83-7.21 (4H, m, Ar-*H*) 7.55-7.57 (2H, m, Ar-*H*) 7.59-7.64 (2H, m, Ar-*H*) 7.82-3.87 (3H, m, Ar-*H*) 8.62 (1H, m, Ar-*H*). **^{13}C{^{1}H} NMR** ($CDCl_3$) 21.45 24.25, 26.35, 51.48, 120.36, 120.55, 121.25, 121.67, 123.95, 125.10, 124.74, 125.28, 129.15, 134.68, 143.27,

149.26, 160.11. **Elemental Analysis** of $C_{26}H_{32}N_2Cl_1Rh_1$, Expected; C 59.3, H 6.1, N 5.3. Found; C 60.2, H 6.2, N 5.3.

Preparation of S-Tether: Silica, 60 Å, 35-70 micron, (20 g) was dried at 100°C under reduced pressure for twenty four hours. To this, 3-aminopropyltrimethoxysilane (3.5 mL, 20.0 mmol) in ethanol (300 mL) was added under nitrogen, and the mixture stirred at room temperature for twenty four hours. The functionalised silica was then filtered and washed with ethanol (3 x 50 mL) and diethyl ether (50 mL). The product was then dried under reduced pressure at 100 °C overnight. **$^{13}C\{^1H\}$ CP/MAS NMR** resonances at 9, 25, 43, 49. **Elemental analysis** Found; C 4.48, H 1.37, N, 1.22.

Preparation of S-Backbone: To **S-Tether** (5 g) was added 2,6-pyridinedicarboxaldehyde (0.70 g, 5.2 mmol) in methanol (75 mL) with stirring for twenty four hours. The resulting mixture was filtered and washed with methanol (3 x 10 mL) and diethyl ether (10 mL). The product was then dried under reduced pressure at 100 °C overnight. **$^{13}C\{^1H\}$ CP/MAS NMR** resonances at 9, 24, 49, 62, 120-140, 160, 200. **Elemental Analysis** Found; C 9.05, H 1.35, N 1.24.

Preparation of S-Me: To **S-Backbone** (1 g) was added *(R)*-(+)-α-Methylbenzylamine (0.13 g, 1.1 mmol) in methanol (15 mL) with stirring for twenty four hours. The resulting mixture was filtered and washed with methanol (3 x 10 mL) and diethyl ether (10 mL). The product was then dried under reduced pressure at 100 °C overnight. **$^{13}C\{^1H\}$ CP/MAS NMR** resonances at 9, 24, 49, 62, 122, 128, 136, 154, 162. **Elemental Analysis** Found C, 8.51, H 1.31, N, 1.18.

Preparation of S-Et: To **S-Backbone** (1 g) was added *(R)*-(+)-α-Ethylbenzylamine (0.15 g, 1.1 mmol) in methanol (15 mL) with stirring for twenty four hours. The resulting mixture was filtered and washed with methanol (3 x 10 mL) and diethyl ether (10 mL). The product was then dried under reduced pressure at 100 °C overnight. **$^{13}C\{^1H\}$ CP/MAS NMR** resonances at 9, 24, 49, 62, 120, 130, 136, 154, 161. **Elemental Analysis** Found; C 8.59, H 1.31, N, 1.19.

Preparation of S-Cy: To **S-Backbone** (1 g) was added *(R)*-(−)-α-Methylcyclohexanemethylamine (0.13 g, 1.1 mmol) in methanol (15 mL) with

stirring for twenty four hours. The resulting mixture was filtered and washed with methanol (3 x 10 mL) and diethyl ether (10 mL). The product was then dried under reduced pressure at 100 °C overnight. **$^{13}C\{^{1}H\}$ CP/MAS NMR** resonances at 9, 24, 49, 62, 120, 136, 154, 161. **Elemental Analysis** Found; C 8.57, H 1.40, N 1.17.

Preparation of S-MeCu: To **S-Me** (1 g) was added copper triflate (0.40 g, 1.1 mmol) in methanol (20 mL) with stirring for twenty four hours. The resulting mixture was filtered and washed with methanol (3 x 10 mL) and diethyl ether (10 mL). The product was then dried under reduced pressure at 100 °C overnight. **Elemental Analysis** Found; C 6.09, H 1.83, N 0.91.

Preparation of S-EtCu: To **S-Et** (1 g) was added copper triflate (0.40 g, 1.1 mmol) in methanol (20 mL) with stirring for twenty four hours. The resulting mixture was filtered and washed with methanol (3 x 10 mL) and diethyl ether (10 mL). The product was then dried under reduced pressure at 100 °C overnight. **Elemental Analysis** Found; C 6.19, H 1.80, N 0.91.

Preparation of S-EtCu: To **S-Cy** (1 g) was added copper triflate (0.40 g, 1.1 mmol) in methanol (20 mL) with stirring for twenty four hours. The resulting mixture was filtered and washed with methanol (3 x 10 mL) and diethyl ether (10 mL). The product was then dried under reduced pressure at 100 °C overnight. **Elemental Analysis** Found; C 6.18, H 1.89, N 0.90.

Preparation of S-MePd: To **S-Me** (0.55 g) was added palladium chloride (0.10 g, 0.56 mmol) in acetonitrile (50 mL) with stirring for twenty four hours. The resulting mixture was filtered and washed with acetonitrile (3 x 10 mL) and diethyl ether (10 mL). The product was then dried under reduced pressure at 100 °C overnight. **$^{13}C\{^{1}H\}$ CP/MAS NMR** resonances at 9, 23, 49, 62, 120, 130-140, 155, 162. **Elemental Analysis** Found; C 5.72, H 1.01, N 0.81.

Preparation of S-EtPd: To **S-Et** (0.55 g) was added palladium chloride (0.10 g, 0.56 mmol) in acetonitrile (50 mL) with stirring for twenty four hours. The resulting mixture was filtered and washed with acetonitrile (3 x 10 mL) and diethyl ether (10 mL). The product was then dried under reduced pressure at 100

°C overnight. **$^{13}C\{^{1}H\}$ CP/MAS NMR** resonances at 9, 25, 48, 62, 123, 130-136, 154, 161. **Elemental Analysis** Found; C 5.71, H 1.13, N 0.86.

Preparation of S-MeRh: Cyclooctadiene rhodium chloride dimer (100 mg, 0.20 mmol) was added to a dry Schlenk which was repeatedly evacuated and backfilled with nitrogen. To this was added dry THF (50 mL) mixture the dimer dissolved with stirring before silver triflate (104 mg, 0.43 mmol) was added. The reaction mixture was left for 30 mins. In a second schlenk **S-Me** (0.40 g) was added and repeatedly degassed and backfilled with nitrogen. The solution from the cyclooctadiene rhodium chloride dimer and silver triflate was cannula filtered into the schlenk containing **S-Me** and was left to stir for twenty four hours. The product was then filtered and washed repeatedly with dry THF (3 x 15 mL) before dried under reduced pressure at 100 °C overnight. **$^{13}C\{^{1}H\}$ CP/MAS NMR** resonances at 9, 20, 24, 28, 42, 49, 64, 120, 130-140, 150, 160. **Elemental Analysis** Found; C 7.72, H 1.48, N 1.00.

Preparation of S-MeRh: Cyclooctadiene rhodium chloride dimer (100 mg, 0.20 mmol) was added to a dry Schlenk which was repeatedly evacuated and backfilled with nitrogen. To this was added dry THF (50 mL) mixture the dimer dissolved with stirring before silver triflate (104 mg, 0.43 mmol) was added. The reaction mixture was left for 30 mins. In a second schlenk **S-Et** (0.40 g) was added and repeatedly degassed and backfilled with nitrogen. The solution from the cyclooctadiene rhodium chloride dimer and silver triflate was cannula filtered into the schlenk containing **S-Et** and was left to stir for twenty four hours. The product was then filtered and washed repeatedly with dry THF (3 x 15 mL) before dried under reduced pressure at 100 °C overnight. **$^{13}C\{^{1}H\}$ CP/MAS NMR** resonances at 9, 20, 24 - 28, 42, 49, 64, 120, 130-140, 150, 160. **Elemental Analysis** Found; C 7.79, H 1.41, N 1.21.

4.2.2. Catalytic Screening

Catalytic performance was evaluated *via* conversion and enantiomeric excess. Conversion was obtained from the ^{1}H NMR spectroscopy of the crude reaction mixture, whereby a percentage was obtained, typically, by:

$$Conversion\ (\%) = \frac{Product\ Integral}{(Product\ Integral)+(Starting\ Material\ Integral)} \times 100$$

Enantiomeric excess of a catalytic reaction is obtained from the chiral HPLC of a crude reaction mixture. Samples were prepared by dissolving 1 mg of material in 1 ml of HPLC grade isopropanol. HPLC analysis was performed on an Agilent Technologies 1120 Compact LC instrument, using an OD-H or OD-J column as appropriate. All solvents used were of HPLC grade. Integration of each enantiomer peak from the GPC trace application of the following equation affords ee (%).

$$ee\ (\%) = \frac{(Integral\ R) - (Integral\ S)}{(Integral\ R) + (Integral\ S)} \times 100$$

Asymmetric Nitroaldol Reaction

Standard Reaction Conditions: The catalyst (0.05 mmol) was placed in a screw top ampoule and dissolved in ethanol (10 mL). To this was added, benzaldehyde (0.10 mL, 1.0 mmol), nitromethane (0.55 mL, 10 mmol) and triethylamine (17 µl, 0.13 mmol). The ampoule was sealed and stirred for 6 hours. The solvent was removed by rotary evaporation and where needed, redissolved in ethanol and filtered through a short plug of silica. The solvent removed by rotary evaporation.

Preparation of Catalysts *in situ*: For the cases where the catalyst was prepared *in situ*, the given metal salt (0.05 mmol) was placed in a screw top ampoule and dissolved in ethanol (10 mL). The required ligand (0.05 mmol) was added and stirred for 30 mins. The standard reaction conditions as above were then followed.

Base Variation Reaction Conditions: For the cases where the base was not triethylamine, the standard reaction conditions were followed and the alternative base used in the same ratio. This is also the case for the investigation of the basic character of the ligand. Diisopropylamine (17 µl, 0.13 mmol), 1-methylpyrrolidine (14 µl, 0.13 mmol), or ligand (0.13 mmol).

Temperature Variation Reaction Conditions: For the investigation of reduced temperature upon the catalysis of the asymmetric nitroaldol reaction, the standard reaction conditions were followed, however the ampoules were suspended in a water-isopropanol bath kept at 0 °C.

Asymmetric Hydrogenation Reaction

Direct Hydrogenation, 5 bar: The catalyst (0.01 mmol) and dimethyl itaconate (0.16 g, 1 mmol) were dissolved in methanol (10 mL) in a glass tube. This was placed into the Parr reactor and sealed. The hydrogen gas flow was opened and the closed reactor pressurised slightly. The flow was stopped and the reaction vessel vented, a process which was repeated three times. Finally the hydrogen gas flow was opened and the closed reaction vessel taken to 5 bar. The gas flow was closed and the hydrogen cylinder removed. The reaction was then stirred at room temperature for the desired length of time. Following this, the reactor was vented, dissembled, and the solvent removed from the reaction mixture by rotary evaporation.

Direct Hydrogenation, atmospheric pressure: The catalyst (0.01 mmol) and dimethyl itaconate (0.16 g, 1 mmol) were dissolved in methanol (10 mL) in round bottom flask, capped by a suba-seal. A latex balloon was filled with hydrogen gas and fitted to a syringe and needle. The reaction vessel was purged of air *via* the flow of hydrogen gas, before the flask was sealed. The reaction was stirred at room temperature for the desired time. Following this, the flask was vented and the solvent removed from the reaction mixture by rotary evaporation.

Transfer Hydrogenation: The catalyst (0.01 mmol) and acetophenone were dissolved in a solution of potassium hydroxide in anhydrous isopropanol (15 ml, 4.29×10^{-5} mol dm^{-3}) in a screw top ampoule. The reaction was sealed and stirred at room temperature for the appropriate length of time. Following the reaction, the solvent was removed by rotary evaporation.

4.3. Chapter 3

4.3.1. Synthesis of starting materials

Preparation of 2,6-Diformyl-p-cresol: To a suspension of 2,6-bis(hydroxymethyl)-*p*-cresol (16.8 g, 0.1 mol) in chloroform (200 mL) was added slowly with stirring activated manganese dioxide, (86.9 g, 1.0 mol, 10 equiv). The mixture was heated to reflux for 2 hours after which the MnO_2 was removed by vacuum filtration with a celite plug. The residue was washed with chloroform, and the solvent removed by rotary evaporation, yielding the dark yellow/green 2,6-diformyl-p-cresol, (12.6 g, 77 %). **^{1}H NMR** ($CDCl_3$) 2.38 (s, 3 H, -CH_3) 7.76 (s, 2 H, Ar-H) 10.20 (s, 2 H, -CHO) 11.44 (br. s., 1 H, -OH) ^{13}C NMR (75 MHz, CHLOROFORM-*d*) δ ppm 20.11 (CH_3) 122.83 (Ar-CH) 129.50 (Ar-CCH_3) 137.93 (Ar-CCO) 161.69 (Ar-O) 192.14 (C=O)

Preparation of 5-Methylsalicylaldehyde[2]: To a solution of 4-methylphenol (20mmol) in acetonitrile (100mL), Dry paraformaldehyde, (135mmol), anhydrous magnesium dichloride (30 mmol) and triethylamine (75 mmol) were added. The mixture was heated under reflux for 4 hours after which the solution was allowed to cool to room temperature before a 5% aqueous HCl solution was added and the product extracted with diethyl ether and dried with magnesium sulphate. Solvent was removed by rotary evaporation and the residue purified by flash column chromatography yielding 5-methylsalicyladehyde. **^{1}H NMR** ($CDCl_3$) 2.31 - 2.41 (m, 3 H, -CH_3) 6.85 - 6.96 (m, 1 H, Ar-H) 7.33 (s, 1 H, Ar-H) 7.35 (s., 1 H, Ar-H) 9.85 (s, 1 H, -CHO) 10.84 (s, 1 H, -OH) 13C NMR (75 MHz, CHLOROFORM-d) 20.17 (-CH_3) 117.34 (Ar) 120.31 (Ar) 129.09 (Ar) 133.36 (Ar) 137.99 (s, 1 C) 159.50 (s, 1 C) 196.53 (s, 1 C)

Preparation of 3,5-di-tert-butyl-2-hydroxybenzyl alcohol[3]: To a solution of 2,4-di-tert-butylphenol (60g, 0.29 mol) in methanol (80 mL), was added dropwise with stirring at room temperature a suspension of paraformaldehyde (9 g, 0.3 mol) and $LiOH.H_2O$ (1 g, 0.024mol) in methanol (80 mL). The mixture was heated to reflux for 6 hours after which the solvent was removed by rotary evaporation, and the orange-brown viscous residue solidified upon cooling. Repeated recrystallisation from hot hexane afforded a colourless precipitate of the title compound. (41 g, 67 %) when washed with copious

amounts of hexane. **^{1}H NMR** ($CDCl_3$) 1.28 (9H, s, $C(CH_3)_3$), 1.42 (9H, s, $C(CH_3)_3$), 4.84 (2H, d J = 6Hz, CH_2), 6.89 (1H, d J = 2.5 Hz, Ar-H), 7.31 (1H, d J = 2.5 Hz, Ar-H), 7.59 (1H, s, OH). **^{13}C{^{1}H}** NMR ($CDCl_3$) 30.0, 31.8, ($C(CH_3)_3$), 34.4, 35.2, ($C(CH_3)_3$), 66.1 (CH_2), 122.8, (Ar-CH), 124.2 (Ar-C), 124.3 (Ar-CH), 136.6, 141.7 (Ar-C), 153.0 (Ar-O).

Preparation of 3,5-di-tert-butyl-2-hydroxybenzyl bromide[3]: To a solution of 3.5-di-tert-butly-2-hydroxybenzyl alcohol, (23.63 g, 0.1 mol) in chloroform (150 ml) with stirring, PBr_3 (11.38 g, 3.95 ml, 0.04 mol) in chloroform (100 mL) was added dropwise. After an hour at room temperature water (100 mL) was added and the organic phase quickly washed three time with water, separated, and dried over MgSO4, and filtered before the solvent was removed by rotary evaporation. Residual solvent was removed under reduced pressure and the product isolated upon scratching of the glassware. (21.40 g, 71.5 %). **^{1}H NMR** ($CDCl_3$) 1.33 (9H, s, C(CH3)3), 1.45 (9H, s, C(CH3)3), 4.60 (2H, s, CH2), 7.11 (1H, d J = 2.5 Hz, Ar-H), 7.41 (1H, d J = 2.5 Hz). **^{13}C{^{1}H} NMR** ($CDCl_3$) 30.1, 31.8, (C(CH3)3), 34.6, 35.0, (C(CH3)3), 71.5 (CH2), 123.7 (Ar-C), 125.3, 126.2 (Ar-CH), 137.7, 143.5 (Ar-C), 152.0 (Ar-O).

4.3.2. Synthetic Procedures

Preparation of 2R-H: To a solution of 2,6-diformyl-p-cresol (0.66 g, 4 mmol) in methanol (10 mL), (*R*)-(+)-methylbenzylamine (0.97 g, 8 mmol) was added. The mixture was stirred over night before the solvent was removed by rotary evaporation. The product was dried under reduced pressure with gentle heating if needed, yielding a Dark yellow/brown viscious oil (1.34 g, 90 %). **^{1}H NMR** ($CDCl_3$) 1.40-1.58 (m, 6 H, $-CH_3$) 2.25 (S, 3 H, Ar-CH_3) 6.75 (d, J=7.5 Hz, 1 H, Ar-H) 6.88-6.90 (m, 1 H, Ar-H) 7.13 - 7.30 (m, Ar-H) 7.28 (d, J=1.5 Hz, 2 H, Ar-H) 8.35 (s, 2 H, CHN) 14.12 (br. s., 1 H, OH). **^{13}C{^{1}H} NMR** ($CDCl_3$) 19.65 ($-CH_3$), 20.21 ($-CH_3$), 20.35 ($ArCH_3$), 76.21-76.77 (CHN), 126.23-128.36 (Ar), 160.19 (CH=N). **m/z** ion M+H Expected; 371.2123, Found; 371.2113.

Preparation of 2S-H: To a solution of 2,6-diformyl-p-cresol (0.66 g, 4 mmol) in methanol (10 mL), (*S*)-(-)-methylbenzylamine (0.97 g, 8 mmol) was added. The mixture was stirred over night before the solvent was removed by rotary evaporation. The product was dried under reduced pressure with gentle

heating if needed, yielding a Dark yellow/brown viscious oil (1.34 g, 90 %). **^{1}H NMR** ($CDCl_3$) 1.42-1.56 (m, 6 H, -CH_3) 2.30 (s, 3 H, Ar-CH_3) 6.91 (d, J=7.5 Hz, 1 H, Ar-H) 6.83-6.88 (m, 1 H, Ar-H) 7.10 - 7.25 (m, Ar-H) 7.24 (d, J=1.5 Hz, 2 H, Ar-H) 8.40 (s, 2 H, CHN) 13.85 (br. s., 1 H, OH). **^{13}C{^{1}H} NMR** ($CDCl_3$) 19.56 (-CH_3), 20.22 (-CH_3), 20.40 (ArCH_3), 76.20-76.80 (CHN), 126.23-128.86 (Ar), 158.49 (CH=N). **m/z** ion M+H Expected; 371.2123, Found; 371.2098.

Preparation of 2E-H: To a solution of 2,6-diformyl-p-cresol (0.66 g, 4 mmol) in methanol (10 mL), (*R*)-(+)-ethylbenzylamine (1.08 g, 8 mmol) was added. The mixture was stirred over night before the solvent was removed by rotary evaporation. The product was dried under reduced pressure with gentle heating if needed, yielding a Dark yellow/brown viscious oil (1.43 g, 90 %). **^{1}H NMR** ($CDCl_3$) 0.7-0.9 (m, 6 H, CH_2-CH_3) 1.75-1.95 (m, 4 H, -CH_2-CH_3) 2.15 (s, 3 H, Ar-CH_3) 6.78 (td, J=7.5, 1.1 Hz, 1 H, Ar-H) 6.89 (d, J=8.3 Hz, 1 H, Ar-H) 7.13 - 7.30 (m, Ar-H) 7.26 (d, J=1.5 Hz, 2 H, Ar-H) 8.28 (s, 1 H, CHO) 13.53 (br. s., 1 H, OH). **^{13}C{^{1}H} NMR** ($CDCl_3$) 11.16 ($CHCH_2CH_3$), 20.34 (ArCH_3), 31.68 ($CHCH_2CH_3$), 76.73-77.58 (ArCH), 126.53-128.56 (Ar), 159.09 (ArCH=N). **m/z** ion M+H Expected; 399.2436, Found; 399.2429.

Preparation of 2N-H: To a solution of 2,6-diformyl-p-cresol (0.66 g, 4 mmol) in CH_2Cl_2 (20 mL), (*R*)-(+)-1-(2-naphthyl)ethylamine (1.37 g, 8 mmol) was added. The mixture was stirred over night before the solvent was removed by rotary evaporation. The product was dried under reduced pressure with gentle heating if needed, yielding a Dark yellow/brown soild (1.61 g, 86 %). **^{1}H NMR** ($CDCl_3$) 1.39-1.56 (m, 6 H, -CH_3) 2.28 (s, 3 H, Ar-CH_3) 6.81 (d, J=7.5 Hz, 1 H, Ar-H) 6.75-6.88 (m, 5 H, Ar-H) 7.10 - 7.25 (m, 6 H, Ar-H) 7.25-7.36 (m, 4 H, Ar-H) 8.51 (s, 2 H, CHN). **^{13}C{^{1}H} NMR** ($CDCl_3$) 18.89 (-CH_3), 21.75 (-CH_3), 20.45 (ArCH_3), 77.82 (CHN), 126.23-128.86 (Ar), 130.89 (Ar), 132.56 (Ar), 158.49 (CH=N), 160.01 (CH=N). **m/z** ion M+H Expected; 471.2436, Found; 471.2401.

Preparation of EH-H: To a solution of *(R)*-ethylbenzylamine (0.81 g, 6 mmol) in methanol (25 mL), salicylaldehyde (0.73 g, 6 mmol) was added. The mixture was stirred over night before the solvent was removed by rotary evaporation. The product was dried under reduced pressure with gentle heating if needed, yielding a Dark yellow/brown viscious oil (1.15 g, 74 %). **^{1}H NMR**

($CDCl_3$) 0.83 (t, J=7.5 Hz, 3 H, -CH_3) 1.88 (quin, J=7.5 Hz, 2 H, -CH_2-) 4.11 (t, J=6.8 Hz, 1 H, N-CH) 6.78 (td, J=7.5, 1.1 Hz, 1 H, Ar-H) 6.89 (d, J=8.3 Hz, 1 H, Ar-H) 7.13 - 7.30 (m, Ar-H) 7.26 (d, J=1.5 Hz, 2 H, Ar-H) 8.28 (s, 1 H, CHO) 13.53 (br. s., 1 H, OH). **$^{13}C\{^1H\}$ NMR** ($CDCl_3$) 10.86 (-CH_3), 31.73 (CH_2), 75.60 (N-CH), 116.89, 118.54, 118.75, 126.75, 127.18, 128.54, 131.33, 132.21, 142.91 (Ar), 161.08 (N=C), 163.81 (C-O). **m/z** ion M+H Expected; 240.1388, Found; 240.1412.

Preparation of E5-H: To a solution of (*R*)-ethylbenzylamine (0.81 g, 6 mmol) in methanol (25 mL), 5-methylsalicylaldehyde (0.82 g, 6 mmol) was added. The mixture was stirred over night before the solvent was removed by rotary evaporation. The product was dried under reduced pressure with gentle heating if needed, yielding a Dark yellow/brown viscious oil (1.2 g, 74 %). **^1H NMR** ($CDCl_3$) 0.83 (t, J=7.5 Hz, 3 H, -CH_3) 1.88 (quin, J=7.2 Hz, 2 H, -CH_2-) 2.19 (s, 3 H Ar-CH_3) 4.11 (t, J=6.8 Hz, 1 H, N-CH) 6.80 (d, J=8.3 Hz, 1 H, Ar-H) 6.95 (d, J=1.5 Hz, 1 H, Ar-H) 7.03 (dd, J=7.9, 2.3 Hz, 1 H, Ar-H) 7.13 - 7.31 (m, 5 H, Ar-H) 8.24 (s, 1 H, -CHO) 13.30 (bs, 1 H, -OH). **$^{13}C\{^1H\}$ NMR** ($CDCl_3$) 10.88 (-CH_3), 20.26 (Ar-CH_3), 31.75 (CH_2), 75.64 (N-CH), 116.64, 118.41, 126.76, 127.15, 127.57, 128.53, 131.39, 133.01, 143.03 (Ar), 158.80 (N=C), 163.82 (C-O). **m/z** ion M+H Expected; 254.1545, Found; 254.1596.

Preparation of EB-H: To a solution of *(R)*-ethylbenzylamine (0.81 g, 6 mmol) in methanol (25 mL), 3,5-di-tert-butylsaliclyaldehyde (1.41 g, 6 mmol) was added. The mixture was stirred over night before the solvent was removed by rotary evaporation. The product was dried under reduced pressure with gentle heating if needed, yielding a Dark yellow/brown viscious oil (1.66 g, 75 %). **^1H NMR** ($CDCl_3$) 0.83 (d, J=7.5 Hz, 3 H, -CH_3) 1.21 (s, 9 H, -C(CH_3)3) 1.37 (s, 9 H, -C(CH_3)3) 1.89 (quin, J=7.5 Hz, 2 H, N-CH) 4.09 (t, J=6.8 Hz, 1 H, Ar-H) 6.99 (d, J=2.3 Hz, 1 H, Ar-H) 7.12 - 7.20 (m, 3 H, Ar-H) 7.21 - 7.33 (m, 5 H, Ar-H) 8.30 (s, 1 H, -CHO) 13.75 (bs,1 H, -OH). **$^{13}C\{^1H\}$ NMR** ($CDCl_3$) 11.05 (-CH_3), 29.45 (, 31.49, 31.76, 34.11, 35.03, 75.80, 117.90, 126.00, 126.91, 127.10, 128.53, 136.61, 140.02, 143.26, 158.03, 164.99. **m/z** ion M+H Expected; 352.264, Found; 352.2671.

Preparation of EC-H: To a solution of *(R)*-ethylbenzylamine (0.81 g, 6 mmol) in methanol (25 mL), 3,5-di-chlorosalicylaldehyde (1.15 g, 6 mmol) was added. The mixture was stirred over night before the solvent was removed by rotary evaporation. The product was dried under reduced pressure with gentle heating if needed, yielding a Dark yellow/brown viscious oil (1.4 g, 71 %). **^{1}H NMR** ($CDCl_3$) 0.85 (t, J=7.5 Hz, 3 H, -CH_3) 1.92 (quin, J=7.2 Hz, 2 H, -CH_2-) 4.21 (t, J=6.8 Hz, 1 H, N-CH) 7.06 (d, J=2.3 Hz, 1 H, Ar-H) 7.17 - 7.34 (m, 6 H, Ar-H) 8.19 (s, 1 H, -CHO) 14.66 (br. s., 1 H, -OH). **^{13}C{^{1}H} NMR** ($CDCl_3$) 10.82 (-CH_3), 31.46, 74.73, 119.31, 122.40, 122.91, 126.77, 127.67, 128.80, 129.04, 132.22, 141.63, 157.10, 162.24. **m/z** ion M+H Expected; 308.0609, Found; 308.0588.

Preparation of NH-H: To a solution of *(R)*-1-(2-naphthyl)ethylamine (0.85 g, 5 mmol) in CH_2Cl_2 (20 mL), salicylaldehyde (0.61 g, 5 mmol) was added. The mixture was stirred over night before the solvent was removed by rotary evaporation. The product was dried under reduced pressure with gentle heating if needed, yielding a Dark yellow/brown viscious oil (1.0 g, 68 %). **^{1}H NMR** ($CDCl_3$) 1.75 (d, J=6.8 Hz, 3 H, -CH_3) 4.77 (q, J=6.4 Hz, 1 H, N-CH) 6.89 (t, J=6.8 Hz, 1 H, Ar-H) 7.04 (d, J=8.3 Hz, 1 H, Ar-H) 7.27 (dd, J=7.5, 1.9 Hz, 1 H, Ar-H) 7.34 (td, J=7.2, 1.5 Hz, 1 H, Ar-H) 7.44 - 7.57 (m, 3 H, Ar-H) 7.77 - 7.90 (m, 4 H, Ar-H) 8.46 (s, 1 H, -CHO) 13.52 (br. s., 1 H, -OH). **^{13}C{^{1}H} NMR** ($CDCl_3$) 24.81 (-CH_3), 68.45, 116.94, 118.59, 118.82, 124.71, 124.85, 125.79, 126.15, 127.61, 127.84, 128.44, 131.39, 132.28, 132.68, 133.37, 141.16, 161.06, 163.64. **m/z** ion M+H Expected; 276.1388, Found; 276.1362.

Preparation of N5-H: To a solution of *(R)*-1-(2-naphthyl)ethylamine (0.85 g, 5 mmol) in CH_2Cl_2 (20 mL), 5-methylsalicylaldehyde (0.68 g, 5 mmol) was added. The mixture was stirred over night before the solvent was removed by rotary evaporation. The product was dried under reduced pressure with gentle heating if needed, yielding a Dark yellow/brown viscious oil (1.07 g, 70 %). **^{1}H NMR** ($CDCl_3$) 1.73 (d, J=6.4 Hz, 3 H, -CH_3) 2.30 (s, 3 H, Ar-CH_3) 4.73 (q, J=6.7 Hz, 1 H, N-CH) 6.91 (d, J=8.3 Hz, 1 H, Ar-H) 7.06 (s, 1 H, Ar-H) 7.14 (dd, J=8.3, 2.3 Hz, 1 H, Ar-H) 7.43 - 7.57 (m, 3 H, Ar-H) 7.78 - 7.90 (m, 4 H, Ar-H) 8.42 (s, 1 H, -CHO) 13.31 (br. s., 1 H, OH). **^{13}C{^{1}H} NMR** ($CDCl_3$) 20.24, 24.80, 68.40, 116.65, 118.44, 124.71, 124.80,125.73, 126.10, 127.57, 127.81, 128.39, 131.43,

132.63, 133.07, 133.35, 141.22, 158.76, 163.64. **m/z** ion M+H Expected; 290.1545, Found; 290.1534.

Preparation of NB-H: To a solution of *(R)*-1-(2-naphthyl)ethylamine (0.85 g, 5 mmol) in CH_2Cl_2 (20 mL), 3,5-di-tert-butylsaliclyaldehyde (1.17 g, 5 mmol) was added. The mixture was stirred over night before the solvent was removed by rotary evaporation. The product was dried under reduced pressure with gentle heating if needed, yielding a yellow solid (1.86 g, 92 %). **^{1}H NMR** ($CDCl_3$) 1.31 (s, 9 H, -C(CH_3)3) 1.48 (s, 9 H, -C(CH_3)3) 1.75 (d, J=6.4 Hz, 3 H, -CH_3) 4.74 (q, J=6.8 Hz, 1 H, N-CH) 7.10 (d, J=2.6 Hz, 2 H, Ar-H) 7.40 (d, J=2.6 Hz, 2 H, Ar-H) 7.44 - 7.52 (m, 2 H, Ar-H, Ar-H) 7.55 (dd, J=8.7, 1.9 Hz, 3 H, Ar-H) 7.79 - 7.91 (m, 4 H, Ar-H) 8.48 (s, 1 H, -CHO) 13.87 (s, 1 H, -OH). **^{13}C{^{1}H} NMR** ($CDCl_3$) 24.74, 29.44, 31.48, 34.11, 35.03, 68.41, 117.94, 124.98, 125.01, 125.75, 126.05, 126.11, 126.97, 127.64, 127.89, 128.39,132.69, 133.42, 136.66, 140.08, 141.39, 158.02, 164.80. **m/z** ion M+H Expected; 388.264, Found; 388.2686.

Preparation of NC-H: To a solution of *(R)*-1-(2-naphthyl)ethylamine (0.85 g, 5 mmol) in CH_2Cl_2 (20 mL), 3,5-di-chlorosalicylaldehyde (0.96 g, 5 mmol) was added. The mixture was stirred over night before the solvent was removed by rotary evaporation. The product was dried under reduced pressure with gentle heating if needed, yielding a orange solid (1.67 g, 92 %). **^{1}H NMR** ($CDCl_3$) 1.75 (d, J=6.4 Hz, 3 H, -CH_3) 4.80 (q, J=6.5 Hz, 1 H, N-CH) 7.12 (d, J=2.3 Hz, 1 H, Ar-H) 7.41 (d, J=2.6 Hz, 1 H, Ar-H) 7.46 - 7.54 (m, 3 H, Ar-H) 7.76 - 7.89 (m, 4 H, Ar-H) 8.31 (s, 1 H, -CHO) 14.73 (br. s., 1 H, -OH). **^{13}C{^{1}H} NMR** ($CDCl_3$) 24.45, 67.66, 119.38, 122.45, 122.91, 124.39, 125.10, 126.09, 126.39, 127.66, 127.86, 128.79, 129.07, 132.24, 132.83, 133.34,139.84, 157.01, 162.06. **m/z** ion M+H Expected; 344.0609, Found; 344.0593.

Preparation of BH-H_2: To a solution of salicylaldehyde (0.5, 4.1 mmol) in methanol (20 mL) was added 2-(aminomethyl)piperidine (0.47 g, 4.1 mmol, 0.5 mL). The resulting mixture quickly changed colour and was stirred over night to obtain a clear solution. Solvent was removed by rotary evaporation to yield a yellow solid (0.67 g, 69.3 %). **^{1}H NMR** ($CDCl_3$) 1.34 - 1.50 (m, 2 H, CH_2), 1.59 - 1.93 (m, 4 H, CH_2) 2.64 (td, J=11.7, 3.0 Hz, 1 H, CH_2) 2.84 - 2.91 (m, 1 H, CH_2)

3.03 - 3.12 (m, 1 H, N-CH_2) 3.39 - 3.47 (m, 1 H, N-CH_2) 3.70 (ddd, J=12.0, 4.43, 1.3 Hz, 1 H, N-CH) 6.88 (td, J=7.54, 1.13 Hz, 1 H, Ar-H) 6.96 (dd, J=8.29, 0.8 Hz, 1 H, Ar-H)7.23 - 7.27 (m, 1 H, Ar-H) 7.32 (ddd, J=8.48, 7.16, 1.70 Hz, 1 H, Ar-H) 8.38 (s, 1 H, N=CH). **$^{13}C\{^1H\}$ NMR** ($CDCl_3$) 24.45(CH_2), 26.14 (CH_2), 30.63 (CH_2), 46.80 (N-CH_2), 56.64 (N-CH_2), 66.12 (N-CH), 116.94 (Ar-H), 118.67 (Ar-H), 129.89 (Ar-C), 131.35 (Ar-H), 132.33 (Ar-H), 161.04 (Ar-OH), 166.24 (N=CH). **m/z** ion M+H calc. 219.1497, found 219.1587. The yellow powder (0.55 g, 2.5 mmol) was dissolved in THF (20 mL), to which a solution of 3,5-di-tert-butyl-2-hydroxybenzyl bromide (0.75 g, 2.5 mmol) in THF (10 mL) was added. Triethylamine (0.25 g, 2.5 mmol, 0.184 mL) was added dropwise, and the mixture was stirred at 80^oC for 24 hours. The white precipitate was filtered off and the solvent removed under reduced pressure. The product was purified via flash chromatography to obtain the title ligand (0.90 g, 82.0 %) **^1H NMR** ($CDCl_3$) 1.27 (s, 9 H, $C(CH_3)_3$), 1.28 - 1.29 (m, 2 H, CH_2), 1.29 - 1.31 (m, 9 H, $C(CH_3)_3$), 1.36 (s, 1 H, CH_2), 1.41 (s, 3 H, CH_2), 1.44 - 1.46 (m, 2 H, CH_2), 1.63 (dd, J=8.3, 3.4 Hz, 2 H, CH_2), 2.13 (td, J=11.5, 3.0 Hz, 1 H, CH_2), 6.76 (d, J=1.1 Hz, 1 H, Ar-H), 6.89 - 6.94 (m, 2 H, Ar-H), 7.16 (d, J=2.3 Hz, 1 H, Ar-H), 7.21 (d, J=2.3 Hz, 1 H, Ar-H) 7.28 - 7.36 (m, 1 H, Ar-H), 8.30 (s, 1 H, N=CH). **$^{13}C\{^1H\}$ NMR** ($CDCl_3$) 23.76 (CH_2), 24.97 (CH_2), 29.55 (CH_2), 29.59 (CH_3), 31.58 (CH_3), 31.74 (CH_2), 34.11 ($C(CH_3)_3$), 34.84 ($C(CH_3)_3$), 61.57 (N-CH_2) 116.93 (Ar-C) 119.00 (Ar-C) 120.87 (Ar-H) 123.07 (Ar-H) 130.45 (Ar-H) 130.98 (Ar-H) 131.40 (Ar-H) 132.36 (Ar-H) 140.36 (Ar-C), 153.31 (Ar-C) 157.77 (N=CH) 161.02 (Ar-OH) 166.22 (Ar-OH). **m/z** calc. 437.3168 found 437.3269.

Preparation of BB-H_2: To a solution of 3,5-di-tert-butylsaliclyaldehyde (0.96, 4.1 mmol) in methanol (20 mL) was added 2-(aminomethyl)piperidine (0.47 g, 4.1 mmol, 0.5 mL). The resulting mixture quickly changed colour and was stirred over night to obtain a clear solution. Solvent was removed by rotary evaporation to yield a yellow powder (1.00 g, 70.2 %). **^1H NMR** ($CDCl_3$) 1.26 - 1.53 (m, 2 H, CH_2) 1.31 (s, 9 H, $C(CH_3)_3$) 1.45 (s, 9 H, $C(CH_3)_3$) 1.59 - 1.89 (m, 4 H, CH_2) 2.65 (td, J=11.7, 3.0 Hz, 1 H, CH_2) 2.85 - 2.93 (m, 1 H, CH_2) 3.04 - 3.14 (m, 1 H, N-CH_2) 3.38 - 3.47 (m, 1 H, N-CH_2) 3.67 - 3.76 (m, 1 H, N-CH) 7.10 (d, J=2.6 Hz, 1 H, Ar-H) 7.39 (d, J=2.6 Hz, 1 H, Ar-H) 8.39 (s, 1 H, N=C). **$^{13}C\{^1H\}$ NMR** ($CDCl_3$) 24.41 (CH_2), 26.02 (CH_2), 29.37($C(CH_3)_3$), 30.53 (CH_2), 31.43

(C(CH_3)$_3$), 34.08 (*C*(CH3)3), 34.98 (*C*(CH3)3), 46.70 (N-CH_2), 56.60 (N-CH_2), 66.04 (N-CH), 117.71 (Ar-H), 126.00 (Ar-H), 126.99 (Ar-C), 136.60 (Ar-C), 140.13(Ar-C), 157.92 (Ar-OH), 167.42 (N=CH). **m/z** ion M+H calc. 331.2749, found 331.2893. The yellow powder (0.83 g, 2.5 mmol) was dissolved in THF (20 mL), to which a solution of 3,5-di-tert-butyl-2-hydroxybenzyl bromide (0.75 g, 2.5 mmol) in THF (10 mL) was added. Triethylamine (0.25 g, 2.5 mmol, 0.18 mL) was added dropwise, and the mixture was stirred at 80^{o}C for 24 hours. The white precipitate was filtered off and the solvent removed under reduced pressure. The product was purified via flash chromatography to obtain the title ligand (1.03 g, 75.3 %) **^{1}H NMR** ($CDCl_3$) 1.27-1.34 (m, 2H, CH_2), 1.49-1.81 (m, 4H, CH_2), 1.30 (s, 9 H, C(CH_3)$_3$), 1.31 (s, 9 H, C(CH_3)$_3$), 1.37 (s, 9 H, C(CH_3)$_3$), 1.46 (s, 9 H, C(CH_3)$_3$), 2.95 - 3.04 (m, 1 H, CH), 3.70 - 3.80 (m, 2 H, CH_2), 3.92 - 4.04 (m, 2 H, CH_2), 4.12 - 4.43 (m, 2 H, CH_2), 6.85 (d, J=2.3 Hz, 1 H, Ar-H), 7.04 (d, J=2.6 Hz, 1 H, Ar-H), 7.20 (d, J=2.3 Hz, 1 H, Ar-H), 7.39 (d, J=2.6 Hz, 1 H, Ar-H), 8.29 (s, 1 H, N=CH). **^{13}C{^{1}H} NMR** ($CDCl_3$) 24.05 (CH_2), 28.23 (CH_2), 28.39 (CH_2), 28.45 (C(*C*H_3)$_3$), 28.60 (C(*C*H_3)$_3$), 30.29 (CH_2), 30.45 (C(*C*H_3)$_3$), 30.68 (C(*C*H_3)$_3$), 33.02 (*C*(CH_3)$_3$), 33.08 (*C*(CH_3)$_3$), 33.79 (*C*(CH_3)$_3$), 33.99 (*C*(CH_3)$_3$), 57.46 (N-CH_2), 60.79 (N-CH), 116.81 (Ar-C), 120.8 (Ar-H), 122.12 (Ar-H), 124.89, 125.97, 134.47 (Ar-C), 135.62 (Ar-C), 138.97 (Ar-C), 139.216 (Ar-C), 153.42 (Ar-OH), 156.90 (Ar-OH), 166.27 (N=CH). **m/z** calc. 549.4420 found 549.4547.

Preparation of BC-H_2: To a solution of 3,5-di-chlorosalicylaldehyde (0.78, 4.1 mmol) in methanol (20 mL) was added 2-(aminomethyl)piperidine (0.47 g, 4.1 mmol, 0.5 mL). The resulting mixture quickly changed colour and was stirred over night to obtain a clear solution. Solvent was removed by rotary evaporation to yield a orange powder (0.96 g, 76.8 %). **^{1}H NMR** ($CDCl_3$) 1.28 - 1.47 (m, 2 H, CH_2) 1.57 - 2.01 (m, 4 H, CH_2) 2.05 - 2.19 (m, 1 H, CH_2) 2.40 - 2.54 (m, 1 H, CH_2) 2.59 - 2.72 (m, 1 H, CH_2) 3.08 (d, J=10.2 Hz, 1 H, N-CH_2) 3.40 - 3.83 (m, 1 H, N-CH_2) 6.96 (d, J=2.6 Hz, 1 H, Ar-H) 7.30 (d, J=2.6 Hz, 1 H, Ar-H) IMINE RESONANCE NOT PRESENT. **^{13}C{^{1}H} NMR** ($CDCl_3$) 23.52 (CH_2), 24.73 (CH_2), 28.84 (CH_2), 48.53 (NH-CH_2), 56.48 (N-CH_2), 63.49 (NH-C), 122.16 (Ar-Cl), 123.33 (Ar-Cl), 124.15 (Ar-C), 128.19 (Ar-H), 129.73 (Ar-H), 152.60 (Ar-OH), IMINE RESONANCE NOT PRESENT. **m/z** ion M+H calc.

287.0718, found 287.0705. The orange powder (0.72 g, 2.5 mmol) was dissolved in THF (20 mL), to which a solution of 3,5-di-tert-butyl-2-hydroxybenzyl bromide (0.75 g, 2.5 mmol) in THF (10 mL) was added. Triethylamine (0.25 g, 2.5 mmol, 0.18 mL) was added dropwise, and the mixture was stirred at 80^{o}C for 24 hours. The white precipitate was filtered off and the solvent removed under reduced pressure. The product was purified via flash chromatography to obtain the title ligand (0.79 g, 62.3 %) **^{1}H NMR** ($CDCl_3$) 1.25 - 1.31 (m, 2 H, CH_2), 1.28 (s, 9 H, C(CH_3)$_3$), 1.29 (s, 9 H, C(CH_3)$_3$), 1.39 - 1.46 (m, 4 H, CH_2), 2.15 (td, J=11.5, 3.0 Hz, 1 H, C*H*), 2.54 - 2.67 (m, 1 H, CH_2), 2.85 - 2.93 (m, 1 H, CH_2), 3.45 - 3.68 (m, 1 H, CH_2), 3.89 (d, J=6.8 Hz, 2 H, N-CH_2), 3.99 (m, 1 H, N-CH_2), 6.44 (d, J=2.6 Hz, 1 H, Ar-H), 6.76 (d, J=2.3 Hz, 1 H, Ar-H), 7.17 (d, J=2.3 Hz, 1 H, Ar-H), 7.21 (d, J=2.6 Hz, 1 H, Ar-H), IMINE RESONANCE NOT PRESENT. **^{13}C{^{1}H} NMR** ($CDCl_3$) 23.43 (CH_2), 24.76 (CH_2), 28.70 (CH_2), 29.50 (CH_2), 28.70 (C(*C*H_3)$_3$), 29.50 (C(*C*H_3)$_3$), 31.68, 34.13 (*C*(CH_3)$_3$), 34.79 (*C*(CH_3)$_3$), 48.7 (N-CH_2), 57.22 (N-CH_2), 58.50 (N-CH_2), 61.27 (N-CH), 120.75 (Ar-C), 121.88 (Ar-C), 122.76 (Ar-H), 123.22 (Ar-Cl), 123.50 (Ar-Cl), 125.60 (Ar-H), 130.20 (Ar-H), 135.86 (Ar- C(CH_3)$_3$), 140.73 (Ar- C(CH_3)$_3$), 152.43 (Ar-OH), 153.73 (Ar-OH) IMINE RESONANCE NOT PRESENT. **m/z** calc. 505.2389 found 505.2379.

Preparation of BA-H_2: To a solution of 3,5-di-adamantlysalicylaldehyde (1.6, 4.1 mmol) in methanol (20 mL) was added 2-(aminomethyl)piperidine (0.47 g, 4.1 mmol, 0.5 mL). The resulting mixture quickly changed colour and was stirred over night to obtain a clear solution. Solvent was removed by rotary evaporation to yield a yellow powder (1.48 g, 71.7 %). **^{1}H NMR** ($CDCl_3$) 1.29 - 1.53 (m, 2 H, CH_2) 1.31 (s, 12 H) 1.61 - 1.92 (m, 4 H) 1.80 (d, J=2.3 Hz, 6 H) 2.10 (br. s., 4 H) 2.17 (br. s., 2 H) 2.19 (d, J=3.0 Hz, 6 H) 2.61 - 2.73 (m, 1 H) 2.86 - 2.98 (m, 1 H) 3.07 - 3.16 (m, 1 H) 3.42 - 3.52 (m, 1 H) 3.73 (ddd, J=12.0, 4.6, 1.1 Hz, 1 H, N-CH) 7.08 (d, J=2.3 Hz, 1 H, Ar-H) 7.34 (d, J=2.6 Hz, 1 H, Ar-H) 8.39 (s, 1 H, CHO). **^{13}C{^{1}H} NMR** ($CDCl_3$) 24.28 (CH_2), 25.83 (CH_2), 29.07 (CH), 30.37 (CH), 31.46 (CH), 34.16 (CH_2), 37.12 (CH_2), 37.18 (CH_2), 40.26 (CH_2), 46.61 (N-CH_2), 56.61 (N-CH_2), 62.74 (N-CH), 117.70 (Ar-H), 125.93 (Ar), 127.06 (Ar), 136.99 (Ar), 140.27 (Ar), 158.20 (Ar-OH), 167.73 (N=CH). **m/z** ion M+H calc. 486.3609, found 486.3599. The yellow powder (1.22 g, 2.5

mmol) was dissolved in THF (20 mL), to which a solution of 3,5-di-tert-butyl-2-hydroxybenzyl bromide (0.75 g, 2.5 mmol) in THF (10 mL) was added. Triethylamine (0.25 g, 2.5 mmol, 0.18 mL) was added dropwise, and the mixture was stirred at 80°C for 24 hours. The white precipitate was filtered off and the solvent removed under reduced pressure. The product was purified via flash chromatography to obtain the title ligand (1.32 g, 74.9 %) **^{1}H NMR** ($CDCl_3$) 1.28-1.34 (m, 2H, CH_2), 1.31 (s, 12 H), 1.33 (s, 9 H), 1.36 (d, J=1.9 Hz, 4 H, CH_2), 1.40 (s, 8 H),1.60-1.90 (m, 4H), 1.79-1.85 (m, 6 H), 2.09-2.14 (m, 4 H), 2.18 (d, J=2.6 Hz, 2 H), 2.19-2.21 (m, 6 H), 2.89 - 3.05 (m, 2, HN-CH_2), 3.68 - 3.80 (m, 1 H, N-CH), 3.89 - 4.03 (m, 2 H, N-CH_2), 6.87 (d, J=2.3 Hz, 1 H, Ar-H), 7.05 (d, J=2.3 Hz, 1 H, Ar-H), 7.21 (d, J=2.3 Hz, 1 H, Ar-H), 7.34 (d, J=2.3 Hz, 1 H, Ar-H), 8.30 (s, 1 H, N=CH). **^{13}C{^{1}H} NMR** ($CDCl_3$) 25.06 (CH_2), 25.14 (CH_2), 28.93 (CH), 29.08 (CH), 29.21 (s, 1 C), 29.48 (s, 2 C), 29.42 - 29.46 (m, 1 C), 29.61 (s, 1 C), 31.47 (C(*C*H_3)$_3$), 31.59 (C(*C*H_3)$_3$), 31.69 (*C*(CH_3)$_3$), 34.79 (*C*(CH_3)$_3$), 37.13, 37.17, 40.16, 40.26, 40.37, 58.55 (N-CH_2), 65.84 (N-CH), 117.81 (Ar-C), 123.14 (Ar-C), 125.28 (Ar-H), 125.78 (Ar-H), 126.98 (Ar-H), 127.69 (Ar-H), 135.49 (Ar-C(CH_3)$_3$), 136.94 (Ar-C(CH_3)$_3$), 140.09 (Ar-C(CH_3)$_3$), 140.30 (Ar-C(CH_3)$_3$), 154.40 (Ar-OH), 158.16 (Ar-OH), 167.43 (N=CH). **m/z** calc. 705.5359 found 705.5348.

Preparation of BM-H_2: To a solution of 3-tert-butyl-5-methylsalicylaldehyde (0.82, 4.1 mmol) in methanol (20 mL) was added 2-(aminomethyl)piperidine (0.47 g, 4.1 mmol, 0.5 mL). The resulting mixture quickly changed colour and was stirred over night to obtain a clear solution. Solvent was removed by rotary evaporation to yield a yellow powder (0.84 g, 65.3 %). **^{1}H NMR** ($CDCl_3$) 1.29 - 1.31 (m, 9 H, C(CH_3)$_3$) 1.33 - 1.49 (m, 2 H, CH_2) 1.56 - 1.92 (m, 4 H CH_2) 2.29 (s, 3 H, CH_3) 2.63 (td, J=11.7, 3.0 Hz, 1 H CH_2) 2.80 - 2.90 (m, 1 H, CH_2) 3.03 - 3.11 (m, 1 H, CH_2) 3.44 - 3.49 (m, 1 H, CH_2) 3.70 (ddd, J=12.0, 4.4, 1.3 Hz, 1 H, N-CH) 7.09 (d, J=2.6 Hz, 1 H, Ar-H) 7.24 (dd, J=2.6, 0.8 Hz, 1 H, Ar-H) 8.37 (s, 1 H, N=CH). **^{13}C{^{1}H} NMR** ($CDCl_3$) 15.72 (CH_3) 24.43 (CH_2) 26.07 (CH_2) 30.55 (CH_2) 31.41 (C(*C*H_3)$_3$) 33.82 (*C*(CH_3)$_3$) 46.75 (N-CH_2) 56.71 (N-CH_2) 65.97 (N-CH) 117.14 (Ar-C) 124.49 (Ar-CH_3) 125.39 (Ar-H) 130.88 (Ar-C) 140.83 (Ar-C) 156.97 (Ar-OH) 166.80 (N=CH). **m/z** ion M+H calc. 288.2201, found 288.2198. The yellow powder (0.72

g, 2.5 mmol) was dissolved in THF (20 mL), to which a solution of 3,5-di-tert-butyl-2-hydroxybenzyl bromide (0.74 g, 2.5 mmol) in THF (10 mL) was added. Triethylamine (0.25 g, 2.5 mmol, 0.18 mL) was added dropwise, and the mixture was stirred at 80^{o}C for 24 hours. The white precipitate was filtered off and the solvent removed under reduced pressure. The product was purified via flash chromatography to obtain the title ligand (0.99 g, 78.2 %) **^{1}H NMR** ($CDCl_3$) 1.30 (s, 9 H, C(CH_3)$_3$) 1.37 (s, 9 H, C(CH_3)$_3$) 2.29 (s, 3 H, CH_3) 2.48 - 2.62 (m, 1 H, CH_2) 2.80 - 2.89 (m, 1 H, CH_2) 2.93 - 3.01 (m, 1 H, CH_2) 3.60 - 3.79 (m, 2 H) 3.88 - 4.04 (m, 2 H) 6.85 (d, J=2.3 Hz, 1 H, Ar-H) 7.04 (d, J=2.6 Hz, 1 H, Ar-H) 7.20 (d, J=2.3 Hz, 1 H, Ar-H) 7.24 (dd, J=2.6, 0.8 Hz, 1 H, Ar-H) 8.28 (s, 1 H, N=CH). **^{13}C{^{1}H} NMR** ($CDCl_3$) 15.72 (CH_3) 24.43 (CH_2) 26.07 (CH_2) 30.55 (CH_2) 31.43 (C(CH_3)$_3$) 31.57 (C(CH_3)$_3$) 31.65 (CH_2) 31.69 (C(CH_3)$_3$) 34.11 (C(CH_3)$_3$) 34.77 (C(CH_3)$_3$) 44.35 (N-CH_2) 48.79 (N-CH_2) 58.45 (N-CH_2) 61.62 (N-CH) 117.24 (Ar-C) 121.03 (Ar-C) 123.13 (Ar-H) 125.23 (Ar-H) 125.31 (Ar-H) 126.15 (Ar-CH_3) 130.88 (Ar-H) 136.74 (Ar-C(CH_3)$_3$) 140.31 (Ar-C(CH_3)$_3$) 140.69 (Ar-C(CH_3)$_3$) 154.40 (Ar-OH) 156.96 (Ar-OH) 166.71 (N=CH). **m/z** calc. 507.3951 found 507.3939.

Preparation of BD-H_2: To a solution of 3,5-di-cumylsalicylaldehyde (1.47, 4.1 mmol) in methanol (20 mL) was added 2-(aminomethyl)piperidine (0.47 g, 4.1 mmol, 0.5 mL). The resulting mixture quickly changed colour and was stirred over night to obtain a clear solution. Solvent was removed by rotary evaporation to yield a yellow powder (1.37 g, 70.9 %). **^{1}H NMR** ($CDCl_3$) 1.09 - 1.51 (m, 2 H, CH_2) 1.70 (m, 4 H, CH_2) 1.66 (s, 3 H, CH_3) 1.67 (s, 3 H, CH_3) 1.70 (s, 6 H, CH_3) 2.51 - 2.62 (m, 1 H, CH_2) 2.73 - 2.82 (m, 1 H, CH_2) 2.97 - 3.06 (m, 1 H, CH_2) 3.31 (s, 1 H) 3.54 - 3.62 (m, 1 H, N-CH) 7.02 (d, J=2.3 Hz, 1 H, Ar-H) 7.09 - 7.30 (m, 10 H, Ar-H) 7.35 (d, J=2.6 Hz, 1 H, Ar-H) 8.25 (s, 1 H, CHO). **^{13}C{^{1}H} NMR** ($CDCl_3$) 24.27 (CH_2) 25.79 (CH_2) 29.20 (CH_3) 29.51 (CH_3) 30.34 (CH_2) 30.83 (CH_2) 42.34 (CH) 46.54 (N-CH_2) 50.53 (N-CH_2) 56.27, 65.92 (N-CH) 117.83 (Ar-C) 125.02, 125.49, 125.58, 126.64, 127.76, 127.96, 129.00, 135.93, 139.67, 150.52, 150.59 (Ar) 157.49 (Ar-OH) 167.04 (N=CH). **m/z** ion M+H calc. 454.2984, found 454.2975. The yellow powder (1.14 g, 2.5 mmol) was dissolved in THF (20 mL), to which a solution of 3,5-di-tert-butyl-2-hydroxybenzyl bromide (0.75 g, 2.5 mmol) in THF (10 mL) was added.

Triethylamine (0.25 g, 2.5 mmol, 0.18 mL) was added dropwise, and the mixture was stirred at 80°C for 24 hours. The white precipitate was filtered off and the solvent removed under reduced pressure. The product was purified via flash chromatography to obtain the title ligand (1.20 g, 71.2 %) **^{1}H NMR** ($CDCl_3$) 1.29 (s, 9 H, $C(CH_3)_3$), 1.31-1.45 (m, 2 H, CH_2),1.39 (s, 9 H, $C(CH_3)_3$), 1.53-1.81 (m, 4H, CH_2),1.65 - 1.69 (m, 6 H, CH_3), 1.71 (s, 6 H, CH_3), 2.58 - 3.18 (m, 3 H, CH_2/CH), 3.43 - 4.00 (m, 4 H , CH_2), 6.82 (d, J=2.3 Hz, 1 H, Ar-H), 7.01 (d, J=2.3 Hz, 1 H, Ar-H), 7.12 - 7.32 (m, 11 H, Ar-H), 7.33 (d, J=2.3 Hz, 1 H, Ar-H), 8.21 (s, 1 H, N=CH). **^{13}C{^{1}H} NMR** ($CDCl_3$) 24.4 (CH_2), 26.01 (CH_2), 29.53 (CH_2), 29.61, 30.12, 30.65, 31.74, 31.74, 34.09, 34.82, 42.12, 42.45, 47.8 (N-CH_2), 50.8 (N-CH_2), 56.76 (N-CH_2), 66.01 (N-CH), 118.00 (Ar-C), 123.42 (Ar-C), 125.01, 125.37, 125.53, 125.58, 126.69, 126.75, 127.75, 127.98, 129.16, 135.96 (Ar), 136.04 (Ar-H), 139.56 (Ar- $C(CH_3)_2$), 142.80 (Ar-$C(CH_3)_2$) 150.65 (Ar-OH) , 150.76 (Ar-OH), 157.0 (N=CH). **m/z** calc. 673.4733 found 673.4735.

Preparation of Zr(2R)$_2$(O^{i}Pr)$_2$: To a solution of **2R**-H_2 (193 mg, 0.52 mmol) in CH_2CL_2 (25 mL) was added zirconium(IV) isopropoxide isopropanol complex (100 mg, 0.26 mmol). The resulting mixture was stirred for two hours, after which time solvent was removed *in-vacuo*. The product was washed with hexane and thoroughly dried under reduced pressure. **^{1}H NMR** ($CDCl_3$) 0.71 - 1.25 (16 H, m) 1.32 - 1.70 (10 H, m) 2.01 - 2.31 (6 H, m) 3.95 - 4.58 (4 H, m) 4.97 - 5.41 (2 H, m) 6.77 (3 H, d, J=4.1 Hz) 6.86 - 7.46 (19 H, m) 7.64 - 8.02 (4 H, m) 8.81 - 9.12 (2 H, m). **^{13}C{^{1}H} NMR** ($CDCl_3$) 20.18, 27.04, 70.08, 71.59, 122.95, 125.94, 126.19, 126.75, 128.40, 133.04, 137.52, 145.53, 157.10, 166.19. **Elemental Analysis** of $C_{60}H_{68}N_4O_4Cl_0Zr_1$. Expected; C 72.03, H 6.85, N 5.6. Found; C 72.1, H 7.1, N 5.6.

Preparation of Zr(2S)$_2$(O^{i}Pr)$_2$: To a solution of **2S**-H_2 (193 mg, 0.52 mmol) in CH_2CL_2 (25 mL) was added zirconium(IV) isopropoxide isopropanol complex (100 mg, 0.26 mmol). The resulting mixture was stirred for two hours, after which time solvent was removed *in-vacuo*. The product was washed with hexane and thoroughly dried under reduced pressure. **^{1}H NMR** ($CDCl_3$) 0.81 (1 H, s) 0.87 - 1.27 (15 H, m) 1.42 - 1.69 (9 H, m) 2.06 - 2.26 (6 H, m) 3.96 - 4.60 (4 H, m) 5.03 - 5.38 (2 H, m) 6.77 (4 H, d, J=6.2 Hz) 6.97 - 7.47 (18 H, m) 7.68 - 8.08 (4 H, m) 8.79 - 9.16 (2 H, m). **^{13}C{^{1}H} NMR** ($CDCl_3$) 20.16, 24.88, 27.01,

71.56, 122.94, 125.93, 126.17, 126.73, 127.64, 128.38, 133.02, 137.46, 145.52, 157.08, 166.15, 166.25. **Elemental Analysis** of $C_{60}H_{68}N_4O_4Zr_1$. Expected; C 72.03, H 6.85, N 5.6. Found; C 72.0, H 7.8, N 5.5.

Preparation of Zr(2E)$_2$(O^{i}Pr)$_2$: To a solution of **2E**-H_2 (207 mg, 0.52 mmol) in CH_2CL_2 (25 mL) was added zirconium(IV) isopropoxide isopropanol complex (100 mg, 0.26 mmol). The resulting mixture was stirred for two hours, after which time solvent was removed *in-vacuo*. The product was washed with hexane and thoroughly dried under reduced pressure. **^{1}H NMR** ($CDCl_3$) 0.38 (2 H, t, J=7.1 Hz) 0.72 (3 H, t, J=7.2 Hz) 0.90 (5 H, t, J=7.3 Hz) 0.94 - 1.09 (4 H, m) 1.17 (7 H, dd, J=14.9, 6.0 Hz) 1.97 (3 H, quin, J=7.2 Hz) 2.19 - 2.39 (5 H, m) 3.96 - 4.27 (2 H, m) 4.29 - 4.46 (1 H, m) 4.75 - 5.22 (2 H, m) 7.03 - 7.13 (3 H, m) 7.14 - 7.24 (5 H, m) 7.24 - 7.31 (3 H, m) 7.32 - 7.41 (3 H, m) 7.41 - 7.53 (3 H, m) 7.81 - 8.16 (3 H, m) 8.96 - 9.14 (1 H, m). **^{13}C{^{1}H} NMR** ($CDCl_3$) 11.28, 11.98, 20.18, 27.00, 69.61, 125.78, 127.14, 128.34, 129.25, 132.99, 144.97, 157.36, 165.57. **Elemental Analysis** of $C_{60}H_{74}N_4O_4Zr_1$. Expected; C 71.6, H 7.41, N 5.57. Found; C 71.4, H 7.7, N 5.7.

Preparation of Zr(2N)$_2$(O^{i}Pr)$_2$: To a solution of **2N**-H_2 (245 mg, 0.52 mmol) in CH_2CL_2 (25 mL) was added zirconium(IV) isopropoxide isopropanol complex (100 mg, 0.26 mmol). The resulting mixture was stirred for two hours, after which time solvent was removed *in-vacuo*. The product was washed with hexane and thoroughly dried under reduced pressure. **^{1}H NMR** ($CDCl_3$) 0.71 - 0.92 (1 H, m) 1.00 - 1.38 (12 H, m) 1.53 - 1.82 (8 H, m) 1.94 - 2.20 (5 H, m) 4.11 - 4.98 (3 H, m) 5.46 (1 H, br. s.) 6.59 - 6.87 (2 H, m) 6.90 - 8.09 (34 H, m) 8.89 - 9.22 (1 H, m). **^{13}C{^{1}H} NMR** ($CDCl_3$) 20.04, 21.71, 23.99, 27.11, 41.69, 62.70, 71.67, 76.62, 77.04, 77.46, 113.43, 113.75, 116.08, 117.03, 119.62, 120.33, 121.49, 121.78, 123.13, 124.30, 124.82, 125.32, 126.06, 126.80, 127.47, 127.95, 128.25, 128.66, 129.06, 133.08, 137.44, 142.90, 154.78, 161.60. **Elemental Analysis** of $C_{72}H_{74}N_4O_4Zr_1$. Expected; C 75.16, H 6.48, N 4.87. Found; C 74.9, H 7.1, N 4.6.

Preparation of Hf(2R)$_2$(O^{i}Pr)$_2$: To a solution of **2R**-H_2 (178 mg, 0.48 mmol) in CH_2CL_2 (25 mL) was added hafnium(IV) isopropoxide isopropanol adduct (100 mg, 0.24 mmol). The resulting mixture was stirred for two hours,

after which time solvent was removed *in-vacuo*. The product was washed with hexane and thoroughly dried under reduced pressure. **^{1}H NMR** ($CDCl_3$) 0.69 - 1.21 (16 H, m) 1.30 - 1.71 (10 H, m) 2.00 - 2.28 (6 H, m) 3.98 - 4.47 (4 H, m) 4.97 - 5.11 (2 H, m) 6.68 (3 H, d, J=4.1 Hz) 6.96 - 7.50 (19 H, m) 7.77 - 8.02 (4 H, m) 8.92 - 9.12 (2 H, m). **^{13}C{^{1}H} NMR** ($CDCl_3$) 20.28, 27.41, 71.65, 123.25, 126.14, 126.22, 126.57, 128.65, 133.22, 137.66, 145.89, 157.31, 165.65. **Elemental Analysis** of $C_{60}H_{68}N_4O_4Hf_1$. Expected; C 66.25, H 6.3, N 5.15. Found; C 65.9, H 6.8, N 5.0.

Preparation of Hf(2S)$_2$(O^{i}Pr)$_2$: To a solution of **2S**-H_2 (178 mg, 0.48 mmol) in CH_2CL_2 (25 mL) was added hafnium(IV) isopropoxide isopropanol adduct (100 mg, 0.24 mmol). The resulting mixture was stirred for two hours, after which time solvent was removed *in-vacuo*. The product was washed with hexane and thoroughly dried under reduced pressure. **^{1}H NMR** ($CDCl_3$) 0.79 (1 H, s) 0.88 - 1.30 (15 H, m) 1.40 - 1.70 (9 H, m) 2.11 - 2.36 (6 H, m) 3.99 - 4.60 (4 H, m) 5.13 - 5.42 (2 H, m) 6.73 (4 H, d, J=6.2 Hz) 6.88 - 7.61 (18 H, m) 7.69 - 8.18 (4 H, m) 8.80 - 9.20 (2 H, m). **^{13}C{^{1}H} NMR** ($CDCl_3$) 20.28, 27.21, 123.12, 126.02, 126.45, 126.77, 127.54, 128.49, 133.13, 137.64, 145.68, 157.18, 165.55, 165.67. **Elemental Analysis** of $C_{60}H_{68}N_4O_4Hf_1$. Expected; C 66.25, H 6.3, N 5.15. Found; C 66.0, H 6.6, N 5.1.

Preparation of Hf(2E)$_2$(O^{i}Pr)$_2$: To a solution of **2E**-H_2 (191 mg, 0.48 mmol) in CH_2CL_2 (25 mL) was added hafnium(IV) isopropoxide isopropanol adduct (100 mg, 0.24 mmol). The resulting mixture was stirred for two hours, after which time solvent was removed *in-vacuo*. The product was washed with hexane and thoroughly dried under reduced pressure. **^{1}H NMR** ($CDCl_3$) 0.36 (2 H, t, J=7.2 Hz) 0.74 (3 H, t, J=7.1 Hz) 0.91 (6 H, t, J=7.3 Hz) 0.93 - 1.21 (11 H, m) 1.97 (3 H, m) 2.12 - 2.35 (5 H, m) 4.01 - 4.28 (2 H, m) 4.29 - 4.50 (1 H, m) 4.75 - 5.25 (2 H, m) 6.93 - 7.03 (3 H, m) 7.19 - 7.30 (6 H, m) 7.32 - 7.40 (6 H, m) 7.42 - 7.52 (3 H, m) 7.72 - 7.87 (3 H, m) 8.50 - 8.65 (1 H, m). **^{13}C{^{1}H} NMR** ($CDCl_3$) 12.28, 20.32, 26.00, 68.79, 71.23, 124.32, 126.25, 127.94, 129.36, 131.56, 145.35, 154.92, 161.17. **Elemental Analysis** of $C_{60}H_{74}N_4O_4Hf_1$. Expected; C 65.89, H 6.82, N 5.12. Found; C 65.9, H 7.3, N 4.9.

Preparation of $Hf(2N)_2(O^iPr)_2$: To a solution of **2N**-H_2 (226 mg, 0.48 mmol) in CH_2CL_2 (25 mL) was added hafnium(IV) isopropoxide isopropanol adduct (100 mg, 0.24 mmol). The resulting mixture was stirred for two hours, after which time solvent was removed *in-vacuo*. The product was washed with hexane and thoroughly dried under reduced pressure. **^{1}H NMR** ($CDCl_3$) 0.8 1(1 H, s) 1.00 - 1.40 (12 H, m) 1.50 - 1.85 (8 H, m) 1.95 - 2.20 (5 H, m) 4.11 - 4.69 (3 H, m) 5.36 (1 H, s) 6.62 - 6.78 (2 H, m) 6.87 - 8.12 (30 H, m) 8.90 - 9.12 (1 H, m). **^{13}C{^{1}H} NMR** ($CDCl_3$) 19.34, 20.36, 23.49, 27.24(1 C, s) 61.42, 112.54, 113.45, 115.77, 116.52, 118.42, 121.11, 121.77, 121.78, 124.26, 124.78, 125.48, 126.18, 127.11, 127.38, 128.04, 128.51, 129.64, 132.78, 142.89, 155.37, 160.86. **Elemental Analysis** of $C_{72}H_{74}N_4O_4Hf_1$. Expected; C 69.86, H 6.03, N 4.53. Found; C 70.1, H 5.1, N 4.4.

Preparation of $Ti(2R)_2(O^iPr)_2$: To a solution of **2R**-H_2 (222 mg, 0.60 mmol) in CH_2CL_2 (25 mL) was added titanium(IV) isopropoxide (0.08 mL, 0.29 mmol). The resulting mixture was stirred for two hours, after which time solvent was removed *in-vacuo*. The product was washed with hexane and thoroughly dried under reduced pressure. **^{1}H NMR** ($CDCl_3$) 0.65 - 1.12 (15H, m), 1.25 - 1.56 (7H, m), 1.59 - 1.69 (4H, m), 1.97 - 2.25 (6H, m), 3.89 - 3.95 (2H, m), 4.58 - 4.63 (1H, m), 4.68 - 4.75 (3H, m), 6.62 - 6.68 (3H, m), 7.01 - 7.45 (16H, m), 7.49 - 7.52 (3H, m), 7.66 - 7.99 (4 H, m), 8.12 (2H, s), 8.34 (2H, s). **^{13}C^{1}H NMR** ($CDCl_3$) 19.99, 21.03, 26.32, 26.84, 71.23, 75.36, 122.36, 122.48, 122.95, 123.34, 123.84, 124.00, 124.59, 127.36, 128.26, 129.73, 130.15, 135.69, 135.87, 136.88, 145.02, 145.68, 158.39, 161.23, 162.35. **Elemental Analysis** of $C_{60}H_{68}N_4O_4Ti_1$. Expected; C 75.3, H 7.16, N 5.85. Found; C 75.3, H 6.5, N 5.2.

Preparation of $Ti(2S)_2(O^iPr)_2$: To a solution of **2S**-H_2 (222 mg, 0.60 mmol) in CH_2CL_2 (25 mL) was added titanium(IV) isopropoxide (0.08 mL, 0.29 mmol). The resulting mixture was stirred for two hours, after which time solvent was removed *in-vacuo*. The product was washed with hexane and thoroughly dried under reduced pressure. **^{1}H NMR** ($CDCl_3$) 0.67 - 1.13 (16H, m), 1.24 - 1.54 (6H, m), 1.60 - 1.71 (4H, m), 1.95 - 2.25 (6H, m), 3.85 - 3.91 (2H, m), 4.86 - 4.75 (H, m), 6.64 - 6.69 (3H, m), 7.03 - 7.42 (17H, m), 7.48 - 7.55 (2H, m), 7.68 - 8.02 (4 H, m), 8.14 (2H, s), 8.32 (2H, s). **^{13}C{^{1}H} NMR** ($CDCl_3$) 20.12, 20.89, 26.75, 27.19, 70.89, 74.80, 121.86, 122.69, 122.94, 128.59, 128.67, 129.56,

130.59, 135.45, 135.84, 137.06, 145.09, 145.72, 158.21, 160.45, 162.11. **Elemental Analysis** of $C_{60}H_{68}N_4O_4Ti_1$. Expected; C 75.3, H 7.16, N 5.85. Found; C 75.4, H 6.3, N 5.3.

Preparation of Ti(2E)$_2$(O^{i}Pr)$_2$: To a solution of **2E**-H_2 (239 mg, 0.60 mmol) in CH_2CL_2 (25 mL) was added titanium(IV) isopropoxide (0.08 mL, 0.29 mmol). The resulting mixture was stirred for two hours, after which time solvent was removed *in-vacuo*. The product was washed with hexane and thoroughly dried under reduced pressure. **^{1}H NMR** ($CDCl_3$) 0.89 - 0.95 (6H, m), 1.15 (3H, s), 1.19 - 1.23 (9H, m), 1.59 - 1.63 (4H, m), 4.05 - 4.54 (2H, m), 6.65 - 6.68 (1H, m), 6.70 - 6.73 (2H, m), 6.84 - 6.87 (1H, m), 7.10 - 7.19 (5H, m), 7.22 - 7.35 (5H, m), 7.64 - 7.71 (2H, m), 8.11 (1H, s), 8.25 (1H, s). **^{13}C{^{1}H} NMR** ($CDCl_3$) 9.98, 10.11, 25.61, 25.68, 28.69, 29.65, 31.23, 31.85, 32.16, 32.26, 33.15, 68.59, 72.69, 73.15, 124.36, 124.89, 125.12, 125.69, 125.87, 126.48, 126.85, 128.23, 129.11, 129.58, 130.25, 131.65, 138.54, 129.26, 135.12, 136.03, 139.65, 140.15, 153.26, 153.29, 160.29, 161.59. **Elemental Analysis** of $C_{60}H_{74}N_4O_4Ti_1$. Expected; C 74.82, H 7.74, N 5.82. Found; C 75.1, H 7.7, N 5.1.

Preparation of Ti(2N)$_2$(O^{i}Pr)$_2$: To a solution of **2N**-H_2 (282 mg, 0.60 mmol) in CH_2CL_2 (25 mL) was added titanium(IV) isopropoxide (0.08 mL, 0.29 mmol). The resulting mixture was stirred for two hours, after which time solvent was removed *in-vacuo*. The product was washed with hexane and thoroughly dried under reduced pressure. **^{1}H NMR** ($CDCl_3$) 1.10 (12H, d, *J*=6.8 Hz), 1.59 - 1.62 (3H, m), 1.65 - 1.67 (3H, m), 2.12 (3H, br. s.), 3.61 - 3.65 (2H, m), 4.53 - 4.69 (4H, m), 6.87 - 6.98 (3H, m), 7.01 - 7.50 (16H, m), 7.58 - 8.02 (13H, m), 8.12 (2H, s), 8.35 (2H, s). **^{13}C{^{1}H} NMR** ($CDCl_3$) 20.15, 20.86, 21.02, 32.26, 70.23, 73.29, 125.36, 125.48, 125.87, 126.01, 126.12, 126.24, 126.35, 126.48, 126.79, 127.59, 128.19, 129.20, 135.12, 135.20, 135.25, 136.17, 157.89, 160.29, 162.25. **Elemental Analysis** of $C_{72}H_{74}N_4O_4Ti_1$. Expected; C 78.1, H 6.74, N 5.06. Found; C 77.8, H 6.0, N 4.8.

Preparation of Al(2R)$_2$(O^{i}Pr)$_2$: To a solution of **2R**-H_2 (296 mg, 0.80 mmol) in Tol (20 mL) was added trimethyl aluminium (0.2 mL, 0.40 mmol). The resulting mixture was stirred for two hours, after which time solvent was removed *in-vacuo*. The product was washed with hexane and thoroughly dried under

reduced pressure. **^{1}H NMR** ($CDCl_3$) 0.98 - 1.08 (14 H, m) 1.18 (3 H, dd, J=6.0, 1.9 Hz) 1.55 - 1.70 (3 H, m) 2.07 - 2.16 (9 H, m) 4.63 (3 H, br. s.) 6.69 - 6.77 (6 H, m) 7.04 (4 H, dd, J=8.5, 2.1 Hz) 7.12 (7 H, br. s.) 7.20 - 7.31 (1 H, m) 7.77 (2 H, s). **^{13}C{^{1}H} NMR** ($CDCl_3$) 11.83, 20.28, 20.97, 25.35, 25.49, 25.52, 45.59, 78.06, 118.88, 120.35, 122.27, 124.30, 126.06, 127.34, 128.29, 128.35, 129.56, 130.88, 133.73, 135.08, 136.54, 161.29. **Elemental Analysis** of $C_{27}H_{32}N_2O_1Al_1$. Expected; C 75.85, H 7.54, N 6.55. Found; C 75.6, H 8.1, N 6.2.

Preparation of Al(2S)$_2$(O^{i}Pr)$_2$: To a solution of **2S**-H_2 (296 mg, 0.80 mmol) in Tol (20 mL) was added trimethyl aluminium (0.2 mL, 0.40 mmol). The resulting mixture was stirred for two hours, after which time solvent was removed *in-vacuo*. The product was washed with hexane and thoroughly dried under reduced pressure. **^{1}H NMR** ($CDCl_3$) 0.96 - 1.05 (14 H, m) 1.16 (3 H, d, J=6.0) 1.53 - 1.71 (3 H, m) 2.11 - 2.17 (9 H, m) 4.61 (3 H, br. s.) 6.71 - 6.76 (6 H, m) 7.05 (4 H, dd, J=8.5, 2.0 Hz) 7.12 (7 H, m) 7.19 - 7.20 (1 H, m) 7.80 (2 H, s). **^{13}C{^{1}H} NMR** ($CDCl_3$) 11.94, 20.36, 25.23, 26.31, 26.62, 45.48, 119.02, 120.87, 121.98, 124.40, 126.23, 127.43, 127.79, 128.13, 129.16, 131.74, 132.35, 135.24, 136.56, 160.76. **Elemental Analysis** of $C_{27}H_{32}N_2O_1Al_1$. Expected; C 75.85, H 7.54, N 6.55. Found; C 75.5, H 7.8, N 6.5.

Preparation of Al(2E)$_2$(O^{i}Pr)$_2$: To a solution of **2E**-H_2 (319 mg, 0.80 mmol) in Tol (20 mL) was added trimethyl aluminium (0.2 mL, 0.40 mmol). The resulting mixture was stirred for two hours, after which time solvent was removed *in-vacuo*. The product was washed with hexane and thoroughly dried under reduced pressure. **^{1}H NMR** ($CDCl_3$) -0.75 (3H, s) 0.84 - 0.98 (6H, m) 1.84 - 2.10 (2H, m) 2.12 - 2.17 (2H, m) 2.34 - 2.41 (3H, m) 4.39 - 4.42 (1H, m) 4.98 - 5.11 (1H, m) 6.12 - 6.36 (2H, m) 7.11 - 7.23 (6H, m) 7.36 - 7.58 (4H, m) 7.69 - 7.75 (1H, m) 8.42 (1H, s) 8.57 (1H, s). **^{13}C{^{1}H} NMR** ($CDCl_3$) 10.12, 10.22, 22.03, 31.16, 31.95, 67.52, 68.12, 120.12, 120.35, 120.40, 121.56, 127.56, 127.84, 127.99, 128.11, 128.36, 129.47, 133.11, 133.25, 133.41, 157.36, 163.21, 164.21. **Elemental Analysis** of $C_{29}H_{36}N_2O_1Al_1$. Expected; C 76.45, H 7.96, N 6.15. Found; C 76.6, H 8.0, N 6.1.

Preparation of Al(2N)$_2$(O^{i}Pr)$_2$: To a solution of **2N**-H_2 (376 mg, 0.80 mmol) in Tol (20 mL) was added trimethyl aluminium (0.2 mL, 0.40 mmol). The

resulting mixture was stirred for two hours, after which time solvent was removed *in-vacuo*. The product was washed with hexane and thoroughly dried under reduced pressure. **^{1}H NMR** ($CDCl_3$) -0.76 (3H, s),1.70 - 1.74 (3H, m), 1.75 - 1.79 (3H, m), 2.23 - 2.29 (3H, m), 4.42 - 4.53 (1H, m), 6.02 - 6.23 (2H, m), 6.74 - 6.85 (4H, m), 7.11 - 7.23 (2H, m), 7.35 - 7.55 (4H, m), 7.72 - 7.79 (1H, m), 7.80 - 7.82 (1H, m), 7.85 - 7.91 (2H, m), 8.12 - 8.23 (2H, m). **^{13}C{^{1}H} NMR** ($CDCl_3$) 19.23, 22.12, 23.69, 70.12, 70.36, 119.25, 119.62, 120.56, 121.84, 122.12, 122.56, 122.78, 123.69, 124.25, 125.48, 127.15, 127.59, 134.26, 135.26, 135.84, 137.26, 138.59, 139.12, 139.65, 153.26, 161.25. **Elemental Analysis** of $C_{35}H_{36}N_2O_1Al_1$. Expected; C 79.67, H 6.88, N 5.31. Found; C 80., H 7.4, N 5.3.

Preparation of Zr(EH)$_2$(O^{i}Pr)$_2$: To a solution of **EH**-H_2 (134 mg, 0.52 mmol) in CH_2CL_2 (25 mL) was added zirconium(IV) isopropoxide isopropanol complex (100 mg, 0.26 mmol). The resulting mixture was stirred for two hours, after which time solvent was removed *in-vacuo*. The product was washed with hexane and thoroughly dried under reduced pressure. **^{1}H NMR** ($CDCl_3$) 0.29 - 0.44 (2 H, m) 0.77 (3 H, br. s.) 0.92 (2 H, d, J=7.2 Hz) 0.98 - 1.03 (1 H, m) 1.05 - 1.16 (4 H, m) 1.18 - 1.27 (3 H, m) 1.37 - 1.41 (1 H, m) 1.64 - 1.87 (2 H, m) 4.11 - 4.25 (1 H, m) 4.29 - 4.41 (1 H, m) 4.82 - 4.95 (1 H, m) 5.26 - 5.41 (1 H, m) 6.64 - 6.78 (3 H, m) 6.93 (2 H, d, J=7.9 Hz) 7.10 (4 H, dd, J=15.6, 7.7 Hz) 7.29 - 7.38 (3 H, m) 7.80 - 7.90 (1 H, m) 8.01 - 8.11 (1 H, m). **^{13}C^{1}H NMR** ($CDCl_3$) 13.37, 13.53, 18.39, 26.76, 37.88, 39.84, 71.51, 77.25, 113.47, 117.02, 120.42, 122.55, 127.49, 128.35, 129.31, 129.92, 132.36, 134.52, 161.02, 163.95. **Elemental Analysis** of $C_{38}H_{48}N_2O_4Zr_1$. Expected; C 66.34, H 7.03, N 4.07. Found; C 66.9, H 6.6, N 4.2.

Preparation of Zr(E5)$_2$(O^{i}Pr)$_2$: To a solution of **E5**-H_2 (141 mg, 0.52 mmol) in CH_2CL_2 (25 mL) was added zirconium(IV) isopropoxide isopropanol complex (100 mg, 0.26 mmol). The resulting mixture was stirred for two hours, after which time solvent was removed *in-vacuo*. The product was washed with hexane and thoroughly dried under reduced pressure. **^{1}H NMR** ($CDCl_3$) 0.29 - 0.39 (2 H, m) 0.77-0.85 (5 H, m) 0.92-0.95 (3 H, m) 1.03 - 1.15 (4 H, m) 1.20 - 1.25 (3 H, m) 1.35 - 1.39 (1 H, m) 1.59 - 1.79 (2 H, m) 4.01 - 4.18 (1 H, m) 4.32 - 4.44 (1 H, m) 4.79 - 4.91 (1 H, m) 6.59 - 6.70 (2 H, m) 6.75 - 6.87 (3 H, m) 7.10-7.13 (4 H, m) 7.31 - 7.37 (3 H, m) 7.80 - 7.95 (1 H, m) 7.99 - 8.09 (1 H, m).

$^{13}C\{^{1}H\}$ NMR ($CDCl_3$) 13.25, 14.56, 17.29, 26.44, 38.02, 39.75, 77.33, 112.84, 117.45, 121.31, 123.49, 127.19, 128.48, 129.45, 131.74, 134.51, 160.82. **Elemental Analysis** of $C_{40}H_{54}N_2O_4Zr_1$. Expected; C 66.9, H 7.58, N 3.9. Found; C 70.1, H 6.9, N 3.8.

Preparation of $Zr(EB)_2(O^iPr)_2$: To a solution of **EB**-H_2 (192 mg, 0.52 mmol) in CH_2CL_2 (25 mL) was added zirconium(IV) isopropoxide isopropanol complex (100 mg, 0.26 mmol). The resulting mixture was stirred for two hours, after which time solvent was removed *in-vacuo*. The product was washed with hexane and thoroughly dried under reduced pressure. **^{1}H NMR** ($CDCl_3$) 0.60 - 0.68 (1 H, m) 0.84 (5 H, t, J=7.3 Hz) 0.99 - 1.10 (5 H, m) 1.22 (14 H, s) 1.38 (14 H, s) 1.49 (8 H, d, J=11.7 Hz) 1.83 - 1.95 (3 H, m) 4.04 - 4.14 (2 H, m) 4.28 - 4.49 (1 H, m) 5.00 - 5.07 (1 H, m) 6.43 - 6.48 (1 H, m) 6.62 - 6.65 (1 H, m) 6.70 - 6.79 (1 H, m) 7.00 (2 H, d, J=2.3 Hz) 7.15 (3 H, s) 7.26 (2 H, s) 7.28 (2 H, s) 7.30 (2 H, d, J=2.3 Hz) 7.34 - 7.36 (1 H, m) 7.39 - 7.43 (1 H, m) 7.78 - 7.84 (1 H, m) 8.31 (2 H, s). **$^{13}C\{^{1}H\}$ NMR** ($CDCl_3$) 9.51, 10.05, 10.40, 26.44, 26.57, 26.59, 28.40, 28.88, 28.97, 30.42, 30.46, 30.57, 30.75, 33.08, 34.00, 34.26, 66.37, 69.73, 69.92, 74.81, 116.85, 121.37, 124.97, 125.55, 125.85, 125.87, 126.07, 126.19, 126.80, 127.23, 127.26, 127.43, 127.50, 127.60, 128.24, 128.29, 135.55, 137.32, 137.81, 138.11, 138.74, 138.97, 142.25, 156.99, 158.84, 163.96, 166.93, 168.23. **Elemental Analysis** of $C_{54}H_{80}N_2O_4Zr_1$. Expected; C 71.08, H 8.84, N 3.07. Found; C 71.6, H 7.9, N 2.8.

Preparation of $Zr(EC)_2(O^iPr)_2$: To a solution of **EC**-H_2 (170 mg, 0.52 mmol) in CH_2CL_2 (25 mL) was added zirconium(IV) isopropoxide isopropanol complex (100 mg, 0.26 mmol). The resulting mixture was stirred for two hours, after which time solvent was removed *in-vacuo*. The product was washed with hexane and thoroughly dried under reduced pressure. **^{1}H NMR** ($CDCl_3$) 1.31 - 1.57 (3 H, m) 1.59 - 1.72 (4 H, m) 1.75 - 2.04 (5 H, m) 4.63 - 5.39 (3 H, m) 6.90 - 6.93 (1 H, m) 7.06 (3 H, d, J=2.4 Hz) 7.26 - 7.29 (2 H, m) 7.39 (2 H, m) 7.44 - 7.47 (1 H, m) 7.56 - 7.58 (1 H, m) 7.69 (2 H, s) 7.94 - 7.99 (1 H, m). **$^{13}C\{^{1}H\}$ NMR** ($CDCl_3$) 23.65, 57.26 - 57.75, 124.25, 126.22, 127.01, 128.02, 128.70, 129.65, 130.59, 131.56, 132.38, 134.24, 156.97, 161.71. **Elemental Analysis** of $C_{38}H_{44}N_2O_4Cl_4Zr_1$. Expected; C 55.27, H 5.37, N 3.39. Found; C 55.5, H 4.8, N 3.1.

Preparation of $Hf(EH)_2(O^iPr)_2$: To a solution of **EH**-H_2 (124 mg, 0.48 mmol) in CH_2CL_2 (25 mL) was added hafnium(IV) isopropoxide isopropanol adduct (100 mg, 0.24 mmol). The resulting mixture was stirred for two hours, after which time solvent was removed *in-vacuo*. The product was washed with hexane and thoroughly dried under reduced pressure. **^{1}H NMR** ($CDCl_3$) 1.05 - 1.19 (1 H, m) 1.36 - 1.75 (8 H, m) 2.08 - 2.22 (4 H, m) 4.43 - 4.96 (2 H, m) 6.85 - 7.15 (4 H, m) 7.19 - 7.41 (12 H, m) 7.92 - 8.00 (2 H, m). **^{13}C{^{1}H} NMR** ($CDCl_3$) 20.04, 21.23, 24.63, 63.04, 70.66, 76.94, 119.75, 126.32, 126.61, 127.25, 127.70, 128.11, 128.31, 128.55, 128.85, 135.41, 137.21, 145.97, 155.76, 163.19. **Elemental Analysis** of $C_{38}H_{48}N_2O_4Hf_1$. Expected; C 58.87, H 6.24, N 3.61. Found; C 60.2, H 5.8, N 3.5.

Preparation of $Hf(E5)_2(O^iPr)_2$: To a solution of **E5**-H_2 (130 mg, 0.48 mmol) in CH_2CL_2 (25 mL) was added hafnium(IV) isopropoxide isopropanol adduct (100 mg, 0.24 mmol). The resulting mixture was stirred for two hours, after which time solvent was removed *in-vacuo*. The product was washed with hexane and thoroughly dried under reduced pressure. **^{1}H NMR** ($CDCl_3$) 0.54 (6 H, d, J=12.4 Hz) 0.88 - 1.04 (2 H, m) 1.20 - 1.42 (2 H, m) 1.55 - 1.82 (2 H, m) 2.55 - 2.78 (1 H, m) 4.60 - 4.96 (3 H, m) 6.70 - 6.90 (2 H, m) 7.03 (1 H, m, J=2.6 Hz) 7.10 - 7.29 (6 H, m) 7.33 - 7.48 (4 H, m) 7.91 (2 H, s). **^{13}C{^{1}H} NMR** ($CDCl_3$) 10.76, 27.70, 77.58, 118.31, 119.65, 121.13, 125.04, 127.45, 128.57, 129.91, 130.91, 155.49, 160.52. **Elemental Analysis** of $C_{40}H_{54}N_2O_4Hf_1$. Expected; C 59.65, H 6.76, N 3.48. Found; C 59.6, H 7.0, N 3.5.

Preparation of $Hf(EB)_2(O^iPr)_2$: To a solution of **EB**-H_2 (177 mg, 0.48 mmol) in CH_2CL_2 (25 mL) was added hafnium(IV) isopropoxide isopropanol adduct (100 mg, 0.24 mmol). The resulting mixture was stirred for two hours, after which time solvent was removed *in-vacuo*. The product was washed with hexane and thoroughly dried under reduced pressure. **^{1}H NMR** ($CDCl_3$) 0.60 (9 H, d, J=13.2 Hz) 0.81 - 0.89 (1 H, m) 1.03 (5 H, s) 1.05 (4 H, s) 1.19 - 1.35 (2 H, m) 1.56 - 1.76 (4 H, m) 1.88 - 1.95 (1 H, m) 2.48 - 2.71 (2 H, m) 4.56 - 4.88 (5 H, m) 6.67 - 6.80 (4 H, m) 6.91 (3 H, d, J=2.6 Hz) 7.10 (7 H, ddd, J=16.7, 4.8, 2.6 Hz) 7.27 (4 H, br. s.) 7.36 (3 H, d, J=2.6 Hz) 7.82 (3 H, s). **^{13}C{^{1}H} NMR** ($CDCl_3$) 10.75, 12.30, 24.30, 24.38, 30.44 - 30.52, 68.84 - 69.43, 76.18, 79.00, 119.40, 122.25, 123.32 - 123.85, 125.77, 126.74, 126.91, 127.45, 127.80, 128.34,

130.21, 132.04, 156.81, 161.24. **Elemental Analysis** of $C_{54}H_{80}N_2O_4Hf_1$. Expected; C 64.88, H 8.07, N 2.8. Found; C 64.6, H 8.5, N 2.6.

Preparation of Hf(EC)$_2$(O^{i}Pr)$_2$: To a solution of **EC**-H_2 (157 mg, 0.48 mmol) in CH_2CL_2 (25 mL) was added hafnium(IV) isopropoxide isopropanol adduct (100 mg, 0.24 mmol). The resulting mixture was stirred for two hours, after which time solvent was removed *in-vacuo*. The product was washed with hexane and thoroughly dried under reduced pressure. **^{1}H NMR** ($CDCl_3$) 0.96 (3 H, t, J=7.3 Hz) 1.10 - 1.31 (6 H, m) 1.54 - 1.70 (1 H, m) 1.95 - 2.09 (1 H, m) 4.18 - 4.27 (1 H, m) 4.42 - 4.64 (1 H, m) 7.12 (1 H, d, J=2.4 Hz) 7.27 (1 H, s) 7.37 - 7.55 (4 H, m) 8.44 (1 H, s). **^{13}C{^{1}H} NMR** ($CDCl_3$) 10.68, 11.37, 16.11, 27.34, 29.40, 33.97, 67.49, 71.02, 77.14, 118.06, 126.20, 126.32, 126.78, 127.05, 127.44, 127.66, 128.10, 128.90, 129.16, 136.71, 138.09, 138.90, 139.35, 143.42, 159.97, 163.49. **Elemental Analysis** of $C_{38}H_{44}N_2O_4Cl_4Hf_1$. Expected; C 49.99, H 4.86, N 3.07. Found; C 49.6, H 5.8, N 2.7.

Preparation of Ti(EH)$_2$(O^{i}Pr)$_2$: To a solution of **EH**-H_2 (154 mg, 0.60 mmol) in CH_2CL_2 (25 mL) was added titanium(IV) isopropoxide (0.08 mL, 0.29 mmol). The resulting mixture was stirred for two hours, after which time solvent was removed *in-vacuo*. The product was washed with hexane and thoroughly dried under reduced pressure. **^{1}H NMR** ($CDCl_3$) 0.96 - 1.26 (2 H, m) 1.40 - 1.79 (18 H, m) 2.03 - 2.24 (10 H, m) 4.50 (3 H, d, J=6.4 Hz) 4.70 - 4.72 (1 H, m) 7.10 - 7.15 (3 H, m) 7.23 (3 H, br. s.) 7.25 (6 H, br. s.) 7.27 - 7.31 (5 H, m) 7.31 - 7.41 (8 H, m) 7.78 - 7.95 (2 H, m) 8.82 (2 H, s). **^{13}C{^{1}H} NMR** ($CDCl_3$) 20.05, 20.91, 24.91, 63.36, 70.06, 77.28, 119.50, 126.46, 126.69, 127.11, 127.86, 128.40, 128.62, 129.09, 135.54, 137.35, 139.27, 145.63, 155.94, 161.47, 169.60. **Elemental Analysis** of $C_{38}H_{48}N_2O_4Ti_1$. Expected; C 70.8, H 7.5, N 4.35. Found; C 71.0, H 7.6, N 4.0.

Preparation of Ti(E5)$_2$(O^{i}Pr)$_2$: To a solution of **E5**-H_2 (163 mg, 0.60 mmol) in CH_2CL_2 (25 mL) was added titanium(IV) isopropoxide (0.08 mL, 0.29 mmol). The resulting mixture was stirred for two hours, after which time solvent was removed *in-vacuo*. The product was washed with hexane and thoroughly dried under reduced pressure. **^{1}H NMR** ($CDCl_3$) 0.96 (3 H, t, J=7.3 Hz) 1.18 (3 H, s) 1.25 - 1.29 (3 H, m) 1.61 (4 H, d, J=11.7 Hz) 1.94 - 2.08 (2 H, m) 4.16 -

4.64 (2 H, m) 6.55 - 6.62 (1 H, m) 6.74 - 6.93 (1 H, m) 7.12 (1 H, d, J=2.4 Hz) 7.27 (1 H, s) 7.33 - 7.44 (5 H, m) 7.45 - 7.55 (1 H, m) 8.44 (1 H, s). **$^{13}C\{^{1}H\}$ NMR** ($CDCl_3$) 10.12, 11.00, 27.05, 29.48, 33.69, 34.87, 66.98, 70.33, 117.45, 125.57, 127.41, 128.10, 136.16, 137.93, 139.34, 139.57, 142.85, 157.60, 159.45, 167.54, 168.84. **Elemental Analysis** of $C_{40}H_{54}N_2O_4Ti_1$. Expected; C 71.2, H 8.07, N 4.15. Found; C 71.3, H 8.7, N 3.8.

Preparation of Ti(EB)$_2$(O^{i}Pr)$_2$: To a solution of **EB**-H_2 (222 mg, 0.60 mmol) in CH_2CL_2 (25 mL) was added titanium(IV) isopropoxide (0.08 mL, 0.29 mmol). The resulting mixture was stirred for two hours, after which time solvent was removed *in-vacuo*. The product was washed with hexane and thoroughly dried under reduced pressure. **^{1}H NMR** ($CDCl_3$) 0.93 (8 H, d, J=5.7 Hz) 1.10 - 1.15 (7 H, m) 1.15 - 1.20 (21 H, m) 1.20 - 1.26 (8 H, m) 1.36 - 1.41 (9 H, m) 1.51 (7 H, d, J=6.4 Hz) 4.81 - 4.93 (2 H, m) 6.67 - 6.79 (1 H, m) 6.83 - 6.87 (1 H, m) 6.88 - 6.97 (1 H, m) 6.98 - 7.01 (1 H, m) 7.16 - 7.22 (1 H, m) 7.22 - 7.24 (1 H, m) 7.25 - 7.32 (3 H, m) 7.33 - 7.35 (1 H, m) 7.35 - 7.37 (1 H, m) 7.39 - 7.41 (1 H, m) 7.41 - 7.44 (1 H, m) 7.45 - 7.47 (1 H, m) 7.48 - 7.51 (1 H, m) 7.97 - 8.00 (1 H, m). **$^{13}C\{^{1}H\}$ NMR** ($CDCl_3$) 11.97, 26.05, 26.64, 27.08, 29.48, 30.27, 31.47, 34.10, 35.26, 68.00, 75.84, 77.70, 121.22, 126.92, 127.02, 127.06, 127.66, 128.20, 128.50, 128.53, 128.87, 129.55, 137.72, 138.50, 139.57, 141.02, 143.29, 159.63, 165.39. **Elemental Analysis** of $C_{54}H_{80}N_2O_4Ti_1$. Expected; C 74.63, H 9.28, N 3.22. Found; C 74.2, H 9.4, N 3.1.

Preparation of Ti(EC)$_2$(O^{i}Pr)$_2$: To a solution of **EC**-H_2 (196 mg, 0.60 mmol) in CH_2CL_2 (25 mL) was added titanium(IV) isopropoxide (0.08 mL, 0.29 mmol). The resulting mixture was stirred for two hours, after which time solvent was removed *in-vacuo*. The product was washed with hexane and thoroughly dried under reduced pressure. **^{1}H NMR** ($CDCl_3$) 1.36 - 1.75 (18 H, m) 2.14 (10 H, s) 4.50 (2 H, d, J=6.4 Hz) 4.88 (2 H, d, J=6.8 Hz) 6.88 (2 H, d, J=2.3 Hz) 7.13 - 7.17 (4 H, m) 7.20 - 7.23 (4 H, m) 7.25 (6 H, d, J=1.9 Hz) 7.29 (3 H, br. s.) 7.31 (2 H, d, J=1.9 Hz) 7.35 (4 H, s) 7.37 (2 H, s) 7.76 - 8.04 (5 H, m) 8.82 (2 H, s). **$^{13}C\{^{1}H\}$ NMR** ($CDCl_3$) 20.07, 20.92, 24.93, 63.39, 70.07, 77.31, 119.52, 126.48, 126.71, 127.11, 127.87, 128.41, 128.63, 129.09, 135.55, 137.38, 139.28, 145.64, 155.95, 161.48, 169.62. **Elemental Analysis** of $C_{38}H_{44}N_2O_4Cl_4Ti_1$. Expected; C 58.33, H 5.67, N 3.58. Found; C 58.7, H 5.5, N 3.3.

Preparation of Al(EH)(Me)$_2$: To a solution of **EH**-H_2 (206 mg, 0.80 mmol) in Tol (20 mL) was added trimethyl aluminium (0.2 mL, 0.40 mmol). The resulting mixture was stirred for two hours, after which time solvent was removed *in-vacuo*. The product was washed with hexane and thoroughly dried under reduced pressure. **^{1}H NMR** ($CDCl_3$) -0.77 (2 H, s) 0.84 (3 H, t, J=7.3 Hz) 0.92 - 1.03 (8 H, m) 1.22 (1 H, s) 1.38 (1 H, s) 1.90 (3 H, quin, J=7.3 Hz) 1.97 - 2.16 (4 H, m) 2.55 - 2.69 (2 H, m) 4.14 (2 H, s) 6.66 (5 H, s) 6.71 - 6.84 (4 H, m) 6.91 (2 H, d, J=1.1 Hz) 7.04 (1 H, d, J=1.5 Hz) 7.07 (1 H, d, J=1.9 Hz) 7.17 (1 H, d, J=1.9 Hz) 7.20 - 7.25 (4 H, m) 7.26 (1 H, d, J=1.9 Hz) 7.27 (3 H, d, J=1.1 Hz) 7.28 - 7.29 (2 H, m) 7.31 (2 H, t, J=2.1 Hz) 7.33 (1 H, d, J=1.5 Hz) 7.44 (1 H, s) 7.46 (1 H, s) 8.07 (4 H, s) 8.32 (2 H, s) 13.54 (1 H, s). **^{13}C{^{1}H} NMR** ($CDCl_3$) 11.88, 11.92, 22.54, 37.82, 45.00, 66.54, 77.24, 91.09, 116.83, 118.63, 120.90, 126.84, 127.72, 127.98, 128.44, 128.65, 128.94, 132.30, 133.39, 139.41, 157.29, 161.13. **Elemental Analysis** of $C_{18}H_{23}N_1O_1Al_1$. Expected; C 72.95, H 7.82, N 4.73. Found; C 73.5, H 7.6, N 4.7.

Preparation of Al(E5)(Me)$_2$: To a solution of **E5**-H_2 (217 mg, 0.80 mmol) in Tol (20 mL) was added trimethyl aluminium (0.2 mL, 0.40 mmol). The resulting mixture was stirred for two hours, after which time solvent was removed *in-vacuo*. The product was washed with hexane and thoroughly dried under reduced pressure. **^{1}H NMR** ($CDCl_3$) -0.81 (1 H, s) 0.81 (1 H, t, J=7.3 Hz) 0.95 (2 H, dt, J=12.8, 7.3 Hz) 1.83 - 1.90 (1 H, m) 1.90 - 2.08 (1 H, m) 2.09 - 2.19 (4 H, m) 2.26 (1 H, s) 2.53 - 2.70 (1 H, m) 4.09 (1 H, t, J=6.8 Hz) 5.12 (1 H, dd, J=10.5, 4.1 Hz) 6.02 (1 H, d, J=8.7 Hz) 6.68 (1 H, d, J=8.3 Hz) 6.75 - 6.84 (1 H, m) 6.87 - 6.95 (1 H, m) 7.00 - 7.37 (7 H, m) 7.44 (1 H, d, J=7.2 Hz) 7.99 (2 H, s). **^{13}C{^{1}H} NMR** ($CDCl_3$) 11.99, 20.24, 28.60, 31.91, 66.20, 66.58, 75.83, 116.76, 118.54, 120.70, 125.72, 126.89, 127.29, 128.10, 128.46, 128.67, 129.02, 131.52, 133.14, 135.35, 158.90, 165.48. **Elemental Analysis** of $C_{19}H_{25}N_1O_1Al_1$. Expected; C 73.52, H 8.12, N 4.51. Found; C 74.1, H 8.7, N 4.5.

Preparation of Al(EB)(Me)$_2$: To a solution of **EB**-H_2 (296 mg, 0.80 mmol) in Tol (20 mL) was added trimethyl aluminium (0.2 mL, 0.40 mmol). The resulting mixture was stirred for two hours, after which time solvent was removed *in-vacuo*. The product was washed with hexane and thoroughly dried under reduced pressure. **^{1}H NMR** ($CDCl_3$) -0.88 (7 H, s) 0.89 (3 H, s) 1.20 (17 H, s)

1.29 (9 H, s) 1.38 (1 H, s) 2.05 - 2.20 (2 H, m) 4.40 - 4.49 (1 H, m) 6.85 - 6.89 (1 H, m) 6.98 - 7.01 (1 H, m) 7.10 - 7.12 (1 H, m) 7.20 - 7.22 (1 H, m) 7.27 (5 H, d, J=3.4 Hz) 7.39 - 7.44 (1 H, m). **$^{13}C\{^{1}H\}$ NMR** ($CDCl_3$) 10.40, 26.11, 28.19, 28.41, 30.29, 30.46, 32.97, 34.16, 70.62, 75.54, 75.96, 76.38, 117.07, 125.86, 127.24, 127.43, 127.48, 127.62, 127.89, 130.70, 137.15, 137.61, 139.26, 160.47, 169.49. **Elemental Analysis** of $C_{26}H_{39}N_1O_1Al_1$. Expected; C 76.43, H 9.62, N 3.43. Found; C 76.3, H 10.3, N 3.4.

Preparation of Al(EC)$_2$(Me)$_2$: To a solution of **EC**-H_2 (261 mg, 0.80 mmol) in Tol (20 mL) was added trimethyl aluminium (0.2 mL, 0.40 mmol). The resulting mixture was stirred for two hours, after which time solvent was removed *in-vacuo*. The product was washed with hexane and thoroughly dried under reduced pressure. **^{1}H NMR** ($CDCl_3$) -0.76 (1 H, s) 1.02 - 1.29 (3 H, m) 2.07 - 2.37 (2 H, m) 5.40 (1 H, br. s.) 6.79 - 6.95 (1 H, m) 6.97 - 7.16 (1 H, m) 7.29 (1 H, dd, J=7.8, 1.8 Hz) 7.32 - 7.36 (1 H, m) 7.39 - 7.63 (7 H, m) 7.68 (1 H, d, J=7.2 Hz) 8.30 (1 H, s). **$^{13}C\{^{1}H\}$ NMR** ($CDCl_3$) 10.22, 11.87, 28.61, 31.56, 66.56, 120.27, 120.90, 127.28, 127.98, 128.93, 131.39, 133.38, 134.82, 162.12, 163.48. **Elemental Analysis** of $C_{18}H_{21}N_1O_1Cl_2Al_1$. Expected; C 59.19, H 5.8, N 3.83. Found; C 58.7, H 5.9, N 3.8.

Preparation of Zr(NH)$_2$(O^{i}Pr)$_2$: To a solution of **NH**-H_2 (153 mg, 0.52 mmol) in CH_2CL_2 (25 mL) was added zirconium(IV) isopropoxide isopropanol complex (100 mg, 0.26 mmol). The resulting mixture was stirred for two hours, after which time solvent was removed *in-vacuo*. The product was washed with hexane and thoroughly dried under reduced pressure. **^{1}H NMR** ($CDCl_3$) 1.16 (2 H, s) 1.43 - 1.49 (2 H, m) 2.00 - 2.15 (6 H, m) 3.31 - 3.44 (2 H, m) 6.50 - 6.67 (2 H, m) 6.69 - 6.78 (1 H, m) 6.82 - 7.11 (4 H, m) 7.28 - 7.34 (4 H, m) 7.38 - 7.55 (2 H, m) 7.59 - 7.61 (2 H, m) 7.65 - 7.80 (3 H, m) 7.88 - 8.03 (1 H, m) 8.25 - 8.27 (1 H, m). **$^{13}C^{1}H$ NMR** ($CDCl_3$) 16.82, 30.67(1 C, s) 72.99, 77.20, 118.66, 122.69(1 C, s) 122.97, 124.85, 125.12, 125.45, 125.96, 127.45, 127.87, 127.89, 128.00, 128.08, 131.99, 134.57, 135.16, 157.60, 162.45. **Elemental Analysis** of $C_{46}H_{52}N_2O_4Zr_1$. Expected; C 70.1, H 6.65, N 3.55. Found; C 70.3, H 6.0, N 3.3.

Preparation of Zr(N5)$_2$(O^{i}Pr)$_2$: To a solution of **N5**-H_2 (160 mg, 0.52 mmol) in CH_2CL_2 (25 mL) was added zirconium(IV) isopropoxide isopropanol

complex (100 mg, 0.26 mmol). The resulting mixture was stirred for two hours, after which time solvent was removed *in-vacuo*. The product was washed with hexane and thoroughly dried under reduced pressure. **^{1}H NMR** ($CDCl_3$) 1.04 - 1.08 (2 H, m) 1.12 (1 H, s) 1.15 (2 H, s) 1.34 - 1.43 (2 H, m) 1.61 - 1.75 (3 H, m) 1.93 - 2.15 (7 H, m) 3.35 - 3.47 (1 H, m) 3.37 - 3.45 (1 H, m) 4.37 - 4.49 (1 H, m) 6.51 - 6.68 (2 H, m) 6.72 - 6.78 (1 H, m) 6.81 - 6.85 (1 H, m) 6.95 - 7.11 (3 H, m) 7.21 - 7.29 (4 H, m) 7.38 - 7.47 (2 H, m) 7.52 - 7.55 (1 H, m) 7.58 - 7.65 (2 H, m) 7.68 - 7.79 (3 H, m) 7.84 - 7.88 (1 H, m) 8.34 - 8.35 (1 H, m). **^{13}C{^{1}H} NMR** ($CDCl_3$) 12.69, 19.12, 22.17, 62.42, 70.32, 121.58, 122.55, 125.78, 126.36, 128.23, 131.58, 133.45, 133.97, 134.65, 136.11, 136.15, 156.02, 156.64, 160.32, 162.85. **Elemental Analysis** of $C_{48}H_{58}N_2O_4Zr_1$. Expected; C 70.46, H 7.14, N 3.42. Found; C 70.8, H 6.5, N 3.0.

Preparation of Zr(NB)$_2$(O^{i}Pr)$_2$: To a solution of **NB**-H_2 (211 mg, 0.52 mmol) in CH_2CL_2 (25 mL) was added zirconium(IV) isopropoxide isopropanol complex (100 mg, 0.26 mmol). The resulting mixture was stirred for two hours, after which time solvent was removed *in-vacuo*. The product was washed with hexane and thoroughly dried under reduced pressure. **^{1}H NMR** ($CDCl_3$) 0.90 (3 H, s) 1.02 (2 H, d, J=6.0 Hz) 1.05 - 1.18 (14 H, m) 1.21 (9 H, s) 1.38 (12 H, s) 1.50 (5 H, s) 1.57 - 1.67 (4 H, m) 4.51 - 4.98 (2 H, m) 6.51 - 6.68 (1 H, m) 6.96 - 7.14 (3 H, m) 7.17 **^{13}C{^{1}H}** 7.40 (6 H, m) 7.41 - 7.53 (2 H, m) 7.65 - 7.79 (6 H, m) 7.87 - 8.00 (1 H, m). **^{13}C^{1}H NMR** ($CDCl_3$) 21.85, 22.26, 24.22, 28.55, 29.74, 30.32, 31.25, 31.74, 34.25, 35.31, 35.64, 62.88, 68.03, 71.54, 116.54,, 118.21, 122.77, 124.72, 125.06, 126.11, 126.48, 127.90, 128.27, 128.94, 129.29, 129.76, 130.11, 131.65, 132.43, 137.24, 138.44, 138.94, 141.17, 14.41, 158.05, 160.03, 164.83. **Elemental Analysis** of $C_{62}H_{84}N_2O_4Zr_1$. Expected; C 73.54, H 8.36, N 2.77. Found; C 73.5, H 7.8, N 2.7.

Preparation of Zr(NC)$_2$(O^{i}Pr)$_2$: To a solution of **NC**-H_2 (188 mg, 0.52 mmol) in CH_2CL_2 (25 mL) was added zirconium(IV) isopropoxide isopropanol complex (100 mg, 0.26 mmol). The resulting mixture was stirred for two hours, after which time solvent was removed *in-vacuo*. The product was washed with hexane and thoroughly dried under reduced pressure. **^{1}H NMR** ($CDCl_3$) 0.98 - 1.26 (7 H, m) 1.28 - 1.36 (2 H, m) 1.42 - 1.64 (2 H, m) 1.67 - 1.89 (4 H, m) 2.08 (1 H, d, J=7.0 Hz) 4.77 (2 H, dd, J=12.4, 6.2 Hz) 6.69 - 7.09 (4 H, m) 7.11 - 7.30

(4 H, m) 7.32 - 7.57 (8 H, m) 7.60 - 7.95 (6 H, m) 7.99 (1 H, br. s.) 8.51 (1 H, s). **$^{13}C\{^{1}H\}$ NMR** ($CDCl_3$) 23.29, 24.98, 25.77, 25.92, 26.64, 64.14, 64.67, 68.15, 80.22, 80.55, 120.52, 120.93, 121.85, 123.03, 123.38, 123.79, 124.22, 124.50, 124.60, 124.85, 124.95, 125.13, 125.51, 125.69, 125.88, 126.46, 126.64, 126.75, 127.03, 127.80, 128.09, 128.24, 128.58, 131.46, 132.97, 133.59, 138.14, 157.33, 157.60, 163.09. **Elemental Analysis** of $C_{46}H_{48}N_2O_4Cl_4Zr_1$. Expected; C 59.67, H 5.23, N 3.03. Found; C 60.1, H 5.4, N 3.1.

Preparation of $Hf(NH)_2(O^iPr)_2$: To a solution of **NH**-H_2 (141 mg, 0.48 mmol) in CH_2CL_2 (25 mL) was added hafnium(IV) isopropoxide isopropanol adduct (100 mg, 0.24 mmol). The resulting mixture was stirred for two hours, after which time solvent was removed *in-vacuo*. The product was washed with hexane and thoroughly dried under reduced pressure. **Elemental Analysis** of $C_{46}H_{27}N_1O_4Hf_1$. Expected; C 66.07, H 3.25, N 1.68. Found; C 65.6, H 3.4, N 1.5.

Preparation of $Hf(N5)_2(O^iPr)_2$: To a solution of **N5**-H_2 (148 mg, 0.48 mmol) in CH_2CL_2 (25 mL) was added hafnium(IV) isopropoxide isopropanol adduct (100 mg, 0.24 mmol). The resulting mixture was stirred for two hours, after which time solvent was removed *in-vacuo*. The product was washed with hexane and thoroughly dried under reduced pressure. **^{1}H NMR** ($CDCl_3$) 0.80 - 0.99 (1 H, m) 1.18 (3 H, d, J=6.0 Hz) 1.20 - 1.40 (7 H, m) 1.40 - 1.64 (8 H, m) 1.67 (3 H, d, J=6.4 Hz) 1.76 (3 H, d, J=6.8 Hz) 2.06 - 2.17 (1 H, m) 4.55 (2 H, s) 6.64 (4 H, br. s.) 6.69 - 6.83 (4 H, m) 6.85 - 7.13 (10 H, m) 7.22 - 7.57 (28 H, m) 7.61 (1 H, d, J=4.5 Hz) 7.64 - 7.78 (7 H, m) 7.78 - 7.98 (6 H, m) 8.05 (5 H, s) 8.47 - 8.50 (1 H, m). **$^{13}C\{^{1}H\}$ NMR** ($CDCl_3$) 18.85, 26.84, 27.07, 30.26, 31.67, 70.99, 72.05, 77.20, 117.14, 118.22, 120.59, 120.69, 122.96, 125.72, 125.91, 125.95, 126.09, 127.29, 127.44, 127.89, 127.95, 128.07, 128.12, 132.49, 133.75, 134.29, 134.96, 139.24, 142.26, 157.60, 161.68, 163.04. **Elemental Analysis** of $C_{48}H_{29}N_1O_4Hf_1$. Expected; C 66.86, H 3.39, N 1.62. Found; C 66.0, H 3.9, N 1.6.

Preparation of $Hf(NB)_2(O^iPr)_2$: To a solution of **NB**-H_2 (195 mg, 0.48 mmol) in CH_2CL_2 (25 mL) was added hafnium(IV) isopropoxide isopropanol adduct (100 mg, 0.24 mmol). The resulting mixture was stirred for two hours, after which time solvent was removed *in-vacuo*. The product was washed with hexane and thoroughly dried under reduced pressure. **^{1}H NMR** ($CDCl_3$) 1.21 (5

H, d, J=7.5 Hz) 1.30 (5 H, d, J=5.7 Hz) 1.41 (3 H, d, J=10.5 Hz) 1.51 (4 H, d, J=6.4 Hz) 1.82 (7 H, br. s.) 1.99 - 2.33 (14 H, m) 4.43 - 4.77 (3 H, m) 6.68 (2 H, br. s.) 6.87 (3 H, d, J=8.7 Hz) 7.16 (6 H, d, J=7.9 Hz) 7.26 - 7.57 (18 H, m) 7.65 (2 H, br. s.) 7.74 (4 H, br. s.) 7.78 - 7.92 (5 H, m) 7.99 (5 H, s). **^{13}C{^{1}H} NMR** ($CDCl_3$) 20.01, 21.67, 26.94, 27.07, 61.94, 70.86, 77.20, 120.38, 122.48, 125.83, 125.87, 125.91, 126.60, 127.04, 127.36, 127.93, 128.02, 132.48, 132.55, 132.79, 132.87, 134.03, 136.00, 136.06, 157.64, 159.63, 163.23. **Elemental Analysis** of $C_{62}H_{43}N_1O_4Hf_1$. Expected; C 71.29, H 4.15, N 1.34. Found; C 71.6, H 4.4, N 1.2.

Preparation of Hf(NC)$_2$(O^{i}Pr)$_2$: To a solution of **NC**-H_2 (174 mg, 0.48 mmol) in CH_2CL_2 (25 mL) was added hafnium(IV) isopropoxide isopropanol adduct (100 mg, 0.24 mmol). The resulting mixture was stirred for two hours, after which time solvent was removed *in-vacuo*. The product was washed with hexane and thoroughly dried under reduced pressure. **^{1}H NMR** ($CDCl_3$) 1.08 (4 H, s) 1.10 (11 H, s) 1.15 (6 H, d, J=6.0 Hz) 1.21 (6 H, s) 1.31 - 1.44 (14 H, m) 1.48 (15 H, s) 1.63 (8 H, t, J=6.6 Hz) 4.39 - 4.53 (2 H, m) 4.54 - 4.68 (1 H, m) 5.44 - 5.55 (1 H, m) 6.57 - 6.61 (1 H, m) 6.63 - 6.70 (2 H, m) 6.98 - 7.01 (1 H, m) 7.12 - 7.15 (1 H, m) 7.35 (9 H, d, J=2.3 Hz) 7.51 - 7.57 (1 H, m) 7.61 - 7.78 (5 H, m) 7.95 (1 H, s) 8.37 (1 H, s). **^{13}C{^{1}H} NMR** ($CDCl_3$) 22.15, 24.76, 27.55, 29.47, 29.83, 31.46, 31.50, 33.94, 34.13, 35.23, 35.29, 61.21, 68.43, 70.93, 77.21, 117.96, 122.69, 124.99, 125.72, 126.06, 126.60, 126.88, 127.30, 127.65, 127.84, 127.89, 128.46, 129.72, 132.35, 132.72, 132.86, 133.44, 138.34, 138.90, 139.21, 140.10, 141.41, 158.05, 160.03, 164.83, 168.54. **Elemental Analysis** of $C_{46}H_{25}N_1O_4Cl_4Hf_1$. Expected; C 56.61, H 2.58, N 1.44. Found; C 56.9, H 3.3, N 1.3.

Preparation of Ti(NH)$_2$(O^{i}Pr)$_2$: To a solution of **NH**-H_2 (176 mg, 0.60 mmol) in CH_2CL_2 (25 mL) was added titanium(IV) isopropoxide (0.08 mL, 0.29 mmol). The resulting mixture was stirred for two hours, after which time solvent was removed *in-vacuo*. The product was washed with hexane and thoroughly dried under reduced pressure. **^{1}H NMR** ($CDCl_3$) **^{13}C{^{1}H} NMR** ($CDCl_3$) 24.44, 24.49, 76.19, 77.46, 116.17, 117.99, 121.73, 124.83, 124.92, 125.44, 126.09, 126.44, 126.96, 131.52, 131.93, 132.76, 133.18, 162.54. **Elemental Analysis** of $C_{46}H_{56}N_2O_4Ti_1$. Expected; C 73.78, H 7.54, N 3.74. Found; C 73.5, H 8.0, N 3.3.

Preparation of Ti(N5)$_2$(O^{i}Pr)$_2$: To a solution of **N5**-H_2 (184 mg, 0.60 mmol) in CH_2CL_2 (25 mL) was added titanium(IV) isopropoxide (0.08 mL, 0.29 mmol). The resulting mixture was stirred for two hours, after which time solvent was removed *in-vacuo*. The product was washed with hexane and thoroughly dried under reduced pressure. **^{1}H NMR** ($CDCl_3$) . 1.08 (12 H, t, *J*=6.8 Hz) 1.37 (3 H, d, *J*=6.8 Hz) 1.54 (5 H, br. s.) 2.05 (7 H, s) 4.73 (2 H, s) 6.57 - 6.85 (5 H, m) 7.01 (3 H, dd, *J*=8.3, 2.3 Hz) 7.12 (1 H, s) 7.23 - 7.54 (10 H, m) 7.64 (4 H, d, *J*=7.9 Hz) 7.86 (3 H, s). **^{13}C{^{1}H} NMR** ($CDCl_3$) 19.10, 24.52, 24.55, 77.11, 117.65, 121.36, 124.78, 124.87, 124.97, 125.07, 126.40, 126.73, 126.89, 126.95, 131.49, 131.92, 132.58, 134.18, 160.43, 163.66. **Elemental Analysis** of $C_{48}H_{62}N_2O_4Ti_1$. Expected; C 74.02, H 8.02, N 3.6. Found; C 73.8, H 9.0, N 3.6.

Preparation of Ti(NB)$_2$(O^{i}Pr)$_2$: To a solution of **NB**-H_2 (243 mg, 0.60 mmol) in CH_2CL_2 (25 mL) was added titanium(IV) isopropoxide (0.08 mL, 0.29 mmol). The resulting mixture was stirred for two hours, after which time solvent was removed *in-vacuo*. The product was washed with hexane and thoroughly dried under reduced pressure. **^{1}H NMR** ($CDCl_3$) 1.02 (2 H, d, *J*=6.4 Hz) 1.08 - 1.15 (8 H, m) 1.21 (9 H, s) 1.38 (9 H, s) 1.51 (6 H, s) 1.63 (4 H, d, *J*=6.4 Hz) 4.77 - 4.96 (1 H, m) 6.66 (1 H, d, *J*=2.3 Hz) 6.99 (1 H, d, *J*=2.3 Hz) 7.11 (1 H, d, *J*=0.8 Hz) 7.30 (1 H, d, *J*=2.6 Hz) 7.32 - 7.41 (4 H, m) 7.44 (1 H, dd, *J*=8.7, 1.9 Hz) 7.48 - 7.54 (1 H, m) 7.62 - 7.85 (6 H, m) 7.94 (2 H, s) 8.37 (1 H, s). **^{13}C{^{1}H} NMR** ($CDCl_3$) 24.82, 26.12, 26.24, 29.53, 30.12, 31.57, 34.08, 34.20, 35.33, 68.49, 77.27, 77.99, 118.03, 122.73, 125.08, 125.82, 126.13, 126.18, 127.05, 127.71, 127.97, 128.47, 132.36, 132.92, 136.74, 140.16, 141.47, 158.11, 160.63, 164.89. **Elemental Analysis** of $C_{62}H_{88}N_2O_4Ti_1$. Expected; C 76.51, H 9.11, N 2.88. Found; C 76.5, H 9.1, N 2.9.

Preparation of Ti(NC)$_2$(O^{i}Pr)$_2$: To a solution of **NC**-H_2 (217 mg, 0.60 mmol) in CH_2CL_2 (25 mL) was added titanium(IV) isopropoxide (0.08 mL, 0.29 mmol). The resulting mixture was stirred for two hours, after which time solvent was removed *in-vacuo*. The product was washed with hexane and thoroughly dried under reduced pressure. **^{1}H NMR** ($CDCl_3$) 0.87 - 1.17 (10 H, m) 1.20 (3 H, d, *J*=6.03 Hz) 1.61 (2 H, d, *J*=6.78 Hz) 1.65 (2 H, d, *J*=6.78 Hz) 1.70 (2 H, br. s.) 1.97 (2 H, d, *J*=6.78 Hz) 4.67 (2 H, dt, *J*=12.62, 6.50 Hz) 6.60 - 6.70 (1 H, m) 6.81 - 6.98 (1 H, m) 7.01 - 7.15 (2 H, m) 7.18 (1 H, d, *J*=2.64 Hz) 7.25 - 7.45 (8

H, m) 7.50 - 7.81 (8 H, m) 7.88 (2 H, br. s.) 8.40 (1 H, s). **$^{13}C\{^{1}H\}$ NMR** ($CDCl_3$) 23.47, 24.40, 24.61, 25.06, 30.37, 34.58, 35.14, 39.39, 40.00, 53.10, 62.74, 63.23, 76.19, 89.85, 118.99, 119.57, 120.48, 121.27, 121.94, 122.35, 123.47, 125.07, 125.16, 126.48, 126.68, 126.88, 127.21, 127.81, 128.08, 130.17, 130.84, 131.59, 131.76, 131.95, 132.21, 132.36, 139.04, 142.76, 149.98, 156.17, 162.53. **Elemental Analysis** of $C_{46}H_{52}N_2O_4Cl_4Ti_1$. Expected; C 62.32, H 5.91, N 3.16. Found; C 62.8, H 6.4, N 2.9.

Preparation of Al(NH)(Me)$_2$: To a solution of **NH**-H_2 (235 mg, 0.80 mmol) in Tol (20 mL) was added trimethyl aluminium (0.2 mL, 0.40 mmol). The resulting mixture was stirred for two hours, after which time solvent was removed *in-vacuo*. The product was washed with hexane and thoroughly dried under reduced pressure. **^{1}H NMR** ($CDCl_3$) -0.73 - -0.55 (3 H, m) 1.78 (2 H, d, J=7.0 Hz) 2.01 (1 H, d, J=6.6 Hz) 5.80 (1 H, d, J=6.8 Hz) 6.52 - 6.58 (1 H, m) 6.89 - 6.96 (1 H, m) 7.07 (1 H, ddd, J=8.5, 7.0, 1.8 Hz) 7.33 - 7.45 (2 H, m) 7.70 - 7.82 (3 H, m) 7.83 - 7.93 (1 H, m) 7.96 - 8.03 (1 H, m). **$^{13}C\{^{1}H\}$ NMR** ($CDCl_3$) 20.09, 21.06, 57.58, 58.89, 76.18, 115.75, 119.18, 119.88, 124.74, 125.12, 125.22, 125.62, 125.65, 126.08, 126.55, 127.05, 127.17, 131.54, 132.07, 132.20, 133.41, 140.09, 162.58, 165.84. **Elemental Analysis** of $C_{22}H_{29}N_1O_1Al_1$. Expected; C 75.4, H 8.34, N 4.0. Found; C 75.9, H 8.4, N 4.0.

Preparation of Al(N5)(Me)$_2$: To a solution of **N5**-H_2 (246 mg, 0.80 mmol) in Tol (20 mL) was added trimethyl aluminium (0.2 mL, 0.40 mmol). The resulting mixture was stirred for two hours, after which time solvent was removed *in-vacuo*. The product was washed with hexane and thoroughly dried under reduced pressure. **^{1}H NMR** ($CDCl_3$) -0.72 - -0.67 (1 H, m) 1.77 (2 H, d, J=7.0 Hz) 2.00 (1 H, d, J=6.8 Hz) 2.03 - 2.11 (3 H, m) 5.80 (1 H, d, J=6.8 Hz) 6.42 (1 H, d, J=8.5 Hz) 6.69 - 6.78 (1 H, m) 6.89 (1 H, dd, J=8.5, 2.1 Hz) 7.32 - 7.46 (2 H, m) 7.70 - 7.83 (3 H, m) 7.83 - 7.96 (3 H, m). **$^{13}C\{^{1}H\}$ NMR** ($CDCl_3$) 18.99, 20.02, 57.51, 58.87, 118.71, 119.61, 124.57, 124.73, 124.90, 125.07, 125.19, 125.62, 125.76, 126.20, 126.55, 127.06, 127.12, 131.54, 131.91, 132.07, 134.43, 138.69, 140.21, 160.59, 166.46. **Elemental Analysis** of $C_{23}H_{31}N_1O_1Al_1$. Expected; C 75.79, H 8.57, N 3.84. Found; C 76.2, H 8.6, N 3.5.

Preparation of Al(NB)(Me)$_2$: To a solution of **NB**-H_2 (324 mg, 0.80 mmol) in Tol (20 mL) was added trimethyl aluminium (0.2 mL, 0.40 mmol). The resulting mixture was stirred for two hours, after which time solvent was removed *in-vacuo*. The product was washed with hexane and thoroughly dried under reduced pressure. **^{1}H NMR** ($CDCl_3$) -0.77 (3 H, s) 1.68-1.88 (2H, m) 2.12 (1 H, s) 6.48 - 6.52 (1 H, m) 6.65 - 6.78 (1 H, m) 7.10-7.12 (1 H, m) 7.30 - 7.36 (2 H, m) 7.75 - 7.95 (2 H, m) 7.99 (1 H, m). **^{13}C{^{1}H} NMR** ($CDCl_3$) 19.56, 20.86, 66.77, 75.28, 119.88, 120.54, 125.47, 125.05, 125.42, 126.55, 127.35, 127.37, 128.25, 132.54, 133.44, 141.69, 161.25. **Elemental Analysis** of $C_{30}H_{45}N_1O_1Al_1$. Expected; C 77.88, H 9.8, N 3.03. Found; C 78.4, H 10.2, N 2.9.

Preparation of Al(NC)(Me)$_2$: To a solution of **NC**-H_2 (290 mg, 0.80 mmol) in Tol (20 mL) was added trimethyl aluminium (0.2 mL, 0.40 mmol). The resulting mixture was stirred for two hours, after which time solvent was removed *in-vacuo*. The product was washed with hexane and thoroughly dried under reduced pressure. **^{1}H NMR** ($CDCl_3$) -0.66 (1 H, m) 1.10 - 1.17 (1 H, m) 1.46 - 1.55 (2 H, m) 1.67 (5 H, d, J=6.4 Hz) 1.74 - 1.89 (4 H, m) 2.27 - 2.30 (1 H, m) 3.35 - 3.45 (1 H, m) 4.66 - 4.80 (2 H, m) 6.71 - 6.86 (2 H, m) 7.06 (2 H, d, J=2.3 Hz) 7.33 (5 H, d, J=2.6 Hz) 7.42 (7 H, s) 7.68 - 7.71 (2 H, m) 7.77 (6 H, s) 8.25 (2 H, s). **^{13}C{^{1}H} NMR** ($CDCl_3$) 15.33, 24.57, 39.80, 42.24, 67.78, 77.25, 124.47, 125.17, 126.17, 126.23, 126.46, 127.74, 127.93, 128.25, 128.86, 129.15, 129.44, 132.32, 133.39, 159.10, 160.96, 162.12, 162.90. **Elemental Analysis** of $C_{22}H_{27}N_1O_1Cl_2Al_1$. Expected; C 63.01, H 6.49, N 3.34. Found; C 62.5, H 6.7, N 2.9.

Preparation of Zr(BH)(O^{i}Pr)$_2$: To a solution of zirconium(IV) isopropoxide isopropanol complex (100 mg, 0.26 mmol) in CH_2Cl_2 (10 mL) **BH**-H_2 (122 mg, 0.28 mmol)was added. The resulting mixture was stirred for two hours or until clear, whichever was longer, after which time solvent was removed *in-vacuo*. The product was washed with hexane and thoroughly dried under reduced pressure. **^{1}H NMR** ($CDCl_3$) 1.05 (d, J=6.0 Hz, 3 H), 1.10 (d, J=6.0 Hz, 3 H), 1.18 (s, 4 H), 1.21 (s, 4 H), 1.25 (s, 4 H), 1.28 (s, 6 H), 1.35 (q, J=2.51 Hz, 3 H), 1.43 - 1.47 (m, 2 H), 1.48 - 1.53 (m, 2 H), 1.53 - 1.57 (m, 2 H), 2.33 - 2.60 (m, 1 H), 3.65 (d, J=7.16 Hz, 1 H), 3.92 - 4.04 (m, 1 H), 4.07 - 4.27 (m, 1 H), 4.28 - 4.59 (m, 1 H), 4.66 - 5.02 (m, 1 H), 5.04 - 5.34 (m, 1 H),n6.14 - 6.28 (m, 1 H),

6.65 (dd, J=8.10, 0.94 Hz, 1 H), 6.74 - 6.79 (m, 1 H), 6.84 (d, J=2.6 Hz, 1 H), 7.05 - 7.14 (m, 1 H), 7.15 - 7.25 (m, 1 H), 8.03 (s, 1 H). **$^{13}C\{^{1}H\}$ NMR** ($CDCl_3$) 26.62, 27.09, 29.76, 29.97, 31.64, 31.73, 31.79, 34.09, 34.67, 70.08, 116.59, 118.46, 121.19, 123.48, 125.92, 129.20, 129.42, 133.69, 135.19, 157.55, 165.21. **Elemental Analysis;** of $C_{34}H_{52}N_2O_4Zr_1$, Expected; C 63.41, H 8.14, N 4.35. Found; C 63.57, H 8.25, N 4.29.

Preparation of Zr(BB)($O^{i}Pr$)$_2$: To a solution of zirconium(IV) isopropoxide isopropanol complex (100 mg, 0.26 mmol) in CH_2Cl_2 (10 mL) **BB**-H_2 (153 mg, 0.28 mmol)was added. The resulting mixture was stirred for two hours or until clear, whichever was longer, after which time solvent was removed *in-vacuo*. The product was washed with hexane and thoroughly dried under reduced pressure. **^{1}H NMR** ($CDCl_3$) 1.06 (s, 2 H) 1.26 (d, J=3.0 Hz, 4 H) 1.27 - 1.30 (m, 8 H) 1.31 (d, J=1.13 Hz, 4 H) 1.33 (d, J=2.3 Hz, 4 H) 1.37 (s, 2 H) 1.45 (d, J=2.3 Hz, 3 H) 1.50 - 1.53 (m, 3 H) 2.90 (s, 1 H) 2.99 - 3.16 (m, 1 H) 3.44 - 3.79 (m, 1 H) 3.91 - 4.03 (m, 1 H) 4.03 - 4.17 (m, 2 H) 4.18 - 4.43 (m, 2 H) 4.44 - 4.59 (m, 1 H) 6.85 (d, J=2.6 Hz, 1 H) 6.95 (d, J=2.6 Hz, 1 H) 7.19 (d, J=2.3 Hz, 1 H) 7.37 - 7.40 (m, 1 H) 8.27 - 8.30 (m, 1 H). **$^{13}C\{^{1}H\}$ NMR** ($CDCl_3$) 19.22 - 19.30, 21.18 - 21.25, 25.37, 27.15, 27.26, 27.35, 29.10, 29.71, 31.46 (s, 10 C) 31.67, 31.84 (s, 9 C) 31.87, 34.63, 35.23, 49.36, 54.10, 56.95, 61.42, 69.75, 121.61, 123.56, 124.16, 128.06, 129.18, 136.21, 138.28, 138.42, 158.98, 159.74, 164.76. **Elemental Analysis;** of $C_{42}H_{68}N_2O_4Zr_1$, Expected; C 66.71, H 9.06, N 3.7. Found; C 66.54, H 9.12, N 3.57.

Preparation of Zr(BC)($O^{i}Pr$)$_2$: To a solution of zirconium(IV) isopropoxide isopropanol complex (100 mg, 0.26 mmol) in CH_2Cl_2 (10 mL) **BC**-H_2 (141 mg, 0.28 mmol)was added. The resulting mixture was stirred for two hours or until clear, whichever was longer, after which time solvent was removed *in-vacuo*. The product was washed with hexane and thoroughly dried under reduced pressure. **^{1}H NMR** ($CDCl_3$) 1.08 - 1.59 (m, 54 H) 1.81 (d, J=9.80 Hz, 2 H) 2.38 - 2.49 (m, 1 H) 2.70 - 2.93 (m, 1 H) 3.49 (d, J=6.78 Hz, 1 H) 3.57 - 3.68 (m, 1 H) 3.71 - 3.91 (m, 1 H) 3.98 - 4.12 (m, 1 H) 4.48 (spt, J=6.00 Hz, 1 H) 4.56 - 4.68 (m, 1 H) 6.08 (d, J=2.3 Hz, 1 H) 6.77 (d, J=2.6 Hz, 1 H) 6.97 (d, J=2.3 Hz, 1 H) 7.01 (d, J=2.6 Hz, 1 H). **$^{13}C\{^{1}H\}$ NMR** ($CDCl_3$) 24.89, 27.27, 28.14, 31.87, 33.28, 33.99, 51.05, 54.86, 63.83, 79.81, 120.84, 121.25, 122.24, 122.97, 123.45,

124.26, 125.83, 126.96, 135.23, 141.49, 158.34, 159.82. **Elemental Analysis;** of $C_{34}H_{60}N_2O_6Cl_2Zr_1$, Expected; C 54.09, H 8.01, N 3.71. Found; C 54.89, H 7.18, N 3.86.

Preparation of Zr(BA)(O^iPr)$_2$: To a solution of **BA**-H_2 (197 mg, 0.28 mmol) in CH_2Cl_2 (10 mL) zirconium(IV) isopropoxide isopropanol complex (100 mg, 0.28 mmol)was added. The resulting mixture was stirred for two hours or until clear, whichever was longer, after which time solvent was removed *in-vacuo*. The product was washed with hexane and thoroughly dried under reduced pressure. **^{1}H NMR** ($CDCl_3$) 1.13 - 1.19 (m, 3 H) 1.22 (d, J=5.65 Hz, 6 H) 1.26 (d, J=1.51 Hz, 4 H) 1.29 (d, J=1.13 Hz, 3 H) 1.30 (s, 5 H) 1.31 (s, 6 H) 1.33 (br. s., 2 H) 1.35 (d, J=2.3 Hz, 3 H) 1.38 (s, 4 H) 1.81 (br. s., 5 H) 2.10 (br. s., 3 H) 2.20 (br. s., 4 H) 3.67 - 3.77 (m, 1 H) 3.93 - 4.02 (m, 1 H) 4.21 - 4.46 (m, 2 H) 6.86 (d, J=2.3 Hz, 1 H) 7.04 (d, J=2.3 Hz, 1 H) 7.20 (d, J=2.6 Hz, 1 H) 7.33 (d, J=2.6 Hz, 1 H) 8.29 (s, 1 H). **^{13}C{^{1}H} NMR** ($CDCl_3$) 25.38, 27.22, 27.40, 29.10, 29.48, 31.46, 31.49, 31.66, 31.70, 31.85, 34.63, 34.80, 37.10, 37.27, 40.23, 40.42, 69.78, 117.77, 121.56, 122.63, 123.15, 125.80, 127.01, 136.80, 136.86, 138.53, 140.14, 140.21, 157.95, 167.43. **Elemental Analysis;** of $C_{54}H_{81}N_2O_4Zr_1$, Expected; C 71.00, H 8.94, N 3.07. Found; C 71.42, H 9.06, N 3.50.

Preparation of Zr(BD)(O^iPr)$_2$: To a solution of **BD**-H_2 (mg, 0.28 mmol) in CH_2Cl_2 (10 mL) zirconium(IV) isopropoxide isopropanol complex (100 mg, 0.28 mmol)was added. The resulting mixture was stirred for two hours or until clear, whichever was longer, after which time solvent was removed *in-vacuo*. The product was washed with hexane and thoroughly dried under reduced pressure. **^{1}H NMR** ($CDCl_3$) 1.09 (s, 3 H) 1.13 - 1.15 (m, 1 H) 1.16 (d, J=2.6 Hz, 1 H) 1.18 (d, J=2.6 Hz, 1 H) 1.19 - 1.25 (m, 6 H) 1.28 (d, J=0.8 Hz, 9 H) 1.30 (d, J=2.3 Hz, 3 H) 1.38 (s, 3 H) 1.51 (d, J=2.3 Hz, 2 H) 1.56 (s, 1 H)1.64 - 1.70 (m, 5 H) 1.70 (s, 1 H) 2.75 - 2.87 (m, 1 H) 2.92 - 3.05 (m, 1 H) 3.55 (s, 1 H) 3.79 - 3.96 (m, 2 H) 3.98 - 4.08 (m, 2 H) 4.34 (m, J=6.0 Hz, 2 H) 6.83 (d, J=2.3 Hz, 1 H) 6.99 (d, J=2.3 Hz, 1 H) 7.01 - 7.33 (m, 11 H) 7.39 (d, J=2.6 Hz, 1 H) 8.19 (s, 1 H). **^{13}C{^{1}H} NMR** ($CDCl_3$) 24.61, 26.01, 26.81, 29.35, 29.49, 31.41, 31.83, 32.87, 33.65, 33.79, 35.55, 35.86, 36.74, 36.80, 36.81, 37.31, 37.75, 38.21, 39.61, 40.54, 40.80, 41.74, 42.35, 50.04, 54.54, 70.33, 75.45, 121.64, 122.22, 122.72, 122.82, 123.75, 124.04, 124.64, 125.24, 126.71, 126.73, 127.66, 127.84, 127.98, 135.98,

136.55, 136.81, 137.56, 148.12, 148.28, 150.71, 150.93, 160.02. **Elemental Analysis;** of $C_{52}H_{78}N_2O_4Zr_1$, Expected; C 70.46, H 8.87, N 3.16. Found; C 71.02, H 7.76, N 3.60.

Preparation of Zr(BM)(O^iPr)$_2$: To a solution of **BM**-H_2 (mg, 0.28 mmol) in CH_2Cl_2 (10 mL) zirconium(IV) isopropoxide isopropanol complex (100 mg, 0.28 mmol)was added. The resulting mixture was stirred for two hours or until clear, whichever was longer, after which time solvent was removed *in-vacuo*. The product was washed with hexane and thoroughly dried under reduced pressure. **^{1}H NMR** ($CDCl_3$) 1.01 (s, 3 H), 1.02 (d, J=2.6 Hz, 2 H), 1.05 (br. s., 2 H), 1.07 (br. s., 1 H), 1.15 (dd, J=6.40, 2.3 Hz, 5 H), 1.22 (d, J=1.88 Hz, 3 H), 1.24 (d, J=2.3 Hz, 5 H), 1.26 (br. s., 4 H), 1.28 (d, J=1.88 Hz, 9 H), 1.32 (d, J=2.6 Hz, 9 H), 1.39 (dd, J=6.0, 1.88 Hz, 2 H), 1.44 (d, J=4.14 Hz, 1 H), 1.47 - 1.56 (m, 5 H), 2.26 - 2.32 (m, 2 H), 4.06 (d, J=5.27 Hz, 1 H), 4.17 - 4.33 (m, 1 H), 6.90 (d, J=2.6 Hz, 1 H), 7.01 (d, J=2.6 Hz, 1 H), 7.15 (d, J=2.3 Hz, 1 H), 7.25 (d, J=2.6 Hz, 1 H), 7.96 (s, 1 H). **^{13}C{^{1}H} NMR** ($CDCl_3$) 26.47, 28.95, 31.42, 31.49, 31.87, 31.89, 32.60, 33.66, 33.94, 34.02, 34.05, 54.69, 59.50, 60.70, 75.02, 120.64, 121.51, 122.55, 123.14, 123.74, 127.83, 129.42, 132.68, 135.58, 136.10, 137.87, 139.18, 153.82, 159.20, 160.69, 160.88. **Elemental Analysis;** of $C_{39}H_{64}N_2O_5Zr_1$, Expected; C 63.98, H 8.81, N 3.83. Found; C 63.93, H 9.54, N 4.03.

Preparation of Hf(BH)(O^iPr)$_2$: To a solution of hafnium(IV) isopropoxide isopropanol adduct (100 mg, 0.24 mmol) in CH_2Cl_2 (10 mL) **BH**-H_2 (105 mg, 0.24 mmol)was added. The resulting mixture was stirred for two hours or until clear, whichever was longer, after which time solvent was removed *in-vacuo*. The product was washed with hexane and thoroughly dried under reduced pressure. **^{1}H NMR** ($CDCl_3$) 1.03-1.05 (m, 3 H), 1.11 (d, J=6.0 Hz, 3 H), 1.20 (s, 4 H), 1.22 (s, 4 H), 1.26 (s, 4 H), 1.29 (s, 6 H), 1.37 (q, J=2.51 Hz, 3 H), 1.42 - 1.48 (m, 2 H), 1.49 - 1.54 (m, 2 H), 1.54 - 1.56 (m, 2 H), 2.30 - 2.60 (m, 1 H), 3.63 (d, J=7.16 Hz, 1 H), 3.90 - 4.00 (m, 1 H), 4.05 - 4.28 (m, 1 H), 4.29 - 4.58 (m, 1 H), 4.61 - 4.95 (m, 1 H), 5.14 - 5.39 (m, 1 H), 6.13 - 6.27 (m, 1 H), 6.55 (dd, J=8, 0.94 Hz, 1 H), 6.75 - 6.78 (m, 1 H), 6.86 (d, J=2.6 Hz, 1 H), 7.02 - 7.15 (m, 1 H), 7.16 - 7.29 (m, 1 H), 8.09 (s, 1 H). **^{13}C{^{1}H} NMR** ($CDCl_3$) 27.01, 27.40, 29.68, 30.13, 31.71, 31.76, 31.83, 33.95, 34.71, 70.67, 116.99, 119.18, 119.4 121.13, 123.48, 125.87, 126.28, 129.29, 129.52, 131.15, 133.60, 135.30, 165.32.

Elemental Analysis; of $C_{34}H_{52}N_2O_4Hf_1$, Expected; C 55.84, H 7.17, N 3.83. Found; C 55.53, H 7.18, N 4.06.

Preparation of Hf(BB)(O^{i}Pr)$_2$: To a solution of hafnium(IV) isopropoxide isopropanol adduct (100 mg, 0.24 mmol) in CH_2Cl_2 (10 mL) **BB**-H_2 (132 mg, 0.24 mmol)was added. The resulting mixture was stirred for two hours or until clear, whichever was longer, after which time solvent was removed *in-vacuo*. The product was washed with hexane and thoroughly dried under reduced pressure. **^{1}H NMR** ($CDCl_3$) 0.90 - 0.93 (m, 2 H) 0.97 - 1.08 (m, 9 H) 1.09 - 1.34 (m, 36 H) 1.47 - 1.60 (m, 3 H) 1.98 - 2.21 (m, 2 H) 2.72 - 2.99 (m, 1 H) 3.05 - 3.18 (m, 1 H) 3.22 - 3.58 (m, 1 H) 4.10 (d, J=13.19 Hz, 2 H) 4.26 - 4.47 (m, 2 H) 4.52 - 4.92 (m, 1 H) 4.93 - 5.28 (m, 1 H) 6.83 - 6.96 (m, 2 H) 7.11 - 7.21 (m, 1 H) 7.38 (d, J=1.88 Hz, 1 H) 7.91 (s, 1 H). **^{13}C{^{1}H} NMR** ($CDCl_3$) 16.61, 21.25, 25.38 27.18, 27.32, 28.94, 31.44, 31.55, 31.74 31.85, 31.87, 33.66, 33.95 - 34.02, 34.35, 49.43 - 49.57, 54.28, 56.97 - 57.21, 61.06, 69.43, 120.86, 121.19, 123.69, 124.04, 127.13, 127.26, 132.91, 136.15, 136.65, 158.85, 159.52, 163.34. **Elemental Analysis;** of $C_{42}H_{70}N_2O_5Hf_1$, Expected; C 58.55, H 8.19, N 3.25. Found; C 58.18, H 9.04, N 3.95.

Preparation of Hf(BC)(O^{i}Pr)$_2$: To a solution of hafnium(IV) isopropoxide isopropanol adduct (100 mg, 0.24 mmol) in CH_2Cl_2 (10 mL) **BC**-H_2 (122 mg, 0.24 mmol)was added. The resulting mixture was stirred for two hours or until clear, whichever was longer, after which time solvent was removed *in-vacuo*. The product was washed with hexane and thoroughly dried under reduced pressure. **^{1}H NMR** ($CDCl_3$) 1.18 (d, J=4.14 Hz, 4 H) 1.20 (s, 3 H) 1.21 - 1.31 (m, 18 H) 1.32 - 1.34 (m, 3 H) 1.35 (d, J=3.39 Hz, 1 H) 1.41 (s, 1 H) 1.42 - 1.45 (m, 1 H) 1.47 (d, J=3.77 Hz, 1 H) 1.49 - 1.54 (m, 2 H) 1.57 (d, J=6.40 Hz, 1 H) 1.81 (d, J=9.80 Hz, 2 H) 2.38 - 2.49 (m, 1 H) 2.70 - 2.93 (m, 1 H) 3.49 (d, J=6.78 Hz, 1 H) 3.57 - 3.68 (m, 1 H) 3.71 - 3.91 (m, 1 H) 3.98 - 4.12 (m, 1 H) 4.48 (spt, J=6.00 Hz, 1 H) 4.56 - 4.68 (m, 1 H) 6.08 (d, J=2.3 Hz, 1 H) 6.77 (d, J=2.6 Hz, 1 H) 6.97 (d, J=2.3 Hz, 1 H) 7.01 (d, J=2.6 Hz, 1 H). **^{13}C{^{1}H} NMR** ($CDCl_3$) 25.30, 27.17, 27.66, 31.23, 33.52, 34.01, 50.55, 57.25, 65.24, 79.90, 120.18, 121.72, 122.36, 123.17, 122.55, 124.73, 125.00, 126.96, 134.13, 140.80, 157.54, 158.71. **Elemental Analysis;** of $C_{34}H_{50}N_2O_4Cl_2Hf_1$, Expected; C 51.04, H 6.30, N 3.50. Found; C 50.93, H 6.49, N 3.60.

Preparation of Hf(BA)(O^iPr)$_2$: To a solution of **BA**-H_2 (mg, 0.24 mmol) in CH_2Cl_2 (10 mL) hafnium(IV) isopropoxide isopropanol adduct (100 mg, 0.24 mmol)was added. The resulting mixture was stirred for two hours or until clear, whichever was longer, after which time solvent was removed *in-vacuo*. The product was washed with hexane and thoroughly dried under reduced pressure. **^{1}H NMR** ($CDCl_3$) 1.01 - 1.04 (m, 2 H) 1.07 (s, 2 H) 1.17 (dd, J=6.0, 3.0 Hz, 4 H) 1.27 (d, J=1.51 Hz, 6 H) 1.31 (br. s., 8 H) 1.31 - 1.32 (m, 7 H) 1.33 (s, 8 H) 1.36 - 1.38 (m, 4 H) 1.39 - 1.42 (m, 5 H) 1.53 - 1.57 (m, 3 H) 1.75 - 1.91 (m, 9 H) 2.12 (br. s., 4 H) 2.22 (br. s., 4 H) 3 Aliphatic Protons short 3.48 - 3.62 (m, 1 H) 3.94 - 4.03 (m, 1 H) 4.06 - 4.21 (m, 2 H) 4.29 - 4.40 (m, 1 H) 4.45 - 4.55 (m, 1 H) 6.88 (d, J=2.6 Hz, 1 H) 7.05 (d, J=2.6 Hz, 1 H) 7.22 (d, J=2.6 Hz, 1 H) 7.35 (d, J=2.6 Hz, 1 H) 8.31 (s, 1 H). **^{13}C{^{1}H} NMR** ($CDCl_3$) 27.49, 27.53, 29.09, 29.12, 29.22, 29.44, 31.46, 31.48, 31.66,31.68, 31.85, 31.87, 33.94, 34.07, 34.80, 37.10, 37.18, 37.25, 40.19, 40.32, 40.42, 57.03, 69.44, 117.77, 122.62, 123.64, 124.46, 125.79, 126.99, 127.92, 136.68, 136.94, 140.00, 140.21 - 140.42, 157.93, 167.43. **Elemental Analysis;** of $C_{54}H_{80}N_2O_4Hf_1$, Expected; C 64.88, H 8.07, N 2.80. Found; C 64.48, H 8.19, N 2.93.

Preparation of Hf(BD)(O^iPr)$_2$: To a solution of **BD**-H_2 (mg, 0.24 mmol) in CH_2Cl_2 (10 mL) hafnium(IV) isopropoxide isopropanol adduct (100 mg, 0.24 mmol)was added. The resulting mixture was stirred for two hours or until clear, whichever was longer, after which time solvent was removed *in-vacuo*. The product was washed with hexane and thoroughly dried under reduced pressure. **^{1}H NMR** ($CDCl_3$) 1.11-1.33 (m, 2H) 1.22 (s, 3 H) 1.24 (s, 3 H) 1.28 (s, 9 H) 1.38 (s, 9 H) 1.48-1.73 (m, 4H) 1.66 (s, 3 H) 1.70 (s, 3 H) 2.63 - 2.93 (m, 2 H) 2.92 - 3.06 (m, 1 H) 3.47 - 3.52 (m, 1 H) 3.52 - 3.60 (m, 1 H) 3.85 - 3.94 (m, 1 H) 3.97 - 4.11 (m, 1 H) 4.42 - 4.49 (m, 2 H) 6.80 (d, J=2.6 Hz, 1 H) 6.99 (d, J=2.3 Hz, 1 H) 7.13 - 7.31 (m, 11 H) 7.32 (d, J=2.3 Hz, 1 H) 8.19 (s, 1 H). **^{13}C{^{1}H} NMR** ($CDCl_3$) 25.34, 25.96, 26.11, 26.22, 26.62, 29.84, 30.88, 31.73, 31.81, 31.84, 33.99, 34.73, 42.15, 42.22, 42.86, 42.88, 42.91, 54.57, 75.23, 121.98, 121.99, 122.90, 123.15, 124.00, 124.02, 124.05, 124.84, 125.31, 125.39, 126.26, 126.76, 126.80, 127.61, 127.75, 127.79, 129.69, 135.58, 136.75, 136.95, 137.01, 140.35, 151.11, 151.30, 161.49. **Elemental Analysis;** of $C_{52}H_{78}N_2O_8rHf_1$, Expected; C 60.19, H 7.58, N 2.70. Found; C 60.31, H 8.33, N 3.13.

Preparation of Hf(BM)(O^iPr)$_2$: To a solution of **BM**-H_2 (mg, 0.24 mmol) in CH_2Cl_2 (10 mL) hafnium(IV) isopropoxide isopropanol adduct (100 mg, 0.24 mmol)was added. The resulting mixture was stirred for two hours or until clear, whichever was longer, after which time solvent was removed *in-vacuo*. The product was washed with hexane and thoroughly dried under reduced pressure. **^{1}H NMR** ($CDCl_3$) 1.21 (s, 2 H), 1.24 (br. s., 2 H), 1.25 (s, 2 H), 1.26 (s, 3 H), 1.29 (s, 9 H), 1.31 (s, 9 H), 1.33 (d, J=1.88 Hz, 5 H), 1.37 (s, 4 H), 1.45 (s, 3 H),1.46 (s, 6 H), 1.52 (s, 3 H), 1.53 (d, J=2.6 Hz, 3 H), 3.69 - 3.79 (m, 1 H), 3.87 - 3.91 (m, 1 H), 3.92 - 4.19 (m, 2 H), 4.20 - 4.53 (m, 2 H), 6.85 (d, J=2.6 Hz, 1 H), 7.04 (d, J=2.6 Hz, 1 H), 7.19 (d, J=2.6 Hz, 1 H), 7.38 (d, J=2.3 Hz, 1 H), 8.29 (s, 1 H). **^{13}C{^{1}H} NMR** ($CDCl_3$) 26.53, 28.75, 31.45, 31.59, 31.77, 31.96, 32.64, 33.71, 33.98, 34.10, 34.18, 54.74, 59.59, 60.74, 75.06, 120.54, 121.56, 122.62, 123.19, 123.32, 127.87, 129.48, 132.48, 135.62, 136.16, 137.92, 139.22, 153.86, 159.23, 160.85, 160.92. **Elemental Analysis;** of $C_{39}H_{68}N_2O_5Hf_1$, Expected; C 56.88, H 8.32, N 3.40. Found; C 57.06, H 9.24, N 3.46.

Preparation of Ti(BH)(O^iPr)$_2$: To a solution of titanium(IV) isopropoxide (74 mg, 0.26 mmol) in CH_2Cl_2 (10 mL) **BH**-H_2 (113 mg, 0.26 mmol)was added. The resulting mixture was stirred for two hours or until clear, whichever was longer, after which time solvent was removed *in-vacuo*. The product was washed with hexane and thoroughly dried under reduced pressure. **^{1}H NMR** ($CDCl_3$) 1.00 - 1.04 (m, 4 H), 1.09 - 1.15 (m, 4 H), 1.17 (s, 1 H), 1.22 - 1.25 (m, 9 H), 1.27 - 1.28 (m, 9 H), 1.29 - 1.33 (m, 1 H), 1.41 (d, J=1.88 Hz, 1 H), 1.43 (d, J=1.88 Hz, 1 H), 1.46 (s, 3 H), 1.49 - 1.52 (m, 2 H), 3.20 - 3.31 (m, 1 H), 3.36 - 3.50 (m, 1 H), 4.16 (d, J=13.56 Hz, 1 H), 4.47 (d, J=13.56 Hz, 1 H), 5.00 (spt, J=6.00 Hz, 1 H), 5.04 (spt, J=6.00 Hz, 1 H), 6.69 - 6.80 (m, 2 H), 6.82 (d, J=2.3 Hz, 1 H), 6.88 (d, J=2.3 Hz, 1 H), 7.12 - 7.16 (m, 1 H), 7.38 (m, J=8.67 Hz, 1 H), 7.93 (d, J=1.88 Hz, 1 H). **^{13}C{^{1}H} NMR** ($CDCl_3$) 25.08, 25.84, 26.18, 29.06, 29.64, 29.66, 31.57, 31.74, 34.91, 55.37, 58.49, 61.22, 116.95, 118.72, 121.44, 122.63, 123.06, 124.25, 125.00, 125.82, 129.00, 133.01, 134.14, 135.17, 160.88. **Elemental Analysis;** of $C_{34}H_{52}N_2O_4Ti_1$, Expected; C 67.99, H 8.73, N 4.66. Found; C 68.0, H 8.81, N 4.63.

Preparation of Ti(BB)(O^iPr)$_2$: To a solution of titanium(IV) isopropoxide (74 mg, 0.26 mmol) in CH_2Cl_2 (10 mL) **BB**-H_2 (142 mg, 0.26

mmol)was added. The resulting mixture was stirred for two hours or until clear, whichever was longer, after which time solvent was removed *in-vacuo*. The product was washed with hexane and thoroughly dried under reduced pressure. **^{1}H NMR** ($CDCl_3$) 1.02 (s, 6 H) 1.06 - 1.15 (m, 7 H) 1.19 - 1.24 (m, 7 H) 1.26 (s, 3 H) 1.27 (s, 3 H) 1.28 - 1.29 (m, 8 H) 1.30 (s, 8 H) 1.35 (s, 3 H) 1.50 (s, 6 H) 3.16 - 3.25 (m, 1 H) 3.46 - 3.54 (m, 1 H) 5.14 (s, 1 H) 6.89 (d, J=2.3 Hz, 1 H) 6.96 (d, J=2.3 Hz, 1 H) 7.14 (d, J=2.6 Hz, 1 H) 7.46 (d, J=2.6 Hz, 1 H). **^{13}C{^{1}H} NMR** ($CDCl_3$) 20.03, 25.20, 28.53, 28.59, 28.65, 28.89, 30.44, 30.69, 30.74, 30.79, 30.85, 32.99, 33.64, 33.88, 34.30, 53.56, 57.39, 60.37, 73.93, 121.04, 122.13, 122.97, 126.62, 128.01, 134.73, 135.97, 136.10, 137.79, 158.39, 160.08, 161.11. **Elemental Analysis;** of $C_{42}H_{72}N_2O_6Ti_1$, Expected; C 67.36, H 9.69, N 3.74. Found; C 66.74, H 9.87, N 4.10.

Preparation of Ti(BC)(O^{i}Pr)$_2$: To a solution of titanium(IV) isopropoxide (74 mg, 0.26 mmol) in CH_2Cl_2 (10 mL) **BC**-H_2 (131 mg, 0.26 mmol)was added. The resulting mixture was stirred for two hours or until clear, whichever was longer, after which time solvent was removed *in-vacuo*. The product was washed with hexane and thoroughly dried under reduced pressure. **^{1}H NMR** ($CDCl_3$) 1.20 - 1.23 (m, 2 H) 1.23 (br. s., 2 H) 1.25 (s, 9 H) 1.25 (s, 2 H) 1.26 (s, 2 H) 1.28 (s, 1 H) 1.28 - 1.31 (m, 3 H) 1.32 (s, 1 H) 1.42 (s, 2 H) 1.43 (s, 2 H) 1.44 (s, 2 H) 1.45 (s, 2 H) 1.46 (s, 6 H) 1.84 - 1.98 (m, 2 H) 2.37 (m, J=9.80 Hz, 2 H) 3.09 - 3.29 (m, 2 H) 3.32 - 3.56 (m, 2 H) 5.01 - 5.16 (m, 2 H) 5.02 - 5.13 (m, 2 H) 6.84 (d, J=2.6 Hz, 1 H) 7.16 (dd, J=2.6, 0.8 Hz, 1 H) 7.21 (d, J=2.3 Hz, 1 H) 7.31 (d, J=2.6 Hz, 1 H). **^{13}C{^{1}H} NMR** ($CDCl_3$) 23.33, 23.68, 24.92, 25.08, 25.29, 28.16, 28.64, 30.60, 33.22, 33.91, 50.45, 54.46, 56.15, 64.23, 80.80, 120.79, 121.99, 122.06, 123.47, 123.55, 123.99, 125.63, 127.86, 134.33, 140.69, 157.44, 157.81. **Elemental Analysis;** of $C_{34}H_{50}N_2O_4Cl_2Ti_1$, Expected; C 60.99, H 7.53, N 4.18. Found; C 60.93, H 7.62, N 4.24.

Preparation of Ti(BA)(O^{i}Pr)$_2$: To a solution of **BA**-H_2 (183 mg, 0.26 mmol) in CH_2Cl_2 (10 mL) titanium(IV) isopropoxide (74 mg, 0.26 mmol)was added. The resulting mixture was stirred for two hours or until clear, whichever was longer, after which time solvent was removed *in-vacuo*. The product was washed with hexane and thoroughly dried under reduced pressure. **^{1}H NMR** ($CDCl_3$) 0.98 (s, 6 H) 1.00 - 1.07 (m, 3 H) 1.14 (dd, J=6.0, 3.39 Hz, 8 H) 1.18 -

1.20 (m, 2 H) 1.20 - 1.24 (m, 6 H) 1.25 - 1.27 (m, 6 H) 1.28 (s, 12 H) 1.30 - 1.32 (m, 12 H) 1.33 - 1.35 (m, 3 H) 1.39 - 1.49 (m, 7 H) 1.50 - 1.58 (m, 1 H) 2.26 (s, 3 H) 3.21 - 3.32 (m, 1 H) 3.47 - 3.69 (m, 1 H) 4.25 (td, J=14.51, 3.39 Hz, 1 H) 4.48 - 4.61 (m, 2 H) 4.99 (spt, J=6.00 Hz, 1 H) 6.88 (d, J=2.3 Hz, 1 H) 6.97 (d, J=2.3 Hz, 1 H) 7.13 (d, J=2.6 Hz, 1 H) 7.33 - 7.36 (m, 1 H) 7.94 (d, J=1.88 Hz, 1 H). **^{13}C{^{1}H} NMR** ($CDCl_3$) 25.56, 25.77, 25.85, 26.11, 29.06, 31.45, 31.67, 31.82, 34.01, 34.48, 51.43, 58.12, 61.04, 120.09, 123.13, 123.77, 126.39, 126.63, 132.40, 135.37, 137.10, 139.57, 158.98, 161.53. **Elemental Analysis;** of $C_{54}H_{80}N_2O_4Til$, Expected; C 74.63, H 9.28, N 3.22. Found; C 73.83, H 9.97, N 3.49.

Preparation of Ti(BD)(O^{i}Pr)$_2$: To a solution of **BD**-H_2 (175 mg, 0.26 mmol) in CH_2Cl_2 (10 mL) titanium(IV) isopropoxide (74 mg, 0.26 mmol)was added. The resulting mixture was stirred for two hours or until clear, whichever was longer, after which time solvent was removed *in-vacuo*. The product was washed with hexane and thoroughly dried under reduced pressure. **^{1}H NMR** ($CDCl_3$) 0.98 (s, 6 H) 1.04 (s, 1 H) 1.07 - 1.09 (m, 1 H) 1.10 (d, J=2.3 Hz, 1 H) 1.11 - 1.13 (m, 2 H) 1.13 - 1.15 (m, 1 H) 1.17 - 1.20 (m, 12 H) 1.20 - 1.22 (m, 2 H) 1.31 (s, 3 H) 1.50 (d, J=1.50 Hz, 2 H) 1.55 (s, 2 H) 1.63 (d, J=2.3 Hz, 1 H) 1.91 (s, 2 H) 2.89 (s, 2 H) 2.97 - 3.06 (m, 1 H) 3.91 - 4.02 (m, 2 H) 4.26 - 4.48 (m, 2 H) 4.55 - 4.69 (m, 1 H) 4.89 (spt, J=5.84 Hz, 1 H) 6.78 (d, J=2.6 Hz, 1 H) 6.79 (d, J=2.6 Hz, 1 H) 6.98 - 7.17 (m, 11 H) 7.18 (d, J=1.13 Hz, 1 H). **^{13}C{^{1}H} NMR** ($CDCl_3$) 23.26, 25.41, 27.84, 28.09, 29.55, 30.18, 30.79, 30.92, 31.73, 34.85, 42.45, 42.46, 50.67, 68.56, 118.01, 125.05, 125.63, 126.50, 126.75, 127.81, 128.03, 128.52, 129.15, 129.17, 129.51, 130.68, 134.92, 136.03, 137.78, 138.19, 138.57, 138.63, 139.59, 140.34, 150.65, 150.77, 157.58. **Elemental Analysis;** of $C_{52}H_{76}N_2O_6Ti_1$, Expected; C 71.54, H 8.77, N 3.21. Found; C 71.78, H 9.45, N 3.41.

Preparation of Ti(BM)(O^{i}Pr)$_2$: To a solution of **BM**-H_2 (132 mg, 0.26 mmol) in CH_2Cl_2 (10 mL) titanium(IV) isopropoxide (74 mg, 0.26 mmol)was added. The resulting mixture was stirred for two hours or until clear, whichever was longer, after which time solvent was removed *in-vacuo*. The product was washed with hexane and thoroughly dried under reduced pressure. **^{1}H NMR** ($CDCl_3$) 1.02 (s, 5 H), 1.08 (d, J=6.0 Hz, 3 H), 1.17 (s, 1 H), 1.18 (s, 1 H), 1.19 (s,

1 H), 1.20 (s, 1 H), 1.21 (d, J=1.13 Hz, 2 H), 1.26 (s, 2 H), 1.28 (s, 9 H), 1.30 (s, 9 H), 1.35 (s, 2 H), 1.44 (s, 1 H), 1.45 (d, J=1.9 Hz, 1 H), 1.47 (s, 1 H), 1.71 - 1.80 (m, 6 H), 1.87 (d, J=11.7 Hz, 4 H), 2.06 (br. s., 2 H), 2.18 (br. s., 2 H), 2.30 - 2.33 (m, 1 H), 3.14 - 3.25 (m, 1 H), 4.62 (spt, J=6.00 Hz, 1 H), 5.10 (spt, J=6.00 Hz, 1 H), 6.88 (d, J=2.3 Hz, 1 H), 6.95 (d, J=2.6 Hz, 1 H), 7.13 (d, J=2.6 Hz, 1 H), 7.40 (d, J=2.6 Hz, 1 H), 7.92 (d, J=1.51 Hz, 1 H). **$^{13}C\{^{1}H\}$ NMR** ($CDCl_3$) 26.31, 26.45, 26.66, 26.85, 29.24, 29.57, 31.50, 31.78, 31.86, 31.92, 34.05, 34.08, 34.68, 37.24, 37.45, 40.72, 51.44, 54.82, 58.25, 61.52, 63.64, 75.18, 121.87, 122.30, 123.15, 123.97, 127.63, 129.19, 135.79, 137.11, 137.46, 138.91, 159.40, 161.61, 162.32. **Elemental Analysis;** of $C_{39}H_{62}N_2O_4Ti_1$, Expected; C 69.83, H 9.32, N 4.18. Found; C 69.9, H 9.41, N 4.18.

Preparation of Al(BH)(Me)$_2$: To a solution of trimethyl aluminium (19 mg, 0.26 mmol) in CH_2Cl_2 (10 mL) **BH**-H_2 (113 mg, 0.26 mmol)was added. The resulting mixture was stirred for two hours or until clear, whichever was longer, after which time solvent was removed *in-vacuo*. The product was washed with hexane and thoroughly dried under reduced pressure. **^{1}H NMR** ($CDCl_3$) -0.48 (s, 3 H), 1.26 (d, J=5.65 Hz, 3 H), 1.31 (s, 7 H), 1.34 (d, J=4.52 Hz, 4 H), 1.45 (s, 4 H), 1.47 - 1.54 (m, 4 H), 1.65 (s, 1 H), 2.54 - 2.73 (m, 1 H), 2.97 (dd, J=10.93, 9.42 Hz, 1 H), 3.21 (dd, J=11.11, 8.10 Hz, 1 H), 3.50 (d, J=12.81 Hz, 1 H), 6.73 - 6.82 (m, 1 H), 6.91 - 6.99 (m, 2 H), 7.23 (dd, J=7.35, 3.20 Hz, 2 H), 7.30 (d, J=2.6 Hz, 1 H), 8.27 - 8.39 (m, 1 H). **$^{13}C\{^{1}H\}$ NMR** ($CDCl_3$) 24.01, 28.17, 29.43, 29.67, 31.65, 31.71, 31.79, 33.96, 34.79, 48.26, 55.30, 57.15, 61.65, 117.49, 120.91, 123.78, 124.47, 128.19, 131.71, 131.86, 137.88, 139.75, 155.21, 158.53, 167.38. **Elemental Analysis;** of $C_{29}H_{43}N_2O_2Al_1$, Expected; C 72.77, H 9.05, N 5.85. Found; C 73.13, H 9.17, N 5.61.

Preparation of Al(BB)(Me)$_2$: To a solution of trimethyl aluminium (19 mg, 0.26 mmol) in CH_2Cl_2 (10 mL) **BB**-H_2 (142 mg, 0.26 mmol)was added. The resulting mixture was stirred for two hours or until clear, whichever was longer, after which time solvent was removed *in-vacuo*. The product was washed with hexane and thoroughly dried under reduced pressure. **^{1}H NMR** ($CDCl_3$) -0.72 (s, 3 H) 1.24 - 1.31 (m, 27 H) 1.31 - 1.39 (m, 4 H) 1.42 - 1.52 (m, 9 H) 1.66 - 1.90 (m, 2 H) 2.63 - 2.75 (m, 1 H) 2.87 - 3.01 (m, 1 H) 3.35 - 3.44 (m, 1 H) 3.45 - 3.74 (m, 1 H) 4.07 (s, 2 H) 4.09 - 4.29 (m, 1 H) 6.89 (d, J=2.6 Hz, 1 H) 6.91 (d, J=2.3

Hz, 1 H) 7.24 (d, J=2.6 Hz, 1 H) 7.50 (d, J=2.6 Hz, 1 H) 8.28 (s, 1 H). **$^{13}C^{1}H$ NMR** ($CDCl_3$) 28.12, 28.67, 29.31, 29.65, 31.27, 31.33, 31.43, 31.52, 31.69, 32.02, 32.79, 33.84, 34.21, 34.65, 35.12, 41.46, 44.65, 50.17, 50.39, 61.31, 120.84, 121.96, 122.88, 124.99, 128.32, 130.13, 137.42, 144.57, 153.23, 154.62, 160.02, 161.20. **Elemental Analysis;** of $C_{37}H_{59}N_2O_2Al_1$, Expected; C 75.21, H 10.06, N 4.74. Found; C 75.39, H 10.17, N 4.56.

Preparation of Al(BC)(Me)$_2$: To a solution of trimethyl aluminium (19 mg, 0.26 mmol) in CH_2Cl_2 (10 mL) **BC**-H_2 (131 mg, 0.26 mmol)was added. The resulting mixture was stirred for two hours or until clear, whichever was longer, after which time solvent was removed *in-vacuo*. The product was washed with hexane and thoroughly dried under reduced pressure. **^{1}H NMR** ($CDCl_3$) -0.46 (s, 3 H) 1.18-1.47 (m, 6H) 1.25 (s, 9 H) 1.36 (s, 9 H) 1.94 (td, J=11.02, 2.83 Hz, 1 H) 2.48 - 2.56 (m, 1 H) 2.56 - 2.63 (m, 1 H) 2.99 (dd, J=10.93, 8.67 Hz, 1 H) 3.27 (dd, J=11.30, 8.67 Hz, 1 H) 3.71 (d, J=12.43 Hz, 1 H) 4.05 (d, J=12.43 Hz, 1 H) 6.69 (d, J=3.0 Hz, 1 H) 6.80 (d, J=2.6 Hz, 1 H) 7.21 (d, J=2.6 Hz, 1 H) 7.31 (d, J=2.6 Hz, 1 H) No Imine Present. **$^{13}C\{^{1}H\}$ NMR** ($CDCl_3$) 24.01, 27.18, 28.63, 29.12, 30.43, 31.87, 32.26, 33.69, 34.90, 48.52, 55.03, 57.30, 62.66, 118.34, 121.09, 123.87, 125.16, 129.39, 132.55, 130.89, 137.78, 140.67, 156.32, 158.33, 159.22, 167.38. **Elemental Analysis;** of $C_{29}H_{39}N_2O_2Cl_2Al_1$, Expected; C 63.85, H 7.21, N 5.14. Found; C 64.28, H 7.62, N 4.87.

Preparation of Al(BA)(Me)$_2$: To a solution of **BA**-H_2 (183 mg, 0.26 mmol) in CH_2Cl_2 (10 mL) trimethyl aluminium (19 mg, 0.26 mmol)was added. The resulting mixture was stirred for two hours or until clear, whichever was longer, after which time solvent was removed *in-vacuo*. The product was washed with hexane and thoroughly dried under reduced pressure. **^{1}H NMR** ($CDCl_3$) -0.66 (s, 3 H) 1.19 (s, 3 H) 1.25 - 1.28 (m, 9 H) 1.29 - 1.30 (m, 9 H) 1.30 (s, 6 H) 1.40 (s, 2 H) 1.45 (t, J=1.88 Hz, 3 H) 1.50 - 1.65 (m, 4 H) 1.71 - 1.90 (m, 10 H) 2.09 (d, J=2.6 Hz, 5 H) 2.16 - 2.28 (m, 5 H) 2.31 (br. s., 3 H) 3.22 - 3.31 (m, 1 H) 3.78 - 3.89 (m, 1 H) 3.97 - 4.08 (m, 1 H) 4.13 - 4.29 (m, 2 H) 6.87 (d, J=2.3 Hz, 1 H) 6.92 (d, J=2.3 Hz, 1 H) 7.24 (d, J=2.6 Hz, 1 H) 7.42 (d, J=2.6 Hz, 1 H) 8.29 (s, 1 H). **$^{13}C\{^{1}H\}$ NMR** ($CDCl_3$) 29.11, 29.21, 31.23, 31.28, 31.66, 31.93, 33.95, 33.99, 34.95, 35.01, 37.20, 37.30, 37.40, 40.26, 40.38, 45.66, 55.53, 116.87, 123.53, 126.48, 128.10, 129.17, 131.74, 136.46, 137.56, 137.88, 140.76, 156.42,

165.25. **Elemental Analysis;** of $C_{49}H_{73}N_2O_4Al_1$, Expected; C 75.35, H 9.42, N 3.59. Found; C 74.47, H 9.26, N 4.04.

Preparation of Al(BD)(Me)$_2$: To a solution of **BD**-H_2 (175 mg, 0.26 mmol) in CH_2Cl_2 (10 mL) trimethyl aluminium (19 mg, 0.26 mmol)was added. The resulting mixture was stirred for two hours or until clear, whichever was longer, after which time solvent was removed *in-vacuo*. The product was washed with hexane and thoroughly dried under reduced pressure. **^{1}H NMR** ($CDCl_3$) - 1.37 (s, 3 H) 1.25 (s, 3 H) 1.29 (s, 9 H) 1.30 (s, 9 H) 1.34 (s, 3 H) 1.62 - 1.71 (m, 4 H) 1.65 (s, 6 H) 2.71 - 2.85 (m, 1 H) 2.85 - 3.00 (m, 1 H) 3.18 - 3.31 (m, 2 H) 3.72 - 3.89 (m, 1 H) 4.00 - 4.20 (m, 1 H) 6.84 (d, J=2.3 Hz, 1 H) 6.88 (d, J=2.3 Hz, 1 H) 7.08 - 7.26 (m, 11 H) 7.29 (d, J=2.3 Hz, 1 H) 8.18 (s, 1 H). **^{13}C{^{1}H} NMR** ($CDCl_3$) 26.21, 26.89, 27.06, 30.31, 31.09, 32.37, 32.55, 31.60, 33.11, 33.44, 35.22, 39.84, 45.46, 50.24, 51.14, 59.93, 117.23, 117.89, 118.21, 118.56, 118.89, 119.56, 120.84, 121.89, 124.28, 125.55, 128.52, 128.93, 136.52, 146.74, 151.87, 155.11. **Elemental Analysis;** of $C_{47}H_{65}N_2O_5Al_1$, Expected; C 73.79, H 8.56, N 3.66. Found; C 74.43, H 8.67, N 4.46.

Preparation of Al(BM)(Me)$_2$: To a solution of **BM**-H_2 (132 mg, 0.26 mmol) in CH_2Cl_2 (10 mL) trimethyl aluminium (19 mg, 0.26 mmol)was added. The resulting mixture was stirred for two hours or until clear, whichever was longer, after which time solvent was removed *in-vacuo*. The product was washed with hexane and thoroughly dried under reduced pressure. **^{1}H NMR** ($CDCl_3$) 0.74 (s, 3 H), 1.24 (s, 3 H), 1.26 (s, 9 H), 1.28 (s, 9 H), 1.29 (s, 9 H), 1.36 (s, 4 H), 1.44 (s, 2 H), 2.25 (s, 1 H), 2.28 (s, 2 H), 2.65 - 2.76 (m, 1 H), 3.19 (dd, J=10.9, 8.7 Hz, 1 H), 3.34 (dd, J=13.9, 4.9 Hz, 1 H), 3.47 - 3.53 (m, 1 H), 3.69 - 3.78 (m, 1 H), 4.04 (d, J=9.80 Hz, 1 H), 6.82 - 6.85 (m, 1 H), 6.90 (d, J=2.6 Hz, 1 H), 7.23 (d, J=2.6 Hz, 1 H), 7.38 (dd, J=2.6, 0.8 Hz, 1 H), 8.26 (s, 1 H). **^{13}C{^{1}H} NMR** ($CDCl_3$) 29.29, 29.59, 31.27, 31.41, 31.55, 31.70, 31.82, 33.64, 34.01, 34.74, 34.92, 40.48, 44.66, 50.12, 50.23, 61.31, 120.63, 120.96, 123.88, 125.89, 128.21, 129.03, 137.15, 145.47, 152.45, 154.31, 161.20. **Elemental Analysis;** of $C_{34}H_{51}N_2O_2Al_1$, Expected; C 74.69, H 9.40, N 5.12. Found; C 74.6, H 9.71, N 5.09.

4.4. References

(1) Sheldrick, G. *Acta Crystallographica Section A* **2008**, *64*, 112.
(2) Hofsløkken, N. U. S., Lars *Acta Chem. Scand.* **1999**, *53*, 258.
(3) Sokolowski, A.; Müller, J.; Weyhermüller, T.; Schnepf, R.; Hildebrandt, P.; Hildenbrand, K.; Bothe, E.; Wieghardt, K. *J. Am. Chem. Soc.* **1997**, *119*, 8889.

Appendices'

Appendix 1. Crystal data and structure refinement for **$Cu(2IM)_2(OTf)_2$**

Identification code	k10mdj25
Empirical formula	C30 H30 Cu F6 N4 O7 S2
Formula weight	800.24
Temperature	150(2) K
Wavelength	0.71073 Å
Crystal system	Monoclinic
Space group	$P2_1$
Unit cell dimensions	a = 8.50900(10) Å alpha = 90.0 ^{0}
	b = 16.0590(2) Å beta = 97.71 ^{0}
	c = 12.96100(10) Å gamma = 90.0 ^{0}
Volume	1687.10(3) $Å^3$
Z	2
Calculated density	1.575 mg/m^3
Absorption coefficient	0.856 mm^{-1}
F(000)	818
Crystal size	0.40 x 0.40 x 0.40 mm
Theta range for data collection	3.54 to 27.49 ^{0}
Limiting indices	-11<=h<=11, -20<=k<=20, -15<=l<=16
Reflections collected	36148
Independent reflections	7674 [R(int) = 0.0356]
Completeness to theta = 27.49	99.5 %
Absorption correction	None
Max. and min. transmission	0.7258 and 0.7258
Refinement method	Full-matrix least-squares on F^2
Data / restraints / parameters	7674 / 1 / 461
Goodness-of-fit on F^2	1.057
Final R indices [I>2sigma(I)]	R_1 = 0.0216, wR_2 = 0.0536
R indices (all data)	R_1 = 0.0228, wR_2 = 0.0543
Absolute structure parameter	0.000(5)
Largest diff. peak and hole	0.239 and -0.416e.$Å^{-3}$

Appendix 2. Crystal data and structure refinement for **Cu_2(Benzoic acid)$_4$**

Identification code	h12mdj16
Empirical formula	C64 H58 Cu4 O20
Formula weight	1401.26
Temperature	150(2) K
Wavelength	0.71073 Å
Crystal system	Monoclinic
Space group	*C2/c*
Unit cell dimensions	a = 46.979(3) Å alpha = 90.0 ^{0}
	b = 6.5670(4) Å beta = 111.11 ^{0}
	c = 21.9790(13) Å gamma = 90.0 ^{0}
Volume	6189.5(6) Å^3
Z	4
Calculated density	1.504 mg/m^3
Absorption coefficient	1.431 mm^{-1}
F(000)	2872
Crystal size	0.10 x 0.10 x 0.10 mm
Theta range for data collection	3.66 to 25.15 ^{0}
Limiting indices	-55<=h<=52, -7<=k<=7, -26<=l<=26
Reflections collected	24163
Independent reflections	5424 [R(int) = 0.1568]
Completeness to theta = 25.15	97.8 %
Absorption correction	None
Max. and min. transmission	0.8701 and 0.8701
Refinement method	Full-matrix least-squares on F^2
Data / restraints / parameters	5424 / 0 / 419
Goodness-of-fit on F^2	1.088
Final R indices [I>2sigma(I)]	R_1 = 0.069, wR_2 = 0.1585
R indices (all data)	R_1 = 0.1337, wR_2 = 0.1945
Absolute structure parameter	-
Largest diff. peak and hole	0.648 and -0.649e.Å^{-3}

Appendix 3. Crystal data and structure refinement for **$Pd(2IC)Cl_2$**

Identification code	h11mdj06
Empirical formula	C28 H40 Cl4 N4 Pd2
Formula weight	787.24
Temperature	150(2) K
Wavelength	0.71073 Å
Crystal system	Monoclinic
Space group	$P2_1$
Unit cell dimensions	a = 13.5380(4) Å alpha = 90.0 ^{0}
	b = 6.2640(2) Å beta = 98.64 ^{0}
	c = 18.7060(7) Å gamma = 90.0 ^{0}
Volume	1559.04(9) $Å^3$
Z	2
Calculated density	1.677 mg/m^3
Absorption coefficient	1.521 mm^{-1}
F(000)	792
Crystal size	0.10 x 0.10 x 0.05 mm
Theta range for data collection	3.60 to 27.47 ^{0}
Limiting indices	-15<=h<=17, -8<=k<=8, -24<=l<=24
Reflections collected	18346
Independent reflections	6767 [R(int) = 0.0788]
Completeness to theta = 27.47	96.9 %
Absorption correction	None
Max. and min. transmission	0.9278 and 0.8628
Refinement method	Full-matrix least-squares on F^2
Data / restraints / parameters	6767 / 1 / 345
Goodness-of-fit on F^2	1.048
Final R indices [I>2sigma(I)]	R_1 = 0.0386, wR_2 = 0.0851
R indices (all data)	R_1 = 0.0633, wR_2 = 0.0969
Absolute structure parameter	-0.02(4)
Largest diff. peak and hole	0.628 and -1.112e.$Å^{-3}$

Appendix 4. Crystal data and structure refinement for **$Pd(2AM)Cl_2$**

Identification code	h10mdj02
Empirical formula	C32 H42 Cl4 N4 O Pd2
Formula weight	853.3
Temperature	150(2) K
Wavelength	0.71073 Å
Crystal system	Monoclinic
Space group	$P2_1$
Unit cell dimensions	a = 12.0460(3) Å alpha = 90.0 ^{0}
	b = 8.8280(2) Å beta = 87.35 ^{0}
	c = 16.6790(4) Å gamma = 90.0 ^{0}
Volume	1759.11(7) $Å^3$
Z	2
Calculated density	1.611 mg/m^3
Absorption coefficient	1.357 mm^{-1}
F(000)	860
Crystal size	0.20 x 0.20 x 0.03 mm
Theta range for data collection	3.64 to 26.72 ^{0}
Limiting indices	-15<=h<=15, -11<=k<=11, -21<=l<=21
Reflections collected	32921
Independent reflections	32921 [R(int) = 0.0000]
Completeness to theta = 26.72	99.4 %
Absorption correction	None
Max. and min. transmission	0.9669 and 0.7730
Refinement method	Full-matrix least-squares on F^2
Data / restraints / parameters	32921 / 1 / 394
Goodness-of-fit on F^2	1.069
Final R indices [I>2sigma(I)]	R_1 = 0.0712, wR_2 = 0.192
R indices (all data)	R_1 = 0.0975, wR_2 = 0.2312
Absolute structure parameter	-0.04(4)
Largest diff. peak and hole	2.517 and -1.155e.$Å^{-3}$

Appendix 5. Crystal data and structure refinement for **$Pd(2AE)Cl_2$**

Identification code	k10mdj16
Empirical formula	C15 H18 Cl2 N2 Pd
Formula weight	403.61
Temperature	150(2) K
Wavelength	0.71073 Å
Crystal system	Monoclinic
Space group	$P2_1$
Unit cell dimensions	a = 9.44100(10) Å alpha = 90.0 ^{0}
	b = 8.58800(10) Å beta = 89.91 ^{0}
	c = 10.0090(2) Å gamma = 90.0 ^{0}
Volume	799.42(2) $Å^3$
Z	2
Calculated density	1.677 mg/m^3
Absorption coefficient	1.486 mm^{-1}
F(000)	404
Crystal size	0.20 x 0.15 x 0.10 mm
Theta range for data collection	3.62 to 27.45 ^{0}
Limiting indices	-12<=h<=12, -10<=k<=11, -12<=l<=12
Reflections collected	14244
Independent reflections	3499 [R(int) = 0.0223]
Completeness to theta = 27.45	98.5 %
Absorption correction	None
Max. and min. transmission	0.8656 and 0.7554
Refinement method	Full-matrix least-squares on F^2
Data / restraints / parameters	3499 / 1 / 186
Goodness-of-fit on F^2	1.033
Final R indices [I>2sigma(I)]	R_1 = 0.0169, wR_2 = 0.0439
R indices (all data)	R_1 = 0.0174, wR_2 = 0.0441
Absolute structure parameter	-0.016(17)
Largest diff. peak and hole	0.291 and -0.670e.$Å^{-3}$

Appendix 6. Crystal data and structure refinement for **$Pd(2AC)Cl_2$**

Identification code	k10mdj02
Empirical formula	C14.50 H23 Cl3 N2 Pd
Formula weight	438.1
Temperature	150(2) K
Wavelength	0.71073 Å
Crystal system	Orthorhombic
Space group	$P2_12_12_1$
Unit cell dimensions	a = 9.1410(5) Å alpha = 90.0 ^{0}
	b = 16.3710(8) Å beta = 90.0 ^{0}
	c = 23.6310(13) Å gamma = 90.0 ^{0}
Volume	3536.3(3) $Å^3$
Z	8
Calculated density	1.646 mg/m^3
Absorption coefficient	1.496 mm^{-1}
F(000)	1768
Crystal size	0.10 x 0.10 x 0.05 mm
Theta range for data collection	3.59 to 25.04 ^{0}
Limiting indices	-10<=h<=10, -17<=k<=18, -28<=l<=28
Reflections collected	21847
Independent reflections	5417 [R(int) = 0.0621]
Completeness to theta = 25.04	92.0 %
Absorption correction	Multi-scan
Max. and min. transmission	0.9289 and 0.8648
Refinement method	Full-matrix least-squares on F^2
Data / restraints / parameters	5417 / 0 / 367
Goodness-of-fit on F^2	1.218
Final R indices [I>2sigma(I)]	R_1 = 0.0698, wR_2 = 0.1678
R indices (all data)	R_1 = 0.0821, wR_2 = 0.1733
Absolute structure parameter	-0.05(9)
Largest diff. peak and hole	1.799 and -1.652e.$Å^{-3}$

Appendix 7. Crystal data and structure refinement for **$Pd(3AM)Cl_2$**

Identification code	k09mdj22
Empirical formula	C24 H29 Cl4 N3 Pd
Formula weight	607.7
Temperature	150(2) K
Wavelength	0.71073 Å
Crystal system	Triclinic
Space group	*P1*
Unit cell dimensions	a = 9.8530(5) Å alpha = 74.56 ^{0}
	b = 10.1620(7) Å beta = 78.08 ^{0}
	c = 14.6090(11) Å gamma = 65.08 ^{0}
Volume	1320.72(15) $Å^3$
Z	2
Calculated density	1.528 mg/m^3
Absorption coefficient	1.124 mm^{-1}
F(000)	616
Crystal size	0.10 x 0.05 x 0.05 mm
Theta range for data collection	3.87 to 23.72 ^{0}
Limiting indices	-10<=h<=11, -11<=k<=10, -16<=l<=16
Reflections collected	6729
Independent reflections	5632 [R(int) = 0.0970]
Completeness to theta = 23.72	91.9 %
Absorption correction	None
Max. and min. transmission	0.9459 and 0.8959
Refinement method	Full-matrix least-squares on F^2
Data / restraints / parameters	5632 / 3 / 566
Goodness-of-fit on F^2	1.043
Final R indices [I>2sigma(I)]	R_1 = 0.066, wR_2 = 0.1549
R indices (all data)	R_1 = 0.0866, wR_2 = 0.1703
Absolute structure parameter	-0.06(7)
Largest diff. peak and hole	1.294 and -0.965e.$Å^{-3}$

Appendix 8. Crystal data and structure refinement for **$Pd(3AN)Cl_2$**

Identification code	k09mdj27
Empirical formula	C32 H34.50 Cl2 N3 O2 Pd
Formula weight	670.43
Temperature	150(2) K
Wavelength	0.71073 Å
Crystal system	Monoclinic
Space group	$P2_1$
Unit cell dimensions	a = 10.0070(3) Å alpha = 90.0 ^{0}
	b = 14.0130(5) Å beta = 105.64 ^{0}
	c = 11.6760(4) Å gamma = 90.0 ^{0}
Volume	1560.36(9) $Å^3$
Z	2
Calculated density	1.427 mg/m^3
Absorption coefficient	0.798 mm^{-1}
F(000)	687
Crystal size	0.10 x 0.05 x 0.05 mm
Theta range for data collection	3.52 to 25.34 ^{0}
Limiting indices	-12<=h<=12, -16<=k<=16, -14<=l<=14
Reflections collected	23223
Independent reflections	5632 [R(int) = 0.0672]
Completeness to theta = 25.34	99.6 %
Absorption correction	Semi-empirical from equivalents
Max. and min. transmission	0.9612 and 0.9244
Refinement method	Full-matrix least-squares on F^2
Data / restraints / parameters	5632 / 1 / 374
Goodness-of-fit on F^2	1.151
Final R indices [I>2sigma(I)]	R_1 = 0.0513, wR_2 = 0.1237
R indices (all data)	R_1 = 0.0669, wR_2 = 0.1329
Absolute structure parameter	0.00(5)
Largest diff. peak and hole	1.445 and -0.582e.$Å^{-3}$

Appendix 9. Crystal data and structure refinement for **Rh(2IM)(COD)(OTf)**

Identification code	db202
Empirical formula	C23 H26 F3 N2 O3 Rh S
Formula weight	570.43
Temperature	150(2) K
Wavelength	0.6889 Å
Crystal system	Orthorhombic
Space group	$P2_12_12_1$
Unit cell dimensions	a = 8.2422(9) Å alpha = 90.0 ^{0}
	b = 11.1607(8) Å beta = 90.0 ^{0}
	c = 25.101(2) Å gamma = 90.0 ^{0}
Volume	2309.0(4) Å^3
Z	4
Calculated density	1.641 mg/m^3
Absorption coefficient	0.882 mm^{-1}
F(000)	1160
Crystal size	0.05 x 0.05 x 0.05 mm
Theta range for data collection	3.61 to 26.57 ^{0}
Limiting indices	-10<=h<=10, -14<=k<=14, -31<=l<=32
Reflections collected	21917
Independent reflections	5249 [R(int) = 0.1362]
Completeness to theta = 26.57	98.9 %
Absorption correction	Semi-empirical from equivalents
Max. and min. transmission	1.00000 and 0.68351
Refinement method	Full-matrix least-squares on F^2
Data / restraints / parameters	5249 / 0 / 298
Goodness-of-fit on F^2	1.072
Final R indices [I>2sigma(I)]	R_1 = 0.0702, wR_2 = 0.1738
R indices (all data)	R_1 = 0.0832, wR_2 = 0.1929
Absolute structure parameter	0.01(6)
Largest diff. peak and hole	1.424 and -2.712e.Å^{-3}

Appendix 10. Crystal data and structure refinement for **3NOMe**

Identification code	k12mdj01
Empirical formula	C24.50 H24.50 Cl4.50 N3 O2
Formula weight	552.5
Temperature	150(2) K
Wavelength	0.71073 Å
Crystal system	Monoclinic
Space group	$P2_1$
Unit cell dimensions	a = 13.4640(1) Å alpha = 90.0 ^{0}
	b = 16.6580(2) Å beta = 119.24 ^{0}
	c = 13.5710(1) Å gamma = 90.0 ^{0}
Volume	2655.97(4) Å^3
Z	4
Calculated density	1.382 mg/m^3
Absorption coefficient	0.523 mm^{-1}
F(000)	1140
Crystal size	0.30 x 0.30 x 0.25 mm mm
Theta range for data collection	3.86 to 30.05 ^{0}
Limiting indices	-18<=h<=18, -23<=k<=22, -19<=l<=19
Reflections collected	56799
Independent reflections	15370 [R(int) = 0.0409]
Completeness to theta = 30.05	99.6 %
Absorption correction	Multi-scan
Max. and min. transmission	0.8804 and 0.8589
Refinement method	Full-matrix least-squares on F^2
Data / restraints / parameters	15370 / 1 / 633
Goodness-of-fit on F^2	1.007
Final R indices [I>2sigma(I)]	R_1 = 0.0454, wR_2 = 0.1065
R indices (all data)	R_1 = 0.0618, wR_2 = 0.1158
Absolute structure parameter	0.04(3)
Largest diff. peak and hole	1.340 and -0.846 e.Å^{-3}

Appendix 11. Crystal data and structure refinement for **$Zr(2R)_2(O^iPr/0_2$**

Identification code	h12mdj03
Empirical formula	C28 H32 N2 O2 Zr0.50
Formula weight	474.17
Temperature	150(2) K
Wavelength	0.71073 Å
Crystal system	Triclinic
Space group	*P1*
Unit cell dimensions	a = 11.5230(7) Å alpha = 100.87 ^{0}
	b = 14.8820(6) Å beta = 96.63 ^{0}
	c = 15.5280(8) Å gamma = 87.0 ^{0}
Volume	2551.9(2) $Å^3$
Z	4
Calculated density	1.234 mg/m^3
Absorption coefficient	0.264 mm^{-1}
F(000)	1000
Crystal size	0.10 x 0.10 x 0.10 mm
Theta range for data collection	3.63 to 27.53 ^{0}
Limiting indices	-14<=h<=14, -19<=k<=18, -20<=l<=20
Reflections collected	47407
Independent reflections	21737 [R(int) = 0.0569]
Completeness to theta = 27.53	98.8 %
Absorption correction	None
Max. and min. transmission	
Refinement method	Full-matrix least-squares on F^2
Data / restraints / parameters	21737 / 3 / 1171
Goodness-of-fit on F^2	0.974
Final R indices [I>2sigma(I)]	R_1 = 0.0416, wR_2 = 0.0931
R indices (all data)	R_1 = 0.0602, wR_2 = 0.104
Absolute structure parameter	-0.006(17)
Largest diff. peak and hole	0.360 and -0.516e.$Å^{-3}$

Appendix 12. Crystal data and structure refinement for **$Zr(2S)_2(O^iPr/0_2$**

Identification code	h12mdj04
Empirical formula	C28 H32 N2 O2 Zr0.50
Formula weight	474.17
Temperature	150(2) K
Wavelength	0.71073 Å
Crystal system	Triclinic
Space group	*P1*
Unit cell dimensions	a = 11.5250(6) Å alpha = 100.84 ^{0}
	b = 14.8890(7) Å beta = 95.78 ^{0}
	c = 15.5270(9) Å gamma = 87.99 ^{0}
Volume	2552.7(2) Å^3
Z	4
Calculated density	1.234 mg/m^3
Absorption coefficient	0.263 mm^{-1}
F(000)	1000
Crystal size	0.20 x 0.20 x 0.10 mm
Theta range for data collection	3.73 to 27.48 ^{0}
Limiting indices	-14<=h<=14, -19<=k<=19, -20<=l<=19
Reflections collected	46302
Independent reflections	21470 [R(int) = 0.0435]
Completeness to theta = 27.48	98.7 %
Absorption correction	None
Max. and min. transmission	
Refinement method	Full-matrix least-squares on F^2
Data / restraints / parameters	21470 / 3 / 1171
Goodness-of-fit on F^2	1.024
Final R indices [I>2sigma(I)]	R_1 = 0.0385, wR_2 = 0.0972
R indices (all data)	R_1 = 0.0468, wR_2 = 0.1038
Absolute structure parameter	-0.024(17)
Largest diff. peak and hole	0.418 and -0.526e.Å^{-3}

Appendix 13. Crystal data and structure refinement for **Ligand**

Identification code	k12mdj15
Empirical formula	C54 H66 N2 O2
Formula weight	775.09
Temperature	150(2) K
Wavelength	0.71073 Å
Crystal system	Orthorhombic
Space group	$P2_12_12_1$
Unit cell dimensions	a = 6.28800(10) Å alpha = 90.0 ^{0}
	b = 9.7190(2) Å beta = 90.0 ^{0}
	c = 39.2460(10) Å gamma = 90.0 ^{0}
Volume	2398.44(9) Å^3
Z	2
Calculated density	1.073 mg/m^3
Absorption coefficient	0.064 mm^{-1}
F(000)	840
Crystal size	0.10 x 0.10 x 0.05 mm
Theta range for data collection	3.60 to 25.00 ^{0}
Limiting indices	-7<=h<=7, -11<=k<=8, -46<=l<=46
Reflections collected	11472
Independent reflections	3709 [R(int) = 0.0916]
Completeness to theta = 25.0	97.1 %
Absorption correction	None
Max. and min. transmission	0.9968 and 0.9936
Refinement method	Full-matrix least-squares on F^2
Data / restraints / parameters	3709 / 0 / 273
Goodness-of-fit on F^2	1.049
Final R indices [I>2sigma(I)]	R_1 = 0.0527, wR_2 = 0.0987
R indices (all data)	R_1 = 0.1053, wR_2 = 0.1177
Absolute structure parameter	-1(3)
Largest diff. peak and hole	0.171 and -0.168e.Å^{-3}